ACTA CHIMICA

ACADEMIAE SCIENTIARUM HUNGARICAE

ADIUVANTIBUS

V. BRUCKNER, GY. DEÁK, K. POLINSZKY,
E. PUNGOR, G. SCHAY, Z. G. SZABÓ

REDIGIT

B. LENGYEL

TOMUS 66 FASCICULUS 1

AKADÉMIAI KIADÓ, BUDAPEST

1970

ACTA CHIM. ACAD. SCI. HUNG.

ACTA CHIMICA

A MAGYAR TUDOMÁNYOS AKADÉMIA KÉMIAI TUDOMÁNYOK OSZTÁLYÁNAK IDEGEN NYELVŰ KÖZLEMÉNYEI

SZERKESZTI

LENGYEL BÉLA

TECHNIKAI SZERKESZTŐK

DEÁK GYULA és HARASZTHY-PAPP MELINDA

Az Acta Chimica német, angol, francia és orosz nyelven közöl értekezéseket a kémiai tudományok köréből.

Az Acta Chimica változó terjedelmű füzetekben jelenik meg, egy-egy kötet négy füzetből áll. Évente átlag négy kötet jelenik meg.

A közlésre szánt kéziratok a szerkesztőség címére (Budapest 112/91 Műegyetem) küldendők.

Ugyanerre a címre küldendő minden szerkesztőségi levelezés. A szerkesztőség kéziratokat nem ad vissza.

Megrendelhető a belföld számára az „Akadémiai Kiadó"-nál (Budapest V., Alkotmány utca 21. Bankszámla 05-915-111-46), a külföld számára pedig a „Kultúra" Könyv- és Hírlap Külkereskedelmi Vállalatnál (Budapest I., Fő utca 32. Bankszámla: 43-790-057-181) vagy annak külföldi képviseleteinél és bizományosainál.

Die Acta Chimica veröffentlichen Abhandlungen aus dem Bereiche der chemischen Wissenschaften in deutscher, englischer, französischer und russischer Sprache.

Die Acta Chimica erscheinen in Heften wechselnden Umfanges. Vier Hefte bilden einen Band. Jährlich erscheinen 4 Bände.

Die zur Veröffentlichung bestimmten Manuskripte sind an folgende Adresse zu senden:

Acta Chimica
Budapest 112/91 Műegyetem

An die gleiche Anschrift ist auch jede für die Redaktion bestimmte Korrespondenz zu richten. Abonnementspreis pro Band: $16.00.

Bestellbar bei dem Buch- und Zeitungs-Außenhandels-Unternehmen »*Kultúra*« (Budapest I., Fő utca 32. Bankkonto No. 43-790-057-181) oder bei seinen Auslandsvertretungen und Kommissionären.

ACTA CHIMICA

ACADEMIAE SCIENTIARUM HUNGARICAE

ADIUVANTIBUS

V. BRUCKNER, GY. DEÁK, K. POLINSZKY,
E. PUNGOR, G. SCHAY, Z. G. SZABÓ

REDIGIT

B. LENGYEL

TOMUS 66

AKADÉMIAI KIADÓ, BUDAPEST

1970

ACTA CHIM. ACAD. SCI. HUNG.

ACTA CHIMICA

TOMUS 66

Fasciculus 1: 1970
Fasciculus 2: 1970
Fasciculus 3: 1970
Fasciculus 4: 1970

INDEX

ASZTALOS, I. s. KISS, A. B.

BARTÓK, M., BOZÓKI–BARTÓK, G. and KOVÁCS, K.: The Chemistry of 1,3-Bifunctional Systems, VII. Mechanism of the Conversion of 1,3-Chlorohydrins in Alkaline Medium 115

BARTÓK, M. and MOLNÁR, Á.: The Chemistry of 1,3-Bifunctional Systems, IX. The Reaction of 1,3-Butanediol and Some of its Cyclic Derivatives with Hydrochloric Acid .. 319

BÁN, S. s. TÖRÖK, T.

BENEDETTI, E. s. PÁLYI, G.

BIANCHI, M. s. PÁLYI, G.

BIENERT, G. s. WILDENHAIN, W.

BLUMBERG, E. A. s. GÁL, D.

BOGA, E. s. MATKOVICS, B.

BOGNÁR, L. s. VÉRTES, A.

BOGNÁR, R. s. MAKLEIT, S.

BOOK REVIEWS— 131, 345, 469

BORSY, J. s. SZILÁGYI, G.

BOZÓKI–BARTÓK, G. s. BARTÓK, M.

BURGER, K. s. VÉRTES, A.

CASTINEIRA, M. s. SZEJTLI, J.

DÉVAY, J. and SAYED SABET ABD EL REHIM: Measurements on A. C. Corrosion Models ... 39

DÉVAY, J., LENGYEL, B. jr. and MÉSZÁROS, L.: The Elimination of Resistance Polarisation in Potentiostatic Investigation 269

DÉZSI, I. s. KOMOR, M.

EMANUEL, N. M. s. GÁL, D.

ERDEY, L. s. SIMON, J.

FARKAS, J. s. KISS, L.

FOGARASI, G.: The Extreme Values of Force Constants and Mean Vibrational Amplitudes of Ethylene-type Molecules, II. C_2F_4, C_2Cl_4, C_2Br_4 87

GADÓ, P. s. HEGEDÜS, A. J.

GADÓ, P. s. KISS, A. B.

GÁL, D., BLUMBERG, E. A., VALENDO, A. Ya. and EMANUEL, N. M.: Data on Competitive Oxidations, I. The Non-Catalytic Cooxidation of Ethylbenzene and Propylene 55

GÁL, S. s. SIMON, J.

GÁTI, Gy. s. ROCKENBAUER, A.

GÉCZY, I.: Synthetische lineare Polymere, XXIX. Zusammenhang zwischen dem spezifischen Drehvermögen und dem Molekulargewicht bei monotonen Oligopeptiden. (Synthetic Linear Polymers, XXIX. Relationship Between the Specific Rotation and the Molecular Weight of Monotone Oligopeptides) 77

GÖRBICZ, M. and UPOR, E.: Some Questions of the Separation of Trace Elements by Precipitation, VII. Determination of Small Amounts of Copper, Zinc, Nickel, Cobalt and Silver in Rocks After Precipitation with Ammonium Hydroxide 373

HEGEDÜS, A. J. s. KISS, A. B.

HEGEDÜS, A. J., GADÓ, P., SCHLOSSER, G. und NEUGEBAUER, J.: Thermokondensation von WO_3 aus 12-Wolframatokieselsäurehydraten. (The Thermocondensation of Tungsten Trioxide from Hydrated 12-Tungstatosilicic Acid) 349

HENRIQUEZ, R. D. s. SZEJTLI, J.

HENSEKE, G. s. WILDENHAIN, W.

HOLLY, S. s. VASVÁRI, G.

HORVÁTH, G. s. KISS, Á. I.

INCZÉDY, J.: László ERDEY (1910—1970) 135

JÓNÁS, K. and SOLYMÁR, K.: Determination of the Mineral Composition of Bauxites by Infrared Spectrophotometry 1

JÓNÁS, K. and SOLYMÁR, K.: Preparation, X-ray, Derivatographic and Infrared Study of Aluminium-substituted Goethites 383

KAMMER, H.: d^N-Elektronensysteme in trigonalen Ligandenfeldern, I. Theorie. (d^N-Electron Systems in Trigonal Ligand Fields, I. Theory) 189

KAMMER, H.: d^N-Elektronensysteme in trigonalen Ligandenfeldern, II. Interpretation der Spektren von V^{3+}-und Cr^{3+}-Ionen. (d^N Electron Systems in Trigonal Ligand Fields, II. Interpretation of the Spectra of V^{3+} and Cr^{3+} Ions) 209

KASZTREINER, E. s. SZILÁGYI, G.

KAZARYAN, N. A., PUNGOR, E.: Application of Ion-Selective Electrodes in Non-Aqueous Media, I. Study on the Application Limits in Some Non-Aqueous Solvents. (Preliminary Communication) 183

KISS, L. und FARKAS, J.: Untersuchung der Ionisation von Metallen und Metallionenneutralisation mit der rotierenden Ringscheibenelektrode, IV. Allgemeiner Zusammenhang für den in *m* Schritten verlaufenden Vorgang. (Investigation of the Ionization and Neutralization of Metals on the Rotary Ring-disk Electrode, IV. General Relationship for Processes Proceeding in *m* Steps) 33

KISS, A. B., GADÓ, P., ASZTALOS, I. and HEGEDÜS, A. J.: New Results Concerning the Thermal Decomposition of Ammonium Heptamolybdate Tetrahydrate 235

KISS, Á. I. and HORVÁTH, G.: Spectroscopic Investigation of Substituted Carbonyl Groups 431

KISS, L. und FARKAS, J.: Untersuchung der Ionisation von Metallen und Metallionenneutralisation mit der rotierenden Ringscheibenelektrode, V. Untersuchung der anodischen Auflösung von Kupfer in sauren Sulfatlösungen. (Investigation of the Ionization and Neutralization of Metals on the Rotary Ring and Disc Electrode, V. Investigation of the Anodic Dissolution of Copper in Acid Sulfate Solutions) 395

KOMOR, M., VÉRTES, A., DÉZSI, I. and RUFF, I.: Investigation of the Electron Exchange Reaction between Iron (II) and Iron (III) by Mössbauer Effect in Solution 285

KOVÁCS, K. s. BARTÓK, M.

KOVÁCS, K. s. SZILÁGYI, G.

KUSZMANN, J. and VARGA, L.: Synthesis of New Sugar Derivatives Having Potential Antitumour Activity, XIII. Synthesis of 1,2 : 5,6-Diepithio-D-mannitolD-glucitol and Some of Their Derivatives 307

LÁSZLÓ, M. s. RATKOVICS, F.

LENGYEL, B. jr. s. DÉVAY, J.

LIPTÁK, A.: Carbohydrate Methyl Ethers, II. A New Synthesis of 3,4-Dimethyl-D-glucose 315

LISZI, J.: The Excess Free Enthalpy and Excess Entropy of Mixing of Acetic-Acid—Carbon Tetrachloride Mixture 47

LISZI, J.: Study of Thermodynamic Properties of Binary Mixtures Containing Acetic Acid. 411

MAKLEIT, S., BOGNÁR, R., MILE, T. and RADICS, L.: The Formation and Structure of Pschorr's 'Bis-Thiocodide' 455

MARKÓ, L. s. ÖTVÖS, I.

MATHERNY, M.: Über die spektrographischen Eigenschaften der Kapillarelektroden, II. (Spectral-analytical Properties of Capillary Electrodes, II) 165

MATKOVICS, B., TEGYEY, Zs., RESCH, M., SIROKMÁN, F. and BOGA, E.: Rearrangements of Steroids, VI. Comparative Examination of the Schmidt Reaction of 3-β-Substituted Cholestan-6- and 7-ones, Cholest-5-en-7-one and the Beckmann Rearrangement of the Corresponding Oximes 333

MÁZOR, L. s. PÁPAY, K. M.

MÉSZÁROS, L. s. DÉVAY, J.

MILE, T. s. MAKLEIT, S.

MINK, J. and PENTIN, Yu. A.: Vibrational Spectra of Organomercuric Compunds, VI. Infrared and Raman Spectra of Divinyl Mercury 277

MOLNÁR, Á. s. BARTÓK, M.

NEUGEBAUER, J. s. HEGEDÜS, A. J.

NYILASI, J., ORSÓS, P. und POMOGATS, E.: Die Reaktion von Osmiumtetroxyd mit Äthylendiamin. (The Reaction of Osmium Tetroxide with Ethylenediamine) 251

ORSÓS, P. s. NYILASI, J.

ÖTVÖS, I., SPEIER, G. and MARKÓ, L.: Chemistry of Transition Metal Nitrogen Complexes, II. Phosphine Exchange in Nitrogen Complexes of Cobalt. (Short Communication) . 27

PAPP, E. s. PUNGOR, E.

PÁLYI, G., PIACENTI, F., BIANCHI, M. and BENEDETTI, E.: Methyniltricobalt Enneacarbonyl Compounds, I. New Method of Preparation of Alkyl Derivatives. (Short Communication) 127

PÁPAY, K. M., MÁZOR, L. and TAKÁCS, J.: Spectrophotometric Determination of Fluorine in Organic Compounds with Thorium Chloranilate after Hydropyrolytic Decomposition of Lead Fluoride 13

PENTIN, Yu. A. s. MINK, J.

PIACENTI, F. s. PÁLYI, G.

POMOGATS, E. s. NYILASI, J.

PUNGOR, E. s. KAZARYAN, N. A.

PUNGOR, E. and PAPP, E.: Electrochemical Study on Ionite Membrane Electrodes 19

RADICS, L. s. MAKLEIT, S.

RATKOVICS, F., SALAMON, T. and LÁSZLÓ, M.: Investigation of the Dielectric and Volumetric Properties of the Acetic Acid—Chloroform Mixture 259

RESCH, M. s. MATKOVICS, B.

RIOLO, C. B., SOLDI, T. F. and SPINI, G.: Oscillometric Study of Complexes Formation. (Short Communication) 29

ROBINSON, P. J.: Integrated Rate-Equations in Chemical Kinetics 407

ROCKENBAUER, A. and GÁTI, Gy.: Electron Spin Resonance Spectra of the Chromium (III) Oxide–Molybdenum (VI) Oxide System 293

RÓNAI, Á. s. SZABOLCS, J.

RUFF, I. s. KOMOR, M.

SALAMON, T. s. RATKOVICS, F.

SAYED SABET ABD EL REHIM s. DÉVAY, J.

SCHLOSSER, G. s. HEGEDÜS, A. J.

SIMON, J., GÁL, S. and ERDEY, L.: Thermal Reactions of Potassium Halates and Perhalates 175

SIROKMÁN, F. s. MATKOVICS, B.

SOLDI, T. F. s. RIOLO, C. B.

SOLYMÁR, K. s. JÓNÁS, K.

SPEIER, G. s. ÖTVÖS, I.

SPINI, G. s. RIOLO, C. B.

SZABOLCS, J., RÓNAI, Á. and TÓTH, Gy.: The Identification of Petaloxanthin 235

SZEJTLI, J., HENRIQUEZ, R. D. and CASTINEIRA, M.: Mechanism of the Acid Hydrolysis of Saccharose and Raffinose 219

SZILÁGYI, G., KASZTREINER, E., KOVÁCS, K. and BORSY, J.: Substituted Benzamidoximes Acting on the Central Nervous System 439

Sztraka, L.: Relationship Between Inversion and Internal-Rotation of Methylamine, II. The Hamilton Operator and the Elements of the Hamilton Matrix 99

Takács, J. s. Pápay, K. M.

Tegyey, Zs. s. Matkovics, B.

Tóth G., s. Szabolcs, J.

Török, T. und Bán, S.: Praktische Verwendung der »Blindwertkorrektion« in der spektrographischen Spurenanalyse. (The Practical Application of Blank Correction in Spectrographic Trace Analysis) 159

Úpor, E. s. Görbicz, M.

Valendo, A. Ya. s. Gál, D.

Vargha, L. s. Kuszmann, J.

Vasvári, G. and Holly, S.: PDPDP and its Derivatives, I. Preparation and Properties of Symmetrically and Asymmetrically Substituted PDPDP Derivatives 459

Vértes, A., Burger, K. and Bognár, L.: Mössbauer Study of Some Iron(II) Complexes in Frozen Aqueous Solutions. (Short Communication) 215

Vértes, A. s. Komor, M.

Wildenhain, W., Henseke, G. und Bienert, G.: Reaktivität phenolischer Verbindungen gegenüber 4-Fluor-3-Nitroacetophenon. (The Reactivity of Phenolic Compounds Towards 4-Fluoro-3-Nitroacetophenon) 447

Acta Chimica Academiae Scientiarum Hungaricae, Tomus 66 (1), pp. 1—11 (1970)

DETERMINATION OF THE MINERAL COMPOSITION OF BAUXITES BY INFRARED SPECTROPHOTOMETRY

K. JÓNÁS* and K. SOLYMÁR**

*(*Institute of General and Inorganic Chemistry, University of Chemical Industries, Veszprém, and **Research Institute for Metal Industry, Budapest)*

Received May 8, 1969

A method has been developed for the infrared spectrophotometric determination of the mineral composition and modulus of bauxites. The 918 and 3700 cm^{-1} kaolinite bands, the 3100 cm^{-1} boehmite band and the 3455 and 3530 cm^{-1} gibbsite bands were used for the analysis. The calibration curves were constructed on the basis of the spectra of bauxites of known chemical and mineral composition. Samples whose structure and crystallinity differed from those used for calibration, were analyzed by a new method, based on the relative intensities of the infrared bands.

The knowledge of the mineral composition of bauxites is very important in bauxite processing. Earlier phase analyses of bauxites were carried out by means of thermogravimetric, X-ray diffraction and derivatographic methods. Infrared spectrophotometry has been introduced into this field only recently. The various methods have widely different applicabilities. Crystal optical methods yield qualitative information on the structure and mineral composition of the bauxites. Up-to-date derivatographic methods [1, 2] give quantitative data for gibbsite, boehmite and diaspore, kaolinite, goethite, calcite, dolomite and pyrite. Though the sensitivity and precision of derivatography is less than that of the X-ray diffraction, certain components (*e.g.* structural water, etc.) can be determined only in this way.

The X-ray diffraction method of NÁRAY-SZABÓ and PÉTER [3, 4] was applied by BÁRDOSSY [5, 6] for the determination of the mineral composition of the bauxite. According to this, the determination of the various components is based on the diffraction data of pure mineral concretions found at the occurrence site of the investigated sample. This method makes possible a total phase analysis in a relatively short time, even in lack of chemical analysis. The difficulty lies in the gathering and preparation of the pure concentrations, which is often a very time-consuming work.

Infrared spectrophotometry has been used for qualitative identification of the components of bauxites mainly by French research workers [7, 8, 9, 10]. A detailed discussion of that problem was given by FREDERICSON [11]. There are, however, no publications dealing with the quantitative infrared phase analysis of bauxite.

The purpose of the present work was the investigation of the applicability of the characteristic infrared bands for quantitative determination of

boehmite, gibbsite, kaolinite and goethite. (There is no significant quantity of diaspore in the Hungarian bauxites.) The possibility of the infrared spectrophotometric determination of the other accompanying minerals (calcite, dolomite, pyrite, hematite, etc.) is precluded due to various reasons.

Experimental

The chemical analyses of the examined Hungarian and foreign bauxites were carried out by generally known procedures, and the mineral compositions were determined by derivatographic and X-ray diffraction methods. The derivatograms were registered on a PAULIK–PAULIK–ERDEY type MOM derivatograph; Müller-Mikro 111 X-ray generator and Phillips diffractometer were used for the diffraction measurements. The infrared spectra were recorded with UR 10 (C. Zeiss, Jena) spectrophotometer, using KBr pellet technique. The pellets contained 2.5–2.8 mg of sample.

The mineral compositions of the Hungarian bauxites used for calibration purposes are summarized in Table I.

Table I

Sample No.	Al_2O_3 (%) in			Fe_2O_3 (%) in	
	Gibbsite	Boehmite	Kaolinite	Goethite	Hematite
1	0.5	43.5	5.8	4.0	20.3
2	23.4	21.5	4.8	14.5	4.9
3	20.5	24.2	2.9	21.9	0
4	18.7	28.1	4.0	17.9	0
5	2.4	44.3	5.6	13.7	6.6
6	5.8	34.0	10.4	10.5	4.9
7	2.2	47.0	6.6	13.1	4.2
8	0	49.4	6.2	18.0	0
9*	2.5	37.4	8.4	5.2	14.8
10	0	42.5	8.0	3.4	18.3
11	3.0	43.8	4.3	5.0	23.8
12	3.8	42.3	3.7	3.4	24.4
13	3.6	42.8	3.2	5.9	22.9
14	3.5	44.0	2.9	5.2	23.4
15	4.2	46.0	3.7	5.1	17.1
16	6.1	38.0	4.7	7.6	16.6
17	22.4	18.7	8.4	4.7	11.4
18	19.0	21.7	6.8	5.7	12.8

* 3.4% Al_2O_3 present as diaspore

The origin of the bauxites listed in Tables I, IV, V, VI and VIII is the following: Samples 1, 5, 6, 7, 8 and 19–23: Halimba; Samples 2, 3, 4, 9, 10, 24, 27, II, IV, VI, VII, X, XII: Iszkaszentgyörgy; Samples 11–16, 25, 26: Nyirád; Samples 17, 18: Fenyőfő, and Sample XIII: Nagyharsány.

Results and discussion

Qualitative phase analysis of bauxites

The wavenumbers of the characteristic infrared absorption bands of the most important mineral constituents of Hungarian bauxites are summarized in Table II. The most intense bands are given in italics. The lattice vibrations of the various AlO_x units appear in the 700–800 cm^{-1} wavenumber range [12], while the bands of the Al—O—H deformation vibrations and the Si—O stretching vibrations are found between 800 and 1200 cm^{-1}. The bands of higher wavenumber belong to the stretching vibrations of O—H groups bounded in hydrogen bridges of different strength.

Table II

Infrared bands of the most important mineral constituents of bauxite (cm^{-1})

Kaolinite	Boehmite	Gibbsite	Goethite
750	*750*	755	*800*
790	*1080*	800	*897*
918	1155 (sh)	840 (sh)	3130
940 (sh)	*3100*	975	
1015	3290	*1030*	
1039		3385	
1110		3400	
3628		*3455*	
3658		*3530*	
3700		3625	

The infrared spectra of Hungarian bauxites are characterized by strong, sharp bands, indicating a high degree of crystallinity (Fig. 1). The wavenumber of the bands is relatively stable, the composition of the sample affects it only slightly.

Regarding the various minerals the following statements can be made:

All given *boehmite* bands — except that appearing at 750 cm^{-1}, which is overlapping with kaolinite and gibbsite bands — are suitable for the qualitative identification. The 3100 cm^{-1} band was found to be the most suitable for quantitative purposes.

The *gibbsite* bands appearing between 700 and 800 cm^{-1} are not characteristic in the presence of boehmite and kaolinite. The bands at 3455 and 3530 cm^{-1} are recommended for quantitative determinations; the others are more

or less disturbed, while those appearing at 3385 and 3400 cm^{-1} are weak, and in samples of low gibbsite content they are not measurable.

The bands of *kaolinite* at 918 and 3700 cm^{-1} are suitable for both quantitative and qualitative purposes. The overlapping absorption of goethite at

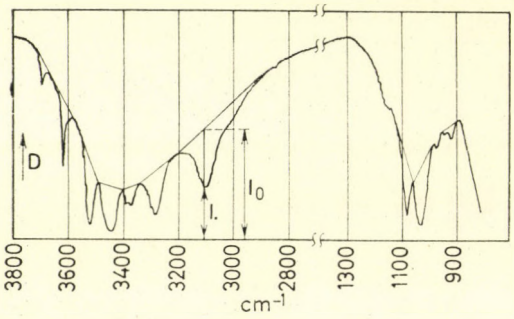

Fig. 1. Infrared absorption spectrum of a Hungarian bauxite, containing gibbsite, boehmite and kaolinite. Base lines for the measurement of extinctions are also given

about 900 cm^{-1} does not produce a significant error even in samples of high goethite content. This is due to the low intensity of the bands of goethite as compared to those of kaolinite. Because of this fact, and since in this range the other aluminium minerals also give rise to bands of various intensities, the infrared spectrophotometric determination of the *goethite* in bauxite is not possible. In the case of red mud, where the mentioned minerals are absent, the determination of goethite also can be accomplished.

Quantitative phase analysis of bauxites

The extinction ($E = \lg I_0/I$) of the analysis bands was measured at the band maxima, and the so-called specific extinction (E/g bauxite) was calculated on the basis of the bauxite content of the pellets. In the knowledge of the mineral composition of the samples, these data were converted into 'ε = E/g Al_2O_3 in the given mineral' values. This value was designated as the specific extinction coefficient.

Evaluation of the spectra of 18 samples (listed in Table I) was carried out and an average specific extinction coefficient ($\bar{\varepsilon}$) was calculated for each analysis band, taking the arithmetical mean of the individual ε values. These data are summarized in the first column of Table III. The infrared spectra of some French, Yugoslav, Greek and Indian bauxites were also evaluated in a

similar manner. The average specific extinction coefficients of these are given in Columns 4, 5, 6 and 7 of Table III. Finally, the spectra of synthetic samples of different composition, prepared from pure mineral concretions collected at the occurrence places of the Hungarian bauxites, were also calculated. The data referring to these samples are found in the third column of Table III.

Table III

Average specific extinction coefficients ($\bar{\varepsilon}$) of the infrared bands of bauxites of different origin

Measured band, cm^{-1}	Hungarian		Synthetic	French	Yugoslav	Greek	Indian
	$\bar{\varepsilon}$	average deviation from $\bar{\varepsilon}$, expressed as % of $\bar{\varepsilon}$	$\bar{\varepsilon}$	$\bar{\varepsilon}$	$\bar{\varepsilon}$	$\bar{\varepsilon}$	$\bar{\varepsilon}$
	1	2	3	4	5	6	7
Kaolinite							
918	794	14.4	480	633	824	353	—
3700	791	17.2	495	735	1000	464	—
Boehmite							
1080	783	8.9	401	477	498	119	—
3100	499	7.9	264	318	291	73.5	—
3290	685	10.9	165	352	455	81	—
Gibbsite							
1030	1529	10.3	403	—	—	—	415
3390	408	8.0	—	—	—	—	155
3455	1647	7.8	231	—	—	—	415
3530	1540	8.4	258	—	—	—	458
3625	577	6.4	141	—	—	—	163

As shown by the data of Table III, synthetic mixtures cannot be used for the construction of calibration curves, since the specific intensities of the bands of the pure concretions are lower than that of those occurring in the bauxites. Further investigations are needed to elucidate this problem. The data of Table III show that significant deviations may exist between the intensities of the corresponding bands of bauxites of different origin, which is due apparently to differences in structure, particle size, degree of crystallinity, etc. Samples obtained, however, from identical or similar geological areas do not show significant differences.

With the average specific data of Table III the mineral composition of five other Hungarian bauxites (not given in Table I) were calculated from their spectra. These results are presented in Table IV. It can be seen that the 1080 and 3290 cm^{-1} boehmite bands and the 1030 and 3625 cm^{-1} gibbsite bands cannot be used for quantitative purposes.

Table IV

Phase composition of bauxites calculated from infrared spectra with the use of the average specific extinction coefficients ($\bar{\varepsilon}$)

Sample No.	19		20		21		22		23	
Band measured, cm^{-1}	Al_2O_3 % bound in the mineral in question									
	A	B	A	B	A	B	A	B	A	B
Kaolinite		5.1		5.0		5.0		6.0		5.5
918	5.8		7.6		6.9		6.8		6.9	
3700	6.8		7.2		7.5		7.9		7.9	
Boehmite		36.5		41.7		30.0		32.4		32.2
1080	31.7		36.6		27.0		26.2		28.5	
3100	36.7		47.6		33.9		34.3		38.5	
3290	27.0		32.9		23.6		24.7		27.3	
Gibbsite		8.2		5.4		13.8		11.1		11.5
1030	9.9		8.5		18.6		14.9		16.5	
3455	7.8		3.4		14.8		11.2		12.8	
3530	8.3		4.0		16.3		11.3		13.0	
3625	9.3		7.2		17.0		12.7		14.1	

A: Data of infrared analysis

B: Data based on chemical, X-ray and derivatographic analyses

Since there is generally no (or only very small amount of) free SiO_2 in the Hungarian bauxites, we have supposed that all SiO_2 is bound in kaolinite, and so it can be calculated from the kaolinite content. Thus the total aluminium oxide content (directly) and the SiO_2 content (indirectly) can be obtained by means of infrared phase analysis. The modulus of the samples No. 19–23 was calculated from these data. The results are given in Table V. In column 4 the total Al_2O_3, determined on the basis of the 3700 cm^{-1} kaolinite, 3455 cm^{-1} gibbsite and 3100 cm^{-1} boehmite bands, while in column 5 the SiO_2 calculated from the kaolinite content are given.

It can be seen that this relatively simple method, which is using the specific extinction coefficients without plotting calibration curves, provides satisfactory information on the chemical and mineral composition and modulus of bauxites.

Table V

Determination of the modulus of bauxite $\left(m = \frac{\Sigma\, Al_2O_3}{SiO_2}\right)$ *from infrared analysis data*

Sample No.	Chemical analysis			Data calculated from 3700, 3455 and 3100 cm^{-1} bands			$\frac{m_1}{m_2}$
	Σ Al_2O_3 (%)	SiO_2 (%)	m_1	Σ Al_2O_3 (%)	SiO_2 (%)	m_2	
	1	2	3	4	5	6	7
19	50.6	6.00	8.46	51.3	8.10	6.34	1.34
20	53.6	5.83	9.20	58.2	8.55	6.80	1.35
21	49.3	5.86	8.42	56.2	8.92	6.30	1.34
22	50.5	7.08	7.14	55.4	9.38	5.90	1.21
23	50.6	7.83	7.83	59.2	9.38	6.30	1.24

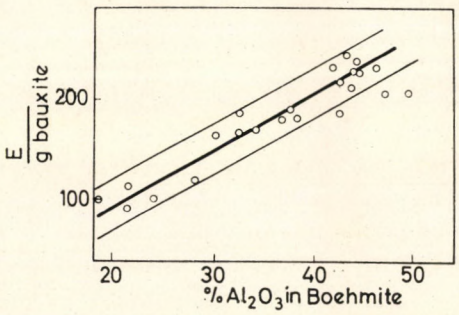

Fig. 2. Calibration curve for 3100 cm^{-1} boehmite band

In the knowledge of the mineral composition of the samples No. 1–18 and 19–23 also calibration curves were constructed, plotting the specific extinction (E/g bauxite) of the corresponding band as a function of the percentage by weight of Al_2O_3 contained in the given mineral. The bisecting line of the area — limited by two parallel lines — which contained all the calibration points (neglecting very divergent ones) was the calibration curve itself. The distance between the calibration curve and one of the limiting parallel lines represents the absolute error of the calibration. Fig. 2 shows an example for such a calibration curve. The error is $\pm 1.7\%$ Al_2O_3 for the 918 cm^{-1} and $\pm 1.6\%$ Al_2O_3 for the 3700 cm^{-1} kaolinite bands; $\pm 1.5\%$ Al_2O_3 for the 3455 cm^{-1} and

$\pm 1.2\%$ Al_2O_3 for the 3530 cm^{-1} gibbsite bands; $\pm 4.6\%$ Al_2O_3 for the boehmite band at 3100 cm^{-1}. The 3100 cm^{-1} boehmite calibration curve cannot be used for analysis in the case of samples containing more than 50% boehmite, and the 3530 cm^{-1} gibbsite curve in the case of samples containing more than 25% gibbsite.

These calibration curves were used for the determination of the mineral composition of further bauxite samples. The results are summarized in Table VI.

Table VI

The mineral composition and modulus of bauxites

Sample No.	Al_2O_3 (%) in kaolinite			Al_2O_3 (%) in gibbsite		
	918 cm^{-1}	3700 cm^{-1}	A*	3455 cm^{-1}	3530 cm^{-1}	A*
24	5.3	4.5	4.8	18.2	19.0	17.0
25	3.0	2.8	4.2	10.8	13.0	14.6
26	10.5	10.7	9.2	6.5	5.2	3.6
27	10.4	10.6	10.8	18.0	16.4	14.5

The agreement between the chemical, X-ray and infrared phase analysis is satisfactory.

The Hungarian bauxites in question (samples 1–27) have identical or similar microstructure, as it is consistent also with their nearly equal specific absorption data. There are, however, in Hungary bauxites with significantly lower specific absorption (less intense infrared bands), which is apparently due to their more amorphous structure (*e.g.* bauxite from Nagyharsány). Of course, the specific absorption coefficients or calibration curves determined for the above series, cannot be used for the analysis of these samples. In order to eliminate that problem a new method has been elaborated, based on the observation that the *relative* intensities of the infrared bands are more independent of the microstructure.

According to this method, the *sum* of the specific extinctions (ΣE/g bauxite) of all significant bands in the infrared spectra of the samples and the percentile participation of each band in the total absorption was calculated. In Table VII the data of a series containing boehmite and gibbsite illustrate the method. On the basis of these data calibration curves were constructed, plotting the quantity of Al_2O_3(%) present in the actual mineral, as a function

of the percentile participation of the corresponding band in the total absorption. It is to be noted that a separate calibration curve is recommended for samples containing boehmite only, since the total absorption of these is lower and also the percentile distribution of the total absorption is different from that of samples containing also gibbsite.

In Table VIII the analysis results got from calibration curves plotted with the absolute, resp. with the relative band intensities are compared. The

determined by means of calibration curves

Al_2O_3 (%) in boehmite		Σ Al_2O_3 (%)		SiO_2 (%)		$m = \frac{\Sigma\ Al_2O_3}{SiO_2}$	
3100 cm^{-1}	A*	3700 + 3530 + 3100 cm^{-1}	A*	3700 cm^{-1}	A*	from infrared	A*
25.6	25.7	49.1	47.5	5.28	5.5	9.30	8.65
29.8	29.4	45.6	48.2	3.30	5.0	13.80	9.65
34.4	36.7	50.3	49.5	11.50	10.8	4.37	4.57
15.0	18.1	42.0	43.4	12.50	12.7	3.36	3.42

A*: Data from chemical, X-ray diffraction and derivatographic analyses

Table VII

The relative intensities of the analysis bands in percentile proportion of the total absorption

Sample No.	ΣE*	Boehmite		Gibbsite		
		Al_2O_3, %	3100 cm^{-1} % of ΣE	Al_2O_3, %	3455 cm^{-1} % of ΣE	3530 cm^{-1} % of ΣE
2	1585.2	21.5	5.80	23.4	23.5	20.9
3	1537.1	24.2	6.70	20.5	23.4	21.7
4	1589.7	28.1	7.62	18.7	20.1	19.3
15	1123.7	46.0	21.0	4.2	2.19	2.04
16	969.0	38.0	19.3	6.1	2.78	3.87
17	1625.5	18.7	6.27	22.4	19.1	18.5
18	1674.4	21.7	6.90	19.0	20.4	19.2
19	1142.8	41.7	20.7	5.4	4.94	5.32
20	1176.7	36.5	15.5	8.2	10.90	10.90
21	1532.4	30.0	11.0	13.8	15.9	16.4
22	1320.2	32.4	12.9	11.1	14.0	13.2
23	1465.2	32.2	13.10	11.5	14.5	13.7

* $\Sigma E = 918 + 1030 + 1085 + 3100 + 3280 + 3455 + 3530 + 3625 + 3700\ cm^{-1}$ bands

relative method apparently eliminates the errors due to differences in the microstructure, thus the analysis of bauxites of widely different origin can be carried out.

Table VIII

Phase analysis of bauxites by means of calibration curves based on absolute resp. relative infrared band intensities

Sample No.	Al_2O_3 in boehmite			Al_2O_3 in gibbsite				
		Infrared (3100 cm^{-1})			Infrared			
	Chemical and X-ray data	absolute	relative	Chemical and X-ray data	absolute		relative	
					3455 cm^{-1}	3530 cm^{-1}	3455 cm^{-1}	3530 cm^{-1}
24	25.7	25.6	25.0	17.0	18.2	19.0	18.0	18.7
25	29.4	29.8	31.2	14.6	10.8	13.0	10.6	13.5
26	36.7	34.4	35.0	3.6	6.5	5.20	5.8	5.1
IV	31.8	19.4	29.1	13.8	10.1	9.35	15.0	13.5
VI	26.4	14.6	27.0	15.2	9.9	9.0	17.8	16.2
VII	30.4	16.9	27.0	19.0	12.1	11.4	18.9	18.1
II	53.0	35.1	51.6					
X	43.2	30.3	45.4					
XII	42.8	23.0	45.0					
XIII	52.9	5.87!	49.6					
French/I	50.4	27.7	46.2					
French/III	47.9	32.4	43.3					

*

The authors' thanks are due to Gy. BÁRDOSSY for supplying the synthetic samples, to T. KOTSIS and Mrs. J. KENYERES for the X-ray diffraction and derivatographic analyses.

REFERENCES

1. ÜVEGES, J.: Fémipari Kutató Intézet Közleményei **III,** 7 (1959)
   ÜVEGES, J.: Symposium sur les Bauxites, Oxydes et Hydroxydes d'Aluminium (Zagreb) **II,** 47 (1964)
2. KOTSIS, T.: Fémipari Kutató Intézet Közleményei **VI,** 7 (1962)
   KOTSIS, T.: Geologie **13,** 159 (1964)
3. NÁRAY-SZABÓ, I., PÉTER, T.: Földtani Közlöny **94,** 444 (1964)
4. NÁRAY-SZABÓ, I., PÉTER, T.: Tschermaks mineralog. petrogr. Mitt. **10,** 120 (1965)
5. BÁRDOSSY, GY.: Bergakademie (Freiberg) **17,** 65 (1965)
6. BÁRDOSSY, GY.: Kohászati Lapok **99,** 355 (1966)
7. CAILLÈRE, S., POBEGUIN, T.: Mémoires du Museum National D'Histoire Naturelle **XII,** (4) 137 (1965)
8. CAILLÈRE, S., POBEGUIN, T.: Travaux du Comité International pour l'Étude des Bauxites, des Oxydes et des Hydroxydes d'Aluminium (Zagreb) No. 1, 9 (1965)

9. CAILLÈRE, S., POBEGUIN, T.: Travaux du Comité International pour l'Étude des Bauxites, des Oxydes et des Hydroxydes d'Aluminium (Zagreb) No. 2, 25 (1966)
10. CAILLÈRE, S.: Travaux du Comité International pour l'Étude des Bauxites, des Oxydes et des Hydroxydes d'Aluminium (Zagreb) No. 2, 35 (1966)
11. FREDERICSON, L. D.: Analytic. Chem. **26,** 1883 (1954)
12. TARTRE, P.: Spectrochim. Acta **23 A,** 2127 (1967)

Klára JÓNÁS; Veszprém, Schönherz Zoltán u. 10. Hungary
Károly SOLYMÁR; Budapest XI., Fehérvári út 144.

Acta Chimica Academiae Scientiarum Hungaricae, Tomus 66 (1), pp. 13—18 (1970)

SPECTROPHOTOMETRIC DETERMINATION OF FLUORINE IN ORGANIC COMPOUNDS WITH THORIUM CHLORANILATE AFTER HYDROPYROLYTIC DECOMPOSITION OF LEAD FLUORIDE

K. M. PÁPAY, L. MÁZOR and J. TAKÁCS

(Institute for General and Analytical Chemistry, Technical University, Budapest)

Received May 19, 1969

Developing an earlier method, a procedure is given for the determination of fluorine in organic compounds. The fluorine bound by a layer of red lead is hydropyrolysed and distilled as hydrogen fluoride, then determined spectrophotometrically in the distillate with thorium chloranilate as reagent. The opinion of American authors is disputed that the colour intensity of chloranilic acid is increased by Methyl Cellosolve. It is shown that this increase in colour intensity is due to iron(III) impurities in Methyl Cellosolve forming a violet complex with chloranilic acid. Fluorine contents of a few organic compounds are reported.

In a previous communication [1] we have described a method for determining the fluorine content of organic compounds. According to this method, the HF-containing pyrolytic products of organic compounds heated in a stream of oxygen flow through a quartz tube whose inner surface is coated with red lead [lead(II, IV) oxide]. Red lead oxidises the pyrolytic products to carbon dioxide and water and binds hydrogen fluoride as heat resistant lead fluoride:

$$2\ PbO_2 + 2\ H_2F_2 = 2\ PbF_2 + 2\ H_2O + O_2$$

The fluorine content of red lead layer was determined after its dissolution either gravimetrically as lead chloride fluoride (PbClF) or by argentometric titration of chloride in the precipitate using Variamin Blue as redox indicator [2]. This method has the drawback that the sensitive spectrophotometric methods are not suitable for the determination of fluorine because of the high lead ion concentration in the analysed solution.

As a development of this method we led stream through the quartz tube containing the red lead and lead fluoride at 700 °C. This operation was performed after determining the carbon and hydrogen content of the organic substances. Lead fluoride decomposes at 700 °C rapidly and fully:

$$PbF_2 + H_2O = PbO + H_2F_2$$

Hydrogen fluoride is transferred into the distillate, containing only traces of lead ions. The temperature required for the hydropyrolytic decompo-

sition of lead fluoride has been determined experimentally. 50 mg of lead fluoride was placed into the quartz tube which was then put into the platinum tube of the apparatus depicted in Fig. 1.

The temperature of the furnace was varied between 300 and 850 °C and hydropyrolysis was performed for 30 min. When the volume of the distillate

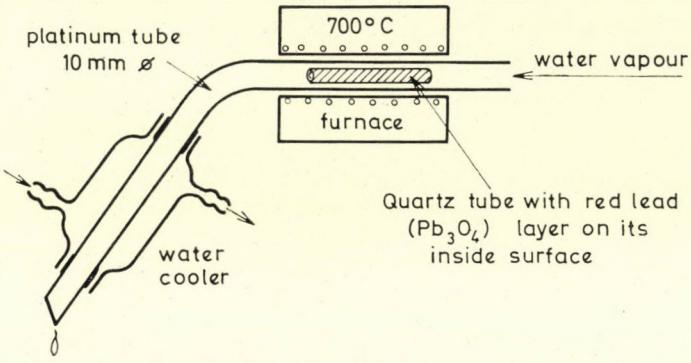

Fig. 1. Apparatus for the hydropyrolysis of lead fluoride

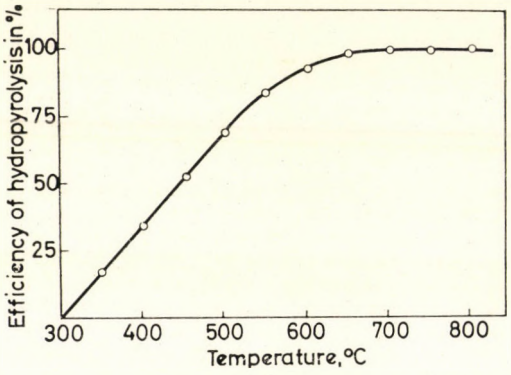

Fig. 2. Relationship between the temperature and efficiency of hydropyrolysis

reached 25 ml, it was neutralized and titrated with thorium nitrate standard solution in the presence of sodium alizarin sulphonate as indicator. The relationship between the amount of fluorine in the distillate and the temperature is shown in Fig. 2. If the amount of fluorine is small in the sample and, consequently, in the distillate, the titration is not sensitive enough and the method is inaccurate for the fluorine determination. Therefore, we intended to find a more suitable spectrophotometric method.

As known, the earlier indirect methods based on the fact that fluorine ion weakens the colour of some metal complexes, are not accurate enough and are suitable for the determination only between narrow concentration limits. Therefore it is more convenient to use methods according to which coloured organic compounds are liberated by fluoride ion from sparingly soluble metal complexes. The colour intensity due to the liberated substance is directly proportional to the fluoride content of the analyzed solution.

Metal (strontium, lanthanum) complexes of chloranilic acid were suggested for the determination of fluoride ion about 10 years ago [3]. A newer method uses as reagent the thorium complex of chloranilic acid [4] which is very slightly soluble in water and at pH 4.7 reacts with fluoride in aqueous solution liberating the violet chloranilic acid:

$$ThCh_2 + 6\,F^- + 2\,H^+ = ThF_6^{2-} + 2\,HCh^-$$

In solutions containing Methyl Cellosolve the following reaction takes place according to the authors:

$$ThCh_2 + 2\,F^- + H^+ = ThF_2Ch + HCh^-$$

The ThF_2Ch complex is dissolved.

This method was discussed later by WEST, BIRKE and HUME [5], who have established that among the water miscible organic solvents only the Methyl Cellosolve increases the intensity of the colour reaction to a significant extent. According to these authors, the reaction takes place as follows:

$$ThCh_2 + 2\,F^- = ThF_2Ch + Ch^{2-}$$

$$ThF_2Ch + 2\,F^- = ThF_4 + Ch^{2-}$$

$$ThCh_2 + 4\,F^- = ThF_4 + 2\,Ch^{2-}$$

and the colour in aqueous solution is caused by Ch^{2-} ions. ThF_2Ch is insoluble in water but becomes soluble, if Methyl Cellosolve is added. This also increases the intensity of the colour.

According to the present studies the colour intensity is not increased by Methyl Cellosolve or other solvents miscible with water (methanol, ethanol, acetone, dioxan) if they are pure. Since the above authors used Methyl Cellosolve in industrial quality, the increased colour intensity is caused by iron impurities in this solvent. Industrial Methyl Cellosolve has a yellow colour and a brownish yellow residue is obtained after distillation. One half of this residue is iron(III) oxide. Methyl Cellosolve used in the present work contained 0.13 mg/ml of iron.

The authors of Ref. [4] used Methyl Cellosolve produced by Union Carbide Chemical Comp., which probably was not of analytical quality. The authors of paper [5] did not report the quality of Methyl Cellosolve used.

Performing a number of experiments we have established that if we use colorless Methyl Cellosolve of analytical grade (Loba Chemie, Wien-Fischamend, Austranal Präparate, B.p. 124 °C), or if we carefully distill yellow industrial Methyl Cellosolve, collecting the fraction which boils at 124 °C and is completely colorless, the obtained solvents do not increase either the solubility of ThF_2Ch or the colour intensity of the pure chloranilic acid solution, regardless of its amount or that of other pure solvents miscible with water.

In order to prove this fact, to identical volumes of fluoride standard solution in test tubes we added water, buffer solution with pH 4.7, and thorium chloranilate, the latter in excess to the amount of fluoride ions. To the solution in the test tubes the following solvents were added in equal volume:

1. methanol, 2. ethanol, 3. acetone, 4. 1,4-dioxane, 5. Methyl Cellosolve p.a., 6. colorless Methyl Cellosolve obtained by distillation of the crude product, 7. water, 8. industrial Methyl Cellosolve, 9. water and 1 ml of iron standard solution (1.4 mg Fe in 1 ml).

These solutions were allowed to stand 2 hours with frequent shaking. The following results were observed:

The contents of test tubes 1–7 showed identical violet colour. The contents of test tubes 8 and 9 were more intensely violet. Upon the addition of 1 ml of iron standard solution (1.4 mg Fe in 1 ml) to test tubes 1–7, we observed the following results. The violet colour of the test solutions immediately increased in intensity. This experiment proves that pure solvents and pure Methyl Cellosolve do not increase the intensity of colour either by dissolving the ThF_2Ch complex or by other interaction between the solvent and Ch^{2-} ions in the solution.

The intensity of colour is increased only by ferric ions. This phenomenon occurs both in the presence and absence of Methyl Cellosolve or other solvents miscible with water. Solely as a result of complex formation between ferric and Ch^{2-} ions the colour of the complex is stronger than that of Ch^{2-}.

The properties of this new complex will be reported in a forthcoming communication.

The fact that iron(III) ions more than double the colour intensity of chloranilic acid, was used for increasing the sensitivity of fluorine determination. We added enough iron standard solution to convert all chloranilic acid to its Fe(III) complex.

The calibration curve in the 0 to 2.5 mg F^-/50 ml concentration range is a straight line, the calculated molar extinction coefficient being equal to 589, while without iron the latter is only 236, referred to fluoride ion.

The use of Methyl Cellosolve or other water miscible organic solvents is not necessary because they do not increase the colour intensity.

The method was used for the analysis of some fluorine containing organic substances. The application of the method is convenient if the available amount of test substance or its fluorine content is small.

Reagents and solutions

Thorium chloranilate. The reagent can be prepared in the following manner. One dissolves 1.0 g of accurately weighed crystalline thorium nitrate [reagent grade $Th(NO_3)_4 \cdot 6\ H_2O$] in 50 ml water. To this solution is added under stirring a chloranilic acid solution in a dropwise manner. This solution is prepared from exactly 0.8 g chloranilic acid and 300 ml boiling water. The precipitated thorium chloranilate settles rapidly, the supernatant liquid is clear and pale violet. The precipitate is filtered on a thick filter paper, washed with distilled water and dried at 110 °C.

Acetic acid–sodium acetate buffer solution. The mixture of 250 ml 0.2 *M* sodium hydroxide and 500 ml 0.2 *M* acetic acid solution. The pH of the buffer is 4.7.

0.001 M iron (III) chloride solution. 0.270 g of $FeCl_3 \cdot 6\ H_2O$ dissolved in 1000 ml of water.

0.001 M sodium fluoride solution. 0.042 g of reagent grade sodium fluoride dissolved in 1000 ml of water.

Procedure. Combustion of organic substance and the determination of carbon and hydrogen is performed as described in a previous paper [1]. After determining the C and H content, the quartz tube containing lead fluoride and the excess of red lead is removed from the combustion tube and put in the platinum tube of the hydropyrolytic apparatus shown in Fig. 1.

The furnace is heated to 700 °C and water vapour is passed through the apparatus for 20 min, collecting 20 ml of distillate in the plastic vessel. Water vapour is carried either by air or nitrogen. After neutralizing the distillate with 1–2 drops of 0.1 *N* sodium hydroxide solution, it is transferred to a 50 ml volumetric flask. 5.0 ml of buffer solution and 5.0 ml iron(III) chloride solution are added followed by dilution with water to 50 ml. After mixing, the solution is poured into a 100 ml glass-stoppered flask and 0.100 g of thorium chloranilate is added. The flask is shaken on a machine for 30 min. The turbid solution is filtered through thick, dry filter paper (⌀ 9 cm) the first portion of the filtrate being discarded.

The extinction of the clear violet solution is measured in a 1 cm cell at 530 nm against a reference solution which is prepared in the same way but without fluoride. The reference solution has a pale violet colour caused by some dissolved thorium chloranilate reagent. The results are read from a calibration curve obtained with 0.001 *M* sodium fluoride prepared in the same way as the analysis solution.

Results

Table 1 shows the results of analysis for some fluorine containing compounds obtained by the present method.

The results are in each case somewhat lower than the theoretical values. This fact can be explained by losses partly in the combustion process, partly in hydropyrolysis. The negative error caused by the losses is not greater than that usually tolerated in microanalysis.

Table I

Analyzed compound	Sample weight, mg	F content of sample, mg	Extinction measured, 1 cm, 530 nm	F found, mg	Δ mg F	Δ %
p-Fluoroacetanilide, C_8H_8NOF, F = 12.40%	4.920	0.610	0.38	0.60	0.01	−1.6
	5.436	0.674	0.41	0.66	0.01	−1.5
	6.146	0.762	0.47	0.75	0.01	−1.3
	7.320	0.908	0.55	0.90	0.01	−1.1
	8.642	1.072	0.66	1.06	0.01	−1.0
	9.830	1.219	0.71	1.19	0.02	−1.6
p-Fluorobenzoic acid, $C_7H_7O_2F$, F = 13.56%	5.146	0.698	0.42	0.68	0.02	−2.8
	6.745	0.915	0.56	0.90	0.02	−2.2
	6.892	0.936	0.58	0.92	0.2	−2.1
	8.328	1.129	0.70	1.11	0.2	−1.8
	9.532	1.293	0.80	1.29	0.01	−0.8
	10.410	1.412	0.84	1.40	0.01	−0.7
p-Fluorotoluene, C_7H_7F, F = 17.25%	3.048	0.526	0.33	0.51	0.02	−1.3
	3.624	0.625	0.38	0.62	0.0	0
	4.542	0.784	0.71	0.77	0.01	−1.2
	6.688	1.154	0.81	1.13	0.02	−1.7
	7.894	1.362	0.88	1.34	0.01	−0.7
	8.246	1.422	0.98	1.40	0.02	−1.3

REFERENCES

1. MÁZOR, L.: Mikrochimica Acta, **1957**, 113
2. ERDEY, L., MÁZOR, L., MEISEL, T.: Mikrochimica Acta, **1958**, 140
3. BERTOLACINI, R. J., BARNEY, J. E.: Anal. Chem. **29**, 281 (1957), **30**, 202 (1958)
4. HENSLEY, A. L., BARNEY, J. E.: Anal. Chem. **32**, 828 (1960)
5. WEST, C. D., BIRKE, R. R., HUME, N. D.: Anal. Chem. **40**, 556 (1966)

Mária K. PÁPAY
László MÁZOR
József TAKÁCS
Budapest XI., Gellért tér 4.

Acta Chimica Academiae Scientiarum Hungaricae, Tomus 66 (1), pp. 19–26 (1970)

ELECTROCHEMICAL STUDY ON IONITE MEMBRANE ELECTRODES

E. PUNGOR and E. PAPP

(Department of Analytical Chemistry, University of Chemical Industries, Veszprém)

Received May 22, 1969

The authors studied the electrochemical behaviour of some heterogeneous cationite and anionite membrane electrodes. The life-time of the electrodes under continuous soaking and the selectivity of the electrodes to individual ionic species were studied. The results confirm the general statement that the solid ion exchanger membrane electrodes are generally perm-selective. In the second part of the study the use of the perchlorate electrode is shown as an example for the possible applications of perm-selective membrane electrodes as a reference electrode.

Recently several research workers have been engaged in the development of ion selective membrane electrodes. A review of the large number of papers published in the literature shows that the membrane electrodes were prepared initially from minerals, then from natural organic ion exchangers and later on from synthetic ion exchange resins (ionites). The evaluation of the results published shows that the ion exchange membrane electrodes developed are selective only to cations or anions, but they are not selective to individual ions. Ion-selective ion-exchanger membrane electrodes could only be prepared from special liquid ion exchangers. Such ion-exchanger electrodes selective *e.g.* for calcium ion [1] and perchlorate ion [2] were developed by ORION Research Inc. However, the selectivity of these special ion-exchanger membrane electrodes is ensured only if their surface is continuously renewed during use.

Ionite membrane electrodes have earlier been investigated in our Laboratory. Heterogeneous ionite and complexonite membrane electrodes of excellent mechanical properties have been developed using silicone rubber as an inert supporting material [3, 4]. The primary aim of these studies was to examine the validity of the theoretical relationships [5–10] obtained with precipitate ion-selective membrane electrodes in the field of ionite and complexonite membrane electrodes also. For this reason, the lower detection limit of the ionite and complexonite membrane electrodes has been studied.

The equation derived shows a relationship between the lower detection limit of electrodes and the dissociation constant of ionites and complexonites built in the electrodes. In a review article the authors give a survey on the types of membrane electrodes used earlier, and on the theoretical interpretation of their behaviour.

In our present work, we report on our investigation concerning the life-time and the selectivity of heterogeneous ionite membrane electrodes and on the practical application of this type of electrodes.

The following ionite membrane electrodes were studied in the present work: chloride, perchlorate, potassium, copper(II) and nickel.

Experimental

For the preparation of the anionite membrane electrodes Varion AD resin (strongly basic) was used, while the cationite membrane plates were prepared from Varion KS ion exchange resin (strongly acidic). 10–20% solution of the appropriate electrolyte was poured over the resin in 300–500% excess depending on the capacity of the resin. After converting the resin into the appropriate form, it was washed with distilled water to remove the excess of the electrolyte. The still wet resin was ground, and subsequently dried. The powder of the suitably prepared ionite resin was mixed with silicone rubber monomer. The total weight of the membrane should contain 40 to 50 per cent ionite resin. Namely, our earlier investigations disclosed that there is no difference in the electrochemical behaviour of electrodes made of membrane plates containing 30, 50 or 70 per cent ionite, while membrane plates containing 50 per cent of ionite showed the most favourable mechanical properties. After cross-linking the mixture of the ionite and the silicone rubber monomer with catalyst, a membrane plate was made. Discs were cut out from the plate, which were sealed to one end of a glass tube. Depending on the types of ions measured, various measuring cells were constructed.

Generally, the following measuring cell was used on our measurements:

Ag/AgCl (standard solution)/ionite membrane/solution to be measured/agar-agar bridge/electrode of second kind.

A Radelkis Blood and Universal pH-meter, resp. were used for all potentiometric measurements.

Results

The operation and the life-time of silicone rubber ionite membrane electrodes depend mainly on the swelling of the membrane plate. In general, at studying the swelling effect the membrane electrodes were continuously soaked in a 10^{-3} M solution of the electrolyte to be measured. In certain intervals, the function of the electrodes was checked by measuring the actual electrode potential in dilute solutions of the ion to be measured, the reproducibility, the results obtained by the electrodes, and the time of obtaining a constant potential value. The activities of the solution were known. Later on, we describe in detail the results obtained with the individual ionite membrane electrodes.

Fig. 1 shows the calibration curve for a potassium ionite membrane electrode taken at the beginning and at the end of the soaking period. The calibration curves were made in a series of KCl solutions (10^{-1} to 10^{-5} M). Figure 1 shows the theoretical $E/\lg a_{KCl}$ curve also. The curves measured at the beginning and at the end of the period investigated differ from each other only at low concentrations (10^{-4} to 10^{-5} M). This shows that the potassium ionite electrode keeps its electrode function during a relatively long soaking period.

In contrary to this, the function of nickel cationite membrane electrodes altered to a greater extent. Results are shown in Fig. 2. After soaking the electrodes in $NiCl_2$ solution for 24 hours they showed higher potential differences in 10^{-1} to 10^{-4} M activity range than were calculated on the basis of the Nernst-equation. However, after soaking the electrodes for two days the potential

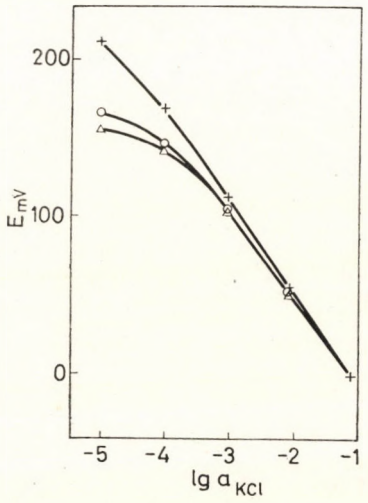

Fig. 1. Relationship between the membrane potential and lg a_{KCl}. Indicator electrode: ionite membrane electrode in the potassium form. +—+ calculated; ○—○ measured after 1 day of soaking; △—△ measured after 50 days of soaking

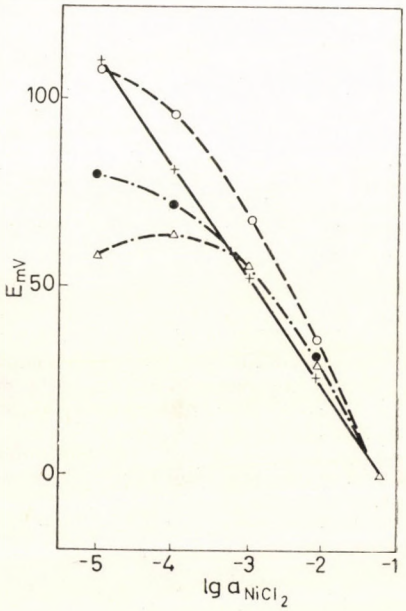

Fig. 2. Relationship between the membrane potential and lg a_{NiCl_2}. Indicator electrode: ionite membrane electrode in the nickel form. +—+ calculated; ○—○ measured after 1 day of soaking; ●— • —● measured after 2 days of soaking; △-..-△ measured after 32 days of soaking

values lowered, and differed only slightly in 10^{-1} to 10^{-3} M activity range from the calculated values. On further soaking, the electrode function did not change in 10^{-1} to 10^{-3} M concentration range, however below 10^{-3} M $NiCl_2$ concentration a decrease was observed in the electrode potentials measured. From the results it can be concluded that under continuous soaking, membrane electrodes are suitable for the direct determination of the nickel ion activity only above 10^{-3} M.

Fig. 3 shows the function of the ionite membrane electrode converted into bivalent copper form after soaking it for 1 day and 15 days, respectively. Calibration curves presented were plotted from values measured in $CuSO_4$ solutions of known activity. The results show no change in the electrode function of the copper cationite electrode during the time of investigation. In the

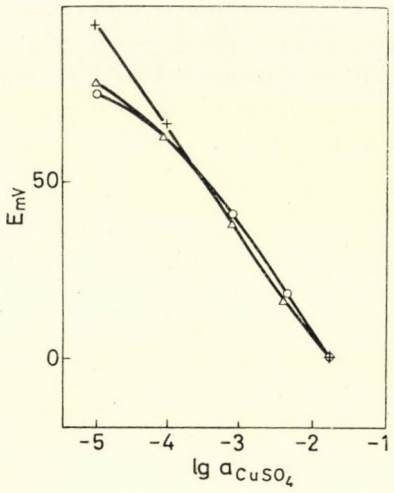

Fig. 3. Relationship between the membrane potential and lg a_{CuSO_4}. Indicator electrode: ionite membrane electrode in the Cu(II) form. +—+ calculated; ○—○ measured after 1 day of soaking; △—△ measured after 15 days of soaking

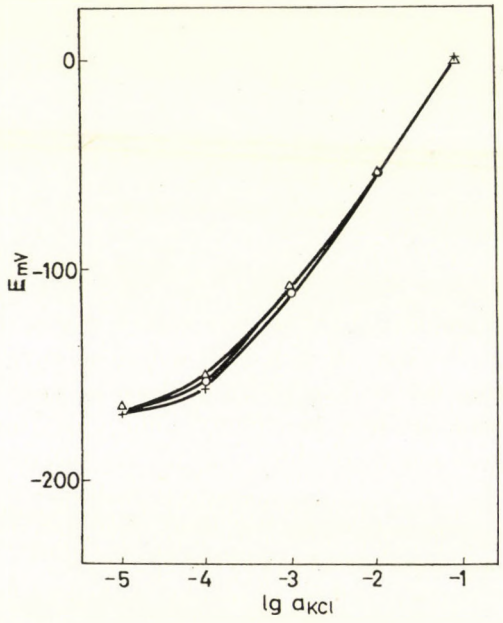

Fig. 4. Relationship between the membrane potential and lg a_{KCl}. Indicator electrode: ionite membrane electrode in the K form. +—+ calculated; ○—○ measured after 1 day of soaking; △—△ measured after 50 days of soaking

following, we show the results obtained during the investigation of some anionite membrane electrodes.

Results obtained with a chloride anionite electrode soaked in a chloride solution continuously are presented in Fig. 4. It can be seen that there is only a little difference between the calibration curves plotted after soaking the electrodes for 1 day and 50 days. Thus, it can be stated that the electrode function of the chloride anionite membrane does not change practically on continuous soaking.

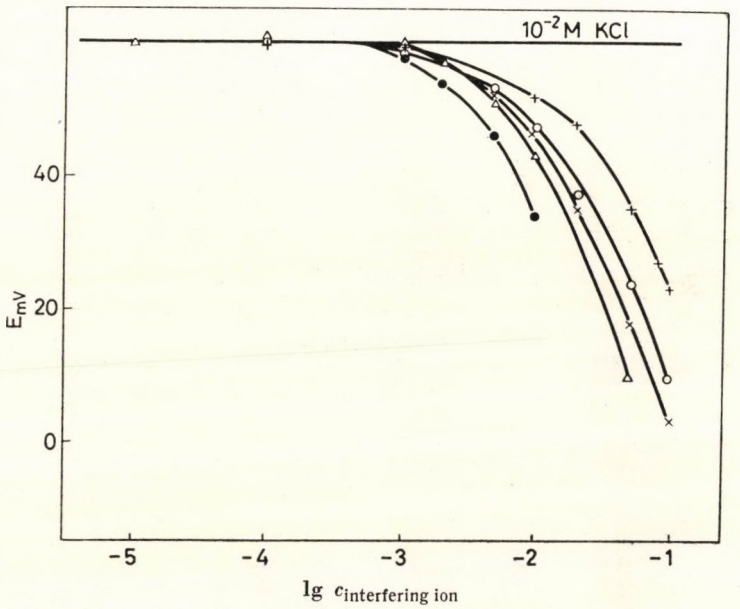

Fig. 5. Relationship between the membrane potential obtained in the investigation of the selectivity of the ionite membrane electrode in the potassium form and lg $c_{\text{interfering ion}}$. Interfering ions: +—+ Li^+. ○—○ Na^+; ×—× Mg^{2+}; △—△ Ca^{2+}; •—• Ba^{2+}

The perchlorate anionite electrode was soaked continuously in 10^{-1} and 1 *M* $NaClO_4$ solutions. We have chosen these solutions of relatively high concentrations for studying the swelling effect, because in practice the electrodes are used mainly in concentrated perchlorate solutions. During 50 days the change in potential was not more than ± 2 mV for the perchlorate anionite electrodes.

During the continuous soaking, the time used for obtaining constant potential values was also measured for some of the ionite electrodes. The investigations show that the time used for obtaining constant potential values increases with the time of swelling. This finding is especially valid in low concentration ranges. However, the time necessary for obtaining the equilibrium potential can be shortened by keeping the electrodes in distilled water for a

few minutes, before using them in solutions of low concentrations. This is sufficient for overcoming the so-called memory effect.

In the second part of our work we investigated the selectivity of ionite electrodes. Our results verified the fact that ionite membrane electrodes are not selective to individual ions, and only selective for cations or anions. However, a slight selectivity of these electrodes was found. Obviously, this is due to the various binding strengths of the individual ions to the resin. For example, Fig. 5 shows the selectivity of potassium cationite electrode to various cations. In these measurements, the concentration of the potassium ion was kept constant (10^{-2} *M*), and the concentration of the various interfering ions changed. It can be seen from Fig. 5 that every ion investigated interferes in the determination of the potassium ion activity in commensurable quantities. However, the interfering effect of the individual ions is different. The order of the ions made according to their interfering effect is the same as the order of their binding strength on the strongly acidic ion exchange resins. The selectivity constants of the perchlorate ionite electrode for the individual ions were determined by EISENMAN's method [11]. The selectivity constants are given in Table I.

Table I

Selectivity coefficient of the perchlorate ionite membrane electrode

Interfering ion	Selectivity coefficient
CH_3COO^-	9.7×10^{-2}
HPO_4^{2-}	1.5×10^{-1}
SO_4^{2-}	2.6×10^{-1}
Cl^-	2.7×10^{-1}
Br^-	4.9×10^{-1}
NO_3^-	5×10^{-1}
I^-	9×10^{-1}

Practical conclusions

The results of our examinations underline the finding that membrane electrodes prepared from solid ion exchange resins are not specific for the individual anions or cations. Their selectivity coefficients approach so closely to unity that the electrodes cannot be used for the specific determination of these ions.

However, the question arises whether the perm-selective properties of the electrodes can be used for practical purposes or not. It is true, that if the

activity coefficient of the solution to be investigated is adjusted with an indifferent electrolyte to a constant value, then these membrane electrodes can be used as a reference electrode, the potential of which is determined by the total activity of the cations or anions in the solution. With this method, the complications due to liquid–liquid interface can be avoided.* Such examinations were carried out with perchlorate ionite membrane electrodes in perchlorate solutions. A perchlorate anionite electrode was used as reference electrode against a glass electrode. This measuring cell was used for potentiometric acid–base titrations and for direct pH-determination in the range of pH 1 to 11. The results obtained with a measuring cell containing a glass electrode and a perchlorate electrode were compared with those obtained with a cell containing a glass electrode and a calomel electrode. In Table I, the pH values measured with the systems containing a glass electrode and a calomel electrode and

Table II

Comparison of the results of pH-measurements obtained with the measuring systems glass electrode—calomel electrode and glass electrode—perchlorate ionite membrane electrode

Measuring system				Δ pH		
1. Glass el.–calomel el.	2. Glass el.–perchlorate el.					
pH values measured in 1 M $NaClO_4$ solutions						
1.33	1.3	1.26	1.3	0.03	0.07	0.03
2.16	2.13	2.1	2.12	0.03	0.06	0.04
3.12	3.12	3.09	3.12	0	0.03	0
4.2	4.19	4.18	4.2	0.01	0.02	0
5.54	5.55	5.56	5.58	0.01	0.02	0.04
6.84	6.81	6.89	6.84	0.03	0.05	0
7.77	7.7	7.72	7.76	0.07	0.05	0.01
8.4	8.39	8.42	8.38	0.01	0.02	0.02
11.22	11.18	11.24	11.26	0.04	0.02	0.04

a glass electrode and a perchlorate electrode, respectively, and the Δ pH-values are given. The solutions measured contained 1 M $NaClO_4$. The data given and the here not discussed results obtained with potentiometric titrations show that the perchlorate anionite membrane electrode can be used successfully in perchlorate solutions of high concentrations (10^{-1} to 1 M) as a reference electrode. The use of the perchlorate electrode is especially advantageous in solutions, where electrodes of the second kind cannot be used because of their high diffusion potential.

* We thank Prof. Dr. Mihály Beck for his valuable suggestion concerning the use of the perchlorate electrode as a reference electrode.

REFERENCES

1. RECHNITZ, G. A.: Anal. Chem. **40,** 696 (1968)
2. RECHNITZ, G. A.: Rec. Chem. Progr. **26,** 4 (1965)
3. PUNGOR, E., HAVAS, J.: Acta Chim. Acad. Sci. Hung. **50,** 77 (1966)
4. PUNGOR, E., HAVAS, J.: Magy. Kém. Folyóirat **72,** 531 (1966)
5. PUNGOR, E., HAVAS, J., TÓTH, K.: Acta Chim. Acad. Sci. Hung. **41,** 239 (1964)
6. PUNGOR, E., HAVAS, J., TÓTH, K.: Z. Chem. **5,** 9 (1965)
7. PUNGOR, E., HAVAS, J., TÓTH, K.: Hung. Sci. Instr. **3,** 2 (1965)
8. PUNGOR, E., TÓTH, K., HAVAS, J.: Acta Chim. Acad. Sci. Hung. **48,** 17 (1966)
9. PUNGOR, E., TÓTH, K., HAVAS, J.: Mikrochim. Acta **4,** 689 (1966)
10. PUNGOR, E., HAVAS, J., TÓTH, K.: Instruments and Control Systems **8,** 105 (1965)
11. EISENMAN, G.: Biophys. J. **2,** 259 (1962)

Ernő PUNGOR
E. HITES-PAPP
Veszprém, Schönherz Z. u. 12, Hungary.

Acta Chimica Academiae Scientiarum Hungaricae, Tomus 66 (1), pp. 27–28 (1970)

CHEMISTRY OF TRANSITION METAL NITROGEN COMPLEXES, II*

PHOSPHINE EXCHANGE IN NITROGEN COMPLEXES OF COBALT

(SHORT COMMUNICATION)

I. Ötvös, G. Speier and L. Markó

(Research Group for Petrochemistry of the Hungarian Academy of Sciences, Veszprém)

Received November 18, 1969

There are only a few reactions of transition metal nitrogen complexes known up to now which do not involve the liberation of gaseous nitrogen.

$Co(N_2)(Ph_3P)_3$ [1], dissolved in benzene, was found to react with n-Bu_3P by stepwise substitution of the triphenylphosphine ligands. The reaction can be followed by infrared spectroscopy, and the following ν_{NN} wavenumbers have been found to be characteristic for the $Co(N_2)(Ph_3)_{3-n}$(n-$Bu_3P)_n$ complexes formed in benzene solution:

n	ν_{NN} (cm^{-1})	n	ν_{NN} (cm^{-1})
0	2091	2	2063
1	2077	3	2047

The exchange reaction was too fast for kinetic measurements.

$Co(N_2)(Ph_3P)_3$ did not react with Ph_3As and Et_2S, but an excess of Et_3As and Ph_3Sb shifted the ν_{NN} band to 2083 and 2085 cm^{-1}, respectively. This suggests the formation of $Co(N_2)(Ph_3P)_{3-n}L_n$ (L = Et_3As, Ph_3Sb) complexes, the first As or Sb containing nitrogen complexes to be reported. The Ph_3Sb containing solution evolved nitrogen. Rapid decomposition of $Co(N_2)(Ph_3P)_3$, without the formation of detectable N_2 containing intermediates, was caused by phosphites, Ph_2PCl, $PhPCl_2$, Ph_2PH and $PhPH_2$.

The trend in the N,N stretching frequencies of $Co(N_2)(Ph_3P)_{3-n}$(n-$Bu_3P)_n$ complexes is in agreement with the lower π-acceptor capacity of the n-Bu_3P ligand as compared with Ph_3P. A similar trend was observed with $Co(N_2)$ $(Ph_{3-m}Et_mP)_3$ complexes, prepared from $Co(acac)_2$, n-BuLi and the appropriate phosphine in tetrahydrofuran solution in a nitrogen atmosphere:

* Part I: see Ref. [1].

m	ν_{NN} (cm^{-1})	m	ν_{NN} (cm^{-1})
0	2093	2	2060
1	2080	3	2050

Both series of nitrogen complexes show that the bonding in the N_2 ligand is influenced by the relative basicity of the other ligands, in a manner similar to carbon monoxide as observed in metal carbonyls [2].

All spectra were measured in a 1.0 mm KBr cell at $10^{-2}M$ concentrations, using a UR-20 (Carl Zeiss, Jena) spectrophotometer.

REFERENCES

1. SPEIER, G., MARKÓ, L.: Inorg. Chim. Acta **3**, 126 (1969)
2. STROHMEIER, W., MÜLLER, F. J.: Chem. Revs. **100**, 2812 (1967)

Irma ÖTVÖS
Gábor SPEIER
László MARKÓ

Veszprém, Schönherz Z. u. 12, Hungary.

Acta Chimica Academiae Scientiarum Hungaricae, Tomus 66 (1), pp. 29—31 (1970)

OSCILLOMETRIC STUDY OF COMPLEX FORMATION

(SHORT COMMUNICATION)

C. B. Riolo, T. F. Soldi and G. Spini

(Istituto Chimica Generale, Università di Pavia, Pavia, Italy)

Received January 31, 1970

The oscillometric method was applied to the study of some reactions of dialkylzinc compounds with 2,2'-bipyridine, ethylenediamine and N,N,N',N'-tetramethylenediamine. Titration curves give information about the stoichiometry and dissociation constant of the complexes.

The study of complex formation of dyalkilzinc compounds with 2,2'-bipyridine (Bipy), ethylenediamine (En) and N,N,N',N'-tetratmethylenediamine (TMED) was investigated by an oscillometric method.

The dipole moments of R_2Zn and the symmetrical molecules of TMED, En and Bipy are close to zero or negligibly small, whereas the complexes $R_2Zn \cdot TMED$, $R_2Zn \cdot En$ and $R_2Zn \cdot Bipy$ have considerable dipole moments. Therefore, when the ligands are added to R_2Zn in benzene, a non-polar solvent, the dielectric constant of the solution increases until complex formation is complete. The changing dielectric properties of the sample produce a corresponding change in the capacitance of the resonant circuit of the HF oscillator. A linear relationship between instrumental scale deflection and cell dielectric constant may be obtained, in the lower range, by the introduction of a variable inductor in the cell circuit.

The meter deflection, which is related to the change in the dielectric properties of the solution, was plotted against the amount of complexing agent: the difference between the deflection at the equivalence point and that obtained by extrapolating to a large excess of complexing agent, is a function of the formation constant of the complex.

Experimental

Dialkylzinc compounds were prepared by direct synthesis from zinc-copper [1] and alkyl halides according to Renshaw and Greenlaw [2], Noller [3] and Soroos and Morgana [4] for dimethylzinc, diethylzinc and diisopropylzinc compounds, respectively.

These dialkyl compounds are extremely sensitive to moisture and oxygen, therefore it is necessary to perform the titration in a dry nitrogen atmosphere. Benzene used for the solutions was rigorously anhydrous. The ligands Bipy, En and TMED were pure grade reagents. A high frequency Sargent oscillator mod. V, with a 10 ml glass vessel, was used. The concentration of dialkylzinc solution ranged from 0.005 *M* to 0.07 *M*.

Solutions were titrated from a micrometer syringe with 0.3 *M* solution of Bipy and 0.5 *M* solutions of TMED and En.

Results and discussion

Since the dipole moments of dialkylzinc compounds and the symmetrical ligand molecules are close to zero or negligibly small, as mentioned above, the change in ε is the result of complex formation.

Figs 1, 2 and 3 show the curves obtained by titration of diethylzinc with Bipy, En and TMED, respectively. The titration curves of dimethylzinc and

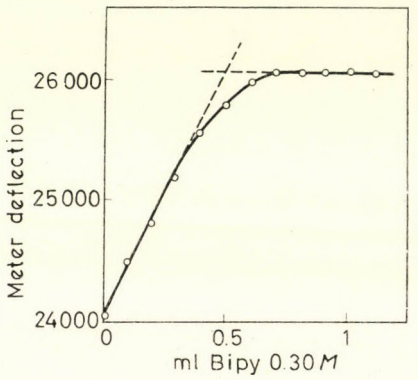

Fig. 1. Representative high-frequency titration curve of 0.140 mmole of $Zn(C_2H_5)_2$ with 0.30 *M* Bipy. $v_0 = 8.60$ ml

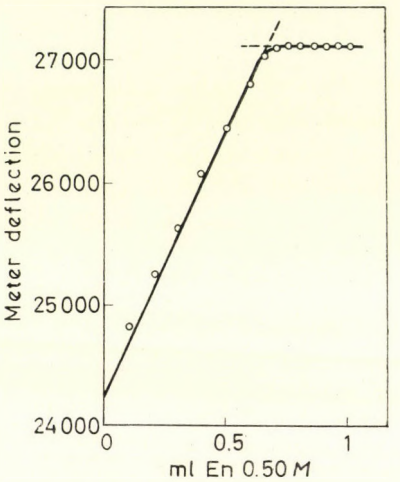

Fig. 2. Representative high-frequency titration curve of 0.330 mmole of $Zn(C_2H_5)_2$ with 0.50 *M* En. $v_0 = 8.0$ ml

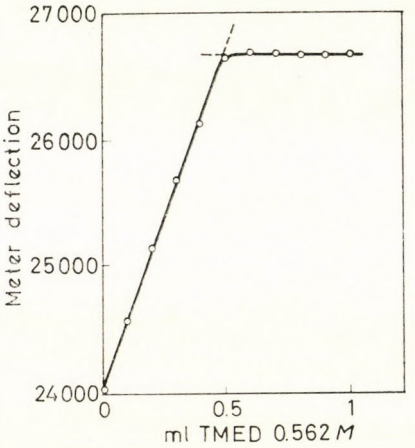

Fig. 3. Representative high-frequency titration curve of 0.270 mmole of $Zn(C_2H_5)_2$ with 0.562 *M* TMED. $v_0 = 6.70$ ml

diisopropylzinc were similar. The molar composition of the complexes corresponds to a ratio R_2Zn/ligand 1 : 1 as reported in the literature [5, 6].

The formation constants of the 1 : 1 complexes have been calculated by GEVERS' graphical method from the equation

$$K_f = \frac{\frac{E_1}{E_2} \cdot \frac{\text{mmoles } R_2Zn}{(v_0 + v)}}{\left(\frac{\text{mmoles } R_2Zn}{(v_0 + v)} - \frac{E_1}{E_2} \cdot \frac{\text{mmoles } R_2Zn}{(v_0 + v)}\right)^2}$$

where E_1 is the value of the meter deflection at the equivalence point and E_2 is the value obtained by extrapolating to a large excess of ligand, v is the volume (ml) of titrant and v_0 is the initial volume (ml) of the solution. The formation constants calculated in this way for $R_2Zn \cdot$ Bipy, $R_2Zn \cdot$ En and $R_2Zn \cdot$ TMED complexes are listed in the Table I.

Table I

Formation constants of $R_2Zn \cdot$ Bipy, $R_2Zn \cdot$ En and $R_2Zn \cdot$ TMED complexes

R_2Zn	K_f		
	Bipy	En	TMED
$(CH_3)_2Zn$	1.78×10^3	4.5×10^4	1.78×10^6
$(C_2H_5)_2Zn$	3.28×10^3	3.6×10^4	5.8×10^4
$(iso\text{-}C_3H_7)_2Zn$	2.44×10^4	2.32×10^4	2.78×10^4

The results show that the stability of TMED and En complexes decreases from dimethylzinc to isopropylzinc, while for Bipy complexes the observed order of stability is Me < Et < iso-Pr, according to NOLTES and BOERSMA [5]. These sequences can be explained only by taking into account the types of bonding involved.

REFERENCES

1. KRUG, R. C., TANG, P. J. C.: J. Amer. Chem. Soc. **76,** 2262 (1954)
2. RENSHAW, R. R., GREENLAW, C. E.: J. Amer. Chem. Soc. **42,** 1472 (1920)
3. NOLLER, C. R.: Org. Synth. **12,** 86 (1932)
4. SOROOS, H., MORGANA, M.: J. Amer. Chem. Soc. **66,** 893 (1944)
5. NOLTES, J. G., BOERSMA, J.: J. Organometal. Chem. **9,** 1 (1967)
6. GEVERS, E. CH. TH.: Recueil, **86,** 572 (1967)

Carla BERTOGLIO RIOLO
Teresa Fulle SOLDI
Giovanni SPINI

Istituto Chimica Generale, Università di Pavia, Pavia, Italy.

Acta Chimica Academiae Scientiarum Hungaricae, Tomus 66 (1), pp. 33–37 (1970)

UNTERSUCHUNG DER IONISATION VON METALLEN UND METALLIONENNEUTRALISATION MIT DER ROTIERENDEN RINGSCHEIBENELEKTRODE, IV

ALLGEMEINER ZUSAMMENHANG FÜR DEN IN m SCHRITTEN VERLAUFENDEN VORGANG

L. KISS und J. FARKAS

(Lehrstuhl für Physikalische Chemie und Radiologie der Eötvös Loránd Universität, Budapest)

Eingegangen am 5. Mai 1969

Es wurde ein Zusammenhang abgeleitet, womit ein Elektrodenvorgang aus m Schritten mit gleichzeitigem Auftreten von Diffusions- und Übertrittspolarisation diskutiert werden kann, in welchem in den einzelnen Schritten bei der Oxydation bzw. Reduktion $n_1, n_2, \ldots n_i, \ldots n_m$ Elektronen übertreten und der Unterschied in der Elektronenzahl des Ausgangsproduktes und des stabilen Endproduktes

$$\sum_{i=1}^{m} n_i = N_m$$

beträgt. Die Unbekannten des inhomogenen linearen Gleichungssystems, welches aufgrund der Ladungs- und Stoffbilanz der verlaufenden Vorgänge aufgeschrieben werden kann, können mit dem Determinantenverfahren berechnet werden und sowohl die Polarisationskurve des Vorganges als auch die Konzentrationen der Intermediärprodukte an der Oberfläche der Elektrode können angegeben werden.

In einer unserer früheren Mitteilungen [1] wurde ein Elektrodenvorgang behandelt, worin die Ionisation bzw. Reduktion eines Metalls in zwei aufeinanderfolgenden Einelektronenschritten verläuft. Es wurden Zusammenhänge bei dem gleichzeitigen Auftreten von Diffusions- und Übertrittspolarisation für die an der rotierenden Scheibenelektrode meßbare Polarisationskurve, für die an der Ringelektrode meßbaren Grenzströme und für die an der Ringelektrode meßbaren Redoxpotentiale bestimmt. Diese Zusammenhänge wurden bei verschiedenen Verhältnissen der reaktionsbestimmenden Parameter [1, 2] und für den Fall der spontanen Auflösung der Metalle [3] diskutiert.

Die Berechnung der Polarisationskurven für den allgemeinen Fall von Elektrodenvorgängen, welche unter Mitwirkung von N_m Elektronen in mehreren Schritten verlaufen, wurde wegen der Kompliziertheit, Unübersichtlichkeit und schwerfälligen Behandelbarkeit dieser Zusammenhänge noch nicht durchgeführt [4]. Deshalb sollen im weiteren allgemeine Zusammenhänge angegeben werden, mit deren Hilfe in m Schritten verlaufende Elektrodenvorgänge behandelt werden können, wo in den einzelnen Schritten bei der Oxydation bzw. Reduktion $n_1, n_2, \ldots n_i, \ldots n_m$ Elektronen übertreten und die Elektronenzahldifferenz zwischen dem Ausgangs- und Endprodukt

$$\sum_{i=1}^{m} n_i = N_m \tag{1}$$

beträgt.

Unsere Untersuchungen wurden zunächst auf den Fall beschränkt, wo das eine Ausgangs- bzw. Endprodukt das Metall *Me*, das andere das Ion $Me^{N_m^+}$ ist. Im weiteren können dann die für diesen Fall, d.h. für die Ionisation bzw. Reduktion des Metalls angegebenen Zusammenhänge leicht in eine Form gebracht werden, die für beliebige Redoxvorgänge anwendbar ist.

Es soll also der in folgenden Teilreaktionen verlaufende Vorgang behandelt werden:

$$\begin{gathered}
Me \underset{k_{k_1}}{\overset{k_{a_1}}{\rightleftarrows}} Me^{N_1^+} + n_1 e \\
Me^{N_1^+} \underset{k_{k_2}}{\overset{k_{a_2}}{\rightleftarrows}} Me^{N_2^+} + n_2 e \\
\cdots\cdots\cdots\cdots\cdots\cdots\cdots\cdots \\
Me^{N_{i-1}^+} \underset{k_{k_i}}{\overset{k_{a_i}}{\rightleftarrows}} Me^{N_i^+} + n_i e \\
\cdots\cdots\cdots\cdots\cdots\cdots\cdots\cdots \\
Me^{N_{m-1}^+} \underset{k_{k_m}}{\overset{k_{a_m}}{\rightleftarrows}} Me^{N_m^+} + n_m e
\end{gathered} \tag{2}$$

wo $N_1, N_2, \ldots N_i \ldots N_m$ die Ladungszahl der in der Reaktion teilnehmenden Ionen, $n_1, n_2, \ldots n_i \ldots n_m$ die Zahl der in den einzelnen Reaktionsschritten übertretenden Elektronen und $k_{a_1}, k_{k_1}, k_{a_2}, k_{k_2}, \ldots k_{a_i}, k_{k_i}, \ldots k_{a_m}, k_{k_m}$-Reaktionsgeschwindigkeitskonstanten sind. Die Bedeutung der letzteren ist nach unseren früheren Mitteilungen:

$$k_{a_i} = k'_{a_i} \exp\left(\frac{\alpha_i n_i F \varphi}{RT}\right) \tag{3}$$

$$k_{k_i} = k'_{k_i} \exp\left(-\frac{(1-\alpha_i) n_i F \varphi}{RT}\right) \tag{4}$$

wo k'_{a_i}, k'_{k_i} (von der Vergleichselektrode abhängige) Geschwindigkeitskonstanten sind, α_i den Übertrittsfaktor und φ das Elektrodenpotential bedeuten; die sonstigen Symbole sind die üblichen.

Nach dem früher mitgeteilten Gedankengang [1] kann, wenn die dort angegebenen Bedingungen bestehen, die stationäre Ladungsbilanz für die Reaktionen (2) aufgeschrieben werden:

$$i = \sum_{i=1}^{m} N_i X_i (c_{i,0} - c_{i\infty}) \tag{5}$$

i = die durch die Elektrode fließende Stromdichte,

$$X_i = 0{,}62 \; F D_i^{2/3} \nu^{-1/6} \omega^{1/2} \tag{6}$$

D_i = die Diffusionskonstante des Me^{N_i+}-Ions,
F = die Faradaysche Zahl,
ν = die kinematische Viskosität der Lösung,
ω = die Winkelgeschwindigkeit der Elektrode,

$c_{i,0}$, bzw. $c_{i,\infty}$ = Konzentration der Me^{N_i+}-Ionen an der Elektrodenoberfläche ($y = 0$), bzw. im Inneren der Lösung ($y = \infty$).

Aufgrund der stationären Stoffbilanz können folgende lineare Gleichungen aufgestellt werden:

$$\begin{aligned}
&\frac{k_{a_1}}{n_1} - \left(\frac{k_{k_1}}{n_1} + \frac{k_{a_2}}{n_2}\right) c_{1,0} + \frac{k_{k_2}}{n_2} c_{2,0} = X_1 (c_{1,0} - c_{1,\infty}) \\
&\frac{k_{a_2}}{n_2} c_{1,0} - \left(\frac{k_{k_2}}{n_2} + \frac{k_{a_3}}{n_3}\right) c_{2,0} + \frac{k_{k_3}}{n_3} c_{3,0} = X_2 (c_{2,0} - c_{2,\infty}) \\
&\frac{k_{a_3}}{n_3} c_{2,0} - \left(\frac{k_{k_3}}{n_3} + \frac{k_{a_4}}{n_4}\right) c_{3,0} + \frac{k_{k_4}}{n_4} c_{4,0} = X_3 (c_{3,0} - c_{3,\infty}) \\
&\cdots\cdots\cdots

$$\begin{aligned}
&\frac{k_{a_2}}{n_2} c_{1,0} - \left(\frac{k_{k_2}}{n_2} + \frac{k_{a_3}}{a_3} + X_2\right) c_{2,0} + \frac{k_{k_3}}{n_3} c_{3,0} = - X_2 c_{2,\infty} \\
&\frac{k_{a_3}}{n_3} c_{2,0} - \left(\frac{k_{k_3}}{n_3} + \frac{k_{a_4}}{n_4} + X_3\right) c_{3,0} + \frac{k_{k_4}}{n_4} c_{4,0} = - X_3 c_{3,\infty} \\
&\cdots\cdots\cdots

die Glieder der Determinante eine wesentlich einfachere Form annehmen und die betreffenden Unbekannten in übersichtlicher Form entwickelt werden können.

LITERATUR

1. Kiss, L., Farkas, J.: Acta Chim. Acad. Sci. Hung. **64,** 241 (1970)
2. Kiss, L., Farkas, J.: Acta Chim. Acad. Sci. Hung. **65,** 7 (1970)
3. Kiss, L., Farkas, J.: Acta Chim. Acad. Sci. Hung. **65,** 141 (1970)
4. Lossew, W. W., Gorodetzky, W. W.: Elektrochimiya **3,** 1961 (1967)
5. Iwanow, Ju. B., Lewitsch, W. G.: Dokl. Akad. Nauk SSSR **126,** 1029 (1959)
6. Nekrassow, L. N.: Elektrokhimiya **2,** 438 (1967)

László Kiss
József Farkas
Budapest VIII., Puskin u. 11—13.

Acta Chimica Academiae Scientiarum Hungaricae, Tomus 66 (1), pp. 39–45 (1970)

MEASUREMENTS ON A.C. CORROSION MODELS

J. DÉVAY and SAYED SABET ABD EL REHIM

(Department of Physical Chemistry, University of Chemical Engineering, and Research Group for Electrochemistry of the Hungarian Academy of Sciences, Veszprém)

Received May 8, 1969

A.c. corrosion model measurements have been performed using a galvanic cell consisting of a dropping mercury electrode immersed in a solution of the Fe^{3+}/Fe^{2+} redox system (cathode) and a hydrogen electrode immersed in solutions of various pH (anode), as well as with an iron electrode immersed in a solution containing quinone. It was found that, depending on their characteristics, anodic and cathodic polarization curves may or may not be affected by a.c. The corrosion observed during the model measurements can be explained by changes in the polarization curves. These investigations have provided an experimental proof for the hypothesis that, depending on circumstances, electrolytic corrosion may or may not be changed by a.c.

In our previous papers [1–22] the corrosive effect of alternating current (a.c.) has been dealt with. These investigations have shown that a.c. influences the electrolytic corrosion of "homogeneous" metal surfaces as well as the corrosion caused by local cells, and leads to the formation of corrosion cells due to its non-uniform distribution on the metal surface. These effects are superimposed on each other.

The above mentioned corrosion effects of a.c. are attributed to changes in the polarization curves of the electrode processes, *i.e.* to alteration of their rates.

Data on the corrosion of "homogeneous" metals can be found in the literature for Hg, Fe, Cu, Zn and Cd. In these cases the corrosion was increased by a.c. However, in principle, there are cases in which a.c. does not alter or even decreases corrosion. Further studies are, therefore, required for the generalization of the conclusions. Our results on this problem are presented in this paper.

1. A.c. corrosion model measurements of the dropping mercury electrode

A suitable model system had to be found for the investigations. The galvanic cell consisting of the redox system Fe^{3+}/Fe^{2+} and a dropping mercury electrode was chosen. The corresponding results are given below.

1.1. *Experimental*

The galvanic cell consisted of a dropping mercury electrode immersed in an aqueous solution of the Fe^{3+}/Fe^{2+} redox system (cathode) and of a hydrogen electrode (anode) placed in a suitable solution. The two electrodes served for modelling local corrosion cells. The circuit

diagram of the applied set-up is shown in Fig. 1. The dropping mercury electrode was immersed into vessel F_1 filled with a solution of $1 \cdot 10^{-3}$ M in Fe^{2+}, $1 \cdot 10^{-3}$ M in Fe^{3+}, $1 \cdot 10^{-1}$ M in oxalic acid, and $2 \cdot 10^{-1}$ M in sodium oxalate. The bottom of vessel F_2 was separated by a cellophane membrane from the solution of in vessel F_1. Vessel F_2 was filled with 0.2 M HCl solution in the first series (1), and with a solution identical to that in vessel F_1 in the second series (2) of experiments. A platinized platinum electrode P_1 with a geometrical surface area of 3 cm² was placed in vessel F_2, through which H_2 (1 atm) was bubbled. The circuit of galvanic cell consisting of the M_1 redox and P_1 hydrogen electrodes was closed through galvanometer A_1 and inductance H_1 (8.7 Hy). Our objective was to determine the influence of a.c. on the above galvanic cell. For this purpose, a 75 Hz a.c. from electronic a.c. generator G_1 was led through

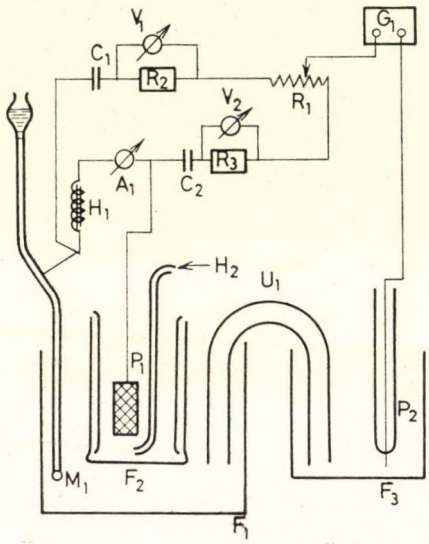

Fig. 1

resistor R_1 (12.000 ohms) to electrodes M_1 and P_1. A.c. was led into the solution by platinum needle electrode P_2 placed in vessel F_3 filled with a solution identical with that in F_1. Vessels F_1 and F_3 were connected by a U-tube containing this solution. The equality of a.c. intensities across eletrodes M_1 and P_1 (with a half-to-half division of current) was achieved by the suitable adjustment of variable resistor R_1. A.c. intensities in different lines of the circuit were determined by means of a.c. vacuum tube voltmeters V_1 and V_2 measuring the voltage drop across resistors R_2 and R_3 (1000 ohms). Capacitors C_1 and C_2 (of capacitance 10 μF each) and inductance H_1 served for the separation of a.c. and d.c. components. (The resistance of the galvanic cell was measured by the a.c. bridge method and it turned out to be a few thousand ohms including the resistance of the instrument.) Considering this fact, the voltages appearing on ohmic resistances due to the low intensity d.c. of the galvanic cell were neglected. To prevent disturbances due to oxygen, pure nitrogen was bubbled through the solution in F_1 and the latter was closed with a stopper not shown in the scheme.

1.2. *Results and discussion*

The d.c. intensities ($i_{=}$) across the galvanic cells described in section 1.1. are shown in Fig. 2 for an a.c. frequency of 75 Hz ($i_{\sim}$). This Figure refers to cathodes (1) and (2) described in section 1.1. From Fig. 2 the conclusion can be drawn that the d.c. across the galvanic cell consisting of a dropping mercury

electrode (cathode) and a hydrogen electrode (anode) decreases with increasing $i_{\sim}$ in case (1) but it remains practically unchanged in case of solution (2). (In Fig. 2, the current intensities corresponding to the maximum surface area of the mercury drop are shown.)

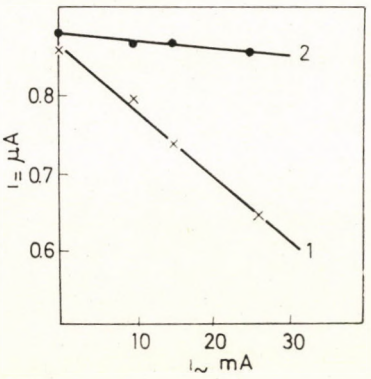

Fig. 2

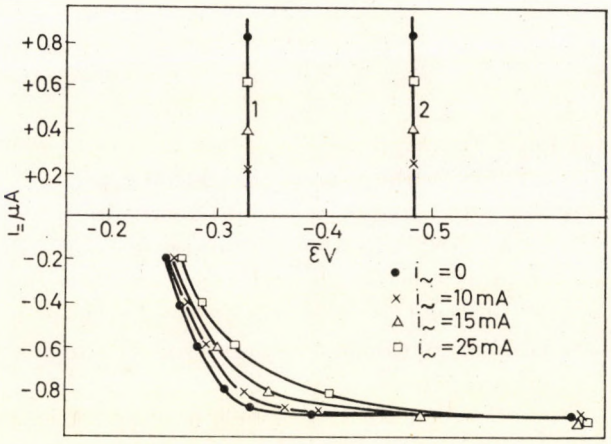

Fig. 3

To explain these phenomena, the cathodic polarization curve of the dropping mercury electrode in redox system Fe^{3+}/Fe^{2+}, and the anodic polarization curves of the hydrogen electrode immersed in solutions (1) and (2) were determined in a suitable set-up [7] under d.c. conditions as well as at different a.c. intensities ($i_{\sim}$) superimposed on d.c. ($\bar{\varepsilon}$ is the potential of the electrode with respect to the normal calomel electrode.) The results are shown in Fig. 3.

As can be seen from Fig. 3, with changing a.c. intensity the potential of the dropping mercury electrode is shifted toward the concave side of the curve. The potential of the hydrogen electrode (anode) is, however, practically independent of $i_{=}$ and $i_{\sim}$, *i.e.* the electrode could not be polarized during the measurements (max. 30 min.).

If the maximum corrosion d.c. intensity ($i_{=}$) that can appear between electrodes of the galvanic cell is calculated from the EVANS diagram [23], the data in Table I are obtained. Satisfactory agreement can be observed between the experimental values and those derived from the polarization curves.

Table I

$i_{=}$ × 10^6 A calculated from the Evans diagram			$i_{=}$ × 10^6 A measured	
$i_{=}$ mA	sol. (1)	sol. (2)	sol. (1)	sol. (2)
0	0.88	0.90	0.86	0.88
10	0.82	0.90	0.80	0.87
15	0.74	0.89	0.74	0.87
25	0.66	0.87	0.65	0.86

Thus, the conclusion can be drawn that, depending on $i_{\sim}$, the corrosion current in the model cell may decrease or remain unchanged. A decrease is observed at potentials where the rate of the cathode process (and the corresponding $i_{=}$) decreases with increasing a.c. intensity (in case of solution (1)). When the cathodic limiting diffusion current of the Fe^{3+}/Fe^{2+} redox system has been reached the extent of corrosion is not altered by changing the a.c. intensity ($i_{\sim}$). This occurs in case (2) where, during the action of the galvanic cell, such potentials are reached at which the magnitude of the corrosion current is controlled by the limiting current.

The above data prove for the first time the hypothesis that a.c. does not enhance corrosion in all cases but can also suppress it or leave it unchanged.

2. A.c. corrosion measurements on iron immersed in a solution of quinone

To extend our knowledge about a.c. corrosion, we have studied the corrosion of an iron electrode immersed in an electrolyte containing quinone. Electrochemical (*e.g.* polarographic) tests have shown that quinone is reduced electrochemically at potentials corresponding to the corrosion of iron.

2.1. *Experimental*

The measurements were performed on a cylindrical iron electrode with a surface area of 4 cm^2 using the experimental set-up described previously [7]. The extent of corrosion was determined using 50 Hz a.c. as described in reference [7]. A 5% KCl solution containing 10^{-3} *M* quinone was used. As ascertained previously [7], quinone does not interfere with the analytical determination of dissolved iron. Oxygen was removed by bubbling N_2 through the solution containing the iron electrode, and the vessel was tightly stoppered.

2.2. *Results and discussion*

The extent of corrosion of iron (k) is shown in Fig. 4 as a function of the d.c. intensity passing across it, at different a.c. densities relative to the iron electrode.

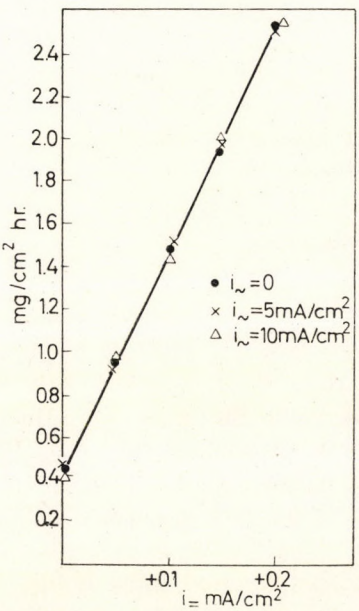

Fig. 4

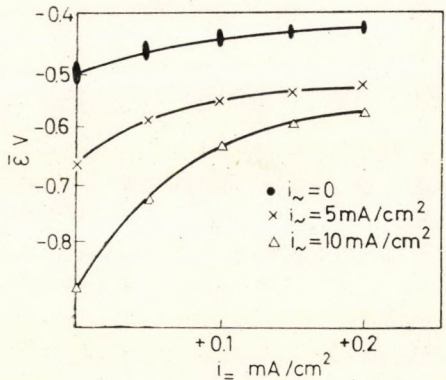

Fig. 5

It can be concluded that the higher the anodic (positive) current, the stronger the corrosion, but the extent of corrosion is practically unaffected by a.c.

During the experiments, the potential of the iron electrode ($\bar{\varepsilon}$) with respect to the normal calomel electrode was also measured. The results are shown in Fig. 5. (The shifts of the experimental points along the ordinate indicate the slow change of the electrode potential during the 4-hour experiment.) The conclusion can be drawn that the higher the current density, the more markedly the electrode potential is shifted by a.c. relative to the d.c. polarization curves.

According to the Faraday law, the current densities corresponding to the anode and cathode processes (i_+ and i_-) can be calculated if the amount of dissolved iron is known. The results of these calculations are shown in Fig. 6. It can be established that the polarization curves for the anode process are affected by a.c. but the electrode can be regarded as ideally polarizable with respect to the cathode process. The cathodic polarization curve shown in Fig. 6 obviously corresponds to the limiting diffusion current of quinone reduction the magnitude of which is not affected by a.c.

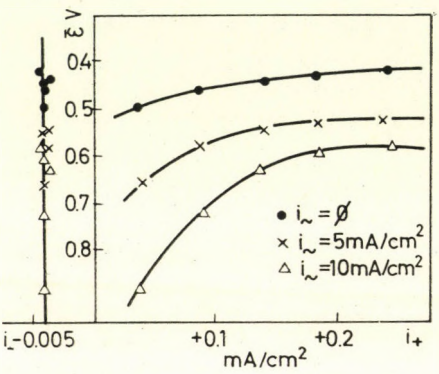

Fig. 6

Thus it is clear that, in agreement with theoretical considerations, a.c. affects the "mixed potential" appearing on electrodes but does not influence corrosion.

In the present a.c. corrosion experiments, an attempt has been made to obtain further information about this phenomenon. Evidence has been gathered to prove that, in agreement with the theory, corrosion is enhanced by a.c. but there are cases in which corrosion is not altered or even is suppressed by a.c.

REFERENCES

1. DÉVAY, J.: Veszprémi Vegyipari Egyetem Közleményei, **10,** 129 (1966)
2. ERDEY-GRÚZ, T., DÉVAY, J., SZEGEDI, R., GÁLDI, A.: Magyar Kém. Foly. **69,** 296 (1963); Acta Chim. Acad. Sci. Hung. **38,** 325 (1963)
3. DÉVAY, J., MÉSZÁROS, L.: Magyar Kém. Foly. **71,** 68 (1965); Acta Chim. Acad. Sci. Hung. **43,** 25 (1965)
4. DÉVAY, J., MÉSZÁROS, L.: Magyar Kém. Foly. **71,** 238 (1965); Acta Chim. Acad. Sci. Hung. **44,** 397 (1965)
5. DÉVAY, J., MÉSZÁROS, L.: Magyar Kém. Foly. **71,** 240 (1965); Acta Chim. Acad. Sci. Hung. **45,** 119 (1965)
6. ERDEY-GRÚZ, T., DÉVAY, J., VAJASDY, I.: Magyar Kém. Foly. **70,** 256 (1964); Acta Chim. Acad. Sci. Hung. **40,** 289 (1964)
7. DÉVAY, J., SAYED SABET ABD EL REHIM, TAKÁCS, V.: Magyar Kém. Foly. **73,** 130 (1967); Acta Chim. Acad. Sci. Hung. **52,** 63 (1967)

8. DÉVAY, J., SAYED ABD EL REHIM, TAKÁCS, V.: Magyar Kém. Foly. **73,** 145 (1967); Acta Chim. Acad. Sci. Hung. **52,** 201 (1967)
9. DÉVAY, J., MÉSZÁROS, L.: Magyar Kém. Foly. **70,** 466 (1964); Acta Chim. Acad. Sci. Hung. **43,** 17 (1965)
10. ERDEY-GRÚZ, T., DÉVAY, J., SZEGEDI, R., VAJASDY, I.: Magyar Kém. Foly. **67,** 512 (1961); Acta Chim. Acad. Sci. Hung. **34,** 301 (1962)
11. ERDEY-GRÚZ, T., DÉVAY, J., SZEGEDI, R.: Magyar Kém. Foly. **67,** 444 (1961); Acta Chim. Sci. Hung. **32,** 355 (1962)
12. ERDEY-GRÚZ, T., DÉVAY, J., SZEGEDI, R.: Magyar Kém. Foly. **68,** 190 (1962); Acta Chim. Acad. Sci. Hung. **37,** 65 (1963)
13. DÉVAY, J., SZEGEDI, R., LÁBODY, I.: Magyar Kém. Foly. **70,** 281 (1964); Acta Chim. Acad. Sci. Hung. **42,** 191 (1965)
14. DÉVAY, J., LENGYEL, B. JR.: Magyar Kém. Foly. **72,** 85 (1966); Acta Chim. Acad. Sci. Hung. **46,** 325 (1956)
15. ERDEY-GRÚZ, T., DÉVAY, J., SZEGEDI, R.: Magyar Kém. Foly. **67,** 535 (1961); Acta Chim. Acad. Sci. Hung. **35,** 29 (1963)
16. DÉVAY, J., MÉSZÁROS, L.: Magyar Kém. Foly. **71,** 277 (1965); Acta Chim. Acad. Sci. Hung. **45,** 37 (1965)
17. DÉVAY, J., MÉSZÁROS, L.: Magyar Kém. Foly. **72,** 167 (1966); Acta Chim. Acad. Sci. Hung. **47,** 185 (1966)
18. DÉVAY, J.: Magyar Kém. Foly. **71,** 198 (1965); Acta Chim. Acad. Sci. Hung. **44,** 385 (1965)
19. DÉVAY, J.: Magyar Kém. Foly. **70,** 497 (1964); Acta Chim. Acad. Sci. Hung. **42,** 255 (1965)
20. DÉVAY, J.: Magyar Kém. Foly. **73,** 146 (1967); Acta Chim. Acad. Sci. Hung. **52,** 57 (1967)
21. DÉVAY, J., SZEGEDI, R., LÁBODY, I.: Magyar Kém. Foly. **70,** 288 (1964); Acta Chim. Acad. Sci. Hung. **42,** 207 (1965)
22. DÉVAY, J., MOSONI, F.: Magyar Kém. Foly. **71,** 476 (1965); Acta Chim. Acad. Sci. Hung. **46,** 97 (1965)
23. AKIMOV, G. D.: Theory and methods of investigation of metal corrosion (in Hungarian), Nehézipari Könyvkiadó, Budapest, 1951.

József DÉVAY
Sayed Sabet ABD EL REHIM } Veszprém, Schönherz Z. u. 10, Hungary.

Acta Chimica Academiae Scientiarum Hungaricae, Tomus 66 (1), pp. 41–53 (1970)

THE EXCESS FREE ENTHALPY AND EXCESS ENTROPY OF MIXING OF ACETIC ACID–CARBON TETRACHLORIDE MIXTURE

J. Liszi

(Department of Physical Chemistry, University of Chemical Engineering, and Research Group for Electrochemistry of the Hungarian Academy of Sciences, Veszprém)

Received May 8, 1969

The excess free enthalpy and entropy of mixing of the acetic acid–carbon tetrachloride mixture have been determined at 20 °C. In the calculations the nominally two-component mixture was regarded as a regular ternary mixture of A–A_2–B type. (A denotes monomeric acetic acid, A_2 dimeric acetic acid, while B carbon tetrachloride.) The excess free enthalpy of mixing has been regarded as the sum of two terms:

i) g^E_{ass} corresponding to the association reaction

ii) g^E_{real} corresponding to the real mixing.

It has been found that in the excess free enthalpy of mixing the above two terms participate in the same order of magnitude.

On investigating the thermodynamical properties of acetic acid–carbon tetrachloride mixture the nominally binary mixture is regarded as a ternary mixture consisting of monomeric acetic acid (A), dimeric acetic acid (A_2) and carbon tetrachloride (B). Contrary to our previous publications [1, 2] none of the mixture pairs of the real (ternary) mixture is regarded as ideal. Every possible mixture pairs (A–A_2, A–B, A_2–B) are supposed to behave regularly, therefore our thermodynamical model can be represented by the following scheme:

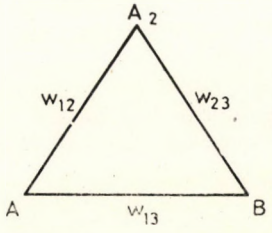

pair exchange energy: A–A_2: w_{12}; A–B: w_{13}; A_2–B: w_{23}

Fig. 1

In the scheme w denotes interchange energy, the indexes 1, 2 and 3 refer to monomeric acetic acid, dimeric acetic acid and carbon tetrachloride, respectively, in the real mixture. During our previous work, using the above model, the following quantities have been determined: the composition at 20 °C [3], the enthalpy of mixing [4], and the vapour–liquid equilibrium data [5] of the ternary mixture, regarded as a real one. This paper deals with the excess

free enthalpy and excess entropy of mixing of the acetic acid–carbon tetrachloride mixture.

1. The excess free enthalpy of mixing of acetic acid–carbon tetrachloride mixture

Acetic acid–carbon tetrachloride mixture is a reactive mixture. The excess free enthalpy of mixing is composed of the free enthalpy of the equilibrium dimerisation reaction

$$2A \rightleftharpoons A_2 \tag{1}$$

and of the excess free enthalpy of mixing corresponding to the formation of a real ternary mixture. Consequently, the excess free enthalpy of mixing of the acetic acid–carbon tetrachloride mixture is given as the sum of two terms:

$$g^E = g^E_{\text{ass}} + g^E_{\text{real}} \tag{2}$$

where

i) g^E_{ass} corresponds to the association reaction, and
ii) g^E_{real} corresponds to the real mixing.

The quantity g^E_{ass}, which corresponds to the association reaction, is evaluated on the basis of the relation known from the literature [6], according to which the chemical potential of the monomer component equals to the chemical potential of the nominal associative component. In the case of acetic acid–carbon tetrachloride mixture this means that the chemical potential of the monomeric acetic acid in the ternary (real) mixture μ_1 equals to that of the acetic acid in the binary (apparent) mixture μ_{ac}:

$$\mu_1 = \mu_{\text{ac}} \tag{3}$$

Regarding that the excess free enthalpy arising from the real nature of the mixture is calculated independently of the effect of the association reaction, g^E_{ass} is calculated using the ideal ternary mixture model. According to the model of ideal ternary mixtures [7] monomer molecules, associated molecules and the solvent form an ideal mixture with each other. The thermodynamical parameters of the apparent mixture differ from those of the ideal one only because the nominal composition of the mixture is not identical to the true composition due to the association phenomenon. In the case of the acetic acid–carbon tetrachloride mixture this means that the chemical potential of the acetic acid, as the component of the nominal mixture should be written as the chemical potential of a component of the real mixture, and the chemical potential of monomeric acetic acid in the ternary mixture should be written as

the chemical potential of a component of the ideal mixture. Accordingly, on the basis of Eq. (3):

$$\mu_{ac}^{0} + RT \ln x_{ac}\gamma_{ac} = \mu_{1}^{0} + RT \ln x_1 \tag{4}$$

where μ_{ac}^{0} and μ_{1}^{0} denote standard chemical potentials, x_{ac} is the nominal molar fraction of acetic acid, x_1 is the real molar fraction of monomeric acetic acid, R is the gas constant, T is absolute temperature, γ_{ac} is the activity coefficient corresponding to acetic acid. It should be emphasized that γ_{ac} is not identical with the activity coefficient of the acetic acid in the nominal mixture, it is a fictive value; and it would be identical with the activity coefficient of the acetic acid in the nominal mixture only if the real (ternary) mixture behaved ideally. From Eq. (4):

$$\gamma_{ac} = \frac{1}{x_1^{\circ}} \frac{x_1}{x_{ac}} \tag{5}$$

where index "0" refers to pure acetic acid. On the basis of similar considerations it can be proved that

$$\gamma_B = \frac{x_3}{x_B} = 1 + x_2 \tag{6}$$

where γ_B is, obviously, a fictive constant having similar meaning as γ_{ac}

Using Eqs. (5) and (6) the excess free enthalpy of mixing arising from the association reaction can be obtained:

$$g_{ass}^{E} = RT\{x_{ac} \ln \gamma_{ac} + x_B \ln \gamma_B\} = RT\left\{x_{ac} \ln\left[\frac{1}{x_1^{\circ}} \frac{x_1}{x_{ac}}\right] + x_B \ln (1 + x_2)\right\} \tag{7}$$

In the calculation of excess free enthalpy of mixing due to the real nature of the mixture it should be considered that acetic acid is in itself a mixture (*i.e.* mixture of monomeric and dimeric acetic acid molecules) and on mixing it with carbon tetrachloride in fact the mixture of monomeric and dimeric acetic acid is diluted. In the course of mixing (*i.e.* of dilution) the association equilibrium is shifted. Therefore the excess free enthalpy of mixing arising from the real nature of the mixture can be calculated by taking into account two partial processes:

i) the separation of the monomeric and dimeric acetic acid corresponding to the association equilibrium taking place in pure acetic acid,

ii) the mixing of carbon tetrachloride with the monomeric and dimeric acetic acid quantity that corresponds to the association equilibrium belonging to the given nominal composition.

Regarding that originally in every case pure acetic acid is present in a quantity corresponding to x_{ac} nominal molar fraction, the excess free enthalpy of the separational process (g^E_{sep}) can be given by the following equation:

$$g^E_{sep} = -x_1^\circ x_2^\circ x_{ac} w_{12}^\circ \tag{8}$$

where index "0" refers to pure acetic acid. On the basis of the theory of regular ternary mixtures, the excess free enthalpy of the mixing process (g^E_{mix}) can be calculated by the following relation:

$$g^E_{mix} = x_1 x_2 w_{12} + x_1 x_3 w_{13} + x_2 x_3 w_{23} \tag{9}$$

In the calculation it should also be taken into account that g^E_{ass} given by Eq. (7) corresponds to 1 mole of nominal mixture, therefore g^E_{real} should also be related to this quantity. As two monomeric acetic acid molecules are required for the formation of one dimeric acetic acid molecule, the true sum of moles in 1 mole of nominal mixture equals to $(1 - N_2)$, where N_2 is the number of moles of dimeric acetic acid. Considering the above facts, on the basis of Eqs. (8) and (9) we obtain:

$$g^E_{real} = (1 - N_2)\{x_1 x_2 w_{12} + x_1 x_3 w_{13} + x_2 x_3 w_{23} - x_1^0 x_2^0 w_{12}^0\} \tag{10}$$

The data (corresponding to 20 °C) required for the calculation are listed in Table I [3, 4].

Table I

x_B	x_1	x_2	x_3	w_{12} cal/mol	w_{13} cal/mol	w_{23} cal/mol
0.0	0.115	0.885	0.000	−3655	−2291	+369
0.2	0.055	0.621	0.324	−4082	−2291	+168
0.4	0.027	0.409	0.564	−4292	−2291	+ 70
0.6	0.012	0.243	0.764	−4391	−2291	+ 24
0.8	0.004	0.109	0.887	−4432	−2291	+ 5
1.0	0.000	0.000	1.000	−4458	−2291	0

Table II shows the calculated excess free enthalpy of mixing as the function of the nominal molar fraction of carbon tetrachloride. The calculations were made using Eqs. (2), (7) and (10), and the data listed in Table I. The data of Table II are related to 1 mole of nominal mixture.

Table II

x_B	g^E_{ass} (cal/mol)	g^E_{real} (cal/mol)	g^E (cal/mol)
0.0	0.0	0.0	0.0
0.2	65.9	94.0	159.9
0.4	109.6	110.0	219.6
0.6	133.7	96.5	230.2
0.8	106.5	59.0	165.5
1.0	0.0	0.0	0.0

The data listed in Table II are shown in Fig. 2. Table II and Fig. 2 show that the nominally binary mixture of acetic acid and carbon tetrachloride has positive deviation on the basis of its excess free enthalpy of mixing. The contribution of the two terms (namely g^E_{ass}, arising from the association reaction and g^E_{real}, arising from the real mixing) to the excess free enthalpy of mixing ranges in the same order of magnitude.

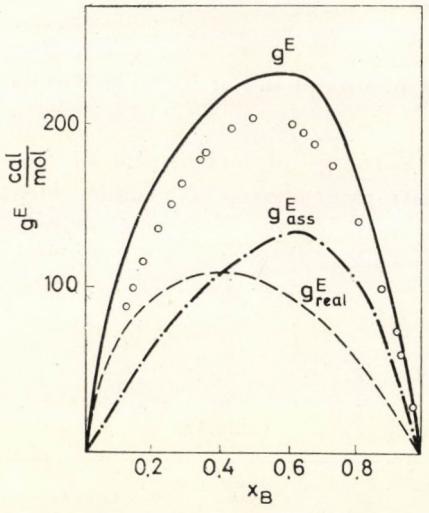

Fig. 2. The excess free enthalpy of mixing of acetic acid-carbon tetrachloride mixture of 20 °C. (The designation ○ refers to the acetic acid–benzene system.)

There is no experimental possibility for the direct determination of the excess free enthalpy of mixing. Unfortunately, there are no published data on the excess free enthalpy of mixing of acetic acid–carbon tetrachloride mixture at 20 °C, either. For the sake of comparison, however, the excess free enthalpy

of mixing of acetic acid–benzene mixture at 20 °C [8] is also shown in Fig. 2. This has been done on the basis of the following considerations:

i) Benzene, a substance regarded as apolar (its permanent dipole moment equals to 0.08 D [9]) has, presumably, the same influence on the equilibrium of the association reaction (1) as carbon tetrachloride.

ii) As the dielectric properties of benzene and carbon tetrachloride utilized for calculating interchange energy differ only to a minor extent (permanent dipole moments: $\mu_{benzene} = 0.08$ D [9], $\mu_{CCl_4} = 0.0$ D [10], mean polarizabilities: $\alpha_{benzene} = 10.7 \cdot 10^{-24}$ cm^3 [11], $\alpha CCl_4 = 10.5 \cdot 10^{-24}$ cm^3 [11]), the interchange energies of the acetic acid–carbon tetrachloride and acetic acid–benzene systems differ only due to the differences in molecular dimensions.

On the basis of the above considerations it can be expected that the excess free enthalpy of mixing of the two mentioned systems (*i.e.* acetic acid–carbon tetrachloride and acetic acid–benzene) does not differ substantially. Consequently, there is a possibility for qualitatively checking the data calculated by us, as well as listed in Table II. The comparison of the data shown in Fig. 2 for acetic acid–carbon tetrachloride and acetic acid–benzene systems indicates that the values of the excess free enthalpy of mixing given in this paper can be regarded as reasonable.

2. The excess entropy of mixing of the acetic acid–carbon tetrachloride mixture

If the excess free enthalpy of mixing and the enthalpy of mixing (h^E) are known, the excess entropy of mixing (s^E) can be calculated according to the following equation:

$$s^E = \frac{h^E - g^E}{T} \tag{11}$$

Table III

x_B	h^E cal/mol	Ts^E cal/mol
0.0	0.0	0.0
0.2	+47.8	−112.0
0.4	+57.2	−162.4
0.6	+50.6	−179.7
0.8	+37.3	−128.1
1.0	0.0	0.0

The excess free enthalpy of mixing can be found in the last column of Table II. The enthalpy of mixing has been determined in our previous work [4] and is listed in Table III. Furthermore, Table III contains the product of the temperature and the excess entropy of mixing calculated according to Eq. (11).

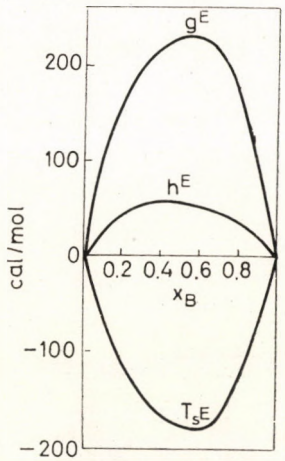

Fig. 3. The excess energy functions of mixing of acetic acid–carbon tetrachloride mixture of 20 °C

In Fig. 3 the product Ts^E, the values of h^E and g^E are plotted against the nominal molar fraction of carbon tetrachloride. In such a way, Fig. 3 gives a summary of the excess energy functions of mixing of the mixture at 20 °C.

REFERENCES

1. Liszi, J., Ratkovics, F., Salamon, T.: Acta Chim. Acad. Sci. Hung. **55**, 165 (1968)
2. Liszi, J., Ratkovics, F., Salamon, T.: Acta Chim. Acad. Sci. Hung. **55**, 179 (1968)
3. Liszi, J.: Acta Chim. Acad. Sci. Hung. **62**, 263 (1969); **62**, 293 (1970)]
4. Liszi, J.: Acta Chim. Acad. Sci. Hung. **63**, 363 (1970); **63**, 371 (1970)
5. Liszi, J.: Acta Chim. Acad. Sci. Hung, **64**, 49 (1970)
6. Prigegine, I., Defay, R.: Chemical Thermodynamics. Longmans (1954)
7. Kehiaian, H.: Bull. Acad. Polan. Sci. Ser. sci. chim. **11**, 591 (1963); **12**, 425, 433, 567 (1964)
8. Werner, G.: J. Prakt. Chem. **29**, 26 (1965)
9. Bretsnaider, Sz.: Svoistva gasov i zhidcostei. Moscow (1966)
10. Moelwyn-Hughes, E. A.: Physical Chemistry, Pergamon Press (1964)
11. Ilič, M.: Hemiiska Industriia (Beograd); **10**, 1879 (1964)

János Liszi; Veszprém, Schönherz Z. u. 10, Hungary.

Acta Chimica Academiae Scientiarum Hungaricae, Tomus 66 (1), pp. 55–76 (1970)

DATA ON COMPETITIVE OXIDATION, I

THE NON-CATALYTIC COOXIDATION OF ETHYLBENZENE AND PROPYLENE

D. GÁL,* E. A. BLUMBERG, A. YA. VALENDO and N. M. EMANUEL

(Institute for Chemical Physics, Academy of Sciences, Moscow, USSR)

Received May 16, 1969

The authors have been studying the so called HALCON-process from kinetic point of view to elucidate the mechanism of this process. Though this reaction takes place in a system of five components (ethylbenzene, ethylbenzene hydroperoxide, oxygen, propylene and catalyst), the investigations were carried out initially in systems with less than five components. The systems studied were as follows: ethylbenzene + oxygen; ethylbenzene + ethylbenzene hydroperoxide; ethylbenzene + ethylbenzene hydroperoxide + propylene; ethylbenzene + ethylbenzene hydroperoxide + propylene + oxygen. From the experimental results obtained at atmospheric pressure and in high pressure experiments — using also literature data — the activation energy of the initiation of the oxidation as well as the rate constants of both the mono- and bimolecular decomposition of the hydroperoxide molecules under the given conditions have been determined. Assuming that the acetophenone molecules in the initial stages of the reaction — due to the small amounts of alcohol molecules present in the system — are formed mainly in the recombination step, the concentration of peroxy radicals has been calculated at varying experimental conditions. For the epoxy formation in the absence of catalyst the TWIGG-mechanism has been accepted and the rate constant of the elementary reaction between propylene and peroxy radicals calculated.

Recently several patents have been published on the direct oxidation of propylene into propylene oxide [1–6]. Since propylene oxide and higher epoxy compounds are used in the manufacture of solvents, anti-freezes, polyesters, polyurethanes, the attention paid to these patents is entirely understandable.

Though from the descriptions it became evident that the direct oxidation was a reaction between propylene and different aryl-alkyl-hydroperoxides, more detailed data were published only on the 7th World Petroleum Congress in the paper by LANDAU, BROWN and RUSSEL [7], giving an account on the so called "HALCON-process".

According to their data this process involves three stages: the first consists of the alkylation of benzene with ethylene yielding ethylbenzene followed by the peroxidation of the latter in the presence of an initiator. In the second stage the ethylbenzene hydroperoxide reacts with propylene in the presence of molybdenum naphthenate as catalyst. The final stage is the separation of propylene oxide (by distillation) and the dehydration of the methyl-phenyl-carbinol formed parallel to the epoxide into styrene.

* 1967–68 Visiting Professor. Present address: Institute for Radiochemistry. József Attila University, Szeged, Hungary.

From chemical point of view the second stage seems very interesting due to its novelty. Reactions of propylene, namely, with aldehydes or peroxyacetic acid have been already applied [8], with hydroperoxides, however, it was not thought suitable due to the low yields.

As far as the mechanism of the propylene–propylene oxide and that of the hydroperoxide–alcohol transition are concerned very few is known about them. LANDAU *et al.* are of the opinion that it proceeds mainly by an ionic mechanism in contrast to the peroxyacetic acid reaction being a typical radical process.

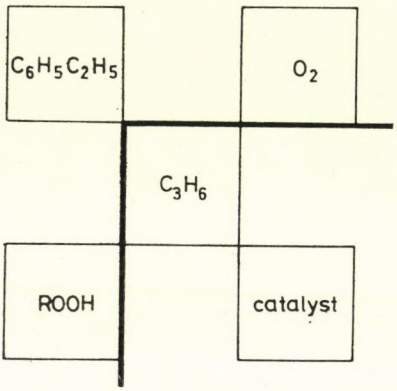

Fig. 1

In spite of the poor knowledge on the actual mechanism the HALCON-process already intruded into the European market and in 1966 a new plant has been built in Spain to manufacture 24 000 tons of propylene oxide and 60 000 tons of styrene per year [9].

These facts justify our studies on the kinetics and mechanism of the process limiting our investigations to the first two stages. The last one, namely, the separation of propylene oxide and dehydration of methyl phenyl carbinol is rather well known.

According to the HALCON-process the interacting system consists of five different compounds: ethylbenzene, ethylbenzene hydroperoxide, oxygen, propylene and the catalyst. Therefore the process can be represented by a system of five components as shown by Fig. 1.

Such system, however, would be too complicated for the study of the corresponding elementary steps. Therefore it seems more appropriate to carry out experiments in *subsystems* with two, three and four components provided that ethylbenzene should be — as both initial compound and solvent — one of them in every subsystem.

Systems of two components

Ethylbenzene + oxygen	(system A)
ethylbenzene + hydroperoxide	(system B)

Further possibilities can be excluded: it is known that under the present experimental conditions ethylbenzene does not react with propylene and the catalysts used do not affect ethylbenzene in the absence of oxygen or propylene.

Systems of three components

Ethylbenzene + oxygen + hydroperoxide	(system C)
ethylbenzene + oxygen + propylene	(system D)
ethylbenzene + oxygen + catalyst	(system E)
ethylbenzene + hydroperoxide + propylene	(system F)
ethylbenzene + hydroperoxide + catalyst	(system G)
ethylbenzene + propylene + catalyst	(system H)

System C can be regarded as an extended system A. Systems D and H are known from literature data [8].

Systems of four components

Ethylbenzene + oxygen + hydroperoxide + propylene	(system I)
ethylbenzene + oxygen + hydroperoxide + catalyst	(system J)
ethylbenzene + oxygen + propylene + catalyst	(system K)
ethylbenzene + hydroperoxide + propylene + catalyst	(system L)

The present paper summarizes our results on non-catalytic systems: A, B, F and I.

Experimental

Materials

Ethylbenzene: commercial product was purified. After prolonged warming with NaOH and separation of the latter it was shaken with hydroxylamine in aqueous solution, followed by treatment with $KMnO_4$ and sulfuric acid. It was washed with water and dried over $CaCl_2$.

Propylene, oxygen and argon were taken from cylinders.

Apparatus

Procedure 1. Experiments were carried out at atmospheric pressure in a glass vessel joined to a reflux. The reaction vessel was immersed into a thermostat and had a stopcock for sampling [10–11]. Flow rate of oxygen was maintained at 1.6 $l/hour^{-1}$. Procedure 2. High pressure experiments were carried out in a stainless steel reactor in air and argon stream, respectively, at 50 atm. Details of the apparatus are shown in the monograph of EMANUEL *et al.* [10].

2 ml of samples were withdrawn from the reactor at different time intervals.

Analyses

Majority of analyses were made by gas chromatography with two different columns. For the separation and determination of acetophenone, methyl phenyl carbinol and ethylbenzene hydroperoxide, special glass column has been developed to avoid decomposition of hydroperoxides as described by VALENDO and NORIKOV [12]. Eventual decomposition of hydroperoxides, namely, would change the amount of other products, too. Support was Celite 545 impregnated by 2% of Na_2CO_3 and 15% of Apiezon-N. It was used at 60 °C in argon flow (2.5–3.5 $l/hour^{-1}$).

Propylene oxide was determined by a metal column of 3 mm internal diameter and of 2.25 m length using brick support (0.25–0.50 in diameter) and impregnated by 20% of NaOH and after drying by 15% of distearate. As carrier gas hydrogen was used at 60 °C.

Both columns were operated with a flame ionization detector.

Beside gas chromatography classical analytical determinations were carried out, too. Hydroperoxides were measured in a chloroform–acetic acid media titrating the iodine with standard thiosulfate solution. Acetophenone was determined photometrically in form of its 2,4-dinitrophenyl-hydrazone derivative.

Oxidation of ethylbenzene

(System A)

Experiments were carried out according to Procedure 1, without initiator at three different temperatures: 90, 107 and 120 °C.

Accumulation of hydroperoxide and acetophenone as well as in some cases that of methyl phenyl carbinol were determined.

The accumulation of hydroperoxide is shown by Fig. 2 at the temperatures mentioned.

Based on the initial stages of the curves the corresponding activation energy of the hydroperoxide accumulation was of 32.7 $kcal/mole^{-1}$.

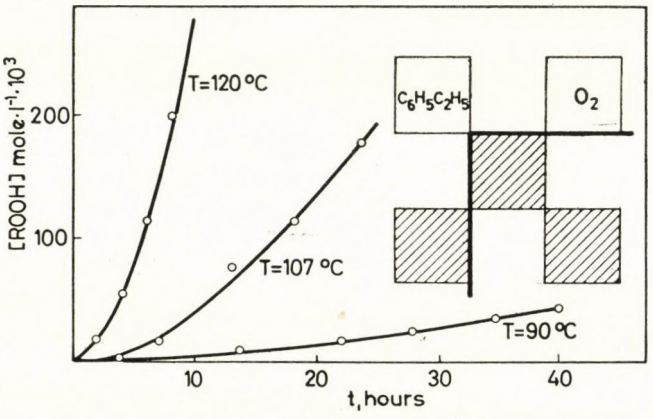

Fig. 2. Kinetics of hydroperoxide accumulation in the oxidation of ethylbenzene at different temperatures in glass vessel

Hydroperoxide is formed by the following elementary steps in liquid phase oxidations:

$$RH \rightarrow R^{\cdot} \qquad (O)$$

$$R^{\cdot} + O_2 \rightarrow RO_2^{\cdot} \qquad (I)$$

$$RO_2^{\cdot} + RH \rightarrow ROOH + R^{\cdot} \qquad (II)$$

The formed ROOH molecules undergo decomposition leading to degenerate branching:

$$ROOH \rightarrow RO^{\cdot} + \dot{O}H \qquad (III)$$

while termination occurs (at high oxygen pressures) in the corresponding recombination:

$$RO_2^{\cdot} + RO_2^{\cdot} \rightarrow \text{products} \qquad (VI)$$

Overall reaction rate expressed in general as the rate of oxygen absorption or as the rate of decrease in the concentration of the hydrocarbon in the first stages of the reaction is proportional to the rate of hydroperoxide formation provided that the decomposition of the hydroperoxide is negligible. The validity of this condition will be proved later.

$$w = -\frac{d[O_2]}{dt} = -\frac{d[RH]}{dt} \sim \frac{d[ROOH]}{dt} \equiv w_{ROOH} \qquad (1)$$

It has been deduced [10] that:

$$w = k_{II}[RH]\sqrt{\frac{w_0}{k_{VI}}} \sim w_{ROOH} \qquad (2)$$

and thus:

$$E_{ROOH} = E_{II} - \frac{1}{2}E_{VI} + \frac{1}{2}E_0 \qquad (3)$$

From the literature [13–14]:

$$E_{II} = 8.5 \text{ kcal/mole}^{-1} \qquad (4)$$

Assuming a closely zero activation energy for the recombination:

$$E_0 = 48.4 \text{ kcal/mole}^{-1} \qquad (5)$$

If hydroperoxide molecules are decomposed according to (III), the products formed may initiate and therefore Equ. (2) should be modified [10]:

$$w_{\mathrm{ROOH}} = k_{\mathrm{II}}\,[\mathrm{RH}]\left(\frac{w_0 + k_{\mathrm{III}}\,[\mathrm{ROOH}]}{k_{\mathrm{VI}}}\right)^{1/2} \tag{6}$$

provided again that the consumption of hydroperoxide is negligible, as shown later.

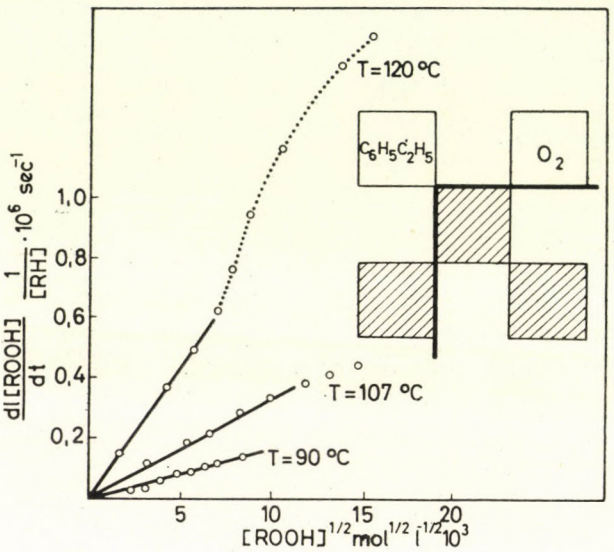

Fig. 3. $w/[\mathrm{RH}]$ as function of $[\mathrm{ROOH}]^{1/2}$ at different temperatures in the oxidation of ethylbenzene

At low w_0 values (as in our case):

$$w_{\mathrm{ROOH}} = k_{\mathrm{II}}\sqrt{\frac{k_{\mathrm{III}}}{k_{\mathrm{VI}}}}\,[\mathrm{RH}]\,[\mathrm{ROOH}]^{1/2} \tag{7}$$

that is $w_{\mathrm{ROOH}}/[\mathrm{RH}]$ plotted against $[\mathrm{ROOH}]^{1/2}$ should give a straight line.

Corresponding experimental data are given by Fig. 3.

As it can be seen at 90 and 107 °C relation (7) is fulfilled, at 120 °C, however, linearity could be observed only in the very beginning of the reaction.

Since according to literature data [13] $k_{\mathrm{VI}} \sim 2.10^7$ and $k_{\mathrm{II}} = 9.6 \cdot 10^5 \exp(-8500/\mathrm{RT})$, we obtain at 90 °C

$$k_{\mathrm{III}} = 0.77 \cdot 10^{-7}\ \mathrm{sec}^{-1} \tag{8}$$

and at 107 °C

$$k_{\mathrm{III}} = 1.26 \cdot 10^{-7}\ \mathrm{sec}^{-1} \tag{9}$$

Assuming a preexponential factor of 10^{12}:

$$E_{III} \sim 32 \text{ kcal/mole}^{-1} \tag{10}$$

The deviations from the linearity at 120 °C and at higher hydroperoxide concentrations at 107 °C in Fig. 3 suggest that with increasing hydroperoxide amounts another degenerate branching becomes predominant assumed first by BATEMAN:

$$\text{ROOH} + \text{ROOH} \rightarrow \text{RO}_2^{\cdot} + \text{H}_2\text{O} + \text{RO}^{\cdot} \tag{IIIa}$$

The RO· radicals formed in the decomposition of hydroperoxides may initiate and terminate. According to ALTES and BERG [15] following reactions should be taken into consideration:

$$\text{RO}^{\cdot} + \text{RH} \rightarrow \text{ROH} + \text{R}^{\cdot} \tag{IIa}$$

$$\text{RO}^{\cdot} + \text{RO}_2^{\cdot} \rightarrow \text{products} \tag{VII}$$

$$\text{RO}^{\cdot} + \text{RO}^{\cdot} \rightarrow \text{products} \tag{VIII}$$

JUNGERS *et al.* [16] have shown that:

$$k_{VII} = \sqrt{k_{VI} \cdot k_{VIII}} \tag{11}$$

and thus it could be deduced:

$$\frac{[\text{RH}]\,[\text{ROOH}]}{w_{\text{ROOH}}} = \frac{1}{k_{II}} \sqrt{\frac{k_{VI}}{k_{IIIa}}} + \frac{1}{k_{II}} \frac{k_{VII}}{k_{IIa}} \frac{[\text{ROOH}]}{[\text{RH}]} \tag{12}$$

(at higher hydroperoxide concentrations).

Plotting $[\text{RH}]\,[\text{ROOH}]/w_{\text{ROOH}}$ against $[\text{ROOH}]/[\text{RH}]$ at 120 °C the corresponding curves are shown by Fig. 4.

As it can be seen the experimental points fit the straight line relation — with exception of the low hydroperoxide concentration range. From Fig. 4:

$$\frac{1}{k_{II}} \sqrt{\frac{k_{VI}}{k_{IIIa}}} = 4.8 \times 10^4 \text{ mole} \cdot \text{sec} \cdot \text{l}^{-1} \tag{13}$$

and

$$\frac{1}{k_{II}} \frac{k_{VII}}{k_{IIa}} = 3.75 \times 10^6 \text{ mole} \cdot \text{sec} \cdot \text{l}^{-1} \tag{14}$$

From literature data [13–14] $k_{II}^{120} = 19.2\ 1 \cdot mole^{-1} \cdot sec^{-1}$ and thus:

$$k_{IIIa}^{120} = 2.26 \times 10^{-5}\ 1 \cdot mole^{-1} \cdot sec^{-1} \tag{15}$$

and

$$\left(\frac{k_{IIa}}{k_{VII}}\right)_{120} = 1.38 \times 10^{-8} \tag{16}$$

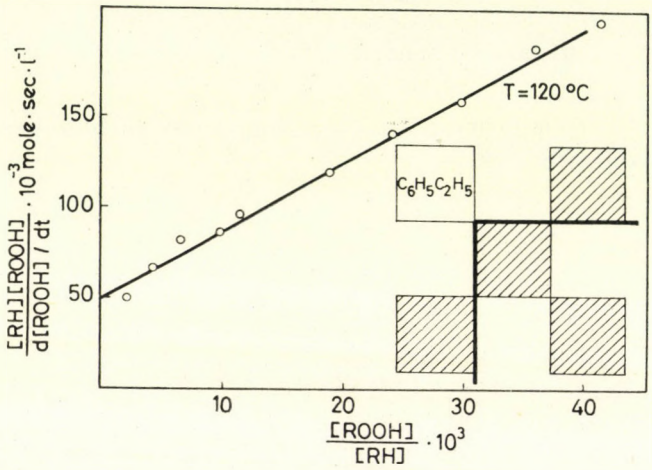

Fig. 4. [RH] [ROOH]/w as function of [ROOH]/[RH] at 120 °C in the oxidation of ethylbenzene

ALTES and BERG obtained an expression for the concentration of the peroxy radicals:

$$[RO_2^{\cdot}] = \frac{\frac{k_{IIa}}{k_{VII}}[RH]}{\sqrt{\frac{k_{VI}}{k_{IIIa}}\frac{1}{[ROOH]}\frac{k_{IIa}}{k_{VII}}[RH]} + 1} \tag{17}$$

At higher hydroperoxide concentrations the first term in the denominator can be neglected (compared to 1) and we obtain a constant value for the maximal concentration of peroxy radicals. At 120 °C:

$$[RO_2^{\cdot}]_{max} \sim \frac{k_{IIa}}{k_{VII}}[RH] = 1.12 \times 10^{-7}\ mole \cdot l^{-1} \geqslant [RO_2]_t \tag{18}$$

At very low hydroperoxide concentrations — *e.g.* 1.10^{-3} mole·l^{-1} — equation (17) yields a value of $7.88 \cdot 10^{-9}$ mole·l^{-1} (at this calculation, how-

ever, in (17) instead of branching (IIIa), (III) should be taken into consideration) and this value increases with increasing hydroperoxide concentration.

Accumulation of acetophenone is shown by Fig. 5.

The amounts of the ketone and of alcohol are very small under present conditions. At 90 °C after 40 hours $44 \cdot 10^{-3}$ mole·l^{-1} hydroperoxide, 1.10^{-3} mole·l^{-1} ketone and roughly the same amount of alcohol are formed. At

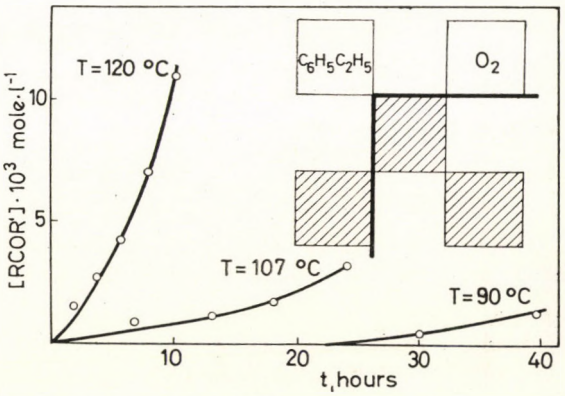

Fig. 5. Kinetics of the accumulation of acetophenone at different temperatures in the oxidation of ethylbenzene

107 °C the corresponding data are 117.10^{-3} mole·l^{-1} hydroperoxide, $1.8 \cdot 10^{-3}$ mole·l^{-1} acetophenone and $3 \cdot 10^{-3}$ mole·l^{-1} methyl phenyl carbinol. This shows that the decomposition of hydroperoxide compared to its formation can be neglected.

Decomposition of ethylbenzene hydroperoxide

(System B)

Experiments were carried out according to Procedure (II) at 50 atmosphere pressure and three different temperatures: 90, 105 and 120 °C. The consumption of hydroperoxide, the accumulation of acetophenone and the formation of methyl phenyl carbinol were measured.

The kinetics of hydroperoxide decomposition at three temperatures are shown in Fig. 6.

Since we used in present experiments ethylbenzene oxidized previously to different extent (at 90 °C) the initial hydroperoxide concentration varied and therefore it seemed more reasonable to plot our data as

$$\log \frac{[\mathrm{ROOH}]_t}{[\mathrm{ROOH}]_{t/T}} \quad vs. \quad t$$

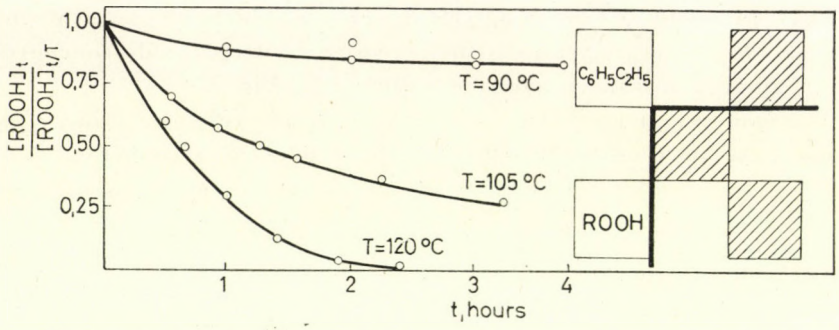

Fig. 6. Kinetics of hydroperoxide decomposition at different temperatures

where $[ROOH]_{t/T}$ means the hydroperoxide concentration at a time t when the reactor reached its working temperature T (usually within 10–15 minutes after the beginning of the experiment). This refers to other products, too.

The activation energy of the decomposition determined from the initial rates is 26.4 kcal/mole^{-1}.

The corresponding hydroperoxide concentrations at the beginning of the decomposition processes are rather high and thus both monomolecular and bimolecular reactions might be taken into account:

$$-\frac{d[ROOH]}{dt} \equiv w_{ROOH} = k[ROOH] + k'[ROOH]^2 \qquad (19)$$

Plotting $w_{ROOH}/[ROOH]$ against [ROOH] at 120 °C we obtain a straight line down to about $25 \cdot 10^{-3}$ mole·l^{-1} concentration (Fig. 7).

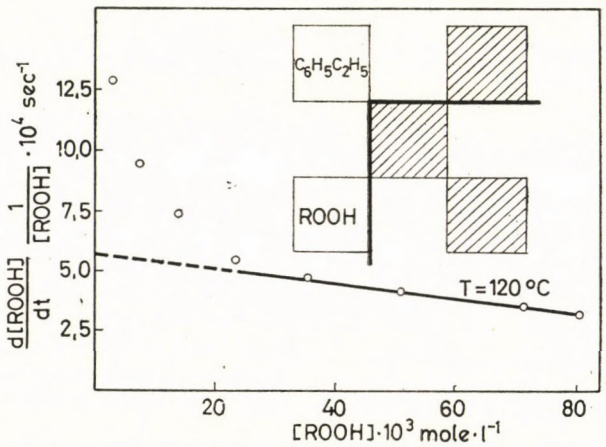

Fig. 7. $w/[ROOH]$ as function of [ROOH] in the decomposition of hydroperoxide in a metal reactor, at 120 °C

At very low hydroperoxide concentrations, however, a sharp deviation can be observed. From Fig. 7

$$k' = 3.15 \cdot 10^{-3} \ \mathrm{l \cdot mole^{-1}} \tag{20}$$

Though the reaction wall (metal surface) could exert a strong catalytic influence, the increase in the value of the rate constant compared to Eq. (15) seems too big and therefore in agreement with TWIGG [17, 19, 20] it should be assumed that due to the fast decomposition the radicals formed from hydroperoxide molecules may contribute to the decomposition, that is parallel to it an initiated decomposition occurs.

Thus further reactions should be added:

$$\mathrm{RO\cdot + ROOH \rightarrow ROH + RO_2} \tag{IIb}$$

$$\mathrm{R\cdot + ROOH \rightarrow ROH + RO\cdot} \tag{IIc}$$

$$\mathrm{\cdot OH + RH \rightarrow H_2O + R\cdot} \tag{IId}$$

including following terminations:

$$\mathrm{R\cdot + R\cdot \rightarrow products} \tag{IV}$$

$$\mathrm{R\cdot + RO_2^{\cdot} \rightarrow products} \tag{V}$$

Radicals formed in branching type IIIa and in propagation type IIb react also with hydroperoxides:

$$\mathrm{RO_2^{\cdot} + ROOH \rightarrow \cdot OH + ROOH + RCOR'} \tag{IIe}$$

From the above scheme a tractable equation cannot be derived and it seems more suitable to use data on acetophenone formation.

$$\frac{\mathrm{d\,[Acetophenone]}}{\mathrm{d}t} \equiv w_{\mathrm{Ac.}} = k_{\mathrm{IIe}}[\mathrm{RO_2^{\cdot}}]\,[\mathrm{ROOH}] + k_{\mathrm{VI}}[\mathrm{RO_2^{\cdot}}]^2 \tag{21}$$

or

$$[\mathrm{RO_2^{\cdot}}] = \frac{-k_{\mathrm{IIe}}[\mathrm{ROOH}] + \sqrt{k_{\mathrm{IIE}}^2[\mathrm{ROOH}]^2 + 4k_{\mathrm{VI}}w_{\mathrm{Ac.}}}}{2k_{\mathrm{VI}}} \tag{22}$$

To use Eq. (22) for the calculations we need the value of k_{IIe}. According to SKIBIDA, MAIZUS and EMANUEL [21] the ratios of the rate constants of reactions between peroxy radicals and ethylbenzene, ethylbenzene hydroperoxide, methyl phenyl carbinol, respectively, are 1 : 9.5 : 12 at 118 °C. Since the value we used for k_{II} at 120 °C was 19.2, for k_{IIe} $2 \cdot 10^2$ can be applied.

Table I

Time, min.	120 °C			105° C		
	[ROOH] mole · l^{-1}	w_{Ac} mole · l^{-1} $sec^{-1} \times 10^6$	[$RO_2^{\cdot}$] mole · $l^{-1} \times 10^7$	ROOH mole · $l^{-1} \times 10^3$	w_{Ac} mole · l^{-1} $sec^{-1} \times 10^6$	[$RO_2^{\cdot}$] mole · $l^{-1} \times 10^7$
15	90.5	5.5	2.4	65.2	2.7	2.2
30	70.5	9.0	4.0	56.5	4.1	3.1
45	50.5	12.0	5.6	48.7	5.2	3.8
60	35.3	8.3	4.9	43.2	5.2	3.9
75	23.5	5.4	4.2	39.3	3.7	3.2
90	14.1	3.5	3.5	35.3	2.7	2.8
105	7.6	2.1	2.9	32.6	2.1	2.4
120	3.5	1.5	2.0	29.8	1.5	2.0
150	—	—	—	25.1	0.8	1.4

Calculated peroxy radical concentrations are given in Table I.

The rate maxima of acetophenone formation supply an activation energy of 31 kcal/mole^{-1} and using the ratio of rate constants as mentioned above ($k_{IIe}/k_{II} \sim 10$), we obtain:

$$k_{IIe} \sim 2.3 \times 10^5 \, e^{-\frac{5600}{RT}} \tag{23}$$

The yield in acetophenone formation, that is the ratio:

$$\frac{\text{moles of acetophenone formed}}{\text{moles of hydroperoxide consumed}}$$

was also calculated and is given at three temperatures in Table II. It is interesting that this ratio increases with increasing temperatures and at given temperatures it increases with the conversion resulting in saturation.

This latter might be explained by an alcohol → ketone transition in the absence of oxygen eventually in a step:

$$ROH + RO_2^{\cdot} \rightarrow 2\,RO^{\cdot} + {}^{\cdot}OH \tag{IIb}$$

followed by the recombination of RO· radicals in the cage of the solvent. This assumption, naturally, is to be proved experimentally. In the laboratory of one of the authors (D.G.) experiments are in course in the presence of labelled methyl phenyl carbinol to study the alcohol → ketone transition in the pres-

Table II

Time, min.	90 °C $\frac{[RCOR'] - [RCOR']_0}{[RCOH]_0 - [ROOH]}$	105 °C $\frac{[RCOR'] - [RCOR']_0}{[ROOH]_0 - [ROOH]}$	120 °C $\frac{[RCOR'] - [RCOR']_0}{[ROOH]_0 - [ROOH[}$
30	0.24	0.34	
60	0.36	0.51	0.08
90	0.38	0.51	
120	0.37	0.51	0.15
150		0.51	
180		0.49	0.20
240			0.36
300			0.44
360			0.51
420			0.58
480			0.63

ence and in the absence of oxygen. Since the real possibility of such transitions would necessarily change Eq. (21) this latter should be conditionally used and only at very low conversions.

It was assumed that the wall of the metal reactor strongly influences the decomposition of the hydroperoxide molecules. To prove this, reactions were carried out in "fresh" reactor* at 120 °C. Fig. 8 shows the comparison between the two reactors. It can be seen that in unused vessel decomposition of hydroperoxide molecules proceeds slower under the same experimental conditions.

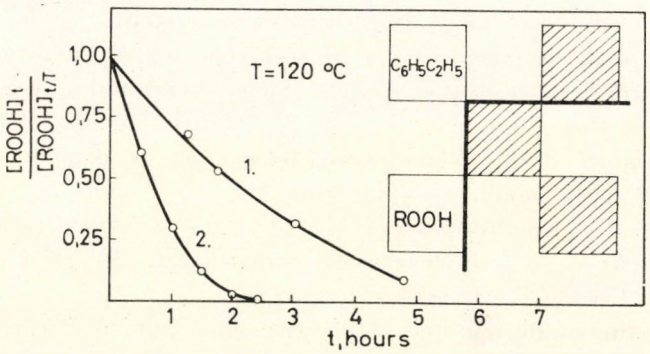

Fig. 8. Kinetics of hydroperoxide decomposition at 120 °C in different reactors: 1: aged metal reactor; 2: "fresh", unused metal reactor

*Authors wish to express thanks to M. BULIGIN performing this run.

Interaction between ethylbenzene, ethylbenzene hydroperoxide and propylene (System F)

Experiments were carried out according to Procedure (II) at 50 atmosphere pressure and three different temperatures. Propylene has been liquefied at low temperature and the liquid propylene added into the reactor containing the mixture of ethylbenzene and of ethylbenzene hydroperoxide previously also cooled down.

Before heating argon bubbled through the mixture prolonged during the whole process. The argon stream previously entered a metal vessel containing

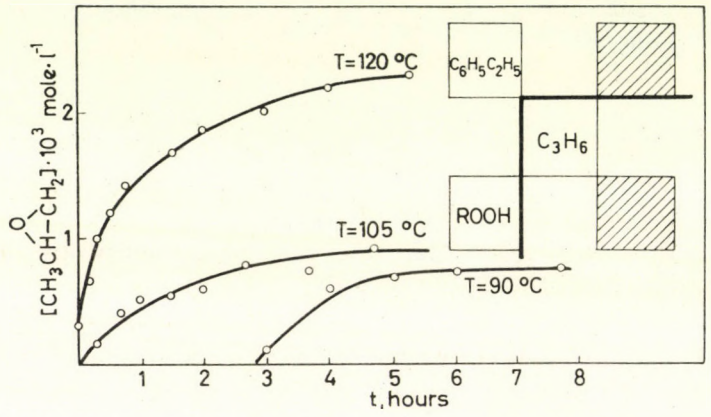

Fig. 9. Kinetics of the formation of propylene oxide at different temperatures

liquid propylene under pressure to maintain a constant propylene concentration in the reactor. Outlets of the reactor were cooled throughout the whole procedure to keep products of low boiling point in the system.

Changes in the concentrations of propylene oxide, hydroperoxide and acetophenone (in some cases that of methyl phenyl carbinol) have been followed in the course of the reaction.

The amounts of propylene oxide formed under present experimental conditions are very small, varying from 0.7×10^{-3} mole·l^{-1} to 2.2×10^{-3} mole·l^{-1} depending on the temperature.

Kinetic curves of propylene oxide formation at 90, 105 and 120 °C are given by Fig. 9.

Despite the small amounts of propylene oxide formed (presumably the consumption of the oxide can be neglected under present conditions and therefore instead of accumulation, formation could be determined), its concentration related to the hydroperoxide amounts consumed during the same time is essentially high. (See Table III.) The decomposition of the hydroperoxide mole-

Table III

T °C	$\frac{[PrO]}{mole \cdot l^{-1} \times 10^3}$	$\frac{[PrO]}{[ROOH]_0 - [ROOH]_{t/T}}$
90	0.77	0.05
105	0.87	0.11
120	2.10	0.21

cules very markedly decreases in the presence of propylene as shown in Fig. 10 (at 90 °C), Fig. 11 (at 105 °C) and Fig. 12 (at 120 °C). In these figures curves 1 refer to experiments in the absence of propylene while curves 2 to the same in its presence.

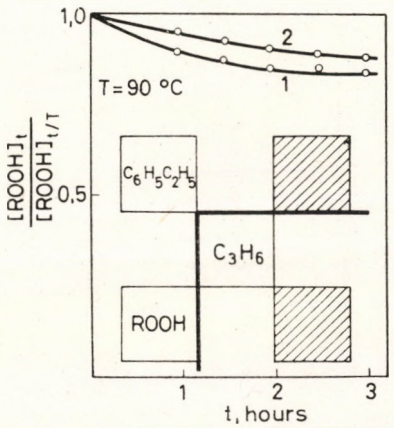

Fig. 10. Kinetics of hydroperoxide decomposition at 90 °C. 1: in the absence of propylene; 2: in the presence of propylene

With respect to the mechanism of propylene oxide formation several suggestions are to be found in the literature.

According to the "PRILEZHAEV-reaction" propylene reacts with peroxyacetic acid forming a π-complex and yielding epoxide by the decomposition of the latter [22]. This mechanism was affirmed also by SWERN [23]. Recently BLUMBERG and coworkers suggested the following complex [24–25]:

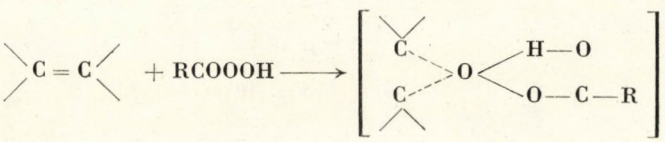

(24)

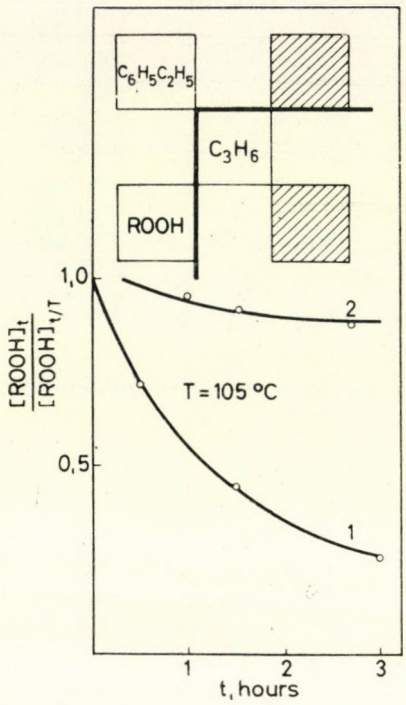

Fig. 11. The same as Fig. 10 at 105 °C

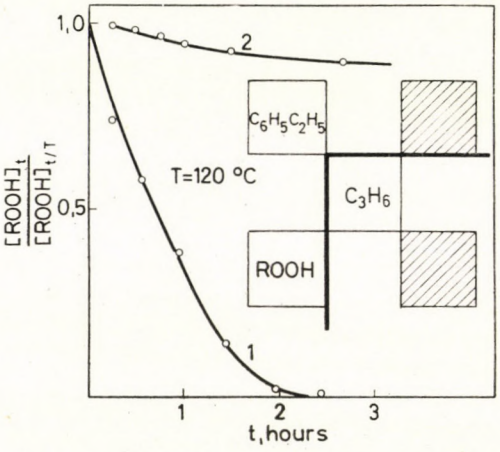

Fig. 12. The same as Fig. 10 at 120 °C

followed by its decomposition:

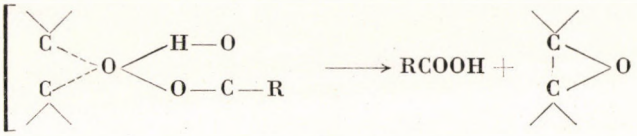

(25)

Several experimental facts can be explained, indeed, by this mechanism. Further studies are needed to explain chemically the second order rate expression for the complex formation with respect to propylene.

According to TWIGG and later to MAYO peroxy radicals react with the unsaturated compound yielding epoxide [20, 26–27]:

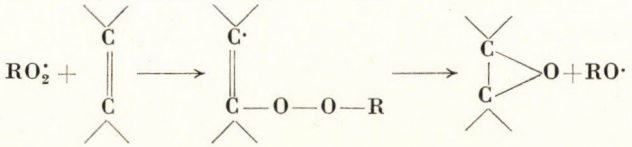

(IIf)

There are suggestions that hydroperoxide molecules decompose into ions and OH^+ formed react with the unsaturated compound. This, however, seems unlikely, due to energetic factors in nonpolar solvents.

In principle there is a possibility for the interaction of hydroperoxide molecules with unsaturated compounds [7]:

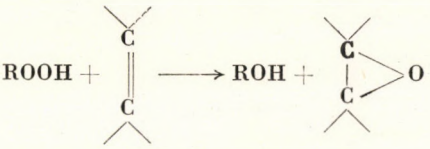

(26)

Under present conditions the probability of the peracetic acid reaction is presumably very low. Traces of acids were not found. (In the "HALCON-process" there is no acid formation being one of the most important advantages of this procedure avoiding thus the application of special non-corrosive materials of construction.)

The remarkable decrease in hydroperoxide decomposition in the presence of propylene due to the strong interaction between radicals and propylene and further the temperature independence of the decomposition suggest that the direct reaction (26) proceeds only in negligible extent if at all.

The most likely is under present conditions the radical mechanism suggested by TWIGG as a general class reaction and assumed also by LANDAU *et al.* in the "non-catalytic HALCON-process" [7]. That is:

$$\frac{\mathrm{d}\,[C_3H_6O]}{\mathrm{d}t} = w_{PrO} = k_{III}\,[RO_2^{\cdot}]\,[C_3H_6] \tag{27}$$

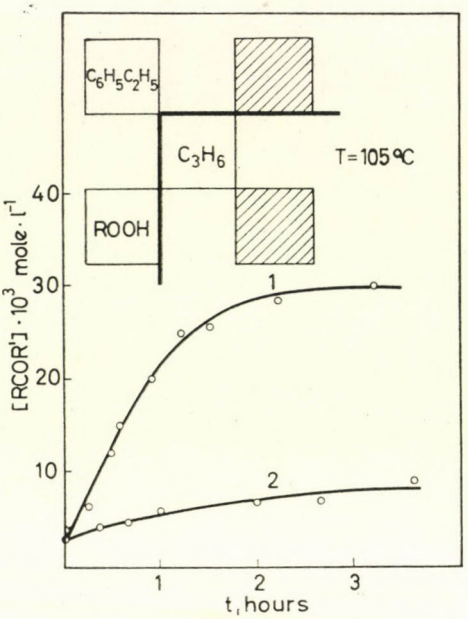

Fig. 13. Kinetics of acetophenone formation at 105 °C. 1: in the absence of propylene; 2: in the presence of propylene

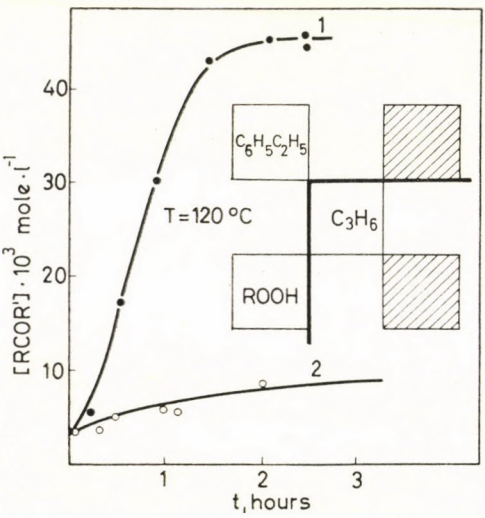

Fig. 14. The same as Fig. 13 at 120 °C

the necessary peroxy radicals can be formed both in reactions (IIIa) and (IIb) that is in decomposition (at higher concentrations) and initiated decomposition.

The corresponding ketone formation in the presence of propylene is shown in Figs 13 and 14.

Assuming that the alcohol–ketone transition can be neglected initially, the contribution of reactions (IIe) and (VI) changes very strongly from the beginning of the reaction. That is, in Eq. (21) the ratio of the two members decreases from a high initial value:

$$\frac{(w_{Ac})_{IIe}}{(w_{Ac})_{VI}} = \frac{k_{IIe}[RO_2^{\cdot}][ROOH]}{k_{VI}[RO_2^{\cdot}]^2} = \frac{2 \cdot 10^2 [RO_2^{\cdot}][ROOH]}{2 \cdot 10^7 [RO_2^{\cdot}]^2} \tag{28}$$

The initial value of this ratio is about 6.7. It seems reasonable to assume that the introduction of propylene capturing the free radicals would even more shift this value to higher ones and therefore in this case it can be written approximatively limiting the calculations for the initial stage of the process:

$$(w_{Ac})_{Pr} \sim k_{IIe}[RO_2^{\cdot}][ROOH] \tag{29}$$

referring thus to the ketone formation in the presence of propylene. Dividing (29) by (27):

$$\frac{(w_{Ac})_{Pr}}{w_{PrO}} \sim \frac{k_{IIe}[ROOH]}{k_{IIf}[C_3H_6]} \tag{30}$$

Substituting the corresponding data at 120 °C:

$$k_{IIf} \sim 1.2 \; l \times mole^{-1} \cdot sec^{-1} \tag{31}$$

The ratio (30) changes strongly also with the temperature, at 105 °C it has a value of 7.2 while at 120 °C of 3.0 implying a faster increase in the yield of epoxide with increasing temperature compared to the yield of ketone.

Table IV

T °C	Without propylene [ROH]/[RCOR']	With propylene [ROH]/[RCOR']
90	0.66	—
105	1.00	2.00
120	1.34	1.30

From this respect data referring to alcohol molecules would be of great importance. Unfortunately, only very few of them are available, shown in Table IV. As it can be seen from the Table, in the absence of propylene the

ratio of alcohol to ketone concentration increases with increasing temperature due presumably to the corresponding activation energy values. On the other hand, however, in the presence of propylene it decreases changing the temperature from 105° to 120 °C. Therefore we have assumed — similar to MAYO [27] in the case of styrene oxidation — that not only the peroxy radicals but also alkoxy radicals react with propylene forming a complex:

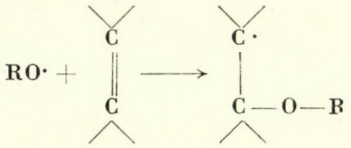

(31)

and thus lessening the formation of alcohol.

Oxidation of ethylbenzene and ethylbenzene hydroperoxide mixtures in the presence of propylene

(System I)

Experiments were carried out according to Procedure (II) at 50 atm. and 120 °C; instead of oxygen, however, compressed air was used to avoid explosion hazards.

Changes in the concentrations of hydroperoxide against reaction time are given in Fig. 15. The same for acetophenone is shown in Fig. 16.

For better comparison curves obtained in the absence of oxygen are also shown. (It should be emphasized, however, that data representing the system ethylbenzene + ethylbenzene hydroperoxide + oxygen can be used only for

Table V

Time, sec.	Without oxygen	With osygen
	[PrO] mole · l^{-1}	[PrO] mole · l^{-1}
30	1.00	0.38
60	1.48	0.48
90	1.80	0.80
120	2.04	1.38
150	2.14	2.08
180	2.18	2.90
210	2.18	3.75

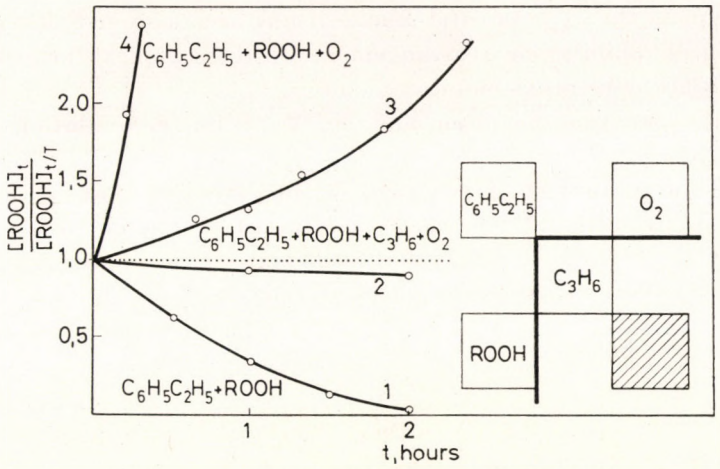

Fig. 15. Changes in the concentration of hydroperoxide at 120 °C. 1: system (B); 2: system (F); 3: system (I); 4: system (C)

qualitative comparison since these experiments were carried out in glass vessel.)

It is interesting that — unexpectedly — in the beginning of the reaction the formation of propylene oxide is smaller compared to reactions in the absence of oxygen. The concentration of hydroperoxide increases already from the start of the reaction.

The kinetics of propylene oxide formation in the absence of oxygen and in its presence are shown in Table V.

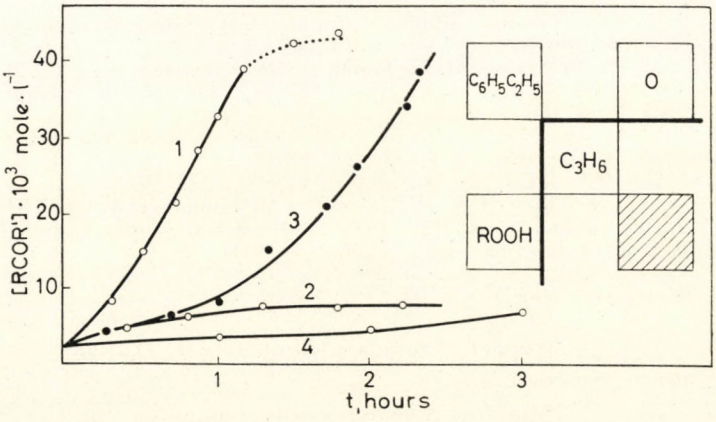

Fig. 16. The same as Fig. 15 with respect to acetophenone

To explain the experimental results it has been assumed that oxygen at high pressures inhibits the rearrangement of the complex formed between peroxy radicals and propylene into epoxide.

Similar suggestion has been made by MAYO for the oxidation of α-diisobutylene [28].

The inhibiting effect of oxygen is of such strength that — though propylene simultaneously inhibits the formation of acetophenone as it can be seen in Fig. 16 — the ratio of the formation rates of acetophenone to that of the propylene oxide at the beginning of the process is as high as:

$$\frac{(w_{Ac})_{PrO}}{w_{PrO}} = 37 \tag{32}$$

Due to our assumption according to which oxygen influences the formation of the epoxide, Eq. (27) cannot be used for the calculation of the corresponding rate constant in the presence of oxygen at high pressures.

REFERENCES

1. Halcon Int. Inc. Neth. Appl. 6, 402, 137; C.A.: **62,** 9106, (1965) (U.A. appl.: January 7, 1964)
2. LANOS, F., ALAGY, J.: Fr. pat. 1, 376, 471; C.A.: **62,** 7726 (1965)
3. Shawinigan Chem. Ltd.: Fr. pat. 1, 386, 354; C.A.: **62,** 1463 (1965)
4. MONSANTO Co.,: Fr. pat. 1 367 762; C.A.: **62,** 4007 (1965)
5. Halcon Int. Neth. Appl. 6, 500, 118: Belg. Pat. 657 838; C.A.: **64,** 2052 (1966)
6. Halcon Int. Inc., Neth. Appl. 6 515 037; C.A.: **65,** 15 321 (1966)
7. LANDAU, R., BROWN, D., RUSSEL, J. L.: 7th Congress Petrole, 1967, P.D. 18. p: 141
8. BLUMBERG, E. A., VALOV, P. I., NORIKOV, YU. D.: Compt. rend. USSR **167,** 579 (1966)
9. European Chem. News. p. 38. Nov. 18, **1966**
10. EMANUEL, N. M., DENISOV, E. T., MAIZUS, Z. K.: Oxidation Chain Reactions of Hydrocarbons in Liquid-Phase. Moscow, 1965. "Nauka", in Russian
11. KNORRE, D. G., MAIZUS, Z. K., EMANUEL, N. M.: Compt. rend. USSR **99,** 415 (1945)
12. VALENDO, A. YA., NORIKOV, YU. D.: Izv. Acad. Sci. USSR **2,** 275 (1969)
13. CEPALOV, V. F., SLYAPINTOKH, V. YA.: Kinetics and Catalysis **3,** 870 (1962)
14. SEMENOV, N. N.: Problems of Chemical Kinetics and Reactivity (Moscow, 1958)
15. ALTES, F. W. K., VAN DEN BERG, P. J.: Rec. Trav. Chim. **85,** 538 (1966)
16. JUNGERS, J. C. et al.: Cinétique Chimique Appliqués, 614, Editions Technique. Paris (1957)
17. TWIGG, G. H.: Disc. Farad. Soc. No 14, 240 **1953**
18. FORDHAM, J. W. L., WILLIAMS, H. L.: Canad. J. Res. **278,** 943 (1949)
19. TWIGG, G. H., GODIN, G. W., BAILEY, H. C., HELDEN, J.: Erdöl und Kohle **15,** 76 (1962)
20. TWIGG, G. H.: Chem. Ind. 4, **1962**
21. SKIBIDA, I. P., MAIZUS, Z. K., EMANUEL, N. M.: Nephtechimia **4,** 82 (1963)
22. PRILEZHAEV, N. A.: Zh. R. F. H. O. **42,** 1387 (1910)
23. SWERN, D.: J. Amer. Chem. Soc. **69,** 1962 (1947)
24. BLUMBERG, E. A., BULIGIN, M. G., EMANUEL, N. M.: Compt. rend. USSR **166,** 353 (1966)
25. VALOV, P. I., BLUMBERG, E. A., FILIPPOVA, T. V.: Kinetics and Catalysis **8,** 760 (1967)
26. TWIGG, G. H.: Chem. Eng. Sci. Spec. Suppl. **3,** 5 (1954)
27. MAYO, F. E.: J. Amer. Chem. Soc. **80,** 2465 (1958)
28. MAYO, F. E.: J. Amer. Chem. Soc. **80,** 2497 (1958)

Dezső GÁL; Szeged, Aradi Vértanúk tere 1, Hungary.

E. A. BLUMBERG
A. Ya. VALENDO
N. M. EMANUEL
} Moscow, Vorobyevskoye chaussée 2b, U.S.S.R.

Acta Chimica Academiae Scientiarum Hungaricae, Tomus 66 (1), pp. 77–85 (1970)

SYNTHETISCHE LINEARE POLYMERE, XXIX*

ZUSAMMENHANG ZWISCHEN DEM SPEZIFISCHEN DREHVERMÖGEN UND DEM MOLEKULARGEWICHT BEI MONOTONEN OLIGOPEPTIDEN

I. GÉCZY

(Zentralforschungslaboratorium für Koloristik, Budapest)

Eingegangen am 20. Mai 1969

In polymerhomologen Reihen monotoner Polypeptide ist der durch Verfasser für Oligosaccharide früher [12] gefundene Zusammenhang zwischen dem spezifischen Drehvermögen der einzelnen Glieder und dem Molekulargewicht gültig:

$$[\alpha]_A^t = \frac{a}{M} + b$$

wobei

$[\alpha]_A^t$ = das spezifische Drehvermögen,
M = das Molekulargewicht,
a und b = Konstanten von denen erstere implizite die Endgruppen, letztere explizite die Zwischenglieder charakterisiert.

Liegt das untersuchte Oligopeptid in der Lösung in helikaler Form vor, so zeigt sich eine Abweichung von der Gleichung. Diese Abweichung macht es also möglich, die Sekundärstruktur von monotonen Oligopeptiden zu bestimmen. Aufgrund der Konstante b wurde das Inkrement des molaren Drehvermögens für einige monotone Oligopeptide in verschiedenen Lösungsmitteln angegeben. Untersuchungen mit Poly-γ-Benzyl-L-Glutamat zeigten, daß infolge des engen Zusammenhanges zwischen dem Drehvermögen und dem Dipolmoment die Sekundärstruktur wahrscheinlich auch mit Messungen des spezifischen Dipolmomentquadrates bestimmt werden kann.

Einleitung

Die optisch-aktiven Polymere bilden ein verhältnismäßig neues, hochinteressantes Gebiet der Polymerchemie.

In den letzten Jahren brachte die Forschung den optisch-aktiven Polymeren erhöhtes Interesse entgegen. Der Grund hierfür ist einerseits darin zu suchen, daß die Erforschung der Sekundärstruktur von Proteinen und Nukleinsäuren in Lösung von hervorragender Bedeutung ist und andererseits in den Erfolgen auf dem Gebiet der stereospezifischen Polymerisation. Die Forschungsarbeiten auf dem Gebiete optisch-aktiver Polymere sind zum Teil ausgedrückt präparativer, während die theoretischen Arbeiten im allgemeinen dadurch gekennzeichnet, daß die erhaltenen Ergebnisse — wegen der unzweckmäßigen

* Synthetische lineare Polymere XXVIII: Acta Chim. Acad. Sci. Hung. *57*, 345 (1968)

Wahl der untersuchten Parameter bzw. wegen ihrer Kompliziertheit — kaum oder nur sehr schwierig nutzbar sind.

So kann z. B. aufgrund der bisherigen Untersuchungen über das Drehvermögen von monotonen Polypeptiden folgende Aussage gemacht werden: Ist das untersuchte Polypeptid statistisch in Form von Knäueln in der Lösung vorhanden (dies ist der Fall in Lösungsmitteln, welche fähig sind, die Wasserstoffbrücken zu spalten), so kann die Rotationsdispersion des Drehvermögens schon mit der sogenannten einfachen oder eingliedrigen DRUDE-Gleichung [1] beschrieben werden:

$$[\alpha]_\Lambda = \frac{A_0}{\Lambda^2 - \Lambda_0^2}, \tag{1}$$

wobei

Λ = Wellenlänge, mμ
$[\alpha]_\Lambda$ = das zur Wellenlänge Λ gehörende spezifische Drehvermögen,
A_0 = Rotationskonstante,
Λ_0 = Dispersionskonstante.

Die Zahlenwerte der Konstanten werden nach YANG und DOTY [2] in folgender Weise bestimmt: Gl. (1) wird linearisiert

$$[\alpha]_\Lambda \Lambda^2 = A_0 + \Lambda_0^2 [\alpha]_\Lambda \tag{2}$$

und die Konstanten durch die graphische Darstellung von $[\alpha]_\Lambda \Lambda^2$ als Funktion von $[\alpha]_\Lambda$ erhalten, wobei der Achsenabschnitt der Geraden den Zahlenwert von A_0, ihre Richtungstangente den Zahlenwert von Λ_0^2 angibt.

Die Polypeptide liegen aber in der Mehrzahl der Fälle in den angewendeten Lösungsmitteln in helikaler Form vor. In diesem Fall können die Verhältnisse nach MOFFIT und YANG [3] beschrieben werden:

$$[M]_\Lambda^0 \equiv \frac{3}{n^2+2} \cdot \frac{M_0}{100} [\alpha]_\Lambda = \frac{a_0 \Lambda_0^2}{\Lambda^2 - \Lambda_0^2} + \frac{b_0 \Lambda_0^4}{(\Lambda^2 - \Lambda_0^2)^2}, \tag{3}$$

wobei

$[M]_\Lambda^0$ = das molare Drehvermögen des Polypeptids bei der Wellenlänge Λ, im Vakuum,
n = Brechungsindex des Lösungsmittels,
M_0 = das Molekulargewicht der sich wiederholenden Einheit,
a_0, b_0, Λ_0 = Konstanten.

Der Wert der Konstante a_0 ist von den sich wiederholenden Einheiten abhängig, während b_0 und Λ_0 von der Natur der vorliegenden Helices abhängig

sind. b_0 ist das Maß des sogenannten Helixgehaltes. Der Zahlenwert von b_0 wird aus den Versuchsergebnissen erhalten, indem die Größe $[M]^0_\Lambda(\Lambda^2-\Lambda_0^2)$ als Funktion von $1/(\Lambda^2-\Lambda_0^2)$ dargestellt wird. Der Wert von b_0 kann aus der Richtungstangente der erhaltenen Geraden berechnet werden. Auf diese Weise läßt sich der Helixgehalt in Abhängigkeit von den Versuchsbedingungen (Lösungsmittel, pH, Temperatur usw.) bestimmen [4, 5].

Solche Untersuchungen wurden von GOODMAN und Mitarbeiter [6–9] mit Oligopeptiden durchgeführt und es wurde festgestellt, daß eine Helixbildung bei Oligo-L-Glutaminsäure-γ-Methylestern in Dichloressigsäure, bzw. in Dimethylformamid schon bei dem Heptamer, während bei Oligo-L-Asparaginsäure-β-Methylester in Chloroform erst bei dem Undekamer auftritt. Die letztere Verbindung ist in Dimethylformamid bzw. in Dichloressigsäure statistisch in Form von Knäueln zugegen.

Auch die Kenntnis dessen, in welchem Maße die einzelnen sich wiederholenden Einheiten zum Endwert des Drehvermögens in den verschiedenen Lösungsmitteln beitragen, ist sehr wichtig. Diese Werte können aufgrund der zur Zeit zu Verfügung stehenden Verfahren nur ziemlich schwierig bestimmt werden.

In einer früheren Mitteilung [12] wurde gezeigt, daß bei Oligosacchariden zwischen dem spezifischen Drehvermögen und dem Molekulargewicht der folgende einfache Zusammenhang besteht:

$$[\alpha]^t_\Lambda = \frac{a}{M} + b \tag{4}$$

wobei

$[\alpha]^t_\Lambda$ = spezifisches Drehvermögen bei der Wellenlänge Λ,
M = Molekulargewicht,
a und b = Konstanten, wobei a implizite die Endgruppen, b explizite die Kettenglieder charakterisiert.

Gl. (4) ist im wesentlichen eine spezielle Form der bereits früher abgeleiteten und angewandten Gleichung [13–21]:

$$\varphi_{sp} = \frac{a}{M} + b \tag{5}$$

wobei φ_{sp} irgendeine aus additiver Größe ableitbare spezifische Eigenschaft ist, während die sonstigen Bezeichnungen die mit den im Text schon vorgekommenen identisch sind. Es wurde gezeigt [10, 11, 14, 15, 20], daß folgende Form der Konstante b in Gl. (5):

$$b = \frac{\varphi_k}{M_k}, \tag{6}$$

wobei φ_k die molare Eigenschaft des Kettengliedes und M_k dessen Molekulargewicht ist, zur Berechnung der molaren Bindungs- bzw. Atominkremente der in der sich wiederholenden Einheit vorhandenen Atome verwendet werden kann. Demgemäß wurden die Zahlenwerte von einigen in der Literatur bisher nicht angeführten Inkrementen angegeben [11,14–17, 22].

Eigene Untersuchungen

In der vorliegenden Arbeit wurde versucht, die Gültigkeit von Gl. (4) auch auf polymerhomologe Reihen von monotonen Oligopeptiden auszudehnen. Die experimentellen Angaben für das Drehvermögen wurden aus der Literatur entnommen. Es wurden nur jene Angaben verwendet, wo in bezug auf eine polymerhomologe Reihe das spezifische Drehvermögen von mindestens drei Gliedern zu Verfügung stand. Es soll vorausgeschickt werden, daß in der Literatur nur spärliche Angaben dieser Art aufzufinden waren. Die untersuchten

Tabelle I

Untersuchte monotone Oligopeptide

Nr.	Benennung	Sich wiederholende Einheit	Molekulargewicht des Zwischengliedes	Literaturzitat
I.	Poly-L-Alanin	$-(NH-\overset{*}{C}H-CO)_n-$ $\quad\quad\quad

monotonen Oligopeptide, zusammen mit der betreffenden Literaturquelle, sind in Tabelle I zusammengefaßt.

In Abb. 1–6 sind die experimentellen Werte des spezifischen Drehvermögens als Funktion des Reziprokwertes des Molekulargewichtes für verschie-

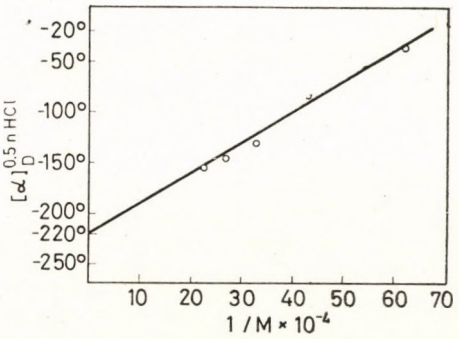

Abb. 1. Spezifisches Drehvermögen von linearen Oligo-L-Alaninen als Funktion des Reziprokwertes des Molekulargewichtes

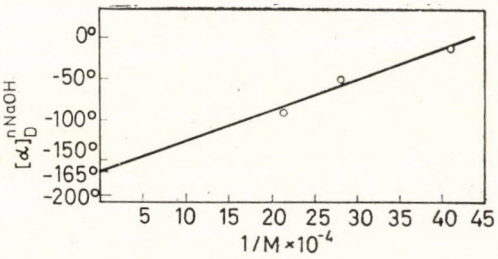

Abb. 2. Spezifisches Drehvermögen von Oligo-L-Leucinen als Funktion des Reziprokwertes des Molekulargewichtes

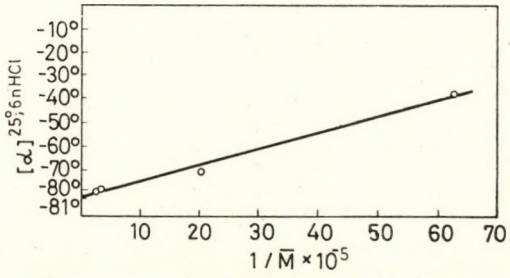

Abb. 3. Spezifisches Drehvermögen von Oligo-ε-Carbo-Benzoxy-Lysinen als Funktion des Reziprokwertes des Molekulargewichtes

dene monotone Oligopeptide dargestellt. Aus den Achsenabschnitten der Kurven wurden die Konstanten b bestimmt und aufgrund von Gl. (6) die Inkremente des molaren Drehvermögens für die verschiedenen sich wiederholenden Einheiten berechnet. Die Ergebnisse sind in Tabelle II zusammengefaßt.

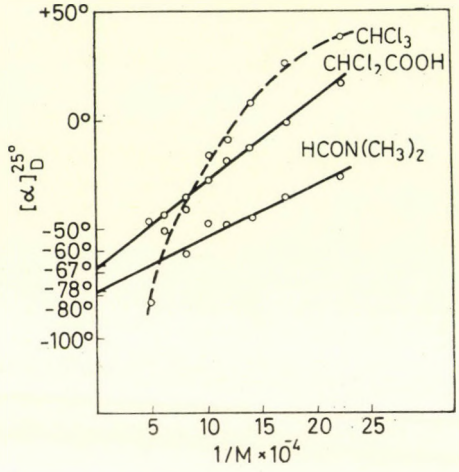

Abb. 4. Spezifisches Drehvermögen von Oligo-β-Methyl-L-Aspartaten als Funktion des Reziprokwertes des Molekulargewichtes, in verschiedenen Lösungsmitteln

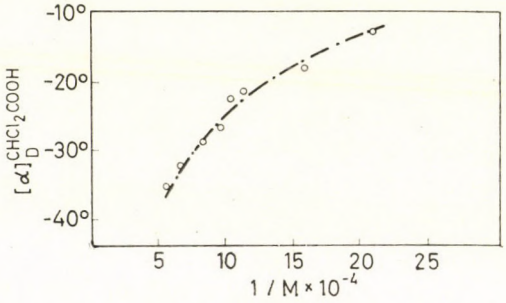

Abb. 5. Spezifisches Drehvermögen von Oligo-L-γ-Methyl-Glutamaten als Funktion des Reziprokwertes des Molekulargewichtes

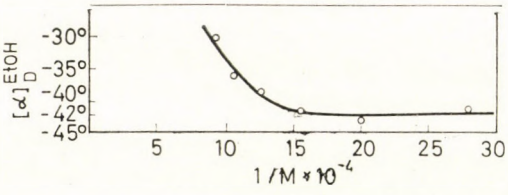

Abb. 6. Spezifisches Drehvermögen von Acetyl-L-iso-Buthyl-Äthylen-Urethan-Oligomeren als Funktion des Reziprokwertes des Molekulargewichtes

Tabelle II

Molares Inkrement des Drehvermögens der sich wiederholenden Einheit der verschiedenen monotonen Oligopeptide, aufgrund von Gl. (6) berechnet

Nr.	Zahlenwert der Konstate b in Gl. (4)	$[M_0]_D$	Lösungsmittel	Temperatur, °C
I.	−220	−156,4	0,5 *n* HCl	23–25
II.	−165	−176,9	1 *n* NaOH	20–23
IV.	− 67	− 86,5	$CHCl_2COOH$	25
IV.	− 78	−100,7	$HCON(CH_3)_2$	25
VI.	− 81	−212.5	6 *n* HCl	25

Diskussion der Ergebnisse

In Abb. 1–4 ergeben die zu Verfügung stehenden experimentellen Punkte in guter Näherung Geraden. Folglich beschreibt Gl. (5) bzw. ihre spezielle Form, d. h. Gl. (4), die Abhängigkeit des spezifischen Drehvermögens der einzelnen Glieder vom Reziprokwert des Molekulargewichtes in polymerhomologen Reihen von monotonen Oligopeptiden recht gut. In diesen Fällen ist das monotone Oligopeptid statistisch vermutlich in Form von Knäueln anwesend. Liegt jedoch das monotone Oligopeptid im untersuchten Lösungsmittel in helikaler Form vor (siehe auch die betreffenden Ergebnisse von GOODMAN und Mitarbeitern [6–9]), so zeigt sich — oberhalb einer bestimmten Molekülgröße — eine wesentliche Abweichung von dem in Gl. (4) enthaltenen linearen Zusammenhang (Kurve bezüglich Chloroform in Abb. 4, sowie Abb. 5 und 6). Gl. (4) bietet also den einfachsten Zusammenhang für das Drehvermögen monotoner Oligopeptide und zugleich eine Möglichkeit zur schnellen Orientierung über die sekundäre Struktur dieser Verbindungen in verschiedenen Lösungsmitteln. Hinsichtlich der Konstanten in Gl. (4) sind offensichtlich alle Zusammenhänge gültig, welche bezüglich der Konstanten in Gl. (5) bereits in den früheren Untersuchungen [13–22] festgestellt wurden. Aus dem Wert von b in Gl. (4) bzw. aus dem Achsenabschnitt der einzelnen Geraden kann der Grenzwert des spezifischen Drehvermögens der sich wiederholenden Einheit bzw. das Inkrement des molaren Drehvermögens bestimmt werden, wie aus Tab. II ersichtlich ist. Dieses Verfahren ist selbstverständlich nicht anwendbar, wenn das Oligopeptid in helikaler Form vorliegt. Gerade aus dieser Tatsache kann dann auf die helikale Form geschlossen werden. Da eine enge Beziehung zwischen dem Wert des Drehvermögens und dem Dipolmoment des Moleküls besteht [27], kann aufgrund des Gesagten erwartet werden, daß bei der Anwendung von Gl. (5) zur Berechnung des spezifischen Dipolmomentquadrates $\left(\frac{\bar{\mu}^2}{M}\right)$ [20] für monotone

Oligopeptide in bestimmten Fällen eine ähnliche Abweichung vom linearen Zusammenhang auftritt. Diese Annahme scheint auch durch die Tatsache unterstützt zu sein, daß das spezifische Dipolmomentquadrat von Poly-γ-Benzyl-L-Glutamat, als Funktion des Reziprokwertes des durchschnittlichen Molekular-

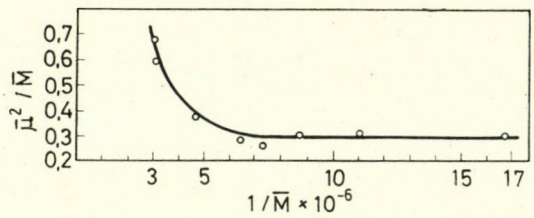

Abb. 7. Spezifisches Dipolmomentquadrat von Poly-γ-Benzyl-L-Glutamaten als Funktion des Reziprokwertes des durchschnittlichen Molekulargewichtes

gewichtes dargestellt, ebenfalls eine Abweichung vom linearen Zusammenhang aufweist (Abb. 7). (Die Dipolmomentangaben stammen aus den Messungen von TSWETKOW und Mitarbeitern in Dichloräthan [28].) Die Anwendung von Gl. (5) auf das Dipolmoment kann also ebenfalls zur Klärung der Sekundärstruktur in dem gegebenen Lösungsmittel verwendet werden, obwohl dies meßtechnisch ziemlich umständlich ist.

LITERATUR

1. DRUDE, P.: Lehrbuch der Optik, S. Hirzel Verlag, Leipzig, 1906
2. YANG, J. T., DOTY, P.: J. Amer. Chem. Soc. **79,** 761 (1957)
3. MOFFIT, W., YANG, J. T.: Proc. Nat. Acad. Sci. U.S. **42,** 596 (1956)
4. GRATZER, W. B., DOTY, P.: J. Amer. Chem. Soc. **85,** 1193 (1963)
5. MOFFIT, W.: J. Chem. Phys. **25,** 467 (1956)
6. GOODMAN, M., SCHMIDT, E. E., YPHANTIS, D. A.: J. Amer. Chem. Soc. **84,** 1283, 1288, 1296 (1962)
7. GOODMAN, M., LISTOWSKY, J., MASUDA, J., BOARDMAN, F.: Biopolymers **1,** 33 (1963)
8. GOODMAN, M., BOARDMAN, F.: J. Amer. Chem. Soc. **85,** 2483 (1963)
9. GOODMAN, M., FELIX, A. M., DEVER, C. M.: Biopolymers **1,** 371 (1963)
10. GÉCZY, I.: Magy. Kém. Foly. **71,** 551 (1965); Polym. Reviews **2,** 556 (1966); J. Polym. Sci. (C), **16,** 2991 (1967)
11. GÉCZY, I.: Magy. Kém. Foly. **72,** 299 (1966); Acta Chim. Acad. Sci. Hung. **51,** 313 (1967)
12. GÉCZY, I.: Kolorisztikai Ért. **8,** 221 (1966); Cellulose Chem. & Techn. **4,** 245 (1970).
13. GÉCZY, I.: Acta Chim. Acad. Sci. Hung. **34,** 323 (1962); Magy. Kém. Foly. **69,** 312 (1963)
14. GÉCZY, I.: Acta Chim. Acad. Sci. Hung. **37,** 435 (1963); Magy. Kém. Foly. **69,** 333 (1963)
15. GÉCZY, I.: Magy. Kém. Foly. **70,** 91 (1964); Vysokomol. Soed. **7,** 642 (1965)
16. GÉCZY, I.: Magy. Kém. Foly. **70,** 99 (1964); Chemische Gesellschaft **11,** 86 (1964); Koll. Z. Polymere **201,** 99 (1965)
17. GÉCZY, I.: Magy. Kém. Foly. **70,** 156 (1964); Makromol. Chem. **90,** 161 (1966)
18. GÉCZY, I.: Magy. Kém. Foly. **70,** 242 (1964); Plaste u. Kautschuk **13,** 11 (1966)
19. GÉCZY, I.: Magy. Kém. Foly. **70,** 244 (1964); Shurn. Prikl. Khim. **40,** 348 (1967)
20. GÉCZY, I.: Magy. Kém. Foly. **71,** 216 (1965); Acta Chim. Acad. Sci. Hung. **45,** 131 (1965)
21. GÉCZY, I.: Kolorisztikai Ért. **8,** 14 (1966); Faserforsch. u. Textiltechn. **17,** 470 (1966)
22. GÉCZY, I.: MTA Kém. Tud. Oszt. Közl. **23,** 285 (1965)

23. BRAND, E., ERLANGER, B. F., SACHS, H.: J. Amer. Chem. Soc. **74**, 1849 (1952)
24. BRANDRUP, I., IMMERGUT, E. H., ELIAS, H. G.: Polymer Handbook 1966. Kap. VII.—47
25. IWAKURA, J., HAYASHI, K., IWATA, K.: Makromol. Chem. **93**, 274 (1966)
26. BECHER, R. R., STAHLMANN, M. A.: J. Amer. Chem. Soc. **74**, 40 (1952)
27. MASON, S. F.: Quarterly Reviews **17**, No. 1, 20 (1963)
28. TSWETKOW, V. N., STENNIKOWA, I. N., RYUMTSEW, E. I., SKASKA, V. S.: Vysokomol. Soed. **7**, 1112 (1965)
29. IWAKURA, J., HAYASHI, K., IWATA, K.: Makromol. Chem. **108**, 296 (1967)

István GÉCZY; Budapest, 62, Pf 182.

Acta Chimica Academiae Scientiarum Hungaricae, Tomus 66 (1), pp. 87–98 (1970)

THE EXTREME VALUES OF FORCE CONSTANTS AND MEAN VIBRATIONAL AMPLITUDES OF ETHYLENE-TYPE MOLECULES, II

C_2F_4, C_2Cl_4, C_2Br_4

G. FOGARASI

(Department of General and Inorganic Chemistry, Eötvös Loránd University of Sciences, Budapest)

Received 30 May, 1969

Applying the parameter method proposed by Török and Pulay on molecules C_2F_4, C_2Cl_4 and C_2Br_4, a large number of series of mean vibrational amplitudes and force constants, reproducing normal frequencies, has been calculated, and their extreme values have been investigated. By the aid of determining extreme values some information can be obtained on bonding relations even in the case when the unambiguous determination of force constants is impossible. The calculated and measured vibrational amplitudes differ considerably very probably due to inaccuracies in electron diffraction measurements.

Introduction

The parameter method suggested by TÖRÖK and PULAY [2, 3, 4] provides the general solution of the inverse eigenvalue problem in a tractable form. By the aid of a computer program, using this method the force constant matrices that reproduce the experimental normal frequencies can be systematically constructed, furthermore mean vibrational amplitudes can be calculated. In order to study the efficiency of this method, investigations on ethylene and ethylene-d_4 molecules were reported in our previous paper [1]; this paper deals with the results of similar investigations on the halogen derivatives. The normal coordinate analysis of these molecules has been carried out by several authors [6, 7, 8].

We aimed to establish that if only normal frequencies are known, as experimental data, *i.e.* force constants cannot be unambiguously determined, what informations can be obtained on chemical bond relations by determining the possible minimum and maximum values of force constants, and, on the other hand, to what extent are mean vibrational amplitudes, as additional experimental data, suitable for fixing the force field more accurately.

Experimental data

Molecular geometry taken from literature, as well as normal frequencies of the compounds studied are listed in Tables I and II. It should be noted

Table I

Geometrical data (ref. [10])

Molecule	C=C (Å)	C—X (Å)	∢ XCX
C_2F_4	1.27	1.33	110°
C_2Cl_4	1.32	1.72	113.5°
C_2Br_4	1.32	1.90	114°

that after beginning our calculations more recent measurements have been published on the molecular geometry of the corresponding compounds [11, 12]. The slight differences in the data, however, do not alter our results substantially.

Calculations

The choice of the symmetry coordinates and the way of the calculations are quite similar to those applied in our previous paper. The parameter method has also been briefly reviewed in that paper. In the $F = G^{-1/2}\, U\Lambda U^T G^{-1/2}$ equation, by which force constants are calculated, the order of the elements of Λ matrix, built up from experimental eigenvalues, *i.e.* the starting assignment is defined in Table II.

Table II

In-plane normal frequencies of the C_2X_4 *molecules* (cm^{-1}). (Ref. [6])

	Assignation	C_2F_4	C_2Cl_4	C_2Br_4
A_g	S_2 (C=C str.)	1872	1571	1535
	S_1 (C—X str.)	778	447	265
	S_3 (CCX bend.)	394	235	144
B_{1g}	S_1 (C—X str.)	1340	1000	880
	S_2 (CCX bend.)	551	347	208
B_{2u}	S_1 (C—X str.)	1337	908	766
	S_2 (CCX bend.)	218	176	119
B_{3u}	S_1 (C—X str.)	1186	777	635
	S_2 (CCX bend.)	558	310	188

Only planar vibrations have been investigated.

Results

Force constants

The total "map" of the force constant sets reproducing normal frequencies is not given here. A part of the calculations concerning species A_g, in connection with the results on vibrational amplitudes, is listed in Tables VII, VIII and IX.

According to our experiences force constants may possess substantially different values even within a relatively narrow parameter interval. Therefore instead of fixing force constants more or less arbitrarily, their extreme values were calculated. In Table III, the minimum values of F_{11} (C—X stretching) and F_{33} (CCX bending) force constants of species A_g are listed, taking into account the whole parameter range. It can be seen that the results, even in themselves, supply some information on the force field, because they limit the minimum at non-evident values, on the other hand their trend in the molecule series reflects

Table III

Minimum values of F_{11} and F_{33} (species A_g)

	F_{11} C—X str. (mdyn Å^{-1})	F_{33} CCX bend. (mdyn Å)
C_2F_4	5.6	3.0
C_2Cl_4	3.6	3.4
C_2Br_4	2.8	3.5

fairly well the variation of bonding relations. The strengths of C—X bond, as it can be expected, decreases in the order F, Cl, Br while the increase of the CCX bending force constant runs parallel with the increase of van der Waals radii.

Nevertheless, the information obtained by using only the condition of reproducing the normal frequencies is, obviously, rather poor; this is indicated also by the fact that the C=C stretching force constant, which is particularly interesting from the point of view of bonding relations, remains quite uncertain. Therefore, the possible ranges of diagonal force constants have been investigated applying some restrictions defined below. The ranges, fixed for certain force constants have been chosen as broad as they should contain the true values by all means, *i.e.* the generality of the solution should not be practically restricted. We have prescribed the following limits:

$$|F_{12}| \leq 2, \quad |F_{13}| \leq 2, \quad |F_{23}| \leq 2$$

$$F_{22}\,(\text{C—X str.}) \geq 9, \quad F_{33}\,(\text{CCX bend.}) \leq 4$$

Under such conditions the possible ranges of force constants become considerably narrower, as it can be seen from the data of Table IV, where the results obtained previously for C_2H_4 and C_2D_4 are also listed. The variation of the range of the F_{22} (C=C stretching) force constant indicates the bond strengths of C=C bonds being decreased in the order: F, H, Cl, Br. The variation of the force constants published in the literature shows the same trend, and our results are also supported by the most recent bond lengths measurements [11, 12]:

Compound	C_2F_4	C_2H_4	C_2Cl_4	C_2Br_4
$R_{C=C}$ (Å)	1.313	1.337	1.354	1.362

Table IV

Constrained maximum and minimum values of the A_g force constants*

			C_2F_4	C_2H_4	C_2D_4	C_2Cl_4	C_2Br_4
F_{11} C–X str.	(mdyn Å^{-1})	min.	6.3	6.0	5.8	4.0	3.2
		max.	10.3	6.8	6.9	4.2	3.7
		ref.	7.28[b]	6.78[a]	6.78[a]	4.27[b]	3.33[b]
F_{22} C=C str.	(mdyn Å^{-1})	min.	9.0	9.0	9.0	9.0	9.0
		max.	13.0	11.7	11.6	11.5	10.7
		ref.	12.85[b]	10.76[a]	10.76[a]	9.35[b]	8.65[b]
F_{33} C=C–X bend.	(mdyn Å)	min.	3.0	1.2	1.3	3.4	3.3
		max.	4.0	1.6	1.6	4.0	4.0
		ref.	3.04[b]	1.40[a]	1.40[a]	3.46[b]	3.61[b]

* See in text. [a] ref. [9], [b] ref. [7]

Table V

Force constants defined by the minimum value of F_{22}

		F_{11} C–X str. (mdyn Å^{-1})		F_{12} str.-bend. (mdyn)		F_{22} C=C–X bend. (mdyn Å)	
B_{1g}	C_2F_4	8.68	(6.34)	1.28	(0.38)	0.73	(0.87)
	C_2Cl_4	5.84	(3.43)	1.03	(0.56)	0.60	(0.77)
	C_2Br_4	5.28	(2.70)	0.90	(0.46)	0.45	(0.66)
B_{2u}	C_2F_4	6.50	(6.41)	0.25	(0.82)	0.66	(0.71)
	C_2Cl_4	3.46	(3.44)	0.40	(0.47)	1.43	(1.39)
	C_2Br_4	2.85	(2.80)	0.56	(0.50)	1.74	(1.72)
B_{3u}	C_2F_4	8.52	(7.28)	−1.56	(−0.17)	3.02	(3.12)
	C_2Cl_4	5.35	(4.28)	−1.39	(−0.19)	2.38	(2.54)
	C_2Br_4	4.61	(3.43)	−1.27	(−0.17)	2.08	(2.36)

In brackets the data of ref. [7] (calculated by a simplified valence force field)

On the basis of the studies on the two-dimensional species we have concluded that in the case of ethylene quite acceptable results can be obtained if the force constants are calculated at the minimum value of F_{22} bending force constant. (Similar calculations have been done by STREY [5] on other molecules.) As it is clear, this method qualitatively results in the fact that bending symmetry coordinate S_2 is assigned with great weight to the lower frequency, *i.e.* in the case of strongly mixed vibrations its applicability is more or less limited. Consequently, the data listed in Table V are numerically less reliable as they were in the case of ethylene; however, as it is supported by the data taken from literature, they seem to be applicable for comparing the values obtained within a series of compounds.

Vibrational amplitudes

A part of the "map" of the mean vibrational amplitudes that reproduce normal frequencies is shown in Tables VII–IX. In these results the contribution of the two-dimensional species is also included, the parameters (and through them force constants), however, have been varied only with species A_g. The fixed force constants of the two-dimensional species are listed in Table VI. The origin of the mapping carried out in species A_g (*i.e.* the 0,0,0 parameter set) is an F matrix that is in the neighbourhood of the data taken from literature, and has been obtained from our calculations, where frequencies were exactly reproduced.

The conclusions drawn in connection with ethylene and ethylene-d_4 molecules are supported by the obtained results. The calculated vibrational amplitudes, even within a broad parameter range, cannot be fitted to the experimental ones, although parameters outside this range yield completely unreal force constant values. It is only the case of C_2Cl_4 molecule where satisfactory

Table VI

Force constants used for calculation of the mean square amplitudes

		C_2F_4	C_2Cl_4	C_2Br_4
B_{1g}	F_{11}	6.121	3.652	3.021
	F_{12}	0.651	0.591	0.480
	F_{22}	0.838	0.761	0.609
B_{2u}	F_{11}	5.766	3.362	2.848
	F_{12}	−0.683	0.232	0.566
	F_{22}	0.864	1.434	1.742
B_{3u}	F_{11}	7.094	4.137	3.318
	F_{12}	−0.498	−0.478	−0.443
	F_{22}	3.318	2.674	2.458

Table VII

A_g force constants and mean square amplitudes of vibrations

Parameters			F_{11}	F_{12}	F_{13}	F_{22}
		−0.1	9.638	−0.875	−0.462	4.282
−0.1	−0.1	0.0	10.007	0.423	0.744	4.709
		0.1	9.974	1.643	2.119	5.568
		−0.1	8.040	−2.263	−3.280	9.282
−0.1	0.0	0.0	8.854	−1.161	−2.166	9.349
		0.1	9.292	−0.054	−0.739	9.794
		−0.1	6.733	−2.254	−4.731	16.653
−0.1	0.1	0.0	7.798	−1.652	−4.014	16.231
		0.1	8.563	−0.983	−2.912	16.028
		−0.1	6.643	−0.048	−1.052	5.200
0.0	−0.1	0.0	7.110	1.166	−0.264	5.821
		0.1	7.264	2.358	0.756	6.891
		−0.1	5.923	0.029	−2.650	11.116
0.0	0.0	0.0	6.622	1.051	−1.719	11.625
		0.1	6.994	2.052	−0.497	12.464
		−0.1	5.614	1.369	−2.883	19.330
0.0	0.1	0.0	6.353	1.892	−2.111	19.565
		0.1	6.799	2.376	−1.061	19.911
		−0.1	5.698	1.499	−2.871	6.045
0.1	−0.1	0.0	6.431	2.855	−2.269	6.992
		0.1	6.874	4.230	−1.325	8.429
		−0.1	5.936	3.038	−3.200	12.535
0.1	0.0	0.0	6.681	4.228	−2.221	13.625
		0.1	7.078	5.353	−0.927	15.037
		−0.1	6.600	5.633	−2.167	21.181
0.1	0.1	0.0	7.168	6.344	−1.107	22.222
		0.1	7.378	6.895	0.168	23.322

* Experimental values of the mean square amplitudes [13].

(10^{-2} Å), C_2F_4 molecule

F_{23}	F_{33}	C=C	C—F	C..F	F..F *cis*	F..F *trans*	F..F *gem.*
−0.266	6.410	4.76	4.27	6.27	10.36	5.98	5.32
−0.597	5.632	4.65	4.26	6.12	10.29	5.70	5.48
−0.358	5.424	4.54	4.28	5.97	10.17	5.47	5.73
2.086	5.204	4.14	4.35	5.99	10.46	6.12	5.29
1.578	3.878	4.12	4.30	5.88	10.39	5.82	5.44
1.632	3.162	4.10	4.28	5.77	10.26	5.56	5.68
7.933	8.268	4.20	4.51	5.75	10.47	6.79	5.27
7.329	6.791	4.27	4.42	5.68	10.40	5.89	5.38
7.110	5.767	4.35	4.35	5.63	10.28	5.62	5.60
−1.458	8.045	4.55	4.35	6.20	10.39	6.07	5.34
−1.847	7.029	4.50	4.34	6.07	10.32	5.79	5.48
−1.675	6.474	4.44	4.36	5.93	10.19	5.54	5.72
0.665	5.143	3.94	4.43	5.90	10.47	6.15	5.33
0.459	3.891	3.92	4.38	5.80	10.39	5.86	5.48
0.799	3.218	3.91	4.35	5.70	10.26	5.59	5.72
6.443	6.587	4.05	4.58	5.64	10.46	6.17	5.32
6.485	5.501	4.10	4.48	5.58	10.39	5.88	5.45
6.885	4.912	4.13	4.41	5.53	10.26	5.61	5.68
−2.783	10.181	4.51	4.43	6.14	10.41	6.13	5.31
−3.233	8.668	4.52	4.42	6.02	10.34	5.84	5.44
−3.072	7.567	4.51	4.44	5.89	10.21	5.58	5.67
−1.036	5.715	3.95	4.52	5.82	10.47	6.16	5.32
−0.956	4.281	3.95	4.46	5.73	10.40	5.86	5.47
−0.283	3.452	3.94	4.43	5.64	10.27	5.60	5.71
4.404	5.486	4.12	4.64	5.56	10.45	6.12	5.33
5.061	4.534	4.12	4.55	5.50	10.37	5.83	5.48
6.123	4.183	4.11	4.47	5.46	10.24	5.57	5.72
		—*	5.6*	9.5*	9.0*	11.4*	8.7*

Table VIII

A_g force constants and mean

Parameters			F_{11}	F_{12}	F_{13}	F_{22}
		−0.1	6.731	−0.372	1.373	2.430
−0.1	−0.1	0.0	6.709	0.481	2.515	2.667
		0.1	6.399	1.226	3.613	3.151
		−0.1	5.575	−1.874	−2.410	7.006
−0.1	0.0	0.0	5.993	−1.173	−1.257	6.813
		0.1	6.123	−0.485	0.068	6.859
		−0.1	4.647	−2.138	−4.395	14.686
−0.1	0.1	0.0	5.323	−1.977	−3.834	13.871
		0.1	5.790	−1.734	−2.959	13.168
		−0.1	3.947	0.559	−0.694	3.414
0.0	−0.1	0.0	4.163	1.353	−0.150	3.876
		0.1	4.195	2.111	0.497	4.603
		−0.1	3.755	1.050	−1.785	9.303
0.0	0.0	0.0	4.074	1.652	−0.916	9.642
		0.1	4.172	2.203	0.098	10.150
		−0.1	3.872	2.610	−1.063	18.213
0.0	0.1	0.0	4.115	2.627	−0.472	18.200
		0.1	4.174	2.580	0.230	18.142
		−0.1	4.488	2.571	−4.447	4.515
0.1	−0.1	0.0	5.132	3.650	−3.964	5.422
		0.1	5.569	4.726	−3.166	6.646
		−0.1	5.335	5.038	−2.835	11.354
0.1	0.0	0.0	5.747	5.909	−1.714	12.456
		0.1	5.874	6.649	−0.413	13.704
		−0.1	6.425	8.323	0.602	21.029
0.1	0.1	0.0	6.424	8.583	1.759	22.057
		0.1	6.138	8.600	2.886	22.951

* Experimental values of the mean square amplitudes [11].

square amplitudes of vibrations (10^{-2} Å), C_2Cl_4 molecule

F_{23}	F_{33}	C=C	C—Cl	C..Cl	Cl..Cl *cis*	Cl..Cl *trans*	Cl..Cl *gem.*
−0.553	8.031	5.58	4.68	6.64	10.02	6.33	6.02
−0.603	8.206	5.48	4.70	6.45	9.88	5.99	6.26
−0.253	8.999	5.35	4.76	6.25	9.67	5.75	6.60
2.257	4.682	4.53	4.76	6.17	10.13	6.44	5.99
1.770	3.763	4.52	4.71	6.04	9.99	6.08	6.23
1.752	3.412	4.52	4.69	5.94	9.77	5.80	6.57
11.112	12.136	5.10	4.99	5.85	10.11	6.48	5.95
10.204	10.405	5.22	4.87	5.81	9.97	6.12	6.16
9.519	9.099	5.32	4.77	5.81	9.76	5.84	6.48
−2.207	10.888	5.26	4.81	6.49	10.06	6.43	6.01
−2.403	10.296	5.27	4.82	6.32	9.92	6.08	6.24
−2.197	10.108	5.25	4.89	6.14	9.71	5.82	6.56
0.731	4.686	4.24	4.90	5.99	10.13	6.47	6.02
0.747	3.742	4.24	4.84	5.87	9.99	6.11	6.26
1.163	3.451	4.24	4.82	5.77	9.77	5.83	6.59
9.929	9.129	4.89	5.11	5.66	10.08	6.44	6.01
10.143	8.482	5.00	4.98	5.63	9.94	6.09	6.24
10.488	8.279	4.99	4.88	5.62	9.73	5.83	6.57
−4.109	14.302	5.34	4.95	6.37	10.09	6.47	5.95
−4.369	12.472	5.46	4.96	6.24	9.95	6.11	6.16
−4.111	11.026	5.56	5.03	6.08	9.74	5.83	6.47
−1.273	5.332	4.50	5.05	5.85	10.13	6.44	5.99
−0.687	4.078	4.50	4.98	5.76	9.99	6.08	6.23
0.382	3.566	4.51	4.97	5.67	9.77	5.81	6.56
7.819	6.777	5.30	5.24	5.53	10.05	6.35	6.02
9.207	6.747	5.20	5.10	5.50	9.91	6.01	6.26
10.776	7.370	5.09	5.00	5.49	9.69	5.76	6.60
		—*	4.8*	5.8*	9.6*	6.4*	6.4*

Table IX

A_g force constants and mean square amplitudes of*

Parameters			F_{11}	F_{12}	F_{13}	F_{22}
		−0.1	10.614	0.191	4.522	1.183
−0.1	−0.1	0.0	10.189	1.074	6.211	1.378
		0.1	9.401	1.761	7.634	1.755
		−0.1	7.430	−3.976	−4.784	6.357
−0.1	0.0	0.0	7.998	−3.231	−3.394	5.741
		0.1	8.241	−2.445	−1.735	5.395
		−0.1	4.952	−5.165	−9.027	18.958
−0.1	0.1	0.0	6.053	−5.387	−9.277	17.180
		0.1	7.018	−5.358	−8.943	15.486
		−0.1	3.664	0.148	1.399	1.722
0.0	−0.1	0.0	3.641	0.734	1.483	2.027
		0.1	3.524	1.309	1.599	2.555
		−0.1	2.935	0.266	−1.724	9.217
0.0	0.0	0.0	3.220	0.725	−1.035	9.437
		0.1	3.342	1.164	−0.190	9.797
		−0.1	3.122	3.144	0.181	24.111
0.0	0.1	0.0	3.258	2.638	0.136	23.834
		0.1	3.307	2.082	0.151	23.343
		−0.1	3.997	2.097	−6.647	2.658
0.1	−0.1	0.0	4.894	3.204	−6.887	3.527
		0.1	5.676	4.414	−6.587	4.758
		−0.1	5.903	6.505	−3.550	11.971
0.1	0.0	0.0	6.421	7.529	−2.278	13.494
		0.1	6.642	8.398	−0.757	15.146
		−0.1	8.605	13.272	4.536	28.377
0.1	0.1	0.0	8.286	13.362	5.987	30.075
		0.1	7.639	13.034	7.177	31.410

* Dimensions: F_{11}, F_{12}, F_{22} — mdyn/Å; F_{13}, F_{23} — mdyn; F_{33} — mdynÅ
** Experimental values of the mean square amplitudes [12].

vibrations (10^{-2} Å), C_2Br_4 *molecule*

F_{23}	F_{33}	C=C	C—Br	C..Br	Br..Br *cis*	Br..Br *trans*	Br..Br *gem.*
0.669	9.965	7.09	4.73	7.46	10.13	6.69	6.29
0.880	11.354	6.84	4.77	7.19	9.99	6.31	6.52
1.412	13.435	6.55	4.84	6.92	9.77	6.03	6.87
4.566	7.119	5.15	4.87	6.61	10.24	6.82	6.25
3.469	5.166	5.14	4.80	6.45	10.10	6.42	6.47
2.838	4.041	5.16	4.76	6.34	9.87	6.10	6.81
22.820	31.140	6.70	5.35	6.16	10.19	6.87	6.22
20.592	27.798	7.00	5.19	6.18	10.07	6.47	6.40
18.372	24.303	7.25	5.03	6.25	9.85	6.14	6.71
−1.490	17.355	6.31	4.92	7.16	10.16	6.80	6.30
−1.857	17.255	6.28	4.96	6.94	10.03	6.42	6.51
−1.967	17.203	6.19	5.05	6.70	9.81	6.11	6.84
1.838	5.039	4.29	5.08	6.24	10.24	6.86	6.30
1.764	4.010	4.29	5.00	6.11	10.11	6.45	6.51
2.035	3.570	4.29	4.95	6.01	9.88	6.13	6.85
19.969	20.205	6.36	5.54	5.80	10.17	6.83	6.29
20.323	20.206	6.45	5.35	5.82	10.03	6.43	6.49
20.478	20.195	6.49	5.18	5.88	9.81	6.13	6.82
−4.613	27.440	6.46	5.18	6.96	10.19	6.86	6.24
−5.522	24.267	6.65	5.22	6.80	10.06	6.46	6.43
−5.924	21.009	6.79	5.32	6.60	9.84	6.14	6.75
−2.213	6.159	4.87	5.36	6.03	10.24	6.83	6.27
−1.250	4.480	4.86	5.26	5.93	10.10	6.43	6.49
0.266	3.641	4.86	5.22	5.83	9.88	6.11	6.83
14.942	11.802	6.95	5.77	5.62	10.13	6.73	6.29
17.838	13.552	6.81	5.56	5.63	10.00	6.34	6.52
80.716	15.953	6.62	5.39	5.66	9.78	6.05	6.86
		—**	4.3**	4.5**	10.7**	7.0**	7.4**

agreement has been found. This fact is remarkable because vibrational amplitudes are generally regarded as additional experimental data besides normal frequencies by which force constants can be more exactly determined. According to our results, this procedure requires a thorough consideration of the reliability of electron diffraction data.

REFERENCES

1. Fogarasi, G., Mezey, P.: Acta Chim. Acad. Sci. Hung. (to be published)
2. Pulay, P., Török, F.: Acta Chim. Acad. Sci. Hung. **44,** 287 (1965)
3. Török, F., Pulay, P.: J. Mol. Struct. **3,** 1 (1969)
4. Török, F.: Acta Chim. Acad. Sci. Hung. (to be published)
5. Strey, G.: J. Mol. Spectry. **26,** 87 (1967)
6. Mann, D. E., Fano, L., Meal, J. H., Shimanouchi, T.: J. Chem. Phys. **27,** 52 (1957)
7. de Alti, G., Galasso, V., Costa, G.: Spectrochim. Acta **21,** 649 (1965)
8. Klochkovskii, Yu. V., Kukina, V. S., Sverdlov, L. M.: Zh. Fiz. Khim. **39,** 1912 (1965)
9. Cyvin, B. N., Cyvin, S. J.: Acta Chem. Scand. **17,** 1831 (1963)
10. Sutton, L. E.: Interatomic Distances, The Chem. Soc. London, 1965
11. Strand, T. G.: Acta Chem. Scand. **21,** 2111 (1967)
12. Strand, T. G.: Acta Chem. Scand. **21,** 1033 (1967)
13. Karle, I. D., Karle, J.: J. Chem. Phys. **18,** 963 (1950)

Géza Fogarasi; Budapest VIII., Múzeum krt. 6–8.

Acta Chimica Academiae Scientiarum Hungaricae, Tomus 66 (1), pp. 99–113 (1970)

RELATIONSHIP BETWEEN INVERSION AND INTERNAL ROTATION OF METHYLAMINE, II

THE HAMILTON OPERATOR AND THE ELEMENTS OF THE HAMILTON MATRIX

L. SZTRAKA

(Department of Physical Chemistry, Technical University, Budapest)

Received October 1, 1969

In the present paper the Hamilton operator of the over-all rotation, internal rotation and inversion motion of the methylamine molecule has been derived, and the elements of the Hamilton matrix were given. It was shown that the theory expounded in this paper provides a more exact and more unified description of the phenomena.

I. Introduction

In a previous paper the classical Hamiltonian describing the over-all rotation, internal rotation and inversion motion of the methylamine molecule has been derived [1]. Formerly, however, an important problem, that of the normal coordinate of inversion had to be solved. This problem is the key to the appropriate treatment of the inversion phenomenon of methylamine.

The present concept of inversion is basically different from those of ITOH [2], and TSUBOI *et al.* [3]. (Their method is dealt with in details in Appendix I.) The wagging motion of the amino-group and the simultaneous internal rotation are treated as an entity, and it is taken into account in the construction of the normal coordinate of the inversion in the following way [1]:

$$Q_I = L_{21}\alpha + iL_{22}\tau \tag{1}$$

where the matrix elements L_{21} and L_{22} are constants independent of τ. Angle α measures the rotation of the methyl group relative to the symmetry plane of the amino-group, while angle τ gives the distance of the plane of the amino-group from the direction of the CN bond.

By the application of the appropriate normal coordinate it is achieved that the classical vibrational kinetical energy of the molecule is split into two parts according to the two types of motion. One part is due to internal rotation, while the other to the combination of the amino-wagging and a simultaneous internal rotation. This combined motion will be called inversion. The classification used up till now results in the fact that the part of the inversion kinetical energy that comes from the rotation of the methyl group appears together with

the kinetical energy of the internal rotation. The contradiction arising from this incorrect classification, which is found among the experimental and calculated data of internal rotation, has been noted by the Japanese authors too, who have tried to eliminate this contradiction in an empirical way [4].

The new classification scheme applied in the present paper introduces two new unknowns, ε and $\left\{\frac{d\alpha}{d\tau}\right\}$ in the Hamiltonian derived. In the following paper these unknowns will be determined together with the potential barriers of inversion and internal rotation. The purpose of the present paper is the derivation of the Hamilton operator and the elements of the Hamilton matrix from the following Hamiltonian [1]:

$$H = \frac{1}{4}\left\{\frac{1}{A} + \frac{B}{B^2+D^2}\right\}(P_x^2 + P_y^2) + \frac{1}{2}\left\{\frac{B+C}{BC-D^2} - \frac{B}{B^2+D^2}\right\}P_z^2 +$$
$$+ \frac{1}{2}\,\frac{BC-D^2}{B[Cf-F^2]-D^2 f}\,P_\alpha^2 + \frac{1}{2}\,\frac{A}{Am-k^2}\,P_\tau^2 + V(\alpha,\tau) +$$
$$+ \frac{1}{4}\left\{\frac{1}{A} - \frac{B}{B^2+D^2}\right\}\{(P_x^2 - P_y^2)\cos 2\varrho\alpha + (P_xP_y + P_xP_y)\sin 2\varrho\alpha\} +$$
$$+ \frac{1}{2}\,\frac{D}{B^2+D^2}\{(P_yP_z + P_zP_y)\cos\varrho\alpha - (P_xP_z + P_zP_x)\sin\varrho\alpha\} \qquad (2)$$

where f and m contain ε and $\left\{\frac{d\alpha}{d\tau}\right\}$ in the following fashion:

$$f = F(1 - \cos^2\varepsilon)$$

$$m = F\cdot\cos^2\varepsilon\left\{\frac{\mathrm{d}\alpha}{\mathrm{d}\tau}\right\}^2 + G$$

and

$$\varrho = \frac{f(B^2+D^2)^{1/2}}{BC-D^2}$$

II. The Hamilton operator

The general method for obtaining the rotational-vibrational Hamilton operator from the classical Hamiltonian was given by WILSON and HOWARD [6, 7] using the results of PODOLSKY [5]. The expressions given by the above authors can be applied also when the elements of the inertial tensor are functions of the normal coordinates. In the present case the tensor elements depend only on the parameter τ.

Let us write the form (1) of the Hamiltonian in the following short form:

$$H = \frac{1}{2} P^+ \mu P + V(\alpha, \tau) \tag{3}$$

where

$$P^+ = \{P_x, P_y, P_z, P_\alpha, P_\tau\} \tag{4}$$

is the row vector of the angular momentum, and the five-dimensional symmetrical tensor μ has the following elements

$$\begin{aligned}
\mu_{xx} &= \frac{1}{2}\left\{\frac{1}{A} + \frac{B}{B^2+D^2} + \left(\frac{1}{A} - \frac{B}{B^2+D^2}\right)\cos 2\varrho\alpha\right\} \\
\mu_{xy} &= \frac{1}{2}\left\{\frac{1}{A} - \frac{B}{B^2+D^2}\right\}\sin 2\varrho\alpha \\
\mu_{xz} &= -\frac{D}{B^2+D^2}\sin\varrho\alpha \\
\mu_{yy} &= \frac{1}{2}\left\{\frac{1}{A} + \frac{B}{B^2+D^2} - \left(\frac{1}{A} - \frac{B}{B^2+D^2}\right)\cos 2\varrho\alpha\right\} \\
\mu_{yz} &= \frac{D}{B^2+D^2}\cos\varrho\alpha \\
\mu_{zz} &= \frac{B+C}{BC-D^2} - \frac{B}{B^2+D^2} \\
\mu_{\alpha\alpha} &= \frac{BC-D^2}{B[Cf-F^2]-D^2 f} \\
\mu_{\tau\tau} &= \frac{A}{Am-k^2}
\end{aligned} \tag{5}$$

The rest of the elements are zero.

According to WILSON and HOWARD the following operator corresponds in quantum mechanics to the classical expression (3):

$$\hat{H} = \frac{1}{2}\sum_i \sum_j \mu^{1/4}\hat{P}_i \mu^{-1/4}\mu_{ij}\mu^{-1/4}\hat{P}_j\mu^{1/4} + V(\alpha,\tau) \tag{6}$$

where $i,j = x,y,z,\alpha,\tau$ and μ is the determinant of matrix μ. The expression of the angular momentum operators $\hat{P}_\alpha$, $\hat{P}_\tau$ is the following, according to the indices: $-i\hbar\dfrac{\partial}{\partial\alpha}$ and $-i\hbar\dfrac{\partial}{\partial\tau}$

The expression for μ is:

$$\mu = \frac{1}{4}\,\frac{1}{A(B^2+D^2)}\left\{\frac{B(B+C)}{BC-D^2} - \frac{D(B-D)}{B^2+C^2}\right\}\times \\ \times \frac{BC-D^2}{B[Cf-F^2]-D^2 f}\,\frac{A}{Am-k^2} \tag{7}$$

Applying the transformation proposed by MAYER and GÜNTHARD [8] for expression (6) we obtain:

$$\hat{H} = \frac{1}{2}\sum_i \sum_j \left\{\hat{P}_i - \frac{i}{4}\hbar\,\frac{\partial \ln \mu}{\partial x_i}\right\}\mu_{ij}\left\{\hat{P}_j + \frac{i}{4}\hbar\,\frac{\partial \ln \mu}{\partial x_j}\right\} + V(\alpha,\tau) \tag{8}$$

where x_i, $x_j = \alpha$, τ.

Since $\ln \mu$ depends only on coordinate τ, all derivatives are zero, except for the derivative according to τ. On the basis of similar considerations all the matrix elements, except for $\mu_{\tau\tau}$, can be taken out. Accordingly, the simplified operator $\hat{H}$ can be grouped into the following four parts:

$$\hat{H}_R = \frac{1}{4}\left\{\frac{1}{A} + \frac{B}{B^2+D^2}\right\}\left(\hat{P}_x^2 + \hat{P}_y^2\right) + \frac{1}{2}\left\{\frac{B+C}{BC-D^2} - \frac{B}{B^2+D^2}\right\}\hat{P}_z^2 \tag{9}$$

Expression (9) is the Hamilton operator of a symmetric top.

The following expression corresponds to the remaining Coriolis interaction arising from the small asymmetry of the molecule [9]. (In equilibrium the value of the asymmetry parameter is $\varkappa_0 = 0.8968$)

$$\hat{H}_c = \frac{1}{4}\left\{\frac{1}{A} - \frac{B}{B^2+D^2}\right\}\left\{\left(\hat{P}_x^2 - \hat{P}_y^2\right)\cos 2\varrho\alpha + \left(\hat{P}_x\hat{P}_y + \hat{P}_y\hat{P}_x\right)\sin 2\varrho\alpha\right\} + \\ + \frac{1}{2}\,\frac{D}{B^2+D^2}\left\{\left(\hat{P}_y\hat{P}_z + \hat{P}_z\hat{P}_y\right)\cos\varrho\alpha - \left(\hat{P}_x\hat{P}_z + \hat{P}_z\hat{P}_x\right)\sin\varrho\alpha\right\} \tag{10}$$

The rotational constants, as functions of τ, can be seen in Figs 1, 2, 3 and 4.

The operator of the large-amplitude internal motions is the following:

$$\hat{H}_{\mathrm{IM}} = \frac{1}{2}\,\mu_{\alpha\alpha}\,\hat{P}_\alpha^2 + \frac{1}{2}\,\mu_{\tau\tau}\,\hat{P}_\tau^2 + V(\alpha,\tau) \tag{11}$$

Figs 5 and 6 depict $\mu_{\alpha\alpha}$ and $\mu_{\tau\tau}$ as functions of τ when $\cos^2\varepsilon = 0$.

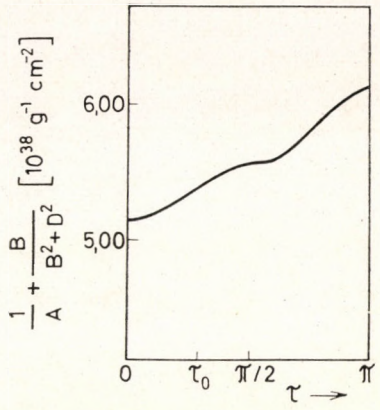

Fig. 1

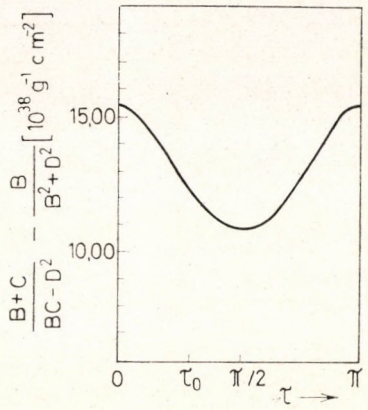

Fig. 2

The fourth term of small significance is given rise due to the dependence of $\mu_{\tau\tau}$ and $\ln \mu$ on τ.

$$\hat{H}' = -\frac{i}{2}\hbar\left\{\frac{\partial \mu_{\tau\tau}}{\partial \tau} + \frac{1}{4}\mu_{\tau\tau}\frac{\partial \ln \mu}{\partial \tau}\right\}\hat{P}_\tau + \\ + \frac{\hbar^2}{8}\left\{\frac{\partial \mu_{\tau\tau}}{\partial \tau}\frac{\partial \ln \mu}{\partial \tau} + \mu_{\tau\tau}\frac{\partial^2 \ln \mu}{\partial \tau^2} + \frac{1}{4}\mu_{\tau\tau}\left(\frac{\partial \ln \mu}{\partial \tau}\right)^2\right\} \qquad (12)$$

The $\ln \mu$ as function of τ when $\cos^2\varepsilon = 0$, can be seen in Fig. 7.

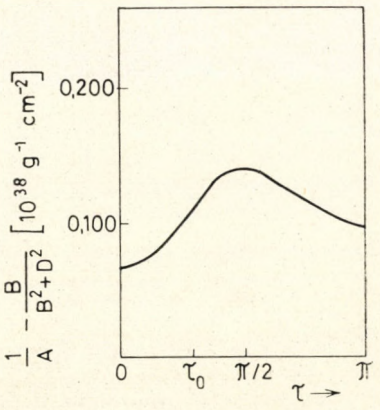

Fig. 3

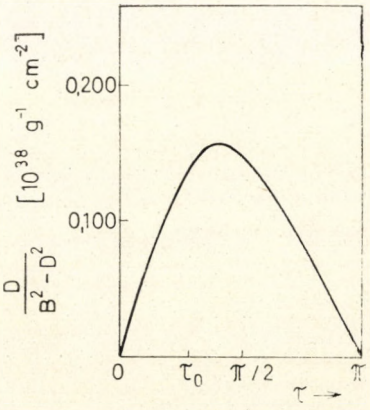

Fig. 4

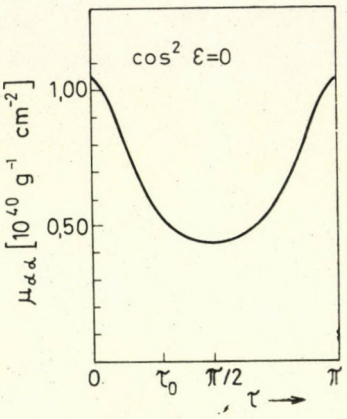

Fig. 5

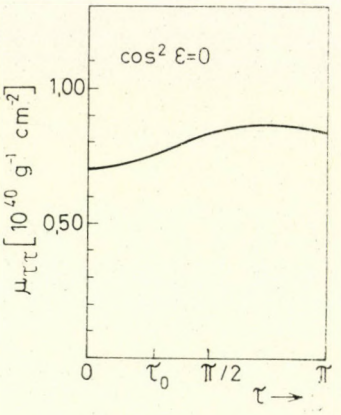

Fig. 6

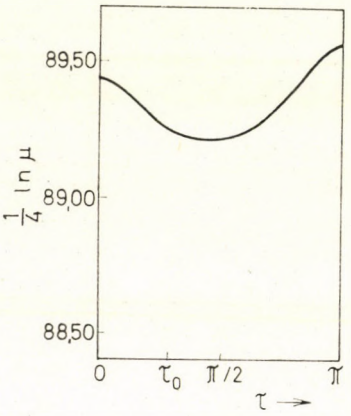

Fig. 7

III. The potential function

The potential energy $V(\alpha, \tau)$ is a two-variable function, which can be expressed as follows:

$$V(\alpha, \tau) = \frac{1}{2} U_{(\tau)} \{1 - \cos 3\alpha\} + V(\tau)$$

The function $U_{(\tau)}$ should be chosen in such a way that it should be even and should vanish for $\tau = 0$. The value $U_{(\tau_0)} = V_0$ can be established in the inver-

sion ground state by the analysis of the internal rotation. The simplest function of such nature, that is easy to treat is:

$$U_{(\tau)} = U_0 \tau^2 \tag{14}$$

The inversion potential function $V(\tau)$ is given here in the form suggested by SWALEN and IBERS [10]:

$$V_{(\tau)} = \frac{1}{2} a\tau^2 + w \cdot \exp(-c\tau^2) \tag{15}$$

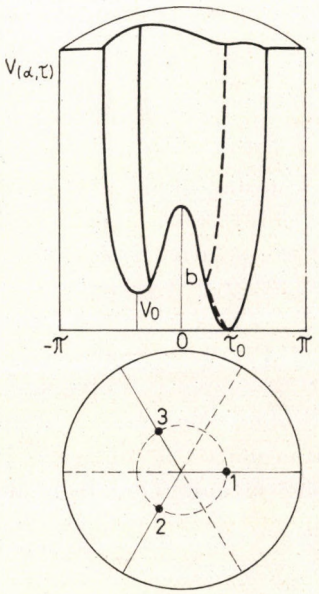

Fig. 8

The potential function $V(\alpha, \tau)$ can be best illustrated in a cylindrical coordinate system (Fig. 8). This depicts very vividly the two dynamical problems. Both the internal rotation and inversion carry the system from one potential minimum into another one via tunnelling effects. During internal rotation the coordinate τ must remain constant while it is easy to see that the coordinate α should change during inversion when the system moves from one to another potential minimum. The zero-point movement is also composed of these two types of motion. Thus the system can also tunnel in its ground state. This is the reason why the term scheme of the ground state is much more complicated than that of any small-amplitude vibration. This complicate structure is manifested by the effect of the ground state internal rotation in the inversion tran-

sitions, and, in turn, by the effect of inversion in the internal rotation transitions.

The only drawback of the above way of description is that it is not suitable for the direct interpretation of the negative τ values, although they must be interpreted, *e.g.*, in the case of studying the symmetry of the basis function. The real source of difficulty is that the potential function has three minima, instead of two. Thus the sign of the τ coordinate of a given potential minimum is relative and it changes steadily during the motion. Let us start *e.g.*, from the first equilibrium position of Fig. 8, whose coordinate τ will be arbitrarily taken positive. By inversion we reach the second or third equilibrium position. It is evident to take the coordinate of the second and third equilibrium positions negative relative to that of the first one. A new inversion can bring the system into the first or third, or the first or second position, depending on the starting position. Accordingly the τ of the first and third positions is positive relative to that of the second, or the τ of the first and second positions is positive relative to that of the third one. By carrying further the above procedure it is seen that the sign of τ coordinate belonging to a given potential minimum is relative and it changes steadily. Fortunately one does not need the absolute sign, only the definition of the positive and negative τ coordinate.

IV. Basis function

The eigenvalues of the above Hamilton operator cannot be given in closed form. Therefore the Hamilton matrix is constructed by means of an appropriately chosen basis function system. The diagonalization of this Hamilton matrix gives the eigenvalues. The following orthonormalized basis function set will be used:

$$\Psi_{JKM\sigma v n\pm} = S_{JKM}\, M_{K\sigma v}\, \psi_{n\pm} \tag{16}$$

where

$$S_{JKM} = \frac{1}{\sqrt{2\pi}} e^{iM\chi}\, e^{iK\varphi}\, \Theta_{JKM(\vartheta)} \tag{17}$$

is the eigenfunction of a symmetric top in the system of the Eulerian angles (χ, φ, ϑ), belonging to operator (9). Quantum numbers J, K and M quantize the total angular momentum, the projection of the latter into the symmetry axis, and the projection of the total angular momentum into one of the axes of the space-fixed coordinate system, respectively.

$$M_{K\sigma v} = e^{-i\varrho K\alpha} \sum_{j=-\infty}^{+\infty} A^{Kv}_{3j+\sigma}\, e^{i(3j+\sigma)\alpha} \tag{18}$$

$M_{K\sigma v}$ is the eigenfunction of the so-called Mathieu differential equation, belonging to the eigenvalue $E_{K\sigma v}$, which is not periodic either according to π or to 2π. This fact is due to the special boundary condition necessitated by the internal axis system. The v is the torsional quantum number, $\sigma = 0, \pm 1$ [9]. In our case the Mathieu differential equation is the following:

$$-\frac{1}{2}\hbar^2 \mu^0_{\alpha\alpha} \frac{\partial^2 M_{K\sigma v}}{\partial \alpha^2} + \frac{1}{2} V_0 \{1 - \cos 3\alpha\} M_{K\sigma v} = E_{K\sigma v} M_{K\sigma v} \tag{19}$$

The matrix elements can be more easily calculated when the coordinate transformation below is applied [9]:

$$\varphi' = \varphi - \varrho\alpha \tag{20}$$

In this case

$$\Psi_{JKM\sigma v n\pm} = S_{JKM(\chi,\varphi',\vartheta)} Q_{K\sigma v} \psi_{n\pm} \tag{21}$$

where

$$Q_{K\sigma v} = \sum_{j}^{+\infty} A^{Kv}_{3j+\sigma} e^{i(3j+\sigma)\alpha} \tag{22}$$

The $\psi_{n\pm}$ is the eigenfunction belonging to the eigenvalue $E_{n\pm}$ of the following differential equation:

$$-\frac{1}{2}\hbar^2 \mu^0_{\tau\tau} \frac{\partial^2 \varphi_{n\pm}}{\partial \tau^2} + \left[\frac{1}{2} a\tau^2 + w \exp\{-c\tau^2\}\right] \psi_{n\pm} = E_{n\pm} \psi_{n\pm} \tag{23}$$

The $\psi_{n\pm}$ eigenfunction is built from harmonic oscillator eigenfunctions (ψ_m) in the following manner [11]:

$$\psi_{n+} = \sum_{m=0}^{+\infty} a^{n+}_m \psi_m \tag{24a}$$

$$\psi_{n-} = \sum_{m=1}^{+\infty} a^{n-}_m \psi_m \tag{24b}$$

The n is the inversion quantum number to each value of which there belong an even (+) and an odd (—) eigenfunction and eigenvalue, respectively. In the case of the even eigenfunctions (ψ_{n+}) only the constants with even index m are different from zero, for the odd eigenfunctions (ψ_{n-}) only the odd ones. Naturally the eigenfunction system $\psi_{n\pm}$ is orthonormalized.

In the methylamine molecule the two hydrogens of the amino group are interchanged relative to the hydrogens of the methyl group during the inversion (Fig. 9). Since the Hamilton operator is invariant with respect to this operation, the eigenfunction $\psi_{n\pm}$ must be either symmetrical or antisymmetrical with respect to inversion. This condition is, in fact, fulfilled since

$$\hat{O}_I \psi_{n+}(\tau) = \psi_{n+}(-\tau) = \psi_{n+}(\tau)$$

$$\hat{O}_I \psi_{n-}(\tau) = \psi_{n-}(-\tau) = -\psi_{n-}(\tau) \tag{25a}$$

where $\hat{O}_I$ is the operator of the inversion.

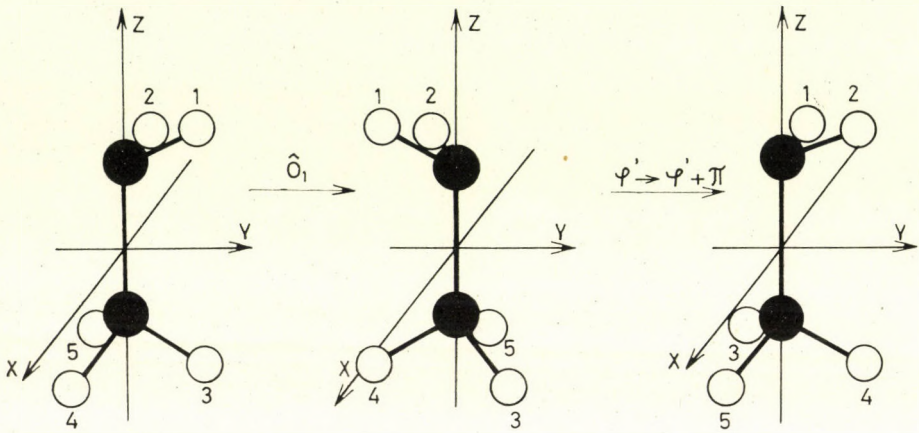

Fig. 9

The Eulerian angle φ' should be changed by π during inversion in order to bring the molecule into an indistinguishable position with regard to the space-fixed system as well. Towards this operation the eigenfunction S_{JKM} is either symmetric or antisymmetric, depending on the value of K

$$\exp\{iK(\varphi' + \pi)\} = (-1)^K \exp\{iK\varphi'\} \tag{26}$$

The following basis function used by the author has a simpler construction than that of the Japanese authors [2, 3]:

$$\Psi_{JKM\sigma vn\pm} = \frac{1}{2} S_{JKM} Q_{K\sigma v} \{(\psi_{n+} + \psi_{n-}) \pm (-1)^K (\psi_{n+} - \psi_{n-})\} \tag{27a}$$

and

$$\Psi_{JKM\sigma vn+} = S_{JKM} Q_{K\sigma v} \psi_{n+} \tag{27b}$$

$$\Psi_{JKM\sigma vn-} = S_{JKM} Q_{K\sigma v} \psi_{n-} \tag{27c}$$

This is so because in the present case the description of the inversion motion already contains the necessary internal rotation.

V. The elements of the Hamilton matrix

The diagonal elements of the Hamilton matrix are the following:

$$\langle JK\sigma vn+|\hat{H}|JK\sigma vn+\rangle = E_{JK}+E_{K\sigma v}+E_{n+}-\frac{1}{2}V_0+$$

$$+\frac{1}{2}V_0\langle n+|\tau^2|n+\rangle+\frac{1}{2}V_0\langle K\sigma v|\cos 3\alpha|K\sigma v\rangle-\frac{1}{2}V_0\langle n+$$

$$+|\tau^2|n+\rangle\langle K\sigma v|\cos 3\alpha|K\sigma v\rangle+\langle n+|\hat{H}'|n+\rangle \qquad (28a)$$

$$\langle JK\sigma vn-|\hat{H}|JK\sigma vn-\rangle = E_{JK}+E_{K\sigma v}+E_{n-}-\frac{1}{2}V_0+$$

$$+\frac{1}{2}V_0\langle n-|\tau^2|n-\rangle+\frac{1}{2}V_0\langle K\sigma v|\cos 3\alpha|K\sigma v\rangle-$$

$$-\frac{1}{2}V_0\langle n-|\tau^2|n-\rangle\langle K\sigma v|\cos 3\alpha|K\sigma v\rangle+\langle n-|\hat{H}'|n-\rangle \qquad (28b)$$

where

$$E_{JK}=\frac{\hbar^2}{4}\left\langle n\pm\left|\frac{1}{A}+\frac{B}{B^2+D^2}\right|n\pm\right\rangle[J(J+1)-K^2]+$$

$$+\frac{\hbar^2}{2}\left\langle n\pm\left|\frac{B+C}{BC-D^2}-\frac{B}{B^2+D^2}\right|n\pm\right\rangle K^2 \qquad (29)$$

Expression (28) contains the τ-average of the rotational constants. This average was determined from the microwave spectrum and it was regarded as the equilibrium value [2].

The off-diagonal elements of the Hamilton matrix are the following:

$$\langle J(K+1)\sigma v'n+|\hat{H}|JK\sigma vn+\rangle =$$

$$=\frac{\hbar^2}{2}\left\langle n\pm\left|\frac{D}{B^2+D^2}\right|n\pm\right\rangle\left(K+\frac{1}{2}\right)\{J(J+1)-$$

$$-K(K+1)\}^{1/2}\langle(K+1)\sigma v'|\cos\varrho\alpha|K\sigma v\rangle \qquad (30a)$$

$$\langle J(K+2)\sigma v'n+|\hat{H}|JK\sigma vn+\rangle =$$

$$=-\frac{\hbar^2}{4}\left\langle n\pm\left|\frac{1}{A}-\frac{B}{B^2+D^2}\right|n\pm\right\rangle\{[J(J+1)-K(K+1)]\times$$

$$\times[J(J+1)-(K+1)(K+2)]\}^{1/2}\langle(K+2)\sigma v'|\cos 2\varrho\alpha|K\sigma v\rangle \qquad (30b)$$

$$\langle JK\sigma v'n+|\hat{H}|JK\sigma vn+\rangle =$$

$$= \frac{1}{2}\{V_0 - U_0\langle n + |\tau^2| n +\rangle\}\langle K\sigma v' |\cos 3\alpha| K\sigma v\rangle \tag{30c}$$

$$\langle JK\sigma v n' + |\hat{H}| JK\sigma v n +\rangle =$$

$$= \frac{1}{2} U_0 \langle n' + |\tau^2| n +\rangle \{1 - \langle K\sigma v |\cos 3\alpha| K\sigma v\rangle +$$

$$+ \langle n' + |\hat{H}'| n +\rangle \tag{30d}$$

$$\langle JK\sigma v n + |\hat{H}| JK\sigma v n -\rangle = \langle n + |\hat{H}| n -\rangle \tag{30e}$$

where

$$\langle K'\sigma v' |\cos 3\alpha| K\sigma v\rangle =$$

$$= \frac{1}{2} \cdot \sum_{-\infty}^{+\infty}{}_j \{A^{K'v'}_{3(j+1)+\sigma} A^{Kv}_{3j+\sigma} + A^{K'v'}_{3j+\sigma} A^{Kv}_{3(j+1)+\sigma}\} \tag{31}$$

$$\langle (K+1)\sigma v' |\cos \varrho\alpha| K\sigma v\rangle = \sum_{-\infty}^{+\infty}{}_j A^{K'v'}_{3j+\sigma} A^{Kv}_{3j+\sigma} \tag{32}$$

$$\langle (K+2)\sigma v' |\cos 2\varrho\alpha| K\sigma v\rangle = \sum_{-\infty}^{+\infty}{}_j A^{K'v'}_{3j+\sigma} A^{Kv}_{3j+\sigma} \tag{33}$$

Similar matrix elements can be obtained for the odd eigenfunctions as well.

The Hamilton matrix is almost diagonal. The selection rules are the following:

$\Delta J = 0, \pm 1$	$\Delta K = 0, \pm 1$
$\Delta\sigma = 0$	$\Delta v = \pm 1, \pm 2, \ldots$
$+ \leftrightarrow -$	$\Delta n = \pm 1, \pm 2, \ldots$

The eigenvalues $E_{K\sigma v}$ can be obtained from Tables for the case $K = 0$; $\sigma = 0$ [12], which also contains the Fourier coefficients necessary for the calculation of the average of $\cos 3\alpha$. In the rest of cases the eigenvalues can be calculated, *e.g.*, by means of the Fourier series given below:

$$E_{K\sigma v} = \frac{V_0}{s} \sum_{i=0}^{+\infty} a^v_{i(s)} \cos \frac{2\pi}{3}\{\varrho K - \sigma\} \tag{34}$$

where the coefficients a^v_i are given as functions of the parameter s [9, 13]. ($s = 8V_0/9\mu_{\alpha\alpha}$).

The eigenvalues E_{n+} and E_{n-} are given by COON *et al.* in tabulated form [11].

In the following paper the values of the potential barriers, $\cos^2 \varepsilon$ and $\left\{\frac{d\alpha}{d\tau}\right\}$ will be determined when the given matrix elements, and the infrared and microwave data will be utilized.

Appendix I

ITOH studied the internal rotation of methylamine in ground state [2]. The Hamilton operator derived by him does not contain inversion term at all, but he proposed the extension of the diagonal elements by a semi-empirical term which has the purpose to describe the inversion splitting. TSUBOI et al. applied this concept for the excited inversion state as well [3].

They have separated in thought the wagging motion of the amino group and the closely associated rotation. They have not distinguished between this rotation and the internal rotation. Due to these reasons the basis function has another construction than the presently applied one.

The eigenfunction of the wagging motion has the following symmetry properties with respect to the inversion:

$$\frac{1}{\sqrt{2}}\left[\psi_{n+}(y) + \psi_{n-}(y)\right] \xrightarrow{\hat{O}_I} \frac{1}{\sqrt{2}}\left[\psi_{n+}(y) - \psi_{n-}(y)\right] \qquad \text{I/1}$$

where y is the normal coordinate of the wagging motion.

The appropriate rotation of the methyl group is taken into account by means of an independent internal motion, by the eigenfunction of the internal rotation.

$$Q_{K\sigma v}(\alpha) \xrightarrow{\hat{O}_I} Q_{K\sigma v}(\alpha + \pi) \qquad \text{I/2}$$

$$\exp\{iK\varphi'\} \xrightarrow{\hat{O}_I} (-1)^K \exp(iK\varphi') \qquad \text{I/3}$$

Using the above functions a symmetric and an antisymmetric basis function is constructed in the following manner:

$$\Phi^s_{JKM\sigma vn} = \frac{1}{2} S_{JKM}\{(\psi_{n+}(y) + \psi_{n-}(y)) Q_{K\sigma v}(\alpha) + (-1)^K (\psi_{n+}(y) - \psi_{n-}(y)) Q_{K\sigma v}(\alpha + \pi)\} \qquad \text{I/4}$$

$$\Phi^a_{JKM\sigma vn} = \frac{1}{2} S_{JKM}\{(\psi_{n+}(y) + \psi_{n-}(y)) Q_{K\sigma v}(\alpha) - (-1)^K (\psi_{n+}(y) - \psi_{n-}(y)) Q_{K\sigma v}(\alpha + \pi)\} \qquad \text{I/5}$$

The basis function (27) used by the author is much simpler.

Using the above basis functions the following diagonal matrix elements are obtained:

$$\langle JK\sigma vns\,|\hat{H}|\,JK\sigma vns\rangle = E_{JK} + E_{K\sigma v} + \\ + \frac{1}{2}(E_{n+} + E_{n-}) - \frac{1}{2}(-1)^K (E_{n-} - E_{n+}) \int_0^{2\pi} Q^*_{(\alpha)}\, Q_{(\alpha+\pi)}\, d\alpha \qquad \text{I/6}$$

$$\langle JK\sigma vn\,a\,|\hat{H}|\,JK\delta vna\rangle = E_{JK} + E_{K\sigma v} + \\ + \frac{1}{2}(E_{n+} + E_{n-}) + \frac{1}{2}(-1)^K (E_{n-} - E_{n+}) \int_0^{2\pi} Q^*_{(\alpha)}\, Q_{(\alpha+\pi)}\, d\alpha \qquad \text{I/7}$$

where

$$\int_0^{2\pi} Q^*_{(\alpha)}\, Q_{(\alpha+\pi)}\, d\alpha = \sum_{-\infty}^{+\infty}{}_j \left\{A^{Kv}_{3j+\sigma}\right\}^2 e^{i(3j+\sigma)\pi}$$

It should be added that the operator applied by the previous authors is a worse approximation than the one used here.

The quantity $(E_{n-}-E_{n+})$ is a hypothetical splitting which would be observed if the inversion would not contain the rotation of the methyl group in addition to the wagging motion. This value is very large, it approaches the magnitude of the inversion splitting in the ammonia molecule. When $n = 0$, $\Delta E_n = 0.9535$ cm^{-1}, for $n = 1$, $\Delta E_n = 31.6$ cm^{-1}. These large splittings are reduced by the overlap integrals, *e.g.* in the case $n = 1$ there is a drop to 6–8 cm^{-1}, which is a still higher value than the experimental value of about 1 cm^{-1}.

The overlap integrals contain the eigenfunction of the internal rotation. This statement can be questioned since the internal rotation is a motion independent of inversion, although there is no doubt that a certain correlation exists between the frequency of the internal rotation and the inversion transition. The inversion frequency of methylamine and the deuterated methylamines is roughly three times larger than the frequency of the internal rotation.

The theory given here gives a more exact and more universal description of the phenomena involved. It is also suitable for giving information about the classical trajectory of the motion of the system in the potential field $V(\alpha, \tau)$ by means of the determination of the quantity $\left\{\frac{d\alpha}{d\tau}\right\}$.

REFERENCES

1. Sztraka, L.: Acta Chim. Acad. Sci. Hung. **65,** 311 (1970)
2. Itoh, T.: J. Phys. Soc. Japan **11,** 264 (1965)
3. Tsuboi, M., Hirakawa, A. Y., Itoh, T., Sasaki, T., Tamagake, K.: J. Chem. Phys. **41,** 2721 (1964)
4. Tamagake, K., Tsuboi, M., Hirakawa, A. Y.: J. Chem. Phys. **48,** 5536 (1968)

5. PODOLSKY, B.: Phys. Rev. **32**, 812 (1928)
6. WILSON, E. B. jr., HOWARD, J. B.: J. Chem. Phys. **4**, 260 (1936)
7. WILSON, E. B. jr., DECIUS, J. C., CROSS, P. C.: Molecular Vibrations (McGraw-Hill, 1955)
8. MEYER, R., GÜNTHARD, Hs. H.: J. Chem. Phys. **49**, 1510 (1968)
9. LIN, C. C., SWALEN, L. D.: Rev. Mod. Phys. **31**, 841 (1959)
10. SWALEN, J. D., IBERS, J. A.: J. Chem. Phys. **36**, 1914 (1962)
11. COON, J. B., NAUGLE, N. W., MCKENZIE, R. D.: J. Mol. Spectroscopy **20**, 107 (1966)
12. Tables Relating to Mathieu Functions (Columbia University Press, New York, 1951)
13. HERSCHBACH, D. R.: Tables for the Internal Rotation Problem. (The Library of Congress Photoduplication Service, Washington, ADI—5339 microfilm)

Lajos SZTRAKA; Budapest XI., Budafoki út 8.

Acta Chimica Academiae Scientiarum Hungaricae, Tomus 66 (1), pp. 115–126 (1970)

THE CHEMISTRY OF 1,3-BIFUNCTIONAL SYSTEMS, VII*

MECHANISM OF THE CONVERSION OF 1,3-CHLOROHYDRINS IN ALKALINE MEDIUM

M. BARTÓK, G. BOZÓKI-BARTÓK and K. KOVÁCS

(Institute of Organic Chemistry, A. József University, Szeged)

Received March 9, 1969

The rates of the alkaline hydrolysis of *n*-butyl chloride and *sec*-butyl chloride have been compared with those of 1,3-chlorohydrins having the same basic skeleton, and the alkaline hydrolysis of 2,2-diethyl-3-chloropropanol was studied by reaction kinetical methods. On the basis of the latter investigations, a mechanism is proposed for the conversion of 1,3-chlorohydrins into oxacyclobutanes.

Within the scope of our investigations on the conversions of 1,3-chlorohydrins and their acetates in alkaline medium, we reported in an earlier work [1] on the preparative utilization of these reactions. The object of the investigations was the preparation of four-membered cyclic ethers. In the course of an examination of the synthesis of oxacyclobutane homologues, conclusions of qualitative character could be drawn concerning the structures of 1,3-chlorohydrins and the direction of their reactions proceeding in the presence of alkalies.

The conversion of 1,3-chlorohydrins by alkalies may take the following principal courses:

1. Formation of four-membered cyclic ethers by intramolecular rearrangement.
2. Formation of olefins and oxo compounds by 1,4-elimination and subsequent fragmentation.
3. Formation of α, β- and β, γ-unsaturated alcohols by 1,2-elimination.
4. Formation of 1,3-diols by bimolecular substitution reactions.

As it has been mentioned, the course of the reaction depends decisively on the structure of the chlorohydrin, besides on the experimental conditions. Results of investigations in this field show that the formation of oxethans, in a degree which can be utilized for preparative purposes, can only be observed with 1,3-chlorohydrins which contain the chlorine atom attached to a primary carbon atom. With compounds containing the chlorine atom in a secondary position, fragmentation and 1,2-elimination are the principal directions of the reaction. 1,3-Chlorohydrins containing a tertiary chlorine atom are very unstable compounds.

* Part VI: Acta Chim. Acad. Sci. Hung. **61**, 315 (1969).

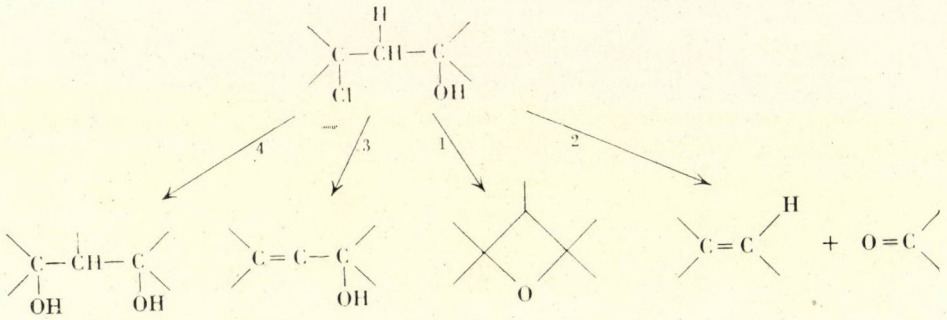

It follows from what has been said above that a study of the alkaline hydrolysis of 1,3-chlorohydrins is interesting for several reasons. It is possible to investigate not only the rate of alkaline hydrolysis in dependence on the structure of the chlorohydrin, but the rates and mechanisms of the different reactions can also be studied.

Several research groups have carried out reaction kinetical investigations of the mechanism of the alkaline hydrolysis of 1,2-chlorohydrins, and this problem can be considered today satisfactorily clarified. It is obvious that an investigation of the alkaline hydrolysis of 1,3-chlorohydrins should start with this mechanism; it is to be considered, how far the above reaction mechanism can be applied to the present case, or how far it must be modified.

We know only of one publication [2] on the kinetics of the reactions of 1,3-chlorohydrins with alkali. Two types of monoalkyl-substituted trimethylene chlorohydrins have been investigated by the author out of compounds of about 20 types.

Our research work was undertaken with the aim to study the reaction directions in the alkaline hydrolysis of 1,3-chlorohydrins of various types, and to investigate the mechanism of the processes by reaction kinetical methods.

Our present communication is an introduction to this research discussing the following problems:

1. The comparative reaction rates of the alkaline hydrolysis of alkyl chlorides and 1,3-chlorohydrins of similar basic skeleton.

2. The mechanism of the alkaline hydrolysis of 1,3-chlorohydrins containing a chlorine atom in primary position.

Comparison of the rates of alkaline hydrolysis of alkyl chlorides and 1,3-chlorohydrins

The rate constants of the alkaline hydrolysis of *n*-butyl chloride and *sec*-butyl chloride have been determined under experimental conditions identical with those used for the corresponding 1,3-chlorohydrins. The experimental

results, together with the data of FORSBERG [2] obtained for 1,3-chlorohydrins, are summarized in Table I.

Comparison of the corresponding rate constants shows that the rate of alkaline hydrolysis is considerably increased on the introduction of a hydroxyl group into the alkyl chloride molecule.

Table I

No.	Formula of the starting substance	k $1 \cdot mole^{-1} \cdot min^{-1}$
1	$CH_3-CH_2-CH_2-CH_2$ $\quad\quad\quad

The presence of a hydroxyl group in γ-position produced a very marked change in the reaction rate, and gave rise to new reaction products.

For the time being, an exact, numerical comparison of compounds containing tertiary chlorine atoms is impossible, as the corresponding 1,3-chlorohydrin — 3-methyl-3-chloro-butanol — could not be prepared so far. This can be explained by the following considerations: the hydrolysis of *t*-butyl chloride proceeds even at 25 °C and in the absence of OH^- ions (in water) at a higher rate ($k = 0.031$), than the alkaline hydrolysis of secondary butyl chloride at 80 °C. Considering the increase of the reaction rate by about two orders of magnitude due to the introduction of the hydroxyl group in γ-position, the instability of chlorohydrins containing tertiary chlorine atom is readily understood.

Mechanism of the conversion in alkaline medium of 1,3-chlorohydrins containing chlorine atom in primary position

Based on theoretical considerations, as well as on a great number of preparative experiments [1], and in view of the mechanism accepted generally for the alkaline hydrolysis of 1,2-chlorohydrins, the mechanism of the reaction of 1,3-chlorohydrins containing chlorine atom in primary position, proceeding in alkaline medium and leading to the formation of oxacyclobutanes, may be represented as follows:

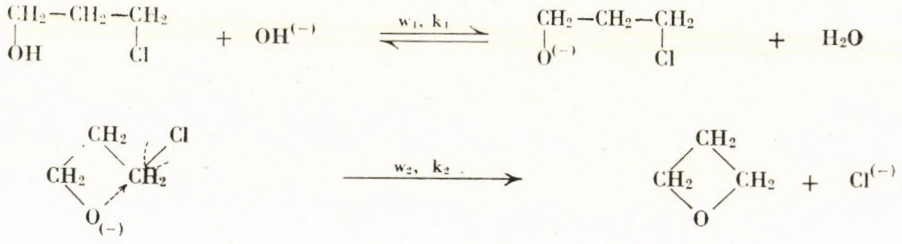

In the first step, the hydroxide ion splits off a proton from the hydroxyl group of the chlorohydrin, and a γ-chloroalkoxy anion is produced as an intermediate. In the second step, intramolecular nucleophilic attack within the alkoxy anion by the negatively charged oxygen atom displaces chlorine from the carbon atom in the form of a chloride and a four-membered cyclic ether is formed.

In order to prove the assumed mechanism, 2,2-diethyl-3-chloropropanol (**I**) was selected as the model substance. Under nearly identical experimental conditions as those used in the kinetical measurements, this compound gives 3,3-diethyloxacyclobutane (**II**) in 80% yield:

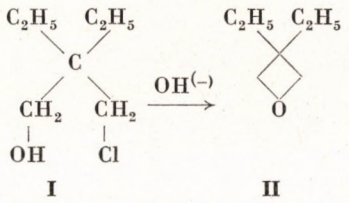

I II

Since it is to be expected that the second step is considerably slower, the rate of formation of the cyclic ether is determined by this step. It follows unequivocally that the rate of the overall process will be influenced by the chlorohydrin concentration.

However, as a first approach, it appears more interesting to determine the effect of the concentration of the hydroxide ions on the reaction rate. Since the rate of formation of 1,3-epoxides is determined by the slowest step, in the present case by the conversion of the γ-chloroalkoxide anion, the reaction rate will depend on the concentration of a single component, the chlorohydrin alcoholate. Thus, the reaction mechanism can be considered monomolecular. However, this statement is true only if the first step, the formation of the alcoholate anion, is instantaneous and, therefore, its rate is not comparable with the second step.

In our experiments the rate of hydrolysis of 2,2-diethyl-3-chloropropanol (**I**) was investigated at different temperatures, and at different chlorohydrin (**I**) and $OH^{(-)}$ concentrations. The results are summarized in Table II.

The partial orders of reaction were determined by the differential method of VAN'T HOFF. Graphic representation of the corresponding experimental data

Table II

No.	°C	[I]	[OH⁻]	($l \cdot mole^{k-1} \cdot min^{-1}$)
1	80	0.01146	0.08177	0.074
2	80	0.01544	0.08177	0.068
3	80	0.01900	0.08177	0.062
4	80	0.02479	0.08177	0.069
5	80	0.00997	0.01400	0.050
6	80	0.01004	0.03197	0.063
7	80	0.01006	0.04590	0.063
8	80	0.01001	0.09510	0.076
9	85	0.01004	0.01623	0.115
10	95	0.00988	0.01305	0.203
11	95	0.01013	0.01305	0.214

shows (Figs 1 and 2) that the rate of formation of 2,2-diethyloxacyclobutane follows first order kinetics, both as a function of the chlorohydrin [I] and $[OH^{(-)}]$ concentrations.

Therefore, the rate of formation of **II** is also dependent on $[OH^{(-)}]$, thus the first step indicated in the reaction scheme is not instantaneous. Though it is more rapid than the second process, the two rates are comparable. Therefore, the rate of formation of the cyclic ether does not depend on the concentration of the intermediate product alone. Evidently, the rate of a composite process, in the present case the rate of formation of the cyclic ether, will be determined

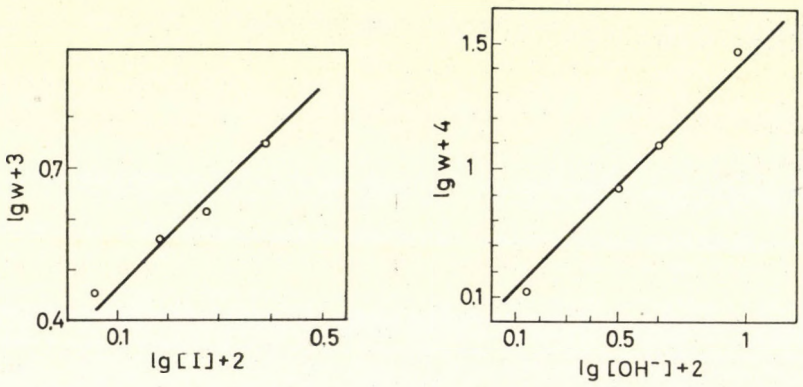

Figs 1 and *2*. Dependence of the reaction rate of 2,2-diethyl-3-chloropropanol (**I**) as a function of the concentration of **I** and the hydroxide ions, respectively

by the slowest step, in our case by the rate S_Ni. However, the rate of further conversion of the intermediate will be determined by all those factors which influence its actual concentration, one of them being the concentration of the hydroxide ion.

On the basis of these considerations, we decided to use the bimolecular rate equation for an evaluation of the reaction kinetic measurements, where the first step of the composite reaction $A + B \rightleftarrows C \rightarrow D$ was regarded as an equilibrium process. This is justified, because water is also present in the reaction mixture. As it is known, composite processes of this kind can be represented in terms of reaction kinetics by a bimolecular reaction scheme, whose rate constant is the product of the equilibrium constant of the first step and the rate constant of the second step. Indeed, the experimental data readily can be interpreted with the bimolecular rate equation. The mechanism proposed is also supported by the value of the activation entropy calculated from the experimental results, which is equal for 2,2-diethyl-3-chloropropanol (**I**) to -10.4 cal/mole/grade. The activation energy of the process is 21.9 kcal/mole.

Experimental

The isomeric butyl chlorides were commercial products, which were purified (distilled) before use. Substances of GLC (gas-liquid chromatographic) purity were used.

2,2-Diethyl-3-chloropropanol (I)

The compound was prepared in 90% yield by the methanolic deacetylation of 2,2-diethyl-3-acetoxypropyl chloride [3]. B. p. (at 40 torr): 116–118 °C; n_D^{28}: 1.4598. After distillation, the substance crystallized.

$C_7H_{15}OCl$ (150.65). Calcd. Cl 23.3%. Found Cl 23.28%.

Alkaline reaction of 2,2-diethyl-3-chloropropanol

1 g of **I** was added to 70 ml of saturated aqueous barium hydroxide solution. The mixture was heated for 4 hrs. at 140 °C. After cooling, it was extracted with 4×20 ml portions of ether, and the combined ethereal solutions were dried. The solvent was removed, using a Vigreux fractionating column. The residue was examined on a Willy Giede GCHF 18/2 gas chromatograph (experimental conditions: dinonylphthalate column of 2 m, 100 °C, 120 ml/min. hydrogen carrier gas). According to the chromatographic investigations, **I** was converted into 3,3-diethyloxacyclobutane (**II**) in about 80% yield. **II** was identified by means of a comparing substance. Under the given experimental conditions, retention time was 18.3 min.

Reaction kinetic measurements

Since the rate of the alkaline hydrolysis of 1,3-chlorohydrins is considerably lower than that of ethylene chlorohydrin homologues, the kinetic measurements must be performed at higher temperatures. Data in the literature show that the rate of alkaline hydrolysis of 1,2-chlorohydrins is considerable even at 20 °C. Our preliminary experiments showed that, in general, a temperature higher than 80 °C was required in our case to obtain experimental data which could be readily evaluated. The measurements were made in an ultrathermostat of 0.01 °C accuracy. (In the measurements above 100 °C, the liquid in the ultrathermostat was a mixture of glycerol and water.)

The rates of the chemical reactions during conversion were determined by measuring the concentration of the chloride ions, formed from the chlorohydrins, by means of VOLHARD's method, as a function of time. Alkaline hydrolysis was carried out with barium hydroxide. Aqueous dioxan (3 : 7) was used as the solvent.

An experimental series may be made as follows. It is advisable to prepare the aqueous dioxan solution of barium hydroxide of the required concentration one week before the beginning of the experiments. During this time, carbon dioxide and carbonate ions, which interfere with the measurements, precipitate as barium carbonate. (Throughout the measurements, all operations must be carried out in an atmosphere free of carbon dioxide, *e.g.*, in a stream of nitrogen.) The concentration of the barium hydroxide solution was checked by titration with 0.01 *N* HCl before each measuring series. The required quantity of chlorohydrin is weighed into a 50-ml volumetric flask, purged with nitrogen, and the flask is filled up to the mark with the standardized barium hydroxide solution in dioxan. From this stock solution, portions of 6 ml are rapidly introduced with a pipette into ampoules which have been rinsed with nitrogen. After sealing, the ampoules are placed into the thermostat which has been adjusted to the required temperature. At regular intervals, depending on the reaction rate, the ampoules are taken out one by one, and placed into icewater to freeze in the reaction. Next, 5.00 ml is taken out from the ampoule, and acidified with nitric acid. 0.01 *N* $AgNO_3$ solution is added in excess, and the concentration of the chloride ions is determined by titrating the excess of $AgNO_3$ with 0.01 *N* ammonium thiocyanate solution. In general, eight samples were examined within one experimental series, and the periods of taking the samples were selected such that about 40% conversion was obtained until the last sample was withdrawn.

The activation energy was calculated by means of the empirical formula of Arrhenius:

$$\Delta E_{act} = \frac{4.576 \cdot T_1 \cdot T_2 \lg \frac{k_2}{k_1}}{T_2 - T_1} ; \; T_2 > T_1$$

and graphically, by means of the function

$$\lg k = f\frac{1}{T} .$$

The activation entropy was calculated from the following equation:

$$S^{\ddagger} = 4.576 \left(\lg k + \frac{\Delta E_{act}}{4.576 \cdot T} - \lg \frac{k}{h} T \right)$$

where k is the Boizmann constant and h is Planck's constant.

Experimental data

In the presentation of the experimental data the following symbols are used:

t	time (min.)
a	initial concentration of the hydroxide ions [$Ba(OH)_2$ g·eq·/litre]
b	initial concentration of chlorohydrin (mole/litre)
x	quantity of chlorohydrin converted at time t (mole/litre)
k	second-order rate constant (litre · $mole^{-1}$ · min^{-1})

$CH_3—CH_2—CH_2—CH_2$
|
Cl

80 °C
$a = 0.01413$
$b = 0.01080$

112 °C
$a = 0.01413$
$b = 0.01007$

No.	t	x	k	t	x	k
1	15	0.00009	0.049	60	0.00068	0.084
2	75	0.00014	0.014	120	0.00122	0.080
3	150	0.00021	0.010	180	0.00167	0.076
4	195	0.00028	0.010	243	0.00222	0.079
5	255	0.00035	0.010	300	0.00272	0.083
6	315	0.00039	0.009	364	0 00279	0.071
7	375	0.00046	0.009	420	0.00327	0.076
8	430	0.00051	0.008	480	0.00340	0.070

$k_{2-8} = 0.010$ $k_{2-8} = 0.077$

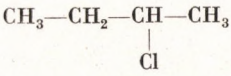

80 °C
$a = 0.01413$
$b = 0.01068$

112 °C
$a = 0.01413$
$b = 0.01111$

No.	t	x	k	t	x	k
1	15	0.00005	0.020	60	0.00274	0.374
2	75	0.00025	0.021	105	0.00392	0.349
3	150	0.00048	0.022	135	0.00464	0.350
4	195	0.00062	0.022	167	0.00555	0.384
5	255	0.00085	0.024	210	0.00612	0.367
6	315	0.00104	0.024	243	0.00656	0.367
7	375	0.00124	0.024	270	0.00688	0.366
8	430	0.00145	0.025	300	0.00711	0.356

$k_{1-8} = 0.023$

$k_{1-8} = 0.364$

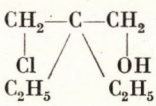

85 °C

$a = 0.01623$

$b = 0.01004$

No.	t	x	k
1	30	0.00044	0.091
2	75	0.00121	0.109
3	120	0.00192	0.116
4	170	0.00251	0.090
5	220	0.00309	0.114
6	270	0.00361	0.116
7	315	0.00399	0.115
8	360	0.00444	0.118

$k_{2,5,6,7,8} = 0.115$

95 °C
$a = 0.01305$
$b = 0.00988$

95 °C
$a = 0.01305$
$b = 0.01013$

No.	t	x	k	t	x	k
1	103	0.00233	0.222	43	0.00121	0.221
2	188	0.00364	0.222	90	0.00203	0.208
3	242	0.00407	0.200	134	0.00286	0.216
4	304	0.00476	0.211	179	0.00351	0.214
5	422	0.00510	0.178	219	0.00403	0.215
6	533	0.00603	0.191	273	0.00463	0.217
7	626	0.00654	0.196	310	0.00485	0.206

$k_{1-7} = 0.203$

$k_{2-7} = 0.214$

Rate measurements for the determination of the partial orders on the basis of the VAN'T HOFF equation $\log w = \log\left(-\frac{\Delta c}{\Delta t}\right)$, where Δc is the quantity of substance (mole/litre) converted during time Δt, and w is the reaction rate (mole/litre/min.)

80 °C $[CH^-]$ = const. = 0.08177 mole/litre
[I] = 0.01146 mole/litre

[I] = 0.01544 mole/litre

No.	t	Δc	$\log w + 3$	No.	t	Δc	$\log w + 3$
1	15	0.00088	0.547	1	15	0.00116	0.667
2	40	0.00247	0.568	2	40	0.00278	0.620
3	70	0.00391	0.519	3	70	0.00468	0.597
4	100	0.00504	0.480	4	100	0.00630	0.578
5	130	0.00616	0.454	5	130	0.00789	0.561
6	160	0.00680	0.406	6	160	0.00887	0.522
7	190	0.00761	0.381	7	190	0.00982	0.492
8	220	0.00820	0.348	8	220	0.01042	0.454

$k = 0.074$

$k = 0.068$

[I] = 0.01900 mole/litre

No.	t	Δc	log w + 3
1	15	0.00092	0.564
2	40	0.00328	0.691
3	70	0.00570	0.683
4	100	0.00725	0.639
5	130	0.00891	0.614
6	160	0.01004	0.576
7	190	0.01113	0.546
8	220	0.01211	0.520

k = 0.062

[I] = 0.02479 mole/litre

No.	t	Δc	log w + 3
1	15	0.00232	0.968
2	40	0.00468	0.847
3	70	0.00771	0.814
4	100	0.01014	0.784
5	130	0.01222	0.751
6	160	0.01405	0.721
7	190	0.01542	0.688
8	220	0.01638	0.650

k = 0.069

[I]	log [I] + 2	log w + 3
0.01146	0.060	0.454
0.01544	0.189	0.561
0.01900	0.279	0.614
0.02479	0.394	0.751

80 °C I = const. + 0.0100 mole/litre
[OH^-] = 0.01400 mole/litre [OH^-] = 0.03197 mole/litre

No.	t	Δc	log w + 4
1	60	0.00029	0.454
2	120	0.00084	0.626
3	180	0.00122	0.604
4	240	0.00133	0.523
5	300	0.00180	0.555
6	360	0.00205	0.535
7	420	0.00233	0.523
8	480	0.00264	0.519

k = 0.050

No.	t	Δc	log w + 4
1	60	0.00121	1.081
2	120	0.00213	1.027
3	180	0.00228	0.881
4	240	0.00351	0.944
5	300	0.00431	0.935
6	360	0.00492	0.914
7	420	0.00531	0.880
8	480	0.00600	0.875

k = 0.063

$[OH^-] = 0.04590$ mole/litre

No.	t	Δc	$\log w + 4$
1	40	0.00105	1.20
2	80	0.00228	1.23
3	120	0.00318	1.20
4	160	0.00364	1.14
5	200	0.00418	1.10
6	240	0.00490	1.09
7	280	0.00528	1.05
8	320	0.00587	1.04

$k = 0.063$

$[OH^-] = 0.09510$ mole/litre

No.	t	Δc	$\log w + 4$
1	20	0.00131	1.59
2	40	0.00259	1.59
3	60	0.00351	1.55
4	80	0.00428	1.51
5	120	0.00590	1.47
6	140	0.00623	1.43
7	160	0.00626	1.37

$k = 0.076$

$[OH^-]$	$\log [OH^-] + 2$	$\log w + 4$
0.01400	0.146	0.523
0.03197	0.505	0.935
0.04590	0.662	1.109
0.09510	0.978	1.470

REFERENCES

1. BARTÓK, M., KOZMA, B., SHUIKIN, N. I., APJOK, J., GILDE, A.: Acta Phys. et Chem. Szeged **8,** 133 (1962); **9,** 25 (1963); Izv. A. N. USSR. Ser. khim. **1966,** 878, 1241; **1967,** 153; Acta Chim. Acad. Sci. Hung. **55,** 365 (1968)
2. FORSBERG, G.: Acta Chim. Scand. **8,** 135 (1954)
3. BARTÓK, M., KOZMA, B., GILDE, A.: Acta Phys. et Chem. Szeged **11,** 35 (1965)

Mihály BARTÓK
Gizella BOZÓKI-BARTÓK
Kálmán KOVÁCS

Szeged, Dóm tér 8, Hungary.

Acta Chimica Academiae Scientiarum Hungaricae, Tomus 66 (1), pp. 127–129 (1970)

METHINYLTRICOBALT ENNEACARBONYL COMPOUNDS, I

NEW METHOD OF PREPARATION OF ALKYL DERIVATIVES

(SHORT COMMUNICATION)

G. PÁLYI,* F. PIACENTI,** M. BIANCHI and E. BENEDETTI

(Institute of Industrial Organic Chemistry, University of Pisa, Pisa, Italy)

Received January 23, 1970

Two main methods are generally used for the preparation of $Co_3(CO)_9CX$ (**I**) compounds. If $Co_2(CO)_6(HC_2R)$ (**II**) (R = alkyl, aryl, or aralkyl) acetylene complexes are heated in acidic medium, the corresponding $Co_3(CO)_9CCH_2R$ (**III**) compounds are obtained [1]. The other possibility [2] is more general; if CY_3X (Y = Cl, Br, I) trihalomethyl derivatives are allowed to react with $Co_2(CO)_8$, $Co_4(CO)_{12}$ or $[Co(CO)_4]^-$ anion, complexes of type **I** can be prepared. The limitation of the first method is that it is suitable only for the preparation of $Co_3(CO)_9CCH_2$ derivatives, while the second has the disadvantage that the preparation of the required trihalomethyl compounds to be used as starting materials is often very difficult.

Recently KIM and HAGIHARA [3] observed that if an acetylenic compound containing a hydroxyl group is used for the preparation of compounds of type **II**, products of type **III** can be obtained by the usual experimental technique: the hydroxyl group is replaced by hydrogen in a reaction which is not yet explored.

Considering that α-(trihalomethyl) alcohols are much more readily accessible than the corresponding trihalomethyl alkanes, attempts have been made to extend the method of KIM and HAGIHARA to the former compounds, supposing that the elimination of the hydroxyl group would take place also in this case.

In fact, when α-(trihalomethyl) alcohols were reacted with $[Co(CO)_4]^-$ anion in THF, the corresponding $Co_3(CO)_9CX$ (X = alkyl) compounds could be isolated; starting from CBr_3CH_2OH, from $CBr_3CH(CH_3)OH$ and from $CCl_3C(CH_3)_2OH$ derivatives, **I** could be prepared (X = Me, Et and *i*-Pr, respectively). The successful synthesis of $Co_3(CO)_9CCH(CH_3)_2$ which has not been described earlier, properly demonstrates the advantage of this method: this compound — as it is obvious from the above considerations — cannot be syn-

* Present address: Research Group for Petrochemistry of the Hungarian Academy of Sciences, Veszprém, Hungary.

** Present address: Institute of Organic Chemistry, University of Firenze, Firenze, Italy.

thesized *via* compounds of type **II**, and the preparation of 1,1,1-trihalo-2-methylpropane which could be used as the starting material for the other method is very difficult.

Experimental

$Co_3(CO)_9CCH_3$

4.6 g of $Co_2(CO)_8$ was allowed to react with 6.1 g of CBr_3CH_2OH in 50 ml of THF at room temperature for 12 hrs. The solvent was then evaporated at reduced pressure and room temperature, the residue extracted with *n*-hexane, and the extract was eluted on a silica gel column. The first violet fraction was sublimed several times in vacuum (2–3 torr, 60–65 °C) and identified on the basis of the following investigations:

$C_{11}H_3O_9Co_3$. Calcd. C 28.98; H 0.66; Co 38.78. Found C 29.54; H 0.72; Co 38.7%.

IR spectrum (in *n*-hexane): CO stretching range: 2102.4(m); 2052.0(vs); 2038.2(s); 2018.0(w) cm^{-1} (± 0.2 cm^{-1}), which data are in good agreement with those reported in the literature [2].

^{1}P-NMR spectrum in C_6D_6 : $\delta = 3.06$ ppm (HMDS internal reference); $\delta = 3.11$ ppm (TMS internal reference), which fairly agrees with the value $\delta = 3.7$ ppm in CCl_3F (reference is not given) published recently [4]. Yield: 9.2% (3 times sublimed substance, calculated for $[Co(CO)_4]^-$).

$Co_3(CO)_9CCH_2CH_3$

4.5 g of $Co_2(CO)_8$ was treated with 7.2 g of $CBr_3(CH_3)OH$ as described above. The first violet chromatographic fraction was identified, after sublimation, on the basis of the following investigations:

$C_{12}H_5O_9Co_3$. Calcd. C 30.67; H 1.07. Found C 31.02; H 1.10%.

IR spectrum (in *n*-hexane): CO stretching range: 2101.2 (m); 2051.5(vs); 2038.0(s); 2017.9(w)$cm^{-1} \pm 0.2$ cm^{-1}, which is in agreement with the CO stretching spectrum of the $Co_3(CO)_9C$-group [2] and consistent with the spectra of the X = Me (see above) and X = *i*-Pr derivatives (see description of the following experiment). IR spectra of this compound have not yet been published in the literature.

^{1}P-NMR spectrum (in CCl_4) : $\delta = 1.62$ ppm (triplet), J = 7.5 cps; $\delta = 3.75$ ppm (quartet), J = 7.5 cps; intensity ratio 3.07 : 2.00 (3 : 2) TMS internal reference, which is in good agreement with the literature data [3]. Yield: 5.1% (3 times sublimed substance, calculated for $[Co(CO)_4]^-$).

$Co_3(CO)_9CCH(CH_3)_2$

5.2 g of $Co_2(CO)_8$ was allowed to react with 3.8 g of $CCl_3C(CH_3)_2OH$ at 45–50 °C for 4.5 hrs, as described above. The structure of the substance in the first violet chromatographic fraction was determined by the following investigations:

$C_{13}H_7O_9Co_3$. Calcd. C 32.68; H 1.46; Co 36.53. Found C 32.67; H 1.63; Co 36.2%.

IR spectrum (in *n*-hexane): CO stretching range: 2102.2(m), 2051.1(vs); 2037.9(s); 2017.1(w) cm^{-1} (± 0.2 cm^{-1}), bands characteristic for the $Co_3(CO)_9C$-group [2]; other characteristic bands (in KBr pellet), (with ± 2.5–3.4 cm^{-1} error): 2955(s); 2870(m); 2840(w) CH_3-group, C–H stretching vibrations; 1458(s) CH_3-group asymmetric deformation vibration; 1375(w); 1355(m) CH-group symmetric deformation vibration; 640(s) C (central)-Co stretching; 531(vs); 521(w); 508(sh, w); 470(m) cm^{-1} C (carbonyl)-Co stretching.

^{1}P-NMR spectrum (in C_6D_6): $\delta = 1.14$ ppm (dublet), J = 6.8 cps; $\delta = 3.31$ ppm (multiplet, 5 observable peaks); intensity ratio 6.27 : 1.00 (6 : 1) (HMDS internal reference). This spectrum can be regarded as characteristic of the *i*-Pr group; the lacking two peaks from the multiplet of the CH group are certainly masked by the background noise, and the solubility of the compound does not permit the investigation of a more concentrated sample.

Molecular weight (osmometric, in C_6H_6): found 485 $\pm$ 14; calculated 484.

Yield 2.8% (5 times sublimed substance, calculated for $[Co(CO)_4]^-$).

*

The authors' thanks are due to Profs. L. MARKÓ (Veszprém) and G. BOR (Padova) for their valuable advice, to Prof. P. GIUSTI, Drs. G. CECCARELLI and V. NUTI for their help in the MW, NMR measurements and elemental analyses. One of the authors (G.P.) is grateful to the Consiglio Nazionale delle Ricerche (Roma) for a research fellowship received in course of this work.

REFERENCES

1. MARKBY, R., WENDER, J., FRIEDEL, R. A., COTTON, F. A., STERNBERG, H. W.: J. Am. Chem. Soc. **80,** 6529 (1958); KRÜECKE, U., HÜBEL, W.: Chem. Ind. (London), 1224 (1960)
2. BOR, G., MARKÓ, B., MARKÓ, L.: Acta Chim. Acad. Sci. Hung. **27,** 295 (1961); BOR, G., MARKÓ, L., FREUND, M.: Hung. Pat. 149.692 (1961); BOR, G., MARKÓ, L., MARKÓ, B.: Chem. Ber. **95,** 333 (1962); DENT, W. T., DUNCANSON, L. A., GUY, R. G., REED, H. W. B., SHAW, B. L.: Proc. Royal Soc. (London), 169 (1961); ERCOLI, R.: Chim. Ind. Milano, **44,** 565 (1962); ERCOLI, R., SANTAMBROGIO, E., TETTAMANTI-CASAGRADE, G.: Chim. Ind. (Milano) **44,** 1344 (1962)
3. KIM, P. J., HAGIHARA, N.: Bull. Chem. Soc. Japan **41,** 1184 (1968)
4. BOOTH, B. L., HASZELDINE, R. N., MITCHELL, P. R., COW, J. J.: J. Chem. Soc. (A), **1969,** 691

Gyula PÁLYI; Veszprém, Schönherz Z. u. 8, Hungary
Franco PIACENTI
Mario BIANCHI
Enzo BENEDETTI
56100 Pisa, Via Risorgimento 35, Italy.

G. C. PIMENTAL and R. D. SPRATLEY: *Chemical bonding clarified through quantum mechanics*, pp. 344.

Holden–Dy Inc., San Francisco–Cambridge–London–Amsterdam, 1969

Books dealing with valence discuss for the greater part the classic theory of bonding; on the other hand, the understanding of books published recently (which are based on quantum mechanics) causes considerable difficulties to readers who do not have a fundamental knowledge in certain fields of chemistry and mathematics. The book "Chemical bonding clarified through quantum mechanics" fills therefore a gap, because it presents the fundamentals of modern bonding theory in an entertaining way to those interested in chemistry. The two authors of the book are engaged in educational work, and their experience in teaching has been put to excellent use in their books which are known all over the world.

This book dealing with chemical bonding begins with a historical review. The way of progress is described as researchers got to the concepts of modern atomic theory through recognition of the corpuscular and wave nature of light and matter. The first chapter discusses line spectra. It is shown by means of vividly dscriptive examples (vibration of a guitar string or a drum) that there are also macroscopic systems, which, similarly to atoms, can take up only definite quantities of energy. The fundamental concepts of quantum chemistry are introduced in such a way that they may be understood by readers without a thorough mathematical background. After showing the connection between the wave function and probability distribution, the hydrogen atom is discussed in detail, and this is followed in the second chapter by the treatment of multi-electron atoms. The fundamental concepts of the theory of chemical bonding (nodal surfaces, PAULI's principle, effective nuclear charge, ionization energy, etc.) are presented with great skill in this part. The formation of the chemical bond is shown for the case of H_2^+, the most simple molecule, and compared with the He^+ ion, having the same number of protons and electrons (if the distance between the protons is more and more decreased in the H_2^+ molecular ion, the molecular orbitals are transformed into the atomic orbitals of a helium ion). The formation of bonding, antibonding and non-bonding molecular orbitals in multi-electron molecules is discussed on the basis of the M.O. method. The fifth chapter deals with older theories on the formation of the chemical bond. A particular merit of this chapter is the presentation of LINNET's electron quartet theory by means of a few examples.

The sixth chapter of the book gives an excellent summary on hybridization, hybrid orbitals and molecular dipole moments. This is followed by a discussion of the covalent bond, ionic bond, dative bond and a few special types of bonds. This part takes a very modern view, and reveals several relationships between the nature of the chemical bond and chemical properties. The last chapter, dealing with the laws of the solid and liquid states and the bonds occurring in these states, is a very valuable part of the book.

Tables in the Appendix (summarizing data on ionization energies, bond energies, bond lengths, force constants and dipole moments) support the statements expounded in the single chapters. The book is completed with a formula index and a subject index.

In summary, the book is characterized by a novel fresh style, modern views and a good gift of teaching. Logical arrangement of the subject-matter, lucid wording and the easy, almost conversational tone all contribute to make the book extremely readable and interesting.

The excellent, well selected figures, supporting the material described in the text, deserve special emphasis. This book of the popular authors will be extremely useful primarily to university students but also to chemists engaged in the various fields of chemistry. The translation of the book into Hungarian is to be recommended.

J. NAGY

L. SZEPESY: *Gas Chromatography*, pp. 384. Akadémiai Kiadó, Budapest, 1970

Gas chromatography is a separation process which finds widespread application. Its theory and practical application are discussed in several books. Among these, only a few are restricted to the theoretical and practical knowledge which is absolutely necessary for those who want to become acquainted with this technique, or for readers specialized in other fields but interested in gas chromatography. One of these works is the book by SZEPESY which has been published earlier in Hungarian and appears now in English, revised and considerably enlarged. The eleven chapters of the book provide the reader with a comprehensive picture on this separation process and give guidance for the acquirement of fundamentals and for the solving of practical problems. A subject index with about 1400 key-words complements the work, which permits to use it also as a hand-book. Numerous references at the end of each chapter, besides referring the reader to a wide field of literature help to acquire deeper insight in a selected topic.

Nowadays, gas chromatography is chiefly used in analytical work. Practical knowledge on gas chromatography, indispensable in routine analytical work, is discussed in Chapters 4—8. This detailed and extensive part (about 60 per cent of the book) gives useful, many-sided help for the solving of practical problems. Chapter 4 deals with the design of analytical instruments. It aims to help in the selection of the appropriate instrument, to obtain optimum operating conditions for the solving of different tasks. It summarizes a great variety of knowledge necessary for such selection on the mechanical, pneumatic, thermostating, electric and detector systems, from which the gas chromatograph is built. Chapter 5 discusses the selection of the chromatographic column best suited for the given analytical task. At the same time, it gives a survey on the various types of columns, on their connection in series, in parallel, or for backflush, and finally, summarizes the factors characteristic of the state of the column in operation. Chapter 6 gives details on the processing of retention data used for qualitative evaluation, and presents also other possibilities of qualitative analysis, thus combined chromatographic, spectrometric, etc. approaches. It summarizes methods used for quantitative analysis. Chapter 7 deals with special methods used for qualitative and quantitative analysis. Chapter 8 lists sources in the literature for several different analyses by gas chromatography.

The first three chapters of the book summarize the theoretical basis necessary for the understanding of practical applications. Chapter 1 is a general introduction to the theoretical and practical problems of gas chromatography. The general survey discusses historical development, presents the forums of discussion and the international organizations of this field and discusses the merits of the most important literature sources. Chapters 2 and 3 treat the pertinent relationships of flow, diffusion and distribution between phases, and discuss the theories relevant to gas chromatographic columns.

Chapters 9—11 report on those possibilities of gas chromatography which are utilized in purification processes on various scales, in the control of industrial processes, and in the measurement of physico-chemical characteristics. With the single problems, details are given also on the instruments and economic factors, directing thereby the interest of the reader to this special field.

Gy. ZÖLLNER

I. NÁRAY-SZABÓ: *Inorganic Crystal Chemistry*, pp. 479. Akadémiai Kiadó (Publishing House of the Hungarian Academy of Sciences), Budapest, 1969

The author of this book has been working as a successful contributor to the science of crystal chemistry for several decades. The determination of a number of crystal structures and the refining or correction of earlier results are associated with his name. His activity in research

has been coupled with the continuous study of literature, enabling the author to give in his book a modern view and a comprehensive survey of the advances in crystal chemistry. Copious references given in the text offer valuable guidance for those who wish to do further research in this branch of science. The book as a whole and in detail comprises the subject of the Hungarian edition published in 1965. Revisions are represented only by slight modifications, bringing up to date the literature, and by the addition of a new chapter (The Crystal Chemistry of Cations).

The first part of the book deals with the general principles of crystal chemistry, discussing the elements of crystal geometry, fundamental structural concepts, isomorphism, mixed crystals, sister structures, polymorphism, and PAULING's electrostatic valency principle.

The principal part of the book gives a systematic description of crystal structures. It comprises the whole domain of inorganic chemistry; as a novel approach, the periodic system has been chosen as the basis of arranging the material. With a thorough knowledge of the subject and critical evaluation, the material is presented concisely, still in sufficient detail. First, a short characterization is given of the groups according to chemical bonds, and this is followed by a detailed discussion. Elementary lattices, intermetallic and alloy structures are dealt with, then crystalline compounds of non-metals, and finally the compounds of metals are described. The mode of discussion of this large material is well balanced. Primarily, the principal types and structural relationships are shown in a modern presentation.

The value of the book is increased by the great number of data compiled in tabular form. These tables have been composed with expert care, and besides facilitating the survey of the subject, they direct the attention to the quantitative differences within lattice types and to the changes of crystal-chemical properties, as the lattice constants, physical data, etc. are shown next to one another.

Special mention must be made of the well selected, rich illustrations. For the illustration of the crystal chemical relations, the sphere-fitting method of R.W.G. WYCKOFF has been predominantly used. The figures are drawn with taste in a uniform style lending a special character to the book, and though slightly overdimensioned in most of the cases, they greatly contribute to the value of the book. On the other hand, it is regrettable that several structural figures are tilted or even turned upside down, while some of the drawings are incomplete or faulty. It may be mentioned that when the sphere-fitting method is used, in certain cases it would be desirable to show a line-diagram of the geometry of the structure and, in particular, the picture of the unit cell (as is indeed done in some of the cases), or at least the bond directions should be indicated on the principal figure. This would promote a better orientation, and give a general impression of the spatial arrangement, because the order of fitting of freely 'floating' spheres is didactically less expressive and such pictures can hardly be memorized.

It must be mentioned further that since the completion of the manuscript of the Hungarian edition of the book at the end of 1964, the crystal chemistry of some groups of compounds has greatly developed to include essential new material on certain details. Thus, for example, a more expressive and up-to-date discussion of borates, according to the categories of simple and more composite borate ions, would be possible today.

Speaking of the structure of the book, in the reviewer's opinion, the material in the first part of the introductory chapter (The Crystalline State) dealing with crystal morphology, and also the fundamentals of structure, could have been discussed in greater detail to yield a complete introduction into crystal chemistry. It can be stated again that some of the figures in this part have been drawn without the accuracy required in crystal geometry or their positions are incorrect. However, these observations hardly affect the great value of the book which has been published in a very attractive presentation. Most certainly, this book will occupy an appreciated position among the works of international scientific literature dealing with crystal chemistry.

K. I. SZTRÓKAY

INDEX

INORGANIC AND ANALYTICAL CHEMISTRY — ANORGANISCHE UND ANALYTISCHE CHEMIE — НЕОРГАНИЧЕСКАЯ И АНАЛИТИЧЕСКАЯ ХИМИЯ

JÓNÁS, K. and SOLYMÁR, K.: Determination of the Mineral Composition of Bauxites by Infrared Spectrophotometry 1

PÁPAY, K. M., MÁZOR, L. and TAKÁCS, J.: Spectrophotometric Determination of Fluorine in Organic Compounds with Thorium Chloranilate after Hydropyrolytic Decomposition of Lead Fluoride 13

PUNGOR, E. and PAPP, E.: Electrochemical Study on Ionite Membrane Electrodes 19

ÖTVÖS, I., SPEIER, G. and MARKÓ, L.: Chemistry of Transition Metal Nitrogen Complexes, II. Phosphine Exchange in Nitrogen Complexes of Cobalt (Short Communication) 27

RIOLO, C. B., SOLDI, T. F. and SPINI, G.: Oscillometric Study of Complex Formation (Short Communication) 29

PHYSICAL CHEMISTRY — PHYSIKALISCHE CHEMIE — ФИЗИЧЕСКАЯ ХИМИЯ

KISS, L. und FARKAS, J.: Untersuchung der Ionisation von Metallen und Metallionenneutralisation mit der Rotierenden Ringscheibenelektrode, IV. Allgemeiner Zusammenhang für den in *m* Schritten verlaufenden Vorgang (Investigation of the Ionization and Neutralization of Metals on the Rotary Ring-Disk Electrode, IV. General Relationship for Processes Proceeding in *m* Steps) 33

DÉVAY, J. and SAYED SABET ABD EL REHIM: Measurements on A. C. Corrosion Models 39

LISZI, J.: The Excess Free Enthalpy and Excess Entropy of Mixing of Acetic Acid–Carbon Tetrachloride Mixture 47

GÁL, D., BLUMBERG, E. A., VALENDO, A. YA. and EMANUEL, N. M.: Data on Competitive Oxidations, I. The Non-Catalytic Cooxidation of Ethylbenzene and Propylene 55

GÉCZY, I.: Synthetische Lineare Polymere, XXIX. Zusammenhang zwischen dem spezifischen Drehvermögen und dem Molekulargewicht bei monotonen Oligopeptiden (Synthetic Linear Polymers, XXIX. Relationship between the Specific Rotation and the Molecular Weight of Monotone Oligopeptides) 77

FOGARASI, G.: The Extreme Values of Force Constants and Mean Vibrational Amplitudes of Ethylene-type Molecules, II. C_2F_4, C_2Cl_4, C_2Br_4 87

SZTRAKA, L.: Relationship between Inversion and Internal-Rotation of Methylamine, II. The Hamilton Operator and the Elements of the Hamilton Matrix 99

ORGANIC CHEMISTRY — ORGANISCHE CHEMIE — ОРГАНИЧЕСКАЯ ХИМИЯ

BARTÓK, M., BOZÓKI-BARTÓK, G. and KOVÁCS, K.: The Chemistry of 1,3-Bifunctional Systems, VII. Mechanism of the Conversion of 1,3-Chlorohydrins in Alkaline Medium 115

PÁLYI, G., PIACENTI, F., BIANCHI, M. and BENEDETTI, E.: Methinyltricobalt Enneacarbonyl Compounds, I. New Method of Preparation of Alkyl Derivatives (Short Communication) 127

BOOK REVIEWS — BUCHBESPRECHUNGEN — РЕЦЕНЗИИ КНИГ 131

Printed in Hungary

A kiadásért felel az Akadémiai Kiadó igazgatója — Műszaki szerkesztő: Farkas Sándor

A kézirat nyomdába érkezett: 1970. VI. 11. — Terjedelem: 11,75 (A/5) ív, 57 ábra

70.69885 Akadémiai Nyomda, Budapest — Felelős vezető: Bernát György

ACTA CHIMICA

ТОМ 66 — ВЫП. 1

РЕЗЮМЕ

Определение состава минералов в бокситах с помощью ИК спектрофотометрии

К. ЙОНАШ и К. ШОЙМАР

Был разработан метод определения содержания минералов в бокситах с помощью ИК спектроскопии. На основе калибровочных кривых, полученных с бокситами с известными химическим и минеральным составом и со строением, подобным изученным образцам, каолинит определялся при 918 $см^{-1}$ и 3700 $см^{-1}$, бемит — при 3100 $см^{-1}$ и гиббсит — при 3455 и 3530 $см^{-1}$. Для анализа же образцов, отличающихся от калибровочных по степени кристалличности и структуре, предлагается метод, основанный на измерении относительной интенсивности полос ИК спектра.

Метод спектрофотометрического определения содержания фтора в органических соединениях с помощью реагента—торий-хлоранилата, используемого после гидропиролитического разложения фтористым свинцом

М. К. ПАПАИ, Л. МАЗОР и Й. ТАКАЧ

Авторами совершенствовался метод определения содержания фтора в органических соединениях. Фтор, закрепленный в слое миния, после гидропиролитического разложения фтористым свинцом, определяется спектрофотометрически в дистилляте с помощью реагента — торий-хлоранилата. Оспаривалось утверждение американских авторов о том, что метил-целлозольв усиливает интенсивность окраски хлораниловой кислоты. На основе экспериментальных исследований было доказано, что усиление окраски происходит за счет примесей железа в метил-целлозольве, т. к. ионы железа(III) образуют с хлораниловой кислотой комплекс с яркой фиолетовой окраской. Приводятся результаты анализа некоторых фторсодержащих органических соединений.

Электрохимическое изучение ионитовых мембранных электродов

Э. ПУНГОР и Э. ПАПП

Авторами изучалось электрохимическое поведение гетерогенно построенных катионитовых и анионитовых мембранных электродов. В первую очередь, изучалось время жизни приготовленных электродов при постоянном вымачивании, а также селективность электродов к отдельным ионам. Результаты подтверждают более раннее заключение о том, что мембранные электроды, приготовленные из нетекучих ионообменных смол, являются пермселективными. Во второй части сообщения, на примере перхлоратного ионитового мембранного электрода, обсуждаются возможности использования пермселективных мембранных электродов.

Изучение ионизации металлов и восстановления ионов металлов с помощью вращающегося дискового электрода с кольцом, IV

Л. КИШ и Й. ФАРКАШ

Была определена зависимость, с помощью которой можно рассматривать многостадийные электродные процессы (число стадий — m) при наличии перенапряжения перехода и диффузии. На отдельных ступенях электродного процесса осуществляется переход $n_1, n_2, n_3, \ldots n_i \ldots n_m$ электронов, а разность числа электронов между исходным и конечным продуктом равна $\sum_{i=1}^{m} n_i = N_m$. На основании материального и зарядного баланса происходящих процессов, можно составить систему линейных неоднородных уравнений, которую можно решить методом определителей. Таким образом, можно получить поляризационную кривую процесса и концентрацию промежуточных продуктов у поверхности электрода.

Некоторые модельные измерения коррозии под влиянием переменного тока

Й. ДЕВАИ и САЙЕД САБЕТ АБД ЭЛЬ РЕХИМ

Модельные измерения коррозии под влиянием переменного тока производились, с одной стороны, в гальваноэлементе с капельным ртутным электродом, как катодом, помещенным в редокси-систему Fe^{3+}/Fe^{2+}, и с водородным электродом как анодом, помещенным в растворы с различными pH, а с другой стороны, на железном электроде, помещенным в раствор хинона. Было установлено, что под влиянием переменного тока кривые поляризации в катодном и анодном процессах, в зависимости от их характера, либо изменяются, либо остаются без изменений. Коррозия, наблюдаемая в течение модельных измерений, объясняется на основе изменения поляризационных кривых. На основе этих измерений удалось доказать экспериментально, что в зависимости от условий, переменный ток может либо уменьшать, либо совсем не изменять электролитическую коррозию металлов.

Изменение свободной энтальпии и энтропии при смешении уксусной кислоты с четыреххлористым углеродом

Й. ЛИСИ

Определялось изменение свободной энтальпии и энтропии при смешении уксусной кислоты с четыреххлористым углеродом при 20°C. Номинально двухкомпонентную смесь в расчетах рассматривали как регулярную трехкомпонентную смесь типа $A—A_2—B$ (где A — мономер уксусной кислоты, A_2 — димер уксусной кислоты и B — четыреххлористый углерод). Изменение свободной энтальпии при смешении преставлялось как сумма двух членов:

1. соответствующего реакции ассоциации — g^E_{ass} и 2. соответствующего реальному смешению — g^E_{rea}. Было установлено, что величины обоих членов g^E_{ass} и g^E_{real}, составляющих изменение свободной энтальпии при смешении, имеют одинаковый порядок.

Совместное окисление, I

Совместное некаталитическое окисление этилбензола и пропилена

Д. ГАЛ, Е. А. БЛЮМБЕРГ, Г. Ю. ВАЛЕНДА и Н. М. ЭМАНУЭЛЬ

Авторами изучался, так называемый, процесс Халкона с кинетической точки зрения с целью выяснения механизма последнего. Несмотря на то, что процесс протекает в пятикомпонентной системе (этилбензол, гидроперекись этилбензола, кислород, пропилен и

катализатор), начальные исследования проводились в системах, содержащих определенное но меньшее пяти число компонентов, а именно: этилбензол + кислород; этилбензол + гидроперекись этилбензола; этилбензол + гидроперекись этилбензола + пропилен; этилбензол + гидроперекись этилбензола + пропилен + кислород. Исходя из данных экспериментов, проводимых при атмосферном и высоком давлениях, а также на основе литературных данных определялись энергия активации зарождения цепей и константы скоростей моно- и бимолекулярного распада гидроперекиси в данных экспериментальных условиях. Полагая, что при начальной стадии реакция образования ацетофенона в присутствии незначительных количеств спирта, в основном, протекает через стадию рекомбинации, рассчитывалась концентрация перекисных радикалов в зависимости от экспериментальных условий.

Полагалось, что образование эпоксида в отсутствии катализатора протекает по радикальному механизму Твигга, и на основе этого определялась константа скорости элементарной реакций взаимодействия пропилена с перекисными радикалами.

Синтетические линейные полимеры, XXIX

Зависимость между удельным оптическим вращением монотонных олигопептидов и их молекулярным весом

И. ГЕЦИ

Зависимость между удельным оптическим вращением и молекулярным весом, найденная автором для олигосахаридов [12], оказалась справедливой и для членов полимерного гомологического ряда монотонных олигопептидов:

$$[\alpha]_\Lambda = \frac{a}{M} + b \,,$$

где $[\alpha]_\Lambda$ — удельное оптическое вращение, M — молекулярный вес, a и b — постоянные, первая из них характеризующая конечную группу в неявной форме, а вторая — промежуточные члены в явной форме. Поскольку исследуемый олигопептид присутствует в геликальной форме, то наблюдается отклонение от вышеприведенного уравнения. Отсюда можно также судить и о вторичной структуре монотонных олигопептидов. На основе постоянной b уравнения автором приводятся инкременты молекулярного оптического вращения в различных растворителях для некоторых изученных олигопептидов. На основе исследований с поли-γ-бензил-L-глутаматом было установлено, что вследствие строгой зависимости между оптическим вращением и дипольным моментом, вероятно, что вторичное строение может быть определено и на основе измерения удельного квадратичного дипольного момента.

Экстремальные значения силовых постоянных и средних амплитуд колебаний молекул типа этилена, II

C_2F_4, C_2Cl_4 и C_2Br_4

Г. ФОГАРАШИ

Применяя параметрический метод Тёрёка и Пулаи к молекулам C_2F_4, C_2Cl_4 и C_2Br_4, была получена многочисленная серия силовых постоянных и средних амплитуд колебаний, воспроизводящих экспериментальные нормальные частоты; изучались их экстремальные значения. Экстремальные значения дают информацию о системе связей даже и в том случае, когда силовые постоянные не могут быть определены однозначно. Измеренные и рассчитанные значения амплитуд колебаний значительно различаются, причиной чего может служить неточность электроннодиффракционных измерений.

Связь между инверсией и внутренним вращением в метиламине, II

Оператор Гамильтона и элементы матрицы Гамильтона

Л. СТРАКА

Были выведены операторы Гамильтона для вращения, внутреннего вращения и инверсии в метиламине, а также приводятся элементы матрицы Гамильтона. Было показано, что изложенная в сообщении теория описывает явления гораздо точнее и более обще, по сравнению с предыдущими.

Химия 1,3-бифункциональных систем, VII

Механизм превращений 1,3-хлоргидринов в щелочных средах

М. БАРТОК, Г. БОЗОКИ-БАРТОК и К. КОВАЧ

Определялись и сравнивались скорости щелочного гидролиза бутилхлорида и втор.-бутилхлорида, а также 1,3-хлоргидринов с соответствующим скелетом. Щелочной гидролиз 2,2-диэтил-3-хлорпропанола (I) изучался кинетическими методом. На основе последних исследований удалось установить механизм превращений 1,3-хлоргидринов, в результате чего образуются оксациклобутаны.

The Acta Chimica publish papers on chemistry in English, German, French and Russian.

The Acta Chimica appear in volumes consisting of four parts of varying size, 4 volumes being published a year.

Manuscripts should be addressed to

Acta Chimica
Budapest 112/91 Műegyetem

Correspondence with the editors should be sent to the same address.

The rate of subscription is $16.00 a volume.

Orders may be placed with "*Kultúra*" Foreign Trade Company for Books and Newspapers (Budapest I., Fő utca 32. Account No. 43-790-057-181) or with representatives abroad.

Les Acta Chimica paraissent en français, allemand, anglais et russe et publient des mémoires du domaine des sciences chimiques.

Les Acta Chimica sont publiés sous forme de fascicules. Quatre fascicules seront réunis en un volume (4 volumes par an).

On est prié d'envoyer les manuscrits destinés à la rédaction à l'adresse suivante:

Acta Chimica
Budapest 112/91 Műegyetem

Toute correspondance doit être envoyée à cette même adresse.

Les prix de l'abonnement est de $16.00 par volume.

On peut s'abonner à l'Entreprise pour le Commerce Extérieur de Livres et Journaux «*Kultúra*» (Budapest I., Fő utca 32. Compte-courant No. 43-790-057-181) ou à l'étranger chez tous les représentants ou dépositaires.

«*Acta Chimica*» издают трактаты из области химической науки на русском, французском, английском и немецком языках.

«*Acta Chimica*» выходят отдельными выпусками разного объема. 4 выпуска составляют один том. 4 тома публикуются в год.

Предназначенные для публикации рукописи следует направлять по адресу:

Acta Chimica
Budapest 112/91 Műegyetem

По этому же адресу направлять всякую корреспонденцию для редакции.

Подписная цена — $16.00 за том.

Заказы принимает предприятие по внешней торговле книг и газет «*Kultúra*» (Budapest I., Fő utca 32. Текущий счет № 43-790-057-181) или его заграничные представительства и уполномоченные.

Reviews of the Hungarian Academy of Sciences are obtainable at the following addresses:

ALBANIA
Drejtorija Qändrone e Pärhapjes dhe Propagandimit tä Librit
Kruga Konferenca e Päzes
Tirana

AUSTRALIA
A. Keesing
Box 4886, GPO
Sydney

AUSTRIA
GLOBUS
Höchstädtplatz 3
A-1200 Wien XX

BELGIUM
Office International de Librairie
30, Avenue Marnix
Bruxelles 5
Du Monde Entier
5, Place St. Jean
Bruxelles

BULGARIA
HEMUS
11 pl Slaveikov
Sofia

CANADA
Pannonia Books
2, Spadina Road
Toronto 4, Ont.

CHINA
Waiwen Shudian
Peking
P. O. B. 88

CZECHOSLOVAKIA
Artia
Ve Smečkách 30
Praha 2
Poštovní Novinová Služba
Dovoz tisku
Vinohradská 46
Praha 2
Mad'arská Kultura
Václavské nám. 2
Praha 1
SLOVART A. G.
Gorkého
Bratislava

DENMARK
Ejnar Munksgaard
Nörregade 6
Copenhagen

FINLAND
Akateeminen Kirjakauppa
Keskuskatu 2
Helsinki

FRANCE
Office International de Documentation et Librairie
48, rue Gay Lussac
Paris 5

GERMAN DEMOCRATIC REPUBLIC
Deutscher Buch-Export und Import
Leninstraße 16
Leipzig 701
Zeitungsvertriebsamt
Fruchtstraße 3—4
1004 Berlin

GERMAN FEDERAL REPUBLIC
Kunst und Wissen
Erich Bieber
Postfach 46
7 Stuttgart S.

GREAT BRITAIN
Blackwell's Periodicals
Oxenford House
Magdalen Street
Oxford
Collet's Subscription Import Department
Dennington Estate
Wellingsborough. Northants.
Robert Maxwell and Co. Ltd.
4—5 Fitzroy Square
London W. 1

HOLLAND
Swetz and Zeitlinger
Keizersgracht 471—487
Amsterdam C.
Martinus Nijhof
Lange Voorhout 9
The Hague

INDIA
Hind Book House
66 Babar Road
New Delhi 1

ITALY
Santo Vanasia
Via M. Macchi 71
Milano
Libreria Commissionaria Sansoni
Vie La Marmora 45
Firenze

JAPAN
Kinokuniya Book-Store Co. Ltd.
826 Tsunohazu 1-chome
Shinjuku-ku
Tokyo
Maruzen and Co. Ltd.
P. O. Box 605
Tokyo-Central

KOREA
Chulpanmul
Phenjan

NORWAY
Tanum-Cammermeyer
Karl Johansgt 41—43
Oslo 1

POLAND
RUCH
ul. Wronia 23
Warszawa

ROUMANIA
Cartimex
Str. Aristide Briand 14—18
Bucureşti

SOVIET UNION
Mezhdunarodnaya Kniga
Moscow G—200

SWEDEN
Almquist and Wiksell
Gamla Brogatan 26
S—101 20 Stockholm

USA
F. W. Faxon Co. Inc.
15 Southwest Park
Westwtood Mass. 02090
Stechert Hafner Inc.
31. East 10th Street
New York, N. Y. 10003

VIETNAM
Xunhasaba
19, Tran Quoc Toan
Hanoi

YUGOSLAVIA
Forum
Vojvode Mišića broj 1
Novi Sad
Jugoslovenska Knjiga
Terazije 27
Beograd

ACTA CHIMICA

ACADEMIAE SCIENTIARUM HUNGARICAE

ADIUVANTIBUS

V. BRUCKNER, GY. DRÁK, K. POLINSZKY,
E. PUNGOR, G. SCHAY, Z. G. SZABÓ

REDIGIT

B. LENGYEL

TOMUS 66 FASCICULUS 2

AKADÉMIAI KIADÓ, BUDAPEST

ACTA CHIMICA

A MAGYAR TUDOMÁNYOS AKADÉMIA KÉMIAI TUDOMÁNYOK OSZTÁLYÁNAK IDEGEN NYELVŰ KÖZLEMÉNYEI

SZERKESZTI

LENGYEL BÉLA

TECHNIKAI SZERKESZTŐK

DEÁK GYULA és HARASZTHY-PAPP MELINDA

Az Acta Chimica német, angol, francia és orosz nyelven közöl értekezéseket a kémiai tudományok köréből.

Az Acta Chimica változó terjedelmű füzetekben jelenik meg, egy-egy kötet négy füzetből áll. Évente átlag négy kötet jelenik meg.

A közlésre szánt kéziratok a szerkesztőség címére (Budapest 112/91 Műegyetem) küldendők.

Ugyanerre a címre küldendő minden szerkesztőségi levelezés. A szerkesztőség kéziratokat nem ad vissza.

Megrendelhető a belföld számára az „Akadémiai Kiadó"-nál (Budapest V., Alkotmány utca 21. Bankszámla 05-915-111-46), a külföld számára pedig a „Kultúra" Könyv- és Hírlap Külkereskedelmi Vállalatnál (Budapest I., Fő utca 32. Bankszámla: 43-790-057-181) vagy annak külföldi képviseleteinél és bizományosainál.

Die Acta Chimica veröffentlichen Abhandlungen aus dem Bereiche der chemischen Wissenschaften in deutscher, englischer, französischer und russischer Sprache.

Die Acta Chimica erscheinen in Heften wechselnden Umfanges. Vier Hefte bilden einen Band. Jährlich erscheinen 4 Bände.

Die zur Veröffentlichung bestimmten Manuskripte sind an folgende Adresse zu senden:

Acta Chimica
Budapest 112/91 Műegyetem

An die gleiche Anschrift ist auch jede für die Redaktion bestimmte Korrespondenz zu richten. Abonnementspreis pro Band: $ 16.00.

Bestellbar bei dem Buch- und Zeitungs-Außenhandels-Unternehmen »*Kultúra*« (Budapest I., Fő utca 32. Bankkonto No. 43-790-057-181) oder bei seinen Auslandsvertretungen und Kommissionären.

Acta Chimica Academiae Scientiarum Hungaricae, Tomus 66 (2), pp. 135—157 (1970)

LÁSZLÓ ERDEY

(1910—1970)

On February 21, 1970, at the age of 60, with tragic suddenness died Dr. László ERDEY, one of the most outstanding Hungarian chemists, twice winner of the Kossuth Prize, Member of the Hungarian Academy of Sciences, Professor of Chemistry and Head of the Department of General and Analytical Chemistry, Technical University of Budapest, chairman and member of numerous Hungarian and foreign international scientific organizations.

László ERDEY was born on February 12, 1910, in Szeged, Hungary, where he also attended elementary and high schools. His interest in and inclination for natural sciences was displayed early and brought him the first prize in a national high-school contest in physics. After completing his studies at the University of Budapest, he received a diploma in chemical and physical education. ERDEY did his graduate work in the No. III Institute of Chemistry, University of Budapest, and obtained his doctor's degree with 'summa cum laude' qualification. As a result of the prevailing high scientific level, the No. III Institute of Chemistry headed by Professor BUCHBÖCK was regarded at that time as the center of Hungarian physical and theoretical chemistry. Numerous associates of the Institute have since become prominent representatives of the reviving chemical science in Hungary.

ERDEY not only recognized but also emphasized, and proved by his life-work, the basic principle that fruitful development of applied sciences is only possible on the basis of extensive knowledge coupled with creative activity in the related branches of science.

After obtaining his diploma and under the difficult war-time conditions, he was employed by the National Institute of Public Health, the Patent Court, and later by the Institute of Chemistry of Budapest. It was while being associated with these institutions that he accumulated the great experience required by successful research in analytical chemistry, and developed his special ability to approach the solution of the most diverse analytical problems.

He maintained a never-ceasing contact with university education. Under the most difficult conditions after the war, he was active in restoring higher education as an instructor and invited lecturer.

The year 1950 marked an important milestone in his life when he was appointed Professor of Chemistry and Head of the Department of General and Analytical Chemistry at the Technical University of Budapest. It was due to his prominence as a scientist and organizer that the Department, soon after its restoration following war-time destruction, achieved scientific results commanding appreciation not only in Hungary but also abroad. As Dean of the Faculty, between 1950 and 1953 he organized and directed the new, independent Faculty of Chemical Engineering and carried out the educational reform.

In recognition of his scientific achievements he was elected Corresponding Member of the Hungarian Academy of Sciences in 1951 and became a full member in 1955. The Hungarian Government awarded him the Kossuth Prize in 1951 and 1958, the Vth grade of the Order of Merit in 1950, the Order of Labour in 1955 and 1960. In 1970, shortly before his death he was awarded the Golden Order of Labour by the State Presidium. His social activity was honoured by the Hanus Medal of the Czechoslovak Chemical Society and the Károly Than Medal of the Hungarian Chemical Society.

ERDEY's scientific work was devoted to the development of analytical chemistry. His life-work is a continuation of the traditions of analytical chemistry in Hungary. However, instead of the old empirical approach he introduced the physico-chemical interpretation of phenomena.

In the course of his graduate work, he studied the behaviour of amalgam electrodes and showed that in the presence of foreign electrolytes the electrode assumes a reproducible potential even in solutions which are extremely dilute with respect to the proper ion. He established the dependence of the potential on the amalgam concentration and explained it quantitatively on the basis of the Gibbs—Helmholtz theory.

The wide experience gained during the years spent in the laboratory and the physico-chemical view in interpreting the facts are reflected in his book entitled "Introduction to Chemical Analysis" published in two volumes, "Qualitative Analysis" (1945) and "Volumetric Analysis" (1947). The scientific, practical and educational importance of these books is best shown by the fact that, with only slight revisions and extensions in the text, "Qualitative Analysis" and "Volumetric Analysis" have been published in 8 and 10 editions respectively. It is very regrettable that during the difficult years of post-war reconstruction publication in foreign languages was impossible, and therefore these volumes written with a fresh and new approach and dealing with the fundamentals and the most important branches of analytical chemistry of that time have remained unknown to non-Hungarian readers.

After his appointment at the Technical University of Budapest, Professor ERDEY restarted his scientific work with great enthusiasm and, considering the possibilities and requirements of that period, he organized research

in the Institute in such a manner that every modern branch of analytical chemistry was represented.

It is impossible on a few pages to give a full account of the research and results achieved in the Institute. There is hardly any field in analytical chemistry in which he, together with his associates, did not perform creative work. Therefore, we can only survey here the chief directions of Professor ERDEY's research, mentioning the most significant results.

In the first years, his attention was directed primarily towards volumetric analysis, and he developed a new reductometric method known as ascorbinometry. This discovery was of great importance since it permitted direct volumetric determination of the most diverse substances. During these years spent in feverish research, new scientific results and methods were produced almost every day, among them the determination of iron(III), chlorate, iodate, iodide, bromate, silver, mercury(II), hexacyanoferrate(III), and other ions.

At the same time, it was discovered in the Institute that Variamine Blue (4-amino-4'-methoxy-phenylamine) can be applied as a redox indicator and a versatile chemical reagent. Variamine Blue proved to be an excellent indicator not only in ascorbinometric titrations but also in iodometry, argentometry and even complexometry.

After the successful application of Variamine Blue as an indicator, he started an extensive research program directed towards the preparation of new reversible redox indicators of the diphenylamine type and towards the elucidation of mechanism of their operation. By introducing nucleophilic and electrophilic substituents into the diphenylamine skeleton, it was possible to influence the basicity of the parent compounds and their standard redox potential. By electrometric and ESR measurements, he showed that the oxidation of the leuco form of Variamine Blue and its derivatives occurred by free radical mechanism. A likely structure and formula were also proposed for the radical ion. An important derivative among the new indicators is 2-hydroxy Variamine Blue which, as opposed to common indicators, behaves reversibly over a very wide pH range (2—11). Another interesting new compound was the thiourea derivative of Variamine Blue, the first indicator which permitted visual end-point detection of redox titrations in non-aqueous media.

Subsequent studies revealed that Variamine Blue was suitable for the determination of numerous elements and ions as a colourimetric reagent and, as an organic precipitant, it could be used for the selective precipitation and determination of tungsten. Utilizing the Variamine Blue–hydrogen peroxide reaction, the determination of ultramicro amounts of iron (2×10^{-9} g/ml) became possible by means of catalytic chronometric methods.

Another important direction of his indicator research was the elucidation of the mechanism of operation and the practical applications of chemi-

luminescent indicators (Lucigenin, Luminol, Lophin, Siloxen). ERDEY successfully clarified the mechanism of the reversible and irreversible chemiluminescent reactions of Lucigenin. It has been shown that in alkaline solutions, Lucigenin peroxide is formed with perhydroxide ions, which then releases oxygen while being converted to an excited molecule in which the two unpaired electrons are in the triplet state. Transition to the singlet state is accompanied by yellow-green luminescence and the resulting compound is converted by perhydroxide ions to the original substance. In the presence of catalysts (alcohol, osmium tetroxide, etc.) Lucigenin is converted irreversibly to inactive methylacridone while emitting a blue light.

The mechanism of the chemiluminescent reactions of Luminol and Lophin were interpreted in a similar manner. ERDEY was the first to apply light-emitting indicators for end-point detection in redox and chelatometric titrations. Using the above indicators, numerous volumetric methods of analysis were developed for cases where this had not been feasible earlier owing to the lack of suitable indicators.

During the study of luminescent indicators, ERDEY discovered that double indicator systems such as Fluorescein–Luminol and Fluorescein–Lucigenin can be applied as reversible acid–base indicators.

Studies on luminescent indicators directed his attention towards a more thorough investigation of the autodecomposition and other reactions of hydrogen peroxide. He established that the cyclic intermediate formed from the perhydroxide ion and hydrogen peroxide had an important role in the autodecomposition observed in pure hydrogen peroxide solutions. He also studied and clarified the mechanism of reaction between hydrogen peroxide and hypohalites. As a result of his studies on the reactions of hydrogen peroxide, new analytical methods were developed in which hydrogen peroxide was applied as a titrant.

Among the results of his studies on reactions occurring in non-aqueous solvents, it is necessary to mention the new redox titration methods worked out in the Institute (*e.g.*, the cyanometric determination of sulfur and selenium), and his new method of qualitative inorganic analysis where the reactions of detection are carried out in formic acid medium.

Simultaneously with basic research, to satisfy urgent needs of the chemical and metallurgical industries, ERDEY and his associates developed a number of new photometric techniques for the determination of germanium, gold, zinc, copper, vanadium, calcium, chromium, silver, and phosphorus impurities in the most diverse substances (bauxite, alumina, noble metals, etc.), utilizing modern separation techniques, such as extraction and ion exchange.

Together with his associates, he developed the theory of analytical application of the Landolt-type reactions which permitted the chronometric and microanalytical determination of numerous metal ions (Fe, Mo, etc.).

The main direction of his research in emission spectrography was the improvement of solution and powder techniques. His objective was to increase the sensitivity and reliability of these methods together with extending their field of application, utilizing the enrichment and separation methods of chemical analysis. The tube-electrode spray technique (earlier referred to as the drilled-electrode method) has found widespread application in the analysis of various industrial raw materials and products. By means of a continuous feeding device, he solved the problem of continuous excitation of powder samples, greatly increasing the accuracy of analysis. The method of 'full evaporation with arc-excitation' has made possible the extensive study of excitation processes.

The first applications of atomic absorption spectrophotometry in Hungary are also due to ERDEY. In addition to determining the optimum conditions for the analysis of numerous metal ions, it has been shown that atomic absorption photometry is also possible using an a.c. arc, *i.e.* with a resolution of the spectra in time.

His main objective in flame-photometry research was the analytical utilization of chemical reactions occurring in flames. Together with his associates he developed the so-called flame-photometric titration method for the determination of calcium ions. The flame-photometric determination of phosphate ions was achieved by an indirect method.

Among the theoretical problems of gravimetric analysis, he was mainly interested in the mechanism of precipitation, in the composition, structure, morphology and thermal properties of precipitates. His three-volume book "Gravimetric Analysis", published in Hungarian (1960), German (1964) and English (1965) is regarded as the most comprehensive treatise of this branch of analytical chemistry. In this book, ERDEY gives a critical survey of the various precipitation methods, based on systematic precipitation and thermoanalytical studies performed in the course of several years in his Institute.

In connection with studies on the thermal behaviour of analytical precipitates, in collaboration with two of his associates, he developed derivatography, a new, complex method of thermal analysis. The method of derivatography is a combination of the earlier methods of thermal analysis with the so-called derivative thermogravimetry invented by them, and thus represents a completely new principle of measurement. The new instrument, derivatograph, developed for the purpose of such measurements, is now manufactured in serial production and exported to various countries. The great significance and impact of derivatography on thermoanalytical research is best demonstrated by the approximately 800 scientific papers that have been published so far about derivatographic studies in various countries.

The derivatograph is a tool for studying the thermal behaviour of solid and liquid substances. With a single sample, one can perform thermogravi-

metric, derivative thermogravimetric, differential-thermoanalytical and thermodilatometric studies, and an accessory part developed recently also allows continuous analysis of the gaseous products formed in the thermal process.

The derivatograph permits not only a systematic study of analytical precipitates, but also the investigation of thermal properties of the most diverse inorganic and organic substances. The derivatographic research group of the Institute has developed analytical methods for the determination of the composition of clay minerals, rocks, drugs, biological substances (tooth, bone, kidney stone), as well as for the technological control of alumina, insulator, semiconductor, ceramics and construction-material processes, for the qualification of coal, for studying the setting of cement and the thermal stability of plastics.

A special field of thermal studies was represented by the projects aimed at elucidating the structure of fused organic salts by determining the conductivity and viscosity of melts.

The mechanism of high-temperature inorganic reactions was interpreted by ERDEY on the basis of a new acid–base theory. The starting point of the theory is the assumption that the variation of chemical bond strength with temperature is determined by the relative acid–base strength or electron affinity of the ions or atomic groups. This theory facilitated the interpretation of the mechanism and temperature dependence of reactions occurring during fusion with alkali carbonates.

With the purpose of studying the morphology and structure of analytical precipitates and other solids, he combined thermal analysis with X-ray diffraction, electron microscopic and infrared measurements. These complex studies have thrown light *e.g.* on the structure of barium sulfate precipitated under different conditions and on the changes occurring during thermal treatment.

With his associates he developed the theory of so-called precipitation exchange reactions which take place between the precipitate and the ions in the surrounding solution, and carried out systematic studies on a number of such reactions, applying radioactive tracer methods. Together with his associates, he worked out volumetric methods for the determination of various ions (chloride, sulfate, etc.) in dilute solutions utilizing precipitation exchange reactions.

The use of precipitation exchange and coordination chemical reactions permitted the radioanalytical determination of micro amounts of various ions. The development of these methods greatly contributed to the improvement of radioanalytical techniques. ERDEY's name is associated also with the first radiometric acid–base titration method.

By means of neutron activation analysis, among others, the problem of determining trace impurities in hydrogenation catalysts has been solved.

ERDEY also contributed to the field of organic analysis by developing methods for the micro determination of phosphorus, sulfur, halogens, carbon, hydrogen and nitrogen in organic substances. The determination of carbon, hydrogen, and nitrogen was solved by a method combining pyrolysis with gas chromatography. In the field of analysis by functional groups, he developed useful methods for the determination of hydroxyl groups and nitroalkanes.

In connection with electroanalysis, he was primarily interested in potentiometry, polarography and in the dead-stop and high-frequency methods. He applied the high-frequency method for end-point detection in redox titrations.

He successfully used thin-layer chromatography in indicator research and developed a number of ion exchange and extraction methods employed in the photometric determination of trace elements.

The research conducted by ERDEY on the theory of gas chromatography is also significant. He developed a new quantitative analytical method which led to a greatly increased accuracy of gas chromatographic measurements. His last research project was also concerned with the theory of gas chromatography. A method was suggested for calculating the retention index from the data obtained by programmed-temperature gas chromatography, and a new equation derived for calculating the error of the retention index.

He was also interested in general theoretical problems of analytical chemistry and in the methodology of research in this field. ERDEY developed methods for the calculation of error in various analytical procedures. In one of his last papers, he discussed the basic principles of analytical chemistry and summarized the criteria necessary for fruitful research and correct data evaluation.

Together with his associates, he tock part in the solution of numerous technological and industrial analytical problems. He developed an instrumental end-point detection method for the basic reaction of industrial sodium dithionite production. In connection with the production of electrolyte capacitors, he devised a new technique for controlling the thickness of the oxide layer on the surface of aluminium foils. He constructed an automatic apparatus for the sterilization of drinking water.

The first Hungarian production of thermoluminescent substances to be used in dosimeters was realized in his Institute.

The scientific achievements of the Institute soon found wide international response. He was indefatigable on his lecturing tours and as participant of numerous international conferences.

In addition to his widespread scientific activity, Professor ERDEY exerted significant organizational activity to promote and co-ordinate the development of natural and engineering sciences in Hungary. He organized the Department of Chemical Sciences in the new Hungarian Academy of Sciences

and was active as its Secretary for nearly 8 years. He held various offices in numerous Hungarian scientific committees and societies.

As member of the governing body of the Analytical Chemistry Division of IUPAC, member of the Standardization Committee of the International Confederation for Thermal Analysis and of CITCE (Comité International de Thermodynamique et de Cinétique Electrochimiques), he also took part in solving international problems of chemical sciences.

As office-holder in various social organizations (Hungarian Chemical Society) and as honorary member of numerous societies (Societé Chimique Industrielle, Czechoslovak Chemical Society) he was often active in organizing scientific meetings and international conferences.

His activities in connection with the publication and edition of scientific journals and books were also significant. He participated in the editorial work of the journals of the Academy, Acta Chimica Hungarica and Kémiai Közlemények. He was a member of the editorial board of Periodica Polytechnica, Magyar Kémikusok Lapja and Magyar Kémiai Folyóirat. He was Chief Editor of the Journal of Thermal Analysis, regional editor of the Journal of Radioanalytical Chemistry and member of the Editorial Board of Talanta.

This short account would be incomplete without the appreciation of ERDEY's outstanding educational work. He has been a teacher almost since his childhood. First as a schoolboy he helped his school-fellows, then as a university professor he taught his students, who listened with close attention to his lectures which he prepared with great care. He was a genuine teacher with a conscious aim to arouse the scientific interest of his students and associates. His brilliant intellect enraptured everyone, filling his audience with enthusiasm.

With his life-work László ERDEY made an outstanding contribution to the science of chemistry and to the international prestige of Hungarian science.

J. INCZÉDY

LIST OF PUBLICATIONS BY PROFESSOR L. ERDEY

1. ERDEY, L.: Amalgámelektródok vizsgálata „saját-ionos" és „idegen-ionos" oldatokban. Bölcsészdoktori értekezés, (Investigation of Amalgam Electrodes in Solutions Containing Proper and Foreign Ions, Ph. D. Thesis), Budapest, 1938
ERDEY-GRÚZ, T., ERDEY, L.: Über das Verhalten von Quecksilberamalgamen in eigenionigen und fremdionigen Lösungen. Z. phys. Chem. A **183,** 401 (1939)
2. ERDEY, L.: Néhány fém mikroanalitikai kimutatása katalitikus reakciókkal. (Microanalytical Detection of some Metals by means of Catalytic Reactions). Magy. Kém. Lapja **3,** 45, 65 (1942)
3. ERDEY, L.: Egészségrontással járó élelmiszerhamisítások (Food-stuff Adulterations Injurious to Health). Magy. Kém. Lapja **3,** 309 (1948)
4. ERDEY, L.: Egy új reduktometriás módszer (A New Reductometric Method). Magy. Kém. Foly. **56,** 262 (1950)

5. ERDEY, L., BODOR, E.: Vas(III)-ionok aszkorbinometriás meghatározása. Magy. Kém. Foly. **56,** 277 (1960)
Ascorbic Acid in Analytical Chemistry. Anal. Chem. **24,** 418 (1952)
6. ERDEY, L., BODOR, E.: Klorát ionok közvetlen meghatározása. Magy. Kém. Foly. **57,** 78 (1951)
Ascorbinometrische Chloratbestimmung. Z. Anal. Chem. **133,** 265 (1951)
7. ERDEY, L., BODOR, E.: Germánium kolorimétéres mikromeghatározása. Magy. Kém. Foly. **57,** 238 (1951)
Colorimetrische Mikrobestimmung des Germaniums. Z. Anal. Chem. **134,** 81 (1951)
8. ERDEY, L., RÁDY, GY.: Kismennyiségű arany kolorimétéres meghatározása. Magy. Kém. Foly. **57,** 267 (1951)
Mikrobestimmung des Goldes. Z. Anal. Chem. **135,** 1 (1952)
9. ERDEY, L., BODOR, E., B. PAP, I.: Jodát- és jodid-ionok aszkorbinometriás meghatározása. Magy. Kém. Foly **57,** 234 (1951)
Ascorbinometrische Jodat- und Jodidbestimmung. Z. Anal. Chem. **134,** 22 (1951)
10. ERDEY, L., BODOR, E., B. PAP, I.: Bromátionok aszkorbinometriás meghatározása. Magy. Kém. Foly. **58,** 129 (1952)
Ascorbinometrische Bromatbestimmung. Z. Anal. Chem. **134,** 412 (1951)
11. ERDEY, L., BODOR, E.: Aszkorbinsav reduktometriás mérőoldat tartósítása. Magy. Kém. Foly. **58,** 295 (1952)
Die Stabilisierung der Ascorbinsäuremaßlösung. Z. Anal. Chem. **136,** 109 (1952)
12. ERDEY, L., RÁDY, GY., BÁNYAI, É.: Kismennyiségű réz meghatározása platinában ditizonnal (Determination of Micro Amounts of Copper in Platinum by Dithizone). Magy. Kém. Foly. **58,** 171 (1952)
13. ERDEY, L., JANKOVITS, L.: Eljárás és készülék szerves anyagok roncsolására. Magy. Kém. Foly. **58,** 106 (1952)
Verfahren und Apparat zur Zerstörung organischer Substanzen. Acta Chim. Acad. Sci. Hung. **3,** 57 (1953)
14. MÁZOR, L., ERDEY, L.: Vanádiummeghatározás káliumperjodát mérőoldattal. Magy. Kém. Foly. **58,** 257 (1952)
Maßanalytische Bestimmung des Vanadins mit Kaliumperjodat. Acta Chim. Acad. Sci. Hung. **2,** 331 (1952)
15. ERDEY, L.: A lucigenin mint sav–bázis indikátor. MTA Kém. Tud. Oszt. Közl. **2,** 425 (1952)
Lucigenin als Säure–Basen-Indikator. Acta Chim. Acad. Sci. Hung. **3,** 81 (1953)
16. ERDEY, L.: A hidrogénperoxid lúgos bomlásának mechanizmusa. MTA Kém. Tud. Oszt. Közl. **2,** 439 (1952)
Mechanismus der alkalischen Zersetzung des Wasserstoffperoxyds. Acta Chim. Acad. Sci. Hung. **3,** 95 (1953)
17. ERDEY, L.: A lucigenin kemilumineszcenciájának mechanizmusa. MTA Kém. Tud. Oszt. Közl. **2,** 447 (1952)
Reaktionsmechanismus der Chemilumines-enz des Lucigenins. Acta Chim. Acad. Sci. Hung. **3,** 105 (1953)
18. ERDEY, L., BÁNYAI, É.: Jodát ionok alkalmazása merkurimetriás titrálások végpontjának jelzésére. MTA Kém. Tud. Oszt. Közl. **3,** 525 (1953)
Anwendung von Jodat zur Bestimmung des Endpunktes bei merkurimetrischen Titrationen. Acta Chim. Acad. Sci. Hung. **3,** 437 (1953)
19. ERDEY, L., BODOR, E.: A 4-amino-4'-metoxi-difenilamin (Variaminkék) mint új redox indikátor. MTA Kém. Tud. Oszt. Közl. **3,** 15 (1953)
Ein neuer Redoxindicator: das 4-Amino-4'-methoxy-diphenylamin (Variaminblau). Z. Anal. Chem. **137,** 410 (1953)
20. ERDEY, L., RÁDY, GY., KÁPLÁR, L.: Gyors módszer cinknyomok meghatározására fehérjék mellett. Magy. Kém. Foly. **59,** 151 (1953)
Eine schnelle Zinkbestimmung neben Proteinen. Acta Chim. Acad. Sci. Hung. **3,** 315 (1953)
21. ERDEY, L., MÁZOR, L.: Vanádiummeghatározás oxidáló mérőoldatokkal II. Magy. Kém. Foly. **59,** 276 (1953)
Vanadinbestimmung mit oxydierenden Maßlösungen II. Acta Chim. Acad. Sci. Hung. **3,** 469 (1953)
22. ERDEY, L.: Promishlennoye znachenie askorbinometrii, Zhurn. Anal. Khimii **8,** 356 (1953)
23. ERDEY, L.: Beszámoló a Kémiai Tudományok Osztályának munkájáról és feladatairól (Report on the Activities and Objectives of the Department of Chemical Sciences). MTA Kém. Tud. Oszt. Közl. **3,** 269 (1953)

24. ERDEY, L., SZABADVÁRY, F.: A vízben oldott oxigén meghatározása aszkorbinsavval. Hidr. Közl. **34**, 8 (1954)
Ascorbinometrische Bestimmung des im Wasser gelösten Sauerstoffes. Acta Chim. Acad. Sci. Hung. **4**, 325 (1954)
25. ERDEY, L., PAULIK, F.: Szulfátok kéntartalmának meghatározása pirogén megbontással. MTA Kém. Tud. Oszt. Közl. **4**, 57 (1954)
Bestimmung des Schwefelgehaltes von Sulfaten durch pyrogene Zersetzung. Acta Chim. Acad. Sci. Hung. **4**, 37 (1954)
26. ERDEY, L., PAULIK, F.: Adalékok a báriumszulfát csapadék összetételének kérdéséhez. MTA Kém. Tud. Oszt. Közl. **4**, 73 (1954)
Beitrag zur Frage der Zusammensetzung des Bariumsulfatniederschlages. Acta Chim. Acad. Sci. Hung. **4**, 97 (1954)
27. ERDEY, L., BUZÁS, I.: Ezüst-ionok aszkorbinometriás meghatározása. MTA Kém. Tud. Oszt. Közl. **4**, 223 (1954)
Ascorbinometrische Bestimmung von Silberionen. Acta Chim. Acad. Sci. Hung. **4**, 195 (1954)
28. ERDEY, L., GEGUS, E.: Spektrokémiai módszer a ciánsávok zavaró hatásának kiküszöbölésére. MTA Kém. Tud. Oszt. Közl. **4**, 309 (1954)
Methode zur Beseitigung der störenden Wirkung von Cyanbanden in der chemischen Spektralanalyse. Acta Chim. Acad. Sci. Hung. **5**, 43 (1954)
29. ERDEY, L., FLEPS, V., BODOR, E.: Kismennyiségű foszfát kolorimetriás meghatározása. MTA Kém. Tud. Oszt. Közl. **4**, 329 (1954)
Kolorimetrische Phosphatbestimmung. Acta Chim. Acad. Sci. Hung. **5**. 65 (1954)
30. JANKOVITS L., ERDEY L.: Kismennyiségű kalcium meghatározása pirazolkékkel. MTA Kém. Tud. Oszt. Közl. **4**, 251 (1954)
Bestimmung kleiner Calciummengen mittels Pyrazolblaus. Acta Chim. Acad. Sci. Hung. **4**, 235 (1954)
31. JANKOVITS, L., ERDEY, L.: Bromanilsav felhasználása az analitikai kémiában. MTA Kém. Tud. Oszt. Közl. **4**, 261 (1954)
Anwendung der Bromanylsäure in der analytischen Chemie. Acta Chim. Acad. Sci. Hung. **4**, 245 (1954)
32. ERDEY, L., VIGH, K., MÁZOR, L.: Kismennyiségű vanádium meghatározása alumíniumban és timföldben. Magy. Kém. Foly. **60**, 79 (1954)
Bestimmung kleiner Vanadinmengen in Aluminium und Tonerde. Acta Chim. Acad. Sci. Hung. **4**, 259 (1954)
33. ERDEY, L., BÁNYAI, É.: Vasszennyezés meghatározása nemesfémekben. Magy. Kém. Foly. **60**, 85 (1954)
Bestimmung der Eisenverunreinigung in Edelmetallen. Acta Chim. Acad. Sci. Hung. **4**, 315 (1954)
34. ERDEY, L., RÁDY, GY., FLEPS, V.: Kismennyiségű ezüst kolorimetriás meghatározása ditizonnal. Magy. Kém. Foly. **60**, 193 (1954)
Kolorimetrische Bestimmung von Silber mit Dithizon. Acta Chim. Acad. Sci. Hung. **5**, 133 (1954)
35. FLEPS, V., SIMÓ, B., ERDEY, L.: Szilikátos kőzetek foszfortartalmának meghatározása. Magy. Kém. Foly. **60**, 89 (1954)
Bestimmung des Phosphorpentoxydgehaltes von Silikatgesteinen. Acta Chim. Acad. Sci. Hung. **5**, 81 (1954)
36. ERDEY, L., INCZÉDY, J.: Króm-nyomok meghatározása fém alumíniumban. Kohászati Lapok **9**, 233 (1954)
Photometrische Schnellmethode zur Bestimmung kleiner Mengen Chroms in metallischen Aluminium. Acta Chim. Acad. Sci. Hung. **4**, 289 (1954)
37. ERDEY, L., ZALAY, E., BODOR, E.: Variaminkék-típusú új redoxindikátorok előállítása és vizsgálata. (Preparation and Study of New Redox Indicators of the Variamin Blue Type). Vegyip. Kut. Int. Közl. **4**, 16 (1954)
38. ERDEY, L., BUZÁS, I.: Lumineszcenciás redoxtitrálások I. Titrálások hidrogénperoxid mérőoldattal. MTA Kém. Tud. Oszt. Közl. **5**, 279 (1954)
Redoxtitrationen mit Lumineszenzindikatoren, I. Bestimmungen mit Wasserstoffperoxyd-Maßlösung. Acta Chim. Acad. Sci. Hung. **6**, 77 (1955)
39. ERDEY, L., BUZÁS, I.: Lumineszcenciás redoxtitrálások II. Nátriumhipobromit mérőoldat alkalmazása. MTA Kém. Tud. Oszt. Közl. **5**, 293 (1954)
Redoxtitrationen mit Lumineszenzindikatoren II. Bestimmungen mit Natriumhypobromit-Maßlösung. Acta Chim. Acad. Sci. Hung. **6**, 93 (1955)

40. ERDEY, L., BUZÁS, I.: Lumineszcenciás redoxtitrálások III. Nátriumhipoklorit mérőoldat alkalmazása. MTA Kém. Tud. Oszt. Közl. **5**, 313 (1954)
Redoxtitrationen mit Lumineszenzindikatoren III. Bestimmungen mit Natriumhypochlorit-Maßlösung. Acta Chim. Acad. Sci. Hung. **6**, 115 (1955)
41. ERDEY, L., BUZÁS, I.: Lumineszcenciás redoxtitrálások IV. Titrálások nátriumarzenit mérőoldattal. MTA Kém. Tud. Oszt. Közl. **5**, 321 (1954)
Redoxtitrationen mit Lumineszenzindikatoren IV. Bestimmungen mit Natriumarsenit-Maßlösung. Acta Chim. Acad. Sci. Hung. **6**, 123 (1955)
42. ERDEY, L., BUZÁS, I.: Lumineszcenciás redoxtitrálások V. Hipohalogenitek meghatározása hidrazinszulfát mérőoldattal. MTA Kém. Tud. Oszt. Közl. **5**, 325 (1954)
Redoxtitrationen mit Lumineszenzindikatoren V. Bestimmungen mit Hydrazinsulfat-Maßlösung. Acta Chim. Acad. Sci. Hung. **9**, 127 (1955)
43. ERDEY, L.: Beszámoló a Kémiai Tudományok Osztályának munkájáról és feladatairól (Report on the Activities of the Department of Chemical Sciences). MTA Kém. Tud. Oszt. Közl. **5**, 3 (1954)
44. ERDEY, L., PAULIK, F., PAULIK, J.: Differential Thermogravimetry. Nature **174**, 885 (1954)
45. ERDEY, L., SZABADVÁRY, F.: 4-Amino-4'-metoxi-difenilamin mint kolorimetriás reagens I. Vas(III)-ionok meghatározása. Magy. Kém. Foly. **60**, 311 (1954)
Kolorimetrische Eisenbestimmung mit 4-Amino-4'-methoxydiphenylamin. Acta Chim. Acad. Sci. Hung. **6**, 131 (1955)
46. ERDEY, L., BODOR, E., PÁPAY, M.: Aszkorbinsav mérőoldat és variaminkék alkalmazása a jodometriában. MTA Kém. Tud. Oszt. Közl. **4**, 365 (1954)
Anwendung von Ascorbinsäuremaßlösung und Variaminblau-Indicator in der Jodometrie. Acta Chim. Acad. Sci. Hung. **5**, 235 (1955)
47. ERDEY, L., INCZÉDY, J.: Adatok a hidrogénperoxid lúgos közegben történő bomlásának kinetikájához. MTA Kém. Tud. Oszt. Közl. **5**, 513 (1955)
Beiträge zur Kinetik der alkalischen Zersetzung des Wasserstoffperoxyds. Acta Chim. Acad. Sci. Hung. **7**, 93 (1955)
48. ERDEY, L., KÁLMÁN, L., ALMÁSY, A.: A ritkaföldfémek csoportjának meghatározása. MTA Kém. Tud. Oszt. Közl. **5**, 443 (1955)
Determination of the Group of Rare Earth Metals. Acta Chim. Acad. Sci. Hung. **6**, 173 (1955)
49. ERDEY, L., PAULIK, F.: Csapadékok termikus vizsgálata I. Fémoxalát csapadékok. MTA Kém. Tud. Oszt. Közl. **5**, 461 (1955)
Thermische Untersuchung von Niederschlägen I. Metalloxalatniederschläge. Acta Chim. Acad. Sci. Hung. **7**, 27 (1955)
50. ERDEY, L., PAULIK, F.: Csapadékok termikus vizsgálata II. Alumíniumhidroxid csapadékok. MTA Kém. Tud. Oszt. Közl. **5**, 477 (1955)
Thermische Untersuchung von Niederschlägen II. Aluminiumhydroxydniederschläge. Acta Chim. Acad. Sci. Hung. **7**, 45 (1955)
51. ERDEY, L., BODOR, E., BUZÁS, I.: Vanádium meghatározása redukáló mérőoldatokkal I. Vanádium közvetlen aszkorbinometriás meghatározása. MTA Kém. Tud. Oszt. Közl. **6**, 89 (1955)
Vanadinbestimmung mit reduzierenden Maßlösungen I. Direkte ascorbinometrische Bestimmung des Vanadins. Acta Chim. Acad. Sci. Hung. **7**, 277 (1955)
52. ERDEY, L., BUZÁS, I., BODOR, E.: Vanádium meghatározása redukáló mérőoldatokkal II. Vanádium közvetett aszkorbinometriás meghatározása. MTA Kém. Tud. Oszt. Közl. **6**, 97 (1955)
Vanadiumbestimmung mit reduzierenden Maßlösungen II. Indirekte ascorbinometrische Vanadinbestimmung. Acta Chim. Acad. Sci. Hung. **7**, 287 (1955)
53. ERDEY, L., VIGH, K., BODOR, E.: Vanádium meghatározása redukáló mérőoldatokkal III. Vanádium meghatározása vas(II)só mérőoldattal. MTA Kém. Tud. Oszt. Közl. **6**, 103 (1955)
Vanadinbestimmung mit reduzierenden Maßlösungen III. Vanadinbestimmung mit Eisen(II)salzmaßlösung. Acta Chim. Acad. Sci. Hung. **7**, 293 (1955)
54. ERDEY, L., GEGUS, E., KOCSIS, E.: Fúrt-elektródos eljárás könnyen illó vegyületek és oldatok színképelemzésére. MTA Kém. Tud. Oszt. Közl. **6**, 113 (1955)
Spektralanalyse von Lösungen unter Anwendung von durchbohrten Elektroden. Acta Chim. Acad. Sci. Hung. **7**, 343 (1955)
55. JANKOVITS, L., ERDEY, L.: Timföld kalciumtartalmának meghatározása. MTA Kém. Tud. Oszt. Közl. **6**, 1 (1955)
Calciumbestimmung in Tonerde. Acta Chim. Acad. Sci. Hung. **7**, 155 (1955)

56. ERDEY, L., BUZÁS, K.: Higany(II)-ionok aszkorbinometriás meghatározása. MTA Kém. Tud. Oszt. Közl. **6**, 395 (1955)
Ascorbinometrische Bestimmung der Quecksilber(II)-ionen. Acta Chim. Acad. Sci. Hung. **8**, 263 (1955)
57. ERDEY, L.: Beszámoló a Kémiai Tudományok Osztálya. munkájáról (Report on the Activities of the Department of Chemical Sciences). MTA Kém. Tud. Oszt. Közl. **7**, 3 (1955)
58. ERDEY, L., PAULIK, F., PAULIK, J.: Differenciál-termogravimetria. MTA Kém. Tud. Oszt. Közl. **7**, 55 (1955)
Ein neues thermisches Verfahren, die Derivationsthermogravimetrie. Acta Chim. Acad. Sci. Hung. **10**, 61 (1956)
59. ERDEY, L., SZABADVÁRY, F.: Variaminkék mint kolorimetriás reagens II. Jódmeghatározás. Magy. Kém. Foly. **61**, 341 (1955)
Kolorimetrische Jodbestimmung mit Variaminblau. Acta Chim. Acad. Sci. Hung. **8**, 191 (1955)
60. ERDEY, L., BUZÁS, I.: Könnyen elkészíthető analitikai üvegszűrő (An Easily Prepared Sintered Glass-Filter for Analytical Purposes). Magy. Kém. Foly. **61**, 445 (1955)
61. ERDEY, L., VIGH, K.: Vanádium meghatározása ferrovanádiumban nátriumnitrites redukció után káliumpermanganáttal titrálva. MTA Kém. Tud. Oszt. Közl. **7**, 277 (1956)
Permanganometrische Vanadinbestimmung in Ferrovanadin nach Reduktion mit Natriumnitrit. Acta Chim. Acad. Sci. Hung. **11**, 73 (1957)
62. BÁNYAI, É., ERDEY, L.: Csapadékcseréléses reakciók alkalmazása az analitikai kémiában I. MTA Kém. Tud. Oszt. Közl. **7**, 165 (1956)
Anwendung von Fällungsaustauschreaktionen in der analytischen Chemie I. Acta Chim. Acad. Sci. Hung. **8**, 383 (1956)
63. ERDEY, L., BÁNYAI, É.: Csapadékcseréléses reakciók alkalmazása az analitikai kémiában II. MTA Kém. Tud. Oszt. Közl. **7**, 175 (1956)
Anwendung von Fällungsaustauschreaktionen in der analytischen Chemie II. Bestimmung von Chloridionen. Acta Chim. Acad. Sci. Hung. **8**, 395 (1956)
64. ERDEY, L., BÁNYAI, É.: Csapadékcseréléses reakciók alkalmazása az analitikai kémiában III. MTA Kém. Tud. Oszt. Közl. **7**, 187 (1956)
Anwendung von Fällungsaustauschreaktionen in der analytischen Chemie III. Bestimmung von Sulfat und Sulfid. Acta Chim. Acad. Sci. Hung. **8**, 409 (1956)
65. ERDEY, L., RÁDY, GY.: Komplexometrische Eisenbestimmung in Anwesenheit von Variaminblau als Indicator. Z. Anal. Chem. **149**, 250 (1956)
Vas komplexometriás meghatározása variaminkék indikátor jelenlétében. MTA Kém. Tud. Oszt. Közl. **8**, 67 (1956)
66. ERDEY, L., SVEHLA, GY.: Ascorbinometrische Bestimmung von Hexacyanoferrat(III). Z. Anal. Chem. **150**, 407 (1956)
67. RÁDY, GY., ERDEY, L.: Komplexometrische Wismutbestimmung. Z. Anal. Chem. **152**, 253 (1956)
Bizmut komplexometriás meghatározása. MTA Kém. Tud. Oszt. Közl. **8**, 371 (1957)
68. ERDEY, L., BUZÁS, I.: Lophine, a New Chemiluminescent Indicator. Anal. Chim. Acta **15**, 322 (1956)
69. ERDEY, L., PÓLOS, L.: Ascorbinometrische Bestimmung von Zink- und Blei-Ionen. Z. Anal. Chem. **153**, 401 (1956)
70. ERDEY, L., PÓLOS, L.: Die Bestimmung von Zink- und Blei-Ionen mit Kaliumhexacyanoferrat(II). Z. Anal. Chem. **153**, 411 (1956)
71. ERDEY, L., SVEHLA, G.: Bestimmung von Calciumionen durch flammenphotometrische Titration. Z. Anal. Chem. **154**, 406 (1956)
Kalciumionok meghatározása lángfotometriás titrálással. M. Kém. Folyóirat **63**, 180 (1957)
72. ERDEY, L., SZABADVÁRY, F.: Variaminblau als colorimetrisches Reagens. Z. Anal. Chem. **155**, 90 (1957)
73. ERDEY, L.: Die Entwicklung der Polarographie in Ungarn. Acta Chim. Acad. Sci. Hung. **9**, 17 (1956)
74. ERDEY, L., KARSAY, A.: Die polarographische Bestimmung der Eisen(III)-ionen mit Ascorbinsäure. Acta Chim. Acad. Sci. Hung. **9**, 43 (1956)
75. ERDEY, L.: Beszámoló a Kémiai Tudományok Osztálya munkájáról (Report on the Activities of the Department of Chemical Sciences). MTA Kém. Tud. Oszt. Közl. **8**, 169 (1957)
76. ERDEY, L.: Untersuchungen mit Hilfe der derivativen Thermogravimetrie. Periodica Polytech. **1**, 35 (1957)

Skumanie Látok derivacnou termogravimetricu. Chemické Zvesti **12,** 352 (1958)
77. ERDEY, L., GEGUS, E., KOCSIS, E.: Spektralanalytische Bestimmung des Magnesium-, Zink-, Vanadium- und Chromgehaltes von Reinaluminium unter Anwendung einer durchbohrten Elektrode. Acta Chim. Acad. Sci. Hung. **11,** 277 (1957)
78. ERDEY, L., KARSAY, A.: Über eine indirekte polarographische Calciumbestimmung. Acta Chim. Acad. Sci. Hung. **11,** 171 (1957)
79. ERDEY, L., INCZÉDY, J.: Über die zwischen Wasserstoffperoxyd und Hypohalogeniten in alkalischem Medium verlaufende Reaktion. Acta Chim. Acad. Sci. Hung. **11,** 125 (1957)
80. ERDEY, L., FLEPS, V.: Bestimmung des Phosphorpentoxydgehaltes in Bauxiten. Acta Chim. Acad. Sci. Hung. **11,** 195 (1957)
81. ERDEY, L., SZABADVÁRY, F.: Variaminkék mint kolorimetriás reagens III. Vanádium- és krómmeghatározás. Magy. Kém. Foly. **63,** 153 (1957)
Photometrisches Verfahren zur Vanadium- und Chrombestimmung mit Variaminblau. Acta Chim. Acad. Sci. Hung. **13,** 335 (1958)
82. ERDEY, L., VIGH, K.: Ferrometrische Bestimmung von Silberionen. Z. Anal. Chem. **157,** 184 (1957)
83. ERDEY, L., SIPOSS, G.: Ascorbinometrische Bestimmung von Kupfer(II)-Ionen. Z. Anal. Chem. **157,** 166 (1957)
84. ERDEY, L.: Derivativ-thermogravimetrische Untersuchung analytischer Hochtemperaturreaktionen. Periodica Polytech. **1,** 91 (1957)
85. PAULIK, F., ERDEY, L.: A derivatív termogravimetria újabb eredményei. MTA Kém. Tud. Oszt. Közl. **9,** 15 (1957)
Neuere Ergebnisse der derivativen Thermogravimetrie. Acta Chim. Acad. Sci. Hung. **13,** 117 (1957)
86. ERDEY, L., BÁNYAI, É., PAULIK, F.: Csapadékcseréléses reakciók alkalmazása az analitikai kémiában IV. Ioncseréléses reakciók. MTA Kém. Tud. Oszt. Közl. **9,** 103 (1957)
Anwendung von Fällungsaustauschreaktionen in der analytischen Chemie IV. Ionenaustauschreaktionen. Acta Chim. Acad. Sci. Hung. **13,** 453 (1958)
87. ERDEY, L., PÓLOS, L.: Chelatometrische Bestimmung von Zink-, Cadmium- und Bleiionen in Anwesenheit von Variaminblau als Redoxindicator. Anal. Chim. Acta **17,** 458 (1957)
88. ERDEY, L.: Titrálások kemilumineszcenciás indikátorok jelenlétében. Magy. Kém. Lapja **13,** 7 (1958)
Analysis for Industry. The Industrial Chemist 459, 523, 575 (1957)
89. ERDEY, L., ZALAY, E., BODOR, E.: Über einige als Redoxindicatoren verwendbare Variaminblauderivate. Acta Chim. Acad. Sci. Hung. **12,** 251 (1957)
90. ERDEY, L., MÁZOR, L., MEISEL, T.: Argentometrische Mikrobestimmung organischer Halogenverbindungen nach Verbrennung, in Anwesenheit von Variaminblau als Indicator. Mikrochim. Acta 140 (1958)
91. ERDEY, L., SZABADVÁRY, F.: Bestimmung von Vanadium in Reinaluminium. Z. Anal. Chem. **160,** 429 (1958)
92. JANKOVITS, L., ERDEY, L.: Kalcium titrálás „Eriochromrot B" indikátor felhasználásával. Magy. Kém. Foly. **64,** 50 (1958)
Calciumbestimmung in Anwesenheit von Eriochromrot B als Indicator. Acta Chim. Acad. Sci. Hung. **15,** 163 (1958)
93. PAULIK, F., PAULIK, J., ERDEY, L.: Der Derivatograph I. Z. Anal. Chem. **160,** 241 (1958)
94. PAULIK, F., PAULIK, J., ERDEY, L.: Der Derivatograph II. Z. Anal. Chem. **160,** 321 (1958)
95. ERDEY, L., BÁNYAI, É.: Über Fällungsaustauschreaktionen. Z. Anal. Chem. **161,** 16 (1958)
96. ERDEY, L., BÁNYAI, É., ZALAY, E., TÉSY, M.: Herstellung und Standardredoxpotentiale von Variaminblauderivaten. Acta Chim. Acad. Sci. Hung. **15,** 65 (1958)
97. ERDEY, L., RÁDY, GY.: Redoxtitrationen in nichtwäßrigen Lösungen. Acta Chim. Acad. Sci. Hung. **15,** 81 (1958)
98. ERDEY, L.: Beszámoló a Kémiai Tudományok Osztálya munkájáról (Report on the Activities of the Department of Chemical Sciences). MTA Kém. Tud. Oszt. Közl. **10,** 87 (1958)
99. ERDEY, L., KÁPLÁR, L.: Maßanalytische Ascorbinsäurebestimmung mit Variaminblau als Indicator. Z. Anal. Chem. **162,** 180 (1958)
100. ERDEY, L., MÁZOR, L., PÁPAY, M.: Mikrobestimmung des Fluors durch direkte argentometrische Titration des Chloridgehaltes des PbClF-Niederschlages. Mikrochim. Acta 482 (1958)
101. ERDEY, L., RÁDY, GY.: Studien über die potentiometrische Goldbestimmung durch Ascorbinsäure. Talanta **1,** 159 (1958)

102. ERDEY, L., SVEHLA, G.: Analytische Anwendungen der ascorbinometrischen Bestimmung von Hexacyanoferrat(III). Teil I. Ascorbinometrische Bestimmung von Hexacyanoferrat(II)-, Chromat- und Permanganationen. Z. Anal. Chem. **163,** 6 (1958)
103. ERDEY, L., INCZÉDY, J.: Über die Zersetzung des Wasserstoffperoxyds in alkalischem Medium bei Anwesenheit eines Kupfer(II)-citratkomplexes. Acta Chim. Acad. Sci. Hung. **17,** 93 (1958)
104. PAULIK, F., ERDEY, L., GÁL, S.: Derivatographische Mikrodestillationsmethode zur Untersuchung von Flüssigkeitsgemischen. Z. Anal. Chem. **163,** 321 (1958)
105. ERDEY, L., BUZÁS, I., VIGH, K.: Argentometrische Titrationen mit Redoxindication I. Bestimmung von Halogeniden, Cyaniden, Rhodaniden und Kalium in Gegenwart von Variaminblau. Talanta **1,** 377 (1958)
106. ERDEY, L.: Titrationen mit Chemilumineszenzindikatoren. Chemie Analyticzna **3,** 269 (1958)
107. ERDEY, L., BUZÁS, I., VIGH, K.: Indirekte ascorbinometrische Bestimmung starker Oxydationsmittel. Periodica Polytech. **3,** 1 (1959)
108. ERDEY, L., SZABADVÁRY, F.: Mikrobestimmung des Eisens mittels Katalyse. Mikrochim. Acta 424 (1959)
109. ERDEY, L., INCZÉDY, J.: Photometrische Bestimmung von Spuren Wasserstoffperoxyd und Kupfer(II)-ionen mit Phlorrhizin. Mikrochim. Acta 438 (1959)
110. ERDEY, L., INCZÉDY, J.: Titrationen mit Wasserstoffperoxyd- und Natriumhypobromitmaßlösungen. Z. Anal. Chem. **166,** 410 (1959)
111. ERDEY, L., SVEHLA, GY.: Analytische Anwendungen der ascorbinometrischen Bestimmung von Hexacyanoferrat(III). II. Mitteilung. Z. Anal. Chem. **167,** 164 (1959)
112. ERDEY, L.: Az Osztályvezetőség beszámolója (Report of the Governing Body of the Department of Chemical Sciences). MTA Kém. Tud. Oszt. Közl. **11,** 217 (1959)
113. BÁNYAI, É., ERDEY, L., SZABADVÁRY, F.: Über die Oxydationsprodukte des 4-Amino-4'methoxy-diphenylamins. Acta Chim. Acad. Sci. Hung. **20,** 307 (1959)
114. PAULIK, F., ERDEY, L., TAKÁCS, J.: Derivatographische Untersuchung von Arzneipulvern und granulierten Arzneimitteln. Z. Anal. Chem. **169,** 19 (1959)
115. ERDEY, L., BUZÁS, I., PÓLOS, L.: Anwendung von Siloxen als Chemilumineszenz-Indicator in der Permanganometrie. Z. Anal. Chem. **169,** 187 (1959)
116. ERDEY, L., BUZÁS, I., PÓLOS, L.: Anwendung von Siloxen als Chemilumineszenz-Indicator in cerimetrischen und chromatometrischen Titrationen. Z. Anal. Chem. **169,** 263 (1959)
117. ERDEY, L., PÓLOS, L., GREGOROWICZ, Z.: Notes on the reduction of nitrates. Talanta **2,** 384 (1959)
118. ERDEY, L., GYIMESI, J., MEISEL, T.: Néhány új komplexképző előállítása és állandóinak meghatározása (Preparation and Characterization of Some New Complexing Agents). Magy. Kém. Foly. **65,** 386 (1959)
119. ERDEY, L., VIGH, K., PÓLOS, L.: Argentometrische Titrationen mit Redoxindikation II. Bestimmung von Ammoniak, Ammonium-Ionen und stickstoffhaltigen organischen Substanzen. Talanta **3,** 1 (1959)
120. ERDEY, L., PÓLOS, L., GREGOROWICZ, Z.: Argentometric Titrations by means of Redox Indication III. Determination of Nitrate Ions and Nitro Compounds. Talanta **3,** 6 (1959)
121. ERDEY, L., BÁNYAI, É., GERE, É. B.: Untersuchung einiger als Redoxindicatoren anwendbaren Variaminblauderivaten. Talanta **3,** 54 (1959)
122. ERDEY, L., BUZÁGH, É., BÁNYAI, É.: Variamine Blue Sulphate as Redox Indicator. Talanta **3,** 209 (1959)
123. ERDEY, L.: Variamine Blue: A Versatile Redox Indicator. Chemist-Analyst **48,** 106 (1959)
124. MÁZOR, L., MEISEL, T., ERDEY, L.: Adatok a szerves vegyületek kéntartalmának mikromeghatározásához (A Contribution to the Microdetermination of Sulfur in Organic Compounds). Magy. Kém. Lapja **14,** 494 (1959)
125. ERDEY, L., PAULIK, F.: Derivatographische Untersuchung der Bauxite. Thermische Zersetzung des Hydrargillits. Acta Chim. Acad. Sci. Hung. **21,** 205 (1959)
126. ERDEY, L., GYIMESI, J., MEISEL, T.: Herstellung einiger neuer komplexbildender Verbindungen und Bestimmung ihrer Konstanten. Acta Chim. Acad. Sci. Hung. **21,** 327 (1959)
127. ERDEY, L., INCZÉDY, J., MARKOVITS, I.: Oxidation-Reduction Reactions on Ion-Exchange-Stannous Columns. Talanta **4,** 25 (1960)
128. ERDEY, L., PÓLOS, L.: Komplexometrische Bestimmung von Aluminium- und Bleiionen in Anwesenheit von Variaminblau als Indicator. Z. Anal. Chem. **174,** 333 (1960)
129. ERDEY, L., BUZÁS, I.: Complexometric and Argentometric Titrations Using Chemiluminescent Indicators. Anal. Chim. Acta **22,** 524 (1960)

130. MÁZOR, L., ERDEY, L., MEISEL, T.: Mikrobestimmung einiger Elemente in organischen Verbindungen nach Aufschluß mit Kalium. I. Halogenbestimmung. Mikrochim. Acta 412 (1960)
131. MÁZOR, L., ERDEY, L., MEISEL, T.: Mikrobestimmung einiger Elemente in organischen Verbindungen nach Aufschluß mit Kalium. II. Schwefelbestimmung. Mikrochim. Acta 417 (1960)
132. ERDEY, L., SVEHLA, GY.: Über die Fehlerberechnung von indirekten Analysen. Z. Anal. Chem. **176,** 8 (1960)
133. BÁNYAI, É., BUZÁGH, É., ERDEY, L.: Complexometric Determination of Mercury(II) and Aluminium Ions. Talanta **4,** 133 (1960)
134. ERDEY, L.: Az analitikai kémiai tudomány helyzete és fejlesztésének fő irányai (Present State and Main Development Trends of Analytical Chemistry). MTA Kém. Tud. Oszt. Közl. **14,** 213 (1960)
135. PAULIK, F., PAULIK, J., ERDEY, L.: Die Derivatographie. Bergakademie **12,** 413 (1960)
136. ERDEY, L., PÓLOS, L.: Beiträge zur jodometrischen Endpunktsindikation. Periodica Polytech. **4,** 157 (1960)
137. BELCHER, R., ERDEY, L., PAULIK, F., LIPTAY, G.: A Derivatographic Study of Potassium Hydrogen Phthalate. Talanta **5,** 53 (1960)
138. RÁDY, G., GIMESI, O., ERDEY, L.: Bestimmung von elementarem Schwefel in nichtwäßrigen Medien. Acta Chim. Acad. Sci. Hung. **28,** 179 (1961)
139. ERDEY, L., VIGH, K., BUZÁS, I.: Maßanalytische Bestimmung von Thalliumionen I. Acta Chim. Acad. Sci. Hung. **26,** 85 (1961)
140. ERDEY, L., VIGH, K., BUZÁS, I.: Maßanalytische Bestimmung von Thalliumionen II. Acta Chim. Acad. Sci. Hung. **26,** 93 (1961)
141. ERDEY, L., BÁNYAI, É., SZABADVÁRY, F.: Radiochemische Untersuchung von Fällungsaustauschreaktionen I. Chloridaustausch mit Silberjodat. Acta Chim. Acad. Sci. Hung. **26,** 211 (1961)
142. ERDEY, L., PORUBSZKY, I., HEGEDÜS, D.: Radiochemische Untersuchung von Fällungsaustauschreaktionen II. Chloridaustausch mit Silberchromat. Acta Chim. Acad. Sci. Hung. **26,** 219 (1961)
143. ERDEY, L., KÁSA, I., KLATSMÁNYI, P., MEISEL, T.: Untersuchung diphenylartiger Redoxsysteme. Acta Chim. Acad. Sci. Hung. **26,** 53 (1961)
144. ERDEY, L., BUZÁGH, É., PÓLOS, L.: Einfluß von Filtration und Altern auf die Ausgestaltung der Niederschläge. Acta Chim. Acad. Sci. Hung. **26,** 43 (1961)
145. PAULIK, F., PAULIK, J., ERDEY, L.: Einfluß der im Inneren der Probe sich ausbildenden Atmosphäre bei den derivatographischen Untersuchungen. Acta Chim. Acad. Sci. Hung. **26,** 143 (1961)
146. RÁDY, GY., GIMESI, O., ERDEY, L.: Bestimmung des Gesamtblei- und Bleioxydgehaltes in Bleichromat. Acta Chim. Acad. Sci. Hung. **28,** 237 (1961)
147. ERDEY, L., MEISEL, T., RÁDY, GY.: Ein neuer Indikator für in nicht-wäßrigen Lösungen ausgeführten Redoxtitrationen. Acta Chim. Acad. Sci. Hung. **26,** 71 (1961)
148. ERDEY, L., SVEHLA, GY.: Determination of Trace Amounts of Metals by means of Chronometric Analysis I. Determination of Molybdenum. Acta Chim. Acad. Sci. Hung. **26,** 85 (1961)
149. PAULIK, J., MACSKÁSSY, H., PAULIK, F., ERDEY, L.: Derivatographische Untersuchung von Polyäthylen I. Plaste und Kautschuk **8,** 588 (1961)
150. ERDEY, L., LIPTAY, G., GÁL, S., PAULIK, F.: Derivatographische Untersuchung von Ammoniumphosphatniederschlägen. Periodica Polytech. **5,** 209 (1961)
151. ERDEY, L., HEGEDÜS, D., PORUBSZKY, I.: Use of Signed Atoms for Investigations of Precipitate Exchange Reactions. Precipitate Exchange with Silver Oxalate. Talanta **8,** 593 (1961)
152. SZABADVÁRY, F., TAKÁCS, J., ERDEY, L.: Untersuchung und analytische Anwendung der *p*-Hydroxy-*m*-nitrophenylarsonsäure. Z. Anal. Chem. **182,** 88 (1961)
153. ERDEY, L., PAULIK, F., SVEHLA, G., LIPTAY, G.: Indirekte derivatographische Bestimmung von Calcium, Strontium und Barium aus einer Einwaage. Z. Anal. Chem. **182,** 329 (1961)
154. MEISEL, T., NÉMETH, Á., ERDEY, L.: Anwendung der Ringofenmethode zum Nachweis einiger Heteroelemente in organischen Verbindungen. Mikrochim. Acta 974 (1961)
155. ERDEY, L., LIPTAY, G., GÁL, S., PAULIK, F.: Thermische Untersuchung von Eisen(III)-hydroxydniederschlägen. Periodica Polytech. **5,** 287 (1961)
156. PAULIK, F., ERDEY, L., GÁL, S.: Derivatographische Untersuchung des Pyrits. Bergakademie **37,** 21 (1962)

157. ERDEY, L., BUZÁS, I.: Die Anwendung von Variaminblau in der Tüpfelanalyse. Mikrochim. Acta 340 (1962)
158. ERDEY, L., PINK, R. C.: An Investigation by Electron-spin Resonance of the Redox Indicator Variamine Blue. Talanta **9**, 329 (1962)
159. ERDEY, L., PICKERING, W. F., WILSON, C. L.: Mixed Chemiluminescent Indicators. Talanta **9**, 371 (1962)
160. BÁNYAI, É., SZABADVÁRY, F., ERDEY, L.: Mikrobestimmung des Chlorids durch radioaktiven Fällungsaustausch. Mikrochim. Acta 437 (1962)
161. GIMESI, O., RÁDY, GY., ERDEY, L.: Die Anwendung von Indikatoren des Typs Arson in der Chelatometrie. Periodica Polytech. **6**, 15 (1962)
162. ERDEY, L., BÁNYAI, É., PORUBSZKY, I., HEGEDÜS, D.: Csapadékcseréléses kloridmeghatározások vizsgálata jelzett atomokkal (Tracer Investigation of Chloride Analysis by Precipitation Exchange). Year-book of the Technical University p. 131. Budapest, 1962
163. ERDEY, L., LIPTAY, G., SVEHLA, G., PAULIK, F.: Indirect Derivatographic Determination of Calcium, Strontium and Barium Ions in the Presence of one another. Talanta **9**, 489 (1962)
164. ERDEY, L., SVEHLA, G., KOLTAI, L.: Analytical Applications of the Determination of Hexacyanoferrate(III) with Ascorbic Acid. Anal. Chim. Acta **27**, 164 (1962)
165. ERDEY, L., GEGUS, E., VÁNDORFFY, M.: Természetes vizek elemzése nagyfrekvenciás titrálással (Analysis of Natural Waters by High-frequency Titration). Magy. Kém. Lapja **17**. 277 (1962)
166. ERDEY, L., PICKERING, W. F., WILSON, C. L.: Chemiluminescence of Luminol and Haemin **9**, 653 (1962)
167. ERDEY, L., KOLTAI, L., SVEHLA, G.: Analytical Applications of the Determination of Hexacyanoferrate(III) with Ascorbic Acid. Part IV. Determination of Hydroxylamine. Anal. Chim. Acta **27**, 363 (1962)
168. TAKÁCS, J., INCZÉDY, J., ERDEY, L.: Bestimmung des Methylbromids und Äthylbromids nebeneinander. J. Chromatography **9**, 247 (1962)
169. ERDEY, L., RÁDY, G., GIMESI, O.: Analyse bleihaltiger Silberlegierungen. Acta Chim. Acad. Sci. Hung. **32**, 151 (1962)
170. ERDEY, L., KOLTAI, L., SVEHLA, G.: Analytical Applications of the Reaction of Hexacyanoferrate(III) with Ascorbic Acid. Part V. Determination of Silver. Anal. Chim. Acta **27**, 498 (1962)
171. PAULIK, F., PAULIK, J., ERDEY, L.: Die Derivatographie. Chem. Techn. **14**, 533 (1962)
172. GIMESI, O., RÁDY, GY., ERDEY, L.: Komplexometrische Bestimmung von elementarem Schwefel und elementarem Selen. Acta Chim. Acad. Sci. Hung. **33**, 381 (1962)
173. ERDEY, L., SZABADVÁRY, F., BÁNYAI, É.: Radiochemische Untersuchung von Fällungsaustauschreaktionen III. Chloridaustausch mit Quecksilber(I)salzen. Acta Chim. Acad. Sci. Hung. **33**, 387 (1962)
174. ERDEY, L., SVEHLA, G.: Determination of Trace Amounts of Metals by Means of Chronometric Analysis. Microchemical Techniques 343 (1962)
175. INCZÉDY, J., ERDEY, L.: The Role of Perhydroxyl Ions in the Reactions of Hydrogen Peroxide. Periodica Polytech. **6**, 195 (1962)
176. ERDEY, L., SVEHLA, G.: Ascorbic Acid as an Analytical Reagent. Chemist-Analyst **52**, 24 (1963)
177. ERDEY, L., GÁL, S.: Thermoanalytical Investigations of High Temperature Fusion Reactions. Talanta **10**, 23 (1963)
178. VIGH, K., INCZÉDY, J., ERDEY, L.: Acél, nyersvas és ferrovanádium meghatározása ioncserélő gyantaoszlop segítségével (Determination of Steel, Pig Iron and Ferrovanadium using Ion Exchange Column). Magy. Kém. Foly. **69**, 73 (1963)
179. ERDEY, L., VÁNDORFFY, M.: Hochfrequenztitrationen mit Ascorbinsäuremaßlösung. I. Bestimmung von Silberionen. Acta Chim. Acad. Sci. Hung. **35**, 381 (1963)
180. ERDEY, L., VIGH, K.: Indirect Determination of Hypochlorite and Hypobromite by Ascorbinometric Titration of Thallium(III) Ions. Talanta **10**, 439 (1963)
181. BUZÁS, I., ERDEY, L.: Titration of Thallium(I) Ions with a Chemiluminescent End-point. Talanta **10**, 467 (1963)
182. ERDEY, L., KÁSA, I., MEISEL, T.: 2-Hydroxy-4-amino-4'-methoxy diphenylamine: a New Redox Indicator. Talanta **10**, 471 (1963)
183. BÁNYAI, É., SZABADVÁRY, F., ERDEY, L.: Microdetermination of Cyanide Ion by Radioactive Precipitate-exchange. Talanta **10**, 499 (1963)
184. ERDEY, L., SVEHLA, G., KOLTAI, L.: The Accuracy of Zinc Determination by Atomic Absorption Method. Talanta **10**, 531 (1963)

185. ERDEY, L., VÁNDORFFY, M.: Hochfrequenztitrationen mit Ascorbinsäuremaßlösung II. Bestimmung von Eisen(III)-Ionen. Acta Chim. Acad. Sci. Hung. **37**, 17 (1963)
186. SZABADVÁRY, F., BÁNYAI, É., ERDEY, L.: Réactions de précipitation échange radioactif et leur application à la microanalyse. Chimie Analytique **45**, 289 (1963)
187. SVEHLA, G., PÁLL, A., ERDEY, L.: Improved Method for Error Calculation of Quantitative Spectrophotometric Measurements. Talanta **10**, 719 (1963)
188. ERDEY, L., KOCSIS, E., TAKÁCS, J.: Levegőszárítás szilikagéllel (Drying of Air with Silica Gel). Épületgépészet **12**, 68 (1963)
189. PAULIK, F., GÁL, S., ERDEY, L.: Determination of the Pyrite Content of Bauxites by Thermal Methods. Anal. Chim. Acta **29**, 381 (1963)
190. SVEHLA, G., KOLTAI, L., ERDEY, L.: The Use of 2,6-dichlorophenol–indophenol as Indicator in Iodometric Titrations with Ascorbic Acid. Anal. Chim. Acta **29**, 442 (1963)
191. PAULIK, F., PAULIK, J., ERDEY, L.: Die Normalisierung der thermoanalytischen Versuchsumstände mit Hilfe des Derivatographen. Periodica Polytech. **7**, 171 (1963)
192. PAULIK, F., LIPTAY, G., ERDEY, L.: Die Bestimmung von Kalzit, Magnesit und Dolomit nebeneinander mit Hilfe des Derivatographen. Periodica Polytech. **7**, 177 (1963)
193. ERDEY, L., LIPTAY, G.: Derivatographische Untersuchung von Metall-anthranilat-Niederschlägen. Periodica Polytech. **7**, 185 (1963)
194. ERDEY, L., GÁL, S.: Thermoanalytische Untersuchung von natürlichen und künstlichen Kryolithen. Periodica Polytech. **7**, 205 (1963)
195. GÁL, S., PAULIK, F., ERDEY, L., BAYER, J.: Derivatographische Untersuchung von Calciumoxalathydraten. **7**, 215 (1963)
196. ERDEY, L., LIPTAY, G.: Derivatographic Study of Metal Pyridine Rhodanide Precipitates. Periodica Polytech. **7**, 223 (1963)
197. SVEHLA, G., ERDEY, L.: The Use of Landolt Reactions in Quantitative Microanalysis I. Theoretical Backgrounds of a New Analytical Principle. Microchem. Journ. **7**, 206 (1963)
198. SVEHLA, G., ERDEY, L.: The Use of Landolt Reactions in Quantitative Microanalysis II. Determination of Traces of Molybdenum by the Hydrogen Peroxide-iodide Reaction. Microchem. Journ. **7**, 221 (1963)
199. KÁSA, I., ERDEY, L.: Bestimmung von Semicarbazid durch Oxydation in alkalischer Lösung. Acta Chim. Acad. Sci. Hung. **39**, 21 (1963)
200. GIMESI, O., RÁDY, GY., ERDEY, L.: Bestimmung von Alkalicyaniden unu Selen mit Schwefelmaßlösung in nichtwäßrigem Medium. Acta Chim. Acad. Sci. Hung. **38**, 303 (1963)
201. ERDEY, L., KÁSA, I.: Untersuchung des Wirkungsmechanismus vom Redoxindikator 2-Hydroxy-4-amino-4'-methoxy-diphenylamin und seine Anwendungen. Talanta **10**, 1273 (1963)
202. PAULIK, F., BUZÁGH, É., PÓLOS, L., ERDEY, L.: Derivatographische Untersuchung von Bariumsulfatniederschlägen I. Acta Chim. Acad. Sci. Hung. **38**, 311 (1963)
203. ERDEY, L., TAKÁCS, J., BUZÁS, I.: Einfluß fluoreszierender Stoffe auf die Chemilumineszenz des Lucigenins. Acta Chim. Acad Sci. Hung. **39**, 295 (1963)
204. KOCSIS, E., ERDEY, L.: Über die Anwendbarkeit von Zerstäubungsvorrichtungen bei Spektrometern. Acta Chim. Acad. Sci. Hung. **39**, 301 (1963)
205. ERDEY, L., GEGUS, E., KOCSIS, E., RÁDY, GY.: Spektralanalytisches Lösungsverfahren zur Bestimmung von Gold mit vorhergehender Anreicherung. Acta Chim. Acad. Sci. Hung. **39**, 313 (1963)
206. INCZÉDY, J., ERDEY, L.: Ioncserélő hártyák néhány analitikai alkalmazása (Analytical Applications of Ion Exchange Membrans). Kolorisztikai Értesítő **6**, 10 (1964)
207. ERDEY, L., KORMÁNY, T., GÁL, S.: Untersuchung von anodisch erzeugten Aluminiumoxidschichten. Teil I. Z. Anal. Chem. **200**, 219 (1964)
208. ERDEY, L., GIMESI, O., RÁDY, GY.: Cyanometric Titrations in Nonaqueous Solutions. Talanta **11**, 451 (1964)
209. ERDEY, L., GÁL, S., LIPTAY, G.: Thermoanalytical Properties of Analytical Grade Reagents. Talanta **11**, 913 (1964)
210. PAULIK, F., PAULIK, J., ERDEY, L.: Derivatography. Hungarian Scientific Instruments. **1**, 3 (1964)
211. ERŐSS, K., SVEHLA, G., ERDEY, L.: The Use of 2,6-dichlorophenol-indophenol as Indicator in Acid–base Titrations. Anal. Chim. Acta **31**, 246 (1964)
212. CSŰRÖS, Z., PETRÓ, J., KÁLMÁN, V., ERDEY, L., PAULIK, F.: A Raney-nikkel katalitikus sajátosságainak alakulása készítésének körülményeitől függően (Variations in the Catalytic Properties of Raney Nickel as a Function of the Preparation Procedure). Magy. Kém. Foly. **70**, 337 (1964)

213. KLATSMÁNYI-GÁBOR, P., MEISEL, T., ERDEY, L.: Oxydation von Thioharnstoffderivaten in Eisessig, I. Acta Chim. Acad. Sci. Hung. **40**, 99 (1964)
214. KÁSA, I., KOVÁCS, L., ERDEY, L.: Studien über die Anregung von Zinksulfid- und Zinkkadmiumsulfid-Leuchtstoffen durch Beta-Strahlen. Periodica Polytech. **8**, 105 (1964)
215. PÁLL, A., SVEHLA, G., ERDEY, L.: Determination of Cobalt(II) Ions by a Differential Spectrophotometric Method. Talanta **11**, 1383 (1964)
216. ERDEY, L., PAULIK, F.: Die Methode der Derivatographie. Wissenschaftl. Zeitschrift d. Techn. Hochschule für Chemie Leuna-Merseburg **6**, 198 (1964)
217. BÁNYAI, É., ERDEY, L.: Redox tulajdonságú színezékek elektrokémiai vizsgálata (Electrochemical Investigation of Dyestuffs with Redox Properties). Kolorisztikai Értesítő 343 (1964)
218. KŐRÖS, E., MARTIN NELSON, S., PAULIK, F., ERDEY, L., RUFF, F.: Néhány kobalt(II)-pirazin vegyes komplex termikus bomlásáról (Thermal Decomposition of Some Cobalt-(II)-Pyrazine Mixed Complexes). Magy. Kém. Foly. **70**, 468 (1964)
219. ERDEY, L., BUZÁS, I., TAKÁCS, J.: Beiträge zum Leuchtmechanismus des Lucigenins. Acta Chim. Acad. Sci. Hung. **41**, 37 (1964)
220. ERDEY, L., KÁSA, I.: Untersuchung des 2-Hydroxy-4-amino-4'-methoxydiphenylamin Redoxindikators. Acta Chim. Acad. Sci. Hung. **41**, 59 (1964)
221. ERDEY, L., PAULIK, F., BUZÁGH, É., PÓLOS, L.: Derivatographische und elektronenmikroskopische Untersuchung von Bariumsulfatniederschlägen II. Acta Chim. Acad. Sci. Hung. **41**, 109 (1964)
222. KHALIFA, H., ERDEY, L., SVEHLA, G.: Accuracy of Silver Determination by Atomic Absorption Methods. Acta Chim. Acad. Sci. Hung. **41**, 187 (1964)
223. LIPTAY, G., DÁVID, P., ERDEY, L.: Villamos szigetelőanyagok és szigetelések hőbomlásának derivatográfiás vizsgálata I. Elektrotechnika **57**, 392 (1964)
Derivatographic Study of Thermal Decomposition of Electrical Insulating Materials and Insulators. Periodica Polytech. El. **8**, 243 (1964)
224. CSŰRÖS, Z., DUSZA, ZS., PETRÓ, J., ERDEY, L., PAULIK, F.: Investigation son Catalysts XL. Acta Chim. Acad. Sci. Hung. **42**, 131 (1964)
225. ERDEY, L., KÁNTOR, T., KOCSIS, E., T. VÁNDORFFY, M.: Vákuumgőzöléssel előállított fémréteg mennyiségi színképelemzése (Quantitative Spectroscopic Analysis of Metal Layers Prepared by Vacuum Deposition). Magy. Kém. Foly. **70**, 557 (1964)
226. LIPTAY, G., HEGYALJAI KISS, G., ERDEY, L.: Investigation by Thermoanalysis of the Pyrolytic Dehydrogenation of Sterols. Acta Chim. Acad. Sci. Hung. **42**, 379 (1964)
227. BÁNYAI, É., ERDEY, L., KOLOS, E.: Eriochromblau S.E. als Redoxindikator. Talanta **12**, 21 (1965)
228. ERDEY, L.: Megemlékezés Winkler Lajos súlyanalitikai munkásságáról (The Contribution of Lajos Winkler to Gravimetric Analysis). Lajos Winkler Memorial Volume, p. 19. Akadémiai Kiadó, Budapest, 1965
229. ERDEY, L., LIPTAY, G., GÁL, S.: Thermoanalytical Properties of Analytical-grade Reagents II. Caesium Salts. Talanta **12**, 257 (1965)
230. INCZÉDY, J., NEMESHEGYI, G., ERDEY, L.: Separation and Determination of Rare Earth Metals by Ion Exchange Chromatography I. Acta Chim. Acad. Sci. Hung. **43**, 1 (1965)
231. INCZÉDY, J., NEMESHEGYI, G., ERDEY, L.: Separation and Determination of Rare Earth Metals by Ion Exchange Chromatography II. Acta Chim. Acad. Sci. Hung. **43**, 9 (1965)
232. ERDEY, L.: Bedeutung der Ionenaustauscher bei der Entwicklung der analytischen Chemie. Ionenaustauscher Symp. Akad. Kiadó, Budapest, 5 (1965)
233. INCZÉDY, J., VIGH, K., ERDEY, L.: Trennung geringer Ionenmengen von störenden Ionen mit Hilfe einer Ionenaustauschersäule. Symposium in Balatonszéplak, 1963. Akad. Kiadó, 181 (1965)
234. INCZÉDY, J., ERDEY, L: Einige analytische Anwendungen von Ionenaustauschermembranen. Symposium in Balatonszéplak 1963. Akad. Kiadó, Budapest, 207 (1965)
235. KHALIFA, H., SVEHLA, G., ERDEY, L.: Precision of the Determination of Copper and Gold by Atomic Absorption Spectrophotometry. Talanta **12**, 703 (1965)
236. ERDEY, L., KÁSA, I., KOVÁCS, L.: Néhány anyag termolumineszcens tulajdonságainak vizsgálata (Investigation of Some Thermoluminescent Substances). Magy. Kém. Foly. **71**, 364 (1965)
237. ERDEY, L., LIPTAY, G., GÁL, S.: Thermoanalytical Properties of Analytical-grade Reagents III. Rubidium Salts. Talanta **12**, 883 (1965)
238. ERDEY, L., LIPTAY, G., BIDLÓ, G.: Investigation of the Polymorphous Transformation of Rubidium Dichromate. J. Inorg. Nucl. Chem. **27**, 2451 (1965)
239. ERDEY, L., KÁSA, I., KOVÁCS, L.: Untersuchung der thermolumineszenten Eigenschaften des Lithiumfluorids. Acta Chim. Acad. Sci. Hung. **45**, 95 (1965)

240. ERDEY, L., HEGYALJAI KISS, G., LIPTAY, G., KISS-ERŐSS, K.: The Identification of a New Polymorphous Modification of Oestron by Derivatographic Method. Acta Chim. Acad. Sci. Hung. **46,** 373 (1965)
241. LIPTAY, G., DÁVID, P., ERDEY, L.: Thermoanalytical Study of Insulating Materials. Periodica Polytech. **9,** 259 (1965)
242. ERDEY, L., SIMON, J., GÁL, S., LIPTAY, G.: Thermoanalytical Properties of Analytical-grade Reagents IV. A. Natrium salts. Talanta **13,** 67 (1966)
243. GÁL, S., ERDEY, L., MEZEI, M., KORMÁNY, T.: Alumíniumoxid-alumíniumhidroxid vékonyrétegek szerkezetének vizsgálata termikus és röntgendiffrakciós módszerrel. (Thermal and X-ray Studies on the Structure of Alumina and Aluminum Hydroxide Layers). Finommechanika **4,** 251 (1965)
244. LIPTAY, G., BERÉNYI, M., ERDEY, L., BABICS, A.: Urológiai eredetű kövek derivatográfiás vizsgálata (Derivatographic Study of Urological Stones). Orvosi Hetilap, 155 (1966)
245. ERDEY, L., KÁSA, I., KOVÁCS, L.: Untersuchung der Thermolumineszenz-Eigenschaften von mit Blei aktiviertem Zinksulfid, von mit Blei und Kupfer aktiviertem Zinksulfid–Strontiumsulfid und von mit Mangan aktiviertem Kalciumfluorid Kristallphosphoren. Periodica Polytech. **9,** 223 (1965)
246. ERDEY, L., KHALIFA, H., SVEHLA, G.: Analytical Applications of the Reaction of Hexacyanoferrate(III) with Ascorbic Acid. Part VII. Determination of Bismuth, Zinc and Manganese. Anal. Chim. Acta **32,** 88 (1965)
247. KŐRÖS, E., NELSON, S. M., PAULIK, F., ERDEY, L., RUFF, F.: The Structure and Thermal Decomposition of some Cobalt(II)-pyrazine Mixed Complexes. Proc. of the Symp. Coord. Chem. Tihany, Hungary, 1964, 295 (1965)
248. MEISEL, T., GYIMESI, J., ERDEY, L.: Bestimmung von Acetessigester und α-Aceto-γ--butyrolaceton nebeneinander. Z. Anal. Chem. **217,** 349 (1966)
249. PAULIK, J., PAULIK, F., ERDEY, L.: Standardization of Experimental Conditions in Thermal Analysis. A New Polyplate Sample Holder. Anal. Chim. Acta **34,** 419 (1966)
250. ERDEY, L., BUZÁS, I., VIGH, K.: Luminol as a Fluorescent Acid-base Indicator. Talanta **13,** 463 (1966)
251. ERŐSS, K., SVEHLA, G., ERDEY, L., VÁZSONYI, É.: Quantitative Infrared Analysis of 2,4--Tolylene Diamine and 2,4-Tolylene Diurea Mixtures. Talanta **13,** 767 (1966)
252. BUZÁGH-GERE, É., PAULIK, F., ERDEY, L.: Electron Microscope Investigation of the Thermal Aging of Barium Sulphate Precipitates. Talanta **13,** 731 (1966)
253. ERDEY, L., KÁNTOR, T.: Porok folyamatos bevitele spektroszkópiai fényforrásokba (Continuous Introduction of Powders into Light Sources). Magy. Kém. Foly. **72,** 268 (1966)
254. KÁNTOR, T., ERDEY, L.: Continuous Introduction of Powdered Samples in Emission Spectroscopy. Talanta **13,** 1289 (1966)
255. ERDEY, L., PAULIK, F., PAULIK, J.: Neuere Ergebnisse der Thermo-Derivatographie. Mikrochim. Acta, 699 (1966)
256. PAULIK, J., PAULIK, F., ERDEY, L.: Kombinierte derivatographische und thermogasanalytische Untersuchungen. Mikrochim. Acta, 886 (1966)
257. PAULIK, F., PAULIK, J., ERDEY, L.: Derivative Dilatometrie. Mikrochim. Acta, 894 (1966)
252. GÁL S., MEISEL, T., HALMOS, Z., ERDEY, L.: Untersuchung der thermischen Eigenschaften von Alkalibenzolsulfonaten. Mikrochim. Acta, 903 (1966)
259. LIPTAY, G., HEGYALJAI-KISS, G., ERDEY, L.: Derivatographische Untersuchung von Verbindungen mit Sterangerüst. Mikrochim. Acta, 926 (1966)
260. MEISEL, T., ERDEY, L.: Empfindliche Reaktion zum Nachweis aliphatischer Nitroverbindungen. Mikrochim. Acta, 1148 (1966)
261. PAULIK, F., PAULIK, J., ERDEY, L.: Derivatography. A Complex Method in Thermal Analysis. Talanta Review. Talanta **13,** 1405 (1966)
262. PAULIK, J., WOLKOBER, Z., PAULIK, F., ERDEY, L.: Derivatographische Untersuchung von PVC. Plaste und Kautschuk **13,** 336 (1966)
263. CSŰRÖS, Z., PETRÓ, J., KÁLMÁN, V., ERDEY, L., PAULIK, F.: Catalytic Properties of Raney-nickel as a Function of its Preparation. Periodica Polytech. **10,** 27 (1966)
264. INCZÉDY, J., GÁBOR-KLATSMÁNYI, P., ERDEY, L.: The Use of Ammonium Sulphosalicylate as Complexing Agent in Ion Exchange Chromatography I. Acta Chim. Acad. Sci. Hung. **50,** 105 (1696)
265. MEISEL, T., GÁL, S., HALMOS, Z., ERDEY, L.: Untersuchung der thermischen Eigenschaften von Benzolsulfonaten II. Erdalkalibenzolsulfonate. Mikrochim. Acta 31 (1967)
266. KOLOS, E., BÁNYAI, É., ERŐSS, K., ERDEY, L.: Malachitgrün, ein empfindlicher Indikator für jodometrische Mikrotitrationen. Mikrochim. Acta 333 (1967)

267. INCZÉDY, J., ERDEY, L.: Polarographic Determination of Rare Earth Ions Solutions Containing Ammonium Lactate. Acta Chim. Acad. Sci. Hung. **51,** 349 (1967)
268. RÁDY, G., ERDEY, L.: Titrimetrische Goldbestimmung mit Ascorbinsäure unter visueller Endpunktsindikation. Talanta **14,** 425 (1967)
269. KISS, T., RÁDY, G., ERDEY, L.: Komplexometrische Bestimmung von Kupfer mit ADTA durch Rücktitrationen gegen Eriochromschwarz. Periodica Polytech. **10,** 303 (1966)
270. ERDEY, L., BUZÁS, I., VIGH, K.: Variamine Blue as a Gravimetric Reagent. Determination of Tungsten. Talanta **14,** 515 (1967)
271. GEGUS, E., KOCSIS, E., ERDEY, L.: Tube-electrode Spray Method in the Emission Spectroscopy of Solutions. Periodica Polytech. **10,** 381 (1967)
272. ERDEY, L., SZABADVÁRY, F.: Some Trends in the Development of Instrumental Analysis in Hungary. Pure and Applied Chem. **13,** 437 (1966)
273. BERÉNYI, M., LIPTAY, G., BABICS, A., ERDEY, L.: Thermoanalytische Untersuchung von Nierensteinen I. Steinkomponenten mit Purinstruktur. Z. f. Urologie **60,** 361 (1967)
274. GIMESI, O., RÁDY, G., ERDEY, L.: Bestimmung quaternärer heterocyclischer Ammoniumbasen und ihrer Salze in Eisessig. Acta Chim. Acad. Sci. Hung. 52. 343. (1967)
275. SIMON, J., GÁL, S., ERDEY, L.: Thermal Reactions of Sodium Halides. Acta Chim. Acad. Sci. Hung. **53,** 105 (1967)
276. ERDEY, L., MEISEL, T., MOHOS, B., TÜDŐS, F.: Electron Spin Resonance Analysis of the Redox Indicator Variamine Blue II. Talanta **14,** 1477 (1967)
277. ERDEY, L., SZABÓ, E.: Az aktivációs analízis hazai helyzete (Activation Analysis in Hungary). Atomtechnika Tájékoztató **10,** 183 (1967)
278. ERDEY, L., MARIK-KORDA, P., LIPTAY, G.: Gravimetric Determination of Copper(II) with *p*-Aminobenzoic Acid. Talanta **15,** 149 (1968)
279. KÁSA, I., RÓKA, O., BUZÁGH-GERE, É., ERDEY, L.: Mangánnal aktivált LiF-MgF_2 alapú foszforok vizsgálata (Investigation of LiF-MgF_2 Phosphors Activated with Manganese. Magy. Kém. Foly. **73,** 515 (1967)
280. KÁNTOR, T., ERDEY, L.: The Role of the Grain-size in the Spectrographic Analysis of Alumina. Proc. XIV. Coll. Spectr. International, Debrecen, 985 (1967)
281. ERDEY, L., SVEHLA, G.: The Calculation of Indicator Error in Oxidation-reduction Titrations. Anal. Chim. Acta **40,** 473 (1968)
282. TOMEK, A., LIPTAY, G., SIMON, J., ERDEY, L.: Derivatographische Untersuchung der Zerreiche I. Holz als Roh- und Werkstoff, **26,** 45 (1968)
283. PAULIK, F., PAULIK, J., ERDEY, L.: Combined Thermo-dilatometric and Derivatographic Examination of Hydrargillite and Barium Chloride Dihydrate. Anal. Chim. Acta **41,** 170 (1968)
284. GÁBOR-KLATSMÁNYI, P., INCZÉDY, J., ERDEY, L.: The Use of Ammonium Sulphosalicylate as Complexing Agent in Ion Exchange Chromatography II. Acta Chim. Acad. Sci. Hung. **57,** 5 (1968)
285. ROKOSZ, A., PAULIK, J., PAULIK, F., ERDEY, L.: Beiträge zur quantitativen Differentialthermoanalyse. Acta Chim. Acad. Sci. Hung. **56,** 221 (1968)
286. GÁL, S., KORMÁNY, T., MEZEY, M., ERDEY, L.: Untersuchung von durch anodische Oxydation erzeugten Aluminiumoxidschichten. II. Z. Anal. Chem. **239,** 106 (1968)
287. PAULIK, J., PAULIK, F., ERDEY, L.: Rolle der Versuchsverhältnisse in den thermischen Untersuchungen I. Form des Probebehälters. Periodica Polytech. **12,** 105 (1968)
288. PAULIK, J., PAULIK, F., ERDEY, L.: Rolle der Versuchsverhältnisse in den thermischen Untersuchungen II. Einfluß der Korngröße der Probe. Periodica Polytech. **12,** 109 (1968)
289. ERDEY, L., SIMON, J., GÁL, S.: Thermoanalytical Properties of Analytical-grade Reagents V. Sodium Halates. Talanta **15,** 653(1968)
290. ERDEY, L., SVEHLA, G., WEBER, O.: Anwendung der ascorbinometrischen Bestimmung von Hexacyanoferrat(III) zu automatischen Mikrotitrationen. Z. Anal. Chem. **240** 91 (1968)
291. KÁSA, I., ERDEY, L., RÓKA, O.: Study of the Thermoluminescence of Manganese-activated LiF-MgF_2 Phosphors. Proc. Int. Conf. on Luminescence 788 (1966)
292. BUZÁGH-GERE, É., ERDEY, L., LÉVÉNYI, M.: Keményfémek elektronmikroszkópos vizsgálata (Electron Microscopic Study of Hard Metals). Kohászat **101,** 319 (1968)
293. ERDEY, L., KÁFIÁR, L.: A nátrium-tetrafenilborát alkalmazása gyógyszerek minőségi és mennyiségi meghatározására. (Application of Sodium Tetraphenylboron in Qualitative and Quantitative Pharmacological Analysis). Acta Pharm. Hung. **38,** 369 (1968)
294. PAULIK, J., PAULIK, F., ERDEY, L.: An Investigation of Barium Oxalate by Combined Derivatographic and Thermo-gas Analysis. Anal. Chim. Acta **44,** 153 (1969)

295. ERDEY, L.: Gravimetry as the Basis of Chemical Analysis. Chemia Analityczna **13,** 969 (1968)
296. ERDEY, L.: Anwendung thermoanalytischer Methoden in der Biochemie und klinischen Chemie. Z. Anal. Chem. **243,** 30 (1968)
297. ERDEY, L.: Nyomelemek meghatározásának különböző módszerei (Methods of Trace Element Analysis). MTA Kém. Tud. Oszt. Közl. **30,** 373 (1968)
298. KÁNTOR, T., HANNA, Z. G., ERDEY, L.: Controlled Evaporation of Materials in a d. c. Arc. Spectrochim. Acta **24B** 37 (1969)
299. SIMON, J., BIHARI-VARGA, M., ERDEY, L., GERŐ, S.: Thermal Decomposition of Glycosaminoglycan. Acta Biochem. et Biophys. Acad. Sci. Hung. **3,** 363 (1968)
300. ERDEY, L., GIMESI, O., SZABADVÁRY, F.: Radiometric Acid-base titrations. Talanta **16,** 445 (1969)
301. ERDEY, L.: Primenenie metoda atomnoy spektroskopii v analiticheskoy laboratorii shirokovo profilya. Zh. anal. khimii **24,** 48 (1969)
302. ERDEY, L.: Nekotorie rezultati v oblasty khimicheskih razdeleniy. Zh. anal. himii **24,** 221 (1969)
303. SIMON, J., BALOGH, K., PETRUCZ, K., ERDEY, L.: Thermal Analysis of Dental Calculi and Duct Calculi. Periodica Polytech. **12,** 395 (1969)
304. KÁNTOR, T., ERDEY, L.: Time-resolved a. c. Arc Spectra for Atomic Absorption Spectroscopy. Spectrochim. Acta **24B** 283 (1969)
305. PAULIK, F., BUZÁGH-GERE, É., ERDEY, L.: Derivatographische Untersuchung des Magnesiumammoniumphosphats. Acta Chim. Acad. Sci. Hung. **61,** 29 (1969)
306. INCZÉDY, J., KLATSMÁNYI-GÁBOR, P., ERDEY, L.: The Use of Complex-forming Agents in Ion Exchange Chromatography, I. Acta Chim. Acad. Sci. Hung. **61,** 261 (1969)
307. HANNA, Z. G., KÁNTOR, T., ERDEY, L.: Distribution of Arc Temperature Using Cathode Excitation. Acta Chim. Acad. Sci. Hung. **61,** 329 (1969)
308. BUZÁGH-GERE, É., ERDEY, L.: Precipitation of Manganese Ammonium Phosphate from Homogeneous Solution. Talanta **16,** 1434 (1969)
309. INCZÉDY, J., KLATSMÁNYI-GÁBOR, P., ERDEY, L.: The Use of Complexing Agent in Ion Exchange Chromatography, II. Acta Chim. Acad. Sci. Hung. **62,** 1 (1969)
310. ERDEY, L., KÁPLÁR, L., TAKÁCS, J., DESSOUKY, Y. M.: Determination of Hydantoins in Pharmaceutical Preparations by Gas Chromatography. J. Chromatogr. **45,** 63 (1969)
311. GÁL, S., MEISEL, T., ERDEY, L.: On the Thermal Analysis of Aliphatic Carboxylic Acids and their Salts. J. Thermal Anal. **1,** 159 (1969)
312. BUZÁGH-GERE, É., PAULIK, F., ERDEY, L.: Thermische Eigenschaften und Aufschlußreaktionen von Natriummetaphosphat. J. Thermal Anal. **1,** 293 (1969)
313. ERDEY, L., BALLA, J., HALMOS, Z., MEISEL, T.: Analysis of the Products of Hydroammonolysis of Acetone. J. Chromatogr. **46,** 312 (1970)
314. KÁNTOR, T., ERDEY, L.: Investigation on the Accuracy of Microphotometers. Acta Chim. Acad. Sci. Hung. (in the press)
315. KÁNTOR, T., ERDEY, L.: Arany spektrográfos meghatározása nemesiszapban (Spectrographic Determination of Gold in Noble Muds). Magy. Kém. Foly. (In the press)
316. ERDEY, L., SZABÓ-ÁKOS, ZS.: Oszillometrische Bestimmung des Lithiums. Acta Chim. Acad. Sci. Hung. (in the press)
317. INCZÉDY, J., KLATSMÁNYI-GÁBOR, P., ERDEY, L.: The Use of Complex Forming Agents in Ion Exchange Chromatography V. Acta Chim. Acad. Sci. Hung. (In the press)
318. PÁLL, A., SVEHLA, G., ERDEY, L.: The Determination of Microgram Amounts of Metals by Chronometric Analysis. Talanta **17,** 211 (1970)
319. ERDEY, L., KÁPLÁR, L., TAKÁCS, J., DESSOUKY, Y. M.: Gyors analitikai módszer hydantoin-származékok gázkromatográfiás meghatározására gyógyszerkészítményekben (Rapid Gas Chromatographic Determination of Hydantoin Derivatives in Pharmacological Preparations). Acta Pharm. Hung. (In the press)
320. ERDEY, L., KÁPLÁR, L.: Rapid Volumetric Method for the Determination of Nitrogen in Nitridized Steels. Periodica Polytech. (In the press)
321. BALLS, J., ERDEY, L.: Quantitative Gas-chromatographic Analysis by Precision Calibration Method I. J. Chromatogr. (In the press)
322. ERDEY, L., MARIK, J.: Szerves oldószerek víztartalmának meghatározása közvetlen termometriás módszerrel (Determination of Water in Organic Solvents by a Direct Thermometric Method). Magy. Kém. Lapja (In the press)
323. ERDEY, L., TAKÁCS, J., KRÁLIK, D.: Error of Determination of Retention Indices. J. Chromatogr. (In the press)
324. ERDEY, L., PÓLOS, L., NÉMETH, A.: Conductometric Studies on Halide Complexes in Formic Acid Medium. Periodica Polytech. (In the press)

325. NÉMETH, Á., ERDEY, L.: Qualitative Tests in Formic Acid Medium. Periodica Polytech. (In the press)
326. ERDEY, L., PÓLOS, L.: How to Report on a New Gravimetric Method of Analysis. Talanta (In the press)
327. ERDEY, L., PÓLOS, L.: A kémiai analízis alapja a gravimetria (Gravimetry — The Basis of Chemical Analysis). Kém. Közlemények (In the press)
328. ERDEY, L.: Redox Titration and Complex Formation. Cronache die Chimica (In the press)
329. SIMON, J., GÁL, S., ERDEY, L.: The Thermal Reactions of Potassium Halates and Perhalates. Acta Chim. Acad. Sci. Hung. (In the press)

BOOKS

1. ERDEY, L.: Bevezetés a kémiai analízisbe I. Minőségi kémiai analízis (Introduction to Chemical Analysis, Vol. 1. Qualitative Chemical Analysis). Természettudományi Társulat. Budapest, 323 pp., 1st Ed. 1945. Tankönyvkiadó Budapest. 2nd Ed. 1951, 3rd Ed. 1955, 4th Ed. 1956, 5th Ed. 1958, 6th Ed. 1961, 7th Ed. 1965, 8th Ed. 1966
2. ERDEY, L.: Bevezetés a kémiai analízisbe II. Térfogatos analízis (Introduction to Chemical Analysis, Vol. 2, Volumetric Analysis). Egyetemi Nyomda, Budapest, 308 pp. 1st Ed. Tankönyvkiadó, Budapest, 1947, 2nd Ed. 1951, 3rd Ed. 1953, 4th Ed. 1954, 5th Ed. 1956, 6th Ed. 1958, 7th Ed. 1962, 8th Ed. 1965, 9th Ed. 1966, 10th Ed. 1969
3. ERDEY, L.: A kémiai analízis súlyszerinti módszerei, I—III. kötet (Gravimetric Methods of Chemical Analysis, Vol. I—III), 1468 pp. Akadémiai Kiadó, Budapest, 1960
4. ERDEY, L.: Theorie und Praxis der gravimetrischen Analyse. Bd. I—III. S. 1524 Akadémiai Kiadó, Budapest 1964
5. ERDEY, L.: Gravimetric Analysis. Vol. I—III. pp. 1421, Pergamon Press, Oxford 1965

PATENTS

1. ERDEY, L. és BUZÁSNÉ PAPP, I.: Eljárás hidrogénperoxid tartósítására (Method for the Stabilization of Hydrogen Peroxide). Hung. Pat. 142.392 (1952)
2. ERDEY, L. és MÁZOR, L.: Eljárás gyorsan ülepedő vörösiszap nyerésére a bauxitnak a Bayer-eljárás szerint való feltárása során (Method for Obtaining Rapidly Settling Red Mud in the Bayer Bauxite Process). Hung. Pat. 145.422 (1956)
3. PAULIK, F., PAULIK, J., ERDEY, L.: Készülék anyagok derivatív termogravimetriás és egyidejű termogravimetriás vizsgálatára (Apparatus for Simultaneous Thermogravimetric and Derivative Thermogravimetric Analysis). Hung. Pat. 144.548 (1954)
4. PAULIK, F., PAULIK, J., ERDEY, L.: Készülék differenciál-termikus elemzés, termogravimetriás és derivatív termogravimetriás vizsgálatok egyidejű elvégzésére és regisztrálására (Apparatus for Differential Thermal Analysis, Thermogravimetric and Derivative Thermogravimetric Studies with Simultaneous Recording of the Results). Hung. Pat. 145.369 (1955)
5. PAULIK, F., PAULIK, J., ERDEY, L.: Eljárás és készülék folyadékok desztillációs görbéjének termogravimetriás úton történő meghatározására. (Method and Apparatus for the Thermogravimetric Determination of Distillation Curves of Liquids). Hung. Pat. 146.464 (1956)
6. PAULIK, F., PAULIK, J., ERDEY, L., ZAGYVAI, I.: Eljárás és készülék szuszpenziók ülepedésére, ill. emulziók kifölöződése által okozott fajsúlyváltozás és ennek sebességének egyidejű meghatározására (Method and Apparatus for Determining the Variation and Rate of Variation of the Specific Weight Due to Sedimentation of Suspensions and to Separation of Emulsions). Hung. Pat. 148.711 (1959)
7. ERDEY, L., PAULIK, F., PAULIK, J.: Eljárás és készülék szuszpenziók ülepedésének és ülepedéssebességének egyidejű meghatározására és automatikus regisztrálására (Method and Apparatus for the Simultaneous Determination and Automatic Recording of Sedimentation and Sedimentation Rate of Suspensions). Hung. Pat. 149.871 (1959)
8. PAULIK, F., PAULIK, J., ERDEY, L.: Eljárás és készülék folyadékok desztillációs görbéjének termogravimetriás úton történő meghatározására (Method and Apparatus for the Thermogravimetric Determination of Distillation Curves of Liquids). Hung. Pat. (Supplement) 146.464 (1960)
9. PAULIK, F., PAULIK, J., ERDEY, L.: Eljárás és készülék vegyületek termikus hőtartalomváltozása, dilatációja és dilatációsebességének egyidejű mérésére (Method and Appara-

tus for the Simultaneous Measurement of the Heat Content, Dilatation and Rate of Dilatation of Compounds). Hung. Pat. 150.905 (1961)

10. PAULIK, F., PAULIK, J., ERDEY, L.: Eljárás és készülék vegyületek termikus súlyváltozásának, súlyváltozás sebességének, entalpiaváltozásának, dilatációjának, dilatációsebességének és hőmérsékletének egyidejű mérésére és automatikus regisztrálására (Method and Apparatus for the Simultaneous Measurement and Automatic Recording of the Thermal Weight-change, Rate of Weight-change, Enthalpy Change, Dilatation, Rate of Dilatation, and Temperature of Compounds). Hung. Pat. 150.906 (1961)
11. PAULIK, J., PAULIK, F., ERDEY, L.: Mintatartó a termoanalitikai vizsgálatok szelektivitásának növelésére (Sample Holder for Increasing the Selectivity of Thermoanalytical Measurements). Hung. Pat. 151.783 (1963)
12. PAULIK, J., PAULIK, F., ERDEY, L.: Termoanalitikai berendezésekhez kapcsolható készülék anyagok hőbomlása során keletkező gázbomlástermékek mennyiségének, ill. gázfejlődés folyamatának és a folyamat sebességének egyidejű automatikus meghatározására (Accessory for Thermoanalytical Instruments, for the Simultaneous Automatic Determination of the Amount of Gaseous Products and the Rate of their Formation During Thermal Decomposition). Hung. Pat. 154.372 (1966)
13. CSERFALVI, T., DEBRECZENI, E., ERDEY, L., MEISEL, T., MÉSZÁROS, P., PÁLMAY, GY.: Eljárás alkálihipokloritok automatikus folyamatos előállítására (Process for the Continuous Automatic Preparation of Alkali Hypochlorites). Hung. Pat. Application No. 16.988 (Dec. 24, 1969)

Acta Chimica Academiae Scientiarum Hungaricae, Tomus 66 (2), pp. 159—164 (1970)

PRAKTISCHE VERWENDUNG DER »BLINDWERTKORREKTION« IN DER SPEKTROGRAPHISCHEN SPURENANALYSE

T. TÖRÖK und S. BÁN

(Institut für Anorganische und Analytische Chemie der L. Eötvös Universität, Budapest)

Eingegangen am 8. Mai 1969

Das zur Ausschaltung des störenden Effektes der Trägerelektroden-Verunreinigungen dienende, früher ausgearbeitete mathematische Verfahren [1] wurde für die Kalziumbestimmung nach dem SCHEIBE—RIVAS Verfahren verwendet. Die Trägerelektrode aus Kohle, Typ TOPOLÁNY war ebenfalls mit Kalzium verunreinigt. Nach eingehender Beschreibung der Versuchsbedingungen wurden die Eichkurven ohne Korrektion mit der Untergrund- und die Trägerelektrodenverunreinigung nur mit Untergrundkorrektion, sowie mit Untergrund- und Trägerelektrodenverunreinigungs-Korrektion dargestellt. Sie beweisen die Brauchbarkeit des Korrektionsverfahrens, sind mit den theoretisch zu erwartenden Effekten im Einklang und geben Aufschluß über das Maß der Trägerelektrodenverunreinigungen.

Einleitung

Bei der spektrographischen Spurenanalyse benötigt man Hilfsmaterialien höchster Reinheit (Trägerelektroden, Gegenelektroden, Lösungsmittel, Aufschließmaterialien, Puffer, inerte Gase usw.), welche im allgemeinen sehr teuer sind, oder oft nicht zur Verfügung stehen. Die Verwendung unreiner Materialien hat aber verschiedene Nachteile. Die Auswertungskurven sind nicht linear, infolgedessen braucht man zu ihrer Aufstellung eine viel größere Zahl von Standards, die Genauigkeit der Analyse vermindert sich, das sog. »leitprobenfreie Verfahren« ist nicht durchführbar, die maschinelle Auswertung wird kompliziert, und die bei der Spurenanalyse oft verwendete Extrapolation kann nicht durchgeführt werden.

Um die Schwierigkeiten zu beseitigen, muß die gemessene Strahlungsintensität der Analysenlinie mit jener Emission korrigiert werden, die aus der Verunreinigung der Hilfsmaterialien stammt. Das diesbezügliche, bereits früher ausgearbeitete Rechnungsverfahren [1] wird durch folgende Gleichungen ausgedrückt:

$$\Delta Y^* = \lg \frac{I_Z + I_{Z0}}{I_G} , \tag{1}$$

$$\Delta Y_0 = \lg \frac{I_{Z0}}{I_G} , \tag{2}$$

$$\Delta Y = \lg \frac{I_Z}{I_G}, \tag{3}$$

wo ΔY^* das zur Analysenaufnahme, ΔY_0 der zu äußeren Verunreinigungen gehörende und ΔY das korrigierte Logarithmus-Intensitätsverhältnis des Analysenlinienpaares ist. Weiterhin bedeuten I_Z bzw. I_{Z0} die Intensität der Analysenlinie des zu bestimmenden Elementes Z, die aus der Probe bzw. von äußeren Verunreinigungen stammt und I_G die Linienintensität des Bezugselementes G. Selbstverständlich bedeuten alle ΔY-Werte mit Untergrund korrigierte Werte.

Das Wesentliche der Blindwertkorrektion ist die Berechnung der ΔY-Werte aus den Werten ΔY^* unter Verwendung der Werte ΔY_0. Nach den Gleichungen (1)—(3) ist die Korrektion der äußeren Verunreinigungen, d. h. die »Blindwertkorrektion«, der Untergrundkorrektion [2] formell gleich. Aufgrund dieser Analogie kann geschrieben werden:

$$\Delta Y = \Delta Y^* - D_{\Delta Y^* - \Delta Y_0} \tag{4}$$

wo D den zum im Index angegebenen Unterschied gehörenden Gauss'schen Subtraktionslogarithmus bedeutet.

Das Ziel dieser Arbeit war die Erprobung der praktischen Verwendbarkeit des Korrektionsverfahrens. Im folgenden fassen wir die Angaben bezüglich der verwendeten Methode, Modell-Materialien, Trägerelektrode und im allgemeinen alle Parameter zusammen, welche wir verwendet haben.

Versuchsverhältnisse

Allgemeine Bedingungen

Versuchsverfahren: Methode nach SCHEIBE—RIVAS [3]
Zusammensetzung der Standardlösungen, angegeben in g/V%:

Ca: $2{,}8 \cdot 10^{-4}$; $8{,}8 \cdot 10^{-4}$; $2{,}8 \cdot 10^{-3}$; $8{,}8 \cdot 10^{-3}$
Al: $1{,}6 \cdot 10^{-1}$

Lösungsmittel: 5,6 *n* HCl
Trägerelektrode: Kohlenelektrode, Typ Topolčany, Durchmesser 6,0 mm, mit abgerundeter Kante und ebener Stirnfläche.
Elektrodenabstand: 3,5 mm
Vorfunkzeit der trockenen Elektroden: 30 s
Aufgetragene Lösungsmenge: 0,1 ml

Anregungsbedingungen

Anregungsgerät: Funkenerzeuger Typ IG-2 (»Tandem-Spark«-System)
Spitzenspannung: 10 kV
Kapazität: 0,02 μF
Selbstinduktion: nicht eingeschaltet
Steuerelektrodenabstand: 0,1 mm
Anzahl der Hauptentladungen: 100/s
Vorfunkzeit: keine
Belichtungszeit: 30 s

Lichtzerlegungsbedingungen

Spektrograph: Dreiprismenglasspektrograph Typ ISzP 51, Brennweite der Kollimatorlinse: 800 mm, der Kammerlinse: 870 mm
Belichtungssystem: Zwischenabbildung
Spaltbreite: 25 μm
Dreistufenfilter: 100/50/10%, bei 395 nm

$$\Delta Y_{100/50} = 0{,}316, \quad \Delta Y_{100/10} = 0{,}960$$

Photographische und photometrische Bedingungen

Spektralplatte: Gevaert Scientia 23 D 56
Entwicklung: in Agfa 1 Entwickler bei 20,5 °C, 4 Minuten
Spektrallinien-Photometer: Zeiss Schnellphotometer
Spaltbreite: 0,20 mm
Analysenlinienpaar: Ca 3968,48/Al 3961,54 Å

Auswertung

Die Rechnungen der zum Analysenlinienpaar gehörenden ΔY-Werte mit und ohne Untergrundkorrektion wurden mit einem elektrischen Auswertegerät [4] analogen Systems — »Spectrator« — durchgeführt. Die Konstanten γ und $\varkappa$ wurden aus den Schwärzungswerten, die an den verschiedenen Stufen der Analysenlinien des Kalziums der Spektralserie gemessen wurden, auch mit dieser Einrichtung berechnet. Wir erhielten folgende Werte:

$$\gamma = 5{,}75$$

$$\varkappa = 2{,}34$$

Zur Bestimmung des für die Berechnung der Verunreinigungskorrektion notwendigen ΔY_0-Wertes wurde eine Serie von Spektren aufgenommen. Hierzu verwendeten wir eine Lösung, die sich von den Standardlösungen darin unterschied, daß keine Kalzium-Stammlösung dazugegeben wurde. Es soll bemerkt werden, daß die äußere Verunreinigung größtenteils von der Kalziumverunreinigung der Trägerelektrode stammt. Die mit dem Bezugselement (Al) und dem Lösungsmittel (5,6 *n* HCl) eingetragene Verunreinigung spielt nur eine untergeordnete Rolle. Es ist jedoch sehr wichtig, daß die Kalziumverunreinigung der Kohlenelektrode homogen verteilt sein soll; diese Bedingung wird aber nicht in jedem Fall erfüllt.

Als Grundwert ΔY_0, der zu unserer Korrektionsmethode nötig ist, wurde der Mittelwert der mit Untergrund korrigierten ΔY-Werte angenommen, die aufgrund der auf die oben angegebene Weise hergestellten Lösungen erhalten wurden. Die Korrektion der Werte ΔY^* wurden mit Hilfe der Gleichung (4) durchgeführt.

Meßergebnisse und Diskussion

Die Kurven 1,2 bzw. 3 in Abbildung 1 veranschaulichen die Eichkurven, die mit Verwendung der Werte des mit dem Untergrund nicht korrigierten ΔY^{**}-, der mit dem Untergrund korrigierten ΔY^{*}-, und des durch dessen Blindwertkorrektion erhaltenen ΔY-Werten aufgestellt wurden.

Aus der Abbildung ist ersichtlich, daß die aus den weder mit Untergrund, noch mit Verunreinigung korrigierten ΔY^{**}-Werten konstruierte Auswer-

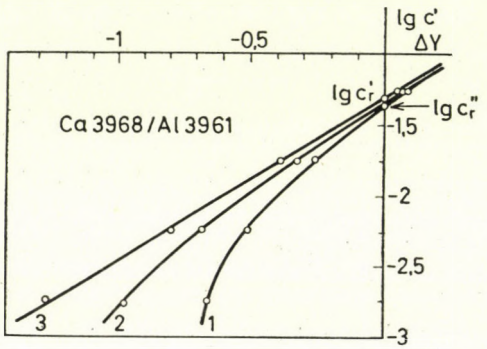

Abb. 1. Unkorrigierte (1), mit Untergrundkorrektion (2) bzw. mit Untergrundkorrektion und Verunreinigungskorrektion (3) erhaltene Auswertungskurven

tungskurve (Kurve 1) nur bei verhältnismäßig hohen Konzentrationen praktisch geradlinig ist, mit abnehmender Konzentration jedoch immer mehr von der Geraden abweicht. Dies ist verständlich, da die störende Wirkung der Untergrundstrahlung und der Verunreinigung die gleiche Richtung aufweist und beide eben bei niedrigen Konzentrationen bedeutend sind. Nach Beseitigung der störenden Wirkung der Untergrundstrahlung gelangen wir noch nicht zur linearen Auswertungskurve (Kurve 2). Es kann jedoch festgestellt werden, daß sich die praktisch lineare Strecke der Kurve verlängert und die Abweichung kleiner wurde. Der Grund der noch bestehenden Deformation liegt in der »äußeren« Verunreinigung. Wenn auch diese in Korrektion genommen wird, so erhalten wir eine völlig lineare Auswertungskurve (Kurve 3). Unsere Versuche ergaben also die erwarteten Resultate. Durch Verwendung der Korrektion können all die Schwierigkeiten beseitigt werden, welche in der Einleitung erwähnt wurden.

Aus der Abbildung ist weiters ersichtlich, daß die mit und ohne Untergrundkorrektion erhaltenen Kurven die Achse lg c' in demselben Punkt schneiden, d. h. daß zu beiden derselbe homologe Konzentrationswert c_r'' gehört. Dies ist leicht verständlich, wenn man bedenkt, daß im Falle von $\Delta Y_{Ca}^{+,+} = Y_{Al}^{**}$ der Wert $Y_{Ca}^{*} = Y_{Al}^{*}$ ist, da die Intensitäten der Untergrunde neben den zueinander nahe liegenden Aluminium- und Kalziumlinien praktisch gleich sind.

Aus der Abbildung geht ferner auch hervor, daß bei Konzentrationen, die kleiner sind als c_r'', die Werte ΔY^{**} ohne jede Korrektion größer sind, als die entsprechenden, mit Untergrund korrigierten Werte ΔY^{*}. Bei Konzentrationen, die höher sind als c'', sind die Verhältnisse umgekehrt. Aus dem vorangehenden folgt — was übrigens auch aus der Abbildung ersichtlich ist, — daß sich die aus den oben erwähnten zweierlei Daten aufgestellten Kurven kreuzen müssen. Der Grund der Erscheinung liegt darin, daß im Falle von $c' < c_r''$ die Werte ΔY^{**} negativ, bei Konzentrationen $c' > c''$ hingegen positiv sind. Im ersten Fall ist die Intensität der Kalziumlinie kleiner, als die des Aluminiums, und so vermindert sich die Intensität der Kalziumlinie bei der Untergrundkorrektion in relativ stärkerem Maße, wie die der intensiveren Aluminiumlinie. Bei Konzentrationen über c'' ist hingegen die Intensität der Aluminiumlinie kleiner und die des Kalziums größer, und so vermindert die Untergrundkorrektion die Intensität der Aluminiumlinie in relativ größerem Maße.

Schließlich geht aus den Kurven der Abbildung auch klar hervor, daß der Wert c_r' der homologen Konzentration im Falle der mit Verunreinigungskorrektion erhaltenen Auswertungskurve höher ist als der Wert c_r'', der zu der ohne Verunreinigungskorrektion erhaltenen Kurve gehört. Der Wert c_r'' bedeutet nämlich diejenige Konzentration, bei welcher die Linienintensität des Kalziums, die ebenfalls von der Verunreinigung und der hinzugegebenen Kalziummenge stammt, der Aluminiumlinienintensität gleich ist. c' bedeutet hingegen diejenige Konzentration, bei welcher die Linienintensität, die von dem in die Standard-Lösung eingewogenen Kalzium stammt, der Linienintensität des Aluminiums gleich ist. So liefert die Differenz $c_r'-c_r''$ Aufschluß über das Maß der äußeren Verunreinigung, dessen Wert in unserem Falle 0,0038 Ca/Al rel. % beträgt.

Über das Maß der äußeren Verunreinigung können wir uns auch auf anderem Wege informieren. Der Konzentrationswert, der zu dem Ordinatenpunkt ΔY_0 der mit Untergrund- und Blindwertkorrektion erhaltenen Auswertungsgerade gehört, ist nämlich umso größer, je größer die äußere Verunreinigung ist.

Es kann festgestellt werden, daß die so ablesbare Konzentration in unserem Falle 0,0016 Ca/Al rel. % beträgt. Dieser Wert stimmt mit dem Wert $c'-c_r''$ nicht überein, da keiner von diesen der tatsächlichen prozentuellen Konzentration der äußeren Verunreinigung gleich ist. Die zu ΔY_0 gehörenden und die $c_r'-c_r''$-Konzentrationswerte können das miteinander verglichene Maß der Verunreinigung der Hilfsmaterialien verschiedener Herkunft nur als mit sich selbst in Vergleich gestellte relative Meßzahlen charakterisieren.

Man erhält die den Grad der Verunreinigung eindeutig charakterisierende Meßzahl in dem Falle, wenn man aufgrund der Gleichung (2) den Wert des Intensitätsverhältnisses I_{Z_0}/I_G berechnet. Dieser ergibt sich aufgrund des Wertes $\Delta Y_0 = -1{,}275$ zu 0,053. Man muß aber zum gleichen Wert gelangen, wenn

man die zu derselben c' Konzentration gehörenden (num lg ΔY^* — num lg ΔY)-Werte berechnet. Diese ergeben nämlich nach den Gleichungen (1) und (3) ebenfalls den von der veränderlichen Konzentration unabhängigen Wert I_{Z_0}/I_G. Für die so berechneten Werte ergab sich — wie wir uns darüber überzeugt haben — innerhalb der Versuchsfehlergrenzen gleichfalls $I_{Z_0}/I_G = 0{,}053$.

Vergleichen wir den Wert $I_{Z_0}/I_G = 0{,}053$ mit dem zur niedrigsten Konzentration gehörenden Wert $(I_Z + I_{Z_0})/I_G = 0{,}105$, so kann der wesentliche störende Effekt der äußeren Verunreinigung festgestellt werden. Dieser Störungseffekt vermindert sich — wie hierauf bereits hingewiesen wurde — mit der Erhöhung der Konzentration, d. h. der unkorrigierten Eichgeraden.

LITERATUR

1. Török, T.: Magy. Kém. Foly., **72**, 433 (1966)
Acta Chim. Acad. Sci. Hung., **49**, 11 (1966)
2. Honerjäger-Sohm, M., Kaiser, H.: Spe trochim. Acta **1**, 396 (1944)
3. Scheibe, G., Rivas, A.: Angew. Chem., **49**, 443 (1936)
4. Török, T., Bajáki, L.: Acta Chim. Acad. Sci. Hung., **41**, 143 (1964).

Tibor Török
Sándor Bán
Budapest VIII., Múzeum-krt. 4.

Acta Chimica Academiae Scientiarum Hungaricae, Tomus 66 (2), pp. 165—173 (1970)

ÜBER DIE SPEKTROGRAPHISCHEN EIGENSCHAFTEN DER KAPILLARELEKTRODEN, II*

M. MATHERNY

(Lehrstuhl für Analytische Chemie der Hüttenmännischen Fakultät der Technischen Hochschule in Košice, Tschechoslowakei)

Eingegangen am 27. Mai 1969

Bei der Vorbereitung der Lösungen ist die genaue Einhaltung der Viskosität wichtiger, als eine Konstanz der Oberflächenspannung. Es ist empfehlenswert, die Gesamtsalzkonzentration in den Lösungen unter der Grenze von 10% zu halten. Weiter ist es richtig, mehrere kürzere, ca. 10 bis 15 Sekunden lange Expositionen mit einer Nachfüllung des Lösungsbehälters zu kombinieren, um eine wahre Proportionalität zwischen der Verdampfung aller zur Anregung kommenden Elemente zu erreichen. Bei einer Änderung des Hauptelementes verursachen die Matrixeffekte im wesentlichen nur eine Parallelverschiebung der Analysenlinie, dagegen verursacht die Änderung der Konzentration des Hauptelementes auch eine Änderung ihrer Richtungstangente.

Die auf die Auswertung von Streudiagrammen sich stützende statistische Methode zeigt, daß es zwischen den verfolgten Linien möglich war, fast immer eine echte Korrelation zu erreichen. Die Werte der orthogonalen Regressionskoeffizienten kann man durch zielbewußtes Aussuchen der Anregungsbedingungen in die Spannbreite der Koeffizienten der Konzentrations- und Temperaturfluktuationen hineinbringen.

Als Schlußfolgerung ist zu erwähnen, daß die Bedeutung der Kapillarelektroden für die spektrochemische Analyse neben den günstigen statistischen Wertungsparametern auch in der überaus einfachen Vorbereitung der Trägerelektroden und Bedienung im Laufe des Anregungsprozesses liegt.

Vom Gesichtspunkt der Klassifikation spektrochemischer Lösungsmethoden kann man die Kapillarelektrodenverfahren [1, 2] in die Gruppe der kontinuierlich arbeitenden Methoden einreihen [3]. Die Kapillarelektroden stellen zur Zeit eine vielversprechende Lösungsmethode dar, es fehlen jedoch ausführliche Studien über ihre Leistungsfähigkeit. Deshalb werden die spektrochemischen Eigenschaften der Kapillarelektroden einer systematischen Untersuchung unterworfen, und ihre Ergebnisse mit den Wertungsparametern von mehreren, teils eingehend überprüften, teils neuentwickelten Verfahren verglichen.

Für die Bewertung der erreichten Leistungsfähigkeit eines spektrochemischen Verfahrens sind drei Bewertungskategorien zu unterscheiden. Die erste bewertet die Methode auf Grund von allgemeinen Eigenschaften, wie z. B. Bedingungen für die Vorbereitung der Lösung zur Analyse, Gang des Anregungsprozesses, Verhalten der Elektroden während der Anregung, Zeitlimite, usw. Die zweite Kategorie stützt sich konsequent auf die Statistik, und deshalb werden hierher die Festlegung der Nachweisgrenzen, Garantiegrenzen [4, 5] und andere statistische Parameter eingereiht, wie z. B. die Kor-

* I. Mitteilung: Acta Chim. Acad. Sci. Hung. **48**, 203 (1966)

relations- und Regressionskoeffiziente, Präzision der analytischen Bestimmung usw., die meist durch Auswertung von Streudiagrammen zu ermitteln sind [6, 7]. Die dritte Kategorie faßt die mit der Verläßlichkeit der analytischen Ergebnisse zusammenhängenden Probleme zusammen, z. B. gehört hierher ein ganzer Komplex von spektrochemischen Matrixeffekten [8], die Möglichkeit des Ausschlusses des Auftretens von systematischen Fehlern usw.

Experimenteller Teil

Für die Durchführung des oben erwähnten Vergleichsstudiums war es notwendig, auch eine umfassende experimentelle Untersuchung anlaufen zu lassen. Bei der Bewertung wurde der Schwerpunkt auf die zweite Kategorie der Wertungsparameter gelegt.

Die Tabelle I enthält die allgemeinen und optischen Versuchsbedingungen, die Tabelle II die Anregungsangaben und die Tabelle III die angewendeten Spektrallinien und ihre Parameter laut Literaturangaben [9, 10]. Bei der Bestimmung von Nachweisgrenzen wurde die Kaisersche statistische Methode [5] angewendet. Die Streudiagramme [6, 7] wurden auf Grund von 35 bis 50 Linienpaaren berechnet und nach dem Vorschlag von HOLDT getestet [11]. Die Tabellen IV bis IX enthalten den Vergleich der aus Streudiagrammen ermittelten statistischen Parameter, die berechneten Koeffizienten der Konzentrations- und Temperaturfluktuationen [12] und zuletzt die gemessenen und berechneten Parameter der analytischen Geraden für die unterschiedlichen Matrizen und für die geprüften Elemente. Die im Text verwendeten Symbole sind am Ende des Artikels zusammengefaßt.

Tabelle I

Allgemeine und optische Versuchsangaben

Spektrograph	Gitterspektrograph PGS—2, C. Zeiss-Jena
Arbeitsbedingungen	einfacher Durchgang ohne Vorzerlegung
	$m = 1$, $\alpha = 5{,}80°$, $D = 7{,}28$ [Å · mm^{-1}]
	$m = 2$, $\alpha = 12{,}03°$, $D = 3{,}64$ [Å · mm^{-1}]
Spektralbereich	für $m = 1$ von 210 [nm] bis 420 [nm]
	für $m = 2$ von 260 [nm] bis 340 [nm]
Abbildungsart	dreilinsige Zwischenabbildung nach Zeiss
Zwischenblende	3,2 [mm]
Spaltbreite	0,04 [mm]
Elektrodenabstand	4,0 [mm]
Elektrodenmaterial	Elektrographit, VEB Elektrokarbon, Topolčany, Tschechoslowakei, und Ringsdorff-Werke G.m.b.H., Bad Godesberg, DBR

Verglichene Methoden	Kapillarelektroden-technik	Scheibe – Rivas Verfahren	Dochtelektrodentechnik
Trägerelektroden	SU — 404	SU — 203	SU — Versuchs-elektroden
	RW — 0038	RW — 0027	RW — 0527
Gegenelektroden	SU — 202	SU — 201	SU — 202
	RW — 0085	RW — 0088	SU — 0085
Emulsionsart	ORWO-Spektralplatten blau extrahart, WU—3		
Entwickler	ORWO-Final-Feinkorn, 10′/20 [°C]		
Geprüfter Konzentrationsbereich	von $5 \cdot 10^{0}$ % bis 10^{-4} %		
Mikrophotometer	Schnellphotometer C. Zeiss-Jena		

Tabelle II

Anregungsbedingungen bei den Vergleichsstudien

Anregungsart	Wärmegezündeter Wechselstrombogen	Elektronisch gesteuerter Abreißbogen
Anregungsquelle	DG — 1	BIG — 100
Netzspannung	220 [V]	220 [V]
Stromintensität	11 bis 12 [A]	5,5 bis 6,5 [A]
Polarität	±	±
Zündungszahl	ca 100 [Sek.$^{-1}$]	100 [Sek.$^{-1}$]
Zündungspunkt	?	$\lambda/4$
Expositionsdauer	6 × 10 [Sek.]	4 × 15 [Sek.]

Tabelle III

Verwendete Spektrallinien und deren Parameter

Element	Wellenlänge in [nm]	Ionisationsspannung in [eV]	Anregungsspannung in [eV]	Intensität im Kupferbogen
Al I	257,51	5,99	4,81	48
Ag I	328,07	7,57	3,78	5500
As I	234,90	9,81	?	85
Au I	242,70	9,22	5,10	200
Bi I	306,80	8,00	5,60	3600
Ca I	300,69	6,11	6,02	7
Co I	271,60	7,88	6,60	10
Co I	304,40	7,88	4,18	160
Co I	304,89	7,88	4,24	22
Cu I	296,02	7,72	9,66	24
Fe I	302,05	7,86	4,19	280
In I	325,61	5,79	4,10	1300
Mg I	277,98	7,65	?	90
Ni I	303,79	7,63	4,11	140
Si I	250,69	8,15	4,95	170
Pb I	283,30	7,42	4,40	950
Te I	238,50			

Diskussion

Was die Vorbereitung der Lösung anbelangt, so ist bei der Bereitung der Vergleichslösungen und Proben die genaue Einhaltung der Viskosität wichtiger als die Gewährleistung der Konstanz der Oberflächenspannung. Eine Änderung der Viskosität um ca. 10% ändert die in das Plasma transportierte Lösungsmenge und dadurch auch die Nachweisgrenzen weitgehend. Die Änderung der Oberflächenspannung von 75 $N \cdot m^{-1}$ bis 60 $N \cdot m^{-1}$ hat fast keinen Einfluß auf die Nachweisgrenzen und auf die Intensitätsfluktuationen [13].

Die Auflösung fester Proben bereitet selbstverständlich einige Schwierigkeiten, die aber größtenteils aus den übrigen Gebieten der analytischen Chemie bekannt und gelöst sind. Es ist möglich mit den Kapillarelektroden auch mit solchen Lösungen im Bogen oder Funken eine regelmäßige Anregung zu erzielen, welche mehr als 10% Salze enthalten, doch ist es zu empfehlen, die Gesamtsalzkonzentration unter dieser Grenze zu halten.

Als einmalige Belichtungszeit muß man die Zeitdauer von 10 bis 15 Sekunden akzeptieren [14, 15, 16], da die Integralintensitätsverdampfungskurven nach PISKO [17] ganz deutlich zeigen, daß sich nach dieser Zeitspanne die Proportionalität der Verdampfung zwischen dem analytischen Element und dem zugegebenen Zusatzelement immer verstellt. Deshalb ist es richtig, nach einer ca. 10 Sekunden dauernden Exposition die Anregung zu unterbrechen, den Behälter mit Lösung nachzufüllen und dann die Exposition fortzusetzen. Eine weitere neue Erkenntnis, die mit der oben erwähnten Erscheinung in Zusammenhang steht, ist die Klärung des Transportmechanismus bei den Kapillarelektroden. Der Transport der Lösung aus dem Behälter zur Elektrodenstirnfläche wird, hauptsächlich bei Bogenanregung, durch Kapillarkräfte hervorgerufen. Von der Elektrodenstirnfläche verdampft die Lösung dann teilweise in das Plasma und kondensiert sich teilweise auf der Gegenelektrode. Aus diesem Kondensat erfolgt dann auf der Stirnfläche der Gegenelektrode die weitere Verdampfung in das Plasma. Diese Behauptung wurde damit bewiesen [16], daß in Spektren, die mit einer durchbohrten Gegenelektrode aufgenommen wurden, die Linienintensitäten um ca. 40 bis 70% schwächer sind als die Linienintensitäten von Spektren, die von normalen, nicht durchbohrten Gegenelektroden stammen. Die Intensitäten von CN-Banden sind dagegen im ersten Fall intensiver als im zweiten Fall, was mit der Senkung des Wasserdampfdruckes und evtl. der OH-Radikalekonzentration zusammenhängt, da diese die Bildung von CN-Radikalen teilweise verhindern.

Einige Vorteile der Kapillarelektroden kann man auch auf Grund des Vergleichs der statistischen Parameter beurteilen, die aus Streudiagrammen zu erhalten sind. In Tabelle IV werden die statistischen Parameter des In/Ag

Tabelle IV

Vergleich der statistischen Parameter der verglichenen Methoden für das In/Ag Linienpaar

Parameter	Dochtelektro-dentechnik	Verglichene Methoden	
		Scheibe – Rivas-Verfahren	Kapillarelektroden-technik
r	0,82	0,92	0,96
$t_{r=0}$	—	—	—
w_{orth}	1,00	1,06	1,03
w_C	1,08	1,08	1,08
w_T	0,76	0,91	0,90
w_x	0,84	0,78	0,96
w_r	0,80	0,80	0,94
ψ	0,34	0,29	0,28
ϱ	0,11	0,06	0,03
$s_{\Delta Y}$	0,07	0,04	0,02

Linienpaares für die Kapillarelektrodentechnik [1, 2], Dochtelektroden nach MALAMAND [18] und das klassische SCHEIBE—RIVAS-Verfahren [19] verglichen. Die erreichte Korrelation ist bei den verglichenen Methoden für eine 99,9%ige statistische Sicherheit immer positiv. Die Bedingungen für die Homologie der Linienpaare sind annähernd erfüllt, da sich der orthogonale Regressionskoeffizient zwischen den Werten w_C und w_T befindet, und diese eine ziemlich enge Spannbreite bilden. Deshalb ist es begründet, über die ausreichenden Analysenbedingungen zu sprechen. Dagegen sind die Reproduzierbarkeitswerte der Kapillarelektroden im Vergleich zu anderen Methoden eindeutig günstiger.

Tabelle V zeigt die Ergebnisse der statistischen Prüfung von mehreren Elementen, die als Haupt- und Nebenkomponente der aufgelösten Kalksteine, Dolomite und Magnesite zur Analyse kommen. Auch in diesem Falle erfüllen die Korrelationskoeffizienten bei einer Testprüfung für die 99,9%ige statistische Sicherheit die signifikante Abweichung von Null. Die orthogonalen Regressionskoeffizienten befinden sich auch hier annähernd in der Mitte der Spannbreite der Koeffizienten w_C und w_T, die die durch Temperatur- und Konzentrationsfluktuationen beeinflußten Werte darstellen. Die Präzision der Konzentrationsbestimmung liegt immer unter dem Grenzwert von 5%.

Tabelle VI faßt die Ergebnisse der statistischen Prüfung von weiteren metallischen Elementen zusammen, die meistens als Spurenelemente in den Elektrolyseschlämmen vorkommen. Auch bei diesen Kombinationen ist die Korrelation ausreichend. Die Regression ist, mit Ausnahme der Au/Co und

Tabelle V

Vergleich der statistischen Parameter einiger Linienpaare, die sich auf Haupt- und Nebenkomponente beziehen

Parameter	Al/Co	Ca/Co	Mg/Co	Fe/Co	Si/Co
r	0,81	0,94	0,92	0,91	0,87
$t_{r=0}$	—	—	—	—	—
w_{orth}	0,73	0,95	0,81	0,99	0,76
w_C	0,73	1,42	?	1,09	1,19
w_T	0,75	0,90	0,80	0,93	0,62
$s_C/C[\%]$	±4,95	±2,53	±3,54	±4,54	±4,95

Bemerkung: Als Bezugslinie wurde bei den Linienpaaren 1 und 3 die Co 271,60 Linie, und bei den Linienpaaren 2, 4 und 5 die Linie Co 304,89 angewendet.

Tabelle VI

Vergleich der statistischen Parameter einiger Linienpaare von Elementen, die in Spurenkonzentrationen auftreten

Parameter	Verglichene Linienpaare							
	As/Co	Ag/Co	Au/Co	Bi/Co	Cu/Co	Ni/Co	Pb/Co	Te/Co
r	0,76	0,85	0,34	0,84	0,76	0,91	0,95	0,41
$t_{r=0}$	—	—	+	—	—	—	—	+
w_{orth}	0,76	1,02	0,27	0,64	1,27	0,99	1,42	1,17
w_C	?	0,92	1,11	0,97	2,31	0,98	1,05	?
w_T	1,23	1,13	1,08	0,60	1,42	1,07	1,50	1,27
$s_{\Delta Y}$	0,08	0,04	0,23	0,07	0,05	0,06	0,12	0,18

Bemerkung: Es wurde ausschließlich die Linie Co 304,40 als Bezugslinie angewendet.

Te/Co Linienpaare, noch ausreichend. Die Koeffizienten w_C und w_T bilden einen ziemlich engen Bereich, und der orthogonale Regressionskoeffizient liegt in diesem Bereich. Dies hat auch einen maßgebenden Einfluß auf die Reproduzierbarkeit (Präzision), die, mit Ausnahme der Au/Co und Te/Co Linienpaare, günstige Werte liefern.

Die Matrixeffekte wurden mit zwei Versuchsserien von Lösungen überprüft. Bei der ersten Serie (Tabelle VII) wurde der Einfluß der Konzentration einer Hauptkomponente auf die Parameter der LOMAKIN—SCHEIBE-Gleichung [20, 21] verfolgt. Die Ergebnisse in Tabelle VII zeigen, daß eine Erhö-

Tabelle VII

Vergleich der Koeffizienten der LOMAKIN—SCHEIBE-*Gleichung für unterschiedliche Matrixkonzentrationen*

Geprüfte Elemente	Al		Fe		Mg	
	Verfolgte Koeffizienten					
Matrixelement	$A_{x,r}$	B_x	$A_{x,r}$	B_x	$A_{x,r}$	B_x
0% CaO	—0,60	0,63	—0,89	0,72	—0,40	0,60
30% CaO	—1,02	0,58	—0,92	0,60	—0,52	0,56
60% CaO	—1,30	0,49	—1,12	0,56	—0,94	0,42

hung der Kalziumkonzentration immer mit einer Änderung der Koeffizienten $A_{x,r}$ und B_x verbunden ist. Diese Änderungen sind bei Eisen gering, bei Magnesium schon bedeutend und bei Aluminium sehr prägnant. Daraus kann geschlossen werden, daß eine unkontrollierbare Änderung der Hauptkomponentenkonzentration immer von einem Matrixeffekt begleitet wird, was bei der Anwendung der fixgelegten analytischen Geraden einen systematischen Fehler bedeutet.

Mit der zweiten Serie (Tabelle VIII) wurde der Einfluß von verschiedenen Elementen gleicher Konzentrationen auf die Koeffizienten der LOMAKIN—SCHEIBE-Gleichung [20, 21] des In/Ag Linienpaares untersucht. Die Ergebnisse in der Tabelle VIII zeigen ein geändertes Bild. Einige Hauptkomponenten, z. B. Blei und Zink, ändern die Koeffizienten nur ganz unbedeutend, Kupfer und Cadmium schon deutlicher, und Wismuth, im Vergleich zu den anderen Elementen, ganz prägnant. Bemerkenswert ist die Tatsache, daß hauptsächlich der Parameter $A_{x,r}$ durch Änderung der Hauptkomponenten beeinflußt wird. Das bedeutet aber, daß die Änderung der Hauptkomponentenkonzentration gleichzeitig eine Änderung der beiden Parameter verursacht, die Änderung der Hauptkomponente im wesentlichen aber nur eine Parallelverschiebung der analytischen Gerade verursacht.

Tabelle VIII

Vergleich der Koeffizienten der LOMAKIN-SCHEIBE-*Gleichung für unterschiedliche Matrizen für das In/Ag Linienpaar*

Matrixelement	Bi	Cd	Cu	Zn	
Koeffizient $A_{x,r}$	—0,02	—0,20	—0,14	—0,06	—0,07
Koeffizient B_x	0,57	0,53	0,40	0,50	0,58

Tabelle IX

Vergleich der Nachweis- und Garantiegrenzen, des Nachweisvermögens und der Präzision für einige Spurenelemente beim Kapillarelektrodenverfahren

Element	Wertungsparameter			
	C_N	C_G	π	τ
Ag	$5 \cdot 10^{-5}$	$8 \cdot 10^{-5}$	$2{,}0 \cdot 10^{5}$	$24{,}2 \cdot 10^{-2}$
As	$7 \cdot 10^{-2}$	$2 \cdot 10^{-1}$	$1{,}4 \cdot 10^{2}$	$8{,}1 \cdot 10^{-2}$
Au	$7 \cdot 10^{-2}$	10^{-1}	$1{,}4 \cdot 10^{2}$	$3{,}7 \cdot 10^{-2}$
Bi	10^{-3}	$5 \cdot 10^{-3}$	10^{3}	$12{,}4 \cdot 10^{-2}$
Cu	10^{-3}	$3 \cdot 10^{-3}$	10^{3}	$11{,}2 \cdot 10^{-2}$
In	10^{-2}	$2 \cdot 10^{-2}$	10^{2}	$43{,}5 \cdot 10^{-2}$
Ni	$3 \cdot 10^{-3}$	$7 \cdot 10^{-3}$	$3{,}3 \cdot 10^{3}$	$16{,}8 \cdot 10^{-2}$
Pb	10^{-2}	$5 \cdot 10^{-2}$	10^{2}	$6{,}4 \cdot 10^{-2}$
Te	$3 \cdot 10^{-2}$	$9 \cdot 10^{-2}$	$3{,}3 \cdot 10^{3}$	$4{,}0 \cdot 10^{-2}$

Symbole

r	Regressionskoeffizient
t	Testprüfung für $\alpha = 0{,}001$
w_{orth}	Orthogonaler Regressionskoeffizient
w_T	Koeffizient der Konzentrationsfluktuation, Verhältnis der Anregungsspannungen E_x/E_r
E_x	Anregungsspannung der Analysenlinie
E_r	Anregungsspannung der Linie des Zusatzelementes
w_C	Koeffizient der Temperaturfluktuation, Verhältnis der Koeffiziente B_x/B_r
B_x	Richtungstangente der analytischen Geraden
B_r	Richtungstangente der Linie des Zusatzelementes
$A_{x,r}$	Koeffizient der LOMAKIN—SCHEIBE Gleichung, $\Delta Y = A_{x,r} - B_x \cdot \log C_x$
w_x	Regressionskoeffizient der analytischen Geraden
w_r	Regressionskoeffizient der Linie des Zusatzelementes
ψ	Länge der größeren Halbachse der Streuellipse
ϱ	Länge der kleineren Halbachse der Streuellipse
$s_{\Delta Y}$	Standardabweichung der Bestimmung von ΔY-Wert
s_C/C	Genauigkeit der analytischen Bestimmung
C_N	Nachweisgrenze in %
C_G	Garantiegrenze in %
π	Nachweisvermögen, $1/C_G$
τ	Präzision

LITERATUR

1. EICHHOFF, H. J., PICKARD, K.: Spectrochim. Acta **7**, 396 (1953)
2. ZINK, T. H.: Appl. Spectroscopy **13**, 75 (1962)
3. MATHERNY, M.: Proc. XIV. Coll. Spectr. Intern., Debrecen, 321 (1967)
4. KAISER, H., SPECKER, H.: Z. anal. Chem., **149**, 46 (1956)
5. KAISER, H.: Z. anal. Chem. **209**, 1 (1965)
6. STRASHEIM, A., KEDDY, R. J.: Appl. Spectroscopy **12**, 29 (1958)
7. HOLDT, G., STRASHEIM, A.: Appl. Spectroscopy **14**, 64 (1960)
8. MATHERNY, M.: Chemia Analityczna **11**, 1053 (1966)
9. MEGGERS, W. F., CORLISS, CH. H., SCRIENER, B. F.: Tables of Spectral Line Intensities. NBS Monograph 32, Part I, Washington

10. SAIDEL, A. N., PROKOFJEW, W. K., RAJSKIJ, S. M.: Spektraltabellen, VEB Verlag Technik, Berlin 1955
11. HOLDT, G.: Emissionsspektroskopie. VEB Akademie-Verlag, Berlin 1964
12. PLŠKO, E.: Coll. Czech. Chem. Commun. **30**, 1246 (1965)
13. MATHERNY, M., PLIEŠOVSKÁ, N.: Chem. zvesti **21**, 417 (1967)
14. MATHERNY, M.: Acta Chim. Acad. Sci. Hung. **48**, 203 (1966)
15. KOLLER, L., MATHERNY, M.: Chem. zvesti **29**, 561 (1966)
16. KOLLER, L., MATHERNY, M., PLIEŠOVSKÁ, N.: Proc. of XIV. Coll. Spectr. Intern., Debrecen, 1057 (1967)
17. PLŠKO, E.: Chem. zvesti **18**, 134 (1964)
18. MALAMAND, F.: Publ. GAMS 207 (1965)
19. SCHEIBE, G., RIVAS, A.: Z. angew. Chem. **49**, 443 (1936)
20. LOMAKIN, B. A.: Z. anorg. allg. Chem. **187**, 75 (1930)
21. SCHEIBE, G., SCHNETTLER, O.: Naturwiss. **19**, 134 (1931).

Mikuláš MATHERNY; Košice, Švermová 5 — Pavilony, ČSSR.

Acta Chimica Academiae Scientiarum Hungaricae, Tomus 66 (2), pp. 175—181 (1970)

THERMAL REACTIONS OF POTASSIUM HALATES AND PERHALATES

J. SIMON, S. GÁL and L. ERDEY†

(Institute of General and Analytical Chemistry, Technical University, Budapest)

Received June 3, 1969

In revised form February 17, 1970

The thermal reactions of potassium halates and perhalates are described on the basis of derivatographic experiments. The observed redox reactions taking place at high temperature have shown that the ionic character of the halogen–oxygen bond is highest for potassium iodate and lowest for potassium chlorate.

We have previously studied acid–base and redox reactions taking place at high temperatures [1].

The results of the investigation of acid–base reactions have been published earlier. In these studies the halides and carbonates of the alkali metals were chosen as model compounds. The latter are important fusing agents in chemical analysis [2, 3].

As a continuation of this work the authors wish to report on the investigation of redox reactions taking place at high temperatures. Potassium halates and perhalates were selected as model compounds.

The derivatographic method [4] proved to be suitable for quantitative interpretation of the reactions of these compounds.

Besides studying decomposition reactions, a qualitative picture of the changing nature of the halogen–oxygen bond as a function of temperature will be presented.

Experimental

Analytical grade potassium chlorate, potassium perchlorate, potassium bromate, potassium iodate and potassium periodate were investigated by means of a F. PAULIK—J. PAULIK—L. ERDEY MOM Derivatograph. Approximately 200 mg samples were ground and passed through a 350 mesh sieve into a platinum crucible. The heating rate was 10 °C/min. The reagents used were made available by E. Merck (Darmstadt, German Federal Republic) for which we would like to express our thanks.

The thermal decomposition of potassium halates proceeds according to the general equation:

$$2\,KXO_3 \xrightarrow{\text{heat}} 2\,KX + 3O_2$$

where X is a halogen atom.

Fig. 1 shows the derivatogram of potassium chlorate. The endothermic peak at 360 °C on the DTA curve shows the melting of the sample, this temperature being in good agreement with the literature values [5, 6]. Decomposition starts with an exothermic process at 380 °C, the peaks on the DTA curve at 520° and 580 °C indicate oxygen evolution. MARKOWITZ *et al.* [7] have reported that the first exothermic process involves two reactions: the decompo-

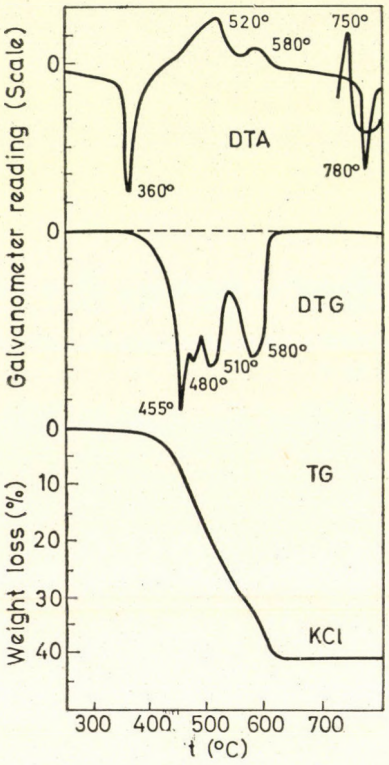

Fig. 1. Derivatogram of potassium chlorate

sition of $KClO_3$ and the formation of $KClO_4$. The second exothermic reaction is due to the decomposition of $KClO_4$. The endothermic peak at 780° C on the DTA curve shows the melting point of potassium chloride formed.

According to the thermal curves, perchlorate is also formed during the decomposition of chlorates. As shown by the DTA curve, the decomposition to potassium chloride proceeds in several steps.

In order to separate the overlapping reactions, a multi-plate sample holder [8] was used. The DTG curve in Fig. 2 shows only two processes. The maximum at 450 °C indicates the decomposition of chlorate, and the peak at 530 °C shows the oxygen evolution from perchlorate formed during the reaction.

The thermal curves of potassium perchlorate in Fig. 3 prove this fact too. The decomposition reaction takes place at maximum rate at 590 °C.

The above mechanism of decomposition can also be proved experimentally. Fig. 4 shows the thermal curves of a 1 : 1 mixture of potassium chlorate and perchlorate. As shown by this measurement, the height of the 590 °C DTG peak characteristic of the decomposition of perchlorate increases relative to that of other peaks.

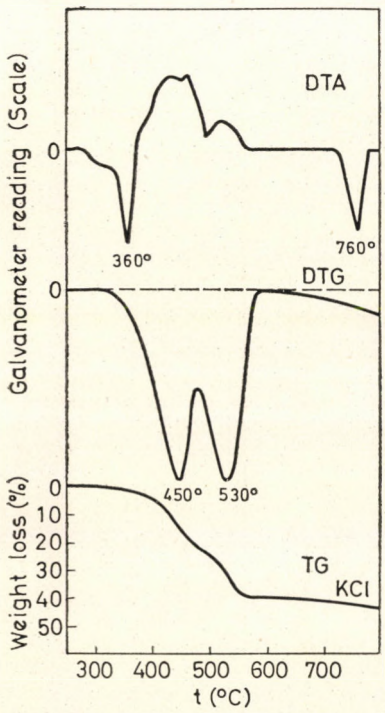

Fig. 2. Derivatogram of potassium chlorate placed on the multi-plate sample holder

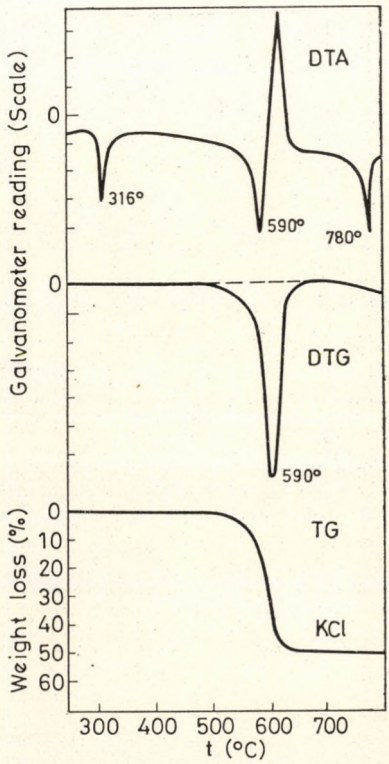

Fig. 3. Derivatogram of potassium perchlorate

It can be established on the basis of these results that the decomposition of chlorate in a crucible occurs in several steps because chloride is formed, therefore the viscosity of the melt increases and in this manner it hinders the departure of oxygen from the melt. Due to the increasing amount of chloride present, the decomposition of perchlorate is shifted to lower temperatures — as indicated by the DTA peak at 580 °C in Fig. 1 — in accordance with the results of SOLYMOSI [9]. Fig. 5 shows the derivatogram of potassium bromate. The decomposition starts in the solid phase to form solid bromide and then the rest of the bromate melts onto the surface of the solid bromide formed. The de-

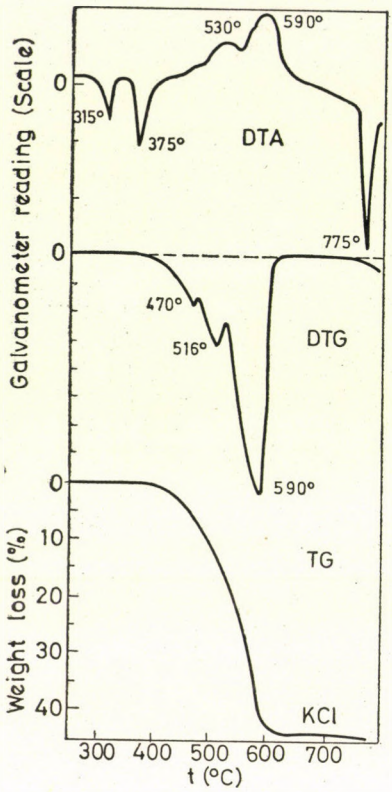

Fig. 4. Derivatogram of a 1 : 1 potassium chlorate–perchlorate mixture

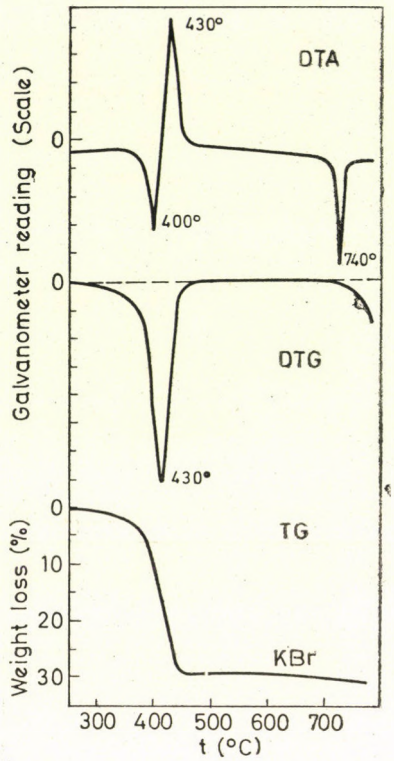

Fig. 5. Derivatogram of potassium bromate

composition product is potassium bromide. The melting point is indicated by the DTA curve as an endothermic peak at 740 °C [7].

The overall enthalpy change consisting of the heats of fusion and decomposition of potassium bromate is positive, *i.e.* the reaction is exothermic.

The decomposition of potassium iodate, similarly to that of the bromate, starts in the solid phase (Fig. 6). The endothermic DTA peak at 540 °C shows the resultant of the heat of fusion and heat of decomposition. As shown by the DTG curve, the decomposition to iodide takes place in two steps, at maximum rates at 540 °C and 565 °C.

The endothermic peak at 675 °C on the DTA curve indicates the melting point of potassium iodide [11].

The derivatogram of potassium periodate is presented in Fig. 7. The first decomposition reaction takes place in the solid phase around 330 °C, accompanied by a positive enthalpy change when potassium iodate is formed in a stoichiometric amount. The decomposition of potassium iodate produced goes

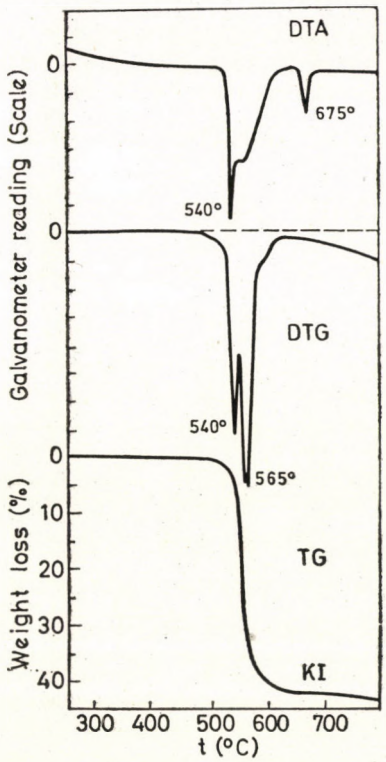

Fig. 6. Derivatogram of potassium iodate

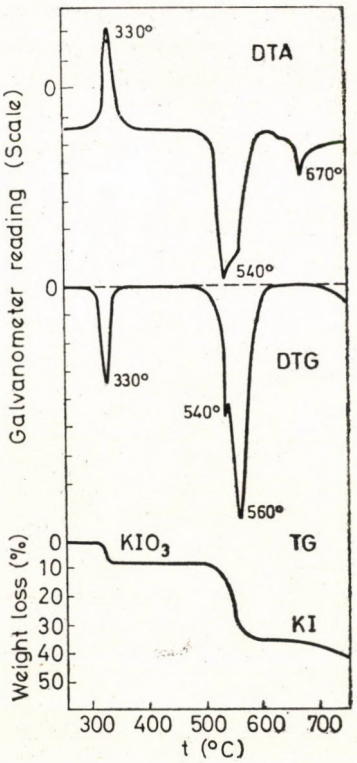

Fig. 7. Derivatogram of potassium periodate

on as given above. The amount of potassium iodide produced during the decomposition of potassium iodate and that of periodate is non-stoichiometric.

The reason for this fact is the thermal decomposition of potassium iodide to potassium oxide and free iodine.

The formation of iodine has been observed by means of visual DTA instruments [12]. The amount of potassium oxide was determined in all cases.

Discussion

On the basis of the measurements, the following statements can be made. In the thermal decomposition of potassium halates the corresponding potassium halides and gaseous oxygen are formed and also iodine in case of iodate.

Experiments performed under dynamic conditions show that the decomposition of all three potassium halates starts in the solid phase and goes to completion above the melting point. This means that a redox reaction occurring at high temperatures in the molten phase, with transfer of 6 electrons,

was investigated. During the decomposition of potassium chlorate, potassium perchlorate is formed as an intermediate; no analogous reaction was observed for the other compounds.

With potassium iodate, the formation of the periodate is not hindered by the electron configuration of iodine, but probably does not occur because periodate decomposes at lower temperatures than potassium iodate.

All three compounds form an ionic lattice in the solid state, containing potassium cations and XO_3^- anions.

Disregarding the polarizing effect of the potassium cation — occurring in all three cases — now we are studying only the thermal cleavage of the halogen–oxygen bond. The shift of melting points towards higher temperatures (350°, 400°, 540 °C) in the order chlorate, bromate, iodate is indicated by the derivatographic curves.

If the halogen–oxygen internuclear distances determined from X-ray data [13, 14] are compared with the sums of the ionic radii, the results presented in the next Table are obtained.

Bond	Measured value Å	Calculated value Å	Δ%
Cl–O	1.42	1.66	16.9
Br–O	1.68	1.79	6.5
I–O	1.82	1.90	4.2

The difference between the measured and calculated distances (Δ) is highest for the Cl–O bond. The smallest difference was obtained for the I–O bond. This phenomenon proves that the ionic nature of these compounds increases in the order $ClO_3^- < BrO_3^- < IO_3^-$.

Similar results are obtained when interpreting the change in the covalent and ionic character of the compounds on the basis of overall enthalpy changes accompanying thermal decomposition. The overall enthalpy change of potassium chlorate and bromate decomposition is exothermic, while that of the decomposition of potassium iodate is endothermic.

The properties of potassium iodate differ markedly from those of the other two salts. The central halogen atoms in the chlorate and bromate ions have a high polarizing effect owing to the high formal positive charges and small radii of the ions ($Cl^{5+} = 0.26$ Å, $Br^{5+} = 0.39$ Å), so that they bind O^{2-} ions by covalent bonds. In the iodate anion the positive charge on the iodine is equal to that on the other two halogens studied, but owing to the larger radius (0.5 Å), the polarizing effect is low. The bonds with O^{2-} ions are therefore more ionic in nature.

REFERENCES

1. ERDEY, L.: Periodica Polytechnica **1,** 91 (1957)
2. SIMON, J., GÁL, S., ERDEY, L.: Acta Chim. Acad. Sci. Hung. **53,** 105 (1967)
3. ERDEY, L., GÁL, S.: Talanta **10,** 23 (1963)
4. PAULIK, F., PAULIK, J., ERDEY, L.: Z. anal. Chem. **160,** 241 (1958)
5. CARPENTER, C. D.: Chem. Met. Eng. **24,** 570 (1921)
6. CAMPBELL, C., TAYLOR, F. R.: Proceedings of the Second International Conference on Thermal Analysis **2,** 812, Academic Press, New York, 1969
7. MARKOWITZ, M., BORYTA, D., STEWART, H. Jr.: J. Phys. Chem. **68,** 2282 (1964)
8. PAULIK, J., PAULIK, F., ERDEY, L.: Anal. Chim. Acta **34,** 419 (1966)
9. SOLYMOSI, F.: Magy. Kém. Foly. **74,** 146 (1968)
10. PHILIPPS, T. E.: J. Am. Chem. Soc. **51,** 1343 (1930)
11. GINNINGS, D. C.: J. Am. Chem. Soc. **52,** 1343 (1930)
12. ERDEY, L., SIMON, J., GÁL, S.: Talanta **15,** 653 (1968)
13. NÁRAY-SZABÓ, I.: Kristálykémia. Akadémiai Kiadó, Budapest, 1965
14. ORMONT, B. F.: Struktury neorganicheskich veshtshestv. Moscow, 1950

Judit SIMON
Sándor GÁL
László ERDEY †
Budapest XI., Gellért-tér 4.

Acta Chimica Academiae Scientiarum Hungaricae, Tomus 66 (2), pp. 183—187 (1970)

APPLICATION OF ION-SELECTIVE ELECTRODES IN NON-AQUEOUS MEDIA, I

STUDY ON THE APPLICATION LIMITS IN SOME NON-AQUEOUS SOLVENTS

(PRELIMINARY COMMUNICATION)

N. A. KAZARYAN* and E. PUNGOR

(Department of Analytical Chemistry, University of Chemical Industries, Veszprém)

Received March 25, 1970

The results lead to the conclusion that the silicone rubber ion-selective membrane electrodes cannot be used in the pure non-aqueous solvents mentioned above. At the same time, the slope of an iodide silicone rubber membrane electrode remains equal to the theoretical value in the non-aqueous solvent–water mixtures studied.

Introduction

Recently the development of ion-selective electrodes has become of great importance. The high selectivity of the electrodes permits the determination of various ions in the presence of each other.

The behaviour and application limits of ion-selective electrodes in aqueous solutions have already been described [1, 2, 3]. Naturally the application field of the electrodes cannot be restricted only to aqueous solutions and, therefore, it seemed interesting to examine their applicability in some non-aqueous solvents. This is especially important because many compounds are only soluble in non-aqueous solvents and, furthermore, it is interesting from the theoretical point of view how the correlations valid in aqueous media would change in non-aqueous solutions. At the same time, the finding that the lowest detection limit of a precipitate-based ion-selective electrode in aqueous media is determined by the solubility of the precipitate composing the electrode, may offer new possibilities, if non-aqueous media are used. It is well known that the solubility of many inorganic precipitates decreases in non-aqueous solvents. Consequently, it can be expected that in non-aqueous media the lowest detection limits of ion-selective electrodes containing such inorganic precipitates also decrease in comparison with that obtained in aqueous solutions.

The precipitate-based ion-selective membrane electrodes can be divided into two groups: homogeneous and heterogeneous ion-selective electrodes [4]. The application of the heterogeneous silicone rubber membrane electrodes in non-aqueous media raises the question of how the swelling of the silicone rubber influences the application limits of the electrodes.

* Permanent address: Mendeleyev Institute of Chemical Technology, Moscow.

The aim of this study was to examine the effect of some non-aqueous solvents: alcohols, acetone, dimethylformamide, acetonitrile, a mixture of benzene and methanol — on the behaviour of the silicone rubber membrane electrodes and furthermore, to choose the solvents in which the silicone rubber membrane electrodes cannot be used because of their swelling or other accompanying phenomena. For a systematic study, water-miscible solvents were chosen and the experiments were carried out in mixtures of the aqueous and non-aqueous solvents.

Experimental

For potentiometric measurements silicone rubber iodide selective electrodes (RADELKIS, Type OP-I-711), a saturated calomel reference electrode and an expanded scale Precision pH-meter Model 205 (RADELKIS, Budapest) were employed. The input resistance of the pH-meter is $10^{12}\Omega$.

On studying the changes in the properties of the membrane layers, silicone rubber membrane plates containing silver iodide precipitate were used. Discs of 2 cm^2 surface area were cut out and were immersed in a mixture of the appropriate aqueous and non-aqueous solvents and the change in their weight was checked in a certain period of time. Parallel to this, the colour change of the appropriate solvent and the change in the properties of the membrane discs were observed visually.

All chemicals used for the studies were of analytical grade. The solvents used were: distilled water, methanol, ethanol, benzene, acetonitrile, and dimethylformamide.

Results and discussion

The experimental results are discussed in two parts. First, the results concerning the swelling and dissolution of the membrane layers are shown. Tables I and II contain the data for the swelling of the membrane discs in various mixtures of distilled water with a non-aqueous solvent such as methanol, *n*-propanol, i-propanol, acetone, acetonitrile, dimethylformamide, and methanol benzene mixture, respectively. The colour change of the appropriate solvent mixture was observed visually. From the results, it can be seen that the silicone rubber ion-selective electrodes can be used in methanol–water and ethanol–water mixtures up to 90% alcohol concentration, while in propanol–water and isopropanol–water mixtures their application limits are at about 60% because above 60% alcohol content the colour of the solvent mixture changes to a great extent on soaking, expecially in case of i-propanol. Furthermore, the dissolution of the membrane discs and the colour change of the solvent-mixture were observed while soaking the discs for a longer period of time in an acetone–water mixture containing more than 40% acetone. For acetonitril–water mixtures this limit is at about 60% acetonitrile concentration, while for dimethylformamide this value lies at an even higher dimethylformamide concentration. At the same time, it also appears from Table II,

Table I

Swelling of silver iodide based silicone rubber membranes in organic solvents and their mixtures with water

Organic solvent content in v/v%	10 min		1 hr.		5 hrs		24 hrs	
	CH_3COCH_3	CH_3CN	CH_3COCH_3	CH_3CN	CH_3COCH_3	CH_3CN	CH_3COCH_3	CH_3CN
10	100	100.3	100	100.3	100	100.1	100.2	100.1
20	100	100.1	99.9	100.2	99.9	100.1	100.1	100.1
40	100	100.2	99.9	100.6	99.9	99.9	99.8	100.5
60	100	100.6	99.9	100.7	100*	99.8	99.8*	99.9
80	100.2	100.6	100	100.6	100*	99.5	99.7*	99.3*
100	94.7	100.6	93.7	99.7	93.5*	98.8	93.6*	98.3*
	$HCON(CH_3)_2$	C_6H_6—CH_3OH	$HCON(CH_3)_2$	C_6H_6—CH_3OH	$HCON(CH_3)_2$	C_6H_6—CH_3OH	$HCON(CH_3)_2$	C_6H_6—CH_3OH
10	100	100.1	100	99.0	100	97.3	99.8	96.7
20	99.6	99.2	99.6	98.0	99.2	96.3	99.6	95.1
40	100.2	98.0	99.8	96.4	99.7	93.9	99.5	93.6
60	100.2	99.2	100.1	97.9	100	96.8	99.7	94.7
80	100.5	96.0	101.1	93.9	100.9	93.7	100.2	93.7
100	100.5	97.8	99.8	98.1	99.1	102.0	98.7	112.5**

* the colour of solvent turns yellow
** the membrane becomes fragile
Data are given in per cent w/w of the original silicone rubber membrane.

that the application limit of the silicone rubber membrane electrodes in benzene–methanol mixtures is at a relatively high alcohol concentration, but this solvent mixture still cannot be used in practice, because it makes the membrane layer fragile.

In the second part of this section, the electrochemical data are discussed. These data are similar to each other, an example of which is presented in Fig. 1 showing the behaviour of an iodide selective electrode in methanol–water mixtures. It can be seen that the behaviour of the electrode is Nernstian in the concentration range of 10^{-3}—10^{-5} *M*. However, the calibration curves of the electrodes are shifted parallel to each other depending on the water content of the solvent mixtures. This may be due to the liquid–liquid junction potentials.

Table II

Swelling of silver iodide based silicone rubber membranes in alcohols and in alcohol–water mixtures

Organic solvent content in v/v%	10 min		1 hr.		5 hrs		24 hrs	
	CH_3OH	C_2H_5OH	CH_3OH	C_2H_5OH	CH_3OH	C_2H_5OH	CH_3OH	C_2H_5OH
10	100.3	100	99.7	99.9	99.7	99.4	99.7	99.9
20	99.6	100.4	99.6	100.3	99.5	99.7	99.5	99.8
40	100.4	100	100.4	99.8	100.2	99.4	100.1	99.1
60	100	99.9	100.5	99.7	99.7	99.2	100	99.7
80	100	100.1	100	100	99.7	99.4	99.5	99.1
100	99.9	99.5	98.3	97.9	97.6	95.5	96.7	95.2
	n—C_3H_7OH	i—C_3H_7OH	*n*—C_3H_7OH	i—C_3H_7OH	*n*—C_3H_7OH	i—C_3H_7OH	*n*—C_3H_7OH	i—C_3H_7OH
10	99.7	99.9	99.7	99.7	99.0	99.4	99.2	99.8
20	100.5	100.2	100.2	100.1	98.4	100.1	99.2	100
40	100.1	100.1	100.1	99.9	100.1	99.8	99.8	99.9
60	99.6	100	99.8	99.9*	99.0	99.8*	98.6	98.7*
80	100	100	99.3	99.5*	98.0	99.2*	97.2**	98.4*
100	99.6	99.4	97.8	98.2*	95.3	97.3*	94.6**	96.1*

* the colour of the solvent turns slightly yellow
** the colour of the solvent turns pink
Data are given in per cent w/w of the original silicone rubber membrane.

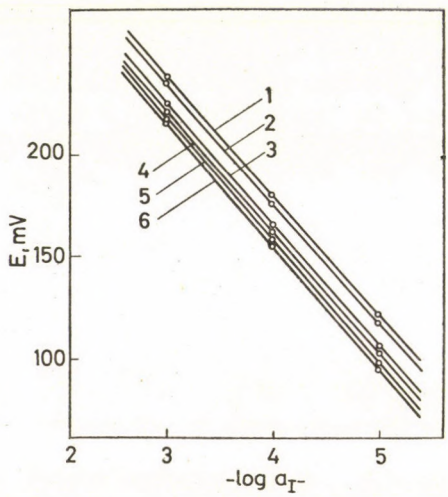

Fig. 1. The behaviour of an iodide selective electrode in various water–metanol mixtures. 1. in distilled water; 2. in 20% methanol–water mixture; 3. in 40% methanol–water mixture; 4. in 60% methanol–water mixture; 5. in 80% methanol–water mixture; 6. in 90% methanol–water mixture

REFERENCES

1. PUNGOR, E.: Anal. Chem. **39**, 28 (1967)
2. PUNGOR, E., TÓTH, K.: Anal. Chim. Acta **47**, 291 (1969)
3. PUNGOR, E., TÓTH, K., HAVAS, J.: Acta Chim. Acad. Sci. Hung. **48**, 17 (1966)
4. PUNGOR, E., TÓTH, K.: Analyst. **95**, 625 (1970)

Ernő PUNGOR; Budapest XI., Gellért tér 4.
Nelly Arissovna KAZARYAN; Mendeleyev Institute of Chemical Technology, Moscow.

Acta Chimica Academiae Scientiarum Hungaricae, Tomus 66 (2), pp. 189—202 (1970)

d^N-ELEKTRONENSYSTEME IN TRIGONALEN LIGANDENFELDERN, I

THEORIE

H. KAMMER

(Bereich Physikalische Chemie, Section Chemie der Technischen Universität Dresden)

Eingegangen am 19. April 1969

Im Rahmen der strong-field-Approximation werden die Energiezustände von Übergangsmetallionen in trigonalen Ligandenfeldern bei Vernachlässigung der Spin-Bahn-Kopplung untersucht. Ein d-Einelektronenzustand spaltet im trigonalen Feld in e, a_1 und ε auf. Die Energieunterschiede zwischen diesen Zuständen werden durch die Parameter D, E und F charakterisiert. In trigonaler Symmetrie existieren die Konfigurationen $e^n a_1{}^p \varepsilon^q$ ($n + p + q = N$ und $0 \leq n, q \leq 4$, $0 \leq p \leq 2$), aus denen nach Einschalten der Coulombschen Wechselwirkung die Terme ${}^{2S+1}\Gamma$ hervorgehen. Die Matrizen der elektrostatischen Energie für ein d^N-Elektronensystem mit $N = 3, 4, 5$ im trigonalen Feld werden aus denen des d^{N-1}-Elektronensystems mit Hilfe einer Induktionsbeziehung berechnet. Für die Konfigurationen d^2, d^3, d^4 und d^5 sind die im trigonalen Ligandenfeld auftretenden Energiematrizen angegeben. Die Matrixelemente der Coulomb-Wechselwirkung werden durch die Racah-Parameter A, B und C ausgedrückt. Außerdem sind die Werte der in den Rechnungen auftretenden Racah-Koeffizienten tabelliert.

Einleitung

Zur Deutung der optischen und magnetischen Eigenschaften von Komplexen der Übergangsmetallionen hat die Ligandenfeldtheorie wesentlich beigetragen. Es sind zwei Näherungen entwickelt worden, die strong-field- und die weak-field-Approximation, die sich durch die Reihenfolge, in der die verschiedenen Störungen berücksichtigt werden, unterscheiden, aber bei konsequenter Durchführung dieselben Ergebnisse liefern.

TANABE und SUGANO [6] berechneten im Rahmen des strong-field-Kopplungsschemas für kubische Symmetrie des Ligandenfeldes die Energiematrizen für alle d^N-Konfigurationen. Neben kubischen Symmetrien treten am häufigsten tetragonale und trigonale Symmetrien in Komplexen auf. TANABE und KAMIMURA [5] diskutierten den Einfluß solcher niederen Symmetrien auf d^N-Elektronensysteme in kubischen Feldern. GILDE und BAN [2] betrachteten die Aufspaltung von d^N-Konfigurationen in trigonalen und rhombischen Symmetrien qualitativ. OTSUKA [3] ermittelte für tetragonale Symmetrie des Ligandenfeldes die Energiematrizen der d^N-Konfigurationen nach der strong-field-Methode.

In der vorliegenden Arbeit werden die Energiezustände für alle d^N-Konfigurationen in trigonaler Symmetrie des Ligandenfeldes nach der strong-field-Methode unter Berücksichtigung der Konfigurationswechselwirkung berechnet. Es ist also zunächst die Aufspaltung der d-Orbitale in trigonalen Feldern zu untersuchen und anschließend die Wechselwirkung zwischen den Elektronen einzuführen.

Das trigonale Ligandenfeld

Das trigonale Potential entsteht durch Verzerrung eines Oktaeders längs einer seiner dreifachen Achsen. Es ist somit als Überlagerung eines oktaedrischen und eines axialen Potentials darstellbar:

$$V_{\text{trig}} = V_{\text{okt}} + V_{\infty},$$

wobei für

$$V_{\text{okt}} = A_4 \left[-Y_{40} + \sqrt{\frac{10}{7}} (-Y_{43} + Y_{4-3}) \right]$$

und für das axiale Potential

$$V_{\infty} = A_2 Y_{20} + A_4' Y_{40}$$

gilt. Die Y_{lm} sind die Kugelflächenfunktionen, und in den A_2, A_4, A_4' sind alle winkelunabhängigen Größen zusammengefaßt:

$$A_2 = \sqrt{\frac{4\pi}{5}}\, eq' \frac{r_<^2}{r_>^3}, \qquad A_4 = \frac{7}{3}\sqrt{\frac{4\pi}{9}}\, eq \frac{r_<^4}{r_>^5}, \qquad A_4' = \sqrt{\frac{4\pi}{9}}\, eq' \frac{r_<^4}{r_>^5},$$

wobei e die Elektronenladung, q, q' effektive Ladungen der Liganden und $r_<$, $r_>$ der kleinere bzw. der größere der beiden Abstände Elektron-Koordinatenursprung und Ligand-Koordinatenursprung sind.

Aufspaltung der d-Orbitale in trigonaler Symmetrie; Konfigurationen und Terme

Wird ein d-Elektron durch ein Feld der Symmetrie D_3 gestört, so spaltet der fünffach bahnentartete D-Term des d-Elektrons in einen einfachen A_1-Term und zwei zweifache E-Terme auf. Die zugehörigen Zustandsfunktionen

induzieren die entsprechenden irreduziblen Darstellungen der Gruppe D_3 und werden daher mit Hilfe dieser Darstellungen klassifiziert. Die hier verwendeten, der trigonalen Symmetrie angepaßten Einelektronenfunktionen haben folgende Gestalt: (Nur die Winkelteile werden angegeben.)

A_1: $$a_1 = \frac{1+i}{\sqrt{2}} Y_{20}$$

E: $$e_1 = \frac{1-i}{2\sqrt{3}} [Y_{2-1} + Y_{21} + \sqrt{2}(Y_{2-2} - Y_{22})]$$

$$e_2 = \frac{1+i}{2\sqrt{3}} [Y_{2-1} - Y_{21} - \sqrt{2}(Y_{2-2} + Y_{22})]$$

$$\varepsilon_1 = \frac{1-i}{2\sqrt{3}} [\sqrt{2}(Y_{2-1} + Y_{21}) - Y_{2-2} + Y_{22}]$$

$$\varepsilon_2 = \frac{1+i}{2\sqrt{3}} [\sqrt{2}(Y_{2-1} - Y_{21}) + Y_{2-2} + Y_{22}]$$

Mit dem oben angegebenen Ausdruck für das trigonale Potential und den Linearkombinationen a_1, e und ε erhält man für die Säkulardeterminante bei Vernachlässigung der Wechselwirkung zwischen e und ε

$$\langle a_1 | V | a_1 \rangle = -\frac{3}{7}\frac{\overline{A_4}}{\sqrt{\pi}} + \left(\frac{3}{7}\frac{\overline{A_4'}}{\sqrt{\pi}} + \frac{\sqrt{5}}{7}\frac{\overline{A_2}}{\sqrt{\pi}}\right)$$

$$\langle e | V | e \rangle = -\frac{3}{7}\frac{\overline{A_4}}{\sqrt{\pi}} - \left(\frac{1}{21}\frac{\overline{A_4'}}{\sqrt{\pi}} + \frac{\sqrt{5}}{14}\frac{\overline{A_2}}{\sqrt{\pi}}\right)$$

$$\langle \varepsilon | V | \varepsilon \rangle = \frac{9}{14}\frac{\overline{A_4}}{\sqrt{\pi}} - \frac{1}{6}\frac{\overline{A_4'}}{\sqrt{\pi}}.$$

An Stelle der Parameter $\overline{A_4}$, $\overline{A_2}$, $\overline{A_4}$, die die Lage der Spaltterme im trigonalen Feld relativ zum ^2D-Term des freien d^1-Ions angeben, können die Parameter D, E, F so eingeführt werden, daß der tiefste Spaltterm Nullpunkt der Energieskala ist:

$$D = \frac{15}{14}\frac{\overline{A_4}}{\sqrt{\pi}} = \frac{5}{3} eq \frac{\overline{r_<^4}}{r_>^5}$$

$$E = \frac{5}{42}\frac{\overline{A_4'}}{\sqrt{\pi}} = \frac{5}{63} eq' \frac{\overline{r_<^4}}{r_>^5}$$

$$F = \frac{\sqrt{5}}{14}\frac{\overline{A_2}}{\sqrt{\pi}} = \frac{1}{7} eq' \frac{\overline{r_<^2}}{r_>^3},$$

wobei die Mittelwerte Integrale des Typs

$$\overline{\frac{r_<^k}{r_>^{k+1}}} = \int_0^\infty dr r^2 \Gamma\Gamma^2 R(r)^2 \frac{r_<^k}{r_>^{k+1}}$$

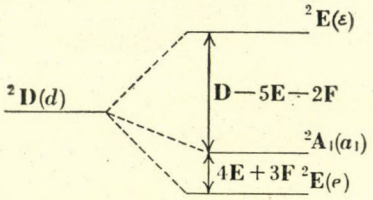

Abb.1. Aufspaltung des ^2D-Terms in trigonaler Symmetrie (schematisch)

sind mit $R(r)$ als der radialen Wellenfunktion. Damit ergibt sich die in Abb. 1 dargestellte Aufspaltung des ^2D-Terms in trigonaler Symmetrie.

Bei dieser Behandlung des Einelektronenproblems unter Einwirkung einer trigonalen Störung werden in der Säkulardeterminante nur die Diagonalelemente berücksichtigt. Tatsächlich sind auch Nichtdiagonalelemente $<e \mid V \mid \varepsilon>$ ungleich Null. Die Rechnung zeigt, daß für

$$\frac{8(F-E)^2}{(D-E+F)^2} \ll 1$$

die Wechselwirkung zwischen den beiden E-Termen vernachlässigbar ist, d. h. der axiale Anteil (Parameter E, F) des trigonalen Feldes muß klein sein gegen den oktaedrischen (Parameter D). Auf diesen Fall wollen wir uns hier beschränken.

Aus obigen Überlegungen ergibt sich, daß in einem System mit N d-Elektronen unter dem Einfluß eines trigonalen Feldes Konfigurationen der Art $e^n a_1^p \varepsilon^q$ auftreten mit $n+p+q=N$, $0 \leq p \leq 2$ und $0 \leq n,q \leq 4$.

Nachdem der Einfluß des Ligandenfeldes betrachtet worden ist, muß im zweiten Schritt die coulombsche Wechselwirkung zwischen den Elektronen berücksichtigt werden. Symmetrieüberlegungen zeigen, welche Terme $^{2S+1}\Gamma$ (S Gesamtspin, Γ irreduzible Darstellung der Gruppe D_3) nach Einschalten der Elektronenwechselwirkung aus der Konfiguration $e^n a_1^p \varepsilon^q$ hervorgehen. Da verschiedene Elektronenkonfigurationen Terme liefern können, die durch die gleichen Quantenzahlen S und Γ charakterisiert sind, muß auch die Wechselwirkung zwischen den entsprechenden Konfigurationen behandelt werden.

Das d^2-Elektronensystem

Im Falle zweier d-Elektronen existieren sechs Konfigurationen. Die aus den Konfigurationen hervorgehenden Terme findet man, indem man die entsprechenden Produktdarstellungen in ihre irreduziblen Bestandteile zerlegt. Die zugehörigen Zustandsfunktionen werden aus antisymmetrischen Produkten von Einelektronenfunktionen aufgebaut und sind in Tabelle I angegeben. Die Matrix des Coulombwechselwirkungsoperators $\frac{e^2}{r_{12}}$ ist diagonal in S, Γ, M_S und M_Γ und unabhängig von den Projektionen M_S und M_Γ. Es sind also Matrixelemente des Typs $\langle \gamma_1^n \gamma_2^{2-n} S\Gamma \left| \frac{e^2}{r_{12}} \right| \gamma_3^{n'} \gamma_4^{2-n'} S\Gamma \rangle$ zu betrachten, wobei $\gamma_i^n \gamma_k^{2-n}$ die Konfiguration bezeichnen soll, aus der der Term $^{2S+1}\Gamma$ hervorgeht.

Tabelle I

Energiematrizen und einige Zustandsfunktionen für d^2

(Zu jedem Diagonalelement ist A zu addieren)

$^1A_1$

ε^2	e^2	$e\varepsilon$	a_1^2
$+8B+4C$ $+2D-2E+2F$	$4B+2C$	0	$\sqrt{2}(2B+C)$
	$+7B+4C$	$2B$	$\sqrt{2}(3B+C)$
		$+2C$ $+D-E+F$	$-2\sqrt{2}B$
			$+4B+3C$ $+8E+6F$

$$e\varepsilon(^1A_1) = \frac{1}{2}[(e_1^+\varepsilon_1^- + e_2^+\varepsilon_2^-) - (e_1^-\varepsilon_1^+ + e_2^-\varepsilon_2^+)]$$

$$e^2(^1A_1) = \frac{1}{\sqrt{2}}[e_1^+e_1^- + e_2^+e_2^-] \qquad a_1^2(^1A_1) = a_1^+a_1^-$$

(Fortsetzung Tab. 1)

$^3A_1$ $\quad -8B + D - E + F$ $\quad e\varepsilon(^3A_1) = \begin{cases} \frac{1}{\sqrt{2}}[e_1^+\varepsilon_1^+ + e_2^+\varepsilon_2^+] \\ \frac{1}{2}[(e_1^+\varepsilon_1^- + e_2^+\varepsilon_2^-) + (e_1^-\varepsilon_1^+ + e_2^-\varepsilon_2^+)] \\ \frac{1}{\sqrt{2}}[e_1^-\varepsilon_1^- + e^-\varepsilon_2^-] \end{cases}$

$^1A_2$ $\quad +4B + 2C + D - E + F$ $\quad e\varepsilon(^1A_2) = \frac{1}{2}[(e_1^+\varepsilon_2^- - e_2^+\varepsilon_1^-) - (e_1^-\varepsilon_2^+ - e_2^-\varepsilon_1^+)]$

$^3A_2$

ε^2	e^2	$e\varepsilon$
$-8B$ $+2D-2E+2F$	0	0
	$-5B$	$-6B$
		$+4B$ $+D-E+F$

$e^2(^3A_2) = e_1^+e_2^+$ $\quad e\varepsilon(^3A_2) = \frac{1}{\sqrt{2}}[e_1^+\varepsilon_2^+ - e_2^+\varepsilon_1^+]$

^1E

ε^2	e^2	$a_1\varepsilon$	ea_1	$e\varepsilon$
$+2C$ $+2D-2E+2F$	$2B$	0	$2\sqrt{2}B$	0
	$+B+2C$	$-2B$	0	$-2B$
		$+2B+2C$ $+D+3E+4F$	$\sqrt{2}B$	$-2B$
			$+B+2C$ $+4E+3F$	$\sqrt{2}B$
				$+2B+2C$ $+D-E+F$

$e^2(^1E) = \begin{cases} \frac{1}{\sqrt{2}}[e_1^+e_2^- - e_1^-e_2^+] \\ \frac{1}{\sqrt{2}}[e_1^+e_1^- - e_2^+e_2^-] \end{cases}$ $\quad ea_1(^1E) = \begin{cases} \frac{1}{\sqrt{2}}[e_1^+a_1^- - e_1^-a_1^+] \\ \frac{1}{\sqrt{2}}[e_2^+a^- - e_2^-a_1^+] \end{cases}$

$e\varepsilon(^1E) = \begin{cases} \frac{1}{2}[(e_1^+\varepsilon_2^- + e_2^+\varepsilon_1^-) - (e_1^-\varepsilon_2^+ + e_2^-\varepsilon_1^+)] \\ \frac{1}{2}[(e_1^+\varepsilon_1^- - e_2^+\varepsilon_2^-) - (e_1^-\varepsilon_1^+ - e_2^-\varepsilon_2^+)] \end{cases}$

Fortsetzung Tab. I)

^3E

$a_1\varepsilon$	ea_1	$e\varepsilon$
$-2B$ $+D+3E+4F$	$-3\sqrt{2}B$	$-6B$
	$-5B$ $+4E+3F$	$3\sqrt{2}B$
		$-2B$ $+D-E+F$

$$ea_1(^3E) = \begin{cases} e_1^+ a_1^+ \\ e_2^+ a_1^+ \\ \cdots \end{cases} \qquad e\varepsilon(^3E) = \begin{cases} \frac{1}{\sqrt{2}}[e_1^+\varepsilon_2^+ + e_2^+\varepsilon_1^+] \\ \frac{1}{\sqrt{2}}[e_1^+\varepsilon_1^+ - e_2^+\varepsilon_2^+] \\ \cdots \end{cases}$$

Diese Matrixelemente werden durch die Racah-Parameter A, B und C [4] ausgedrückt:

$$A = F_0 - 49F_4 \qquad B = F_2 - 5F_4 \qquad C = 35F_4,$$

wobei die F_k Slater—Condon-Parameter [1] sind. Die Ergebnisse sind in Tabelle I zusammengestellt.

d^N-Elektronensysteme mit $N > 2$

Die Matrizen der elektrostatischen Energie für ein d^N-Elektronensystem mit $N = 3$, 4 und 5 werden aus denen des d^{N-1}-Systems mit Hilfe einer Induktionsbeziehung bestimmt.

Ein aus der Konfiguration $e^n a_1^p \varepsilon^q$ hervorgehender Zustand wird durch $|\, e^n(S_1\Gamma_1)a_1^p(S_2\Gamma_2)\{S_1\Gamma_1\}\varepsilon^q(S_3\Gamma_3)S\Gamma M_S M_\Gamma\rangle$ bezeichnet. Dieser Schreibweise kann man die Kopplung der Terme von e^n, a_1^p und ε^q entnehmen, die zu dem vorliegenden Zustand führt. Es liefert nämlich die Kopplung von $S_1\Gamma_1$ und $S_2\Gamma_2$ zunächst $S_1\Gamma_1$, und die Kopplung von $S_1\Gamma_1$ und $S_3\Gamma_3$ ergibt schließlich $S\Gamma$.

Um die elektrostatischen Energiematrizen für ein d^N-Elektronensystem zu erhalten, müssen Matrixelemente der Art $\langle K_1\, S\Gamma \,|\, V_N \,|\, K_2\, S\Gamma\rangle$ berechnet werden, wobei die K_i für verschiedene Konfigurationen stehen und $V_N = \sum_{1\leq i<j\leq N} \frac{e^2}{r_{ij}}$ die elektrostatische Abstoßung zwischen den N Elektronen darstellt. Man erhält folgende Induktionsformel (vgl. Anhang I):

$$\langle e^n (S_1\Gamma_1)\, a_1^p\, (S_2\Gamma_2)\{S_I\Gamma_I\}\varepsilon^q\, (S_3\Gamma_3)\, S\Gamma \mid V_N \mid e^{n'}\, (S_4\Gamma_4) a_1^{p'} (S_5\Gamma_5)\{S_{II}\Gamma_{II}\}\varepsilon^{q'}\, (S_6\Gamma_6)\, S\Gamma\rangle$$

$$= \frac{\sqrt{nn'}}{N-2} \sum_{\substack{S_1'\Gamma_1'\bar{S}\bar{\Gamma} \\ \bar{\bar{S}}\tilde{\Gamma}\, S_4'\Gamma_4' \\ \tilde{S}\tilde{\Gamma}}} \langle [E\Gamma_1'(\Gamma_1)\Gamma_2](\Gamma_I)\Gamma_3\Gamma \mid E, [\Gamma_1'\Gamma_2(\bar{\Gamma})\Gamma_3](\bar{\bar{\Gamma}})\Gamma\rangle \cdot$$

$$\cdot \left\langle \left[\frac{1}{2}\, S_1'(S_1)S_2\right](S_I)S_3S \mid \frac{1}{2}, [S_1'S_2(\bar{S})S_3](\bar{\bar{S}})S\right\rangle \cdot$$

$$\cdot \langle e^n S_1\Gamma_1\{ \mid e, e^{n-1}(S_1'\Gamma_1'), S_1\Gamma_1\rangle \cdot$$

$$\cdot \langle e^{n-1}(S_1'\Gamma_1')a_1^p(S_2\Gamma_2)\{\bar{S}\bar{\Gamma}\}\varepsilon^q(S_3\Gamma_3)\bar{\bar{S}}\bar{\bar{\Gamma}} \mid V_{N-1} \mid e^{n'-1}(S_4'\Gamma_4')a_1^{p'}(S_5\Gamma_5)\{\tilde{S}\tilde{\Gamma}\}\varepsilon^{q'}(S_6\Gamma_6)\bar{\bar{S}}\bar{\bar{\Gamma}}\rangle \cdot$$

$$\cdot \langle E, [\Gamma_4'\Gamma_5(\tilde{\Gamma})\Gamma_6](\bar{\bar{\Gamma}})\Gamma \mid [E\Gamma_4'(\Gamma_4)\Gamma_5](\rangle \cdot \Gamma_{II})\Gamma_6\Gamma\rangle \cdot$$

$$\cdot \left\langle \frac{1}{2}, [S_4'S_5(\tilde{S})S_6](\bar{\bar{S}})S \mid \left[\frac{1}{2}\, S_4'(S_4)S_5\right](S_{II})S_6S\right\rangle \cdot$$

$$\cdot \langle e, e^{n'-1}(S_4'\Gamma_4'), S_4\Gamma_4 \mid \}e^{n'}S_4\Gamma_4\rangle$$

$$+ (-1)^{np+\alpha(\Gamma_1\Gamma_2\Gamma_I)+S_1+S_2-S_I} \cdot (-1)^{n'p'+\alpha(\Gamma_4\Gamma_5\Gamma_{II})+S_4+S_5-S_{II}} \cdot$$

$$\cdot \frac{\sqrt{pp'}}{N-2} \sum_{\substack{S_2'\Gamma_2'\bar{S}\bar{\Gamma} \\ \bar{\bar{S}}\tilde{\Gamma}\, S_5'\Gamma_5' \\ \tilde{S}\tilde{\Gamma}}} \langle [A_1\Gamma_2'(\Gamma_2)\Gamma_1](\Gamma_I)\Gamma_3\Gamma \mid A_1, [\Gamma_2'\Gamma_1(\bar{\Gamma})\Gamma_3](\bar{\bar{\Gamma}})\Gamma\rangle \cdot$$

$$\cdot \left\langle \left[\frac{1}{2}\, S_2'(S_2)S_1\right](S_I)S_3S \mid \frac{1}{2}, [S_2'S_1(\bar{S})S_3](\bar{\bar{S}})S\right\rangle \cdot$$

$$\cdot \langle a_1^{p-1}(S_2'\Gamma_2')e^n(S_1\Gamma_1)\{\bar{S}\bar{\Gamma}\}\varepsilon^q(S_3\Gamma_3)\bar{\bar{S}}\bar{\bar{\Gamma}} \mid V_{N-1} \mid a^{p'-1}(S_5'\Gamma_5')e^{n'}(S_4\Gamma_4)\{\tilde{S}\tilde{\Gamma}\}\varepsilon^{q'}(S_6\Gamma_6)\bar{\bar{S}}\bar{\bar{\Gamma}}\rangle \cdot$$

$$\cdot \langle A_1, [\Gamma_5'\Gamma_4(\tilde{\Gamma})\Gamma_6](\bar{\bar{\Gamma}})\Gamma \mid [A_1\Gamma_5'(\Gamma_5)\Gamma_4](\Gamma_{II})\Gamma_6\Gamma\rangle \cdot$$

$$\cdot \left\langle \frac{1}{2}, [S_5'S_4(\tilde{S})S_6](\bar{\bar{S}})S \mid \left[\frac{1}{2}\, S_5'(S_5)S_4\right](S_{II})S_6S\right\rangle$$

$$+ \frac{\sqrt{qq'}}{N-2} \sum_{\substack{S_3'\Gamma_3'\bar{S}\bar{\Gamma} \\ S_6'\Gamma_6''}} \langle \Gamma_I, \Gamma_3'E(\Gamma_3)\Gamma \mid \Gamma_I\Gamma_3'(\bar{\Gamma})E\Gamma\rangle \langle S_I, S_3' \frac{1}{2}\, (S_3)S \mid S_IS_3'(\bar{S})\, \frac{1}{2}\, S\rangle \cdot$$

$$\cdot \langle \varepsilon^q S_3\Gamma_3\{ \mid \varepsilon^{q-1}(S_3'\Gamma_3')\varepsilon S_3\Gamma_3\rangle \cdot$$

$$\cdot \langle e^n(S_1\Gamma_1)a_1^p(S_2\Gamma_2)\{S_I\Gamma_I\}\varepsilon^{q-1}(S_3'\Gamma_3')\bar{S}\bar{\Gamma} \mid V_{N-1} \mid e^{n'}(S_4\Gamma_4)a_1^{p'}(S_5\Gamma_5)\{S_{II}\Gamma_{II}\}\varepsilon^{q'-1}(S_6'\Gamma_6')\bar{S}\bar{\Gamma}\rangle \cdot$$

$$\cdot \langle \Gamma_{II}\Gamma_6'(\bar{\Gamma})E\Gamma \mid \Gamma_{II}, \Gamma_6'E(\Gamma_6)\Gamma\rangle \langle S_{II}S_6'(\bar{S})\frac{1}{2}S \mid S_{II}, S_6'\frac{1}{2}(S_6)S\rangle \cdot$$

$$\cdot \langle \varepsilon^{q'-1}(S_6'\Gamma_6')\varepsilon S_6\Gamma_6 \mid \}\varepsilon^{q'}S_6\Gamma_6\rangle$$

Ein Matrixelement $M = \langle K_1\, S\Gamma \mid V_N \mid K_2\, S\Gamma\rangle$ wird also im allgemeinsten Falle aufgebaut aus drei Teilen, die ihrerseits Matrixelemente vom Typ $\langle K_1'\; S'\Gamma' \mid V_{N-1} \mid K_2'\; S'\Gamma'\rangle$ enthalten. In der obigen Beziehung gilt: $n + p + q = n' + p' + q' = N$ und

$$\alpha(\Gamma_i\Gamma_j\Gamma_k) = \begin{matrix} 1, \text{ wenn } (\Gamma_i\Gamma_j\Gamma_k) = (EEA_2) \\ 0 \text{ sonst.} \end{matrix}$$

Die Racah-Koeffizienten wurden aus Clebsch—Gordan-Koeffizienten berechnet und sind teilweise im Anhang II angegeben. Die Clebsch—Gordan-Koeffizienten findet man leicht aus Symmetrieüberlegungen (vgl. Tabelle II).

Tabelle II

Clebsch-Gordan-Koeffizienten $\langle \Gamma_1\Gamma_2 M_1 M_2 \mid \Gamma_1\Gamma_2\Gamma M\rangle$

A_2XA_2	A_1 / a_1
$a_2\ a_2$	1

A_2XE	E / e_1	e_2
$a_2\ e_1$	0	−1
$a_2\ e_2$	1	0

EXE		A_1 / a_1	A_2 / a_2	E / e_1	e_2
e_1	e_1	$2^{-1/2}$	0	0	$2^{-1/2}$
e_1	e_2	0	$2^{-1/2}$	$2^{-1/2}$	0
e_2	e_1	0	$-2^{-1/2}$	$2^{-1/2}$	0
e_2	e_2	$2^{-1/2}$	0	0	$-2^{-1/2}$

Es gilt $\langle \Gamma_1\Gamma_2 M_1 M_2 \mid \Gamma_1\Gamma_2\Gamma M\rangle = \langle \Gamma_2\Gamma_1\, M_2 M_1 \mid \Gamma_2\Gamma_1\Gamma M\rangle$, wenn nicht $(\Gamma_1\Gamma_2\Gamma) = (EEA_2)$ ist. Die analogen Koeffizienten für den Spin wurden [1] entnommen.

Weiterhin erscheinen in der obigen Beziehung coefficients of fractional parentage (cfp) vom Typ $\langle e^{n-1}(S'\Gamma')e\ S\Gamma \mid\} e^n S\Gamma\rangle$. Die hier interessierenden cfp werden aus (vgl. [4] und Anhang I) $\sum_{S''\Gamma''} \langle e, ee(S''\Gamma''), S\Gamma \mid e^2(S'\Gamma')eS\Gamma\rangle \langle e^2(S'\Gamma')e\ S\Gamma \mid\} e^3\ S\Gamma\rangle = 0$ bestimmt, wobei $S\Gamma = {}^2E$, $S'\Gamma' = {}^1A_1, {}^3A_2, {}^1E$ und $S''\Gamma'' = {}^3A_1, {}^1A_2, {}^3E$ sind (vgl. Tabelle III).

Tabelle III

cfp $\langle e^2(S'\Gamma')e\ S\Gamma \mid\} e^3\ S\Gamma\rangle$

$S\Gamma$ \ $S'\Gamma'$	$^1A_1$	$^3A_2$	^1E
^2E	$6^{-1/2}$	$2^{-1/2}$	$-3^{-1/2}$

Außerdem gilt für die cfp (vgl. [4]):

$$\langle e, e^2(S'\Gamma'), {}^2E \mid\} e^3\ {}^2E\rangle = (-1)^{S'} \langle e^2(S'\Gamma')e\ {}^2E \mid\} e^3\ {}^2E\rangle$$

und

$$\langle e^3\ {}^2E\{ \mid e^2(S'\Gamma')e\ {}^2E\rangle = \langle e^2(S'\Gamma')e\ {}^2E \mid\} e^3\ {}^2E\rangle.$$

Mit Hilfe der angegebenen Induktionsformel wurden die in Tabelle IV aufgeführten elektrostatischen Energiematrizen für die d^N-Elektronensysteme mit $N = 3$, 4 und 5 berechnet. Wegen der Teilchen-»Loch«-Äquivalenz folgen

die Matrizen der elektrostatischen Wechselwirkung für d^N-Systeme mit $N > 5$ aus den Energieausdrücken der entsprechenden d^N-Systeme mit $N < 5$. Man erhält folgende Beziehung zwischen den Zuständen komplementärer Elektronensysteme

$$| e^n a_1^p(S_1\Gamma_1)\varepsilon^q S\Gamma\rangle \mathrel{\hat{=}} (-1)^{np+pq+nq} c_1 c_2 \, | e^{4-n} a_1^{2-p}(S_1\Gamma_1)\varepsilon^{4-q} S\Gamma\rangle$$

mit

$$c_1(c_2) = \begin{cases} -1, \text{ wenn } n(q) = 2 \text{ und } S\Gamma = {}^3A_2, {}^1E \\ 1 \text{ sonst.} \end{cases}$$

Ein konstanter Beitrag der Elektronenwechselwirkung, der komplementäre d^N-Systeme unterscheidet, ist unwesentlich, da er lediglich eine konstante Verschiebung aller Terme bedingt.

Anhang I

Ableitung der Induktionsformel

Ausgangspunkt ist die in N Elektronen antisymmetrische Funktion

$$| F\rangle = | e^n(S_1\Gamma_1)a_1^p(S_2\Gamma_2)\{S_1\Gamma_1\}\varepsilon^q(S_3\Gamma_3)S\Gamma\rangle.$$

Da $| F\rangle$ total antisymmetrisch ist, erhält man beim Abkoppeln des N-ten Elektrons Ausdrücke des Typs

$$| e,\ e^{n-1}(S_1'\Gamma_1')(S_1\Gamma_1)a_1^p(S_2\Gamma_2)\{S_1\Gamma_1\}\varepsilon^q(S_3\Gamma_3)S\Gamma\rangle \qquad \text{(x)}$$

und entsprechende für die a_1- und ε-Konfigurationen. Diese Funktionen enthalten nun aber auch symmetrische Anteile (die obige bspw. in $n-1$ Elektronen symmetrische Anteile), was man beim Übergang zu einem anderen Kopplungsschema sofort sieht:

$$\begin{aligned} &| e,\ e^{n-1}(S_1'\Gamma_1')(S_1\Gamma_1)a_1^p(S_2\Gamma_2)\{S_1\Gamma_1\}\varepsilon^q(S_3\Gamma_3)S\Gamma\rangle \\ &= \sum_{S_1''\Gamma_1''} \langle e^{n-1}(S_1''\Gamma_1'')\, eS_1\Gamma_1 \,|\, e,\ e^{n-1}(S_1'\Gamma_1')\, S_1\Gamma_1\rangle \cdot \\ &\qquad \cdot | e^{n-1}(S_1''\Gamma_1'')e(S_1\Gamma_1)a_1^p(S_2\Gamma_2)\{S_1\Gamma_1\}\varepsilon^q(S_3\Gamma_3)\, S\Gamma\rangle, \end{aligned} \qquad \text{xx}$$

denn die Summation läuft natürlich über alle $S_1''\Gamma_1''$.

$| F\rangle$ kann man also nur als Linearkombination der Funktionen (x) erhalten, wobei über die $S_1'\Gamma_1'$ zu summieren ist:

$$| F\rangle = \sum_{\substack{S_1'\Gamma_1' \\ +\cdots}}' \langle e,\ e^{n-1}(S_1'\Gamma_1')S_1\Gamma_1 \,|\, \}\, e^n S_1\Gamma_1\rangle \cdot | e,\ e^{n-1}(S_1'\Gamma_1')(S_1\Gamma_1)a_1^p(S_2\Gamma_2)\{S_1\Gamma_1\}\varepsilon^q(S_3\Gamma_3)S\Gamma\rangle$$

Aus dem Vergleich mit (xx) sieht man sofort, daß für die cfp gelten muß:

$$\sum_{\cdot}' \langle e,\ e^{n-1}(S_1'\Gamma_1')S_1\Gamma_1 \,|\, \}\, e^n S_1\Gamma_1\rangle \langle e^{n-1}(S_1''\Gamma_1'')eS_1\Gamma_1 \,|\, e,\ e^{n-1}(S_1'\Gamma')S_1\Gamma_1\rangle = 0$$

für alle verbotenen Zustände $S_1''\Gamma_1''$.

Das N-te Elektron kann nun vollständig abgekoppelt werden. Man erhält

$$\begin{aligned} F\rangle = \sum_{\substack{S_1\Gamma_1' \\ \Gamma \\ \bar{S}\bar{\Gamma} \\ +\cdots}}' &\langle e, e^{n-1}(S_1'\Gamma_1')S_1\Gamma_1 \,|\}\, e^n S_1\Gamma_1\rangle \cdot \langle E, [\Gamma_1'\Gamma_2(\bar{\Gamma})\Gamma_3]\bar{\bar{\Gamma}})\Gamma \,|\, [E\Gamma_1'(\Gamma_1)\Gamma_2](\Gamma_1)\Gamma_3\Gamma\rangle \langle S\,|\rangle \cdot \\ &\cdot | e,\ e^{n-1}(S_1'\Gamma_1')a_1^p(S_2\Gamma_2)\,\{\bar{S}\bar{\Gamma}\}\varepsilon^q(S_3\Gamma_3)[\bar{\bar{S}}\bar{\bar{\Gamma}}]S\Gamma\rangle \end{aligned} \qquad \text{(xxx}$$

Energiematrizen für d^3, d^4 und d^5

(Zu jedem Diagonalelement ist 3A zu addieren)

d^3

$^2A_1$

$-3B+4C$	0	$3B+C$	0	0	$-6B$	$-2\sqrt{3}B$	$4\sqrt{2}B$	$\sqrt{2}(2B+Q)$	$-2B$	$\sqrt{3}B$
	$-8B+4C$ $+3D-3E+3F$	0	0	$\sqrt{2}(2B+Q)$	0	0	$-2B$	0	0	$-2\sqrt{2}B$
		$-3B+4C$ $+8E+6F$	$5\sqrt{2}B$	0	B	$-\sqrt{3}B$	$\sqrt{2}B$	$\sqrt{2}(2B+Q)$	0	$2\sqrt{3}B$
			$+2B+4C$ $+D+7E+7F$	$\sqrt{2}B$	0	0	0	$\sqrt{3}B$	$\sqrt{2}B$	$\sqrt{6}B$
				$-6B+3C$ $+4E+3F$	$2B$	$5B$	$-\sqrt{3}B$	0	0	$-\sqrt{3}B$
					$-2B+3C$ $+2D+2E+5F$	0	0	$\sqrt{2}B$	$-5\sqrt{2}B$	$-\sqrt{6}B$
						$+5B+5C$ $+D-E+F$	$-5\sqrt{2}B$	$-1/2\sqrt{6}B$	$-B$	$-5B$
							$-3B+3C$ $+D-E+F$	$-\sqrt{6}B$	$3/2\sqrt{2}B$	$3/2\sqrt{6}B$
								$-B+3C$ $+D-E+F$	B	$-\sqrt{3}B$
									$+6B+5C$ $+2D-2E+2F$	0
										$-6B+3C$ $+2D-2E+2F$

^4E

$d^3(^4A_2)_2$	$a_1a_2(^4E)$	$a_1(^2E)$
$-9B$ $+D-E+F$	$3\sqrt{2}B$	$6B$
	$-12B$ $+2D-2E+2F$	$3\sqrt{2}B$
		$-9B$ $+D+3E+4F$

$^4A_1$ $a_1a_2(^4E)$ $\quad -15B+D+3E+4F$

d^3

$^2A_2$

$e^1(^4A_2)_1$	$a_1a_2(^4A_2$	$e^1(^2E)$	$e^2(^2E)$	$e_1(^2E)$	$e_1(^2E)$
$-6B+3C$ $+4E+3F$	0	$-\sqrt{6}B$ $+2D+2E+5F$	$2\sqrt{3}B$	$3\sqrt{3}B$	$\sqrt{3}B$
	$-6B+3C$ $+2D+2E+5F$	$-\sqrt{6}B$	$2\sqrt{3}B$	$\sqrt{3}B$	$-3B$
		$-B+3C$ $+D-E+F$	$-\sqrt{2}B$	$5\sqrt{2}B$	$\sqrt{6}B$
			$-2B+3C$ $+2D-2E+2F$	B	$-\sqrt{3}B$
				$+4B+3C$ $+D+3E+4F$	$-\sqrt{3}B$
					$+3C+D$ $+3E+4F$

d^4

$^2A_1$

$e^1(^2E)^2$	$a_1^2e^1(^2A_1)$	$e^1(^2E)e$	$e^1(^2A_1)e^1(^2A_1)$	$e^1(^2E)e_1(^2E)e$	$e^1(^2E)e_1(^2E)e$	$e_1(^2E)$
$-3B+5C$ $+D-E+F$	$4B+C$	$3B+C$	$4B$	$6B$	$2B$	$-\sqrt{2}B$
	$-8B+5C$ $+3D-3E+3F$	$2B+C$	$6B$	$2B$	$4B$	$-3\sqrt{2}B$
		$-13B+5C$ $+D+7E+7F$	$2B$	$4B$	$-2\sqrt{2}B$	
			$-13B+4C$ $+2D-2E+2F$	$2B$	$-2\sqrt{2}B$	
				$-10B+4C$ $+D+3E+4F$	$\sqrt{2}B$	
					$-9B+4C$ $+2D+2E+5F$	

$^4A_1$ $e^2(^2A_2)e^2(^2A_2)$ $\quad -21B+2D-2E+2F$

d^4 $\quad ^1A_1$ (Zu jedem Diagonalelement ist 6A zu addieren)

e^4	$e^4(^1A_1)e^1$	$e^1(^1A_1)e^1(^1A_1)$	$e^4(^1E)e$	$ee_1^1(^1E)e$	$e^1(^1A_1)e^1(^1A_1)$	$e^4(^1E)e^1(^1E)e$	$e^4(^1E)e_1(e_1(^1E)e$	$ee_1(^1E)e^1(^1E)$
$-6B+8C$	0	$\sqrt{2}(3B+Q)$	0	$-10\sqrt{2}B$	0	0	$2\sqrt{2}B$	0
	$-16B+8C$ $+4D-4E+4F$	0	$\sqrt{2}(2B+Q)$	0	0	0	$-2\sqrt{2}B$	$-4B$
		$-3B+9C$ $+8E+6F$	$2(2B+Q)$	0	0	0	$-2\sqrt{2}B$	$-2\sqrt{2}B$
			$+8B+9C$ $+2D+6E+8F$	0	$-2B$	0	0	$-10\sqrt{2}B$
				$+5B+7C$ $+D-E+F$	$4B+C$	$3B+C$	$2\sqrt{6}B$	$-\sqrt{2}B$
					$+7C+3D$ $-3E+3F$	$2B+C$	$\sqrt{2}B$	$-\sqrt{2}B$
						$-5B+7C$ $+D+7E+7F$	$\sqrt{2}B$	$\sqrt{6}B$
							$+11B+10C$ $+2D-2E+2F$	$5\sqrt{2}B$
								$-9B+6C$ $+2D-2E+2F$

d^4

$^3A_1$

$e^4(^3E)e$	$ee_1^2(^3E)e$	$e^4(^3E)e^1(^3A_1)$	$e^4(^3B)e_1(^3E)e$	$e^4(^3E)e_1(^3E)e$	$ee_1(^3E)$
$-3B+5C$ $+D-E+F$	$4B+C$	$3B+C$	$4B$	$6B$	$-\sqrt{2}B$
	$-8B+5C$ $+3D-3E+3F$	$2B+C$	$6B$	$2B$	$-3\sqrt{2}B$
		$-13B+5C$ $+D+7E+7F$	$2B$	$4B$	$-2\sqrt{2}B$
			$-13B+4C$ $+2D-2E+2F$	$2B$	$-2\sqrt{2}B$
				$-10B+4C$ $+D+3E+4F$	$\sqrt{2}B$
					$-9B+4C$ $+2D+2E+5F$

$^3A_2$

$e^4(^3E)^2$	$a_1^2e^4(^3A_2)^2$	$e^4(^3E)e$	$ee_1^2(^3E)e$	$e^4(^3A_2)e^4(^3A_2)$	$e^4(^3E)e_1(^3E)e$	$ee_1(^3E)$
$-15B+5C$ $+8E+6F$	0	$2B$	0	$4B$	$\sqrt{2}(2B+Q)$	$-2B$	0
	$-8B+5C$ $+2D+6E+8F$	0	$2B$	$10B$	$\sqrt{2}(3B+Q)$	0	$2B$	$2\sqrt{2}B$
		$-11B+5C$ $+D-E+F$	C	$3B+C$	$-6\sqrt{2}B$	$2\sqrt{2}B$	$-6B$	$\sqrt{2}B$
			$-16B+5C$ $+3D-3E+3F$	$2B+C$	$-\sqrt{2}B$	$-3\sqrt{2}B$	$-2B$	$3\sqrt{2}B$
				$+5C+D$ $+7E+7F$	$\sqrt{2}B$	$\sqrt{2}B$	$-4B$	$2\sqrt{2}B$
					$-5B+6C$ $+2D-2E+2F$	0	$5\sqrt{2}B$	$-2B$
						$-B+6C$ $+2D-2E+2F$	$\sqrt{2}B$	$-\sqrt{2}B$
							$-10B+4C$ $+D+3E+4F$	$\sqrt{2}B$
								$-9B+4C$ $+2D+2E+5F$

d^2

^4E *(Zu jedem Diagonalelement ist 10A zu addieren)*

$e^3(^2E)e^2(^1A_1)$	$e^3(^2A_2)\ ^1(^1E)$	$e^3(^2A_2)a_2^1\{^3A_2\}\ e$	$ea_1^1\{^3E\}e^3(^2A_2)$	$e^3(^2E)a_1\{^2E\}e$	$ea_1\{^3E\}e^3(^2E)$	$e^3(^2A_1)a_2\{^1A_2\}e^2(^1E)$	$e^3(^1E)a_1\{^2E\}e^2(^1A_2)$
$-19B+6C$ $+2D-2E+2F$	$-2\sqrt{2}B$	$-\sqrt{2}B$	$3B+C$	$-2\sqrt{2}B$	$-\sqrt{2}B$	$2B$	0
	$-21B+6C$ $+3D-3E+3F$	$2B+C$	$-\sqrt{2}B$	$-2B$	$-4B$	0	$-\sqrt{2}B$
		$-21B+6C$ $+D+7E+7F$	$-2\sqrt{2}B$	$-4B$	$-2B$	0	$\sqrt{2}B$
			$-19B+6C$ $+2D+6E+8F$	$-\sqrt{2}B$	$-2\sqrt{2}B$	$-2B$	0
				$-21B+6C$ $+D+3E+4F$	$2B+C$	$-\sqrt{2}B$	$-\sqrt{2}B$
					$-21B+6C$ $+3D+E+6F$	$\sqrt{2}B$	$\sqrt{2}B$
						$-21B+5C$ $+2D+2E+5F$	$-2B$
							$-20B+6C$ $+2D+2E+5F$

					$-22B+9C$ $+D+3E+4F$	0	C	$3/2\sqrt{2}B$	$-3/2\sqrt{2}B$	$\sqrt{3}B$
						$-18B+9C$ $+3D+E+6F$	$-\sqrt{3}B$	$-5/2\sqrt{6}B$	$1/2\sqrt{6}B$	$-3B$
							$-22B+9C$ $+3D+E+6F$	$3/2\sqrt{2}B$	$-3/2\sqrt{2}B$	$-\sqrt{3}B$
								$-10B+10C$ $+2D+2E+5F$	0	0
									$-4B+10C$ $+2D+2E+5F$	0
										$-12B+8C$ $+2D+2E+5F$

$^4A_2$

$e^3(^2E)a_1\{^2E\}e$	$ea_1\{^2E\}e^3(^2E)$	$e^3(^1A_1)a_1\{^3A_1\}e^2(^3A_2)$	$e^3(^1A_2)a_1\{^3A_2\}e^2(^1A_1)$
$-25B+6C$ $+D+3E+4F$	C	$3\sqrt{2}B$	0
	$-25B+6C$ $+3D+E+6F$	$3\sqrt{2}B$	0
		$-16B+7C$ $+2D+2E+5F$	0
			$-13B+7C$ $+2D+2E+5F$

d^8

^1E *(Zu jedem Diagonalelement ist 10A zu addieren)*

$e^4(^1E)e^0(^1A_1)$	$e^3(^1A_1)\ ^1(^1E)$	$e^3(^1A_1)a_1^1\{^3A_2\}\ e$	$ea_1^1\{^3E\}e^3(^1A_2)$	$e^3(^3E)a_1\{^3E\}\ e$	$ea_1\{^3E\}e^3(^1E)$	$e^3(^1A_1)a_2\{^1A_2\}e^3(^1E)$	$e^3(^1E)a_1\{^3E\}e^3(^1A_2)$
$-19B+6C$ $+2D-2E+2F$	$-2\sqrt{2}B$	$-\sqrt{2}B$	$3B+C$	$-2\sqrt{2}B$	$-\sqrt{2}B$	$2B$	0
	$-21B+6C$ $+3D-3E+3F$	$2B+C$	$-\sqrt{2}B$	$-2B$	$-4B$	0	$-\sqrt{2}B$
		$-21B+6C$ $+D+7E+7F$	$-2\sqrt{2}B$	$-4B$	$-2B$	0	$\sqrt{2}B$
			$-19B+6C$ $+2D+6E+8F$	$-\sqrt{2}B$	$-2\sqrt{2}B$	$-2B$	0
				$-21B+6C$ $+D+3E+4F$	$2B+C$	$-\sqrt{2}B$	$-\sqrt{2}B$
					$-21B+6C$ $+3D+E+6F$	$\sqrt{2}B$	$\sqrt{2}B$
						$-21B+5C$ $+2D+2E+5F$	$-2B$
							$-20B+6C$ $+2D+2E+5F$

d^5

^2E

$e^4(^1A_1)\varepsilon$	$ee^4(^1A_1)$	$e^3(^2E)a_1^2$	$a_1^2e^3(^2E)$	$e^3(^2E)e^3(^1A_1)$	$e^3(^2E)e^3(^3A_2)$	$e^3(^2E)e^3(^1E)$	$e^3(^1A_1)e^3(^2E)$	$e^3(^1A_2)e^3(^2E)$	$e^3(^1E)e^3(^2E)$	$e^3(^1A_1)a_1^2(^1A_1)\varepsilon$	$e^3(^1A_2)a_1^2(^1A_2)\varepsilon$	$e^3(^1E)a_1^2(^1E)\varepsilon$	$ea_1^2(^2E)e^3(^1A_1)$	$ea_1^2(^2E)e^3(^1A_2)$	$ea_1^2(^2E)e^3(^2E)$	$e^3(^2E)a_1(^1E)\varepsilon$	$e^3(^2E)a_1(^2E)\varepsilon$	$ea_1(^1E)e^3(^2E)$	$ea_1(^2E)e^3(^2E)$	$e^3(^1A_1)a_1(^2A_1)e^3(^2E)$	$e^3(^1A_2)a_1(^2A_2)e^3(^1E)$	$e^3(^1E)a_1(^2E)e^3(^2E)$	$e^3(^1E)a_1(^2E)e^3(^1A_1)$	$e^3(^1E)a_1(^2E)e^3(^2A_2)$
$-10B+10C$ $+D-E+F$	0	$\sqrt{2}B$	0	$5B$	$5\sqrt{3}B$	$5\sqrt{2}B$	$\sqrt{2}(2B+C)$	0	$2B$	$\sqrt{2}(3B+C)$	0	0	0	0	0	$-5\sqrt{2}B$	$-\sqrt{6}B$	0	0	0	0	$-\sqrt{2}B$	$-B$	$-\sqrt{3}B$
	$-20B+10C$ $+4D-4E+4F$	0	$\sqrt{2}B$	$\sqrt{2}(2B+C)$	0	$2B$	$-B$	$-3\sqrt{3}B$	$\sqrt{2}B$	0	0	0	$\sqrt{2}(2B+C)$	0	0	0	0	$-B$	$3\sqrt{3}B$	$\sqrt{2}B$	$-\sqrt{6}B$	$2B$	0	0
		$-20B+10C$ $+8E+6F$	0	$\sqrt{2}(2B+C)$	0	0	0	0	0	$-B$	$3\sqrt{3}B$	$-\sqrt{2}B$	$\sqrt{2}(2B+C)$	0	$-2B$	B	$-3\sqrt{3}B$	0	0	$-\sqrt{2}B$	$-\sqrt{6}B$	$2B$	0	0
			$-10B+10C$ $+3D+5E+9F$	0	0	0	$\sqrt{2}(3B+C)$	0	0	$\sqrt{2}(2B+C)$	0	$-2B$	$5B$	$-5\sqrt{3}B$	$-5\sqrt{2}B$	0	0	$5\sqrt{2}B$	$\sqrt{6}B$	0	0	$-\sqrt{2}B$	B	$-\sqrt{3}B$
				$-B+11C$ $+2D+2E+2F$	0	$5\sqrt{2}B$	$-3\sqrt{2}B$	$-\sqrt{6}B$	$4B$	$1/2\sqrt{2}B$	$1/2\sqrt{6}B$	$-B$	$3B+C$	0	0	$2\sqrt{2}B$	$-\sqrt{6}B$	$-1/2\sqrt{2}B$	$1/2\sqrt{6}B$	$-5B$	$-5\sqrt{3}B$	$5\sqrt{2}B$	0	0
					$-13B+9C$ $+2D-2E+2F$	$\sqrt{6}B$	$3\sqrt{6}B$	$-\sqrt{2}B$	$4\sqrt{3}B$	$1/2\sqrt{6}B$	$-1/2\sqrt{2}B$	$\sqrt{3}B$	0	$3B+C$	0	$-2\sqrt{6}B$	$-\sqrt{2}B$	$-1/2\sqrt{6}B$	$-1/2\sqrt{2}B$	$-\sqrt{3}B$	B	$-\sqrt{6}B$	0	0
						$-9B+9C$ $+2D-2E+2F$	$6B$	$-2\sqrt{3}B$	0	B	$-\sqrt{3}B$	0	0	0	$3B+C$	0	0	0	0	0	0	$5\sqrt{2}B$	$-\sqrt{6}B$
							$-7B+11C$ $+3D-3E+3F$	0	$5\sqrt{2}B$	$2B+C$	0	0	$1/2\sqrt{2}B$	$-1/2\sqrt{6}B$	$-B$	$-2B$	0	$5B$	$-\sqrt{3}B$	0	$-5B$	$5/2\sqrt{2}B$	$-5/2\sqrt{6}B$
								$-15B+9C$ $+3D-3E+3F$	$-\sqrt{6}B$	0	$2B+C$	0	$-1/2\sqrt{6}B$	$-1/2\sqrt{2}B$	$-\sqrt{3}B$	0	$-2B$	$\sqrt{3}B$	$-7B$	0	0	$-\sqrt{3}B$	$-1/2\sqrt{6}B$	$-1/2\sqrt{2}B$
									$-13B+9C$ $+3D-3E+3F$	0	0	$2B+C$	B	$\sqrt{3}B$	0	0	0	0	0	$-5B$	$-\sqrt{3}B$	0	0	0
										$-7B+11C$ $+D+7E+7F$	0	$-5\sqrt{2}B$	$-3\sqrt{2}B$	$-3\sqrt{6}B$	$-6B$	$-5B$	$\sqrt{3}B$	$2B$	0	0	0	$-5B$	$-5/2\sqrt{2}B$	$-5/2\sqrt{6}B$
											$-15B+9C$ $+D+7E+7F$	$-\sqrt{6}B$	$\sqrt{6}B$	$-\sqrt{2}B$	$-2\sqrt{3}B$	$\sqrt{3}B$	$-7B$	0	$-2B$	0	0	$\sqrt{3}B$	$-1/2\sqrt{6}B$	$1/2\sqrt{2}B$
												$-13B+9C$ $+D+7E+7F$	$-4B$	$4\sqrt{3}B$	0	0	0	0	0	$-5B$	$\sqrt{3}B$	0	0	0
													$-B+11C$ $+2D+6E+8F$	0	$-5\sqrt{2}B$	$1/2\sqrt{2}B$	$-1/2\sqrt{6}B$	$-2\sqrt{2}B$	$\sqrt{6}B$	$5B$	$-5\sqrt{3}B$	$5\sqrt{2}B$	0	0
														$-13B+9C$ $+2D+6E+8F$	$\sqrt{6}B$	$-1/2\sqrt{6}B$	$-1/2\sqrt{2}B$	$-2\sqrt{6}B$	$-\sqrt{2}B$	$-\sqrt{3}B$	$-B$	$\sqrt{6}B$	0	0
															$-9B+9C$ $+2D+6E+8F$	0	0	0	0	0	0	0	$5\sqrt{2}B$	$\sqrt{6}B$
																$-13B+9C$ $+D+3E+4F$	0	$2B+C$	0	$5/2\sqrt{2}B$	$-1/2\sqrt{6}B$	0	$-3/2\sqrt{2}B$	$3/2\sqrt{6}B$
																	$-15B+9C$ $+D+3E+4F$	0	$2B+C$	$3/2\sqrt{6}B$	$3/2\sqrt{2}B$	0	$-1/2\sqrt{6}B$	$-1/2\sqrt{2}B$
																		$-13B+9C$ $+3D+E+6F$	0	$5/2\sqrt{2}B$	$1/2\sqrt{6}B$	0	$-3/2\sqrt{2}B$	$-3/2\sqrt{6}B$
																			$-15B+9C$ $+3D+E+6F$	$3/2\sqrt{6}B$	$-3/2\sqrt{2}B$	0	$-1/2\sqrt{6}B$	$1/2\sqrt{2}B$
																				$-6B+10C$ $+2D+2E+5F$	0	0	$-10B$	0
																					$-12B+8C$ $+2D+2E+5F$	0	0	$2B$
																						$-12B+8C$ $+2D+2E+5F$	0	0
																							$-4B+10C$ $+2D+2E+5F$	0
																								$-16B+8C$ $+2D+2E+5F$

Es sind Matrixelemente des Typs $M = \langle F \mid V_N \mid F \rangle$ zu berechnen, wobei $V_N = \sum_{1 \le i < j \le N} \frac{e^2}{r_{ij}}$ ist. Mit $\langle F \mid V_N \mid F \rangle = \frac{N}{N-2} \langle F \mid V_{N-1} \mid F \rangle$ und (xxx) erhält man sofort den oben angegebenen Ausdruck für M. Die in (xxx) auftretenden Racah-Koeffizienten werden wie folgt aus Clebsch—Gordan-Koeffizienten aufgebaut:

$$\langle E, [\Gamma_1' \Gamma_2(\bar{\Gamma}) \Gamma_3](\bar{\bar{\Gamma}}) \Gamma \mid [E\Gamma_1'(\Gamma_1)\Gamma_2](\Gamma_1)\Gamma_3\Gamma \rangle =$$
$$\sum_{\substack{\gamma_1\gamma_2\gamma_3\gamma_1\gamma_2 \\ \gamma_1'\gamma_e\bar{\gamma}\bar{\bar{\gamma}}}} \langle \Gamma_1\Gamma_3\gamma_1\gamma_3 \mid \Gamma_1\Gamma_3\Gamma\gamma \rangle \langle \Gamma_1\Gamma_2\gamma_1\gamma_2 \mid \Gamma_1\Gamma_2\Gamma_1\gamma_1 \rangle \langle E\Gamma_1'\gamma_e\gamma_1' \mid E\Gamma_1'\Gamma_1\gamma_1 \rangle \cdot$$
$$\cdot \langle \Gamma_1'\Gamma_2\bar{\Gamma}\bar{\gamma} \mid \Gamma_1'\Gamma_2\gamma_1'\gamma_2 \rangle \langle \bar{\Gamma}\Gamma_3\bar{\bar{\gamma}} \mid \bar{\Gamma}\Gamma_3\bar{\gamma}\gamma_3 \rangle \langle E\bar{\bar{\Gamma}}\Gamma\gamma \mid E\bar{\bar{\Gamma}}\gamma_e\bar{\bar{\gamma}} \rangle .$$

Anhang II

1. *Tabellen der in den Rechnungen auftretenden Racah-Koeffizienten*

$$\langle \Gamma_1, \Gamma_2\, \Gamma_3(\Gamma^{\mathrm{I}})\Gamma \mid \Gamma_1\ \Gamma_2(\Gamma^{\mathrm{II}})\Gamma_3\Gamma \rangle$$

und

$$\langle \Gamma_1, [\Gamma_2\Gamma_3(\Gamma^{\mathrm{I}})\Gamma_4](\Gamma^{\mathrm{II}})\Gamma \mid [\Gamma_1\Gamma_2(\Gamma^{\mathrm{III}})\Gamma_3](\Gamma^{\mathrm{IV}})\Gamma_4\Gamma \rangle$$

$\langle E, \Gamma_2 E(E)\Gamma \mid E\Gamma_2(E)E\Gamma \rangle$

Γ_2	A_2			E		
Γ	A_1	A_2	E	A_1	A_2	E
A_1	—1			1		
A_2		—1			—1	
E			1			0

$\langle E, EE(\Gamma^{\mathrm{I}})E \mid EE(\Gamma^{\mathrm{II}})EE \rangle$

Γ^{II} \ Γ^{I}	A_1	A_2	E
A_1	1/2	—1/2	$1/\sqrt{2}$
A_2	1/2	—1/2	$-1/\sqrt{2}$
E	$1/\sqrt{2}$	$1/\sqrt{2}$	0

$\langle A_2, EE(\Gamma^{\mathrm{I}})\Gamma \mid A_2E(E)E\Gamma \rangle$

Γ^{I} \ Γ	A_1	A_2	E
A_1		1	
A_2	—1		
E			—1

$\langle E, EA_2(E)\Gamma \mid EE(\Gamma^{\mathrm{II}})A_2\Gamma \rangle$

Γ^{I} \ Γ	A_1	A_2	E
A_1		—1	
A_2	1		
E			—1

$\langle E, \Gamma_2 A_2(\Gamma^{\mathrm{I}})E \mid E\Gamma_2(E)A_2E \rangle$

Γ^{I} \ Γ^2	A_1	A_2
A_1		—1
A_2	1	

$\langle A_2, \Gamma_2 E(E)E \mid A_2\Gamma_2(\Gamma^{\mathrm{II}})EE \rangle$

Γ^{I} \ Γ_2	A_1	A_2
A_1		—1
A_2	1	

$\langle E, [EA_1(E)E](\Gamma^{\mathrm{II}})\Gamma \mid [EE(\Gamma^{\mathrm{III}})A_1](\Gamma^{\mathrm{III}})E\Gamma \rangle$

Γ	A_1	A_2	E		
Γ^{III} \ Γ^{II}	E	E	A_1	A_2	E
A_1			1/2	—1/2	$1/\sqrt{2}$
A_2			1/2	—1/2	$-1/\sqrt{2}$
E	1	—1	$1/\sqrt{2}$	$1/\sqrt{2}$	0

$\langle E, A_2A_1(A_2)E \mid (E)\Gamma \mid [EA_2(E)A_1](E)E\Gamma\rangle$

Γ	A_1	A_2	E
A_1	−1		
A_2		−1	
E			1

$\langle E, [EA_1(E)A_2](E)\Gamma \mid [\Sigma E(\Gamma^{III})A_1](\Gamma^{III})A_2\Gamma\rangle$

Γ^{III} \ Γ	A_1	A_2	E
A_1		−1	
A_2	1		
E			−1

Alle anderen in den Rechnungen auftretenden Racah-Koeffizienten obigen Typs sind 1.

2. *Tabellen der in den Rechnungen auftretenden Racah-Koeffizienten*

$$\langle S_1,S_2S_3(S^I)S \mid S_1S_2(S^{II})S_3S\rangle$$

und

$$\langle S_1,[S_2S_3(S^I)S_4](S^{II})S \mid [S_1S_2(S^{III})S_3](S^{IV})S_4S\rangle$$

$\langle 1/2,\ 1/2\ 1/2(S^I)1/2 \mid 1/2\ 1/2(S^{II})1/2\ 1/2\rangle$

		1
0	$-1/2$	$\sqrt{3/2}$
1	$\sqrt{3/2}$	$1/2$

$\langle 1,\ 1/2\ 1/2(S^I)1 \mid 1\ 1/2(S^{II})1/2\ 1\rangle$

S^{II} \ S^I	0	1
1/2	$-1/\sqrt{3}$	$\sqrt{2/3}$
3/2	$\sqrt{2/3}$	$1/\sqrt{3}$

$\langle 1/2,\ 1/2\ 1(S^I)1 \mid 1/2\ 1/2(S^{II})1\ 1\rangle$

S^{II} \ S_I	1/2	3/2
0	$-1/\sqrt{3}$	$\sqrt{2/3}$
1	$\sqrt{2/3}$	$1/\sqrt{3}$

$\langle 1/2,\ 1\ 1/2(S^I)1 \mid 1/2\ 1(S^{II})1/2\ 1\rangle$

S^{II} \ S^I	1/2	3/2
1/2	$-1/3$	$2/3\sqrt{2}$
3/2	$2/3\sqrt{2}$	$1/3$

$\langle 1/2,\ 1\ 1(S^I)S \mid 1/2\ 1(S^{II})1S\rangle$

S	1/2		3/2	
S^{II} \ S^I	0	1	1	2
1/2	$-1/\sqrt{3}$	$\sqrt{2/3}$	$-1/\sqrt{6}$	$\sqrt{5/6}$
3/2	$\sqrt{2/3}$	$1/\sqrt{3}$	$\sqrt{5/6}$	$1/\sqrt{6}$

$\langle 3/2\ 1/2\ 1/2(S^I)3/2 \mid 3/2\ 1/2\ (S^{II})1/2\ 3/2\rangle$

S^{II} \ S^I	0	1
1	$-1/2\sqrt{3/2}$	$1/2\sqrt{5/2}$
2	$1/2\sqrt{5/2}$	$1/2\sqrt{3/2}$

$\langle 1,\ 1\ 1/2(1/2)S \mid 1\ 1(S^{II})1/2S\rangle$

S \ S^{II}	0	1	2
1/2	$-1/\sqrt{3}$	$\sqrt{2/3}$	
3/2		$-1/\sqrt{6}$	$\sqrt{5/6}$

$\langle 1/2,[1/2\ 1/2(S^I)1/2](S^{II})S \mid [1/2\ 1/2(0)1/2](1/2)1/2S\rangle$

S	0		1	
S^{II} \ S_I	0	1	0	1
1/2	$-1/2$	$\sqrt{3/2}$	$-1/2$	$-1/2\sqrt{3}$
3/2				$\sqrt{2/3}$

$\langle 1/2,[1/2\ 1/2(S^{I})1/2](S^{II})S \mid [1/2\ 1/2(1)1/2](S^{IV})1/2S\rangle$

S	0		1			
S^{IV}	1/2		1/2		3/2	
S^{II} \ S^{I}	0	1	0	1	0	1
1/2	$\sqrt{3}/2$	1/2	$\sqrt{3}/2$	$-1/6$	0	$2\sqrt{2}/3$
3/2				$\sqrt{2}/3$		1/3

$\langle 1/2,[1/2\ 0(1/2)1/2](S^{II})1/2 \mid [1/2\ 1/2(S^{III})0](S^{II})\ 1/2\ 1/2\rangle$

S^{III} \ S^{II}	0	1
0	$-1/2$	$\sqrt{3}/2$
1	$\sqrt{3}/2$	1/2

$\langle 1/2,[1/2\ 1(S^{I})1/2](S^{II})S \mid [1/2\ 1/2(0)1](1)1/2S\rangle$

S	1/2		3/2	
S^{II} \ S^{I}	1/2	3/2	1/2	3/2
0	$-1/2$			
1	$-1/2\sqrt{3}$	$\sqrt{2/3}$	$-1/\sqrt{3}$	$-1/2$ $1/\sqrt{6}$
2				$1/2$ $\sqrt{5/2}$

$\langle 1/2,[1/2\ 1/2(S^{I})0](S^{I})1/?\ '\ [1/2\ 1/2(S^{III})1/2](1/2)0\ 1/2\rangle$

S^{III} \ S^{I}	0	1
0	$-1/2$	$\sqrt{3/2}$
1	$\sqrt{3/2}$	1/2

$\langle 1/2,[1/2\ 1/2(S^{I})1](S^{II}T)S \mid [1/2\ 1/2(0)1/2](1/2)1S\rangle$

S	1/2		3/2	
S^{II} \ S^{I}	0	1	0	1
0		$-1/2$		
1	$-1/2$	$1/\sqrt{2}$	$-1/2$	$-1/2\sqrt{2}$
2				$1/2\sqrt{5/2}$

$\langle 1/2,[1/2\ 1/2(S^{I})1](S^{II})S \mid [1/2\ 1/2(1)1/2](S^{IV})1S\rangle$

S	1/2				3/2			
S^{IV}	1/2		3/2		1/2		3/2	
S^{II} \ S^{I}	0	1	0	1	0	1	0	1
0		$-1/2\sqrt{3}$		$\sqrt{2/3}$				
1	$\sqrt{3}/2$	$1/\sqrt{6}$	0	$1/\sqrt{3}$	$\sqrt{3}/2$	$-1/2\sqrt{6}$	0	$\sqrt{5/6}$
2						$1/2\sqrt{5/6}$		$1/\sqrt{6}$

$\langle 1/2[0\ 1/2(1/2)\ 1/2](S^{II})1/2 \mid [1/2\ 0(1/2)1/2](S^{IV})1/2\ 1/2\rangle$

S^{IV} \ S^{II}	0	1
0	$-1/2$	$\sqrt{3}/2$
1	$\sqrt{3}/2$	$1/2$

$\langle 1/2, [1\ 1/2(S^{I})1/2](S^{II})S \mid [1/2\ 1(1/2)1/2](S^{IV})1/2S\rangle$

S	1/2				3/2	
S^{IV}	0		1		1	
S_{II} \ S_I	1/2	3/2	1/2	3/2	1/2	3/2
0	$-1/2$		$-1/2\sqrt{3}$			
1	$\sqrt{3}/2$	0	$-1/6$	$2\sqrt{2}/3$	$-1/3$	$-1/3\sqrt{2}$
2						$\sqrt{5/6}$

Alle anderen in den Rechnungen auftretenden Racah-Koeffizienten obigen Typs sind 1.

Herrn Professor Dr. Dr. K. SCHWABE danke ich herzlich für seine ständigen Bemühungen um den Fortgang der Arbeit.

LITERATUR

1. CONDON, E. U., SHORTLEY, G. H.: The Theory of Atomic Spectra, 3. Auflage, Cambridge University Press, 1953
2. GILDE, F. J., BAN, M. I.: Acta Phys. Hung. **12**, 13 (1960)
3. OTSUKA, J.: J. Phys. Soc. Japan **21**, 596 (1966)
4. RACAH, G.: Phys. Rev. **62**, 438 (1942)
   ibid. **63**, 367 (1943)
5. TANABE, Y., KAMIMURA, H.: J. Phys. Soc. Japan **13**, 394 (1958)
6. TANABE, Y., SUGANO, S.: J. Phys. Soc. Japan **9**, 753 (1954)
   ibid. **9**, 766 (1954).

Hans KAMMER; 8027 Dresden, Bergstraße 66c, DDR.

Acta Chimica Academiae Scientiarum Hungaricae, Tomus 66 (2), pp. 203—207 (1970)

d^N-ELEKTRONENSYSTEME IN TRIGONALEN LIGANDENFELDERN, II

INTERPRETATION DER SPEKTREN VON V^{3+}- UND Cr^{3+}-IONEN

H. KAMMER

(Bereich Physikalische Chemie, Sektion Chemie der Technischen Universität Dresden)

Eingegangen am 19. April 1969

Die in I. erhaltenen Säkulardeterminanten für das d^2- und d^3-System werden unter bestimmten Voraussetzungen gelöst und die erhaltenen Ergebnisse mit denen aus gemessenen Absorptionsspektren für V^{3+}- und Cr^{3+}-Ionen in trigonaler Umgebung verglichen.

Einleitung

Die in I. dargestellte Theorie soll mit einigen für d^2- und d^3-Systeme erhaltenen experimentellen Ergebnissen verglichen werden. Dazu muß zunächst etwas über die in der Theorie auftretenden Ligandenfeldparameter D, E, F und die Elektronenwechselwirkungsparameter B, C gesagt werden.

Die Parameter

Im kubischen Ligandenfeld tritt neben den Racah-Parametern nur der Parameter D auf. Bei trigonaler Verzerrung erscheinen zusätzlich die Parameter E und F. Im folgenden wird angenommen, daß sich die Racahparameter und D in oktaedrischer und trigonaler Symmetrie nicht unterscheiden. Für F/E erhält man (vgl. I)

$$\frac{F}{E} = \frac{9}{5} \frac{\overline{r_<^2}}{r_>^3} \Big/ \frac{\overline{r_<^4}}{r_>^5} \equiv \frac{9}{5} Q .$$

E und Q werden durch Vergleich mit dem Experiment bestimmt.

In der Literatur werden die trigonalen Parameter verschieden bezeichnet: v, v' [6], K, K' [7], Ds, Dt [4], $D\sigma$, $D\tau$ [2]. E und F hängen wie folgt mit diesen Parametern zusammen:

$$F = -Ds = D\sigma \qquad E = 5\,Dt = \frac{5}{3} D\tau$$

$$K = -\frac{1}{3} v = -F - \frac{4}{3} E \qquad K' = v' = \sqrt{2}(F - E)$$

V^{3+}-Ion in trigonaler Umgebung

GRIFFITH [1] gibt für den Vanadiumoxalat-Komplex $D = 17\,800$ und $B = 550\ cm^{-1}$ an. Weiterhin wird hier $C = 5B$ gesetzt. PIPER und CARLIN [4] haben Q für V^{3+} unter Zugrundelegung verschiedener Abstände R Ligand-Zentralion mit Hartree—Fock-Funktionen berechnet und Werte zwischen 2 und 5 erhalten.

Aus dem von PIPER und CARLIN [5] für den Vanadiumtrisoxalat-Komplex gemessenen Spektrum konnte für $E = 65\ cm^{-1}$ und $Q = 1$ entnommen werden. Man erhält also $F = 1{,}8\ E$. Es folgt damit $K = -200\ cm^{-1}$ in relativ guter Übereinstimmung mit dem von PIPER und CARLIN [5] ermittelten Wert $K = -230\ cm^{-1}$.

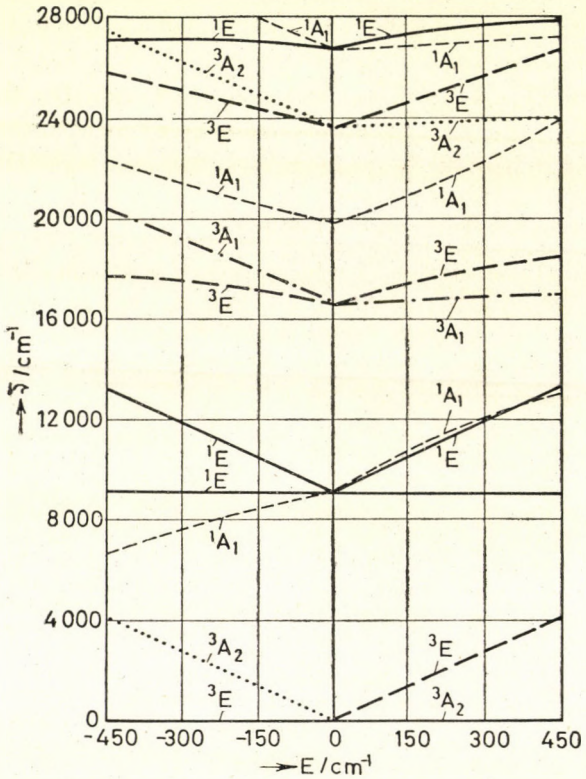

Abb. 1. Termdiagramm für die Konfiguration d^2 in trigonaler Symmetrie. Parameter: $B = 550\ cm^{-1}$; $C = 5B$; $D = 17\,800\ cm^{-1}$; $F = 1{,}8\ E$

Abb. 1 zeigt die Terme für V^{3+} in trigonaler Symmetrie, die berechnet wurden mit den oben angegebenen Werten für D, B, C, F und E im Bereich zwischen -450 und $+450\ cm^{-1}$. In diesem Bereich ist $\frac{8(F-E)^2}{(D-E+F)^2} \leq$

$\leq 3 \cdot 10^{-3}$. Für $E > 0$ ist $^3A_2$ und für $E < 0$ ^3E Grundzustand. Wegen des Jahn—Teller-Theorems müßte also die trigonale Verzerrung unter den vorliegenden Bedingungen immer zu einem gestreckten Oktaeder (E, $F > 0$) führen.

In Tabelle I sind die von PIPER und CARLIN [5] gemessenen mit den berechneten Werten (für $E = 65$ und $100\ cm^{-1}$) zusammengestellt. Alle Terme, die mehr als $28\,000\ cm^{-1}$ über dem $^3A_2$-Grundzustand liegen, sind nicht in Tabelle I aufgeführt. σ und π beziehen sich auf die Polarisationsrichtung des zur Untersuchung verwendeten Lichtes (vgl. [5]).

Für $E = 100\ cm^{-1}$ und $Q = 1$ ist $K = -310\ cm^{-1}$.

Aus Abb. 1 können auch einige Angaben über den Vanadiumtrisacetylacetonat-Komplex entnommen werden. Es muß aber darauf hingewiesen werden, daß in solchen Komplexen mit Sicherheit kovalente Effekte auftreten, die von dem hier zugrundegelegten Ionenmodell nicht erfaßt werden. Die ermittelten Termlagen können daher durch diese Einflüsse beträchtlich verschoben werden. Wir nehmen an, daß sich die Parameter B, C, D und Q für trigonale Oxalat- und Acetylacetonat-Umgebung nicht unterscheiden. PIPER und CARLIN [5] geben für V $(acac)_3 K \approx -900\ cm^{-1}$ an. Daraus folgt $E \approx$

Tabelle I

Gemessene [5] *und berechnete Termlagen für V^{3+} in trigonaler Oxalatumgebung*

Parameter: $D = 17\,800$, $B = 550$, $C = 5B$, $F = 1{,}8E$.
(Alle Zahlenangaben in cm^{-1})

Term	Gemessen	Berechnet	
		$E = 65$	$E = 100$
^3E		610	930
^1E		9 090	9 100
^1E	9 615 σ	9 740	10 070
$^1A_1$		9 840	10 230
$^3A_1$	16 670 σ	16 670	16 700
^3E	17 230 π	16 970	17 140
$^1A_1$	20 480 τ	20 290	20 540
$^3A_2$	23 500 π	23 740	23 760
^3E		24 060	24 270
$^1A_1$	26 300 π	26 790	26 820
^1E		27 040	27 170

Tabelle II

Berechnete Termlagen für V $(acac)_3$

Parameter: vgl. Tab. I, $E = +300$. (Alle Zahlenangaben in cm^{-1})

^3E	^1E	^1E	$^1A_1$	$^3A_1$	^3E	$^1A_1$	$^3A_2$	^3E	$^1A_1$
2790	9100	11 940	12 080	16 850	18 000	22 300	23 920	25 620	27 040

$\approx +300\ cm^{-1}$. Damit würden sich die in Tabelle II angegebenen Termlagen ergeben.

Man sieht, daß der Energieunterschied zwischen den Folgetermen $^3A_1$ und ^3E des $^3T_{2g}$-Terms wesentlich größer ist als im Falle des Oxalats und daß die Termlagen nach größeren Wellenzahlen hin verschoben sind.

Cr^{3+}-Ion in trigonaler Umgebung

Zur Interpretation des von PIPER und CARLIN gemessenen Spektrums des Chromoxalat-Komplexes wurden folgende Parameterwerte den Rechnungen zugrundegelegt: $B = 620\ cm^{-1}$, $D = 17\,500\ cm^{-1}$ und $C = 5B$ (vgl. [1]). Außerdem wurden verschiedene Sätze von E- und F-Werten gewählt: *a)* Dem gemessenen Spektrum entnimmt man $E = -50$ und $F_1 = -230\ cm^{-1}$; *b)* wählt man $Q = 1$, ergibt sich $E = -230\ cm^{-1}$ und $F = 1{,}8\ E$; *c)* für $Q \approx$ $\approx 10{,}5$ folgt $E = -10$ und $F = -190\ cm^{-1}$. In allen drei Fällen ist $\frac{8(F-E)^2}{(D-E+F)^2} \approx 10^{-3}$.

Tabelle III

Gemessene [5] *und berechnete Termlagen für* Cr^{3+} *in trigonaler Oxalatumgebung*

Gewählte Parameterwerte siehe im Text. (Alle Zahlenangaben in cm^{-1})

Term	Gemessen	Berechnet		
		a)	*b)*	*c)*
$^2E(^2E_g)$	14 455 14 476	13 877	13 479	13 915
$^2E(^2T_{1g})$	15 216	14 437	14 373	14 450
$^2A_2(^2T_{1g})$	15 284 15 323	14 498	14 506	14 497
$^4A_1(^4T_{2g})$	17 316 π	17 316	17 316	17 316
$^4E(^4T_{2g})$	17 620 σ	17 736	18 228	17 632
$^2A_1(^2T_{2g})$	20 555	21 127	21 172	21 116
$^2E(^2T_{2g})$	20 704 21 119	21 241	21 767	21 172
$^4A_2(^4T_{1g})$		23 681	23 676	23 681
$^4E(^4T_{1g})$	23 670 σ	24 188	25 000	24 054

Man erhält aus diesen E- und F-Werten die folgenden Werte für K: *a)* $K = 300\ cm^{-1}$, *b)* $K = 720\ cm^{-1}$, *c)* $K = 200\ cm^{-1}$. Erwartungsgemäß stimmt $K_{a)}$ am besten mit dem von PIPER und CARLIN [5] aus dem Spektrum gewonnenen Wert $K = 270\ cm^{-1}$ überein.

Tabelle IV

Vergleich des in [3] *gemessenen und berechneten Absorptionsspektrums von cis—Cr $(CN)_3$ $(H_2O)_3$ mit dem nach der strong-field-Approximation berechneten.*

Parameter: $B = 575$, $C = 5{,}25B$, $D = 21\,400$, $E = 170$, $F = 1{,}8E$.
(Alle Zahlenangaben in cm^{-1})

Term	Gemessen [3]	Berechnet	
		weak-field-App. [3]	strong-field-App.
$^2E(^2E_g)$	13 870	13 250	13 230
$^2E(^2T_{1g})$	14 545	13 825	13 846
$^2A_2(^2T_{1g})$		13 950	13 936
$^4E(^4T_{1g})$	21 433	20 662	20 753
$^2A_1(^2T_{2g})$			20 833
$^2E(^2T_{2g})$			21 141
$^4A_1(^4T_{2g})$		21 536	21 536
$^4E(^4T_{1g})$	27 624	27 062	27 158
$^4A_2(^4T_{1g})$		27 633	27 738

In Tabelle III sind die von PIPER und CARLIN [5] gemessenen und die hier berechneten Termlagen aufgeführt. Die bei den Dubletts auftretenden geringen Aufspaltungen werden durch Spin-Bahn-Kopplung hervorgerufen.

Von PERUMAREDDI *et al.* [3] wurden das Absorptionsspektrum von *cis*-$Cr(CN)_3(H_2O)_3$ gemessen und die Termlagen mit Hilfe einer weak-field-Approximation bestimmt. Unter Verwendung der in [3] angegebenen Parameter liefert die hier durchgeführte strong-field-Approximation die in Tabelle IV zusammengestellten Ergebnisse. Man sieht, daß die Resultate beider Näherungen gut übereinstimmen.

*

Herrn Professor Dr. Dr. K. SCHWABE danke ich herzlich für seine ständigen Bemühungen um den Fortgang der Arbeit.

LITERATUR

1. GRIFFITH, J. S.: The Theory of Transition-Metal Ions. Cambridge, 1961
2. PERUMAREDDI, J. R.: J. Phys. Chem. **71**, 3155 (1967)
3. PERUMAREDDI, J. R., *et al.*: Inorg. Chem. **6**, 1338 (1967)
4. PIPER, T. S., CARLIN, R. L.: J. Chem. Phys. **33**, 1208 (1960)
5. PIPER, T. S., CARLIN, R. L.: J. Chem. Phys. **35**, 1809 (1961); Inorg. Chem. **2**, 261 (1963)
6. PRYCE, M. H. L., RUNCIMAN, W. A.: Discussions Faraday Soc. **26**, 34 (1958)
7. TANABE, Y., SUGANO, S.: J. Phys. Soc. Japan **13**, 880 (1958).

Hans KAMMER, 8027 Dresden, Bergstraße 66c. DDR.

Acta Chimica Academiae Scientiarum Hungaricae, Tomus 66 (2), pp. 209—212 (1970)

MÖSSBAUER STUDY OF SOME IRON(II) COMPLEXES IN FROZEN AQUEOUS SOLUTIONS

(SHORT COMMUNICATION)

A. VÉRTES*, K. BURGER** and L. BOGNÁR***

(Departments of Physical Chemistry and Radiology, Inorganic and Analytical Chemistry**, and Minerology***, L. Eötvös University, Budapest)*

Received September 1, 1969

The Mössbauer parameters of some high-spin iron(II) complexes (iron(II)-oxalates, iron(II)-iminodiacetate and iron(II)-nitrilotriacetate) were measured in frozen aqueous solutions. The Mössbauer parameters provided information on the covalency of the bond between the ligands and the central iron atom.

The Mössbauer study of frozen solutions containing iron [1—4] suggested the idea that the Mössbauer parameters of the ice obtained by rapid freezing of the aqueous solutions of iron complexes forming stepwise, may furnish information also on the complexes dissolved [4, 5, 6]. High-spin iron(II) complexes seem to be suitable as model substances for these investigations, since the large quadrupole splitting characteristic of the $t_{2g}^4 e_g^2$ electron configuration is very sensitive to changes in the electron configuration of iron, and seems to be therefore a promising indicator. Unfortunately, the number of water soluble high-spin iron(II) complexes, suitable for these studies, is rather limited, which restricts the scope of these investigations. Changes in the coordination sphere of iron cause only small absolute shifts in the Mössbauer parameters of high-spin iron(III) complexes and of low-spin iron complexes, so that this circumstance limits the information which can be obtained from Mössbauer measurements on these complexes.

The present communication reports on the Mössbauer study of frozen aqueous solutions of oxalate, iminodiacetate and nitrilotriacetate complexes of iron(II).

Experimental

The apparatus described in an earlier work [7] was used for the Mössbauer measurements. The samples of the solutions were frozen by quick cooling to the temperature of liquid air (rate of cooling ~ 20 °K/s), and the measurements were undertaken immediately after freezing. Cobalt-57 isotope, diffused into stainless steel, was used as the source.

For the X-ray diffraction investigations, complementing the Mössbauer measurement, a Siemens Kristalloflex-4 diffractometer was used. (Principal data of the instrument: Fe anode 35 kV, 14 mA, manganese filter; scintillation counter 631.5 V, base line: 10 V, channel width: 10 V, attenuation 1×5, sensitivity 1×10^4 imp/min).

Chemicals used for the measurements were A. R. grade commercial products.

As starting material, the iron-57 isotope, enriched to 80 per cent was used.

The composition of the solutions investigated, together with the Mössbauer parameters are listed in Table I. The Mössbauer spectrum of iron(II)-iminodiacetate is shown in Fig. 1.

In the case of the iron oxalate system, the relatively poor solubility of sodium oxalate n water on the one hand, and the minimum quantity of iron required by the Mössbauer meth-

od on the other hand, determined the workable concentration range. Therefore, solutions of such composition that would contain only a single stepwise complex, could not be prepared. The solutions were prepared so that the $Fe(C_2O_4)_2^{2-}$ complex ion should be predominant in one case and the $Fe(C_2O_4)_3^{4-}$ complex ion in the other. The concentration of the species in the solution has been calculated with the aid of the stability constants determined by BAILAR *et al.* [8]. On the basis of our earlier investigations [1, 3, 4, 5, 6], it was assumed that in the quickly frozen solutions the complex formation equlibria are aslso 'frozen', so that from the Mössbauer parameters measured in the ice conclusions may be drawn also on the dissolved system.

From solutions 0.03 *M* with respect to iron or solutions of higher concentration, a precipitate separated on standing, even in the presence of excess $Na_2(COO)_2$. The Mössbauer investigation of this precipitate was also carried out. The precipitate was identified by X-ray diffraction.

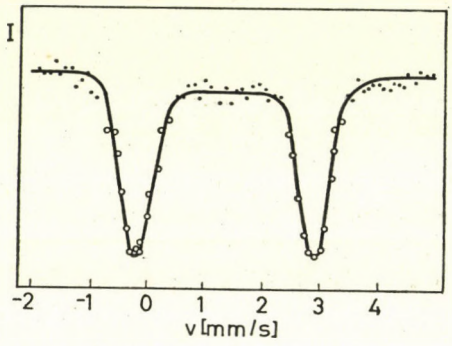

Fig. 1

Table I

Composition and Mössbauer parameters of frozen aqueous solutions containing iron(II) complexes

Iron concentration (mole/l)	Ligand concentration (mole/l)	p	Dominant complex	Isomer shift mm/s		Quadrupole splitting mm/s	
			(II)-oxalate system				
			$Fe(C_2O_4 \cdot 2H_2O$ (solid)	1.16		2.03	
0.13	0.3		$Fe(C_2O_4)_2^{2-}$	1.28		2.13	
0.03	Saturated $Na_2(C_2O_4)$ solution	6.6	$Fe(C_2O_4)_3^{4-}$ + $Fe(C_2O_4)_2^{2-}$ *	1.30	(1.28)	2.70	(2.13)
			$Fe(C_2O_4)$ precipitate	1.24		2.07	
			Iron(II)-iminodiacetate system				
0.075	2.32	8.3	$Fe(IDA)_2$	1.36		3.11	
			Iron(II)-nitrilotriacetate system				
0.031	0.83	7.25	Fe(NTA)	1.34		3.05	

* At these concentrations $Fe(C_2O_4)_3^{4-}$ and $Fe(C_2O_4)_2^{2-}$ are present simultaneously in the solution, so that a superimposed spectrum is observed.

In the investigation of the iminodiacetate (IDA) complex of iron, the pH of the solution (pH = 8.3) and the concentration of the metal and the ligand, respectively, were adjusted so as to ensure quantitative formation of the $Fe(IDA)_2$ complex.

Nitrilotriacetic acid (NTA) forms with iron(II) only a 1 : 1 metal : ligand complex. A sample prepared by freezing a solution warranting quantitative formation of this complex has been investigated.

Results and discussion

A comparison of the Mössbauer parameters of solid $FeC_2O_4 \cdot 2\ H_2O$ with the corresponding data of the frozen solutions containing the complexes $Fe(C_2O_4)_2^{2-}$ and $Fe(C_2O_4)_3^{4-}$, respectively, shows that upon increasing the oxalate content of the species investigated, the value of both the isomer shift (δ) and the quadrupole splitting (ΔE) increases. This means that the electron density at the iron nucleus decreases in the order

$$Fe(C_2O_4), > Fe(C_2O_4)_2^{2-}, > Fe(C_2O_4)_3^{4-}$$

while the electric field gradient increases along the above series. In view of the fact that with high-spin iron(II) complexes of the $t_{2g}^4 e_g^2$ electron configuration both the increase of electron density at the nucleus (diminishing δ) and the decrease of electric field gradient at the nucleus (diminishing ΔE) are indicative of an increased covalency of the iron compound, the above series of complexes formed stepwise corresponds to the order of decreasing covalency of their coordinate bond.

The Mössbauer parameters of the precipitate formed during standing from solutions containing iron oxalate complexes, were approximately the same as the corresponding data of crystalline $Fe(C_2O_4) \cdot 2\ H_2O$. The two substances were investigated also by X-ray analysis. According to these investigations, the X-ray diffraction pattern of $Fe(C_2O_4) \cdot 2\ H_2O$ could be identified with the rhombic crystal structure listed on the ASTM card No. 14-703 (Table II, column 1).

The X-ray diffraction pattern of the precipitate separating from the solution shows a lower degree of order (Table II, column 2), but essentially, it represents a similar structure. Derivatographic studies of the latter substance show that it contains water of crystallization in excess of two molecules ($\sim$2.5).

The Mössbauer parameters of the iminodiacetate and the nitrilotriacetate complexes were the same within experimental errors, which indicates the similarity of their coordination sphere, or with other words, the same electron configuration of iron in the two complexes.

Table II

X-ray diffraction data

(1 — Data for $Fe(C_2O_4)\cdot 2H_2O$; 2 — Data for the precipitate separating from iron oxalate solutions)

1 dÅ	I/I_0	2 dÅ	I/I_0	ASTM 14-703 dÅ	ASTM 14-703 I/I_0
5.35	5				
4.78	100	4.83	100	4.75	100
3.900	22	3.869	25	3.83	25
3.602	27	3.698	3	3.58	25
3.325	2	3.600	2		
3.186	4	3.491	2		
3.007	50	3.098	28	2.98	35
2.938	2	2.984	5		
2.791	2	2.811	4		
2.659	25				
2.623	20	2.613	16	2.61	35
2.402	2	2.379	5		
2.359	2				
2.269	10	2.262	2	2.23	5
2.231	2				
2.127	8	2.123	9	2.09	6
2.027	11	2.004	8	2.02	6
1.953	10				
1.934	8			1.936	
1.897	11	1.890	9	1.87	6
1.819	16	1.820	3	1.81	12

REFERENCES

1. Dézsi, I., Keszthely, L., Pócs, L., Korecz, L.: Phys. Letters **14**, 14 (1965)
2. Dézsi, I., Keszthely, L., Molnár, B., Pócs, L.: Phys. Letters **18**, 28 (1965)
3. Nozik, A. K., Kaplan, M.: J. Chem. Phys. **47**, 2960 (1967)
4. Vértes, A.: Magy. Kém. Foly. **75**, 175 (1969); Acta Chim. Acad. Sci. Hung. (In the press
5. Burger, K., Vértes, A. N., Czakó, I.: Magy. Kém. Foly. **75**, 257 (1969)
6. Vértes, A., Dézsi, I., Suba, M.: Acta Chim. Acad. Sci. Hung. (In the press)
7. Soós, J., Vértes, A.: Magy. Kém. Lapja **23**, 690 (1968)
8. Schapp, W. B., Laitiene, H. A., Bailar, J. C.: J. Am. Chem. Soc. **76**, 5868 (1954).

Attila Vértes
Kálmán Burger
László Bognár
Budapest VIII., Múzeum krt. 4—6.

Acta Chimica Academiae Scientiarum Hungaricae, Tomus 66 (2), pp. 213—227 (1970)

MECHANISM OF THE ACID HYDROLYSIS OF SACCHAROSE AND RAFFINOSE*

J. SZEJTLI,** R. D. HENRIQUES and M. CASTIÑEIRA

(Escuela de Bioquímica-Farmacéutica, Universidad de la Habana, Cuba)

Received May 30, 1969

Raffinose can be regarded as a saccharose molecule in which a galactose is attached to the glucose unit. Therefore a comparative study of the acid hydrolysis of raffinose and saccharose may furnish important conclusions concerning the mechanism of the reaction. A specific feature of saccharose is that essentially two glycosidic components are linked together by the bridge oxygen atom, without any nonsugar (aglycone) component being present.

According to our determinations, in dilute carbohydrate solutions in the range of 0.001—1.0 N HCl, the rate constant of the hydrolysis of saccharose is as follows: $\log k = 1.038 \cdot \mathrm{pH} + 16.754 - 0.4343 \cdot 25541/1.987 \cdot T$.

The rate of splitting of the glucosyl-fructosyl bond in raffinose is lower by about 19%, and that for the galactosyl-glucose bond is lower by about three orders of magnitude.

The conclusion that can be drawn from the experimental facts is that, in contrast to the general case, proton addition in saccharose does not take place to the bridge oxygen atom, but to the ring-oxygen atom of the furanose ring. As a consequence, splitting of the glycosidic linkage does not involve the formation of a pyranosyl carbonium cation; instead of this, a furanosyl cation is produced. The furanose ring by itself does not explain the rapid hydrolysis of saccharose, since turanose, from which a tertiary cation cannot be formed, is much more stable than saccharose. On the other hand, the possibility of the formation of a tertiary cation, in other cases, also causes a great velocity of hydrolysis. The entropy of activation (+8.07 e.u. for saccharose and +8.34 e.u. for raffinose) points to an A-1 mechanism.

Introduction

The acid hydrolysis of saccharose is a classical example of reactions of first order as well as of catalysis in homogeneous phase. The importance of this reaction need not be emphasized; among all disaccharides, saccharose is produced in the greatest amounts, and it is the most sensitive against acids.

WILHELMY [49] was the first to study the acid hydrolysis of saccharose; this process is called generally 'inversion' because, as a consequence of hydrolysis, the optical rotation is reversed. Since then, a great deal of research has been devoted to this reaction; full elucidation of the mechanism, however, has not been achieved. Few and controversial data are available for the entropy of activation [10, 44]. Only a few publications deal with the acid hydrolysis of raffinose [43], rate constants have been published only by one author [31],

* The present paper is a part of a series; the previous part has been published in Acta Chim. Acad. Sci. Hung. **56**, 175 (1968)

** Present address: Chinoin Pharmaceutical and Chemical Works Ltd., Budapest

and this does not allow to draw conclusions concerning the mechanism of acid hydrolysis of the glucopyranosyl–fructofuranosyl linkages. A comparison of the hydrolysis of saccharose (in the following = SA) with that of raffinose (in the following = RAF) permits the investigation of the fission of the glycosidic linkage of a non-reducing end-group (fructose = F), when it is bound to a monosaccharide (glucose = G) and a disaccharide (melibiose = Ga-G), respectively.

The first step in the acid hydrolysis of pyranosides is the formation of a conjugated acid, followed by a change of the conformation of the pyranoside ring [14, 17].

The conversion of the C1 conformation of the pyranoid ring to half-chair form is the precondition of the formation of a planar carbonium cation. The bulkier the substituents on the pyranoid ring, the more difficult is this conformational change, *i.e.* the more slowly will hydrolysis take place [15, 42]. RAF may be considered as a SA molecule which contains a galactosyl substisuent attached to the C_4 atom of its glucopyranoside ring. If the glucopyranotyl moiety controls the process of hydrolysis, as it is common in most cases [38], the galactosyl substituent has to decelerate the hydrolysis. If the fructofuranosyl moiety determines the rate of hydrolysis, the difference between the rates of hydrolysis of SA and RAF must be rather small, however, in this case there are again two possibilities. The first is that the entropy of activation is negative, as in the case of alkyl aldofuranosides; *i.e.* the reaction is of A-2 type. The other possibility is that the ΔS^+ is positive, *i.e.* the reaction is of type A-1; in this case the extraordinary sensitivity to acids of the G—F bond requires an explanation.

The aim of the present work was to clarify these problems.

Experimental

Materials: Saccharose (sucrose), p. a., and raffinose, p. a., $[\alpha]_D^{20} = +102—104°$ ($c = 4$, in water), were used.

Hydrolysis: 500 mg of SA or 750 mg of RAF was dissolved in 25 ml of water which had been warmed to the temperature of the proposed hydrolysis; 25 ml of HCl of the same temperature and appropriate concentration (2.12; 0.212; 0.0212; or 0.00212 *N*) was added and the solution was let to stand in an ultrathermostate. 2 ml samples were withdrawn at regular intervals, and they were mixed with 2 ml of 1.2 or 0.12 *N* LiOH. (To avoid volume discrepancies caused by temperature differences, the 2 ml samples of LiOH solutions were pipetted into the test tubes at the temperature of the hydrolysis). In every experiment 19 samples were taken. The residual solution (12 ml) was then heated in a boiling water bath for 30 min. (in cases of low acid concentrations 1 drop of cc. HCl was added); in the 20th sample withdrawn after this procedure, the splitting of the glucopyranosyl-fructofuranosyl linkage was complete.

Analysis: As a rather small difference was expected between the rates of hydrolysis of SA and RAF (or strictly speaking: between the rates of formation of F from SA and from RAF, since only half of the hydrolysis of RAF — its splitting to F and of melibiose — was studied), the application of polarimetry, which is the most frequently used — and most convenient — method in similar investigations has been disregarded. The limit value of the optical rotation may considerably influence the value of k, as it has been pointed out by MANTOVANI

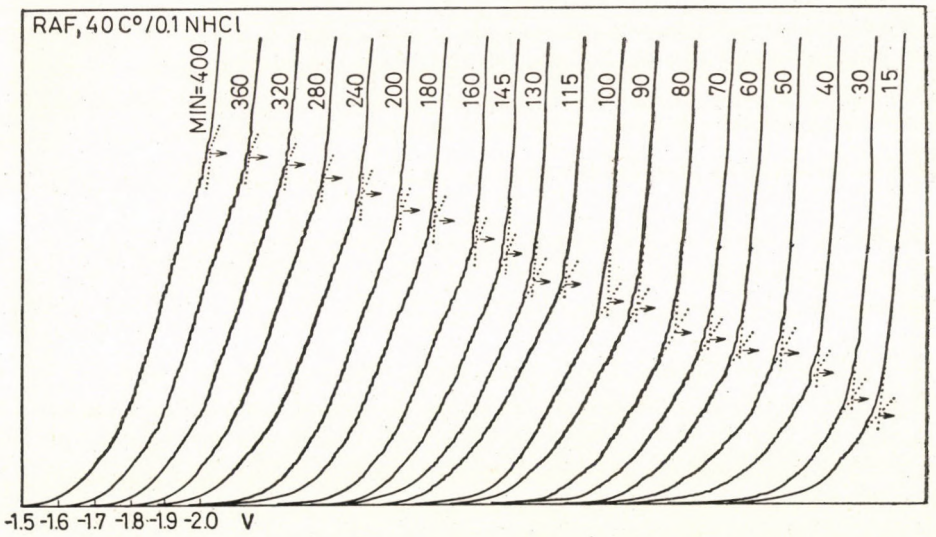

Fig. 1. Polarographic curves of raffinose hydrolyzates. Hydrolysis at 40 °C; 750 mg raffinose/ /50 ml 0.106 *N* HCl. The samples were taken after 15, 30, 40, etc. minutes, as indicated beside the curves. Polarograph: LP-60; sensitivity: 1/100; damping = 2, 200 mV and 40 mm paper/ min. Abscissa: voltage; recording from —1.5 V; the second, third, fourth, etc. curves are displaced by distances corresponding to 0.1, 0.2, 0.3, etc. V. Ordinate: intensity of current passing through the cell (in mm)

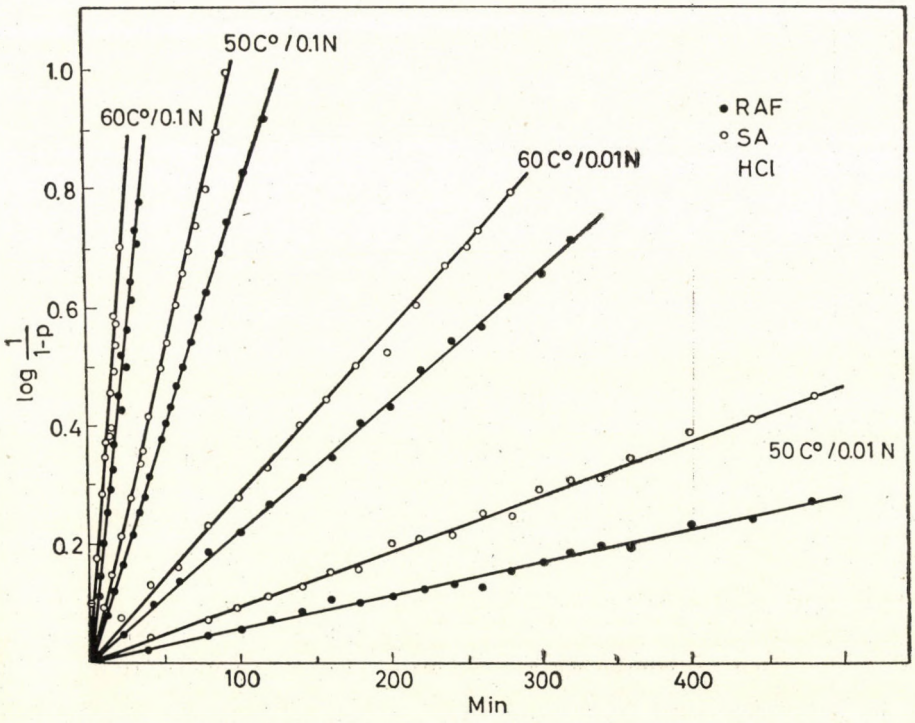

Fig. 2. Logarithmic hydrolysis curves, from polarographic measurements

and INDELLI [30]. In case of SA it does not mean a problem, but in a partial hydrolyzate of RAF F may be accompanied by G, Ga (= galactose), Ga-G (= melibiose), and some SA, therefore the correlation between the optical rotation and the concentration of F is not unambiguous. Thus, a polarographic method has been applied, which is selective for fructose [12]. To check the results of the polarographic determinations, and to detect occasional hydrolysis of the other (Ga-G) linkage of RAF, the reducing power has also been determined simultaneously with the polarographic determinations.

0.5 ml of the neutralized hydrolyzate (from 2 ml sample + 2 ml LiOH) and 4 ml of 0.12 *N* LiOH (from a solution of 7.5 mg gelatine in 100 ml 0.12 *N* LiOH) was placed into a polarographic cell. After passing N_2 through the solution, the polarogram was recorded from

Table I

Rate constants and entropies of activation

t, °C	[HCl] *N*	pH*	$k \cdot 10^3$ min^{-1}	ΔS^{+**}	$k \cdot 10^3$ min^{-1}	ΔS^{+**}	Determined by P = polarography; F = photometry
			Saccharose		Raffinose		
30.0	0.106	1.040	1.78	8.44	1.35	8.54	P
			1.78	8.44	1.42	8.68	F
	1.06	—0.087	20.4	7.94	16.0	8.52	P
			19.2	7.82	16.5	8.54	F
40.0	0.0106	2.011	0.582	8.04	0.486	8.35	P
			0.541	7.90	0.449	8.19	F
	0.106	1.040	7.21	8.43	6.17	8.79	P
			7.12	8.41	6.17	8.79	F
	1.06	—0.087	100.4	8.36	78.4	8.86	P
			85.0	8.69	72.7	8.71	F
50.0	0.00106	2.986	0.198	7.92	0.155	8.07	P
			0.194	7.87	0.159	8.12	F
	0.0106	2.011	2.17	8.04	1.57	8.05	P
			2.21	8.08	1.84	8.36	F
	0.106	1.040	23.5	8.16	17.6	8.24	P
			21.7	8.00	17.5	8.23	F
60.0	0.00106	2.986	0.625	7.74	0.544	8.09	P
			0.608	7.68	0.523	8.01	F
	0.0106	2.011	6.52	7.76	5.20	7.94	P
			8.05	8.19	6.75	8.46	F
	0.106	1.040	69.0	7.84	51.6	7.89	P
			68.8	7.84	57.5	8.11	F
Average:				8.07 ± 0.057		8.34 ± 0.061	

* = pH calculated as follows:

if [HCl] < 0.2 *N* pH = $0.091 - 0.973 \cdot \log$ [HCl]

if $1{,}2 >$ [HCl] > 0.2 *N* pH = $-0.058 - 1.170 \cdot \log$ [HCl]

$$** = \Delta S^+ = 1.987 \cdot 2.303 \cdot \left[\log k_r - \log\left(60 \cdot 2.0842 \cdot 10^{10} \cdot T \cdot e^{-\frac{E_a - RT}{RT}}\right)\right]$$

—1.5 V on. A series of such polarograms is illustrated in Fig. 1. The extrapolated intersections and a calibration curve were used to calculate the amount of F in the sample. The value of k was calculated as follows: $k = \frac{2.3}{\tau} \log \frac{1}{1-p}$, where τ is the time in min., and p denotes the relation of fructose concentrations measured at time τ and in the 20th sample. Fig. 2 shows the $\log(1/1-p)$ values as a function of τ for some experiments.

In order to determine the reducing power, 1 ml of neutralized hydrolyzate was mixed with 9 ml of 0.05 N $NaHCO_3$, then 2 or 5 ml of this solution was completed to 10 ml with water, and 2 ml of Somogyi—Nelson A—B solution [35] was added. After mixing it was kept for 20 min. in a boiling water-bath; after cooling 2 ml of Somogyi—Nelson C solution was added, the volume completed to 50 ml with water, and the optical density was determined at 500 mμ in a 1 cm cuvette. The extent of hydrolysis was calculated by means of a calibration curve constructed for invert sugar, and k was calculated as above. The Ga-G linkage in RAF hydrolyzed so slowly (its stability being higher by nearly three orders of magnitude than the stability of the G-F linkage) that the value of k calculated from samples 1—19 on the basis of the reducing power was practically the same as the one calculated from the polarographic results; a considerable amount of galactose was only detected in the 20th sample; therefore, in this case the reducing power, which is expectable after 100% hydrolysis of the G–F linkages, was calculated on the basis of the theoretical amount of SA in the RAF.

The rate constants determined at different temperatures and acid concentrations are shown in Table I. The differences between the polarographic and photometric results are within the limits of experimental error.

Effect of acid concentration

The increase of rate constant in hydrochloric acid is a little faster than the increase of the acid concentration, as it is illustrated in Fig. 3. HAMMETT and PAUL [19], studying the hydrolysis of saccharose in aqueous solutions of strong mineral acids, stated that the correlation between $\log k$ and H_0 was linear and $\frac{\Delta \log k}{\Delta H_0} = 1.00$ for any strong mineral acid. The only deviation from

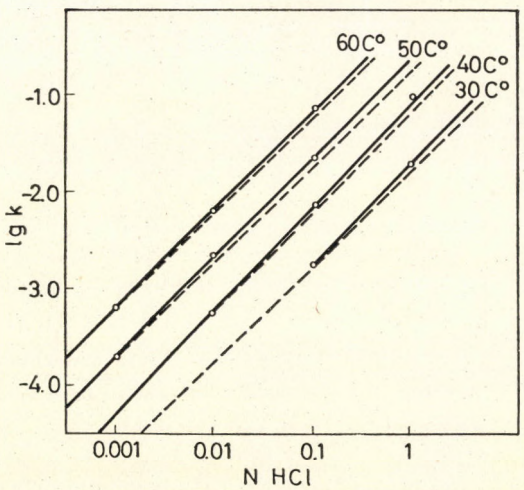

Fig. 3. Rate constants of saccharose hydrolysis determined polarographically as a function of the acid concentration. The dashed line represents the $\Delta \log k/\Delta \log HCl = 1.00$ relation; the full line connects the points determined actually

this linearity has been observed in the case of trichloroacetic acid; in this acid $\log k$ increases much faster than H_0. This may be explained by assuming the formation of a more easily hydrolyzable saccharose trichloroacetic acid ester; a more probable explanation is that the H_0-function does not hold for relatively weak organic acids [29].

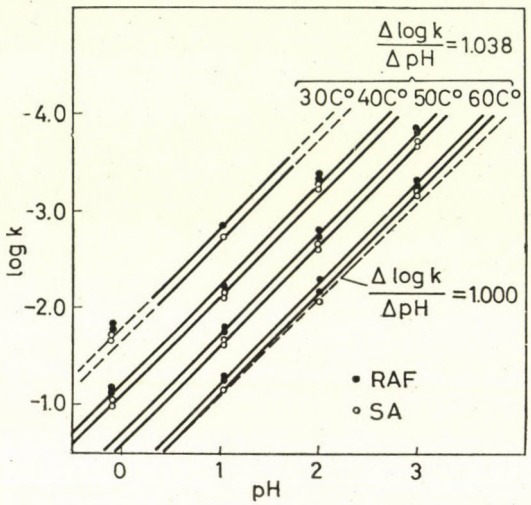

Fig. 4. Correlation of log k and the pH in the hydrolysis of saccharose and raffinose. (The deviation of the points of the 30 °C/1.06 N HCl curve from the general trend cannot be fully explained by experimental error; probably it may be attributed to secondary reactions (reversion and destruction of the formed monosaccharides) occurring more readily at higher acid concentrations)

KRIEBLE [25, 26] studying the hydrolysis at 20 °C in HCl up to 10 mole/l, in H_2SO_4 up to 6.5 mole/l, LEININGER and KILPATRICK [27] between 0 and 40 °C in HCl up to 6 mole/l, stated (or from their published data it may be seen) that the correlation between log k and H_0 is influenced to a certain extent by the temperature.

The relation between a_{H+} and k was found to be slightly exponential in some thoroughly studied cases [38, 39, 40]. As it is seen in Fig. 4, the same is true for saccharose: the correlation between log k and pH is linear, however, its slope is higher than 1.00. The $g(= \Delta \log k/\Delta \text{ pH})$ values calculated from the data of Table I are shown in Table II. It may be established that the rate constants of hydrolysis of the glucopyranosyl–fructofuranosyl linkages both SA and RAF depend on the pH as follows [38, 40]:

$$k = k_r \cdot (a_{H+})^g, \text{ i.e. } \log k_r = \log k + g \cdot \text{pH}$$

where k_r is the reduced rate constant, corresponding to pH = 0.

Table II

Values of g

t, °C	[HCl] *N* range	Saccharose	Raffinose	Determined by P = polarography; F = photometry
30.0	0.106—1.06	0.941	0.954	P
		0.918	0.945	F
40.0	0.0106—0.106	1.128	1.138	P
		1.150	1.170	F
	0.106—1.06	1.017	0.980	P
		0.956	0.954	F
50.0	0.00106—0.0106	1.063	1.031	P
		1.082	1.082	F
	0.0106—0.106	1.065	1.081	P
		1.021	1.008	F
60.0	0.00106—0.0106	1.042	1.005	P
		1.150	1.139	F
	0.0106—0.106	1.041	1.026	P
		0.960	0.960	F
	Average:	1.038±0.013	1.033±0.019	

The effect of temperature

The relation between $\log k$ and $1/T$ is illustrated in Fig. 5. The E_a and d values calculated from Table I are shown in Table III. On the basis of this data, k in diluted saccharose solutions and in 0.001—1.0 N HCl may be calculated as follows:

$$\log k = 1.038 \cdot \mathrm{pH} + 16.754 - 0.4343 \cdot 25541/1.987 \cdot T.$$

Controversial data have been reported concerning the temperature-dependence of this reaction. According to LEININGER and KILPATRICK [27], *e.g.*, an increase in both the temperature and acid concentration results in a decrease of E_a. The value of $\Delta E_a/\Delta T$ is about −70 cal/°C at 10 °C, but it decreases at higher temperatures. According to MOELWYN-HUGHES [32], in a 5% saccharose solution at 33.6 °C this value is −94 cal/°C. It is emphasized that this is an apparent value, which may be explained by the temperature-dependence of the dissociation of mineral acids, or their apparent activity in catalyzing the hydrolysis.

According to other authors, E_a has a constant value. In order to clarify this problem, VUKOV [47] made a statistical study of the accessible data. His

compilation, completed by us with further data, resulted in $E_a = 25.55 \pm$ $\pm$ 0.26 kcal/mole, which is an average of the values given by numerous authors [1—8, 11, 16, 20, 22—24, 27, 28, 31, 36, 37, 44, 46, 51, 52]. The agreement with the E_a value of Table III is excellent.

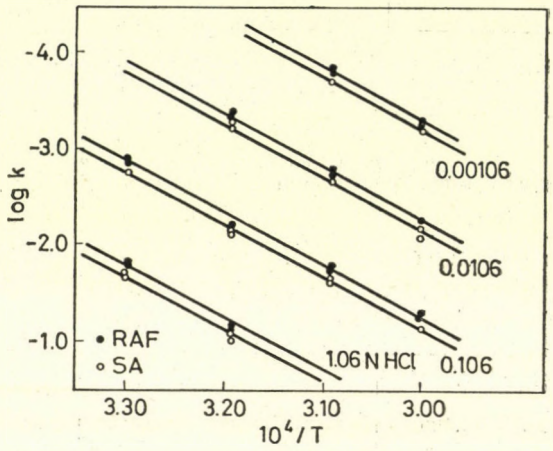

Fig. 5. Correlation of log k and $1/T$ in the hydrolysis of saccharose and raffinose

Table III

Determination of E_a and d

[HCl] N	t, °C	Saccharose		Raffinose		Determined by P = polarography; F = photometry
		E_a, kcal/mole	d	E_a, kcal/mole	d	
1.06	30—40	30.008	19.894	29.922	19.806	P
		28.057	18.457	27.927	18.379	F
0.106	30—40	26.366	17.372	28.621	18.881	P
		26.106	17.184	27.667	18.214	F
	40—50	23.755	15.516	21.115	13.605	P
		22.412	14.572	20.977	13.508	F
	50—60	23.072	15.053	23.023	14.895	P
		24.748	16.152	25.488	16.559	F
0.0106	40—50	26.441	17.304	23.569	15.301	P
		28.339	18.597	28.385	18.629	F
	50—60	23.565	15.360	25.635	16.760	P
		27.657	18.136	27.805	18.236	F
0.00106	50—60	24.600	16.033	26.917	17.600	P
		24.452	15.924	25.487	17.243	F
Average:		25.541±0.57	16.825±0.41	25.895±0.74	16.973±0.52	

An examination of values reported by various authors shows that E_a has no definite trend between 0 and 130 °C, so its value may be considered constant within this temperature range and within the limits of experimental error.

The apparent value of E_a also depends on the concentration of electrolytes and carbohydrates; the investigation of this problem was, however, beyond the scope of the present work.

Results

No significant difference has been found between the values of k calculated from the reducing power and from the polarographic curves (*cf.* the results for RAF in Table I); it may be concluded that the rupture of Ga–G bond is slower by about 3 orders of magnitude than the hydrolysis of the G–F linkage. Considering that the rate of splitting of the non-reducing end-group is the same in both cellotriose and cellobiose [18], and that the same is true for amylose and maltose, the assumption seems to be justified that the rate of rupture of the Ga–G linkages in RAF is the same as in melibiose. For the latter some data have been reported in the literature [33]; *e.g.*, at 60 °C in 1.0 N HCl the k value of melibiose is $0.775 \cdot 10^{-3}$ min $^{-1}$, while under the same conditions k for the rupture of the G–F bond in RAF is 0.74; thus the hydrolysis of the G–F bond is $0.74/0.775 \cdot 10^{-3} = 955$ times faster than that of Ga–G linkage.

It is very probable that the hydrolysis of the Ga–G linkage occurs by A-1 mechanism, as it is generally accepted for pyranosides. In principle, the complete hydrolysis of RAF may consist of four reactions:

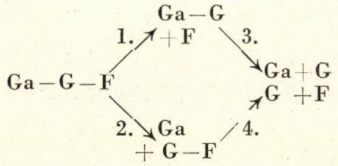

Actually, Reaction 1 is nearly a thousand times faster than Reaction 2, therefore Reaction 4 also remains negligible. In practice, the kinetics are simplified to two simultaneous reactions:

$$p = 1 - 0.5\,(e^{-k_R \cdot \tau} + e^{-k_M \cdot \tau})$$

where p is the ratio of the ruptured bonds, k_R is the rate constant of formation of melibiose, and k_M is the rate constant of the hydrolysis of melibiose.

OVEREND *et al.* [34] presume that furanosides are generally hydrolyzed by an A-2 mechanism, resulting in a low or negative ΔS^+ value. The ΔS^+ val-

ues for α-methyl-galacto-, -gluco-, and -xylo-furanosides are between −8 and −11 e.u. [10]. In spite of the numerous papers devoted to the acid hydrolysis of SA, only a few ΔS^+ values have been published for this reaction. According to TIMELL [44], its value is +2.3 e.u., while a value of +8.11 e.u. can be calculated from the k values published by LEININGER and KILPATRICK [27], which agrees quite well with our own result (see in Table I). (The value of −26.9 e.u., which is to be found in BEMILLER's monograph [10], is a misprint.) RAF also has a positive entropy of activation: +8.34 e.u. The fact that TIMELL obtained a lower value probably can be attributed to the use of sulfuric acid in his experiments; as it has been pointed out [39], this acid is not very convenient for hydrolysis-kinetical studies. The dissociation, and the hydrolysis-catalyzing activity of this acid is a rather complex function of temperature and acid concentration, which may lead to incorrect E_a and ΔS^+ values. The most appropriate acid for such investigations is hydrochloric acid.

The mentioned ΔS^+ values prove that the entropy of activation of the hydrolysis of furanosides is not always negative, thus the A-2 mechanism cannot be generalized.

Discussion

The following facts and consideration may serve as a basis for investigating the reaction mechanism of the acid hydrolysis of the fructofuranosyl-glucopyranosyl linkage.

(1) The rate-determining step can hardly be the formation of a glucopyranosyl cation; in such a case the inevitable conversion of the C1 conformation to a half-chair form should be retarded by the bulky galactosyl substituent in RAF; as a consequence, the splitting off of the fructose from RAF should be slower by at least 50% as compared with the hydrolysis of SA. Actually, the ratio of k_{RAF}/k_{SA} is 0.812, *i.e.* the difference is only 18.8% or:

$$\overset{1}{\text{G–F}} \text{ and } \text{Ga–}\overset{0.8}{\text{G}}\text{–F}$$

(The numbers above the bonds represent the relative rate constants.)

In the case of cellobiose and cellotriose [18], the ratio $k_{disaccharide}/k_{trisaccharide}$ is 0.65; however, this value is the average of two k's characteristic of the rupture of both in the trisaccharide, thus:

$$\overset{1}{\text{xG–G}} \text{ and } \text{xG–}\overset{1}{\text{G}}\text{–}\overset{0.3}{\text{G}}$$

(xG = reducing end-group). Hydrolysis experiments with C^{14}-labelled amylose have shown that its non-reducing end-group splits off about three times faster

than the reducing one [21]. In this case a conformational effect seems to be probable [41], while in case of SA it is hardly conceivable.

(2) The furanoside ring is practically planar; therefore no conformational change is necessary in the conversion of the C_2-atom into a carbonium cation. It is well known that the formation of a cyclopentyl cation occurs more readily than that of a cyclohexyl cation [10].

(3) The small difference between the rates of hydrolysis of SA and RAF presumably is caused by a lower concentration of the conjugated acid in the case of RAF. The Ga–O–G bridge withdraws one part of the hydronium ions from the fructofuranosyl part. The fact that the reaction proceeds faster in D_2O than in H_2O [9, 48] verifies that the rate-determining step is preceded by an equilibrium between the glycoside and its conjugated acid.

(4) If the hydrolysis takes place at the furanosyl–O bond, it leads to the formation of a tertiary carbonium cation. It is well known that tertiary cations are formed much more readily than primary ones. As it is seen from Table IV, the values of k as well as of E_a allow to presume that the G–F linkage is hydrolyzed in SA and RAF in the same way as it is characteristic of aglycones bound through a tertiary carbon atom.

(5) Both SA and RAF belong to the particular type of glycosides, in which two glycosyl parts are attached to the glycosidic oxygen atom; as a matter of fact, there is no real aglycon part. It is conceivable that such a special structure is hydrolyzed by other than the usual mechanism. It is known that the hydrolysis of 2-desoxyglycosides is a much faster process than that of 3- or 4-desoxyglycosides [34]. The decrease of stability may be attributed in part to a decrease in the hindrance of rotation which takes place during the conformational change, but mainly to the disappearance of the inductive stabilizing effect of the C_2—OH group. The electron density around the bridge oxygen atom is diminished by the electron-withdrawing effect of the C_2—OH group, which results in less intense formation of the conjugated acid. In cases when there are two C_2—OH groups close to the bridge oxygen atom, *e.g.* in α,α-trehalose, the extent of proton addition to the bridge atom becomes rather suppressed, while the addition of a proton to the ring-oxygen—which introduces an *axial* substituent into the ring, or such a substituent which in the first step of the hydrolysis becomes *axial* — does not result in hydrolysis. A secondary carbonium cation is formed only 2—3 times easier than a primary one, so in case of tetrahalose this effect is too small to compensate the inductive stabilizing effect. Therefore, α,α-tetrahalose is one of the most stable disaccharides [38].

In determining the stability of SA, the glucopyranosyl part cannot play an important role, as it has been shown under (1). Considering the very low stability of 2-desoxyglycosides and the extraordinary stability of α,α-trehalose, it may be concluded that proton addition to the bridge-oxygen must also have a subordinate importance. Therefore, the key to the hydrolysis of sac-

Table IV

Effect of the aglycone moiety on the stability of

Aglycone moiety		Glycosyl moiety: β-D-glucopyranoside		
Connected by		$k \cdot 10^4$ min^{-1}	k_{rel}	$\Delta k_{rel} > 0.5$
—C<	methyl-	3.75[c]	1.00	
primary C-atom	$\Delta k_{rel} < 0.5$			
—C—C<	ethyl-	4.04[a]	1.08	
	n-propyl-	4.76[a]	1.27	
	n-butyl-	4.19[a]	1.12	
	n-pentyl-			
	n-hexyl-			
	6-D-glucopyranosyl- (gentiobiose)	3.42[f]	1.13	
secondary C-atom	$0.5 < \Delta k_{rel} < 3.5$			
>C(—C)—C<	i-propyl-	6.77[a]	1.80	0.80
	3-pentyl-	3.08[d]	1.51	0.51
	cyclopentyl-			
	cyclohexyl-	8.34[a]	2.22	1.22
	2-D-glucopyranosyl- (sophorose)	7.02[f]	2.62	1.62
tertiary C-atom	$90 < \Delta k_{rel} < 8670$			
>C(—C)(—C)—C<	t-butyl-	1750[a]	466	465
	1,1-dimethylpropyl-	111.7[e]	1071	1070
	triethylmethyl-	860[a]	230	229
>C(—O—C)—C<	2-D-fructofuranosyl- (saccharose)	72.1[g]	8671	8670

[a] = TIMELL[44], 1.0 *N* H_2SO_4, 70 °C
[b] = DE BRUYNE and VAN WIJNENDAELE [13] 0.5 *N* HCl, 80 °C
[c] = SZEJTLI [39]
[d] = VEIBEL and HJORTH [45], 1.0 *N* HCl, 60 °C;
$k_{\beta\text{-Me-glucopyranoside}} = 2.05 \cdot 10^{-4}$ (SZEJTLI [39])

charose has to be found in the fructofuranosyl part. It is probable that the first step is proton addition to the ring-oxygen (I → II → III) which is not impeded by any conformational effect in this case, as the furanosyl ring has nearly planar structure. This conjugated acid can easily be heterolyzed to a tertiary cation without ring opening.

(6) The hypothesis of the splitting of SA involving the formation of a tertiary carbonium cation intermediate is also supported by the hydrolysis of turanose. Turanose [3-(α-D-glucopyranosyl)-fructofuranose; IV] consists of the same monosaccharides as SA, but the glycosidic linkage is attached to the C_3-atom of the furanose ring, thus the formation of a tertiary cation is impossible. Therefore, the rate of hydrolysis is practically the same as that of maltose (*cf.* Table V). It may be stated that the presence of a furanose ring in itself does not give rise to rapid hydrolysis.

β-D-alkyl-glucopyranosides and of β-D-alkyl-xylopyranosides

		Glycosyl moiety: β-D-xylopyranoside[b]				
E_a, kcal/mole	ΔE_a > 1.5	$k \cdot 10^4$ min^{-1}	k_{rel}	Δk_{rel} > 0.5	E_a, kcal/mole	ΔE_a, > 1.5
33.3		64.8	1.00		33.2	
33.8		86.4	1.33		32.3	
32.9		90.5	1.40		32.1	
33.6		86.4	1.35		31.8	
		88.2	1.36		32.5	
		93.0	1.43		31.7	
33.7						
33.2		181.7	2.80	1.80	—	—
—		292	4.51	3.51	31.4	—2.9
		160.1	2.47	1.47	30.7	—2.5
33.5		204.2	3.16	2.16	30.8	—2.4
28.9	—4.4					
29.3	—4.0	6000	92.5	91.5	30.3	—2.9
—	—	19420	299	298	29.2	—4.0
26.0	—7.3					
25.5	—7.8					

[e] = VEIBEL and HJORTH [45], 1.0 *N* HCl, 40 °C;
$k_{\beta\text{-Me-glucopyranoside}} = 0.109 \cdot 10^{-4}$ (SZEJTLI [39])
[f] = WOLFROM, THOMPSON and TIMBERLAKE [50], 0.1 *N* HCl, 80 °C;
$k_{\beta\text{-Me-glucopyranoside}} = 3.02 \cdot 10^{-4}$ (SZEJTLI [39])
[g] = from present work, 0.106 *N* HCl, 40 °C;
$k_{\beta\text{-Me-glucopyranoside}} = 0.00831 \cdot 10^{-4}$ (SZEJTLI [39])

(7) Since a tertiary carbonium cation is substantially more stable than a primary or secondary one, it is very probable that the rate-determining step is its monomolecular formation and not a nucleophilic attack of water on the conjugated acid. This hypothesis can explain the positive value of the entropy of activation, as well as the low value of energy of activation and the relatively high rate of reaction.

As it has been mentioned, the hydrolysis of aldofuranosides occurs probably by an A-2 mechanism. Such a mechanism is conceivable if the probability of a bimolecular collision (nucleophilic attack) between water molecule and the conjugated acid is higher than the probability of monomolecular heterolysis of the acid. If the ring-oxygen were protonated, similarly as it has been assumed in the cases of SA and RAF, only a monomolecular mechanism would be conceivable; since the bimolecular collision of such a conjugated acid can-

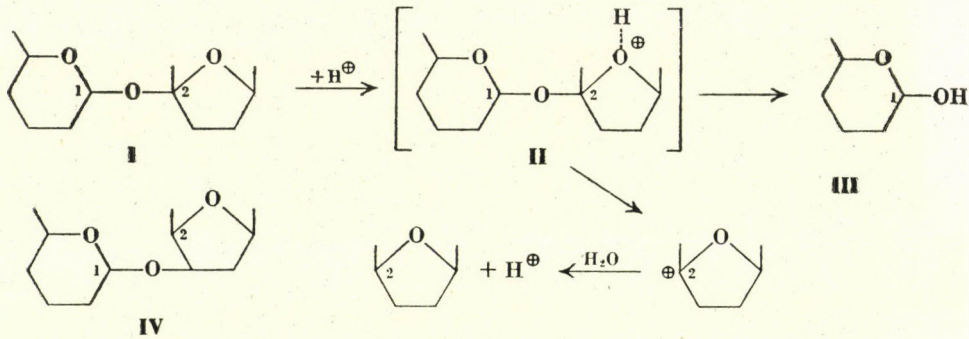

Table V

Values of k_r at 100 °C in HCl (min^{-1})

	$k_{r,100°C}$	k, published	Author
Saccharose	56.360	present work, Table I.	
Raffinose	48.750	present work, Table I.	
Melibiose	0.114	60 °C, 1.0 *N* HCl $k = 7.75 \cdot 10^{-4}$	MOELWYN-HUGHES [33]
Turanose	0.080	80 °C, 1.0 *N* HCl $k = 106.2 \cdot 10^{-4}$	MOELWYN-HUGHES [33]
Maltose	0.094	80 °C, 0.1 *N* HCl $k = 9.30 \cdot 10^{-4}$	WOLFROM *et al.* [50]

not result in the rupture of the glycosidic bond, as in this case the real reaction center, the bridge oxygen, is not activated.

The difference between the mechanism of acid hydrolysis of aldo- and ketofuranosides is that the former are split by protonation of the bridge oxygen and a subsequent A-2 mechanism, while the latter undergo protonation on the ring-oxygen and are hydrolyzed involving the monomolecular formation of a tertiary carbonium cation.

We thank Dr. E. VÁNDOR, Budapest, for correcting the galley proofs of this paper.

REFERENCES

1. AHARI, D., GENOTELLE, J.: Ind. Aliment. Agric. **78**, 742 (1961)
2. ANDERSEN, E.: Int. Sugar Journ. **58**, 133 (1956)
3. ASPINALL, G. O.: Compt. Rend. 10. Ass. CITS, Londres, 1957. p. 14
4. ASSELBERGS, C. J., *et al.*: Compt. Rend. 10. Congr. Int. Ind. Agr., Madrid, 1954. Tom. 2, 1187
5. ATHENSTEDT, M.: Zuckerind. Z. **11**, 605, 661 (1961)
6. BAMFORD, C. H., BAMFORD, D., COLLINS, J. R.: Proc. Roy. Soc. (London), **A204**, 62, 85 (1951)

7. BAMFORD, C. H., COLLINS, J. R.: Proc. Roy. Soc. (London), A**228**, 100 (1955)
8. BARTA, GY.: Enzimek, Élelmiszeripari Kiadó, Budapest, 1954
9. BELL, R. P.: Acid-Base Catalysis, Oxford Univ. Press, London, 1941
10. BEMILLER, J. N.: Adv. Carbohydrate Chem. **22**, 25 (1967)
10a. CAPON, B., THACKER, D.: J. Am. Chem. Soc. **87**, 4199 (1965)
11. BODAMER, G., KUNIN, R.: Ind. Engng. Chem. **43**, 1082 (1951)
12. BREZINA, M., ZUMAN, P.: Polarography, p. 281. Interscience, New York, 1958
13. DE BRUYNE, C. K., VAN WIJNENDAELE, F.: Carbohydrate Res. **6**, 367 (1968)
14. EDWARD, J. T.: Chem. Ind. (London) **1955**, 1102
15. FEATHER, M. S., HARRIS, J. F.: J. Org. Chem. **30**, 153 (1965)
16. FODOR, J., HAJÓS, Z.: MTA Kémiai Tud. Oszt. Közl. **5**, 545 (1955)
17. FOSTER, A. B., OVEREND, W. G.: Chem. Ind. (London) **1955**, 566
18. FREUDENBERG, K.: J. Polymer Sci. **23**, 791 (1957)
19. HAMMETT, L. P., PAUL, M. A.: J. Am. Chem. Soc. **56**, 830 (1934)
20. HEIDT, L. J., PURVES, C. B.: J. Am. Chem. Soc. **60**, 1206 (1938); **66**, 1385 (1944)
21. HOLLÓ, J., LÁSZLÓ, E., SZEJTLI, J., ZALA, GY.: Stärke **16**, 211 (1964)
22. HONIG, P.: Principles of Sugar Technology, Vol. I., Chapter I. (by H. Hirschmüller); Elsevier, Amsterdam, 1958
23. JACKSON, R., GILLIS, C.: Z. Ver. Deutsch. Zuckerind. **70**, 521 (1920)
24. JACKSON, R., GILLIS, C.: Sci. Pap. Bur. Standards **16**, 141, 375 (1920)
Natl. Bur. Standards Circular **C440**, 132 (1942)
25. KRIEBLE, V. K.: J. Am. Chem. Soc. **57**, 15 (1935)
26. KRIEBLE, V. K., REINHART, F. M.: J. Am. Chem. Soc. **57**, 19 (1935)
27. LEININGER, P. M., KILPATRICK, M.: J. Am. Chem. Soc. **60**, 1268, 2891, (1938); **61**, 2510 (1939)
28. LITVAK, I. M., REVA, L. P.: Trudü KTIPP **24**, 8 (1961)
29. LONG, F. A., PAUL, M. A.: Chem. Revs. **57**, 1, 1935 (1957)
30. MANTOVANI, G., INDELLI, A.: Zucker **17**, 593 (1964)
31. MOELWYN-HUGHES, E. A.: Trans. Faraday Soc. **24**, 309, 321 (1928)
32. MOELWYN-HUGHES, E. A.: Z. physik. Chem. **B26**, 281 (1934)
33. MOELWYN-HUGHES, E. A.: Trans. Faraday Soc. **25**, 503 (1929)
34. OVEREND, W. G., REES, C. W., SEQUEIRA, J. S.: J. Chem. Soc. **1962**, 3429
35. PARCH, K., TRACEY, M. V.: Moderne Methoden der Pflanzenanalyse, Vol. II. Springer Verlag, Berlin, 1955
36. PINDAT, M. A.: Sucr. Franç. **98**, 176 (1957)
37. STADLER, F. G.: Arch. Suikerind., Nederl. Ind. **39**, 689 (1931)
38. SZEJTLI, J.: Stärke **19**, 145 (1967)
39. SZEJTLI, J.: Acta Chim. Acad. Sci. Hung. **56**, 175 (1968)
40. SZEJTLI, J.: Acta Chim. Acad. Sci. Hung. **45**, 141, 153 (1965); **46**, 77 (1965)
41. SZEJTLI, J.: Stärke **18**, 274 (1966)
42. SZEJTLI, J.: Ernährungsforschung **13**, 371 (1968)
43. TÄUFEL, K., RUTTLOFF, H.: Ernährungsforschung **4**, 44 (1959)
44. TIMELL, T. E.: Canadian J. Chem. **42**, 1456 (1964)
45. VEIBEL, S., HJORTH, E.: Acta Chem. Scand. **6**, 1353 (1952)
46. VERHAART, M. L. A., DE VISSER, N. H. M.: Compt. Rend. 10. Ass., CITS, Londres 1957, p. 203.; Z. Zuckerind. **9**, 446 (1959)
47. VUKOV, K.: Cukoripari Kutató Intézet Közl. (Budapest) **8**, 7 (1963)
48. WIBERG, K. B.: Chem. Revs. **55**, 713 (1955)
49. WILHELMY, L.: Pogg. Ann. **81**, 413, 499 (1850)
50. WOLFROM, M. L., THOMPSON, A., TIMBERLAKE, C.: Cereal Chem. **40**, 82 (1963)
51. WOOTTON, A. E.: Compt. Rend. 10. Ags. CITS, Londres, 1957, p. 66.
52. ZHIDKOV, A. A. *et al.*: Trudy CINS **4**, 180 (1956)

József SZEJTLI
R. D. HENRIQUES
M. CASTIÑEIRA

Escuela de Bioquímica-Farmacéutica, Universidad de la Habana, Cuba

Acta Chimica Academiae Scientiarum Hungaricae, Tomus 66 (2), pp. 229—233 (1970)

THE IDENTIFICATION OF PETALOXANTHIN

J. SZABOLCS, Á. RÓNAI and GY. TÓTH

(Chemical Institute of the Medical University, Pécs)

Received June 5, 1969

A reinvestigation of petaloxanthin has revealed that it is a mixture of zeaxanthin and lutein, which may occasionally contain antheraxanthin impurity. Tables showing the distribution of the carotenoids present in *Cucurbita pepo* flowers are presented.

Petaloxanthin was isolated from the blossoms of *Cucurbita pepo* by ZECHMEISTER, BÉRES and UJHELYI [1, 2] in 1936. Its great similarity to antheraxanthin was soon recognized, and even the identity of the two substances has been suggested (KARRER *et al.* [3], 1950). The existence of petaloxanthin has repeatedly been questioned, and so far no unequivocal evidence has been given for its presence in nature.

According to our experiments, petaloxanthin is a mixture of lutein and zeaxanthin (about 1 : 3), which may occasionally contain some antheraxanthin impurity. Under the conditions used by ZECHMEISTER *et al.* for the isolation of petaloxanthin, lutein occurring in the blossoms of *Cucurbita pepo* is precipitated and adsorbed together with zeaxanthin. Although, on a calcium carbonate column, lutein or zeaxanthin accumulates at the top of the zeaxanthin–lutein (petaloxanthin) zone, depending on what solvent is used (from carbon disulfide zeaxanthin, and from a 1 : 1 mixture of benzene and petroleum ether lutein will remain at the top), and appears as a separate band, there is no sharp line of separation between the two components. Re-chromatography of the petaloxanthin zone furnishes, apart from a small amount of zeaxanthin, a homogeneous band from which petaloxanthin can be crystallized (CS_2–petroleum ether; m.p. 190 °C). This sample of petaloxanthin has the same physical and chemical properties as those described for petaloxanthin in the literature (Table I). The light blue colour reaction of petaloxanthin which, according to ZECHMEISTER *et al.*, is obtained in ether with hydrogen chloride, is most probably due to antheraxanthin impurity. It should be noted that our rechromatographed samples of petaloxanthin did not give blue colouration with HCl.

When a very dilute solution of petaloxanthin was subjected to chromatography on calcium carbonate from a mixture (1 : 10) of benzene and petroleum ether (b.p. 50—60 °C), and the concentration of benzene was gradually increased up to 2 : 10, lutein was adsorbed above zeaxanthin in a sharp layer. If the concentration of benzene was higher, the two pigments merged into each other yielding petaloxanthin. The lutein and zeaxanthin in the zone of

Table I

Properties of 'petaloxanthin'

	M.p.	Absorption maxima (mμ)			Partition between petroleum ether and 90% methanol	Colour reaction in ether with 37% aqueous HCl
		CS_2	Benzene	Ethanol		
Petaloxanthin [1, 2, 3]	202 °C (Berl block)	515.5 481	494 460.5	483 451.5	hypophasic	pale blue
'Petaloxanthin' (Zeaxanthin–lutein zone)	190 °C (Boetius app.)	515 481	494 460	483.5 451.5	hypophasic (rel. polarity: 1.92)	*

* Depends on the presence of traces of antheraxanthin impurity.

Table II

Quantitative distribution of carotenoids in Cucurbita pepo petals

(In the vicinity of Pécs (Hungary), August, 1968)

Pigment	Concentration, mg/g dry wt.	Percentage of total pigments	λ_{max}(mμ) in benzene	λ_{max}(mμ) in HCl-benzene	Partition between petroleum ether and 90% methanol
Cis-xanthopylls[a,b]	0.075	12.0	484 453	460 436	hypophasic
Violaxanthin	0.077	12.3	484 454	437	hypophasic
Antheraxanthin	0.080	12.8	491 458	466 436	hypophasic
Lutein	0.051	8.2	489 458	—	hypophasic
Zeaxanthin	0.210	33.6	496 462	—	hypophasic
β-Cryptoxanthin	0.115	18.4	496 462	—	epiphasic
β-Carotene	0.017	2.7	496 463	—	epiphasic
Total	0.625				

[1] Pigments belonging to this zone were identified after re-chromatography (see p. 232)
[a] Calculated for violaxanthin

Table III

Quantitative distribution of Carotenoids in Cucurbita pepo anthers
(In the vicinity of Pécs (Hungary) August, 1968)

Pigment	Concentration, mg/g dry wt.	Percentage of total pigments	λ_{max}(mμ) in benzene	λ_{max}(mμ) in HCl—benzene	Partition between petroleum ether and 90% methanol
Neoxanthin } [b]	0.342	42.4	480	(460)	hypophasic
Violaxanthin }			450	437	
3,3'-Dyhydroxyluteochrom[b]	0.080	9.9	460	437	hypophasic
			431		
Violaxanthin	0.181	22.4	484	437	hypophasic
			453		
Lutein	0.204	25.3	489	—	hypophasic
			458		
Total	0.807				

[b] Calculated for violaxanthin

petaloxanthin can also be separated by paper chromatography (the R_F values of zeaxanthin and lutein on Whatmann No. 3 paper in light petroleum containing 5% ethanol are 0.48 and 0.41, respectively).

Thus we believe that it was this mixed zone of lutein with zeaxanthin that was described as petaloxanthin. This assumption was confirmed in the present model experiments using authentic lutein, zeaxanthin and antheraxanthin.

In the course of our investigation of petaloxanthin, several quantitative analyses of the carotenoids occurring in the petals and anthers of *Cucurbita pepo* were carried out, and the results are summarized in Tables II and III. It is noteworthy that neoxanthin was found in the anthers, whereas the petals contained neoxanthin-X.

Experimental

The routine procedures and measurements used here have been summarized elsewhere [4]. Petaloxanthin was isolated from the yellow flowers of *Cucurbita pepo* collected in the vicinity of Pécs, Hungary.

Isolation of petaloxanthin

After extraction of the dried (at 45 °C) and finely ground male pumpkin blossoms (310 g) with ether at room temperature, the ethereal extract was concentrated in vacuum to 2 l and saponified with 30% methanolic potassium hydroxide (130 ml) for 18 hrs. The colourless impurities were then filtered off, and the ethereal solution was allowed to stand with fresh

alcoholic potassium hydroxide for another 20 hrs. The completeness of saponification was checked by a partition test, then the methanolic phase was transferred into a separatory funnel and diluted with ether and water for the extraction of the pigments present in the methanol phase. The combined ethereal extracts were washed free from alkali, dried over anhydrous sodium sulfate and evaporated in vacuum. The residue was dissolved in benzene and diluted with three volumes of methanol in order to precipitate the colourless impurities. After standing overnight at —10 °C, the colourless precipitate was filtered off, and the mother liquor evaporated in vacuum. The residue was dissolved in benzene and mixed with petroleum ether (b. p. 50—60 °C). The yield of two successive precipitations amounted to 650 mg of phytoxanthin. Separation of the pigments was effected by chromatography on calcium carbonate from a mixture (1 : 3) of benzene and petroleum ether (b.p. 50—60 °C).

Zone	Pigment	λ_{max} in benzene	
1. 4 yellow		484	453
2 —			
2. 5 yellow	violaxanthin	484	454
10 —			
3. 10 yellowish-ochre			
2 —	antheraxanthin	491	458
4. 10 diffuse ochre			
(unsharp zone)	'petaloxanthin'	493	461
5. 40 light orange	zeaxanthin	496	462
50 —			
6. 40 orange	β-cryptoxanthin	496	463

Further processing was carried out in the usual manner.

Band 1 consisted of neoxanthin-X, *cis*-zeaxanthins, and violaxanthin. Accordingly, re-chromatography on calcium carbonate of Band 1 from a mixture of benzene and petroleum ether (1 : 2) gave the following zones:

Zone	Pigment	λ_{max} in benzene		λ_{max} in HCl–benzene	
11. 2 yellow	neoxanthin-X	484	453	460	432
12. 2 ochre	*cis*-zeaxanthin	489	456	490	457
1 —					
13. 1 yellow	*cis*-lutein (?)	486	453	486	453
14. 2 ochre	*cis*-zeaxanthin	490	460	490	459
1 —					
15. 1/2 pale yellow	unidentified	—	—	—	—
25 —					
16. 6 diffuse yellow	violaxanthin	484	453	—	437
40 —					
17. 10 diffuse orange	unidentified	(493)	(459)	(493)	(459)

Violaxanthin (2), antheraxanthin (3), zeaxanthin (5) and β-cryptoxanthin (6) were crystallized from methanol. This gave 16 mg of violaxanthin (m.p. 164 °C), 21 mg of antheraxanthin (m.p. 181 °C), 48 mg of zeaxanthin (m.p. 182 °C) and 20 mg of β-cryptoxanthin (m.p. 153 °C).

Petaloxanthin (4) was subjected to re-chromatography on calcium carbonate from a mixture (1 : 3) of benzene and petroleum ether with the following result:

Zone	Pigment	λ_{max} in benzene	
1. 1 ochre	neolutein B	486	458
90 —			
2. 8 diffuse ochre	'petaloxanthin'	492.5	460
3. 6 orange	zeaxanthin	496	463

After the usual work-up, petaloxanthin was crystallized from a 1 : 2 mixture of carbon disulfide and petroleum ether to obtain 2 mg of the product, m.p. 190 °C. The properties of petaloxanthin are presented in Table I.

Separation of petaloxanthin into lutein and zeaxanthin

2 mg of petaloxanthin was dissolved in a large amount of a mixture (1 : 10) of benzene and petroleum ether, and poured on a calcium carbonate column. The concentration of benzene was gradually increased up to 20% during the chromatographic run. Petaloxanthin separated into 2 distinct zones,

Zone	Pigment	λ_{max} in benzene	
1. 1 ochre	neolutein B	486	457
60 —			
2. 10 ochre	lutein	490	457
8 —			
3. 8 orange	zeaxanthin	496	462

Both zeaxanthin and lutein were identified in mixed chromatograms with authentic samples, and by other tests.

Quantitative analysis. The petals and anthers of 16 g of blossoms were removed and separated from each other to form two batches; either of them was ground separately in a Turmix-type grinder, in the presence of methanol, and the finely ground material was dehydrated with methanol at room temperature. Ethereal extraction, saponification, etc. of the two batches were carried out as described above. The results are presented in Tables II and III (the pigments are listed in the sequence of decreasing adsorption affinities).

*

The skilfull technical assistance of Miss M. HÁM and Mrs. I. NAGY is gratefully acknowledged. The present work was supported by a grant from the Hungarian Ministry of Health.

REFERENCES

1. ZEICHMEISTER, L., BÉRES, T., UJHELYI, E.: Ber. **68**, 1321 (1935)
2. ZECHMEISTER, L., BÉRES, T., UJHELYI, E.: Ber. **69**, 573 (1936)
3. KARRER, P., JUCKER, E.: Carotenoids, translated by E. A. Braude. Elsevier, Amsterdam, 1950
4. SZABOLCS, J., RÓNAI, Á.: Acta Chim. Acad. Sci. Hung. **61**, 301 (1969).

József SZABOLCS
Ádám RÓNAI
Gyula TÓTH
Pécs, Rákóczi út 80. Hungary,

INDEX

INORGANIC AND ANALYTICAL CHEMISTRY — ANORGANISCHE UND ANALYTISCHE CHEMIE — НЕОРГАНИЧЕСКАЯ И АНАЛИТИЧЕСКАЯ ХИМИЯ

INCZÉDY, J.: László Erdey (1910—1970) 135

TÖRÖK, T. und BÁN, S.: Praktische Verwendung der »Blindwertkorrektion« in der spektrographischen Spurenanalyse. (The Practical Application of Blank Correction in Spectrographic Trace Analysis) 159

MATHERNY, M.: Über die spektrographischen Eigenschaften der Kapillarelektroden, II. (Spectral-analytical Properties of Capillary Electrodes, II) 165

SIMON, J., GÁL, S. and ERDEY, L.: Thermal Reactions of Potassium Halates and Perhalates 175

KAZARYAN, N. A., PUNGOR, E.: Application of Ion-Selective Electrodes in Non-Aqueous Media, I. Study on the Application Limits in Some Non-Aqueous Solvents (Preliminary Communication) 183

PHYSICAL CHEMISTRY — PHYSIKALISCHE CHEMIE — ФИЗИЧЕСКАЯ ХИМИЯ

KAMMER, H.: d^N-Elektronensysteme in trigonalen Ligandenfeldern, I. Theorie (d^N Electron Systems in Trigonal Ligand Fields, I. Theory) 189

KAMMER, H.: d^N-Elektronensysteme in trigonalen Ligandenfeldern, II. Interpretation der Spektren von V^{3+}- und Cr^{3+}-Ionen. (d^N Electron Systems in Trigonal Ligand Fields, II. Interpretation of the Spectra of V^{3+} and Cr^{3+} Ions) 203

VÉRTES, A., BURGER, K. and BOGNÁR, L.: Mössbauer Study of Some Iron(II) Complexes in Frozen Aqueous Solutions. (Short Communication) 209

ORGANIC CHEMISTRY — ORGANISCHE CHEMIE — ОРГАНИЧЕСКАЯ ХИМИЯ

SZEJTLI, J., HENRIQUES, R. D. and CASTIÑEIRA, M.: Mechanism of the Acid Hydrolysis of Saccharose and Raffinose 213

SZABOLCS, J., RÓNAI, Á. and TÓTH, GY.: The Identification of Petaloxanthin 229

ACTA CHIMICA

ТОМ. 66 — ВЫП. 2

РЕЗЮМЕ

Практическое использование поправки на глухую величину в спектрографическом анализе следов элементов

Т. ТЁРЁК и Ш. БАН

Математический метод, разработанный ранее для исключения помех примесей в носителе электрода (4), был использован в практике для определения кальция в растворе по Шейбе—Ривасу. Вспомогательные угольные электроды производства *Тополь чяни* были также загрязнены кальцием. После подробного описания экспериментальных условий приводятся кривые, полученные без поправки на примеси в фоне и в носителе, лишь с поправкой на фон, а также с поправкой на примеси в фоне и в носителе. Эти кривые подтверждают возможность использования метода поправки, находятся в согласии с теоретически ожидаемыми эффектами, а также дают информацию о степени загрязнения носителя электрода.

Свойства капиллярных электродов; примененных в спектральном анализе, II

М. МАТЕРНИ

При спектральном анализе, проведенном при помощи капиллярных электродов изменение внутреннего сопротивления растворов оказывает гораздо более значительное влияние на обнаруживаемость элементов, нежели изменение поверхностного натягивания растворов. Общее содержание соли в растворах не должно превышать 10%. При одном заряде не рекомендуется использовать время освещения, превышающее 15 сек, т. к. в противном случае изменяется отношение концентраций исследуемого и эталонного элементов наблюдаются две разного типа влияния матрицы. В первом случае, вследствие изменения концентрации основного компонента, кривые оценки смещаются параллельно и изменяется их тангенс угла наклона, в других же случаях различные основные компоненты вызывают лишь параллельное смещение. Корреляция между элементами и оптимальная комбинация полос изучались с помощью статистических методов оценки.

Термические реакции галогенатов и пергалогенатов калия

Й. ШИМОН, Ш. ГАЛ и Л. ЭРДЕИ

Термические реакции галогенатов и пергалогенатов калия изучались дериватографическим методом. Окислительно-восстановительные реакции, протекающие при высоких температурах, указывают на то, что химическая связь обладает наиболее высоким ионным характером в случае иодата калия и наинизшим — в случае хлората калия.

Электронные системы d^N в тригональном лигандном поле, I.

Теория

Х. КАММЕР

В рамках приближения силового поля изучались энергетические состояния ионов переходных металлов в тригональном лигандном поле с пренебрежением спин-орбитального взаимодействия. d-Электронное состояние расщепляется в тригональном поле на e, a_1 и э состояния. Разница энергий этих состояний характеризуется параметрами D, E и F. В случае тригональной симметрии существуют следующие конфигурации: $e^n a_1{}^p \varepsilon^q$ ($n + p + q = N$, и $0 \leq n, q \leq 4, 0 \leq p \leq 2$), из которых при кулоновском взаимодействии образуются тэрмы $^{2S+1}\Gamma$. Матрицы электростатической энергии электронной системы d^N в тригональном поле в случае $n = 3, 4, 5$ рассчитываются с помощью индукционной зависимости из электронной системы d^{N-1}. Приводятся энергетические матрицы, справедливые для конфигураций d^2, d^3, d^4 и d^5 в тригональном лигандном поле. Элементы матрицы кулоновского взаимодействия выражаются параметрами Рацаха A, B, C. Помимо этого, в табличной форме приводятся фигурирующие в расчетах величины параметров Рацаха.

Электронные системы d^N в тригональном лигандном поле, II.

Интерпретация спектров ионов V^{3+} и Cr^{3+}

Х. КАММЕР

Вековые определители, полученные в 1-ом сообщении для систем d^2 и d^3, решаются при определенных условиях, и полученные результаты сравниваются с результатами, полученными из абсорбционных спектров ионов V^{3+} и Cr^{3+} в тригональной среде.

Механизм кислотного гидролиза рафинозы и сахарозы

Й. СЕЙТЛИ, Д. Р. ЭНРИКЕЗ и М. КАСТИНЕЙРА

Рафиноза может быть рассмотрена как молекула сахарозы, в которой к глюкозному звену присоединяется ещё галактоза. Сравнение кислотного гидролиза сахарозы и рафинозы позволяет сделать заключения относительно механизма реакции. Особенностью сахарозы является то, что в последней, по существу, два глюкозила связаны непосредственно друг с другом и без агликона.

Константа скорости гидролиза сахарозы, на основе измерений в разбавленных углеводных растворах в пределах концентраций HCl, равной 0,001 ÷ 1,0 N, может быть описана следующим уравнением:

$$\log k = 1{,}038 \cdot \mathrm{pH} + 16{,}754 - 0{,}4343 \cdot 25541/1{,}987 \cdot T$$

Связь глюкоза-фруктоза в рафинозе разрывается со скоростью ниже на 19% скорости, получаемой по вышеприведенному уравнению, а скорость разрыва связи глюкоза-галактоза на три порядка ниже этого.

На основе экспериментальных результатов можно заключить, что в данном случае, в противоположность общему случаю, портонируется не кислород водородного мостика, а кислород кольца фуранозы. Вследствие этого, связь расщепляется с образованием не первичного глюкозил-карбониевого катиона, а третичного фуранозильного катиона. Присутствие фуранозного кольца, само по себе, еще не объясняет быстрый гидролиз сахарозы, т. к., например, тураноза, из которой не образуется третичный катион, значительно стабильнее, чем сахароза, а возможность образования третичного катиона приводит и в других случаях к высокой скорости гидролиза. Положительное значение энтропии активации (для сахарозы +8,07 и для рафинозы +8,34) указывает на механизм распада типа A—1.

Идентификация петалоксантина

Й. САБОЛЬЧ, А. РОНАИ и ДЬ. ТОТ

При возобновленном изучении петалоксантина было обнаружено, что он представляет собой смесь зеаксантина и лутеина, содержащую в некоторых случаях примеси антераксантина. В табличной форме приводятся данные количественного анализа каротиноилов, найденных в цветах Cucurbita pepo.

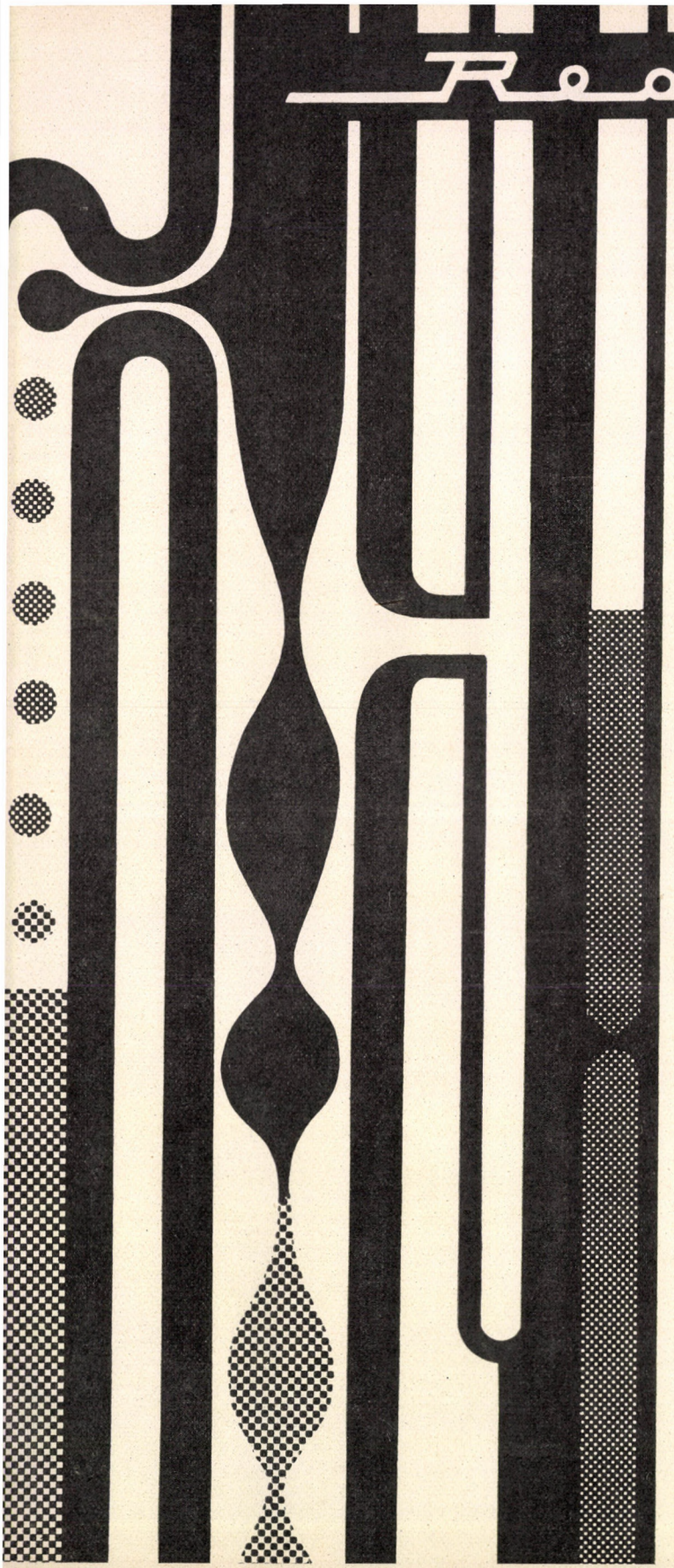

ANORGANISCHE UND ORGANISCHE FEINCHEMIKALIEN

Garantiert reine Reagenzien
für analytische Zwecke

Laboratoriumspräparate
für die Forschung
und Technik

Biochemikalien:

Aminosäuren und Derivate
Peptide und Derivate
Enzyme und Koenzyme
Nukleoproteide · Purine

Indikatoren

Tetrazoliumsalze

Präparate für Mikroskopie und Biologie

Kohlenhydrate

REANAL
FABRIK FÜR
FEINCHEMIKALIEN
Budapest · Ungarn

INFORMATION
UND LITERATUR
MEDIMPEX
BUDAPEST 5 · POSTFACH 126

Printed in Hungary

A kiadásért felel az Akadémiai Kiadó igazgatója — Műszaki szerkesztő: Farkas Sándor

A kézirat nyomdába érkezett: 1970. VII. 2. — Terjedelem: 9 (A/5) ív, 18 ábra, 2 melléklet

70.70012 Akadémiai Nyomda, Budapest — Felelős vezető: Bernát György

The Acta Chimica publish papers on chemistry in English, German, French and Russian.

The Acta Chimica appear in volumes consisting of four parts of varying size, 4 volumes being published a year.

Manuscripts should be addressed to

Acta Chimica
Budapest 112/91 Műegyetem

Correspondence with the editors should be sent to the same address.

The rate of subscription is $ 16.00 a volume.

Orders may be placed with "*Kultúra*" Foreign Trade Company for Books and Newspapers (Budapest I., Fő utca 32. Account No. 43-790-057-181) or with representatives abroad.

Les Acta Chimica paraissent en français, allemand, anglais et russe et publient des mémoires du domaine des sciences chimiques.

Les Acta Chimica sont publiés sous forme de fascicules. Quatre fascicules seront réunis en un volume (4 volumes par an).

On est prié d'envoyer les manuscrits destinés à la rédaction à l'adresse suivante:

Acta Chimica
Budapest 112/91 Műegyetem

Toute correspondance doit être envoyée à cette même adresse.

Le prix de l'abonnement est de $ 16.00 par volume.

On peut s'abonner à l'Entreprise pour le Commerce Extérieur de Livres et Journaux «*Kultúra*» (Budapest I., Fő utca 32. Compte-courant No. 43-790-057-181) ou à l'étranger chez ous les représentants ou dépositaires.

«*Acta Chimica*» издают трактаты из области химической науки на русском, французском, английском и немецком языках.

«*Acta Chimica*» выходят отдельными выпусками разного объема. 4 выпуска составляют один том. 4 тома публикуются в год.

Предназначенные для публикации рукописи следует направлять по адресу:

Acta Chimica
Budapest 112/91 Műegyetem

По этому же адресу направлять всякую корреспонденцию для редакции.

Подписная цена — $ 16.00 за том.

Заказы принимает предприятие по внешней торговле книг и газет «*Kultúra*» (Budapest I., Fő utca 32. Текущий счет № 43-790-057-181) или его заграничные представительства и уполномоченные.

Reviews of the Hungarian Academy of Sciences are obtainable at the following addresses:

ALBANIA
Drejtorija Qändrone e Pärhapjes dhe Propagandimit të Librit
Kruga Konferenca e Päzes
Tirana

AUSTRALIA
A. Keesing
Box 4886, GPO
Sydney

AUSTRIA
GLOBUS
Höchstädtplatz 3
A — 1200 Wien XX

BELGIUM
Office International de Librairie
30, Avenue Marnix
Bruxelles 5
Du Monde Entier
5, Place St. Jean
Bruxelles

BULGARIA
HEMUS
11 pl Slaveikov
Sofia

CANADA
Pannonia Books
2, Spadina Road
Toronto 4, Ont.

CHINA
Waiwen Shudian
Peking
P. O. B. 88

CZECHOSLOVAKIA
Artia
Ve Směčkách 30
Praha 2
Poštovní Novinová Služba
Dovoz tisku
Vinohradská 46
Praha 2
Mad'arská Kultura
Václavské nám. 2
Praha 1
SLOVART A. G.
Gorkého
Bratislava

DENMARK
Ejnar Munksgaard
Nörregade 6
Copenhagen

FINLAND
Akateeminen Kirjakauppa
Keskuskatu 2
Helsinki

FRANCE
Office International de Documentation et Librairie
48 rue Gay Lussac
Paris 5

GERMAN DEMOCRATIC REPUBLIC
Deutscher Buch-Expor und Impor
Leninstraße 16
Leipzig 701
Zeitungsvertriebsamt
Fruchtstraße 3—4
1004 Berlin

GERMAN FEDERAL REPUBLIC
Kunst und Wissen
Erich Bieber
Postfach 46
7 Stuttgart S.

GREAT BRITAIN
Blackwell's Periodicals
Oxenford House
Magdalen Street
Oxford
Collet's Subscription Import Department
Dennington Estate
Wellingborough, Northants.
Robert Maxwell and Co. Ltd.
4 — 5 Fitzroy Square
London W. 1

HOLLAND
Swetz and Zeitlinger
Keizersgracht 471—487
Amsterdam C.
Martinus Nijhoff
Lange Voorhout 9
The Hague

INDIA
Hind Book House
66 Babar Road
New Delhi 1

ITALY
Santo Vanasia
Via M. Macchi 71
Milano
Libreria Commissionaria Sansoni
Via La Marmora 45
Firenze

JAPAN
Kinokuniya Book-Store Co. Ltd.
826 Tsunohazu 1-chome
Shinjuku-ku
Tokyo
Maruzen and Co. Ltd.
P. O. Box 605
Tokyo-Central

KOREA
Chulpanmul
Phenjan

NORWAY
Tanum-Cammermeyer
Karl Johansgt 41 — 43
Oslo 1

POLAND
RUCH
ul. Wronia 23
Warszawa

ROUMANIA
Cartimex
Str. Aristide Briand 14—18
Bucureşti

SOVIET UNION
Mezhdunarodnaya Kniga
Moscow G—200

SWEDEN
Almquist and Wiksell
Gamla Brogatan 26
S—101 20 Stockholm

USA
F. W. Faxon Co. Inc.
15 Southwest Park
Westwood Mass. 02090
Stechert Hafner Inc.
31. East 10th Street
New York, N Y 10003

VIETNAM
Xunhasaba
19, Tran Quoc Toan
Hanoi

YUGOSLAVIA
Forum
Vojvode Mišića broj 1
Novi Sad
Jugoslovenska Knjiga
Terazije 27
Beograd

28. XII. 1970

Index: 26.007

ACTA CHIMICA

ACADEMIAE SCIENTIARUM HUNGARICAE

ADIUVANTIBUS

V. BRUCKNER, GY. DEÁK, K. POLINSZKY,
E. PUNGOR, G. SCHAY, Z. G. SZABÓ

REDIGIT

B. LENGYEL

TOMUS 66 FASCICULUS 3

AKADÉMIAI KIADÓ, BUDAPEST

1970

ACTA CHIM. ACAD. SCI. HUNG.

ACTA CHIMICA

A MAGYAR TUDOMÁNYOS AKADÉMIA KÉMIAI TUDOMÁNYOK OSZTÁLYÁNAK IDEGEN NYELVŰ KÖZLEMÉNYEI

SZERKESZTI

LENGYEL BÉLA

TECHNIKAI SZERKESZTŐK

DEÁK GYULA és HARASZTHY-PAPP MELINDA

Az Acta Chimica német, angol, francia és orosz nyelven közöl értekezéseket a kémiai tudományok köréből.

Az Acta Chimica változó terjedelmű füzetekben jelenik meg, egy-egy kötet négy füzetből áll. Évente átlag négy kötet jelenik meg.

A közlésre szánt kéziratok a szerkesztőség címére (Budapest 112/91 Műegyetem) küldendők.

Ugyanerre a címre küldendő minden szerkesztőségi levelezés. A szerkesztőség kéziratokat nem ad vissza.

Megrendelhető a belföld számára az „Akadémiai Kiadó"-nál (Budapest V., Alkotmány utca 21. Bankszámla 05-915-111-46), a külföld számára pedig a „Kultúra" Könyv- és Hírlap Külkereskedelmi Vállalatnál (Budapest I., Fő utca 32. Bankszámla: 43-790-057-181) vagy annak külföldi képviseleteinél és bizományosainál.

Die Acta Chimica veröffentlichen Abhandlungen aus dem Bereiche der chemischen Wissenschaften in deutscher, englischer, französischer und russischer Sprache.

Die Acta Chimica erscheinen in Heften wechselnden Umfanges. Vier Hefte bilden einen Band. Jährlich erscheinen 4 Bände.

Die zur Veröffentlichung bestimmten Manuskripte sind an folgende Adresse zu senden:

Acta Chimica
Budapest 112/91 Műegyetem

An die gleiche Anschrift ist auch jede für die Redaktion bestimmte Korrespondenz zu richten. Abonnementspreis pro Band: $16.00.

Bestellbar bei dem Buch- und Zeitungs-Außenhandels-Unternehmen »*Kultúra*« (Budapest I., Fő utca 32. Bankkonto No. 43-790-057-181) oder bei seinen Auslandsvertretungen und Kommissionären.

Acta Chimica Academiae Scientiarum Hungaricae, Tomus 66 (3), pp. 235—249 (1970)

NEW RESULTS CONCERNING THE THERMAL DECOMPOSITION OF AMMONIUM HEPTAMOLYBDATE TETRAHYDRATE

A. B. KISS, P. GADÓ, I. ASZTALOS and A. J. HEGEDÜS

(Tungsram Research Laboratories, Budapest)

Received June 2, 1969

The thermal decomposition of ammonium heptamolybdate was studied applying various experimental techniques. Prior to the formation of MoO_3, that of two intermediary phases of unknown structure was detected. On the basis of chemical analyses, formulas referred to 1 R_2O are $(NH_4)_2O \cdot Mo_{14}O_{42}$, and $(NH_4)_2O \cdot Mo_{22}O_{66}$. The infrared spectrum data of the decomposition series were recorded in the Mo–O stretching vibration range. By X-ray diffraction the dimensions of the 2.5-, 14-, and 22-molybdate unit cells were determined. Comparison of processes in the solid phase with polycondensation in solution has revealed similar and dissimilar feature of the intermediary polycondensates obtained. Correlations suggest that also in the solid phase polycondensations occur.

The thermal decomposition of ammonium heptamolybdate tetrahydrate (paramolybdate) has been studied by a number of authors [1—5]. Based on the results of thermo-analytical and X-ray diffraction experiments the decomposition reaction may be written as the sequence of the following steps:

$$(NH_4)_6[Mo_7O_{24}] \cdot 4\,H_2O \xrightarrow{50-110\,^\circ C}$$
$$(NH_4)_2O \cdot 2.5\,MoO_3 \xrightarrow{110-210\,^\circ C}$$
$$(NH_4)_4[Mo_8O_{26}] \xrightarrow{300\,^\circ C} MoO_3.$$

FUNAKI has reported [2] results somewhat different, since he supposed the intermediate corresponding to the 2.5-molybdate to be without water of crystallization of heptamolybdate; and RODE [4] has described the initial heptamolybdate by the erroneous empirical formula $5(NH_4)_2O \cdot 12\,MoO_3 \cdot 12\,H_2O$. HEGEDÜS [3, 15] claimed the formation of an unidentified substance with a molecular weight between 145.95 and 146.57 before MoO_3 is produced.

Thus available information suggests that in the course of the thermal decomposition of heptamolybdate to molybdenum trioxide two intermediary phases, each of a distinct structure, ought to be produced according to thermogravimetric data. The composition of these intermediates has been determined by several authors [1—5]. The lattice structure of the initial substance [6, 7], that of the second intermediary (octamolybdate) [8], and that of the final product [9—12] are known, of the first intermediary only the composition has

been elucidated (that is why, in order to discriminate between the two cases, in the latter the composition referred to one R_2O is formulated).

By studying the decomposition reaction with various methods, further intermediary phases of unknown structure have been detected.

Experimental

The materials used were of Analar p.a., and of Tungsram grade. Both corresponded to the formula $(NH_4)_6[Mo_7O_{24}] \cdot 4\ H_2O$, X-ray diffraction and data of chemical analyses showed their structure to be that well known for the heptamolybdate.

Joint thermogravimetry and infrared spectroscopy measurements — a method of which the particulars have been published [13, 14] — yielded the records shown in Fig. 1.

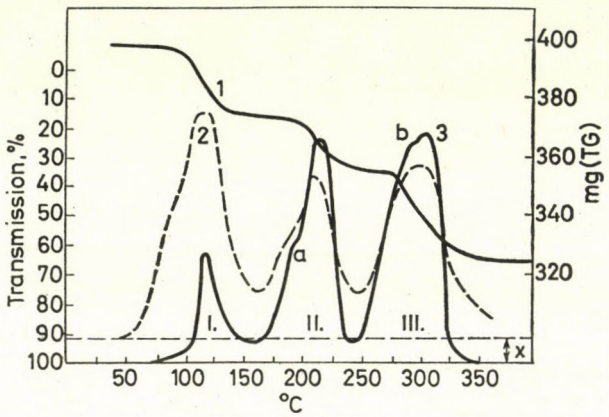

Fig. 1. TG curve and IR spectrum of the gaseous products of thermal decompositions. Sample weight: 400 mg. Air flow rate: 16.65 litres per hour. Heating rate: 300 °C per hour. 1. TG curve. 2. IR curve for H_2O. 3. IR curve for NH_3. X denotes the equilibrium moisture content of the carrier gas

In agreement with the decomposition reaction mentioned, three TG steps, and three intensive maxima on the IR-records on gases, can be discerned in Fig. 1. However, the inflexions at points *a* and *b* on the maximum curves II and III, respectively, cannot be interpreted by this scheme of the decomposition process. A similar case is presented by the derivatographic records of the process carried out in the presence of air, as shown in Fig. 2.

Here, on the TG and DTG curves, and corresponding to point *a*, and somewhat removed from inflexion *b*, of Fig. 1, the retardation of the reaction *a'*, *b'* or peaks *a''*, *b''*, can be seen. The first inflexion *a* is revealed also by the DTA curve, while, no doubt, the second is superimposed by the great endothermic peak due to the enthalpy-change of process III. Also in former experiments on the decomposition of ammonium heptamolybdate, thermograms revealed inflexions that forced us to suppose the appearance of H_2MoO_3 or $9MoO_3 \cdot H_2O$ [15], perhaps of the so-called [3] genotype-hydroxide $Mo_5O_5(OH)_{10}$, intermediaries with the same molecular weight between 1022 and 1026, referred to the initial substance.

In consequence of these findings there emerged the possibility that some correlation may exist between the phenomena noted at various occasions and that these might be connected with the finer details of the decomposition process. Thus we started to study the process more thoroughly, and, to accomplish this task, two methods were mainly applied.

1. In a high temperature X-ray diffraction chamber the change of the diffraction pattern in functions of the stepwise raised temperature was followed up to the formation of MoO_3.

2. Parallel to this, in the oven of the thermobalance the known intermediaries were prepared from 8 to 10 mg samples of the heptamolybdate placed in the centre of a 15 mm ⌀

quartz plate, on the other hand, further specimens were prepared at 10 °C intervals around the inflexions *a* and *b* of Fig. 1. The IR spectra in KBr pellets and also X-ray patterns of every sample were recorded. Thus the optimum conditions of formation of each phase were obtained. Knowing these, from Analar and Tungsram substances the respective samples were repeatedly prepared and identified by diffraction- and spectrum-data.

In this way we found that the inflexion at *a* on the IR gas curve is due to an octamolybdate of a slightly different structure, and that *b* is connected with the formation of two structurally similar yet well distinguishable, hitherto unknown intermediates. Among these the one formed at lower temperature was prepared also in the oven of the thermobalance, the one

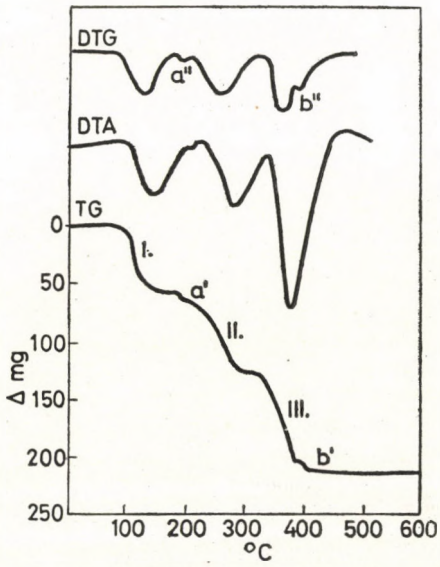

Fig. 2. Derivatographic record of thermal decomposition. Sample weight: 1.3029 g. Sensitivity TG 500 mg, DTG : $\frac{1}{5}$. DTA: $\frac{1}{20}$. Heating rate: 600 °C per hour

formed at higher temperature could be isolated only in the high temperature adapter of the diffractometer, by continuous recording of the changes.

From experimental data there could be deduced the conclusion that in normal atmosphere the domains of existence of the several intermediates of the decomposition series fall within the following limits:

Heptamolybdate	20 ⟶	100 °C
2.5-Molybdate	110 ⟶	160 °C
Octamolybdate	210 ⟶	260 °C
New phase I	260 ⟶	270 °C
New phase II	275 ⟶	280 °C
MoO_3	280 ⟶	°C

The somewhat different octamolybdate structure indicated by the inflexion *a* is formed between 160 and 210 °C.

Determination of the composition of the new phases

The new phases of hitherto unknown structure are formed within a rather narrow temperature range. This causes the difficulty of preparing the new substances in quantities and purity needed for chemical analysis. Thus, with 50 to 100 mg heptamolybdate samples, for example, the mixtures of the phases were obtained because temperature distribution within the

sample was not uniform. The determination of compositions became feasible thereby that compounds with the same IR and X-ray diffraction characteristics as those of the phases obtained by thermal decomposition could be separated from solutions. These compounds obtained by preparative methods were suitable both from the point of view of quantitative analysis and purity.

Though structures with the same spectra and X-ray diffraction pattern need not be of the same composition, we supposed that the compound separated from solution has the same composition as that of "new phase I" obtained by thermal decomposition. This supposition was supported by the experimental fact that "new phase I" was converted via "new phase II" to MoO_3, no matter whether it was prepared from solution or obtained in a thermal process.

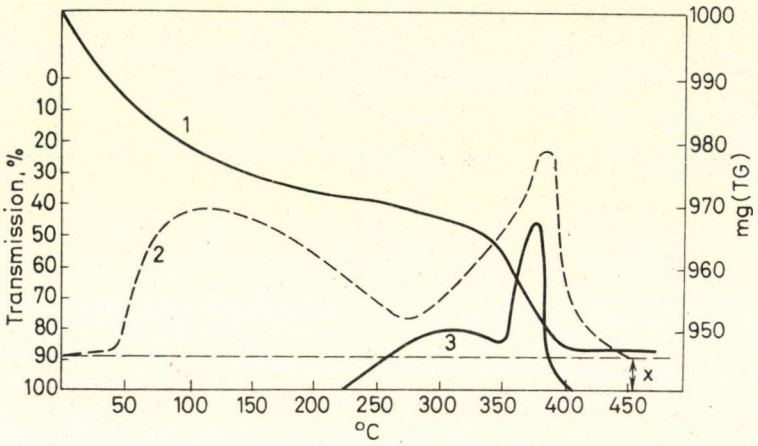

Fig. 3. TG curve and IR spectrum of the gaseous products of 14-molybdate precipitated from solution. Sample weight: 1.00 g. Air flow rate: 16.65 litres per hour. Heating rate: 300 °C per hour. 1. TG curve; 2. IR curve of H_2O; 3. IR curve of NH_3, X denotes the equilibrium moisture content of the carrier gas

Precipitation was carried out as follows: the pH of a 1.8 to 2.6 moles per litre solution of ammonium heptamolybdate tetrahydrate was adjusted to 1.5 with concentrated nitric acid under vigorous stirring. This mixture was heated on a waterbath for two hours, and allowed to settle for 20 hours. The precipitate was collected on a G-4 filter, washed with much water, then with a little alcohol, and dried for one hour in air passed through it by suction.

The same substance was obtained when hydrochloric acid was used for acidification. TG-records and IR gas spectra of the ammonium molybdate of unknown composition thus separated from solution are shown in Fig. 3.

According to Fig. 3, in the decomposition reaction three processes can be distinguished. Up to 220 °C, *i.e.* in the first section of the curve, H_2O is removed. Then, as shown by the ammonium curve of the IR spectra, ammonium is removed in two steps and a further amount of H_2O is set free. In IR spectra and X-ray diagrams of samples heated to various temperatures,

Table I

Analytical data of the composition of new phase I, and new phase II

Substance	per cent			Empirical formulas
	MoO_3	NH_3	H_2O	
Initial	94.81	1.59	3.59	$(NH_4)_2$ 0.14 $MoO_3 \cdot$ 3.3 H_2O
At 360 °C	96.83	1.04	2.13	$(NH_4)_2$ 0.22 $MoO_3 \cdot$ 2.1 H_2O

Table II

Characteristic vibration frequencies of the decomposition series in the domain between 400 and 1000 cm^{-1} (Wave numbers for 14-, and 22-molybdates precipitated from solutions, or thermally prepared, are the same)

7-molybdate 4 H_2O	2.5-molybdate	8-molybdate	14-molybdate	22-molybdate	MoO_3
					485
			526	533	
			650	610	600
		728		710	
	798	754			
841	835				820
868	855	861			
880	873	887			
895	895	895	876	876	880
918		913	915	915	
923	921				
935	933				
		944			
		948			
		958			
			975	978	995

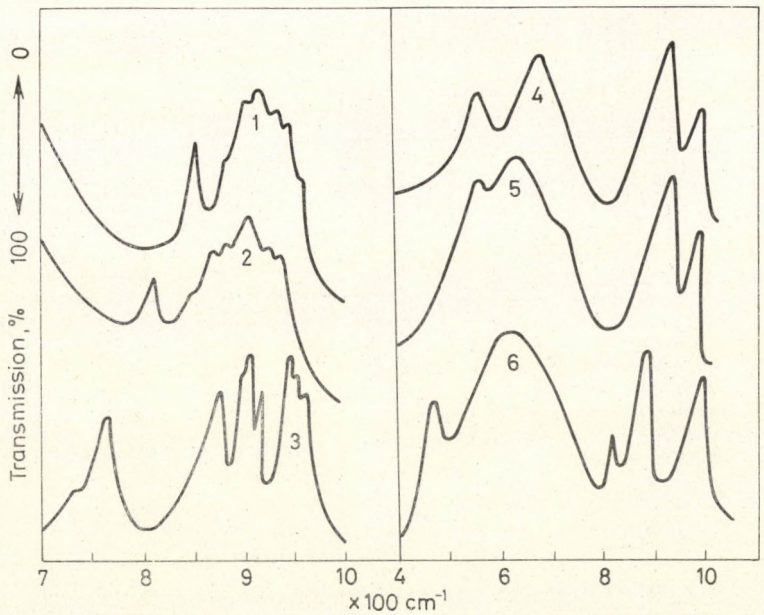

Fig. 4. IR spectra of several phases. 1. 7-molybdate·4 H_2O; 2. 2.5-molybdate; 3. 8-molybdate; 4. 14-molybdate 3. 3 H_2O or 14-molybdate; 5. 22-molybdate 2.13 H_2O, or 22-molybdate; 6. MoO_3

Table III

X-ray diffraction data of 2.5-molybdate powder samples

1	2	3	4	5
d	$\sin^2_{meas.}\theta$	I_{rel}	$\sin^2_{calc.}\theta$	hkl
10.582	0.00528	50	00500	110
8.788	00775	60	00776	112
7.704	01005	60	01000	200
6.618	01353	100	01354	104
6.386	01496	80	01526	212
5.895	01726	50	01725	005
5.264	02137	20	02106	204
4.985	02377	30	02354	214
4.731	02642	30	02621	223
4.105	03522	50	03526	322
3.623	04530	20	04526	412
3.500	04860	15	04871	413
3.451	05010	80	05000	420
3.360	05290	30	05276	422
3.282	05521	50	05604	334
3.068	06316	40	06319	501
3.036	06480	30	06500	510
2.919	06963	30	06984	336
2.877	07230	20	07250	520
2.773	07737	15	—	—
2.623	08617	5	08626	443
2.541	09254	20	09250	610
2.441	10069	30	10069	621

the data characteristic of new phase II emerge between 350 and 360 °C. Table I shows composition according to chemical analysis of samples heated to 360 °C, and of the initial substance.

On the basis of the formulas, the designations 22-molybdate, and 14-molybdate, respectively, will be used for them in what follows, by analogy with the first, the 2.5-molybdate. intermediate. Comparison of Figs. 1 and 3 shows that the substance represented by Fig. 3 is converted to molybdenum trioxide at a higher temperature than is the heptamolybdate. The cause of this resides probably in that the morphological properties, and defect structure of the precipitated 14-molybdate differ from those of the 14-molybdate formed in thermal decomposition.

X-ray diffraction, and IR-spectra, characteristic to the phases

In Fig. 4 the Mo–O stretching vibrations between 800 and 1000 cm^{-1} of the phases isolated during thermal decomposition and of the 14-molybdate precipitated from solution are given. Where it seemed necessary, also the details between 400 and 800 cm^{-1} of the spectrum were considered. Table II contains the wave numbers characteristic of the phases.

Table IV

X-ray diffraction data of new phase I (14-molybdate) powder samples (The diffraction patterns of 14-molybdates prepared thermally, or precipitated from solutions, do not differ)

1	2	3	4	5
d	$\sin^2_{meas.}\theta$	I_{rel}	$\sin^2_{calc.}\theta$	hkl
9.224	0.00737	50	0.00713	110
5.301	02151	5	02138	112
4.585	02863	25	02850	220
3.462	04990	100	04987	123
3.046	06420	70	06413	330
2.889	07146	3	07125	240
2.641	08525	5	08585	224
2.534	09275	60	09263	134, 150
2.153	12840	3	12825	600, 244
2.096	13530	10	13538	235, 116
1.994	14938	20	14963	145
1.947	15660	10	15675	622
1.862	17125	30	17100	444
1.825	17801	10	17913	345, 170
1.757	19214	1	19238	172, 255
1.724	19941	1	19950	642
1.638	22078	40	22088	156, 237
1.588	23485	5	23513	455
1.564	24207	3	24225	802
1.520	25642	1	25650	660
1.499	26359	5	26363	347
1.390	30645	1	30638	556
1.359	32070	5	32063	903

Since the structure of hepta- [6, 7], and octa-molybdate [8], and that of MoO_3 are known [9—12] from X-ray diffraction patterns, only the data from powder diagrams of the 2.5-molybdate, and those of the two new intermediate phases will be given here. Table III contains data of Guinier X-ray records made on 2.5-molybdate with CuK_α rays; Tables IV and V those made on 14-molybdate, and 22-molybdate with FeK_α rays. Column 3 lists intensity values visually estimated; column 4 lists $\sin^2\theta$ values calculable from the edge-length of elementary cells corresponding to the indices in column 5. For all the three substances, the differences between measured and calculated $\sin^2\theta$ values yielded WOLFF—VISSER factors [16] higher than 10, thus indexing can be said to be reliable.

The 2.5-molybdate can be characterized by a tetragonal elementary cell $a = 15.42$ Å, $c = 29.32$ Å; 14-molybdate by a cubic elementary cell $a = 12.90$ Å, 22-molybdate by a hexagonal elementary cell $a = 10.52$ Å, $c = 3.725$ Å.

In connexion with the last two phases it is interesting to note that the dimensions of the cubic cell of the 14-molybdate and those of the hexagonal cell of the 22-molybdate are not quite independent from each other since

$$a_{22,\,hex} \approx \frac{\sqrt{2\,a_{14\,cubic}}}{\sqrt{3}}$$

Table V

X-ray diffraction data of new phase II (22-molybdate) powder samples
The diffraction patterns of 22-molybdate prepared thermally, or precipitated from solutions, do not differ

1	2	3	4	5
d	$\sin^2_{meas.}\theta$	I_{rel}	$\sin^2_{calc.}\theta$	hkl
9.219	0.00687	50	0.00700	100
5.333	02084	5	02100	110
4.616	02781	25	02800	200
3.483	04866	60	04900	210
3.458	04958	60	04980	101
3.053	06367	70	06300	300
2.878	07061	3	07080	201
2.657	08402	5	08400	220
2.543	09173	60	09100	310
2.163	12680	3	12680	221
2.109	13337	10	13300	320
			13380	311
2.006	14744	20	14700	410
1.955	15520	10	15480	401
1.862	17118	30	17120	002
1.837	17581	10	17580	321
1.645	21932	40	21780	501
1.640	22040	30	22020	212
1.597	23283	5	23180	331
1.573	23987	3	23880	421
1.365	31878	5	31900	412

and

$$c_{22,\,hex} = \frac{a_{14\ cubic}}{2\sqrt{3}}$$

A structural relationship between the two compounds is suggested also by their diffraction patterns and infrared spectra. The X-ray record of the 22-molybdate differs from that of the 14-molybdate only in that some lines split into two components and some small shifts occur. In the IR spectrum the band at 650 cm^{-1} is shifted to 610 cm^{-1} and band 530 cm^{-1} is more in coalescence with that at 610 cm^{-1}. Should in the above expressions of parameter a a strict equality prevail, with the hexagonal cell thus resulting the X-ray diffraction pattern of the 14-molybdate could be indexed quite as exactly as with the cubic cell previously used. However, this kind of connexion is trivially given for any cubic cell, and general custom requires that always the possibly largest cell with the highest symmetry should be taken into consideration. The appearance of the 22-molybdate thus raises the question whether it would not be more correct to give a hexagonal cell also for the 14-molybdate. For in this case the transformation between the two molybdates could be regarded as a change of the $\frac{c}{a} = 0.353$ ratio of hexagonal axes to the ratio $\frac{c}{a} = 0.354$ and this would produce the slight splitting of the several spectrum lines.

Table VI

Densities of the several phases

φ	7-molybdate 4 H_2O	2.5-molybdate	8-molybdate	14-molybdate	MoO_3
g/cm³	2.86	3.05	3.13	3.57	4.71

Also the density values of the phases of the decomposition series show continuous change. Data found are listed in Table VI. These dimensions of the unit cells, and densities, being known, it seems to be highly probable the 2.5-molybdate having the formula: $(NH_4)_8[Mo^{O}_{10}{}_{34}]$.

In our further work we try to disclose the molecular and crystal structure of the three phases.

Discussion

According to our results the decomposition of ammonium heptamolybdate tetrahydrate to MoO_3 in air proceeds as follows:

$$(NH_4)_6[Mo_7O_{24}] \cdot 4\,H_2O \xrightarrow{\sim 100\,^\circ C} (NH_4)_2O \cdot Mo_{2.5}O_{7.5} \longrightarrow$$

$$\xrightarrow{\sim 160\,^\circ C} \text{pseudo octamolybdate} \xrightarrow{\sim 210\,^\circ C} (NH_4)_4[Mo_8O_{26}]$$

$$\xrightarrow{\sim 260\,^\circ C} (NH_4)_2O \cdot Mo_{14}O_{42} \xrightarrow{\sim 275\,^\circ C} (NH_4)_2O \cdot Mo_{22}O_{66} \longrightarrow$$

$$\xrightarrow{\sim 280\,^\circ C} MoO_3 < O \cdot 145\,H_2O \xrightarrow{\geqq 300\,^\circ C} MoO_3$$

Thus the number of intermediates with distinct structures in the pathway of thermal decomposition is not less than four. However, the real formulas of the new phases need not be those as given for 14- or 22-molybdates, they can be multiples of these. This will be decided, however, only after detailed determination of the relevant structures.

In the *a* inflexion part of maximum II in Fig. 1, X-ray analysis of the solid phase, and IR spectra, do not suggest a structure fundamentally different from those of known phases. A compound of the composition $(NH_4)_2O \cdot 3.4\,MoO_3$ formed between 160 and 210 °C is well distinguishable from the 2.5-molybdate and differs also from the octamolybdate, though on the grounds of spectral and X-ray diffraction data, octamolybdate structure predominates in it. The existence of 3-molybdate, close to it in composition, has not been verified yet [5]. LINDQVIST supposed [17] that the 3-molybdate is the double salt of hepta- and octamolybdates, but according to MA [5] the structural moiety beside the predominant octamolybdate cannot be heptamolybdate. In view of the decomposition sequence the composition $(NH_4)_2O \cdot 3.4\,MoO_3$ found by us could be approached with a double salt of the 2.5- and octamolybdates

$$(NH_4)_2O \cdot 2.5\,MoO_3 + (NH_4)_2O \cdot 4\,MoO_3 : 2 = (NH_4)_2O \cdot 3.25\,MoO_3.$$

In this way one can suppose that in this domain a double salt of this kind is produced. MA [5] isolated a 3-molybdate phase of similar composition by the thermal decomposition of various molybdates and pointed out the double-salt character of this molybdate. While in the case of the other phases passage through a relatively narrow temperature interval involves rapid rearrangement of the crystal lattice after the collapse of the preceding phase, conversion of 2.5-molybdate into octamolybdate seems not to be such a sharp transition. According to what has been said, the emergence of octamolybdate seems to be preceded by the formation of a double salt, and this process is revealed by point II. in Fig. 2 through a small endothermic peak. Since in the structure here evolved the characteristics of octamolybdate predominate, in the scheme of the decomposition series the designation pseudo-octamolybdate has been written. By further heating above 260 °C, the arrangement of octamolybdate crystal lattices begins.

Prior to the formation of MoO_3, the IR spectrum of the solid phase between 280 and 300 °C shows Mo–O stretching vibrations characteristic to MoO_3. However, at 3420 and 1635 cm^{-1}, respectively, *i.e.* for νHOH, and δHOH frequencies still a weak absorption occurs which is not due to moisture of the potassium bromide pellets. MoO_3 without OH bonds cannot be prepared but by long heating above 300—320 °C. Accordingly, preceding the formation of MoO_3 a species of $MoO_3 \cdot xH_2O$ is produced where $x < 0.1454$ according to our thermogravimetric measurements [3].

Correlations between polycondensation reactions in solution and in solid phase

Comparing the thermal decomposition of heptamolybdate and the polycondensation of molybdate in solution no principal difference can be observed. Thus, in fact, instead of thermal decomposition a thermally effected polycondensation reaction occurs. In solution, polymerisation involving loss of water is caused mainly by the increase of H^+ ion concentration, in the solid phase by heat. During the thermal processes the chemical equilibria, or reversibility, are not assured through overall and partial pressures in the gas-phase while in solution equilibrium conditions exist.

Considering the polycondensation products the polycondensation reactions display both some similarities and some differences.

On perusal of the literature that deals with the processes in solution, the development of two fundamental views may be perceived. According to JANDER *et al.* [18], ions of polycondensation grades 3, 6, 12, and 24 are formed with the decrease of pH values. Other authors, who refer mainly to LINDQVIST [6, 8, 17, 19, 20], accept the existence of mono-, hepta- and octamolybdates

and that of the monomeric cation. In Table VII we compiled the polycondensation products deduced, by the two authors named, from experimental data and, in parallel, the polycondensation products of the thermal decomposition of ammonium paramolybdate, as found by others and by us.

Later authors (DANIELLE [21], GLEMSER [22], AVESTON [23], HALÁSZ and PUNGOR [24]) have supported the view of LINDQVIST (Table VII). How-

Table VII

Comparison of polycondensates formed in solutions, with those formed in solid–phase reactions
Z stands for proton uptake by one mole molybdate calculated from pH and amount of acid added. In order to simplify the notation of polyanions, processes in connexion with protonation are not considered. Since the structures of 2.5-, 14-, and 22-molybdates are not yet definitely established, formulas indicate possible and probable structures

In solutions				In solid phase reactions	
pH	JANDER	*Z*	LINDQVIST	°C	Present authors
>6.5	MoO_4^{2-}		MoO_4^{2-}	20—100	$[Mo_7O_{24}]^{6-}$
6.5—4.5	$[Mo_3O_{11}]^{4-}$			110—160	$[Mo_5O_{17}]^{4-}$ or $[Mo_{10}O_{34}]^{8-}$
4.5—2.5	$[Mo_6O_{21}]^{6-}$	1.14	$[Mo_7O_{24}]^{6-}$	210—260	$[Mo_8O_{26}]^{4-}$
2.5—1.5	$[Mo_{12}O_{41}]^{10-}$	1.5	$[Mo_8O_{26}]^{4-}$	260—275	$[Mo_{14}O_{43}]^{2-}$ or $[Mo_{28}O_{86}]^{4-}$
1.5—0.9	$[Mo_{24}O_{78}]^{12-}$			275—280	$[Mo_{22}O_{67}]^{2-}$ or $[Mo_{42}O_{134}]^{4}$
~0.9	$MoO_3 \cdot xH_2O$			280—300	$MoO_3 \cdot xH_2O$
<0.9	MoO^{4+}	>1.5	MoO_2^{2+}	>300	MoO_3

ever, it is still not clear what happens in the domain between the formation of octamolybdate and that of the monomeric cation.

No doubt, experimental difficulties obstruct the way of the explorations that would elucidate the polycondensation steps in solutions beyond the octamolybdate species. The diffusion method has been criticized by CARPENI [25], SOUCHAY [26], and later by BAKER and POPE [27]. It has been shown that determinations of molecular weights based upon the measurement of the diffusion constants of polyanions is not reliable enough, because the degree of hydration of the ions is not known to sufficient accuracy, and this fact casts some doubt upon the reality of the molybdate condensates proposed by JANDER. With increasing acidity, the accuracy of pH measurements becomes lower; also, due to the similarity of the absorption curves, potentio-spectrophotometric measurements become increasingly difficult to evaluate. Thus, owing to experimental difficulties, processes brought about by stronger acidification could not yet be satisfactorily explained.

Beside those mentioned, others also supposed the existence of the monomeric cation [28, 29] which has been suggested by JANDER *et al.* [30]. The

supporters of LINDQVIST's view allow the existence of ion species substantially fewer in kind than does JANDER, so that according to the former, 2- and 3-molybdates are present in the solution only as intermediates.

There are others whose ideas closely approach JANDER's by accepting the existence of more polycondensation products. Accordingly, di-, tri- and octamolybdate [31, 32], tetramolybdate [33—36], deka- or dodekamolybdate [37], hexa- and dodekamolybdates too [38] are formed in solutions.

Thus this point cannot be considered, by far, as being settled, since the various studies refer to various techniques under various experimental conditions. We wish to compare the polycondensation reactions in solution with those in the solid phase always supposing that in principle, conditions permitting polycondensates identified by several authors can occur in both.

The main common feature of thermal and solution polycondensations is the production of the two polyanions of LINDQVIST, *i.e.* of the hepta- and the octamolybdate, in solution as well as in the solid phase.

The decisive evidence for this was produced by Raman spectra recorded by AVESTON [23]. He measured the Raman-shifts of the solid hepta- and octamolybdates and, through this, has proved the formation of these ions also by polycondensation reactions carried out in solution.

As far as JANDER's series is considered, in possession of the evidence furnished by the authors named, and by AVESTON in particular, we should say that $[Mo_6O_{21}]^{6-}$ is in fact $[Mo_7O_{24}]^{6-}$. BYÉ [39, 40] has shown by conductometric measurements that the ratio $Z = \frac{7\,H^+}{6\,MoO_4^{2-}}$ measured by JANDER for the formation of para-molybdate is, more accurately $Z = \frac{8}{7}$ and from such a system isolated LINDQVIST the heptamolybdate with a composition of $[Mo_7O_{24}]^{6-}$ [6, 17]. It is interesting that the 2.5-molybdate is formed only in solid-state polycondensation. Neither JANDER, nor LINDQVIST and other authors ever mentioned the existence of this species.

The thermal polycondensation subsequent to the formation of octamolybdate proceeds in steps distinctly similar to those suggested by JANDER. There is a certain similarity between the composition of JANDER's 12- or 24-molybdate and the composition of the 14- or 22-molybdate detected in the thermal reaction, of which we leave the charges of the polycondensates out of consideration. However, our experiments suggest that 22-molybdate as well as 24-molybdate may exist each in itself. NEUGEBAUER [41] separated from solution ammonium molybdate with a composition identical with JANDER's 24-molybdate: 5.14 per cent NH_3, 88.0 per cent MoO_3, and 6.8 per cent H_2O. By recoring the infrared spectrum (Fig. 5) and the X-ray diffraction pattern (Table VIII) of this substance, characteristics rather different from those of known ammonium molybdate structures emerge.

Table VIII

X-ray diffraction data of powdered samples of a molybdate with the composition $(NH_4)_2O \cdot Mo_4O_{12}$

Monoclinic, $a = 9.66$ Å, $b = 11.06$ Å, $c = 16.28$ Å, $\beta = 85.4°$

1	2	3	4	5
d	$\sin^2_{found}\theta$	I_{rel}	$\sin^2_{calc}\theta$	hkl
9.6	0.00643	80	0.00643	100
9.2	00712	20	00712	011
7.2	01145	30	01128	110
6.5	01405	30	01431	102
6.0	01649	90	01671	102
5.5	01963	10	01940	020
5.2	02195	10	02167	021
4.8	02577	10	02572	200
4.65	02746	5	02750	121
4.03	03654	30	03632	004, 122
3.90	03903	10	03993	023
3.80	04112	5	04117	014
3.78	04156	10	04205	212
3.70	04335	20	04365	030
3.62	04529	10	04512	220
3.59	04606	20	04619	221
3.47	04931	25	04985	203
3.43	05045	25	05000	114
3.39	05166	25	05175	131
3.30	05450	100	05470	213
3.24	05653	20	05675	005
3.20	05795	20	05787	300

Comparison of spectra in Figs 4 and 5 reveals that the stoichiometrical 24-molybdate has, in fact, a structure that is different from that of the new phase II of the decomposition series. This, at the same time, proves that only similarity exists and that the unusual composition of the new phases is not a consequence of some experimental error.

It may be of interest to note that JANDER builds up the condensation process by a stepwise increase of negative charges, while in the process according to LINDQVIST, at least for the existing members, and in thermal polycondensation, the amount of negative charges decreases.

Though it was not our aim in this work to disclose some questions concerning polycondensation in solutions, our experimental results prompt us to suggest some conclusions. The fact that from not too concentrated solutions,

say from 10^{-1} to 10^{-2} moles per litre, JANDER's 24-molybdate could be precipitated, as could the thermally obtained 14-molybdate, speaks without doubt for the formation, under certain conditions, of ions with polycondensation grades higher than eight. The existence of further, perhaps not yet isolated, polyanions in higher or lower concentrations according to circumstances, may be legitimately supposed. The experimental methods used up to now would

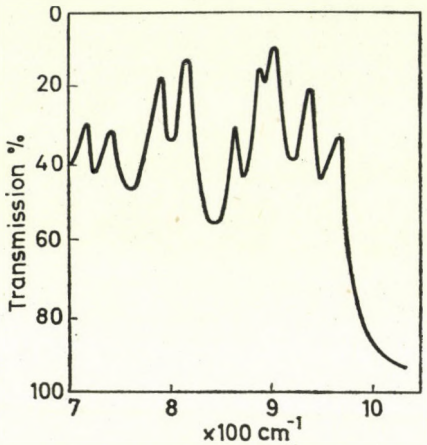

Fig. 5. IR spectrum of a molybdate with the composition $(NH_4)_2O \cdot Mo_4O_{12}$, 712, 742, 790, 816, 863, 900, 938, and 959 cm^{-1}

not be adequate for their study. Neither of the two ways discussed can be said to have been closed, especially the detection of a number of polymers between the monomeric cation and the octamolybdate seems to be possible. Knowledge of the Raman-spectra of the molybdates prepared by us, and of other polymolybdates, allows us to expect that the extension of Raman-spectrometry according to AVESTON will help to elucidate the phenomena not yet fully understood.

REFERENCES

1. DUVAL, C.: Inorganic Thermogravimetric Analysis. pp. 96, 426. Elsevier, Amsterdam, 1963
2. FUNAKI, K., SEVGEWA, T.: J. Electrochem. Soc. Japan **18,** 152 (1950)
3. HEGEDÜS A. J., SASVÁRI, K., NEUGEBAUER, J.: Z. anorg. allg. Chem. **293,** 56 (1957)
4. RODE E. J., TVERDOKHLEDOV, V. N.: Zh. neorg. Khim. **3,** 2343 (1958)
5. MA, E.: Bull. Chem. Soc. Japan **37,** 171 (1964); **37,** 648 (1964)
6. LINDQVIST I.: Arkiv Kemi **2,** 325 (1950); Acta Cryst. **3,** 159 (1950); Acta Chem. Scand. **4,** 1066 (1950)
7. MA (shimao) E.: Bull. Chem. Soc. Japan **40,** 1609 (1967)
8. LINDQVIST, I.: Arkiv Kemi **2,** 349 (1950)
9. BRACKKEN, H.: Z. Krist. **80,** 504 (1931)
10. WOOSTER, N.: Z. Krist. **78,** 484 (1931)
11. ANDERSSON, G., MAGNELI, A.: Acta Chem. Scand. **7,** 793 (1950)
12. KHILBORG, L.: Arkiv Kemi **21,** 357 (1963)
13. HEGEDÜS, A. J., KISS, B. A.: Acta Chim. Acad. Sci. Hung. **51,** 251 (1967); Magy. Kém. Foly. **73,** 41 (1967)

14. KISS, B. A.: Acta Chim. Acad. Sci. Hung. **61**, 207 (1968); Magy. Kém. Foly. **75**, 303 (1968)
15. HEGEDÜS, A. J.: Magy. Kém. Lapja **8**, 146 (1953)
16. DE WOLFF, P. M., VISSER, J. W.: Acta Cryst. **21**, A—11 (1966)
17. LINDQVIST, I.: Nova Acta Regiae Soc. Sci. Upsalic. Ser. IV. 15. No. 1, 1 (1950)
18. Gmelins Ho. anorg. Chem. S-Nr. **53**, 119—121 (1935)
19. LINDQVIST, I.: Acta Chem. Scand. **5**, 568 (1951)
20. SASAKI, I., LINDQVIST, I., SILLÉN, L. G.: J. Inorg. Nucl. Chem. **9**, 93 (1959)
21. DANIELE, G.: Gazz. Chim. Ital. **90**, 1371 (1960)
22. GLEMSER, O., HOLZNAGEL, W., IFTIKHAR Ali S.: Z. Naturforsch. **3**, 192 (1965)
23. AVESTON, J., ANACKER, E. W., JOHNSON, J. S.: Inorg. Chem. **3**, 735 (1964)
24. HALÁSZ, A., PUNGOR, E.: Magy. Kém. Foly. **74**, 545 (1964)
25. CARPENI, G.: Bull. Soc. Chim. France **5**, 14, 484 (1947)
26. SOUCHAY, P.: Bull. Soc. Chim. France **5**, 14, 914 (1947)
27. BAKER, L. C. W., POPE, M. T.: J. Am. Chem. Soc. **82**, 4176 (1960)
28. STRICKLAND, J. D. H.: J. Am. Chem. Soc. **74**, 862 (1952)
29. BABKO, A. K., NABIVANIT, B. J.: Zh. Neorg. Khim. **2**, 2085 (1957)
30. JANDER, C., JAHR, K., HENKESHOVEN, W.: Z. anorg. Chem. **194**, 383 (1930)
31. BELTRAM, J., PUERTA, F.: Anales Real. Soc. Espan. Fis. Quim.; Ser. B. **59**, 271 (1963)
32. RIPAN, R., DUCAN, A., CALU, CL.: Studii Cercetari Chim. (Cluj) **9**, 19 (1958)
33. CANNON, P.: J. Inorg. Nucl. Chem. **9**, 252 (1959)
34. DOUCET, Y., BUGNON, S.: J. Chim. Phys. **54**, 155 (1957)
35. RICHARDSON, E.: J. Inorg. Nucl. Chem. **9**, 267 (1951)
36. COOPER, M. K., SALMON, J. E.: J. Chem. Soc. (London) **1962**, 2009
37. CHALMERS, A. R., SINCLAIR, A. G.: Anal. Chim. Acta **33**, 384 (1965)
38. SCHRIEVER, K., LEETSCH, W.: Naturwiss. **17**, 392 (1962)
39. BYÉ, J.: Bull. Soc. Chim. France **5**, 9, 626 (1942)
40. BYÉ, J.: Ann. Chim. **20**, 463 (1945)
41. NEUGEBAUER, J.: not published

András B. KISS
Pál GADÓ
Iván ASZTALOS
András J. HEGEDÜS

Budapest IV., Váci út 77.

Acta Chimica Academiae Scientiarum Hungaricae, Tomus 66 (3), pp. 251—258 (1970)

DIE REAKTION VON OSMIUMTETROXYD MIT ÄTHYLENDIAMIN

J. NYILASI, P. ORSÓS und E. POMOGÁTS

(Institut für Allgemeine und Anorganische Chemie, Eötvös Loránd Universität, Budapest)

Eingegangen am 11. Juni 1969

Es wurde die Reaktion von Äthylendiamin mit Osmiumtetroxyd untersucht, um zu bestimmen, welcher Anteil des Stickstoffgehalts des Diamins in 0,5 *n* NaOH bei 100 °C in Form von Ammoniak freigesetzt wird bzw. nach dem Ablauf der Reaktion mit dem Kjeldahl-Verfahren bestimmt werden kann.

Es wurde festgestellt, daß die Erhöhung der OsO_4-Konzentration bei gegebenem Äthylendiamingehalt bis zum Molverhältnis 1 Mol Diamin : 2 Mol OsO_4 die Desaminierung begünstigt. Bei einer weiteren Steigerung des OsO_4-Gehalts nimmt das Maß der Ammoniakabspaltung ab und bei einem Molverhältnis von 1 Mol Diamin : 8 Mol OsO_4 wird überhaupt keine Ammoniakentwicklung beobachtet.

Nach der Desaminierung kann solange kein Stickstoff mit dem Kjeldahl-Verfahren gefunden werden, bis 2 oder mehr Mol OsO_4 pro Mol Diamin vorliegen. Die Summe des in Form von Ammoniak bestimmten und des sich als Stickstoffdefizit meldenden Stickstoffgehalts (in Grammatomen) steht in Übereinstimmung mit den Grammatomen Osmium, die im System vorliegen. Die sogenannten Stickstoffdefizitwerte werden aus dem eingewogenen Stickstoffgehalt und der Summe des in Form von Ammoniak frei werdenden bzw. nach dem Kjeldahl-Verfahren bestimmten Stickstoffgehaltes berechnet. Werden die Gemische nach der Desaminierungsreaktion mit Dewarda-Legierung in alkalischem Medium reduziert, so werden Ammoniakstickstoffwerte erhalten, die mit den Stickstoffdefizitwerten identisch sind.

Aufgrund unserer bisherigen Untersuchungen nehmen wir an, daß bei der Reaktion von Äthylendiamin mit Osmiumtetroxyd verschiedene stickstoffhaltige Osmiumkomplexe bzw. in den Osmiumkomplexen verschiedenartig gebundene Stickstoffatome entstehen.

Nach unseren früheren Beobachtungen katalysiert das Osmiumtetroxyd die oxydative Desaminierungsreaktion von zahlreichen Aminen in hohem Maße [1]. Die Deutung des Wirkungsmechanismus des OsO_4-Katalysators wird jedoch durch den Umstand erschwert, daß nur wenig Literaturangaben über die Wechselwirkung zwischen den Aminen und Osmiumverbindungen zu Verfügung stehen. Daher hielten wir die Durchführung solcher Untersuchungen für zweckmäßig.

In der vorliegenden Arbeit wird über unsere Erfahrungen bezüglich der Reaktion von Äthylendiamin mit Osmiumtetroxyd berichtet.

Die Untersuchungen wurden in 0,5 *n* NaOH bei 100 °C durchgeführt. Es wurden Gemische von 7,5 ml Volumen hergestellt, indem zur Lösung von Äthylendiamin (BDH) zuerst das Osmiumtetroxyd (Merck p.a.) und dann das Natriumhydroxyd (Chemapol p.a.) zugegeben wurde. Die Kolben mit den Mischungen wurden sofort in ein Wasserbad von 100 °C gestellt und Stickstoffgas wurde mit einer Geschwindigkeit von 20 Liter/Stunde durchgeleitet.

Der Stickstoff wurde zur Entfernung seines Sauerstoffgehaltes durch eine alkalische Pyrogallollösung und zur Entfernung von eventuellen Ammoniakverunreinigungen durch Schwefelsäure geleitet. In den Absorptionskolben, welche über einen Kühler an die Reaktionskolben angeschlossen waren, befand sich eine bekannte Menge 1/70 *n* Schwefelsäure; durch Rücktitration dieser Schwefelsäure (mit 1/30 *n* NaOH, unter Anwendung von einer Mischung aus Methylrot und Methylenblau als Indikator) in bestimmten Zeitabständen, wurde die Ammoniakbildung im Laufe der Reaktion verfolgt.

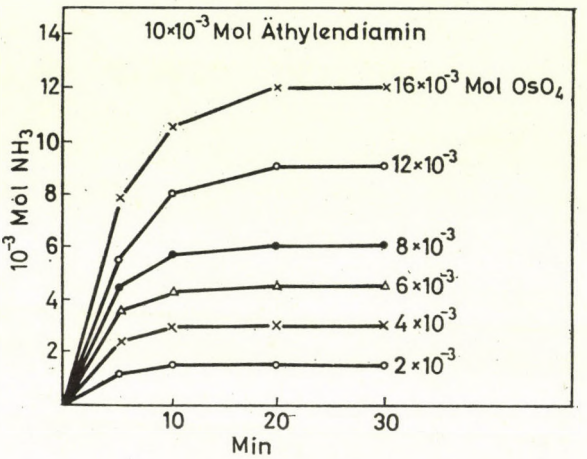

Abb. 1. Zeitliche Änderung der bei 100 °C freiwerdenden Ammoniakmenge. Äthylendiaminkonzentration $10 \cdot 10^{-3}$ Mol

In Abb. 1 ist die zeitliche Änderung der Menge des freigesetzten Ammoniaks bei Gemischen dargestellt, die hinsichtlich ihrer Äthylendiaminkonzentration von $10 \cdot 10^{-3}$ *m* waren und deren Osmiumtetroxydgehalt zwischen $2 \cdot 10^{-3}$ und $16 \cdot 10^{-3}$ Mol lag.

Da die Ammoniakentwicklung auch bei anderen Mol verhältnismäßig rasch aufhört, werden im weiteren nur die im Laufe von 30 Minuten freigewordenen Ammoniakmengen aufgegeben.

In Tab. I sind die aus Mischungen verschiedener Mengen von Äthylendiamin und Osmiumtetroxyd bei 100 °C im Laufe von 30 Minuten abdestillierbaren Mengen von Ammoniakstickstoff angegeben sowie die Ergebnisse der nach der Desaminierung durchgeführten Kjeldahl-Stickstoffbestimmungen. Die letzteren wurden wie folgt ausgeführt: nach halbstündiger Desaminierung wurden zum Gemisch konz. Schwefelsäure, Katalysator (Kupfersulfat, Natriumselenid) und zur Erhöhung des Siedepunktes Kaliumsulfat zugefügt und die Gemische wurden ca. 24 Stunden lang zum Sieden erhitzt. Aus dem Rückstand wurde der Ammoniakgehalt in einer Parnasschen Destil-

Tabelle I

10^{-3} Grammatome Stickstoff	10^{-3} Mol Äthylendiamin							
	1	2	3	4	5	6	8	10
				$4 \cdot 10^{-3}$ Mol OsO_4				
Ammoniak-N	1,5	1,4	1,6	1,3	1,5	1,7	1,4	1,5
Kjeldahl-N	—	2,2	3,8	6,1	8,0	10,0	14,1	18,1
N-Defizit	0,5	0,4	0,6	0,6	0,5	0,3	0,5	0,4
				$4 \cdot 10^{-3}$ Mol OsO_4				
Ammoniak-N	0,9	2,9	3,1	3,0	3,1	2,8	3,2	3,1
Kjeldahl-N	—	—	1,9	3,8	6,0	8,1	11,8	15,8
N-Defizit	1,1	1,1	1,0	1,2	0,9	1,1	1,0	1,1
				$6 \cdot 10^{-3}$ Mol OsO_4				
Ammoniak-N	0,4	2,4	4,5	4,3	4,7	4,5	4,4	4,5
Kjeldahl-N	—	—	—	2,3	3,8	6,2	9,9	13,9
N-Defizit	1,6	1,6	1,5	1,4	1,5	1,3	1,7	1,6
				$8 \cdot 10^{-3}$ Mol OsO_4				
Ammoniak-N	—	2,0	3,9	5,8	6,1	5,9	5,9	6,2
Kjeldahl-N	—	—	—	—	1,9	3,8	8,0	11,8
N-Defizit	2,0	2,0	2,1	2,2	2,0	2,3	2,1	2,0
				$12 \cdot 10^{-3}$ Mol OsO_4				
Ammoniak-N	—	1,1	3,0	5,1	6,9	8,8	9,2	9,1
Kjeldahl-N	—	—	—	—	—	—	3,8	7,7
N-Defizit	2,0	2,9	3,0	2,9	3,1	3,2	3,0	3,2
				$16 \cdot 10^{-3}$ Mol OsO_4				
Ammoniak-N	—	—	1,8	3,7	5,8	7,9	11,8	11,9
Kjeldahl-N	—	—	—	—	—	—	—	3,8
N-Defizit	2,0	4,0	4,2	4,3	4,2	4,1	4,2	4,3

liervorrichtung durch Zugabe von 40%iger Natronlauge freigesetzt und mit Wasserdampf in 2%ige Borsäurelösung abdestilliert.

In Tab. I sind außerdem die Werte des sogenannten Stickstoffdefizits angegeben. Letzterer ergibt sich aus dem Vergleich des Stickstoffgehalts der eingewogenen Amminmenge und der Summe des Ammoniak- bzw. Kjeldahl-Stickstoffs.

Aus den Angaben der Tabelle kann festgestellt werden, daß kein Ammoniak frei wird, wenn pro Grammatom Stickstoff 4 Grammatome Osmium oder mehr vorliegen. Bei Erhöhung der Äthylendiaminkonzentration erfolgt Desaminierung, jedoch nur bis zum Molverhältnis von 1 Mol Äthylendiamin : 2 Mol Osmiumtetroxyd. Durch weitere Steigerung des Äthylendiamingehalts wird keine weitere Ammoniakentwicklung herbeigeführt.

Nach der Desaminierung kann mit der Kjeldahl-Methode nur dann Stickstoff nachgewiesen werden, wenn das Molverhältnis von 1 Mol Diamin : 2

Mol OsO_4 überschritten war. Außerdem kann beobachtet werden, daß die Summe der in Form von Ammoniak bestimmten Stickstoff-Grammatome und der Stickstoffdefizit mit der Grammatomzahl des im System befindlichen Osmiums übereinstimmt.

Bezüglich des Stickstoffdefizits dachten wir zunächst an die Bildung von Nitrit oder Nitrat. Jedoch konnte die Gegenwart solcher Verbindungen im Rückstand nach der Desaminierung nicht festgestellt werden. Es muß also angenommen werden, daß bei der Reaktion solche stickstoffhaltige organische Verbindungen oder Osmiumkomplexe entstehen, deren Stickstoffgehalt mit dem Kjeldahl-Verfahren nicht bestimmt werden kann. Als weitere Möglichkeit konnte an das Entweichen von molekularem Stickstoff aus dem System gedacht werden.

Um diese Frage zu prüfen, wurden Versuche mit verschiedenen Gemischen durchgeführt. Zum Rückstand wurde nach der Desaminierung Dewarda-Legierung gegeben, und ungefähr eine Stunde lang wurde Stickstoffgas durch das alkalische Reaktionsgemisch geleitet, wobei das entweichende Ammoniak in 1/70 *n* Schwefelsäure aufgefangen wurde.

Die auf diese weise bestimmten Stickstoffmengen sind in Tab. II angeführt. Ein Vergleich mit den entsprechenden Stickstoffdefizitwerten in Tab. I

Tabelle II

Nach halbstündiger Desaminierung durch Reduktion mit Dewarda-Legierung in alkalischem Medium in Form von Ammoniak bestimmte Stickstoffmengen

OsO_4, 10^{-3} Mol	Äthylendiamin, 10^{-3} Mol	Ammoniak-N, 10^{-3} Grammatome
2	1	0,4
2	2	0,6
2	4	0,5
2	8	0,6
4	1	1,0
4	2	0,8
4	4	1,1
4	8	0,9
8	1	1,8
8	2	2,0
8	4	2,2
8	8	2,1
16	1	1,8
16	2	4,1
16	4	4,3
16	8	4,3

zeigt gute Übereinstimmung. Diese Beobachtung — obwohl sie keine Erklärung für den Ursprung des Stickstoffdefizits liefert — schließt die Möglichkeit aus, daß die Ursache des Stickstoffdefizits in der Bildung von molekularem Stickstoff zu suchen wäre.

Sämtliche angeführten Untersuchungen wurden auch so ausgeführt, daß anstelle von Stickstoffgas Argongas durch das Reaktionsgemisch geleitet wurde. Jedoch ergaben sich dabei keinerlei Abweichungen außerhalb der Versuchsfehlergrenzen, im Vergleich zu den mit Stickstoff erhaltenen Ergebnissen.

Das Ziel unserer weiteren Versuche war, festzustellen, welche Stickstoffdefizite auftreten, wenn die alkalischen Gemische 30 Minuten lang bei 100 °C stehen gelassen werden, ohne Stickstoffgas durchzuleiten.

In Tab. III sind die nach halbstündigem Stehen und anschließender Zerstörung mit Schwefelsäure bestimmten Kjeldahl-Stickstoffwerte und die aufgrund der eingewogenen Diaminmengen berechneten Stickstoffdefizitwerte angegeben.

Beim Vergleich der Stickstoffdefizitwerte in Tab. I und III zeigt sich, daß diese Werte nur bei dem Molverhältnis 16 Mol OsO_4 : 2 Mol Diamin (d. h.

Tabelle III

Nach halbstündigem Stehen bei 100 °C bestimmte Stickstoffmengen

OsO_4, 10^{-3} Mol	Äthylendiamin 10^{-3} Mol	Kjeldahl-N 10^{-3} Grammatome	N-Defizit 10^{-3} Grammatome
2	2	3,2	0,8
2	4	6,9	1,1
2	8	14,8	1,2
4	2	1,9	2,1
4	4	6,1	1,9
4	8	13,8	2,2
6	2	1,0	3,0
6	4	5,2	2,8
6	8	13,1	2,9
8	2	—	4,0
8	4	4,1	3,9
8	8	12,0	4,0
12	2	—	4,0
12	4	2,3	5,6
12	8	9,8	6,2
16	2	—	4,0
16	4	—	8,0
16	8	7,8	8,2

4 Mol OsO_4 : 1 Grammatom N) übereinstimmen. Bei Gemischen, wo eine Desaminierung zu beobachten war, sind die Stickstoffdefizitwerte in Tab. I und III in sämtlichen Fällen unterschiedlich.

Um die Übersicht zu erleichtern, sind die Meßergebnisse zusammenfassend auch in Abb. 2 und 3 dargestellt.

Die Angaben in Abb. 2 beziehen sich auf diejenigen Versuche, in denen die Molzahl von OsO_4 konstant gehalten und die Molzahl des Äthylendiamins verändert wurde. In den in Abb. 3 angeführten Versuchen war dagegen der Äthylendiamingehalt konstant und die Molzahl des OsO_4 wurde verändert.

Aufgrund der bisherigen Ergebnisse kann entweder angenommen werden, daß bei der Reaktion von Äthylendiamin und OsO_4 in alkalischer Lösung verschiedene stickstoffhaltige Verbindungen bzw. Osmiumkomplexe entstehen, oder aber, daß in den entstehenden Verbindungen bzw. Komplexen verschiedenartig gebundene Stickstoffatome vorhanden sind.

Bezüglich der letzteren Annahme sollen die Mitteilungen von WATT, POTRAFKE und MCMORDIE [2] erwähnt werden, nach denen bei der Reaktion von Osmiumtetroxyd mit flüssigem oder gasförmigem Ammoniak Komplexe folgender Struktur entstehen:

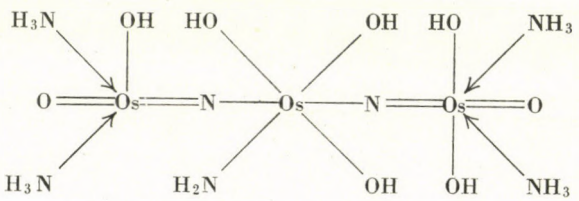

Von den im Komplexmolekül befindlichen sieben Stickstoffatomen werden durch Einwirkung von Natriumhydroxyd nur vier Atome in Form von Ammoniak abgespalten.

Unsere eigenen Versuche zeigten folgendes: werden verschiedene Mengen von Osmiumtetroxyd mit einer wäßrigen Ammoniaklösung vermischt und wird soviel NaOH zugegeben, daß eine 0,5 *n* Lösung ensteht, worauf das Gemisch eine halbe Stunde lang bei 100 °C stehen gelassen und danach eine halbe Stunde mit Stickstoffgas begast wird, so ergibt sich auch in diesen Versuchen ein Stickstoffdefizit, dessen Wert dem Verhältnis 1 Mol OsO_4 : 1 Grammatom N entspricht (Tab. IV).

Unter diesen Bedingungen besteht die Möglichkeit der Bildung von Nitridoosmat $[OsO_3N]^-$ [3]. Diese Verbindung wurde auch auf präparativem Wege hergestellt [4] und es wurde festgestellt, daß ihr Stickstoffgehalt in 0,5 *n* NaOH bei 100 °C auch in Gegenwart von OsO_4 nicht in Form von Ammoniak abgespalten wird. Der Stickstoffgehalt von Kaliumnitridoosmat (VIII) kann auch nach der Zerstörung mit konz. Schwefelsäure nicht gemessen wer-

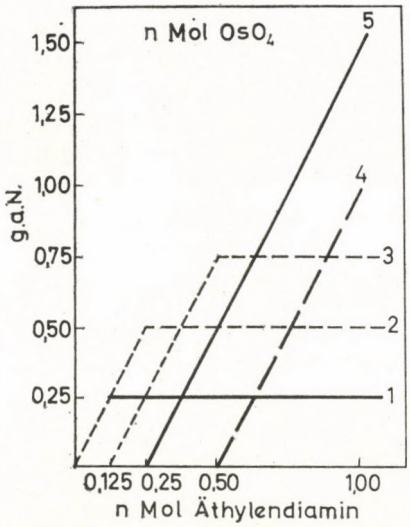

Abb. 2. Nach halbstündigem Stehen bei 100 °C bzw. nach der Desaminierung gemessene Stickstoffmengen bei verschiedenen Molverhältnissen des Äthylendiamins zu *n* Mol Osmiumtetroxyd. 1 — Stickstoffdefizit nach der Desaminierung; 2 — Stickstoffdefizit nach halbstündigem Stehen; 3 — bei N_2-Begasung in Form von Ammoniak freiwerdender Stickstoff; 4 — nach der Desaminierung mit dem Kjeldahl-Verfahren gemessener Stickstoff; 5 — nach halbstündigem Stehen mit dem Kjeldahl-Verfahren gemessener Stickstoff

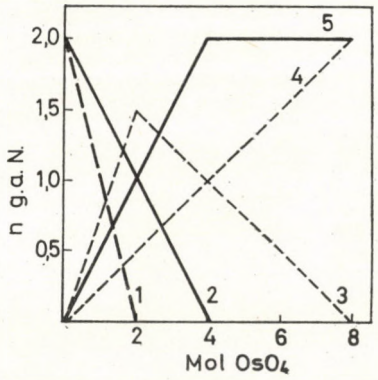

Abb. 3. Nach halbstündigem Stehen bei 100 °C bzw. nach der Desaminierung gemessene Stickstoffmengen bei verschiedenen Molverhältnissen des Osmiumtetroxyds zu *n* Mol Äthylendiamin. 1 — Nach der Desaminierung mit dem Kjeldahl-Verfahren gemessener Stickstoff; 2 — nach halbstündigem Stehen bei 100 °C mit dem Kjeldahl-Verfahren gemessener Stickstoff; 3 — bei N_2-Begasung in Form von Ammoniak freiwerdender Stickstoff; 4 — Stickstoffdefizit nach der Desaminierung; 5 — Stickstoffdefizit nach halbstündigem Stehen

den, läßt sich hingegen nach Reduktion mit Dewarda-Legierung in alkalischem Medium quantitativ bestimmen.

Da bezüglich der Reaktion des Osmiumtetroxyds mit Äthylendiamin noch verschiedene Fragen offen bleiben, setzen wir unsere diesbezüglichen Untersuchungen weiter fort.

Tabelle IV

Nach halbstündigem Stehen bei 100 °C bestimmte Stickstoffmengen

OsO_4, 10^{-3} Mol	NH_4OH, 10^{-3} Mol	Ammoniak-N, 10^{-3} Grammatome	N-Defizit, 10^{-3} Grammatome
2	2	—	2,0
2	4	2,1	1,9
2	8	5,8	2,2
4	2	—	2,0
4	4	—	4,0
4	8	4,2	3,8
8	2	—	2,0
8	4	—	4,0
8	8	—	8,0

LITERATUR

1. NYILASI, J.: Magy. Kém. Foly. **66,** 313 (1960); **67,** 52, 269 (1961). Acta Chim. Acad. Sci. Hung. **25,** 49 (1961); **30,** 221 (1962)
NYILASI, J., SOMOGYI, P.: Ann. Univ. Sci. Budapest. Sect. Chim. **6,** 139 (1964)
2. WATT, G. W., POTRAFKE, E. M.: J. Inorg. Nucl. Chem. **17,** 248 (1961)
WATT, G. W., MCMORDIE, W. C.: J. Inorg. Nucl. Chem. **27,** 2013 (1965)
GRIFFITH, W. P.: The chemistry of the rarer platinum metals. Interscience Publishers, London—New York—Sidney, 1967
3. WERNER, A., DINKLAGE, K.: Berichte **34,** 2698 (1901)
JAEGER, F. M., ZANSTRA, J. E.: Proc. Acad. Amsterdam, **35,** 610 (1932); Rev. Trav. Chim. P. B. **51,** 1031 (1932)
4. CLIFFORD, A. F., KOBAYASHI, C. S.: Inorg. Synth. **6,** 204 (1960)

János NYILASI
Piroska ORSÓS
Erzsébet POMOGÁTS
Budapest VIII., Múzeum krt. 6—8.

Acta Chimica Academiae Scientiarum Hungaricae, Tomus 66 (3), pp. 259—267 (1970)

INVESTIGATION OF THE DIELECTRIC AND VOLUMETRIC PROPERTIES OF THE ACETIC ACID–CHLOROFORM MIXTURE

F. RATKOVICS, T. SALAMON and M. LÁSZLÓ

(Physico-Chemical Department of the Chemical University, Veszprém, Research Group for Electrochemistry of the Hungarian Academy of Sciences, Budapest)

Received June 30, 1969

The authors studied the system acetic acid–chloroform, and report on experimental results obtained in the investigation of the change in mixing volume, the dependence of the dielectric constant and the refractive index in visible light on the composition. These investigations show that the dielectric properties of the mixture cannot be interpreted on the basis of the model for the ternary system A–A_2–B, discussed in earlier communications, because presumably monomeric acetic acid forms also with chloroform an associate of the type AB by hydrogen bonding.

In our earlier communications the properties of mixtures have been studied, in which the molecules of one of the components form associated by the formation of one or more hydrogen bondings [1, 2]. The other component mixed with the associative component was generally a hydrocarbon or carbon tetrachloride. Changes in the mixing properties were explained on the basis of a model established for the ternary system A–A_2–B. In continuation of this work, we wished to investigate a system, in which associates of other composition than A_2 may also be formed. We studied the dielectric properties of the acetic acid–chloroform mixture, and could not explain the properties of this mixture on the basis of the model A–A_2–B, so that presumably this mixture contains besides A_2 also associates of other composition.

Measuring method and experimental results

Substances used in the experiments were purified as follows: An appropriate amount of acetic anhydride was added to a 96 per cent acetic acid of commercial grade, and the mixture was repeatedly distilled. The product, which contained about 0.1 per cent of water, was further purified by repeated freezing (4 to 5 times) until a freezing point of 16.26 °C was reached. The required purity was checked by the measurement of the dielectric constant, because the slightest water impurity renders acetic acid conductive. Pure acetic acid was protected from atmospheric humidity during the measurements.

The purity of chloroform of analytical grade was checked after repeated distillation on a packed column by the measurement of the refractive index. The refractive index of the chloroform used in the experiments, referred to the Na_D line was 1.4486 at 15 °C, in accordance with data reported in the literature [3].

The change in volume on mixing of the acetic acid–chloroform mixture was determined from density data. The density of the mixture was measured at 20 and 40 °C with a picnometer, in function of the nominal composition.

The dielectric constant was measured in function of the composition with a Model TR-9701 dielectric constant and loss factor measuring bridge. Our investigations showed that

the dielectric constant of the mixture can be readily measured in the frequency range from 100 to 300 KHz. Dielectric constants were calculated from capacity values measured at a frequency of 200 KHz. For the measurements at 20 and 40 °C, an acid-resistant steel measuring cell of 10 pF basic capacity, surrounded by a thermostat jacket, was used. Since pure acetic acid is strongly hygroscopic, the cell was air-tightly sealed with Teflon during the measurements. The error of the dielectric constant measurement was found to be less than 2 rel. per cents. The refractive index of the mixture in function of the nominal composition was measured with an Abbé refractometer. For the characterization of the dispersion properties of the mixture, the Abbé-number $\left(\nu_m = \frac{n_D - 1}{n_F - n_C}\right)$ was also determined, however, incertitudes in the determination of dispersion do not permit a quantitative evaluation. (ν_m is the Abbé-number, while n_D, n_F and n_C are the refractive indexes measured in the given order at the wavelengths of the D line of sodium and the β and α lines of hydrogen.)

Experimental results measured at 20 and 40 °C are summarized in Table I in dependence of the nominal composition of the mixture, and plotted in Figs 1—4.

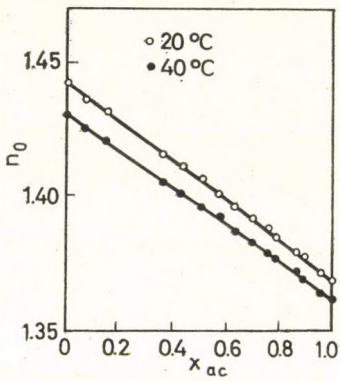

Fig. 1

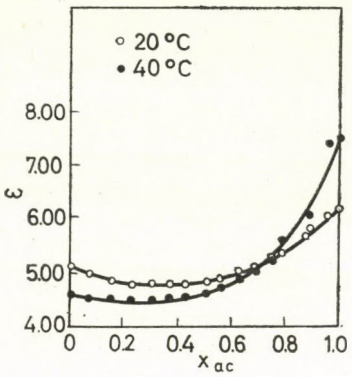

Fig. 2

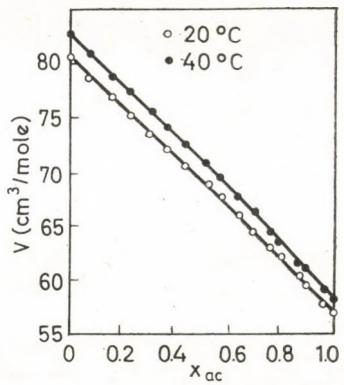

Fig. 3

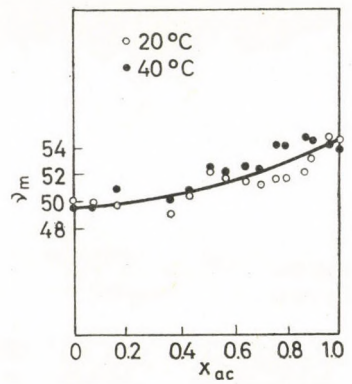

Fig. 4

Table I

Volumetric and dielectric data of the system acetic acid–chloroform

X_{ac}	ε		V cm³ · mole⁻¹		n_D		v_m	v_m
	t(°C) 20	40	20	40	20	40	20	40
0.0000	5.10	4.59	80.789	82.874	1.4427	1.4303	50.0	49.6
0.0822	4.97	4.55	78.916	81.006	1.4367	1.4254	49.8	49.5
0.1640	4.84	4.51	77.070	79.043	1.4318	1.4204	49.7	50.9
0.2331	4.81	4.48	75.481	77.508	—	—	—	—
0.3097	4.78	4.49	73.713	75.727	—	—	—	—
0.3691	4.77	4.51	72.404	74.332	1.4160	1.4059	49.1	50.2
0.4356	4.77	4.55	70.880	72.755	1.4109	1.4010	50.5	50.8
0.5083	4.80	4.60	69.168	70.967	1.4066	1.3964	52.1	52.4
0.5658	4.90	4.74	68.027	69.794	1.4016	1.3929	51.8	52.1
0.6342	5.00	4.90	66.198	67.983	1.3958	1.3870	51.5	52.6
0.6942	5.10	5.06	64.752	66.410	1.3922	1.3831	51.3	52.4
0.7577	5.32	5.23	63.182	63.827	1.3887	1.3792	51.8	54.2
0.7928	5.38	5.58	62.332	63.827	1.3855	1.3771	51.7	54.1
0.8710	5.71	—	60.422	61.824	1.3796	1.3715	52.1	54.7
0.8967	5.83	6.08	59.788	61.168	1.3775	1.3698	53.2	54.5
0.9674	6.06	7.43	58.014	59.325	1.3720	1.3642	54.7	54.1
1.0000	6.20	7.53	57.173	58.453	1.3693	1.3613	54.5	53.9

Discussion

First the deviation of the molar volume of the mixture from the additivity valid for ideal mixtures was investigated. Table II contains the $V—V^*$ values, that is to say, the difference between the measured molar volumes and those calculated for ideal mixtures, at 20 and 40 °C in dependence of the composition. It will be seen that the deviation from additivity is positive and increases with increasing temperature, however, it amounts only to a few tenths per cent of the molar volume. The results are shown in Fig. 5.

Next, the mole polarization of the mixture was calculated in dependence of the composition by means of the following relationship:

$$P_{M\,\text{mixture}} = \frac{\varepsilon - 1}{\varepsilon + 2} \cdot V \qquad (1)$$

where

P_M is the mole polarization and
ε is the dielectric constant.

Table II

The excess mol volume of the acetic acid–chloroform mixture

X_{ac}	$V-V^*$ at 20 °C	$V-V^*$ at 40 °C
0.0000	0.00	0.00
0.0822	0.05	0.14
0.1640	0.15	0.17
0.2332	0.20	0.33
0.3097	0.24	0.42
0.3691	0.33	0.47
0.4356	0.38	0.52
0.5083	0.39	0.51
0.5658	0.60	0.74
0.6342	0.39	0.60
0.6942	0.36	0.49
0.7066	0.37	0.46
0.7577	0.29	0.36
0.7928	0 27	0.31
0.8710	0.20	0.22
0.8967	0.17	0.19
0.9522	0.09	−0.15
0.9674	0.07	0.07
1.0000	0.00	0.00

The mole polarization of the mixture, considered as ideal, was then calculated from the mole polarization of the pure components with the aid of the following relationship:

$$P^*_{M\,\text{mixture}} = \sum_i P_{Mi} X_i \qquad (2)$$

The difference, $P^*_{M\,\text{mixture}} - P_{M\,\text{mixture}}$, representing the magnitude of deviation from the ideal value, was plotted in function of the nominal composition. It was found that the mole polarization of the mixture differs substantially from the mole polarization of the ideal mixture. This difference increases with increasing temperature, and amounts to about 10 per cent.

When the above calculations were applied to the mole refractions, calculated from the refractive index and density data with the substitution $\varepsilon = n_D^2$, it was found that the mole refraction of our mixture follows the rule of additivity valid for ideal mixtures with a relative deviation of less than 1 per cent. Our calculations pertinent to mole polarization and mole refraction are contained in Table III, and shown in Figs 6, 7 and 8.

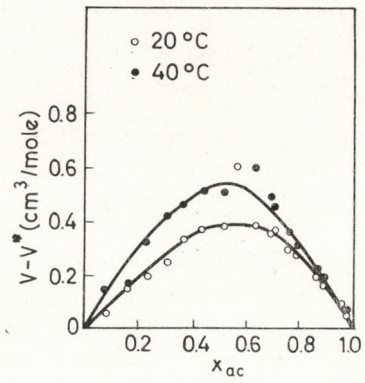

Fig. 5

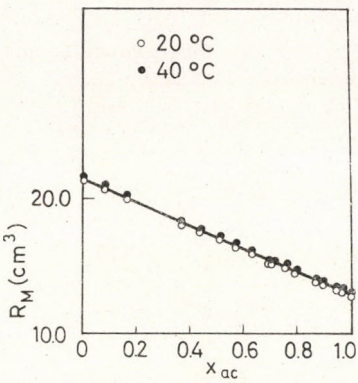

Fig. 6

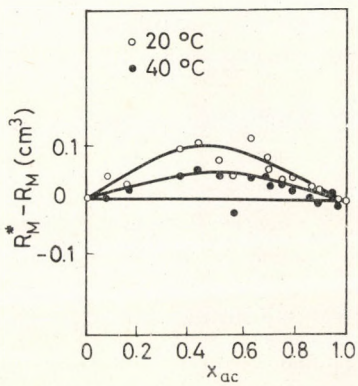

Fig. 7

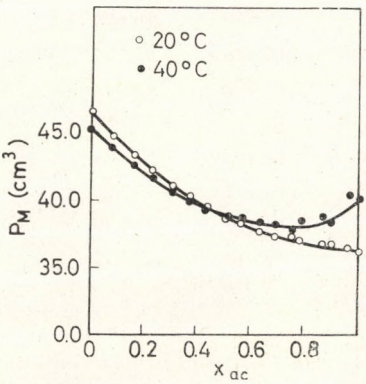

Fig. 8

Since the mole refraction is practically independent of the interaction of adjacent molecules, and neither can atom polarization change perceptibly during association, it was assumed that changes taking place during mixing do not influence the displacement polarization of the mixture.

This assumption means that the deviation of the mole polarizations from additivity is caused by a change in directional polarizations. The change of directional polarization was interpreted as a phenomenon due to the association of the components. For the determination of the directional polarization of the mixture a knowledge of the directional polarization of the pure components is necessary.

The directional polarization of pure acetic acid was calculated as follows. From the known values of the dielectric constant and the mole volume the mole polarization was calculated. From this value, the displacement polarization, calculated from the refractive index relative to light of infinite wavelength

Table III

Polarizations in the acetic acid–chloroform mixture

X_{ac}	R_M 20 °C	R_M 40 °C	$R_M^*-R_M$ 20 °C	$R_M^*-R_M$ 40 °C	P_M 20 °C	P_M 40 °C
0.0000	21.405	21.430	0.000	0.000	46.647	45.141
0.0822	20.662	20.729	0.044	0.002	44.942	43.897
0.1640	19.981	20.019	0.031	0.018	43.266	42.612
0.2331	—	—	—	—	42.224	41.621
0.3097	—	—	—	—	41.095	40.718
0.3691	18.169	18.254	0.100	0.043	40.314	40.072
0.4356	17.595	17.676	0.109	0.056	39.465	39.425
0.5083	17.012	17.067	0.075	0.048	38.651	38.705
0.5658	16.550	16.653	0.048	−0.026	38.449	38.721
0.6342	15.899	16.004	0.118	0.042	37.825	38.423
0.6942	15.426	15.494	0.081	0.043	37.387	38.185
0.7577	14.932	14.966	0.036	0.032	37.283	37.868
0.7928	14.624	14.683	0.046	0.017	36.987	38.564
0.8790	13.982	14.034	0.024	0.003	36.905	38.868
0.8967	13.767	13.828	0.020	−0.009	36.877	38.456
0.9674	13.185	13.229	0.002	−0.011	36.415	40.447
1.0000	12.910	12.942	0.000	0.000	36.253	40.051

(n_∞) [4] was subtracted. In calculating the displacement polarization, consideration was given to the fact that the value of $P_{\text{displ.}}$ does not change with temperature. According to our calculations, the directional polarization of pure acetic acid is 15.584 cm³ at 20 °C, and 19.379 cm³ at 40 °C. The increase of the directional polarization is caused by the suppression of the dimerization equilibrium, because the permanent dipole moment of the monomeric molecules is larger than that of dimeric acetic acid, where the dipole moments of the associating monomeric molecules compensate at least partly each other. (Some authors consider the dipole moment of dimeric acetic acid as zero [5].)

The directional polarization of pure chloroform was determined from the mole polarizations calculated from data measured at 20 and 40 °C [6]. We obtained for the dipole moment 1.0644 Debye, for the displacement polarization 21.901 cm³ at 20 °C and 21.9904 cm³ at 40 °C, and for n_∞ 1.45325 at 20 °C and 1.44250 at 40 °C. Considering the displacement polarization as independent of temperature, this resulted for the directional polarization 24.6974 cm³ at 20 °C and 23.1915 cm³ at 40 °C.

The directional polarization of the mixture considered as ideal (P_i^*) was calculated from the directional polarizations of the pure components on

the basis of the following relationship

$$P_i^*{}_{\text{mixt.}} = \sum_j P_{i,j} X_j \tag{3}$$

The true directional polarization of the mixture was determined by the relationship

$$P_i = P_M - P_{\text{displ., mixture}} \tag{4}$$

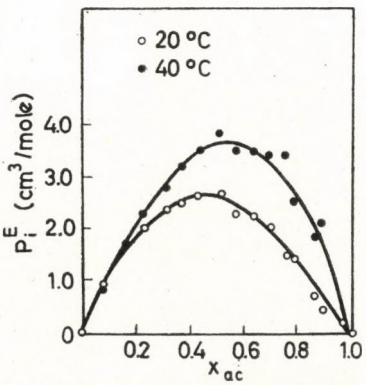

Fig. 9

where P_M is the mole polarization of the mixture according to Eq. (1), while the displacement polarization, considered as additive, is:

$$P_{\text{displ., mixture}} = \sum_j P_{\text{displ.}\,j} X_j \tag{5}$$

In these calculations, the value of the displacement polarization was considered as additive, since it is to be presumed that it changes only to a very slight degree due to possible complex formation. The excess value of directional polarization, defined by the equation

$$P_i^E = P_i^* - P_i\,,$$

representing the deviation of the directional polarization from additivity, was considered as a measure of the association. It can be seen from Fig. 9 that the maximum of the curve P_i^E *vs.* X_{ac} is exhibited near the value $X_{\text{ac}} = 0.5$, which permits to follow on the formation of associates of the type A_iB_i besides the type A_2 (where X_{ac} is the nominal mole fraction of acetic acid). P_i^E data are given in Table IV.

Table IV

Excess values of the directional polarization of the acetic acid–chloroform system

X_{ac}	P_f^E 20 °C	P_f^E 40 °C
0.0000	0.00	0.00
0.0822	0.85	0.83
0.1640	1.67	1.69
0.2331	2.00	2.33
0.3097	2.33	2.85
0.3691	2.49	3.19
0.4356	2.65	3.50
0.5083	2.71	3.85
0.5658	2.31	3.54
0.6342	2.23	3.49
0.7577	1.49	3.42
0.7928	1.42	2.54
0.8710	0.69	1.84
0.8967	0.45	2.12
0.9674	0.18	−0.23
1.0000	0.00	0.00

In the whole concentration range, the true (measured) directional polarization of the mixture is smaller than the directional polarization of the mixture considered as ideal. Thus, the value of the average dipole moment corresponding to one molecule is diminished in the mixture by the processes taking place during mixing. If this phenomenon would be interpreted by an increase in number of the associates of type A_2, that is to say, if it would be assumed that the equilibrium of the dimerization reaction is shifted towards association under the action of the solvent, the place of the maximum should shift towards the value $X_{ac} = 1$. However, since the maximum is exhibited in the vicinity of $X_{ac} = 0.5$, it must be assumed that the associate A_iB_i is also formed in the mixture besides the associate A_2.

Further investigations are planned for the final answer to this problem. However, on the basis of work done so far, it seems as proved that in the system acetic acid–chloroform also acetic acid–chloroform associates are formed besides dimeric acetic acid. The question, how many acetic acid molecules and how many chloroform molecules are linked to the associate of type A_iB_i could not be unequivocally cleared on the basis of data available so far. However, we presume the existence of 1 : 1 associates, that is to say that one acetic acid molecule is linked to one chloroform molecule.

Symbols

n_D	refractive index referred to the D line of sodium
$P_{\text{displ.}}$	displacement polarization
P_i	directional polarization
P_i^*	calculated directional polarization of the mixture considered as ideal
P_i^E	excess value of directional polarization
P_M	mole polarization
P_M^*	calculated mole polarization of the mixture considered as ideal
R_M	mole refraction
R_M^*	calculated mole refraction of the mixture considered as ideal
V	molar volume of the mixture
V^*	calculated molar volume of the mixture considered as ideal
X_{ac}	mole fraction of acetic acid in the mixture
ε	dielectric constant
ν_m	Abbé number

REFERENCES

1. Ratkovics, F.: Magy. Kém. Foly. **72,** 186 (1966)
2. Liszi, J., Ratkovics, F., Salamon, T.: Magyar Kém. Foly. **72,** 546 (1966)
3. D'ans Lax: Taschenbuch für Chemiker und Physiker II. Springer-Verlag, Berlin, 1964
4. Liszi, J.: Magy. Kém. Foly. **75,** 159 (1969)
5. Affsprung, H. E., Findenegg, G. H., Kohler, F.: J. Chem. Soc. A **1968,** 1364
6. Erdey-Grúz, T., Schay, G.: Elméleti Fizikai Kémia I. Tankönyvkiadó, Budapest, 1962

Ferenc Ratkovics
Tamás Salamon
Mária László

Veszprém, Schönherz Z. u. 12. Hungary.

Acta Chimica Academiae Scientiarum Hungaricae, Tomus 66 (3), pp. 269—275 (1970)

THE ELIMINATION OF RESISTANCE POLARIZATION IN POTENTIOSTATIC INVESTIGATIONS

J. DÉVAY, B. LENGYEL jr. and L. MÉSZÁROS

(Department for Physical Chemistry, University for Chemical Engineering, Veszprém and Research Group for Electrochemistry of the Hungarian Academy of Sciences, Budapest)

Received June 9, 1969

A method was developed for the measurement and the automatic compensation of the ohmic potential drop arising on the cell resistance during polarization experiments carried out by means of a potentiostat. The method is based on the following principle: An a.c. current having an amplitude proportional to the intensity of the d.c. current flowing through the cell under investigation is superimposed on the cell current, hence the a.c. voltage measured between the reference electrode and the working electrode is proportional to the d.c. potential arising on the resistance of the solution. The a.c. voltage is amplified and is added, after rectification, to the d.c. voltage controlling the potentiostat. Thus the potential of the working electrode is always maintained at a desired value, independently of the resistance of the cell.

Potentiostatic measuring techniques are widely used in electrochemical investigations and corrosion studies. In potentiostatic measurements a three-electrode cell configuration is employed. The measuring electrode is maintained at a desired potential as compared to the reference electrode by means of an electromechanical or electronic device. This is attained by changing the output voltage of the supply source, *i.e.* the direct current flowing between the counter-electrode and the measuring electrode, proportional to the difference between the potential of the measuring electrode as compared to the reference electrode and the adjusted voltage, until this difference becomes zero.

It is obvious from what was said above that the potentiostat stabilizes the potential between the reference electrode and the measuring electrode, or changes this potential according to a predetermined program. However, this potential differs from the actual potential of the electrode, because a considerable voltage drop may arise on the layer of solution between the reference electrode and the working electrode, particularly when high currents or solutions of a high resistance are used. The difference between the actual potential of the electrode and the potential adjusted on the potentiostat will be particularly high if surface layers of high resistance are also formed on the surface of the electrode.

Several procedures are known [1—7] for the elimination of the errors described above. These essentially involve the increase of the control voltage of the potentiostat by the voltage produced across the ohmic resistance of the

solution between the reference electrode and the measuring electrode, that is to say, the sum of the desired potential and the voltage established across the ohmic resistance is adjusted between the reference and the measuring electrodes by the potentiostat. The voltage established across the ohmic resistance is taken into correction by connecting in series the measuring electrode and a resistance equal to the resistance of the solution between the reference and the measuring electrodes, and by adding twice the value of the voltage

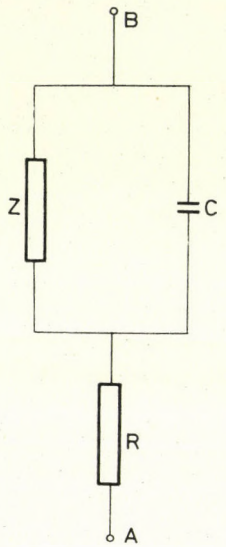

Fig. 1. Equivalent circuit of the impedance established between the measuring and the reference electrodes

established across this resistance to the direct voltage controlling the potentiostat.

A disadvantage of this approach is that it can be used only if the resistance of the solution between the two electrodes does not change during the measurement. (This resistance may also change within the polarization cycle.)

The deficiency of the above methods can be eliminated only by the continuous measurement of the resistance in the solution or rather of the voltage established across this resistance, and by the continuous feedback of the latter voltage.

The voltage arising across the resistance of the solution can be measured on the basis of the following considerations. Fig. 1 shows the simplest equivalent circuit of the impedance established between the measuring electrode and the reference electrode, where the impedance of the former is represented by the parallel resultant of the capacity C of the double layer and the imped-

ance Z of the electrode process. The resistance R of the solution is connected in series with the electrode impedance. If the direct current flowing through the cell is denoted by $i_{=}$, the voltage arising across the resistance of the solution is

$$E_{=} = i_{=} \cdot R. \tag{1}$$

Let us superimpose on the direct current of the cell an alternating current of amplitude i and of angular frequency (ω), and let us select the angular frequency (ω) so that

$$\frac{1}{\omega C} \ll R. \tag{2}$$

i.e. the impedance of the double layer capacity, and thus the whole electrode impedance, should be negligibly small as compared to the resistance of the solution. In this case, the alternating voltage arising between the reference electrode and the measuring electrode (on Fig. 1, A and B) will be

$$U_{\sim} = i_{\sim} \cdot R. \tag{3}$$

If $i_{\sim}$ is proportional to $i_{=}$, so that

$$i_{\sim} = K \cdot i_{=}, \tag{4}$$

(where K is the proportionality factor), the alternating voltage measured between the points A and B will be proportional to the voltage $\Delta E_{=}$, *i.e.* considering (1), (3) and (4)

$$U_{\sim} = i_{\sim} \cdot R = K \cdot i_{=} \cdot R = K \cdot \Delta E_{=}. \tag{5}$$

Thus, when the alternating voltage arising between the reference electrode and the measuring electrode is suitably amplified (in order to eliminate the proportionality factor K), and subsequently rectified, the voltage $\Delta E_{=}$ is obtained. By adding the latter to the control voltage of the potentiostat, the effect of the resistance of the solution can be compensated.

It should be noted that the above method can be applied only if the geometry of the cell is designed in such a way that the spatial distribution of the direct and alternating currents can be considered as identical. The simplest way to attain this is *e.g.* to arrange coaxially the cylindrical measuring and counter electrodes.

Even if the resistance of the solution changes, this method permits the continuous measurement or the correction of the voltage across this resistance.

Our measuring equipment is shown in Fig. 2. The direct current flowing through the three-electrode cell (1) is fed in the unit consisting of the modulator (5) and the a.c. voltage amplifier (6), which generates an alternating current proportional to the direct current, and supplies the cell with alternating current through the resistance (7) and the condenser (8). The capacity (8) serves to separate the direct current and alternating current circuits, and the resistance (7) ensures the functioning of the amplifier (6) as a current generator,

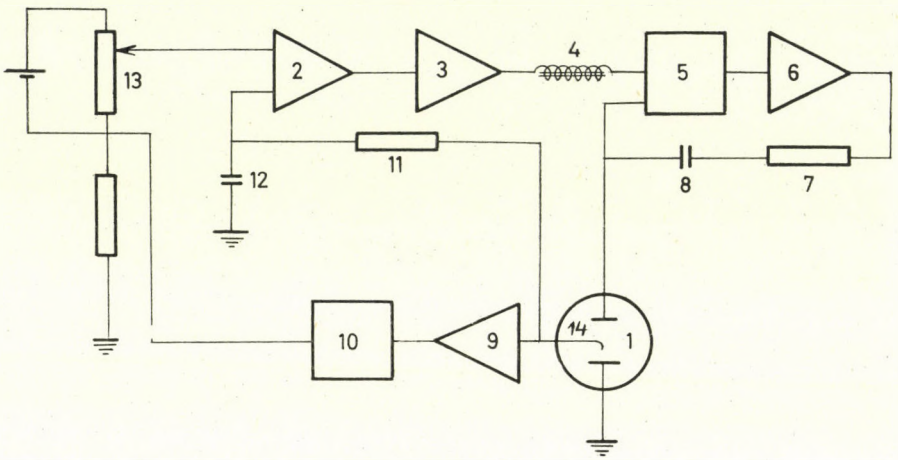

Fig. 2. Block diagram for the continuous automatic compensation of the resistance polarization

that is to say, the alternating current flowing through the cell shall be independent of the resistance of the cell.

The reference electrode (14) is connected to the input of the differential amplifier (2) through the filters (11, 12), as well as to the a.c. voltage amplifier (9) and the demodulator (10). The output voltage of the demodulator, which is equal to the voltage across the ohmic resistance, is added to the polarization voltage adjusted on the potentiometer (13), and fed to the second input of the differential amplifier (2). The filter circuit (11, 12) prevents the alternating voltage between the reference and the measuring electrodes to get to the input of the differential amplifier. The inductivity (4) prevents the shunting of the cell by the output impedance of the potentiostat from the viewpoint of the alternating current.

The range of the a.c. measuring frequency can be determined from the frequency characteristics of the impedance of the measuring cell. The dependence of the electrode impedance on frequency is shown in Fig. 3. In the range of frequencies where Z is independent of f, the reactance of capacity C shown in the equivalent circuit in Fig. 1 is considerably lower than resistance R,

so that the alternating current flowing through the cell is only determined by the ohmic resistance.

The application of the above method was examined on the model cell shown in Fig. 4. In this model cell, the resistance (10 Ω) and the capacitor (50 μF), connected in parallel, represented the electrode process and the capacity of the double layer, respectively, while the variable resistance (1—100 Ω) and the resistance of 50 Ohms connected in series with them the resistance of

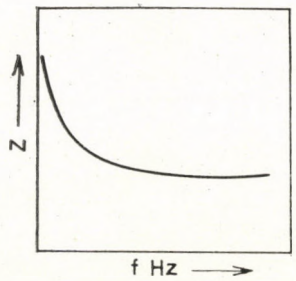

Fig. 3. Dependence of the electrode impedance on frequency

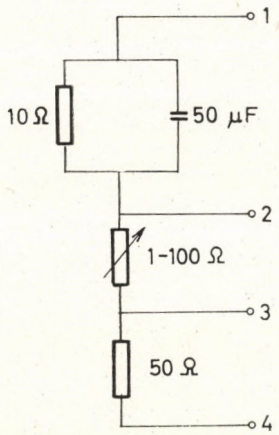

Fig. 4. Circuit diagram of the model cell investigated

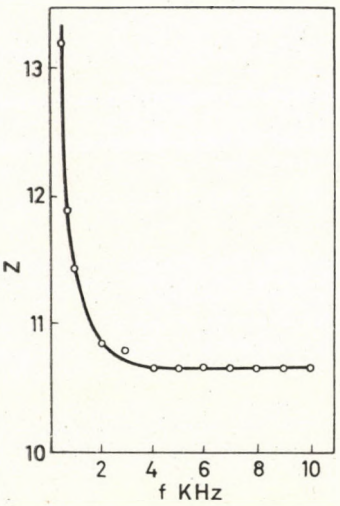

Fig. 5. Dependence on frequency of the impedance of the model cell

the solution between the reference and the measuring electrode, and the internal resistance of the cell, respectively.

First, the frequency characteristics of the cell impedance were investigated. The results are shown in Fig. 5. It is apparent that the impedance of the cell is independent from the frequency in the range from 4 to 10 KHz, and therefore, our investigations were undertaken at 5 KHz.

Point 1 of the model cell shown in Fig. 4 corresponds to the measuring electrode, point 3 to the reference electrode, while point 4 was connected to the clamp of the potentiostat, corresponding to the input terminal of the counter electrode.

Our object was to demonstrate that a potentiostat provided with the auxiliary equipment recommended will actually stabilize the potential of the electrode irrespective of the magnitude of the ohmic resistance. To prove this, the voltage between points 1 and 2 was measured with a d.c. valve voltmeter, while the resistance between points 2 and 3 varied and the potentiostat was adjusted to constant voltage. The results of our measurements are summarized in Table I. The table contains the voltage values as measured between points

Table I

Voltage adjusted on the potentiostat: 100 mV

Resistance adjusted between points 2 and 3	Voltage measured between points 1 and 2, mV	
	with automatic correction	without automatic correction
1	100	90
10	100	50
20	100	35
30	100	27
40	100	21
50	100	18
60	100	16
70	100	15
80	100	14
100	100	12

1 and 2, when the potentiostat was adjusted to a constant voltage of 100 mV while the resistance between points 2 and 3 was changed from 1 to 100 Ohms For comparison, data are also presented for the case when automatic correction for the voltage across the resistance between points 2 and 3 was not applied.

It is apparent from the data in the table that the voltage of 100 mV adjusted on the potentiostat appears between the points 1 and 2 in every case, independently of the magnitude of the resistance between points 2 and 3, while in the case when no automatic correction is employed the voltage appearing between points 1 and 2 depends on the resistance between points 2 and 3. This means, however, that not the potential between the measuring and the reference electrodes, but actually the electrode potential is stabilized and con-

trolled in the required way by the potentiostat even in case of a possible change of the resistance of the solution.

Thus, in summary, it can be established that the device makes automatic corrections for the voltage existing across the resistance between points 2 and 3, so that in each case the voltage adjusted on the potentiostat appears between points 1 and 2, independently of the magnitude of the resistance between points 2 and 3. With this method, it becomes possible to eliminate automatically in potentiostatic investigations the resistance-polarization, whether constant or changing with time. Moreover, our method has the advantage over methods described in the literature [1—7] that the voltage across the resistance is measured with an a.c. method so that no positive feedback is necessary from the output terminal of the potentiostat. Hereby, possible instabilities arising from circuitries employed in the other methods can be avoided.

REFERENCES

1. Booman, G. L., Holbrook, W. B.: Anal. Chem. **35,** 1973 (1963)
2. Booman, G. L., Holbrook, W. B.: Anal. Chem. **37,** 795 (1965)
3. Pouli, D., Huff, J. R., Pearson, J. C.: Anal. Chem. **38,** 382 (1966)
4. Bewick, A.: Electrochim. Acta **13,** 825 (1968)
5. Brown, E. R., Smith, D. E., Booman, G. L.: Anal. Chem. **40,** 1411 (1968)
6. Brown, E. R., Hung, H. L., McCord, T. G., Smith, D. E., Booman, G. L.: Anal. Chem. **40,** 1424 (1969)
7. Clavilier, I. Lamy, C., Malaterre, P.: C. R. Acad. Sci. Paris **267,** 362 (1968)

József Dévay
Béla Lengyel jr.
Lajos Mészáros
Veszprém, Schönherz Z. u. 10. Hungary

Acta Chimica Academiae Scientiarum Hungaricae, Tomus 66 (3), pp. 277—284 (1970)

VIBRATIONAL SPECTRA OF ORGANOMERCURIC COMPOUNDS, VI*

INFRARED AND RAMAN SPECTRA OF DIVINYL MERCURY

J. MINK** and YU. A. PENTIN***

*(**Institute of Isotopes of the Hungarian Academy of Sciences, Budapest, ***Department of Chemistry, Moscow State University, Moscow)*

Received June 13, 1969

The infrared spectrum of divinyl mercury, gas and liquid, and the Raman spectrum of the liquid and the low temperature crystalline phase were measured and the observed frequency bands were assigned to the characteristic molecular vibrations. The observed frequencies suggest linear or closely linear CHgC skeleton. It is also apparent that the spectra taken in each the gas, liquid and solid phase cannot be explained by assuming the presence of a single type of the symmetry groups C_{2v}, C_{2h}, C_2, $D_{\infty h}$. The normal coordinate analysis of the spectra, performed on computer, gives for the force constant of the CHg stretching frequency $4.02 \cdot 10^6$ cm^{-2} [2.58 mdyn/Å].

The infrared spectrum of liquid divinyl mercury has been studied by several authors [1—3]. The infrared spectrum of perfluoro-divinyl mercury is also known [4]. The low frequency infrared region and the Raman spectrum of this organo-mercury compound have not been investigated so far.

Experimental

Divinyl mercury was prepared by the reaction of C_2H_3MgBr with $HgCl_2$. The analytical data of the product are as follows. B.p. 63—65 °C (23 torr); refractive index n_D^{25} 1.5983 (1.5978, Ref. [5]). Analyses: found C 18.92%; H 2.41%; calculated C 18.86%; H 2.37%.

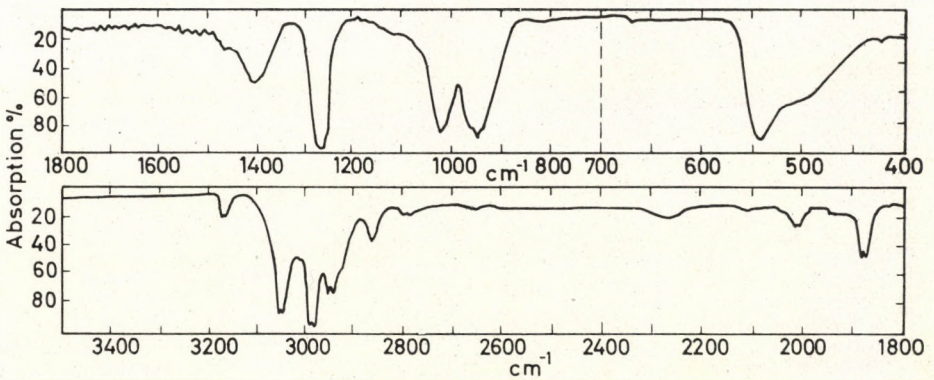

Fig. 1. Infrared absorption spectra of $(CH_2{=}CH)_2Hg$ gas at 72 °C in a 13 cm cell with KBr windows, pressure 35 mm

* For Part V, *cf.* Ref [6].

Table I

Experimental frequencies of vibrational spectra of divinyl mercury

Infrared			Raman			Assignments
Liquid		Gas	Liquid		Crystalline	
νcm^{-1} from Ref. [2]	νcm^{-1}	νcm^{-1}	νcm^{-1}	ϱ	νcm^{-1}	
1.	2.	3.	4.	5.	6.	7.
			172			δ'CHgC ν_1
			203			
	265 w		259 m	0.66	268 m	δ^SCCHg ν_2
	304 s		291 m	0.60	310 m	δ^ACCHg ν'_2
			347			$\nu_7 - \nu_5$
		418 vw	423			$\nu_{14} - \nu_3$
			456 m	0.86	463 m	w^{S}CH ν_{13}
	495 m, sh	500 m, sh	489		494	w^{A}CH ν'_{13}
	515 m, sh		513 vs	0.42	521 s	ν^SCHg ν_3
	537 s	541 s(A)				ν^ACHg ν'_3
			559			$\nu_2 + \nu'_2$
	670	667				$\nu_1 + \nu_3$
943 s	938 vs	937 vs(C)	937 vw	dp	943 vw	wCH$_2$ ν_{14}
1008 s	1009 vs	1019 vs(A)	1002 vw	(0.37)	992 vw	rCH$_2$, tCH$_2$ ν_4, ν_{15}
		1060	1052			$\nu_3 + \nu'_3$
		1120	1115			
1165 w	1165	1168 vw				
		1200				
1255 s	1252 vs	1263 vs(A)	1262 vs	0.39	1262 s	bCH ν_5
			1352			
1398 s	1395 vs	1400 m	1388 vs	0.5	1388 s	bCH$_2$ ν_6
1465 w	1463 vw	1462 w	1460	dp		$\nu_{13} + \nu_{15}$
			1490			
	1520		1520			$\nu_3 + \nu_4$
1588 w	1589 m	1603 w(B)	1578 s	0.32	1578 m	νC=C ν_7
			1614			
1650 vw	1641		1652			$\nu_2 + \nu_6$
1740 vw						
	1773					$\nu_3 + \nu_5$
1793 vw						
1890 m	1879 s	1879 m(B)				$2\nu_{14}$
1955 vw	1943 vw	1944 vw				$\nu_{14} + \nu_{15}$
2025 w	2010 w	2007 w(B)				$2\nu_{15}$
	2100	2107				$\nu_3 + \nu_7$

Table I continued

Infrared			Raman			Assignments	
Liquid		Gas	Liquid		Crystalline		
ν, cm^{-1} from Ref. [2]	ν, cm^{-1}	ν, cm^{-1}	ν, cm^{-1}	ϱ	ν, cm^{-1}		
1.	2.	3.	4.	5.	6.	7.	
2260 w	2244 w	2252 w				$\nu_4 + \nu_5$	
	2503						
	2560						
2660 vw	2640 vw	2659 vw				$\nu_5 + \nu_6$	
	2775 w	2790 w(B)	2785 vw.	0.56		$2\nu_6$	
2805 w							
	2814 vw		2818	0.59			
2850 m, sh	2853	2855 w	2868	0.57		$\nu_5 + \nu_7$	
2900 m, sh							
2975 s, sh	2926 vs	2944 s(B)	2928 s	0.45	2926 w	$\nu^{(S)}CH_2$	ν_8
3010 s	2964 vs	2985 vs(B)	2963 vs	0.47	2965 s	ν CH	ν_9
	2979 sh		2978 sh				
3100 s	3036 vs	3051 vs(B)	3034 s	0.34	3042 s	$\nu^{(A)}CH_2$	ν_{10}
3200 w	3148 m	3165 w(B)	3143	0.77		$2\nu_7$	
	3295						

Designation of band intensity: vs — very strong, s — strong, m — medium, w — weak, vw — very weak, sh — shoulder; of vibrational modes: ν — stretching, b — bending, w — wagging, t — twisting, r — rocking, δ — skeletal deformation, τ — torsional, dp — depolarized Raman line; (*S*) — symmetrical, (*A*) — asymmetrical vibrations (by local symmetry of groups); A, B and C — type of contoures of vibrational bands.

The infrared spectra of divinyl mercury, liquid and gas were measured on an UR-10 double-beam spectrometer in the range from 400 to 3500 cm^{-1} (Fig. 1). The IR spectra in the low frequency region from 200 to 400 cm^{-1} were taken in benzene solution on an IKS-21 single beam spectrometer with CsI prism. The Raman spectra of the neat liquid (Fig. 2) and of the crystalline (at low temperature) samples were measured on a DSF-12 greating spectrograph with photoelectric detector. The measured frequencies are listed in Table I along with those measured by KAESZ and STONE [2].

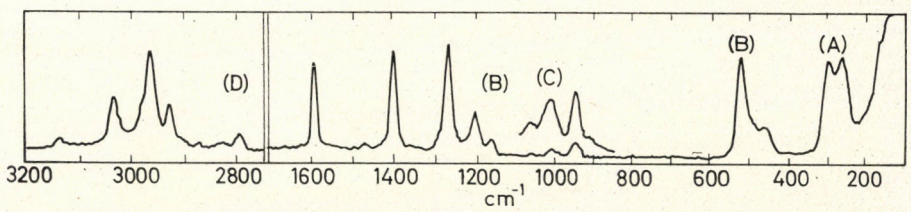

Fig. 2. Raman spectra of liquid $(CH_2{=}CH)_2Hg$ recorded at different slits: (A) — 0.35, (B) — 0.20, (C) — 0.40, (D) — 0.15 mm

Frequency assignments

Theoretically, divinyl mercury has 27 fundamental frequencies. In the present measurements, as to be expected for the R_2Hg-type compounds [6], only 14 intense bands could be observed.

The CH stretching frequency (ν_8, ν_9, ν_{10}) is thought to be responsible for the three most intense infrared and Raman active bands, the polarization of which is probably due to local C_s symmetry of the vinyl groups. The infrared spectrum of the liquid is in good agreement with the data reported by KAESZ and STONE [2], except for the difference of about 50 cm^{-1} in the region of CH stretching frequency.

The C=C stretching frequency (ν_7) is thought to be well apparent in the Raman spectra, while in the infrared spectrum of the gas it was difficult to identify it, because the atmospheric water vapor marked the very weak band appearing at 1603 cm^{-1}.

The $=CH_2$ group has theoretically four deformation frequencies. Only three intense bands were observed which could be assigned to this group. The intense bands at 1400 cm^{-1} in each of the spectra was attributed to the bending frequency (ν_6). It seemed reasonable to assign the high intensity band in the infrared spectrum at 1010 cm^{-1} to both the rocking (ν_4) and the twisting (ν_{15}) frequencies of the CH_2 group, while the intense band at 940 cm^{-1} in the infrared spectrum which appears in the Raman spectrum as a weak depolarized line, was attributed to the CH_2 wagging (ν_{14}) frequency.

The vibrational frequency of the planar deformation (ν_5, bCH) of the >CH group is thought to produce the well observable band at 1260 cm^{-1} in each of the spectra. The out-of-plane bending frequency splits into a symmetric Raman active depolarized band (ν_{13}) and an asymmetric infrared band (ν'_{13}) observed at 456 cm^{-1} and 500 cm^{-1}, respectively.

The CHg stretching is held responsible for the strongly polarized Raman line at 513 cm^{-1} (ν_3) which is thought to be the symmetric, and for the intense infrared band at 541 cm^{-1} (ν'_3) which is thought to be the asymmetric contribution.

The polarized Raman lines at 259 and 291 cm^{-1} were assigned to the symmetric and asymmetric contributions ν_2 and ν'_2, respectively, to the deformation of the CCHg valence angle. These bands were observable in the infrared spectrum of the benzene solution and in that of the low temperature crystalline sample, too.

No frequency bands were observed which could be attributed to two of the deformation frequencies (ν_1, ν'_1) of CHgC and to the rotational frequency (ν_{11}) of the vinyl groups around the CHgC axis (omitting free rotation).

The properties of the CHg stretching frequencies suggest linear or nearly linear CHgC structure. The spectra taken in different phases of the compound

are essentially similar. The properties of the w $\geqslant$CH, ν CHg and δ CCHg bands which are split because of the interaction between the two vinyl groups cannot be explained with the assumption of single C_{2v}, C_{2h}, C_2 or free rotation in terms of $D_{\infty h}$ point groups. Taking the $(CH_2{=}CH)_2$ Hg molecule to be slightly deformed with symmetrical top, the ratio of the rotational constants B/A $\sim$ 0.12—0.13. The contours observed in the infrared spectrum of the gas (Fig. 1) do not yield any useful information about the configuration because of the poor molecular symmetry.

Results of calculations

Normal coordinate analysis was performed by the methods described in [6] assuming for divinyl mercury a configuration of two groups: one of C_{2v}, the other of C_{2h} planar symmetry (Fig. 3). The displacements in bond distances

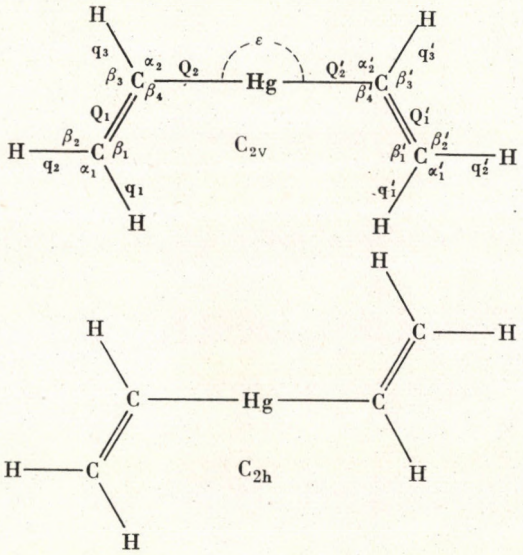

Fig. 3. The internal in-plane coordinates of divinyl mercury

and valence angles due to in-plane vibrations are computed in terms of the internal coordinates shown in Fig. 3. For out-of-plane vibrations, the displacements were computed for the internal coordinates of the CHgC valence angle (ε') normal to the plane, the angles 2 ϱ_1 and 2 ϱ_2 of the C=C bond and the planes HCH and HCHg, respectively; 2 χ_1, the angle between the HCH and HCHg planes and χ_2, the angular displacement of the two vinyl groups around the CHgC axis. Because of redundance the coordinates β_2, β_4, β'_2, β'_4 were omitted.

No geometric parameters being available, valence angles of 120° and linear CHgC skeleton were assumed with bond distances CH, C=C and CHg of 1.07, 1.34 and 2.20 Å, respectively.

The elements of the kinetic energy matrix and the symmetry transformations were evaluated on a computer [9]. The values of the force constants in zero approximation were taken from the data reported on diethyl mercury [6] and the vinyl-halogenides [7]. The values were fitted by the method of least squares [8] to the environment of the Hg-atom for C_{2v} symmetry. The force field thus obtained was used for computing the fundamental frequencies for C_{2h} symmetry. The computed values are listed in Table II.

The measured values were taken from the infrared spectrum of the gas and the Raman spectrum of the liquid.

Table II

Observed and computed fundamental frequencies

	Experimental frequency ν, cm^{-1}	Computed frequency, ν, cm^{-1}				Assignment	
		C_{2v}		C_{2h}			
		A_1	B_1	A_g	B_u		
In-plane vibrations	—	78			79	δCHgC	ν_1
	259			269			ν_2
	291	289				δCCHg	
	291		283		303		ν'_2
	513	513		508		ν^SCHg	ν_2
	541		541		543	ν^ACHg	ν'_3
	1019	1015	1014	1012	1016	rCH_2	ν_4
	1263	1263	1262	1264	1266	bCH	ν_5
	1402	1402	1402	1399	1401	bCH_2	ν_6
	1603	1603	1600	1600	1599	νC=C	ν_7
	2944	2944	2945	2944	2944	$\nu^{(S)}CH_2$	ν_8
	2985	2985	2984	2985	2985	νCH	ν_9
	3051	3051	3051	3051	3050	$\nu^{(A)}CH_2$	ν_{10}
		A_2	B_2	A_u	B_g		
Out-of-plane	—	119		120		τCCHgCC	ν_{11}
	(170)		145	146		δ'CHgC	ν_{12}
	456	456			456		ν_{13}
	495		495	494		wCH	ν'_{13}
	937	938	935	938	935	wCH_2	ν_{14}
	1019*	1002	1019	1019	1002	tCH_2	ν_{15}

* Frequency used twice.

By the use of the same force field the computed δ CCHg frequencies were found to be very closely spaced in the case of C_{2v} symmetry (289 and 283 cm^{-1}), while the values computed for C_{2h} point group reproduce fairly well the observed values of ν_2 and ν_2'. The rest of the computed frequencies proved to be insensitive to differences in configuration.

The rotational frequency of the two vinyl groups is probably nearly zero. The value of the force constant ($K\varkappa_2$) was chosen arbitrarily and the value of $\nu_{11} = 120\ cm^{-1}$ thus obtained seems to be fallacious.

The vibrational modes (eigenvectors) show that in addition to the CH stretching frequencies, the frequencies ν_1 and ν_{12} are characteristic of fundamental vibrational modes. The vibrations of the CHg valence angles exhibit considerable CCHg angular deformation.

The force constants of divinyl mercury are listed in Table III. The CH stretching frequencies are observed in a wavelength region on the average by

Table III

*Force constants of divinylmercury**

Force constant		10^6 cm^{-2}	Force constant		10^6 cm^{-2}
For in-plane vibrations					
K_{Q_1}		14.05	$H_{Q_2q_3}$		0.11
K_{Q_2}		4.02	$H_{Q_2Q_2'}$		−0.07
K_{q_i}	(i = 1, 2)	8.31	$A_{Q_1\beta_i}$	(i = 1, 2)	0.40
K_{q_3}		8.27	$A_{Q_1\beta_3}$		0.33
K_{α_1}		0.44	$A_{Q_1\beta_4}$		0.45
K_{β_i}	(i = 1, 2)	0.66	$A_{Q_2\alpha_1}$		1.09
K_{α_2}		1.47	$a_{Q_2\beta_4}$		0.38
K_{β_3}		0.38	$a_{q_1\beta_1}=a_{q_2\beta_2}=a_{q_3\beta_3}$		0.66
K_{β_4}		1.04	$a_{q_i\alpha_i}$	(i = 1, 2, 3)	0.43
K_ε		0.45	$A_{q_3\alpha_2}$		0.60
$H_{Q_1q_i}$	(i = 1, 2, 3)	0.10	$m_{\beta_1\beta_3}=m_{\beta_2\beta_4}$		0.09
$h_{q_1q_2}$		−0.03	$n_{\beta_1\beta_4}=n_{\beta_2\beta_3}$		−0.02
$H_{Q_1Q_2}$		0.37	$n_{\alpha_2\varepsilon}=m_{\beta_4\varepsilon}$		0.06
For out-of-plane vibrations					
K_{ϱ_1}		0.31	$u_{\varrho_1\varrho_2}$		0.05
K_{ϱ_2}		0.25	$u_{\varrho_1\varkappa_1}$		0.01
$K_{\varkappa_1}$		0.75	$u_{\varrho_2\varkappa_1}$		−0.04
$K_{\varkappa_2}$		0.10	$u_{\varrho_2\varrho_1'}$		0.03
$K_{\varepsilon'}$		0.45	$u_{\varkappa_1\varkappa_1'}$		−0.01

*K — diagonal elements, $H(h)$ elements of valence–valence, $A(a)$ — elements of valence–angle, m, n — elements of angle–angle interactions and u — non-diagonal elements of out-of-plane coordinates.

70 cm^{-1} lower than that observed for vinyl halogenides. This is reflected by the decrease of the force constant from $8.8 \cdot 10^6$ cm^{-2} [7] to $8.3 \cdot 10^6$ cm^{-2}. This phenomenon is frequently encountered if one compares the spectra and force fields of RX and R_2Hg-type compounds.

*

This work was performed at the Chemical Department of the Moscow State University. The authors are indebted to Dr. I. P. BELETSKAYA and her co-workers for their help in the synthesis, and for their useful advices.

REFERENCES

1. REYNOLDS, G. F., DESSY, R. E., JAFFE, H. H.: J. Org. Chem. **23,** 1217 (1958)
2. KAESZ, H. G., STONE, F. G. A: Spectrochim. Acta **15,** 360 (1959)
3. HUGGINS, D. K., KAESZ, H. D.: Progress in Solid State Chemistry **1,** 417 (1964)
4. STADFORD, S. L., STONE, F. G. A.: Spectrochim. Acta **17,** 412 (1961)
5. MAKAROVA, L. G., NESMEYANOV, A. N.: Methods of Elemental Organic Chemistry Vol. 4, Mercury. North-Holland, Amsterdam, 1967
6. MINK, J., PENTIN, Yu. A.: Acta Chim. Acad. Sci. Hung. **65,** 273 (1970)
7. SVERDLOV, L. L., KLOTSKOVSKY, Y. V., KUKINA, V. S.: Inzh. Fizh. Zhurn. **12,** 43 (1958)
8. MINK, J., MINK, L. M., PENTIN, YU. A.: Vestnik Mosc. Univ. (In press)
9. MINK, J., MINK, L. M., PENTIN, YU. A.: Zhurn. Prikl. Spectr. **9,** 129 (1968)

János MINK; Budapest XII., Konkoly Thege u.
YU. A. PENTIN; Chemistry Department, Moscow State University, Moscow B-234 USSR.

Acta Chimica Academiae Scientiarum Hungaricae, Tomus 66 (3), pp. 285—292 (1970)

INVESTIGATION OF THE ELECTRON EXCHANGE REACTION BETWEEN IRON(II) AND IRON(III) BY MÖSSBAUER EFFECT IN SOLUTION

M. KOMOR, A. VÉRTES, I. DÉZSI*, and I. RUFF**

(Institute of Physical Chemistry, L. Eötvös University, Budapest)

Received June 16, 1969

The electron exchange reaction

$$^{57}Fe^{3+} + Fe^{2+} = Fe^{3+} + {}^{57}Fe^{2+}$$

has been studied. Iron(III) perchlorate solution was labelled with ^{57}Fe and its mixture with iron(II) perchlorate solution of natural isotopic composition was investigated at a concentration of 0.13 M and in the pH range from 0 to 2.50. The exchange of various hydrolysis products of iron(III) was followed by measuring the effect due to iron(II) in the spectrum. It was found that $Fe(H_2O)_6^{3+}$ and $FeOH^{2+}$ exchange their electrons very rapidly and its kinetics could not be measured by the technique applied in this work, the rate constant of the exchange being $k \geqq 1.8\ M^{-1}sec^{-1}$. Other hydrolysis products again show no exchange.

The concentration of the various hydrolysis products of iron(III) was calculated from the intensity of the Mössbauer effect and compared with the data computed using HEDSTRÖM's equilibrium measurement [1].

Introduction

Several papers have appeared on Mössbauer study of frozen solutions of iron salts. DÉZSI *et al.* [3, 4, 5] investigated the phase properties of ice in frozen solutions of iron(II) salts. Similar measurements have been outlined by NOZIK and KAPLAN [6]. RUBY *et al.* [7] determined the dependence of the Mössbauer parameters on the rate of freezing-in and showed that with a rate larger than 8 °K/sec the parameters remain unchanged. By studying iron(II) solutions, VÉRTES *et al.* [8—11] and BURGER *et al.* [12] were able to follow the change of the solvation sphere due to the change in the composition of the mixed solvent for several systems.

All these investigations, thus, showed that the structure as well as the change in the structure of solutions could be studied by means of Mössbauer spectroscopy.

0.04 M iron(II) and iron(III) perchlorate solutions have been studied by DÉZSI *et al.* [13—15]. The iron(II) solutions of various pH resulted identical spectra with a quadrupole splitting of $\Delta E = 3.30$ mm/sec and an isomeric

* Central Research Institute for Physics, Budapest.
** Institute of Inorganic and Analytical Chemistry, L. Eötvös University, Budapest.

shift $\delta = 1.44$ mm/sec, and the value of the line intensity was also identical within 10 per cent for identical times of measurement.

The spectra of iron(III) perchlorate solutions differ at various pH (see Fig. 1). According to data in the literature [1, 2], the following ions exist in iron(III) solutions depending on the pH: $Fe(H_2O)_6^{3+}$, $Fe(OH)^{2+}$, $Fe(OH)_2^{+}$,

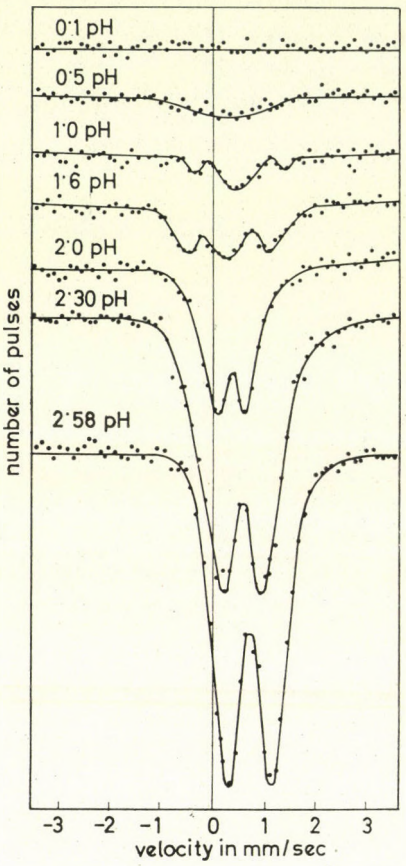

Fig. 1. Mössbauer spectra of frozen aqueous solution of iron(III) perchlorate

$Fe_2(OH)_2^{4+}$. As it is seen from Fig. 1, the hexaquo iron(III) complex dominating at low pH values gives no Mössbauer effect, while the peak appearing at pH = 2.0 with a quadrupole splitting of 0.60 mm/sec can be assigned to the so-called dimer. According to HEDSTRÖM [1] and MULAY and SELWOOD [2], besides the hexaquo complex and the dimer, all the other hydrolysis products do not exceed 7 per cent of the total iron(III). In contradiction to this, the concentration of the complex ion, with a quadrupole splitting of 1.65 mm/sec in the Mössbauer spectra of solutions of intermediate pH values, be at least 10 per cent of the total iron to produce such a large effect as observed. On the

basis of calculations of electric field gradient [15], such a quadrupole splitting would result in a *trans*-$Fe(OH)_2^+$ ion. To assign this spectral line with more certainty, and to indicate the hexaquo complex, electron transfer reactions were investigated.

Usually two groups of electron transfer reactions are distinguished: the electron transfer reactions of finite net enthalpy change are called oxidation-reduction reactions, while those of zero net enthalpy change are quoted as electron exchange reactions [16]. Several theoretical approaches have been outlined for the interpretation of the kinetics of this type of reactions [17, 18]. One of the fundamental criteria of these reactions is the satisfaction of the FRANCK—CONDON principle which requires an appropriate symmetry of the environment of the ions in the activated complex in course of the electron exchange.

In general two types of mechanism are believed to exist: the outer sphere mechanism, which takes place between ions of substitution inert coordination spheres, and the inner sphere mechanism when a common ligand serves as a bridge for the transferring electron.

Iron(II)—iron(III) electron exchange reaction was one of the first ones studied. Due to the rather fast exchange, 10^{-4}—10^{-5} *M* solutions were applied, measured using the isotopic exchange technique, which requires the separation of the reactants [19]. The use of Mössbauer effect to study electron exchange reactions has an advantage: it requires separation and so the exchange rate can be measured in solid systems, too.

Experimental

$^{57}Fe(ClO_4)_3$ solutions of 80 per cent ^{57}Fe content were prepared by dissolving metallic iron in 35 per cent perchloric acid and by heating with concentrated perchloric acid.

$Fe(ClO_4)_2$ solutions were obtained by dissolving metallic iron in 0.5 *M* perchloric acid.

All the other chemicals (sodium perchlorate, sodium hydrogen carbonate, perchloric acid) were of analytical grade. pH was measured by a Radelkis-type pH-meter and was adjusted by adding saturated sodium hydrogen carbonate solution.

The concentrations of the solutions investigated were 0.13 *M* with respect to both reactants (the exact concentrations are shown in Table I, in mg/g units), the constant ionic strength was 3 *M* ($NaClO_4$). The pH of the solutions varied from 0 to 2.25.

Some oxidation-reduction reactions between iron(III) and metallic copper were measured in a system of iron(III) perchlorate reduced by a copper sheet.

The iron(II) and iron(III) perchlorate solutions were mixed at —15 °C, and immediately frozen by liquid nitrogen in a sample-holder. The time elapsed from mixing to freezing was about 3 sec. In another series of runs the mixed samples were kept for 24 hours at room temperature before measuring their Mössbauer spectra.

The Mössbauer apparatus was the same as described earlier [20] with a ^{57}Co source diffused in stainless steel. $^{57}Fe_2O_3$ was used for calibration.

Results

In Tables I and II the Mössbauer parameters of the solutions mixed at —15 °C and room temperature, respectively, are summarized (c: concentration is given in mg iron/g solution; δ: isomeric shift, ΔE: quadrupole splitting,

Table I

The Mössbauer parameters of the iron perchlorate solutions
(Mixed at —15 °C and immediately frozen by liquid nitrogen)

pH	Fe(II)				Fe(III)			
	c mg/g	ΔE mm/sec	δ mm/sec	T cm²	c mg/g	ΔE mm/sec	δ mm/sec	T cm²
0.05	5.92	3.32	1.52	13.97	6.21	—	—	—
1.10	5.85	3.31	1.58	9.88	6.00	0.00	0.50	46.89
						1.67	0.76	
1.85	5.37	3.23	1.47	9.06	4.93	0.70	0.45	36.25
2.25	6.12	3.27	1.49	2.52	5.72	0.69	0.54	89.20

Table II

The Mössbauer parameters of the iron perchlorate solutions

(The mixed samples were kept at room temperature for 24 hours before measuring)

pH	Fe(II)			Fe(III)		
	ΔE mm/sec	δ mm/sec	T cm²	ΔE mm/sec	δ mm/sec	T cm²
0.05	3.27	1.48	14.50	—	—	—
1.10	3.30	1.54	12.07	0.00	0.43	41.35
				1.60	0.72	
1.85	3.32	1.54	9.97	0.70	0.51	34.99
2.25	3.28	1.50	2.55	0.65	0.58	83.07

T: integral line intensity). The spectra obtained with the solutions mixed at —15 °C are shown in Fig. 2.

The integral intensity of the Mössbauer lines (T) was determined by a planimeter. For the case of iron(II), only that of the two lines is given, which does not overlap other lines. The calculation of the concentrations was also based on the intensity of this line, so the difference in the f values of different products of hydrolysis could be eliminated. The area of the iron(III) peak was calculated by that overlapped by the other peak of iron(II), subtracting this latter one that was known from the former calculation.

The spectrum of the iron(II), (see Fig. 2) appearing with 3.27 and 1.48 mm/sec values of quadrupole splitting and isomeric shift, respectively, shows that the exchange between iron(II) and some hydrolysis products of iron(III) took place. The increase in the extent of the exchange would mean an increase

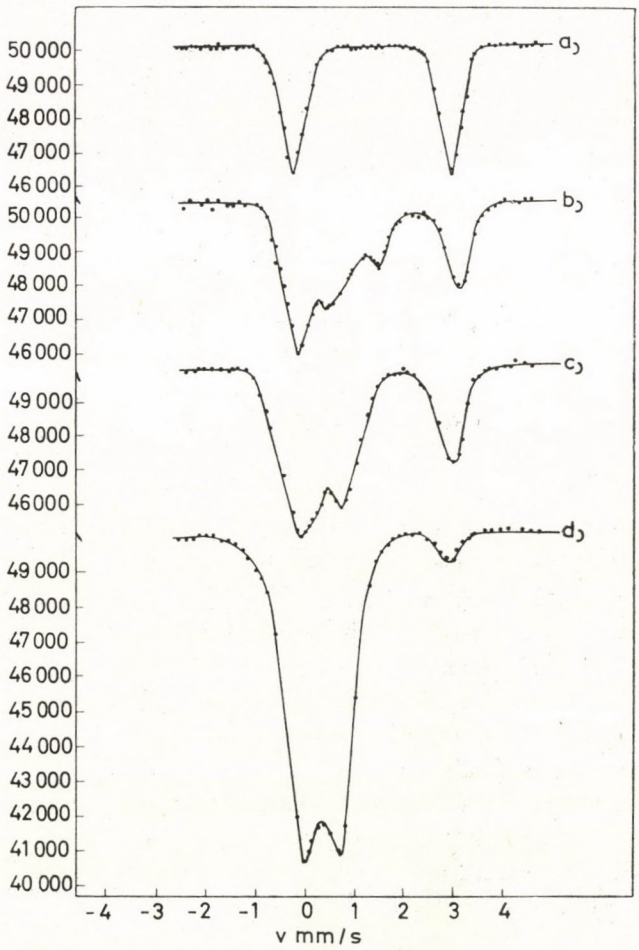

Fig. 2. Mössbauer spectra of frozen aqueous solution of mixtures of $Fe^{(II)}$ and $^{57}Fe^{(III)}$ perchlorate

in the line intensity of the iron(II) spectrum. However, the spectra of different samples, prepared in this way, showed no change even if standing for several days at room temperature. The values of the line intensity agree within 10 per cent. It is obvious that within a few seconds from mixing to freezing the exchange reaction proceeded completely. Therefore the rate constant is

$$k \geqq 0.69/3 \cdot 0.13 \geqq 1.8\ M^{-1}\,\mathrm{sec}^{-1}.$$

From the comparison of the first and second spectra it can be seen that the peaks of 1.67 and 0.69 mm/sec quadrupole splitting and 0.76 and 0.54 mm/sec isomeric shift do not change, *i.e.* the iron species producing these spectra do not exchange their electrons.

The assignment of the hydrolysis products can be done just on this basis. Considering the exchange rate measured by SILVERMAN and DODSON [19], it appears to be proved that, first of all, the two hexaquo forms react. Similarly, this can be deduced theoretically as well, since the inner coordination spheres of the two reactant iron species are chemically identical and so a relatively low free energy of activation is required. The symmetry requirement of the environment of the reactants can be also easily satisfied in the case of the monohydroxo iron(III), as it can be seen from the following mechanism:

$$(H_2O)_5\,Fe^{(II)}-\underset{\underset{H}{|}}{OH}\cdots\underset{\underset{H}{|}}{O}-{}^{57}Fe^{(III)}\,(H_2O)_5 \rightleftharpoons$$

$$\rightleftharpoons (H_2O)_5Fe^{(III)}-\underset{\underset{H}{|}}{O}\cdots\underset{\underset{H}{|}}{HO}-{}^{57}Fe^{(II)}\,(H_2O)_5$$

and the electron jump is accompanied by a simultaneous proton transfer.

Not this is the case, however, for the dihydroxo complex, because if it is of *cis*-form, one would expect a double-bridged mechanism, but the *cis*-form itself is by all means not the case [13]. On the other hand, for a *trans*-form, there is not any reasonable geometry that would satisfy the symmetry restrictions.

The exchange with the dimeric form of iron(III) is entirely excluded theoretically and this is really observed.

By accepting that none but the hexaquo- and monohydroxo iron(III) are reactive, the common concentration of these two species and that of the dihydroxo and dimeric complexes can be calculated from the spectra. These data could be compared with those computed using HEDSTRÖM's equilibrium constants which are the following:

$$Fe^{3+} + H_2O = FeOH^{2+} + H^+ \qquad K_{11} = (9.0 \pm 1.0) \cdot 10^{-4}$$
$$Fe^{3+} + 2\,H_2O = Fe(OH)_2^+ + 2\,H^+ \qquad K_{12} = (4.9 \pm 1.0) \cdot 10^{-7}$$
$$2\,Fe^{3+} + 2\,H_2O = Fe_2(OH)_2^{4+} + 2\,H^+ \qquad K_{22} = (1.2 \pm 0.1) \cdot 10^{-3}$$

In Table III this comparison in shown.

The discrepancy found between the data by HEDSTRÖM [1] and those obtained by Mössbauer measurements can be attributed most probably to the deviation in individual concentration of the dihydroxo ions.

Though the spectra measured at the intermediate pH values cannot be used for calculations because of their complicated manner, but, since the dihydroxo complex undoubtedly appears in the spectrum, its concentration should exceed 10 per cent of the total amount of iron(III), unlike the value calculated by HEDSTRÖM's data ranging from zero to 0.4 per cent.

Table III

Concentrations of the iron(III) hydrolysis products

pH	$Fe(H_2O)_6^{3+} + FeOH^{2+}$		$Fe_2(OH)_2^{4+} + Fe(OH)_2^{+}$	
	Data of HEDSTRÖM %	Data from Mössbauer measurements %	Data of HEDSTRÖM %	Data from Mössbauer measurements %
0.05	100	100	0	0
1.10	96	74	4	26
1.85	73	68	26	32
2.25	31	10	68	90

Some qualitative observations have been done on oxidation-reduction reactions too: the iron(III) solutions of different pH have been reduced by metallic copper. These spectra agree with those of the electron exchange investigation. At pH = 0.05 one gets the peaks due to the iron(II) perchlorate with a quadrupole splitting of 3.35 mm/sec and an isomeric shift of 1.42 mm/sec. At pH = 1.45, the superposition of the iron(II) and the hydrolysis products of iron(III) have been obtained, while at pH = 2.30 no reduction could be observed. These qualitative tests accord well with the predictions that the electron-exchange and oxidation-reduction reactions proceed via similar mechanism.

It can be concluded that the Mössbauer effect is a useful method for investigating some problems concerning the structure of solutions, as well as for studying electron transfer reactions. The kinetics of the reactions can be studied also in solid state, if the reaction is slow enough.

REFERENCES

1. HEDSTRÖM, B. D. A.: Arkiv Kemi **6,** 1 (1953)
2. MULAY, L. N., SELWOOD, P. W.: J. Am. Chem. Soc. **77,** 2693 (1955)
3. DÉZSI, I., KESZTHELYI, L., MOLNÁR, B., PÓCS, L.: Central Research Institute for Physics, Budapest, Hungary. Preprint 9 (1967)
4. DÉZSI, I., KESZTHELYI, L., MOLNÁR, B., PÓCS, L.: Phys. Letters **18,** 18 (1965)
5. DÉZSI, I., KESZTHELYI, L., PÓCS, L., KORECZ, L.: Phys. Letters **18,** 14 (1965)
6. NOZIK, A. J., KAPLAN, M.: J. Chem. Phys. **47,** 2960 (1967)
7. RUBY, S. L., TSENG, P. K., HWA-SHENG CHENG, HI, N. C.: Chem. Phys. Letters, **2,** 39 (1968)
8. VÉRTES, A.: Magyar Kém. Foly. **75,** 175 (1969)
9. VÉRTES, A., BURGER, K., SUBA, L : Acta Chim. Acad. Sci. Hung. **63,** 123 (1970)
10. VÉRTES, A., DÉZSI, I., SUBA, L.: Acta Chim. Acad. Sci. Hung. **64,** 347 (1970)
11. VÉRTES, A., KISS, L., VARSÁNYI, M.: Acta Chim. Acad. Sci. Hung. **65,** 67 (1970)
12. BURGER, K., VÉRTES, A., CZAKÓ, I. N.: Acta Chim. Acad. Sci. Hung. **63,** 115 (1970)
13. DÉZSI, I., VÉRTES, A., KOMOR, M.: Inorg. Nucl. Chem. Letters **4,** 649 (1968)
14. DÉZSI, I., GOROBCHENKO, V. D., LUKACHEVICH, I. I., VÉRTES, A.: Chem. Phys. Letters **2,** 665 (1968)
15. DÉZSI, I., KOMOR, M., VÉRTES, A., GOROBCHENKO, V. D., LUKACHEVICH, I., I., CIKISHWILLI, K. F.: to be published

16. RUFF, I.: Quart. Rev. **22**, 199 (1968)
17. MARCUS, R. A.: Ann. Revs. Phys. Chem. **15**, 155 (1964)
18. ZWOLINSKY, B. J., MARCUS, R. J., EYRING, H.: J. Phys. Chem. **58**, 432 (1954)
19. SILVERMAN, J., DODSON, R. W.: J. Phys. Chem. **56**, 846 (1952)
20. SÓS, J., VÉRTES, A.: Magyar Kémikusok Lapja **12**, 690 (1968)

Mária KOMOR, Attila VÉRTES } Budapest VIII., Puskin u. 11/13
István DÉZSI; Budapest XII., Konkoly Thege M. u.
Imre RUFF; Budapest VIII., Múzeum-krt. 6/8.

Acta Chimica Academiae Scientiarum Hungaricae, Tomus 66 (3), pp. 293—306 (1970)

ELECTRON SPIN RESONANCE SPECTRA OF THE CHROMIUM(III) OXIDE–MOLYBDENUM(VI) OXIDE SYSTEM

A. ROCKENBAUER* and GY. GÁTI**

*(*Central Research Institute for Chemistry of the Hungarian Academy of Sciences and **High Pressure Research Institute, Budapest)*

Received June 30, 1969

The paramagnetic resonance spectrum of chromium–molybdenum mixed oxides has been investigated at various chromium : molybdenum ratios in case of various starting materials and at various ignition temperatures. The spectra exhibited lines of two types. One of them was a structureless broad singlet, which was attributed to the Cr^{3+} ions in $Cr_2(MoO_4)_3$, the other was a narrow signal with anisotropic g and hyperfine structure, presumed by the authors to arise from Cr^{5+} ions located in the MoO_3 lattice. These Cr^{5+} ions of restricted number are formed only in special centres where OH^- groups are also present. The Cr^{5+} ion is surrounded by oxygens arranged in square-pyramidal symmetry. The strongest chromium–oxygen bond is formed with the oxygen located at the vertex on the fourfold axis. The bonding pattern of the structure is analogous to that of $(CrOCl_4)^-$, however, the in-plane σ bond is stronger, and the charge transfer excitation energies are larger. Spectra in the X-band exhibit besides the lines of the ^{53}Cr isotope also a super-hyperfine structure arising from hydrogen.

I. Introduction

In an earlier study, the solid state reactions and the catalytic properties of the chromium oxide–molybdenum oxide system have been investigated [1]. These investigations gave an evidence that chromium molybdate ($Cr_2(MoO_4)_3$) is formed by annealing a mixture of the two oxides [2]. It was also shown that dispersed molybdenum ions can be incorporated in the lattice of chromium oxide, when the chromium content exceeds considerably that of molybdenum. There was no information, however, available for samples containing small amounts of chromium. We have recorded electron spin resonance spectra of mixed oxides. The ESR spectra can supply information first of all for samples of low chromium concentration, since the diamagnetic molybdenum(VI) oxide gives no signal and the paramagnetic centres, formed by ignition even in a very low concentration, can be observed.

II. Experimental part

For the preparation of the mixed oxides, the following substances of analytical grade have been used:

A: chromium(III) oxide
B: chromium(III) nitrate
C: molybdenum(VI) oxide
D: ammonium paramolybdate

Marking of the samples prepared from the above substances:

AC: A mixture of preannealed chromium(III) oxide and molybdenum(VI) oxide of an atomic ratio of 1 : 1 was ignited at various temperatures (300—700 °C).

AD: Chromium(III) oxide was impregnated with an aqueous solution containing various amounts of ammonium molybdate, and the samples were ignited for 10 hours at 700 °C.

BC: Molybdenum(VI) oxide, preannealed at 700 °C, was impregnated with an aqueous solution of chromium nitrate, the samples were dried, and ignited at various temperatures (300—700 °C).

BD: Chromium nitrate was mixed with the aqueous solution of ammonium molybdate, and the samples were dried at various temperatures (300—700 °C).

The electron spin resonance spectra were taken in X-band with a JEOL Model JES-P-10 spectrometer, and in Q-band with a VARIAN Model E3 spectrometer both at room temperature and at liquid nitrogen temperature.

III. Characterization of the spectra

The spectra contained a broad symmetric singlet ($g = 1.97$) and a composite asymmetric signal consisting of narrow lines (Fig. 1). With some of the samples, signal components occurred, which are characteristic of one of the start-

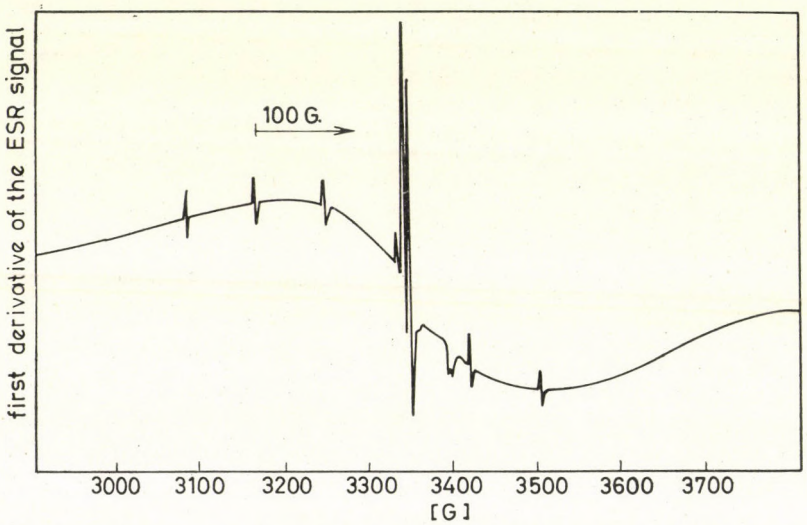

Fig. 1. X-band electron spin resonance spectrum of chromium–molybdenum mixed oxide containing 0.1 per cent of chromium

ing materials, and not of the mixed oxide. Thus, for example, in samples of high chromium concentration the signal of the antiferromagnetic-paramagnetic chromium(III) oxide [3] could be observed, while in samples containing ammonium paramolybdate and ignited at a temperature below 400 °C, signals to be ascribed to the Mo(V) ion appeared. We will not discuss here signals of the two latter types.

a) Broad singlet line

The intensity of the broad singlet line exhibits in function of the chromium concentration a maximum at 40 per cent (referred to atomic ratio). Below 40 per cent, the intensity of the signal is proportional to the concentration of chromium, above 40 per cent to that of molybdenum (Fig. 2). The concentration dependence of signal intensity, plotted in Fig. 2, supports the fact

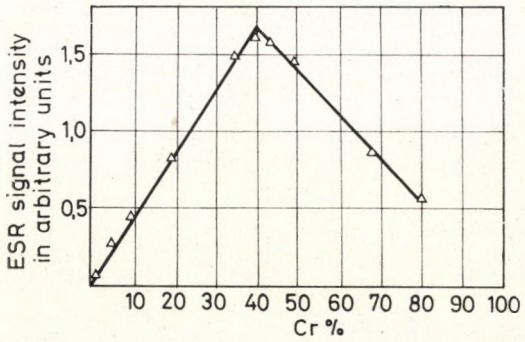

Fig. 2. Signal intensity of the electron spin resonance spectrum of chromium–molybdenum mixed oxides in function of the chromium content

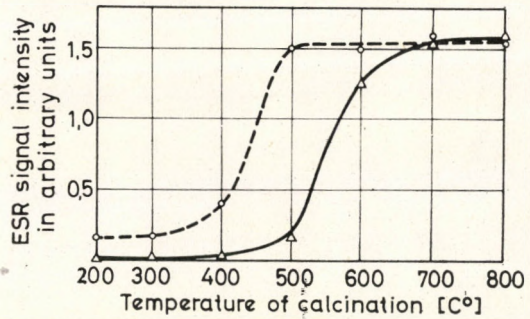

Fig. 3. Signal intensity of the electron spin resonance spectrum of chromium–molybdenum mixed oxides in function of the ignition temperature, - - - - *AD* and *BD* samples; ———— *AC* samples

that a paramagnetic mixed oxide ($Cr_2(MoO_4)_3$) is formed [2], when a mixture of diamagnetic molybdenum(VI) oxide and antiferromagnetic chromium(III) oxide is heated at high temperatures. In samples containing less than 70 per cent of chromium, the width of the signal is 200—350 Gauss. Presumably, the moderate width of the signal is due to a strong exchange interaction between the chromium(III) ions. In samples containing more than 70 per cent of chromium, the line width increases (maximum line width observed was 700 Gauss), which is indicative of the fact that a phase, richer in chromium than

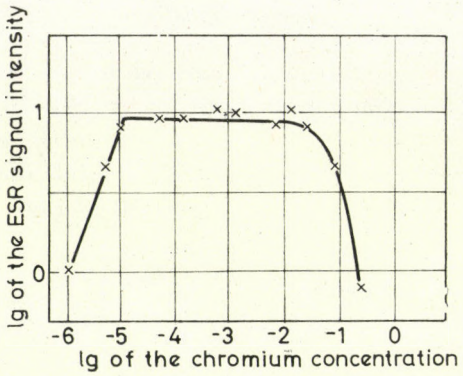

Fig. 4. Intensity dependence of narrow signal on chromium concentration in the electron spin resonance spectrum of chromium–molybdenum mixed oxide

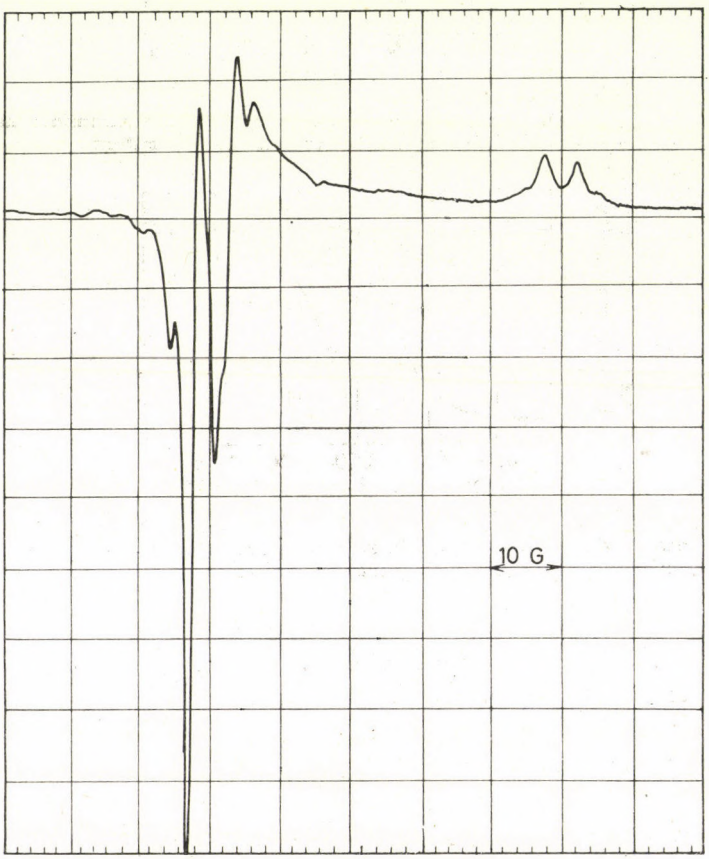

Fig. 5. X-band electron spin resonance spectrum of mixed oxides containing 0.01 per cent of chromium at 77 °K

chromium(III) molybdate has been formed. Though signals in the half-field region (about 1500 Gauss in X-band spectra) were not observed, the existence of dispersed chromium(III) ions in molybdenum oxide cannot be excluded, since lack of this signal component can be caused by the small value ($D \leq 0.2$ cm^{-1}) of the zero field term [4].

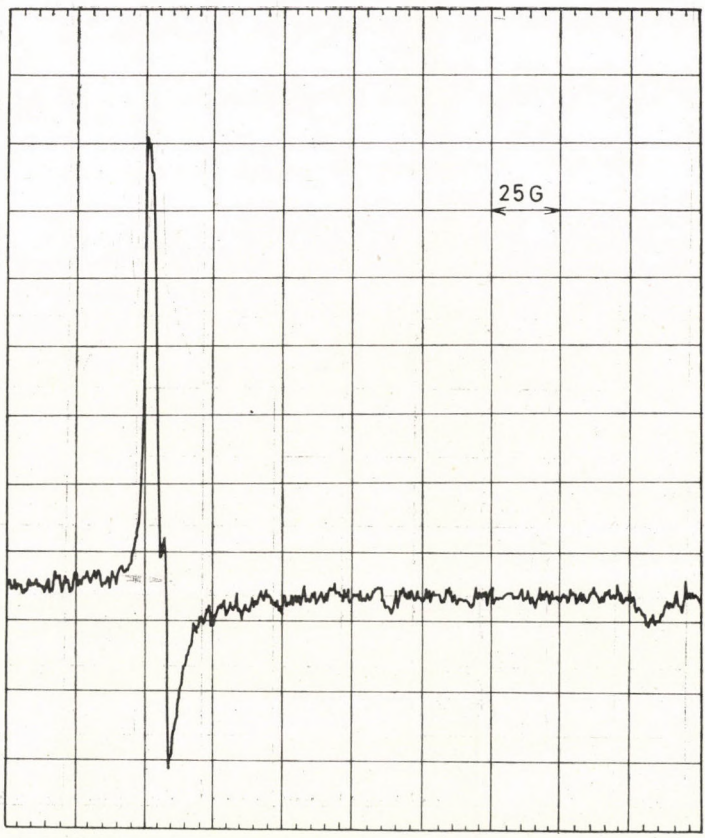

Fig. 6. Q-band electron spin resonance spectrum of mixed oxides containing 0.01 per cent of chromium at 77 °K

The temperature of the formation of chromium(III) molybdate can be established from the intensity dependence of the broad signal on the ignition temperature (Fig. 3). It can be seen from the diagram that the temperature necessary for the solid state reaction is 600 °C for the metal oxide mixture (sample *AC*) and about 450 °C for impregnated samples (*AD* and *AC*).

b) Narrow composite signal

The narrow asymmetric signal was observed with samples of less than 10 per cent chromium content, when the ignition temperature was higher than 400 °C. Remarkably, within a wide range (between a chromium concentration

from 0.001 to 5 per cent) the signal intensity was found to be independent of the concentration, while below 0.001 per cent it was proportional to the chromium concentration, and above 5 per cent to the excess concentration of molybdenum, not participating in the solid state reaction (Fig. 4).

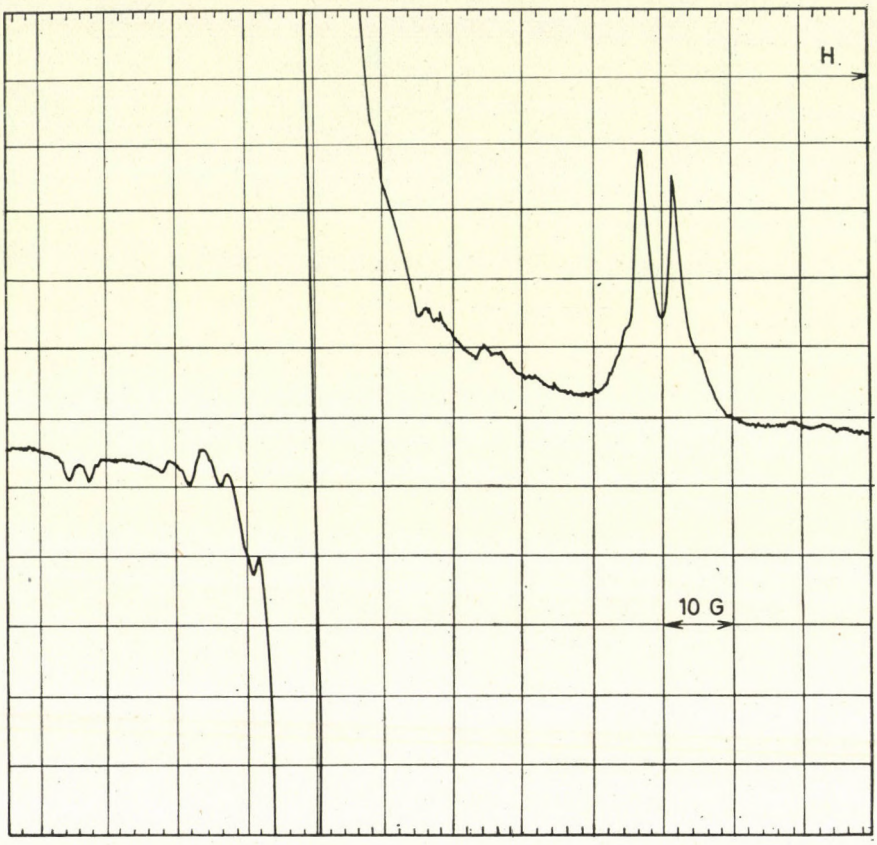

Fig. 7. X-band electron spin resonance spectrum of mixed oxides containing 0.01 per cent of chromium at 77 °K (increased amplification)

The signal intensity is influenced only slightly by ignition temperature, while it is affected considerably by the mode of preparation. Thus, when the mixture of preannealed metal oxides (*AC*) is ignited, the intensity of the signal is by an order of magnitude smaller than that of samples (*BD*) impregnated with ammonium molybdate.

In order to identify unambiguously the particular signal components, the spectra were recorded both in the X- and Q-bands (Figs 5 and 6). In the spectrum taken in the Q-band, the hyperfine structure merges almost completely, and the axial character of the g tensor can be clearly seen. In the $g_{||}$ part of the X-band spectrum a doublet of $4 \cdot 10^{-4}$ cm^{-1} separation, and in the $g_{\perp}$

part a more composite line structure (two larger and two smaller lines) can be observed. In spectra of high amplification further lines appear, the amplitude of which is by 40 to 100 times smaller than that of the principal lines (Fig. 7).

The shape of the spectrum is almost independent of the preparational technique. Slight changes were observed, when the ignition temperature (760 °C) approximated the sublimation temperature of molybdenum(VI) oxide. The width of each line in the hyperfine patterns is nearly identical, being at room temperature 1.2 Gauss, and at liquid nitrogen temperature 0.8 Gauss.

IV. Discussion of the results

We concluded that the narrow signal of composite pattern arises also from chromium ions, because the intensity of the signal is proportional to the concentration of chromium when the concentration does not exceed 0.001 per cent. On the other hand, the diminution of signal intensity in the concentration range, where the quantity of molybdenum participating in the solid state reaction is considerable, indicates that paramagnetic chromium ions are incorporated in the molybdenum(VI) oxide lattice or in its surface layer. The characteristic g values and small line width [5] suggest that the observed centres are Cr(V) ions.

The doublet observed in the $g_{||}$ part of the spectrum can be interpreted as hyperfine splitting arising from a nuclear spin of $I = 1/2$. However, since none of the mixed oxide components have a nuclear spin of 1/2, it must be assumed that the doublet splitting arises from an impurity playing an important role in the formation of the paramagnetic centre. An impurity of this type may be hydrogen of a nuclear spin of $I = 1/2$, which is able to stabilize Cr^{5+} ions at the site of Mo^{6+} ions, by compensating the charge deficiency. For the verification of our assumption, 1 per cent of sodium hydroxide was added before ignition to the mixed oxide. This brought about a broadening of the signal and an increase of its intensity. Paramagnetic centres formed during ignition proved to be stable when subjected to various treatments. The signal intensity and shape did not change significantly when samples were boiled in water or in cyclohexane.

The following alternative explanations may be given for the complexity of the spectrum in the $g_{\perp}$ region:

1. The hyperfine tensor of the proton has three different principal values.
2. The hyperfine tensor of the proton is axial, but the direction of its principal axis is perpendicular to the principal axis of the g tensor.
3. There exist paramagnetic centres of different kinds.

This latter interpretation is supported by the fact that after repeated ignition at 760 °C, the amplitude of the doublet in the $g_{||}$ part diminishes as

compared to the amplitude of the lines in the $g_\perp$ part, and the two larger lines in the $g_\perp$ part are saturated easier than the two smaller ones.

An examination of the low intensity lines of the spectrum indicates also that centres of more than one type are present. Besides the hyperfine lines of the ^{53}Cr isotope of about 10 per cent natural abundance and a nuclear spin of $I = 3/2$, additional small lines could be observed. In the assignment of the hyperfine lines, it was assumed on the one hand that the hyperfine coupling tensor associated with chromium is also axial and its principal axis is parallel to that of the g tensor, and on the other hand, only those lines were taken into consideration, the amplitude of which was by about 40 times less than that of the corresponding main lines.

The spin Hamiltonian neglecting the super-hyperfine coupling of proton is:

$$\mathcal{H} = g_{||} S_z H_z + g_\perp (S_x H_x + S_y H_y) + A_{||}^{^{53}Cr} I_z S_z + A_\perp^{^{53}Cr} (I_x S_x + I_y S_y).$$

The principal values were evaluated by the method of SANDS [6]:

$$g_{||} = 1.949 \pm 0.001 \qquad g_\perp = 1.976 \pm 0.002$$

$$|A_{||}^{^{53}Cr}| = (38.5 \pm 1) 10^{-4}\ cm^{-1},$$

$$|A^{^{53}Cr}| = (\ 9.1 \pm 1) 10^{-4}\ cm^{-2}.$$

According to VAN REIJEN and COSSEE [7], besides from the spin Hamiltonian parameters, the spin-lattice relaxation time can also supply information about the geometrical environment of Cr(V) ions. The procedure is based upon that spin-lattice relaxation is weak, when the ground state is a singlet well separated from the excited states. However, a well separated singlet ground state occurs only in a crystal field of square-pyramidal symmetry, while the ground state of the $3d$ electron is degenerated in case of octahedral or tetrahedral symmetry. In our case, the small width of the spectrum lines (1.2 Gauss) observed at room temperature shows a weak spin-lattice relaxation, indicative of the fact that the Cr^{5+} ion is surrounded by oxygen ions arranged according to square-pyramidal symmetry. The question may arise, however, whether such a square-pyramidal arrangement can be formed when a Mo^{6+} ion is substituted by Cr^{5+} ion in the molybdenum(VI) oxide lattice.

According to X-ray diffraction structural determinations [8], molybdenum is surrounded by six oxygens in a distorted octahedral arrangement in the molybdenum(VI) oxide lattice. Four oxygens are situated on the *ac* plane (O_I, O_{II}, O_{III}, O_{IV}) and form an almost regular square, their distance from central molybdenum is 1.88 Å and 1.96 Å, resp. The remaining two oxygens of octahedron are spaced at a greater distance. O_V is located in the direction of the *b* axis at a distance of 2.1 Å, and O_{VI} at a distance of 2.43 Å (Fig. 8a). O_V has

a distinguished position, because this is the only oxygen, which is coordinated to a single molybdenum ion. Owing to this fact, when molybdenum is substituted with another ion, the distance of O_V from the metal ion can change without producing any other distortion in the lattice. The geometry of Mo^{5+} in $MoOPO_4$, surrounded similarly by six oxygens [9], differs from the structure of molybdenum(VI) oxide by the very fact that the distance Mo–O_V is

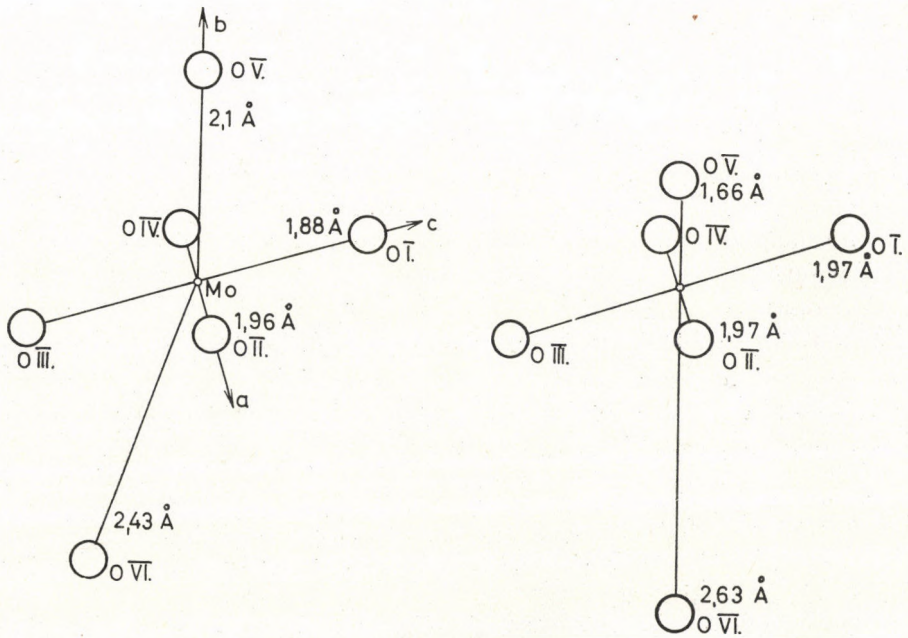

Fig. 8. Geometrical arrangement of oxygens in the MoO_3 and $MoOPO_4$ lattices

considerably less: 1.6 Å (Fig. 8b). The shortening of the Cr–O_V distance on substitution of the Mo^{6+} ion with Cr^{5+} ion is supported by the following facts:

1. The radius of the Cr^{5+} ion is smaller than that of the Mo^{6+} ion.

2. In square-pyramidal Cr^{5+} structures, thus *e.g.* in $(CrOCl_4)^-$, the Cr–O bond is very strong [10].

3. JAHN—TELLER effect. In a regular octahedral crystal field, the lowest energy level of the $3d^1$ electron is a triplet (t_2), which is split into a singlet ($b_2(d_{xy})$) and a doublet ($e(d_{xz}, d_{yz})$) by axial distortion. In the molybdenum(VI) oxide lattice, the environment of the Mo^{6+} ion is approximately a tetragonally elongated octahedron, and consequently, if substitution of the Cr^{5+} ion would take place without a change in the position of the oxygens, the ground state would be a doublet. If, however, the distance Cr–O is shortened, the ground state is a singlet.

It follows from the foregoing that a square-pyramidal symmetry can result when the Cr^{5+} ion is built into the interior of the molybdenum(VI) oxide lattice. However, the possibility cannot be excluded that the Cr^{5+} ion is incorporated on the surface, since a square-pyramidal arrangement can be realized in this case, too [7b].

Let us denote the centre in question by the formula $(CrO_5)^{5-}$. An analogy can be shown between the groups $(CrO_5)^{5-}$ and $(CrOCl_4)^-$ on the basis of principal values of g tensor and hyperfine tensor. KON and SHARPLESS [11] pointed to the covalent character of bondings in $(CrOCl_4)^-$. These authors showed that the anomal order of $g_{||} < g_\perp$ values is caused by a low-lying charge transfer excitation. They are of the opinion that, owing to the weak Cr–Cl bondings, the energy required for the excitation of an electron from the filled b_1 bonding orbital to the b_2 antibonding orbital is nearly the same as the energy required for the excitation of the unpaired electron from the b_2 antibonding orbital to the b_1 antibonding orbital (Fig. 9). Thus, the orbital contributions to $g_{||}$ coming from antibonding and bonding b_1 orbitals compensate each other. In our case, due to the stronger Cr–O bondings, the charge transfer transition energies are of such magnitude that these states need not be taken into consideration in the second order perturbation procedure, and thus, it is sufficient to restrict ourselves to antibonding orbitals. The antibonding molecular orbitals belonging to square-pyramidal symmetry are:

$$b_2 = \alpha_1 d_{xy} - \alpha_1' \pi_{xy} ,$$

$$e = \begin{cases} \alpha_2 d_{xz} - \alpha_2' \pi_{xz} , \\ \alpha_2 d_{yz} - \alpha_2' \pi_{yz} , \end{cases}$$

$$b_1 = \alpha_3 d_{x^2-y^2} - \alpha_3' \sigma_{x^2-y^2} ,$$

omitting the α_1 antibonding orbital, because it does not give second order contribution to the g values. In the above molecular orbitals σ and π denote linear combinations of $2s$ and $2p$ oxygenic atomic orbitals of proper symmetry, α and α' are the appropriate molecular orbital coefficients.

In order to calculate the g factors, a perturbation was carried out through second order, using the ABRAGAM—PRYCE perturbation Hamiltonian [12]. In the formulae of hyperfine coupling constants only the first order terms are retained and integration is limited over the metal atom when a matrix element contains the factor $\langle r^{-3} \rangle$. The resulting equations are:

$$g_{||} - g_0 = \frac{8\xi_m}{E_{b_1} - E_{b_2}} \alpha_1 \alpha_3 (\alpha_1 \alpha_3 - \alpha_1' \alpha_3') ,$$

$$g_\perp - g_0 = \frac{2\xi_m}{E_e - E_{b_2}} \alpha_1^2 \alpha_2^2 ,$$

$$A_{||}^{^{53}Cr} = -P\left(\varkappa + \frac{4}{7}\right)\alpha_1^2,$$

$$A_{\perp}^{^{53}Cr} = -P\left(\varkappa - \frac{2}{7}\right)\alpha_1^2,$$

where

$$P = 2\beta\beta_N g_N \langle r^{-3}\rangle .$$

Notations used in the expressions: g_0 is the g factor of the free electron, g_N the g factor of the ^{53}Cr nucleus, β BOHR's magneton, β_N the nuclear magneton and $\varkappa$ the Fermi constant. Spin–orbit couplings (ξ_m) are taken into consideration only for the $3d$ orbitals of chromium, while the effect of the ligand orbitals has been neglected. Overlap integrals have also been neglected. Crystal field energy levels are designated by E_{b_1}, E_{b_2} and E_e, resp.

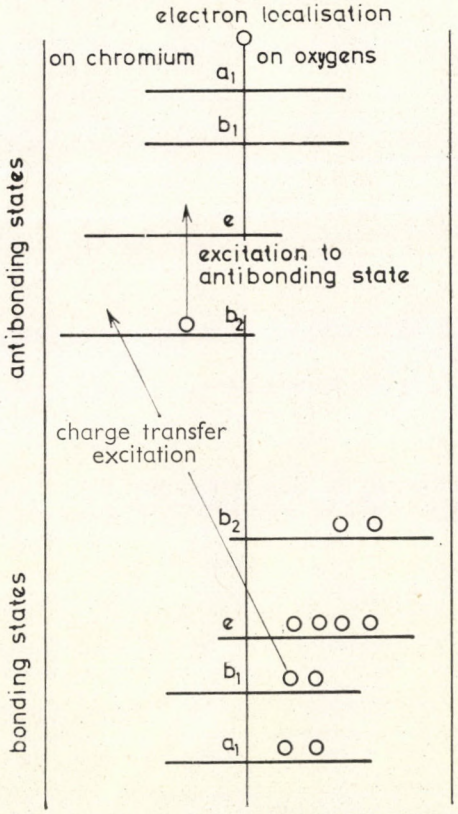

Fig. 9. Energy level diagram of molecular orbitals for the $(CrO_5)^{5+}$ group. The horizontal shifts illustrate the charge localization in the particular molecular orbitals

If the value of P is known, conclusions may be drawn from the experimental values of the hyperfine constants on the magnitude of the Fermi term and on the strength of the π bonding in the ground state. The theoretical value of P is known only for the free Cr^{5+} ion, and this value may change substantially for a Cr^{5+} ion participating in a chemical bond, so that the value $P = 35.5\ 10^{-4}\ cm^{-1}$, determined by KON and SHARPLESS [11] in $(CrOCl_4)^-$ is taken as a basis in our calculations. Supposing that $\varkappa$ has about the same value as in case of $(CrOCl_4)^-$, the sign of both hyperfine constants has to be taken as negative. Then we obtain:

$$\varkappa = 0.552 \text{ and } \alpha_1^2 = 0.965 .$$

It can be seen from Table I that the bonding in the ac plane is weaker in $(CrO_5)^{5-}$ than in $(CrOCl_4)^-$.

Table I

Substance	α_1^2	α_2^2	α_3^2	ω	Ref.
$(CrOCl_4)^-$	0.868	0.814	0.818	2.24	[11]
Cr^{5+}/MoO_3	0.965	0.802	0.633	2.56	present commun.

For the calculation of the further molecular orbital parameters, the values of the E_e and E_{b_1} energy levels must also be known. As no optical data are available, the values determined by MISHRA and SYMONS [13] from the optical spectrum of $(CrO_3)^-$ in oleum are used:

$$E_e - E_{b_2} = 13{,}700\ cm^{-1} \text{ and } E_{b_1} - E_{b_2} = 18{,}000\ cm^{-1} .$$

The almost completely identical magnetic parameters of Cr^{5+} ion in oleum [13, 14] and in molybdenum(VI) oxide permit to assume a good agreement of the optical data (Table II).

Table II

Substance	$g_\parallel$	$g_\perp$	$\lvert A_\parallel \rvert$ $10^{-4}cm^{-1}$	$\lvert A_\perp \rvert$ $10^{-4}cm^{-1}$	Ref.
Cr^{5+}/MoO_3	1.949	1.976	38.5	9.1	present commun.
$(CrO_3)^-$ (in oleum)	1.949	1.975	39	9	[14]
$(CrO_3)^-$ (65% oleum)	1.951	1.970	—	—	[13]
$(CrOCl_4)^-$	1.988	1.979	36.1	9.2	[11]

According to the calculations of DUNN [15], the value of the ξ_m spin–orbit coupling constant is strongly dependent on the number of electrons actually localized around chromium, that is to say, on the covalent character of the bonds. Let us assume temporarily that the amount of charge backdonation to chromium does not differ substantially in the case of $(CrO_5)^{5-}$ and $(CrOCl_4)^-$, and use the value

$$\xi_m = 230 \text{ cm}^{-1},$$

determined by KON and SHARPLESS [11]. Then α_2 and α_3 can be calculated by using the experimental values of g factors. In Table I the bonding parameters and charge backdonation produced by the b_1, b_2 and e bonding and antibonding orbitals:

$$\omega = 8 - (\alpha_1^2 + 4\,\alpha_2^2 + 2\,\alpha_3^2)$$

are compared for $(CrO_5)^{5-}$ and $(CrOCl_4)^-$. Though the charge backdonation calculated in this way is larger for $(CrO_5)^{5-}$ than for $(CrOCl_4)^-$, the difference is so small that it does not influence considerably the value of the spin–orbit coupling constant. It can be seen from Table I that the out-of-plane π-bond has almost the same degree of covalent character in the two cases, while the in-plane σ bond is considerably stronger in $(CrO_5)^{5-}$, which is in accordance with the expectation that the Cr–O bonds have a stronger covalent character than the Cr–Cl bonds.

Since the principal values of the super-hyperfine tensor of hydrogen cannot be determined unambiguously, the location of hydrogen can be determined only approximately. The small value of the doublet splitting (4 Gauss) indicates that the hydrogen is not coordinated directly to the Cr^{5+} ion, so that it gives only a small contribution to the crystal field. In free radicals, in the —ĊOH groups, the coupling constant of hydrogen [16] has the same order of magnitude as the doublet separation observed by us. Thus, it may be assumed that hydrogen is not attached directly, but through oxygen to the Cr^{5+} ion.

*

We wish to thank D. J. OCKWELL working in Zürich at VARIAN AG laboratory for recording of the Q-band spectra.

REFERENCES

1. GÁTI, GY., MÁNDY, T.: Fourth Internat. Conf. Catalysis. Moscow 1968
2a. NASSAU, K., LEVINSTEIN, H. J., LOIACONO, G. M.: J. Phys. Chem. Solids **26**, 1805 (1965)
2b. TRUNOV, V. K., KOVBA, L. M.: Izv. Akad. Nauk USSR. Neorgan. Materialy **2**, 151 (1966)
2c. CLARK, G. M., DOYLE, W. P.: Spectrochim. Acta **22**, 1441 (1966)
2d. DOYLE, W. P., MC GUIRE, G., CLARK, G. M.: J. Inorg. Nucl. Chem. **28**, 1185 (1966)

3a. TROUNSON, E. P., BLEIL, D. E., WANGSNESS, R. K., MAXWELL, L. R.: Phys. Rev. **79**, 542 (1950)
3b. MAXWELL, L. R., MC GUIRE, T. R.: Rev. Mod. Phys. **25**, 279 (1953)
3c. DAYHOFF, E. S.: Phys. Rev. **107**, 84 (1957)
4a. O'REILLY, D. E.: Advances in Catalysis **12**, 31 (1960)
4b. O'REILLY, D. E., MAC IVER, D. S.: J. Phys. Chem. **66**, 276 (1962)
5. GARRETT, B. B., DE ARMOND, K., GUTOWSKY, H. S.: J. Chem. Phys. **44**, 3393 (1966)
6. SANDS, R. H.: Phys. Rev. **99**, 1222 (1955)
7a. VAN REIJEN, L. L., COSSEE, P., VAN HAREN, H. J.: J. Chem. Phys. **38**, 572 (1963)
7b. VAN REIJEN, L. L., COSSEE, P.: Disc. Faraday Soc. **41**, 277 (1966)
7c. BANKS, E., GREENBLATT, M., MC GARVEY, B. R.: J. Chem. Phys. **47**, 3772 (1967)
8. ANDERSSON, G., MAGNÉLI, A.: Acta Chem. Scand. **4**, 793 (1950)
9. KIERKEGARD, P., WESTERBAND, M.: Acta Chem. Scand. **18**, 2217 (1964)
10a. GRAY, H. B., HARE, C. R.: Inorg. Chem. **1**, 363 (1962)
10b. BALLHAUSEN, C. J., GRAY, H. B.: Inorg. Chem. **2**, 246 (1963)
11. KON, H., SHARPLESS, N. E.: J. Chem. Phys. **42**, 906 (1965)
12. ABRAGAM, A., PRYCE, M. H. L.: Proc. Roy. Soc. **206**, 164 (1954)
13. MISHRA, H. C., SYMONS, M. C. R.: J. Chem. Soc. **1963**, 4490
14. VAN REIJEN, L. L.: Thesis (Eindhoven 1964)
15. DUNN, T. M.: Trans. Faraday Soc. **57**, 1441 (1961)
16. RAO, D. V. G. L. N., GORDY, W.: J. Chem. Phys. **35**, 362 (1961)

Antal ROCKENBAUER; Budapest II., Pusztaszeri út 59/67
Gyula GÁTI; Budapest, 5 P.O.B. 208.

Acta Chimica Academiae Scientiarum Hungaricae, Tomus 66 (3), pp. 307—314 (1970)

SYNTHESIS OF NEW SUGAR DERIVATIVES HAVING POTENTIAL ANTITUMOUR ACTIVITY, XIII*

SYNTHESIS OF 1,2 : 5,6-DIEPITHIO-D-MANNITOL, -D-GLUCITOL AND SOME OF THEIR DERIVATIVES

J. KUSZMANN and L. VARGHA

(Research Institute for Pharmaceutical Chemistry, Budapest)

Received June 30, 1969

The synthesis of 1,2 : 5,6-diepithio-D-mannitol, -D-glucitol and some of their derivatives, starting from 1,2 : 5,6-dianhydro-3,4-O-isopropylidene-L-iditol and 3,4-O-isopropylidene-D-glucitol, and the properties of the new compounds are described.

In a previous publication [1] the synthesis and properties of 1,2 : 5,6--diepithio-L-iditol have been described. It is known from former investigations carried out in these laboratories that the cytostatic activity of different carbohydrate derivatives with similar structures markedly depend on their configuration. Therefore, the synthesis of new diepithio-hexitols possessing similar structures, but different configurations, was attempted. Of the stereoisomeric diepithio-hexitols to be synthesized, the D-mannitol derivative was the most interesting as far as the biological activity was concerned, because in similar investigations with other hexitol derivatives the mannitol configuration was shown to have the strongest cytostatic activity [2] (*e.g.*, among the 2-chloroethylamino-, or methanesulfonyl derivatives).

For the synthesis of 1,2 : 5,6-diepithio-D-mannitol, 1,2 : 5,6-diepoxi--3,4-O-isopropylidene-L-iditol (**I**) prepared in this laboratory some years ago [3] could be used as the starting material. Treatment of this L-iditol derivative, **I**, with thiourea according to CREIGHTON and OWEN [4] should lead, with Walden inversion at C-2 and C-5 to the required diepithio-mannitol derivative, **II**. This reaction could be carried out in 45% yield using acetone as solvent instead of methanol [5]; in the latter solvent, owing to fast polymerization of the formed episulfide, the yield was lower than 10%. The presence of epithio rings in **II** could be proved by the IR spectrum, which showed a band at 3080 cm^{-1} corresponding to the νCH of strained rings, and by conversion into 3,4-O-isopropylidene-1,2,5,6-tetrathio-1,2 : 5,6-bis-thiocarbonyl-D-mannitol (**III**) on treatment with carbon disulfide and potassium hydroxide [4]. The structure of **II** was also verified by thin-layer chromatography, as the compound gave a single spot on detection with 4-(*p*-nitrobenzyl)-pyridine, showing the presence of an alkylating agent [6].

* Part XII: Carbohydrate Research **11**, 165 (1969)

The protecting O-isopropylidene group of compound **II** was removed by treatment with methanolic hydrogen chloride, without cleavage of the epithio rings. The structure of the 1,2 : 5,6-diepithio-D-mannitol (**IV**) obtained was proved by the positive reaction with 4-(*p*-nitrobenzyl)-pyridine, by the IR spectrum showing a strained *v*CH band at 3065 cm^{-1}, and by the IR and NMR spectra of the O-diacetyl derivative (**V**).

1,2 : 5,6-diepithio-3,4-O-isopropylidene-D-mannitol (**II**) rapidly undergoes polymerization in methanolic solution in the presence of sodium methoxide

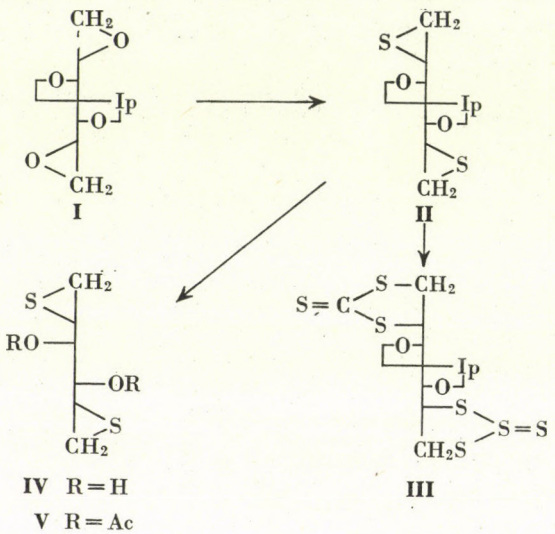

Fig. 1

to give an insoluble amorphous compound, whose IR spectrum showed no bands for SH, OH or epithio groups. This fact leads to the conclusion that the polymerization of **II** takes place by C—S—C cross-linking. After removal of the O-isopropylidene group, the diepithio compound, **IV**, suffers a rearrangement in aqueous solution, yielding partly a polymer and partly a hydrolyzed derivative, as the solution contains 28% dithio-hexitol, on the basis of the SH groups present, determined by titration with 0.1 *N* iodine solution.

For the synthesis of the 1,2 : 5,6-diepithio-D-glucitol isomer, 3,4-O-isopropylidene-1,2,5,6-tetra-O-methanesulfonyl-D-glucitol (**VI**) [7] was chosen first as the starting material. Treatment of **VI** with potassium thiolbenzoate gave an amorphous 1,6-di-S-benzoyl-2,5-di-O-methanesulfonyl-1,6-dithio-D--glucitol (**VII**) which yielded the required 1,2 : 5,6-diepithio-3,4-O-isopropylidene-D-glucitol (**VIII**) on treatment with methanolic sodium methoxide. Compound **VIII** could be purified by distillation, giving a crystalline product. During the formation of the epithio rings, Walden inversion takes place at C-2 and C-5 in this case too, but due to the special configuration of glucitol,

a simultaneous change at the asymmetric centres mentioned above, leads to glucitol derivatives again.

As the preparation of the 1,6-di-S-benzoyl intermediate **VII** in acetone solution involved experimental difficulties (precipitation of an extremely thick potassium methanesulfonate) making the isolation of the product laborious, the synthesis of **VIII** was also attempted through the previously unknown 3,4-O-isopropylidene-1,2,5,6-tetra-O-toluene-*p*-sulfonyl-D-glucitol (**IX**). Compound **IX** was obtained by treatment of the known 3,4-O-isopropylidene-

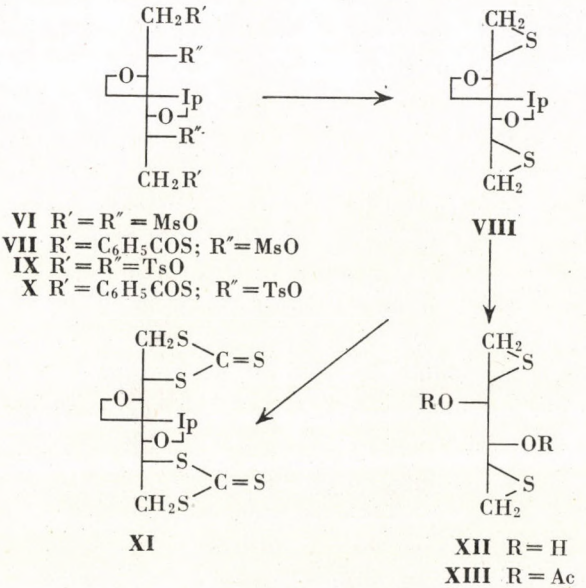

Fig. 2

-D-glucitol [3] with toluene-*p*-sulfonyl chloride, giving a mixture of three compounds (*a*, *b* and *c*) which could be separated by column chromatography. The slowest moving fraction (*c*) representing the main component (68%) proved to be the required compound **IX**, as it could be converted with potassium thiolbenzoate into an amorphous 1,6-di-S-benzoyl-3,4-O-isopropylidene-1,6--dithio-2,5-di-O-toluene-*p*-sulfonyl-D-glucitol (**X**), which gave the diepithio-derivative **VIII** described above in a good yield on treatment with methanolic sodium methoxide. The structures of components *a* and *b* (representing 7% and 27%, respectively) were not elucidated unambiguously. Analytical and IR data suggest that *a* has the structure of an anhydro-di-O-toluene-*p*-sulfonyl--hexitol and that *b* is an isomer of *c*. For comparative studies we also synthesized 3,4-O-isopropylidene-1,2,5,6-tetra-O-toluene-*p*-sulfonyl-D-mannitol; this compound is mentioned in the literature [8] but physical constants, analytical or other experimental data have not been reported. The obtained crystalline compound was not identical with component *b*, as shown by TLC.

The diepithio derivative **VIII** gave a positive reaction with 4-(nitrobenzyl)pyridine, it polymerized readily in methanolic solution in the presence of sodium methoxide to give an insoluble product, and its IR spectrum showed the νCH bands (3080 and 3070 cm^{-1}) characteristic of strained rings. Treatment of compound **VIII** with carbon disulfide and potassium hydroxide gave the corresponding trithio-carbonate (**XI**), proving the anticipated structure. The protecting O-isopropylidene group was removed in a similar manner as in the case of the mannitol derivative described above. 1,2 : 5,6-Diepithio-D--glucitol (**XII**) was obtained in a somewhat lower yield (35%), and its structure was proved by the same reactions as mentioned for the mannitol derivative (**IV**). Compound **XII**, when dissolved in hot water, suffered polymerization and hydrolysis, the latter being indicated by the appearance of SH groups. In pyridine solution it suffered a fast polymerization like the mannitol and iditol analogues, therefore the compound was acetylated with a mixture of pyridine and acetic anhydride. The IR and NMR spectra of the di-O-acetyl derivative (**XIII**) were in full agreement with the structure supposed.

The synthesized 1,2 : 5,6-diepithio-hexitols displayed a very weak cytostatic effect. Walker s.c. carcinoma and Ehrlich ascites carcinoma were not influenced by doses of $LD_{50}/10$. The L-iditol derivative was ineffective on S 180 s.c. sarcoma, but the D-glucitol (**IV**) and the D-mannitol derivatives (**XII**) produced 17% and 30% inhibition, respectively. The prolongation of life-time caused by these three compounds, tested on S 180 asc. sarcoma, showed a similar order (20%, 25% and 47%). These results indicate that the epithio--hexitols are much weaker cytostatics than their epoxi analogues (probably due to easy polymerization of the episulfides), but the hitherto unexplained general rule holds even for this series of hexitol derivatives, the most effective configuration being that of mannitol.

Experimental

Melting points are uncorrected. Thin-layer chromatography (TLC) was carried out on plates (7.5×2.5 cm) coated with Kieselgel G, using carbon tetrachloride–ethyl acetate 3 : 1 (*A*), 5 : 1 (*B*) and 9 : 1 (*C*) as solvent systems. The detecting agents used were 0.1 *M* potassium permanganate–2 *N* sulfuric acid 1:1; 4-(*p*-nitrobenzyl)-pyridine [6], and iodine. Chloroform solutions were dried over sodium sulfate; the evaporations were carried out in a rotary evaporator under diminished pressure. The light petroleum used has b.p. 60—80 °C. Optical rotations were determined in chloroform solution at $c = 1$, unless stated otherwise. The IR spectra were recorded with a U.R. 10 instrument, and the NMR spectra with a JEOL J. N. M.-C-60 spectrometer.

1,2 : 5,6-Diepithio-3,4-isopropylidine-D-mannitol (II)

A slurry of 1,2 : 5,6-dianhydro-3,4-isopropylidene-L-iditol (I) [3] (1.9 g) and thiourea (2.5 g) in methanol (10 ml) was stirred for 1 hr. At the beginning a gentle exothermic reaction took place, and the solution became clear in 30 min. After evaporating the solvent the residue was treated with chloroform–water, the organic layer washed with water, dried and evaporated. The solid residue was extracted with ether, the filtered solution evaporated, and

the remaining material extracted with light petroleum (3×5 ml). The solution was concentrated to 10 ml, and cooled. Pure compound **II** crystallized in needles (0.22 g; 10%), m.p. 97—99 °C; $[\alpha]_D^{20}$ —117.2°; R_f 0.9 (solvent *B*); ν_{max}^{KBr} 3080 (epithio CH) 2990, 1390, 1380, 1185, 1160 (isopropylidene CH) 1060, 1050, 870 cm^{-1} (O-isopropylidene); NMR data: δ 3.5 (2-proton multiplet, H-3 and H-4), δ 2.85 (2-proton multiplet, H-2 and H-5), δ 2.6 (4-proton multiplet, H-1 and H-6), δ 1.40 (6-proton singlet, isopropylidene H).

$C_9H_{14}O_2S_2$ (218.3). Calcd. C 49.51; H 6.46; S 29.37. **Found** C 49.73; H 6.42; S 29.48%.

The same compound (**II**) was obtained in 45% yield using acetone instead of methanol, but the reaction time had to be prolonged to 55 hrs. The filtered solution was worked up as described above.

Polymerization of II

Compound **II** (0.22 g) was dissolved in 0.2 *N* sodium methoxide (10 ml) and kept overnight at room temperature. The precipitated polymer was filtered off and washed with methanol (0.2 g). This product had no definite m.p.; from 215 °C 'softening' occurs gradually and at 275 °C decomposition takes place. The IR spectrum (KBr) showed no absorption between 3600—3000 (OH) and 2600—2500 cm^{-1} (SH).

3,4-O-Isopropylidene-1,2,5,6-tetrathio-1,2 : 5,6-bis-thiocarbonyl-D-mannitol (III)

Potassium hydroxide (2.3 g) was dissolved in methanol (10 ml) and to the warm solution carbon disulfide (2.9 ml) and compound **II** (1.5 g) were added. The reaction mixture was stirred for 24 hrs., the yellow crystals were filtered off and washed with methanol (2.3 g; 90.5%). Pure compound **III** (1.9 g; 74.7%) was obtained after recrystallization from benzene (12 ml)–light petroleum, m.p. 147—148 °C; $[\alpha]_D^{20}$ —353.6°; R_f 0.4 (solvent *C*). ν_{max}^{KBr} 2985, 2930 (CH), 1240 (C = S), 1075, 880, 870, 850 cm^{-1} (C—S); NMR data: δ 3.8—4.8 (8-proton multiplet, Hexitol H), δ 1.5 (6-proton singlet, isopropylidene H).

$C_{11}H_{14}O_2S_6$ (370.6). Calcd. C 35.66; H 3.81; S 51.91. Found C 35.55; H 3.85; S 51.98%.

1,2 : 5,6-Diepithio-D-mannitol (IV)

A solution of compound **II** (10.9 g) in warm methanol (350 ml) was cooled to 20 °C and mixed with 3 *N* HCl-methanol (150 ml). After 30 min. the solution was poured, with strong stirring and simultaneous ice-cooling, on solid $NaHCO_3$ (70 g). The filtered solution was evaporated below 30 °C, the dry residue extracted with chloroform, filtered and evaporated. The remaining material was extracted with hot ethyl acetate (150 ml), the filtered solution concentrated to 30 ml and, after cooling, the crystalline compound **IV** was filtered off and washed with ether (2.6 g; 29.2%), m.p. 128—129 °C (in a bath pre-heated to 125 °C); $[\alpha]_D^{20}$ —19.36°; R_f 0.15 (solvent *A*); ν_{max}^{KBr} 3065, 2985 (epithio CH), 3500—3000, 800—550 (OH), 1010 cm^{-1} (C—OH).

$C_6H_{10}O_2S_2$ (178.3). Calcd. C 40.42; H 5.65; S 35.97. Found C 40.35; H 5.80; S 35.82%.

3,4-Di-O-acetyl-1,2 : 5,6-diepithio-D-mannitol (V)

A solution of **IV** (0.9 g) in a mixture of pyridine (5 ml) and acetic anhydride (2 ml) was allowed to stand at room temperature overnight. The precipitate obtained on dilution of the solution with ice was filtered off, washed with water and dried. The crude ester **V** (0.85 g; 64.8%) was recrystallized from methanol (3 ml) to give 0.5 g (37.2%) of the product, m.p. 117—119 °C; $[\alpha]_D^{20}$ —40.8°; R_f 0.6 (solvent *A*); ν_{max}^{KBr} 3080 (epithio CH); 1745, 1220, 1085, 1050, 1020, 1010 cm^{-1} (ester); NMR data: δ 4.8 (2-proton multiplet, H-3 and H-4), δ 3.0 (2-proton multiplet, H-2 and H-5), δ 2.45 (4-proton multiplet, H-1 and H-6), δ 2.15 (6-proton singlet, acetyl).

$C_{10}H_{14}O_4S_2$ (262.4). Calcd. C 45.78; H 5.38; S 24.45. Found C 45.97; H 5.23; S 24.45%.

1,6-Di-S-benzoyl-3,4-O-isopropylidene-2,5-di-O-methanesulfonyl-1,6-dithio-D-glucitol (VII)

The syrupy tetramethanesulfonyl derivative **VI** obtained from 0.2 mole of 3,4-isopropylidene-D-glucitol [3] was dissolved in acetone (2 l). To this solution potassium thiolbenzoate (70 g) was added, and the reaction mixture was heated on a steam bath for 1 hr. The very dense

suspension was filtered after cooling, and washed with acetone. The filtrate was evaporated, the residue dissolved in chloroform, washed with water and dried. After evaporation of the solvent, a solid foam was obtained which could not be crystallized (117 g; 94.5%); $[\alpha]_D^{20}$ + 17.2°; R_f 0.8 and 0.55 (the latter being dominant) (solvent *A*).

$C_{25}H_{30}O_{10}S_4$ (618.7). Calcd. S 20.73. Found S 20.42%.

Compound **VII** was purified by column chromatography on silica (CCl_4) using CCl_4–ethyl acetate (9 : 1) as the eluting solvent. The slower moving component (R_f 0.55) was recovered by evaporation in 80% yield as a solid foam, $[\alpha]_D^{20}$ + 14.56°. (Found S 20.32%).

1,2 : 5,6-Diepithio-3,4-O-isopropylidene-D-glucitol (VIII)

For the synthesis of **VIII**, the chloroform solution of compound **VII** (prepared from 0.2 mole of 1,2-O-isopropylidene-D-glucitol) was used without any further purification. The solution was concentrated to remove traces of water by azeotropic distillation, then diluted with dry chloroform to 1 l. and chilled to 0 °C. To the stirred solution 2 *N* sodium methoxide was added over a period of 10 min., stirring was continued for another 10 min. and the reaction mixture was poured onto ice. The separated organic layer was neutralized in the presence of ice with a stream of CO_2, then washed with water, dried and the solvent evaporated. The residue was distilled at 1.5 torr. First methyl benzoate was distilled off up to 60 °C and then the main fraction at 80—85 °C, which soon became solid. It was recrystallized from the same volume of light petroleum to yield pure **VIII** (26 g; 59.6%), m.p. 55—56 °C; $[\alpha]_D^{20}$ —30.3°; R_f 0.9 (solvent *B*); ν_{max}^{KBr} 3080, 3060 (epithio CH), 2995, 2990, 2985, 1395, 1380, 1190, 1170 (isopropylidene CH) 1070, 1055, 870 cm^{-1} (O-isopropylidene).

$C_9H_{14}O_2S_2$ (218.3). Calcd. C 49.51; H 6.46; S 29.37. Found C 49.37; H 6.56; S 29.48%.

The ditoluene-*p*-sulfonyl derivative **Xc** (20 g) gave on a similar treatment 3.5 g (67.4%) of the distilled compound **VIII**; after recrystallization the yield was 3.15 g (60.5%).

Starting from the ditoluene-*p*-sulfonyl derivative **Xb**, only traces of **VIII** could be detected after a similar treatment.

Polymerization of the diepithio compound **VIII** was carried out in the same way as that of compound **II**. The polymer formed (0.2 g) had similar m.p. and IR spectrum as the mannitol isomer.

3,4-O-Isopropylidene-1,2,5,6-tetra-O-toluene-p-sulfonyl-D-glucitol (IX)

To a solution of 3,4-O-isopropylidene-D-glucitol [3] (44.2 g) in pyridine (400 ml) toluene-*p*-sulfonyl chloride (172 g) was added without cooling. The solution was kept for two days at room temperature, and then poured into water. The precipitated oil was extracted with chloroform, washed, dried and evaporated to yield a solid foam (153 g; 91%). On TLC three spots could be detected with iodine: R_f 0.8; 0.65 and 0.5 (solvent *B*). These components (*a*, *b*, *c*) were separated by chromatography on a silica column (CCl_4), using CCl_4–ethyl acetate (9 : 1) as the eluting solvent. The combined fractions gave after evaporation *a* as a yellow syrup (4.5%; $[\alpha]_D^{20}$ —1.1°. Found S 11.70%); *b* (27%; $[\alpha]_D^{20}$ +8.0°. Found S 15.25%), and *c* (68.5%; $[\alpha]_D^{20}$ +14.6° Found S 15.15%) as solid foams. ($C_{37}H_{42}O_{14}S_4$ (839.0) Calcd. S 15.28%.)

Treatment of component IXa with sodium iodide

A solution of the former syrup **IXa** (3.4 g) and sodium iodide (4 g) in acetone (60 ml) was heated in a sealed tube for 20 hrs. at 100 °C. After cooling, the precipitate was filtered off and the filtrate evaporated. The syrupy residue was dissolved in chloroform, the solution washed with water and 1*N* sodium thiosulphate, dried, and evaporated. The remaining yellow oil was kept over paraffin at 10^{-2} torr for 5 hrs. R_f 0.65 (solvent *B*), $[\alpha]_D^{20}$ 0 °C.

$C_{16}H_{21}O_6SI$ (468.3). Calcd. S 6.83; I 27.03. Found S 6.41; I 28.05%.

3,4-O-Isopropylidene-1,2,5,6-tetra-O-toluene-p-sulfonyl-D-mannitol

A solution of 3,4-O-isopropylidene-D-mannitol (4.4 g) and *p*-toluene-sulfonyl chloride (19 g) in pyridine (40 ml) was kept for two days at room temperature, and worked up as described above. The syrupy product which remained after evaporation of the solvent was dissolved

in ethanol (100 ml) and allowed to stand overnight in a refrigerator. The needles of the tetraester were filtered off, washed with ethanol and recrystallized from ethanol (200 ml) to yield 8 g (47.5%), m.p. 142—143 °C, $[\alpha]_D^{20}$ +6.57°, R_f 0.4 (solvent *B*; detection by iodine).

$C_{37}H_{42}O_{14}S_4$ (839.0). Calcd. C 52.88; H 5.15; S 15.63. Found C 52.96; H 5.05; S 15.28%.

Evaporation of the mother liquor gave a syrup, showing on TLC two spots: R_f 0.55 and 0.4 (solvent *B*: iodine detection).

1,6-Di-S-benzoyl-3,4-O-isopropylidene-1,6-dithio-2,5-di-O-toluene-p-sulfonyl-D-glucitol (X)

A solution of compound **IXc** (25 g) and potassium thiolbenzoate (10.5 g) in acetone (250 ml) was treated as described for compound **VII**. The solid foam obtained after evaporating the chloroform solution was 20.7 g (90%): $[\alpha]_D^{20}$ +16.2°; R_f 0.7 (solvent *B*).

$C_{37}H_{38}O_{10}S_4$ (770.9). Calcd. C 57.64; H 4.97; S 16.64. Found C 57.15; H 5.13; S 16.25%.

Compound **IXb** gave on similar treatment an amorphous material in 94% yield: $[\alpha]_D^{20}$ 0°; R_f 0.7 (solvent *B*). (Found C 57.20; H 5.22; S 16.80%).

3,4-O-Isopropylidene-1,2,5,6-tetrathio-1,2 : 5,6-bis-thiocarbonyl-D-glucitol (XI)

Potassium hydroxide (1.5 g) was dissolved in methanol (7 ml) and, after cooling, carbon disulfide (2 ml) and compound **VIII** (1 g) were added to the solution. The reaction mixture was stirred until dissolution was complete (5 min.) and then kept for two days at room temperature. After 15 min. the yellow solution became turbid and an oil separated. The mixture was evaporated and the residue was dissolved in chloroform–water; the organic layer was washed with water, dried and evaporated to a syrup (1.2 g; 70%). This could be crystallized from benzene (4 ml) to give pure compound **XI** (0.6 g; 35%), m.p. 142—144 °C; $[\alpha]_D^{20}$ —103.2; R_f 0.45 (solvent *C*); ν_{max}^{KBr} 2995, 2980, 2940, 2920 (CH), 1240 (C=S), 1040, 890, 880, 870, 850 cm^{-1} (C—S); NMR data: δ 3.9—4.6 (8-proton multiplet, hexitol H), δ 1.5 (6-proton singlet, isopropylidene H).

$C_{11}H_{14}O_2S_6$ (370.6). Calcd. C 35.66; H 3.81; S 51.91. Found C 35.73; H 4.05; S 52.00%.

1,2 : 5,6-Diepithio-D-glucitol (XII)

Compound **VIII** (10.9 g) was treated with HCl-methanol for 10 min. as described for the mannitol derivative **VI**. The evaporated residue was extracted with hot ethyl acetate 3×100 ml), the combined and filtered solutions were evaporated to 10 ml, the crystalline epithio compound **XII** was filtered off and washed with ether (3.1 g; 35%), m.p. 120—121 °C; $[\alpha]_D^{20}$ +4.68° (c = 1, methanol); R_f 0.2 (solvent *A*); ν_{max}^{KBr} 3060 (epithio CH), 3600—3000, 800—500 (OH), 1090 cm^{-1} (C—OH).

$C_6H_{10}O_2S_2$ (178.3). Calcd. C 40.42; H 5.65; S 35.97. Found C 40.69; H 5.79; S 36.03%.

3,4-Di-O-acetyl-1,2 : 5,6-diepithio-D-glucitol (XIII)

Compound **XII** (0.9 g) was acetylated in the same way as the mannitol derivative **V** to yield the crude diester **XIII** (0.9 g; 68%). Recrystallization from methanol (3 ml) gave pure **XIII** (0.6 g; 46.7%), m.p. 89—91 °C; $[\alpha]_D^{20}$ 0° (c = 5, chloroform); R_f 0.65 (solvent *A*), ν_{max}^{KBr} 3080 (epithio CH), 1750, 1740, 1220, 1080, 1055, 1020 (ester); NMR data: δ 4.85 (2-proton multiplet, H-3 and H-4), δ 3.05 (2-proton multiplet, H-2 and H-5), δ 2.4 (4-proton multiplet, H-1 and H-6) δ 2.1 (6-proton singlet, acetyl).

$C_{10}H_{14}O_4S_2$ (262.4). Calcd. C 45.78; H 5.38; S 24.45. Found C 45.80; H 5.37; S 24.15%.

*

The authors are indebted to Dr. P. SOHÁR (Research Institute for Pharmaceutical Chemistry) for determining and evaluating the IR and NMR spectra, and to Dr. E. CSÁNYI and Dr. M. HALÁSZ for the antitumour assays.

REFERENCES

1. KUSZMANN, J., VARGHA, L.: Carbohydrate Research **11**, 165 (1969)
2. VARGHA, L., TOLDY, L., KASZTREINER, E.: Acta Chim. Acad. Sci. Hung. **19**, 295 (1953); VARGHA, L., FEHÉR, Ö., HORVÁTH, T., TOLDY, L., KUSZMANN, J.: Acta Chim. Acad. Sci. Hung. **25**, 361 (1960)
3. VARGHA, L., KASZTREINER, E.: Ber. **92**, 2506 (1959)
4. CREIGHTON, A. M., OWEN, L. N.: J. Chem. Soc. **1960**, 1024, 1030
5. HALL, L. D., HOUGH, L., PRITCHARD, R. A.: J. Chem. Soc. **1961**, 1537
6. FRIEDMAN, D. M., BOGER, E.: Anal. Chem. **33**, 906 (1961)
7. BOURNE, E. J., MCSWEENY, G. P., STACEY, M., WIGGINS, L. F.: J. Chem. Soc. **1952**, 1408
8. KARRER, P., DAVIS, P. C.: Helv. Chim. Acta **31**, 1611 (1948); FLETCHER, H. G. Jr., DIEHL. H. W.: J. Am. Chem. Soc. **74**, 3797 (1952)

János KUSZMANN
László VARGHA
Budapest IV., Szabadságharcosok útja 47.

Acta Chimica Academiae Scientiarum Hungaricae, Tomus 66 (3), pp. 315—318 (1970)

CARBOHYDRATE METHYL ETHERS, II

A NEW SYNTHESIS OF 3,4-DIMETHYL-D-GLUCOSE

A. LIPTÁK

(Biochemical Laboratory, L. Kossuth University, Debrecen, Hungary)

Received July 10, 1969

α-Methyl-D-glucoside (**I**) gives with two moles of benzoyl chloride in pyridine at 0 °C 2,6-dibenzoyl-α-methyl-D-glucoside (**II**), which can be methylated in dichloromethane solution with diazomethane in the presence of catalytical amounts of boron trifluoride etherate to yield 2,6-dibenzoyl-3,4-dimethyl-α-methyl-D-glucoside (**III**). Debenzoylation with sodium methoxide followed by acid hydrolysis gives 3,4-dimethyl-D-glucose (**V**) in 70% yield.

In the structural investigation of oligo- and polysaccharides by methylation, the formation of 3,4-dimethyl-D-glucose is to be expected if a D-glucopyranose unit, participating in 2,6-branching, is present within the polymer molecule investigated.

3,4-Dimethyl-D-glucose was synthesized first by DEWAR *et al.* [1, 2] by the methylation of β-methyl-D-glucoside-2,6-dinitrate, further by the subsequent methylation of 2-benzoyl-6-trityl-β-methyl-D-glucoside and 2-benzoyl-3-methyl-6-trityl-β-methyl-D-glucoside. The methylations were accomplished in acetone solution with methyl iodide, in the presence of silver oxide. Under such reaction conditions, migration of the benzoyl group did not occur, and the 12-step synthesis gave crystalline 3,4-dimethyl-D-glucose.

In 1962 MITRA *et al.* [3] published a new process for the preparation of 3,4-dimethyl-D-glucose by the methylation of 2,6-dimesyl-α-methyl-D-glucoside.

The process reported in the present work starts with 2,6-dibenzoyl-α-methyl-D-glucoside (**II**), which is formed in 40—45% yield when α-methyl-D-glucoside (**I**) is acylated in pyridine with 2 moles of benzoyl chloride [4]. This compound cannot be methylated by the usual methods (*i e.* with dimethyl sulfate and alkali, or methyl iodide in the presence of silver oxide), because it either undergoes saponification, or acyl migration takes place.

A possibility for methylation is offered by the observation that alcoholic hydroxyl groups can be methylated with diazomethane in the presence of catalysts of the Lewis acid type [5, 6], and partially acetylated sugar derivatives can thus be methylated in very good yields; the process is not accompanied by acyl migration [7]. Recently, 6-methyl-α-D-glucose [7, 8], 2-methyl-β-D-glucose [8], 4-methyl-D-glucose [8], 2-methyl-β-D-galactose [8], 2-methyl-

-D-mannose [9], 2,6-dimethyl-D-mannose [10], and 1,2,6,2',3',4',6'-hepta-acetyl-3-methyl-β-D-maltose [11] have been prepared in this way.

2,6-Dibenzoyl-α-methyl-D-glucoside (**II**) was methylated at —5 °C in dichloromethane with diazomethane in the presence of catalytic amounts of boron trifluoride etherate. 2,6-Dibenzoyl-3,4-dimethyl-α-methyl-D-glucoside (**III**) was obtained in a high yield as a chromatographically homogeneous syrup, which was saponified with sodium methoxide to give 3,4-dimethyl-α-methyl-D-glucoside (**IV**). This compound is crystalline, and chromatographically homogeneous.

The acid hydrolysis of 3,4-dimethyl-α-methyl-D-glucoside gave crystalline 3,4-dimethyl-D-glucose (V) in very good yield; the purity of the product was checked by paper and thin-layer chromatography, and by the preparation of its crystalline N-phenyl-D-glucopyranosylamine-3,4-dimethyl ether derivative.

The steps of the synthesis can be represented as shown below:

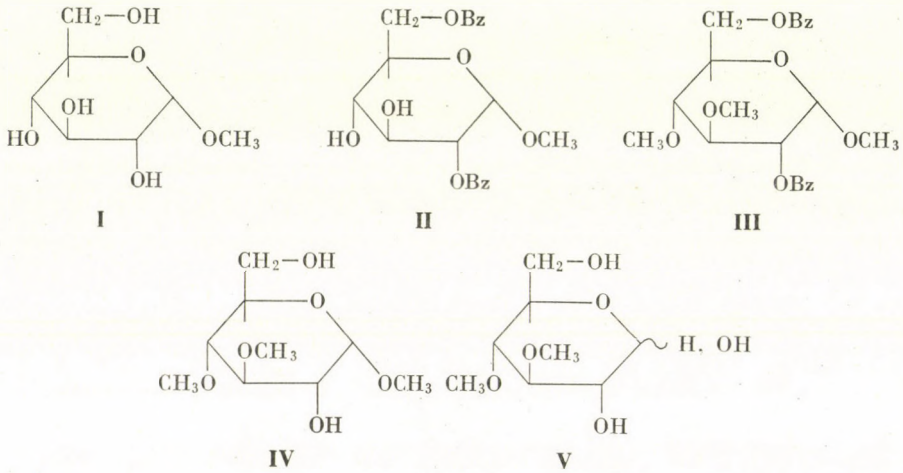

Fig. 1

This new synthesis of 3,4-dimethyl-D-glucose has several advantages over the methods known up to now: starting from glucose, the end product is obtained in 5 steps, and in each step an excellent yield is attained; this can be ascribed primarily to the extremely mild reaction conditions. The isolation and identification of the intermediate products can readily be accomplished.

At the same time, this synthesis proves that methylation with diazomethane in the presence of boron trifluoride etherate catalyst, used up to the present only in the field of sugar acetates, can also be applied to sugar benzoates without the danger of acyl migration.

Experimental

All m.p.'s were determined on a Küstner apparatus, and are uncorrected. Specific rotations were measured with a Bellingham and Stanley polarimeter, using tubes 2 dm.

The paper chromatographic tests were made on Schleicher—Schüll 2043/b paper, using a 5 : 1 : 4 *n*-butanol–ethanol–water (*A*) solvent system [12]. The detecting agent was anilin hydrogen phthalate [3] (*a*).

For the thin-layer chromatography Kieselgel G plates were used. The plates were prepared according to the standard method of Stahl. The following solvent systems were used: methyl ethyl ketone saturated with water (*B*), 9 : 1 benzene–methanol (*C*), and 95 : 5 benzene–methanol (*D*).

In each case, the chromatograms were run in a saturated system. The detecting agent was 50% (v/v) sulfuric acid (*b*) at 140 °C, or anilin hydrogen phthalate (*a*) at 100—105 °C.

2,6-Dibenzoyl-α-methyl-D-glucoside (II)

38.80 g (0.2 mole) of α-methyl-D-glucoside (**I**) was dissolved in 200 ml of abs. pyridine. After cooling to 0 °C, 50 ml (0.43 mole) of benzoyl chloride was added dropwise, with stirring, during 1 hr. The reaction mixture was kept for another hour at 0 °C, and subsequently for 8 hrs at room temperature. The solution was then poured into 1 l of ice-water containing 5% acetic acid, and the syrup which separated was washed free of pyridine by the repeated change of ice-water. The solid reaction product was dissolved in 400 ml of chloroform, the solution washed with 4×5 ml portions of water, and dried over $CaCl_2$. Evaporation in vacuum yielded a syrup. This was dissolved in 400 ml of hot ether, treated with 2 g of clarifying carbon and, after filtration, mixed with petroleum ether until the mixture became turbid (200 ml). A crystalline product (32 g) was obtained, m.p. 140—143 °C. Further 200 ml of petroleum ether was added to the mother liquor which was then allowed to stand overnight in a refrigerator to give a second crop (13.8 g), m.p.: 139—142 °C. Thus the total yield was 56.9%.

Recrystallization from 100 ml of 70% (v/v) methanol gave m.p. 143—144 °C (lit. [4] m.p. 144 °C); $[\alpha]_D^{22}$ +81.00° (in chloroform, $c = 4.0$) (lit. [4] $[\alpha]_D^{23}$ +80.37° (in chloroform)). R_f 0.42 (solvent: *C*; detecting agent: *b*).

2,6-Dibenzoyl-3,4-dimethyl-α-methyl-D-glucoside (III)

5.03 g (0.0125 mole) of 2,6-dibenzoyl-α-methyl-D-glucoside (**II**) was dissolved in 60 ml of dichloromethane and cooled to —5 °C. 0.2 ml of boron trifluoride etherate was added to this solution, followed by the dropwise addition, in the course of 30 min., of a solution of diazomethane (prepared from 30 g of N-nitrosomethylurea) in 300 ml of dichloromethane, which had been chilled to —5 °C. The reaction mixture was kept for further 30 min. at —5 °C. Polymethylene which precipitated during the reaction was filtered off, the solution was washed first with 2×20 ml portions of a 10% $NaHCO_3$ solution, then with water until it gave a neutral reaction, and dried over Na_2SO_4.

Evaporation in vacuum gave a syrup (4.85 g; 90.6%) which was found homogeneous by chromatography; $[\alpha]_D^{23}$ +100.1° (in chloroform, $c = 1.0$).

R_f 0.62 (solvent: *D*; detecting agent: *b*).

$C_{23}H_{26}O_8$ (430.4). Calcd. C 64.17; H 6.08; OCH_3 21.62. Found C 65.02; H 6.11; OCH_3 21.82%.

3,4-Dimethyl-α-methyl-D-glucoside (IV)

3.85 g of 2,6-dibenzoyl-3,4-dimethyl-α-methyl-D-glucoside (**III**) was dissolved in 50 ml of abs. methanol, and mixed with 0.2 ml of a 0.1 *N* $NaOCH_3$ solution. After standing overnight, no starting substance could be detected by chromatography (System *C*). The pH of the solution was adjusted with acetic acid to 6—7, and the solution was evaporated in vacuum. The residual syrup was dissolved in 100 ml of chloroform, washed first with water, then with $NaHCO_3$ solution and again with water, and dried over Na_2SO_4. Evaporation gave a syrup which solidified on standing to give a crystalline mass. Recrystallization from ether–hexane gave 1.80 g (90.9%), m.p. 55—56 °C (lit. [3] m.p. 53.5—55.5 °C); $[\alpha]_D^{22}$ +179.3° (in chloroform, $c = 1.0$) (lit. [3] $[\alpha]_D^{23}$ +179° (in chloroform)). R_f 0.31 (solvent: *B*; detecting agent: *b*).

$C_9H_{18}O_6$ (222.2). Calcd. C 48.64; H 8.16; OCH_3 41.89. Found C 48.50; H 8.10; OCH_3 42.01%.

3,4-Dimethyl-D-glucose (V)

1.66 g (0.0075 mole) of 3,4-dimethyl-α-methyl-D-glucoside was dissolved in 100 ml of 1 *N* HCl and kept for 4 hrs at 100 °C. The solution was cooled, agitated overnight with 50 ml of Amberlite IR 45 (OH) anion exchanger resin, filtered from the resin, and evaporated in vacuum. The crystalline residue was dissolved in 25 ml of ethyl acetate, the solution dried over K_2CO_3, and treated with 0.1 g of clarifying carbon. After evaporation in vacuum to 4—5 ml, crystallization began to give 1.08 g (69.6%), m.p. 108—118 °C. Repeated recrystallizations from ethyl acetate gave m.p. 115—119 °C (lit. [3] m.p. 114—118.5 °C); $[\alpha]_D^{22}$ +80.95° → +75° (12 hrs.) (in water, $c = 1.0$) (lit. [3] $[\alpha]_D^{33}$ +80.0° → +76°).

R_f 0.24 (solvent: *B*; detecting agent: *a*). R_{TMG} 0.52 (solvent: *A*; detecting agent: *a*).

$C_8H_{16}O_6$ (208.2). Calcd. C 46.14; H 7.74; OCH_3 29.81. Found C 46.29; H 7.56; OCH_3 30.02%.

N-Phenyl-D-glucopyranosylamine-3,4-dimethyl ether

29.8 mg of 3,4-dimethyl-D-glucose and 12 mg of aniline were boiled for 3 hrs with 2 ml of 96% ethanol. Evaporation in vacuum gave a solid residue. The excess of aniline was extracted with 1 ml of ether, decanted, the solid residue dissolved in 0.5 ml of warm n-butanol, and mixed with 2.5 ml of petroleum ether (b.p. 120 °C). On standing in a refrigerator, the solution deposited long crystal needles, m.p. 170—172 °C (lit. [3] m.p. 171—173 °C); $[\alpha]_D^{22}$—98.5° (in ethanol, $c = 0.05$) (lit. [3] $[\alpha]_D^{33}$ —102° (in ethanol)).

*

The author's thanks are due to Prof. P. NÁNÁSI for his valuable advice and his interest in this work, and to Mr. L. JÁNOSSY for his help in the synthesis of the starting materials.

REFERENCES

1. DEWAR, J., FORT, G.: J. Chem. Soc. **1944,** 496
2. DEWAR, J., FORT, G., MCARTHUR, N.: J. Chem. Soc. **1944,** 499
3. MITRA, A. K., BELL, D. H., LONG, L.: J. Org. Chem. **27,** 160 (1962)
4. LIESER, T., SCHWEIZER, R.: Ann. **519,** 271 (1935)
5. MÜLLER, E., RUNDEL, W.: Angew. Chem. **70,** 105 (1958)
6. NEEMAN, N., CASERIO, M. C., ROBERTS, J. D., JOHNSON, W. S.: Tetrahedron **6,** 36 (1959)
7. GROS, E. G., FLAMETTI, S. M.: Chem and Ind. **1966,** 1556
8. MASTRONARDI, J. O., FLAMETTI, S. M., DEFERRARI, J. O., GROS, E. G.: Carbohydr. Res. **3,** 177 (1966)
9. DEFERRARI, J. O., GROS, E. G., MASTRONARDI, J. O.: Carbohydr. Res. **4,** 432 (1967)
10. PERRY, M. B., WEBB, A. C.: Canad. J. Chem. **47,** 31 (1969)
11. DICK, W. E., BAKER, B. G., HODGE, J. E.: Carbohydr. Res. **6,** 52 (1968)
12. HIRST, E. L., JONES, J. K. N.: J. Chem. Soc. **1949,** 1659
13. PARTRIDGE, S. M.: Nature **164,** 443 (1949)

András LIPTÁK; Debrecen 10. Hungary.

Acta Chimica Academiae Scientiarum Hungaricae, Tomus 66 (3), pp. 319—331 (1970)

THE CHEMISTRY OF 1,3-BIFUNCTIONAL SYSTEMS, IX*

THE REACTION OF 1,3-BUTANEDIOL AND SOME OF ITS CYCLIC DERIVATIVES WITH HYDROCHLORIC ACID

M. BARTÓK and Á. MOLNÁR

(Institute of Organic Chemistry, A. József University, Szeged)

Received July 10, 1969

The routes of the conversion of butanediol-1,3 and some of its cyclic derivatives, such as the cyclic sulphite, cyclic carbonate and cyclic formal, with concentrated hydrochloric acid, and with dry gaseous hydrogen chloride have been established, and the mechanisms of the processes have been studied.

The reaction of the cyclic sulphate of butanediol-1,3 with hydrogen halides has been studied first by LICHTENBERGER *et al.* [1, 2] who have established that only one of the isomers is formed in the process. Thus, for example, 3-chlorobutanol-1 (**I**) was formed in the reaction with hydrochloric acid. However, recent investigations have shown [3, 4] that if the reaction is carried out under similar conditions (in the presence of concentrated hydrochloric acid, refluxing the cyclic sulphate on a water bath or heating it in a pressure tube), both chlorohydrine isomers can be detected by gas-liquid chromatography (70—80% of **I** and 20—30% of **II**):

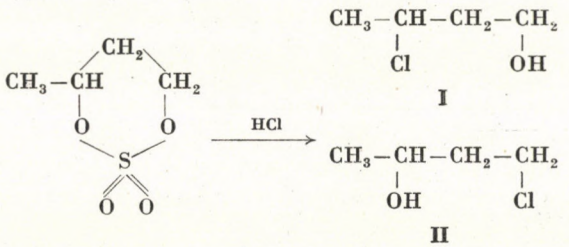

With the aim to draw more general conclusions, we investigated the reaction of butanediol-1,3 and some of its cyclic derivatives (such as cyclic formal, sulphite and carbonate) with hydrochloric acid under the conditions mentioned above, and also under anhydrous conditions.

Results and discussion

Investigation of the reactions with concentrated hydrochloric acid

Similarly to the case of the cyclic sulphate [3] in the reaction of the cyclic sulphite, carbonate and formal of butanediol-1,3 with conc. hydrochloric acid,

* Part VIII: Acta Phys. et Chem. Szeged (In the press.)

the formation of the following liquid products was observed under normal conditions:

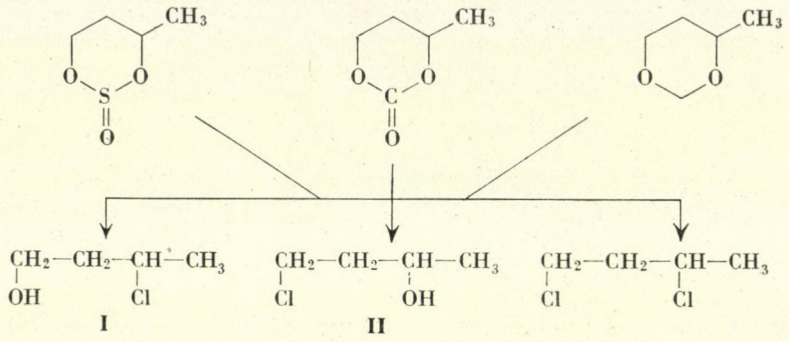

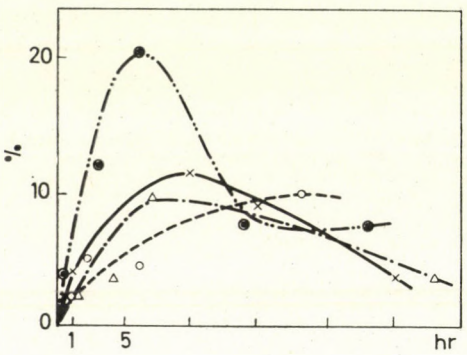

Fig. 1. Variation of the yield of 1-chlorobutanol-3 (**II**) as a function of the reaction time, in the presence of concentrated hydrochloric acid. ——×—— butanediol-1,3 cyclic sulphite; --○-- butanediol-1,3 cyclic carbonate; ---△--- 4-methyl-1,3-dioxan; ---●--- butanediol-1,3*

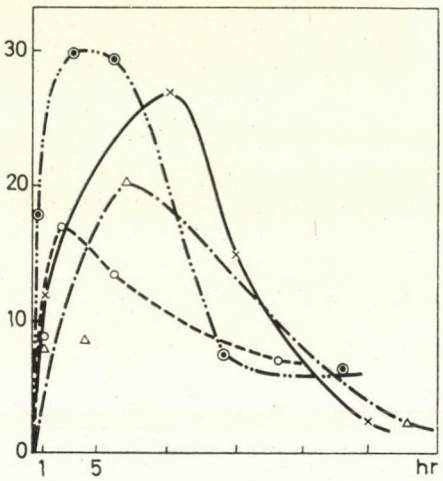

Fig. 2. Variation of the yield of 3-chlorobutanol-1 (**I**) as a function of the reaction time, in the presence of concentrated hydrochloric acid

It was established that the amount of the two chlorohydrine isomers increases up to a limiting value with increasing reaction time. Simultaneously, the amount of 1,3-dichlorobutane also increases. However, after a certain reaction time, the amount of chlorohydrines diminishes, and at the same time, the ratio of the isomers shifts in favour of 1-chlorobutanol-3 (**II**), the compound containing a primary chlorine atom, and the amount of 1,3-dichlorobutane also increases (Table I; Figs 1, 2, 3). Thus, the amount of the two chlorohydrine

* The notation used in Fig. 1 refers also to Figs 2—6.

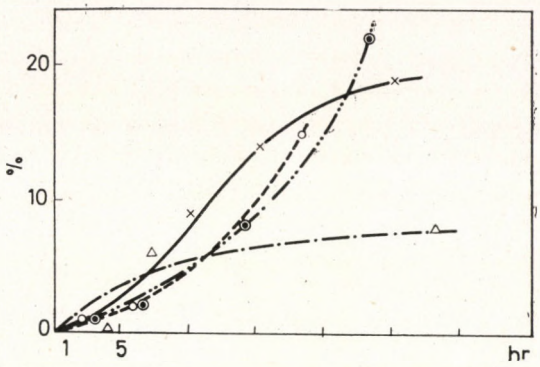

Fig. 3. Variation of the yield of 1,3-dichlorobutane as a function of the reaction time, in the presence of concentrated hydrochloric acid

Table I

The reaction of butanediol-1,3 and some of its cyclic derivatives with conc. hydrochloric acid at 110—120 °C

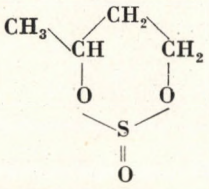

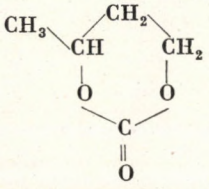

Reaction time (hrs.)	Chloro-butanol yield (%)	Ratio II/I	1,3-Dichloro-butane yield (%)	Reaction time (hrs.)	Chloro-butanol yield (%)	Ratio II/I	1,3-Di-chlorobutane yield (%)
1	16	25 : 75	traces	1	11	20 : 80	traces
10	39	30 : 70	9	2	22	22 : 78	1
15	24	38 : 62	14	6	18	26 : 74	2
25	6	62 : 38	19	18	17	58 : 42	15

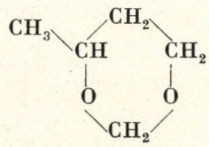

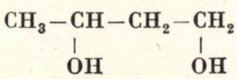

1	10	20 : 80	—	0.5	22	18 : 82	—
4	12	30 : 70	0.5	3	42	28 : 72	1
7	30	32 : 68	6	6	50	41 : 59	2
28	6	63 : 37	8	14	15	51 : 49	8
				23	14	55 : 45	22

isomers varies with the reaction time along a curve exhibiting a maximum, which proves that the primary process is accompanied by secondary changes.

The reaction of butanediol-1,3 reveals the same features under similar conditions. We concluded from this that the first step in the reaction of cyclic derivatives is probably the hydrolytic cleavage of the ring. This assumption is supported by several works published in literature, dealing with the mechanism of the acid-catalyzed conversion of cyclic sulphites, carbonates and acetals into diols. After primary hydrolysis, the diol semiester or hemiacetal, or the diol itself reacts with hydrochloric acid resulting in the formation of chlorohydrines.

This mechanism also explains the initial ratio of the chlorohydrine isomers. Actually, in the case of butanediol-1,3, two hydroxyl groups of different reactivity, a primary and a secondary one, are present (formed during hydrolysis) in the molecule, and under the given experimental conditions the substitution of the secondary hydroxyl group occurs at a higher rate than that of the primary one, consequently, more 3-chlorobutanol-1 (**I**) is formed.

The shift of the initial ratio of the two chlorohydrines during the reaction is due either to transisomerization of the two compounds, or to further reactions of the isomers. The overall rate of these reactions must be greater in the case of **I**, than in that of **II**. However, in the reaction of pure **I** with conc. hydrochloric acid, **II** could not be detected among the reaction products, indicating that no isomerization takes place. Subsequently, the second possibility had to be verified. For this purpose, the reaction vessels were connected to receivers cooled with salt ice mixture to recover low-boiling products possibly formed and released during the reaction. Actually, volatile products were obtained both in the case of butanediol-1,3 and its cyclic derivatives, as well as in the reaction of the pure chlorohydrine isomers.

On the basis of products identification by gas-liquid chromatography, the reaction of butanediol-1,3 with concentrated hydrochloric acid takes place according to the scheme on top of p. 323.

(Besides the above products, an unidentified substance was obtained in 12%. The percentages indicated are relative ratios of the products. Besides chlorohydrines, unreacted diol is also present in the reaction mixture after a short reaction time. At the end of the reaction dichlorobutane, chlorobutanes and isopropyl chloride are found in the mixture.)

In the further conversion of chlorohydrines formed in the first step, the order of reaction rates is reversed: the dehydration or second substitution of 3-chlorobutanol-1 (**I**) formed in the fast substitution of the secondary hydroxyl group, are slower processes than the corresponding reactions of 1-chlorobutanol-3 (**II**), since these reactions take place already at a primary hydroxyl group, while in the case of **II** these reactions concern a secondary hydroxyl group. Accordingly, the higher rate of the further conversion of **I** can be

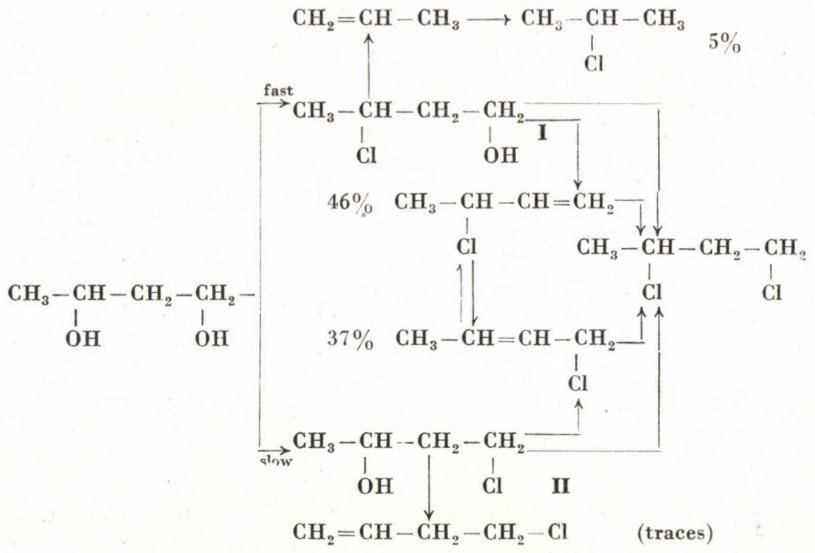

interpreted by assuming fast fragmentation [5] under the formation of propylene:

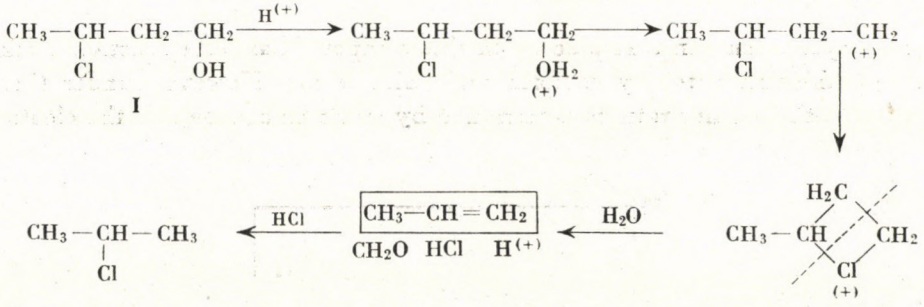

Conversions under the influence of dry gaseous hydrogen chloride

The reaction of the four compounds with hydrogen chloride under anhydrous conditions did not show such unequivocal changes as those observed in the reactions with concentrated hydrochloric acid (Table II; Figs 4, 5, 6).

In the reaction of the cyclic carbonate, already during a short reaction time, the ratio of the two isomers is reversed with respect to that observed in aqueous medium, and this proportion remains practically unchanged with time. This means that in this case, chloride ion attacks preferentially at the primary carbon atom. This is due to the fact that under anhydrous conditions

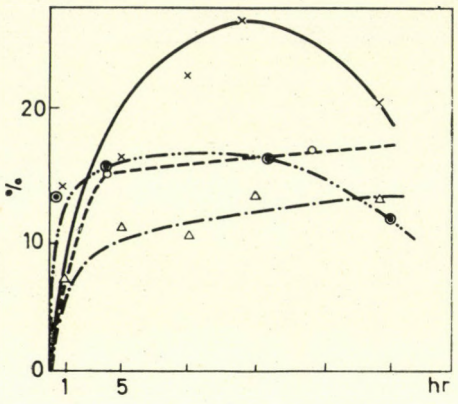

Fig. 4. Variation of the yield of 1-chlorobutanol-3 **(II)** as a function of the reaction time, in the presence of dry gaseous hydrogen chloride

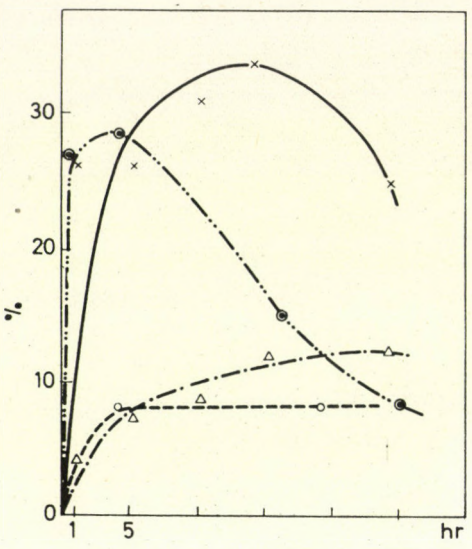

Fig. 5. Variation of the yield of 3-chlorobutanol-1 **(I)** as a function of the reaction time, in the presence of dry gaseous hydrogen chloride

no ring hydrolysis can take place with this compound, and the reaction occurs between the unreacted cyclic form and chloride ion. However, under these conditions the isomer ratio is determined by steric hindrance and the electro-

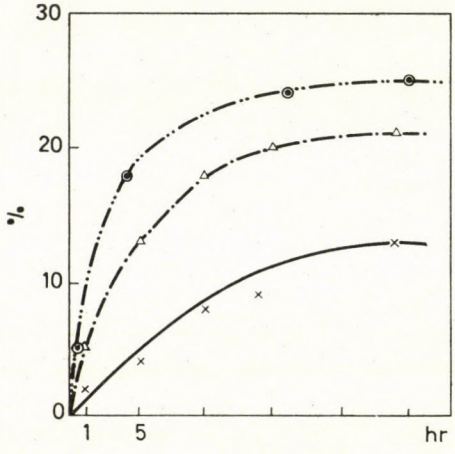

Fig. 6. Variation of the yield of 1,3-dichlorobutane as a function of the reaction time, in the presence of dry gaseous hydrogen chloride

philic character of the two carbon atoms (α and γ) that can be attacked by chloride:

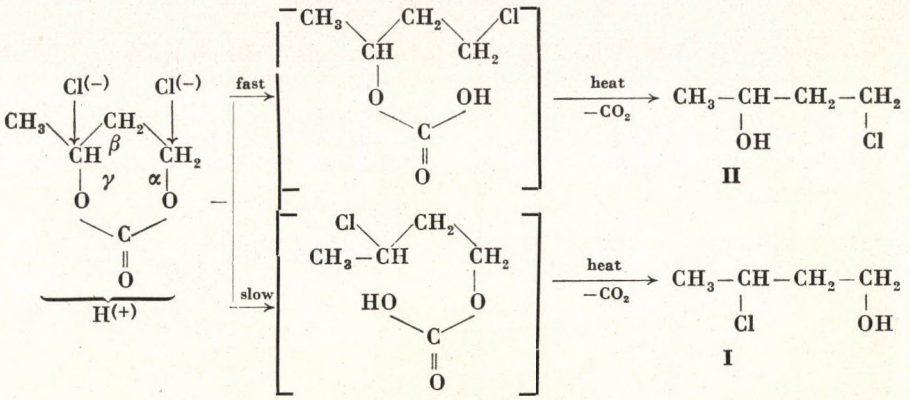

Owing to the space requirement and the positive inductive effect of the methyl group attached to the γ carbon atom, chloride ion attack is less favourable at this position with respect to both factors. This results in an isomer mixture containing more of compound **II.** With increasing reaction time, the ratio of the chlorohydrines remains unchanged because, even after introducing hydrogen chloride over a longer period, the cyclic carbonate is able to absorb only much less than the equimolecular amount of hydrogen chloride. This also explains the absence of 1,3-dichlorobutane among the products.

Contrary to findings in the case of concentrated hydrochloric acid, the conversion of 4-methyl-1,3-dioxan under similar conditions yields also more of compound **II,** *i.e.* here too the process is governed by factors described for the reaction of the cyclic carbonate:

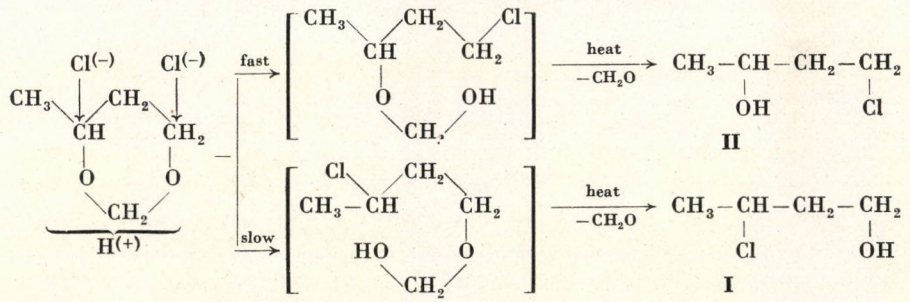

In the saturation of this compound with hydrogen chloride, an excess of about 0.5 mole in hydrogen chloride was achieved. Therefore, increased reaction times changed also the ratio of the isomers. This change acts in the direction of equalizing the amounts of the two isomers. This is mainly due to the fact that with changing reaction conditions, the rates of secondary reactions are

Table II

The reaction of butanediol-1,3 and some of its cyclic derivatives in a pressure tube, in the presence of dry gaseous hydrogen chloride

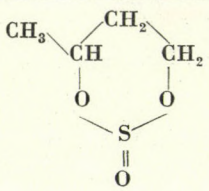

120 °C

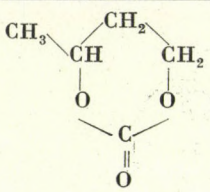

105 °C

Reaction time (hrs.)	Chloro-butanol yield (%)	Ratio II/I	1,3-Dichloro-butane yield (%)	Reaction time (hrs.)	Chloro-butanol yield (%)	Ratio II/I	1,3-Dichloro-butane yield (%)
1	40	35 : 65	2	4	23	65 : 35	—
5	42	38 : 62	4	19	25	68 : 32	—
10	53	42 : 58	8	75	30	68 : 32	—
14	60	44 : 56	9				
24	45	45 : 55	13				

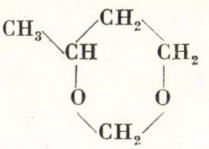

120 °C

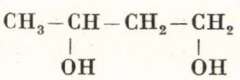

120 °C

1	11	63 : 37	5	0.5	40	33 : 67	5
5	18	60 : 40	13	4	44	35 : 65	18
10	19	54 : 46	18	16	31	52 : 48	24
15	25	53 : 47	20	25	20	58 : 42	25
24	25	51 : 49	21				

also changed, in such a manner that elimination and fragmentation leading to the formation of volatile components (chlorobutenes and isopropyl chloride) are suppressed, and the formation of 1,3-dichlorobutane predominates. Owing to the considerably reduced fragmentation rate, the conversion of the two chlorohydrines to 1,3-dichlorobutane will be the predominant secondary process. However, of these two reactions, the conversion of 1-chlorobutanol-3, containing the secondary hydroxyl group, is faster, therefore its relative amount diminishes.

We wish to mention here that in the reaction of each compound, a substance was formed in very small amounts, the largest yield being observed in

the reaction of 4-methyl-1,3-dioxane with anhydrous hydrogen chloride (about 2—3%). It could not be identified exactly due to a comparing substance, but its retention time was very close to that of bis(4-chloro-2-butyl)ether, prepared by us. The unknown compound is most probably an ether formed from 3-chlorobutanol-1, or the mixed ether of the two chlorobutanols. The conversion of this intermediate also leads to the formation of 1,3-dichlorobutane.

The results obtained for the reactions of butanediol-1,3 and the cyclic sulphite under anhydrous conditions are the same as found in the case of concentrated hydrochloric acid. With butanediol-1,3, this is obviously explained by the fact that the initial step, *i.e.* substitution leading to the formation of chlorohydrine, is accompanied by the formation of water regardless of the hydroxyl group at which it occurs. Thus, factors characteristic of aqueous conditions are operative from the beginning.

Since in the case of the cyclic sulphite of butanediol-1,3 there is no water liberation at the beginning of the reaction, it should be assumed that this ring is considerably less stable than either the cyclic carbonate or the cyclic acetal, and its protonation is immediately followed by cleavage of the ring even without the simultaneous action of chloride ions. (This is in contrast with the two rings discussed previously, where after protonation the oriented chloride attack gives rise to ring cleavage which favours bonding of chlorine to the primary carbon atom):

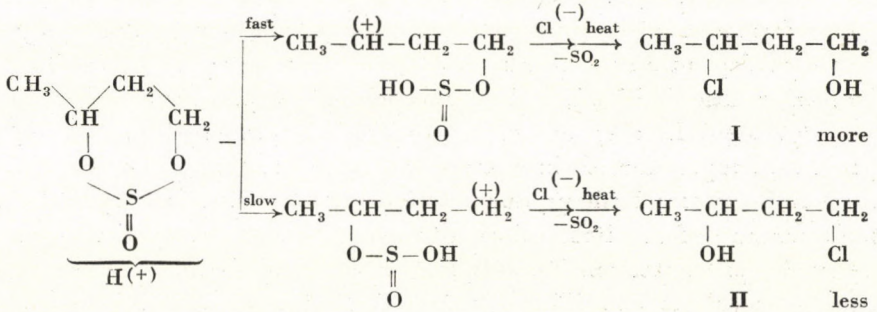

Obviously, the formation of the secondary carbonium ion will be favoured, because due to the $+I$ effect of the methyl group, it assists the formation of the following intermediate:

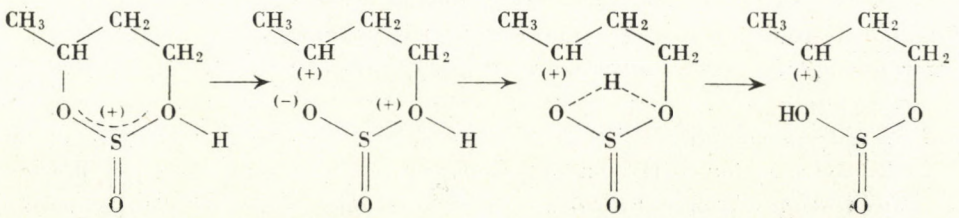

On comparing the reactions investigated by us in aqueous and anhydrous media, the following general conclusions can be drawn.

Both reaction conditions applied favour processes of the ionic type, and in each case the reaction begins with protonation. In aqueous media, the protonated rings open under the influence of water in the primary process proper, resulting in the formation of butanediol-1,3 hemiacetals or semiesters, which in turn can be converted to butanediol-1,3. The ratio of isomers is determined in this case by the difference in substitution rates of functional groups on the primary and secondary carbon atoms, favouring the formation of 3-chlorobutanol-1 (I).

In the presence of dry gaseous hydrogen chloride, as shown by the cyclic carbonate of butanediol-1,3 and by stable cyclic derivatives of 4-methyl-1,3-dioxan, simultaneously with protonation or immediately following it, the chloride ion attacks predominantly at the primary carbon atom of the ring, which is spatially less hindered and is more electrophilic. In this case, the opening of the six-membered ring occurs upon the action of chloride ion, consequently, 1-chlorobutanol-3 (II) will be formed in greater amounts in the case of the two compounds mentioned above. The cyclic sulphite, which is less stable, decomposes immediately in the primary process up on protonation, regardless of other external factors. In a decomposition under these conditions, formation of a secondary carbonium ion and, consequently, the formation of 3-chlorobutanol-1 (I) is favoured, similarly as in the presence of water.

The formation of isomeric chlorohydrines is followed by secondary processes which depend on the conditions. These secondary processes change the initial isomer ratio and lead to the formation of new products as the reaction time is increased. In reactions carried out in the presence of dry hydrogen chloride, the suppression of elimination and fragmentation is supported partly by the formation of volatile products only in trace amounts, partly by the fact that the amount of 1,3-dichlorobutane is, with the exception of the reaction of the cyclic carbonate, considerably higher than that found in reactions with aqueous hydrochloric acid (Tables I and II). Besides the fact that less hydrogen chloride is present, this is the other reason why in the anhydrous reaction of the cyclic sulphite, contrary to its reaction in the presence of concentrated hydrochloric acid, the isomer ratio only shifts but does not invert at an almost identical reaction time.

Since with the cyclic carbonate of butanediol-1,3 and with 4-methyl-1,3-dioxan the isomer ratios are opposite, and these ratios change with time in a different manner under different reaction conditions, the reactions of these two compounds permit to compare the time-course of the reactions in aqueous and anhydrous media.

In the reaction with concentrated hydrochloric acid, the overall yield of chlorohydrines changes for both compounds along a curve exhibiting a maxi-

mum, the same being true for the yield of the single chlorohydrines. At the same time, the amount of 1,3-dichlorobutane increases. The corresponding data plotted for the reactions under anhydrous conditions give in each case a saturation curve. This can be ascribed to the fact that in the latter case the excess of hydrogen chloride was lower than that ensured with concentrated hydrochloric acid. (In the case of concentrated hydrochloric acid, the reactions were carried out at a fivefold excess of hydrogen chloride, while in the case of anhydrous media not more than a 1.5-fold excess of hydrogen chloride could be achieved.) Owing to this, secondary reactions becoming more important with increasing reaction times, *i.e.* chlorohydrine dehydration and fragmentation, cannot take place, or occur only to a small degree. In reactions of butanediol-1,3 and its cyclic sulphite, the curves of chlorohydrine yield were similar in each case, exhibiting a maximum. The ratio of chlorohydrines also changed in an identical direction, while the amount of 1,3-dichlorobutane gave, here, too, a saturation curve.

As for the preparative utilization of the reactions studied, *i.e.* preparation of the two chlorohydrine isomers, it can be established that butanediol-1,3, as the most easily available substance, can be used as starting material. Besides the experiments described so far, further studies were carried out at a 1 : 1 mole ratio of butanediol-1,3 and concentrated hydrochloric acid, to determine the highest chlorohydrine yield. The experimental results are summarized in Table III.

In the first case, gaseous hydrogen chloride partly left the reaction mixture, so that the relative excess in hydrochloric acid, necessary for the secondary reactions to occur, could not be achieved. Therefore, the yields are higher in this case.

Table III

Reaction of a 1 : 1 mixture of butanediol-1,3 and concentrated hydrochloric acid at 120 °C, under reflux (A) and in a pressure tube (B)

	Reaction time (hrs.)	Yield of chlorobutanol (%)	Ratio II/I	Yield of 1,3-dichlorobutane (%)
A	3	25	28 : 72	traces
	6	35	34 : 66	traces
	10	40	36 : 64	1
	15	44	37 : 63	1
B	3	28	49 : 51	2.5
	6	21	61 : 39	5
	10	19	69 : 31	6
	15	13	74 : 26	7

Comparing the experimental data in Tables I, II and III, it can be seen that in a static system the production of chlorohydrine mixture by the reaction of butanediol-1,3 with hydrogen chloride cannot be raised above a yield of 50%.

Experimental

Cyclic sulphite of butanediol-1,3

A freshly distilled product, manufactured by Chemische Werke Hüls, was used. B.p. 95—97 °C (33 mmHg); $n_D^{25} = 1.4405$.

Cyclic carbonate of butanediol-1,3

Using the method described in Ref. [6] and starting from 180 g butanediol-1,3, 116 g (50%) of the substance was obtained. B.p. 173—176 °C (35 mmHg); $n_D^{29} = 1.4406$. (Ref. [8]: b.p. 113—115 °C (0.2 mmHg); $n_D^{15} = 1.4465$.)

4-Methyl-1,3-dioxan

A product by Chemische Werke Hüls was used. B.p. 114 °C; $n_D^{20} = 1.4168$.

Butanediol-1,3

A product of Chemische Werke Hüls has been used after distillation. B.p. 108—110 °C (16 mmHg); $n_D^{20} = 1.4394$.

The reaction of butanediol-1,3, butanediol-1,3 cyclic sulphite, cyclic carbonate, and 4-methyl-1,3-dioxan with concentrated hydrochloric acid

0.01 mole of the above substances was refluxed in the presence of 5 ml of concentrated hydrochloric acid at 110—120 °C. During the reaction, a dark brown phase separated. At the end of the reaction, the mixture was diluted with an identical volume of water saturated with sodium chloride, and extracted with 30 ml of ether. The ether extract was washed with a $NaHCO_3$ solution and evaporated. The evaporation residue was analyzed by gas chromatography. The individual components of the mixture obtained in a vessel cooled by salt ice were identified by comparison of their infrared spectra, gas-liquid chromatography, and after fractional distillation, by microanalysis.

Reactions with dry gaseous hydrogen chloride in a pressure tube

0.01 mole of the starting material was introduced into a micro-pressure tube with a volume of about 5 ml, and, under cooling with ice, a measured quantity of gaseous hydrogen chloride, dried over sulphuric acid, was introduced. Referred to 1 mole, butanediol-1,3 and 4-methyl-1,3-dioxan absorbed 1.5 mole of hydrogen chloride, butanediol-1,3 cyclic sulphite about 1 mole, while the cyclic carbonate absorbed only about 0.5 mole of hydrogen chloride, even when the latter was introduced for several hours. The pressure tubes were sealed and heated at temperatures and for times given in Table II. The pressure tubes were allowed to cool, and before opening were placed into iced water. After opening, the reaction mixture was poured into 5 ml of saturated NaCl solution, also cooled with iced water. The mixture was extracted with 3×5 ml of ether, dried over Na_2SO_4, and after the evaporation of ether, analyzed by gas chromatography.

For gas-liquid chromatography, a Willy Giede Modell GCHF 18/2 (column 1 m) chromatograph and a Carlo Erba Mod GV (column 1.5 m) chromatograph were used.

Conditions of chromatography:

	1	2	3
Length of column (m)	1.5	1	1.5
Partition liquid	ODPN*	DNP**	CWAX 20000***
Carrier	Thermolite	Thermolite	Thermolite
Temperature of thermostat (°C)	60	130	160
Carrier gas	Hydrogen	Hydrogen	Hydrogen
Flow-rate of carrier gas (ml/min)	120	60	120
Detector current (mA)	150	160	150

* β,β'-Oxydipropionitrileether
** Dinonylphthalate
*** Polyethylene Glycol 20000

Retention times of the reaction products (min):

	1	2	3
Unidentified product	26 sec		
Isopropyl chloride	1.3		
3-Chlorobutene-1	3.1		
1-Chlorobutene-3	5.0		
1-Chlorobutene-2	6.6		
1,3-Dichlorobutene		3.4	1.7
Dichlorobutyl ether		5.4	4.1
1-Chlorobutanol-3		6.0	5.6
3-Chlorobutanol-1		7.0	7.4

REFERENCES

1. LICHTENBERGER, J., LICHTENBERGER, R.: Bull. Soc. Chim. France **15**, 1002 (1948)
2. LICHTENBERGER, J., DÜRR, L.: Bull. Soc. Chim. France **1956**, 664
3. BARTÓK, M., APJOK, J., FÉNYI, SZ.: Acta Phys. et Chem. Szeged **8**, 143 (1962)
4. MILLER, J. J.: J. Org. Chem. **27**, 2680 (1962)
5. FORSBERG, G.: Acta Chem. Scand. **8**, 136 (1954)
6. SEARLES, S., HUMMEL, D. G., NUKINA, S., THROCKMORTON, P. E.: J. Am. Chem. Soc. **82**, 2928 (1960)
7. SAREL, S., POHORYLES, L. A., BEN-SHOSHAN, R.: J. Org. Chem. **24**, 1874 (1959)

Mihály BARTÓK
Árpád MOLNÁR
Szeged, Dóm-tér 8. Hungary.

Acta Chimica Academiae Scientiarum Hungaricae, Tomus 66 (3), pp. 333—343 (1970)

REARRANGEMENTS OF STEROIDS, VI

COMPARATIVE EXAMINATION OF THE SCHMIDT REACTION OF 3β-SUBSTITUTED CHOLESTAN-6- AND 7-ONES, CHOLEST-5-EN-7-ONE AND THE BECKMANN REARRANGEMENT OF THE CORRESPONDING OXIMES

B. MATKOVICS, ZS. TEGYEY, M. RESCH, F. SIROKMÁN and E. BOGA

(Institute of Organic Chemistry, A. József University, Szeged)

Received January 31, 1969; revised October 20, 1969

3β-Acetoxy- and 3β-benzoyloxycholestan-6-one and their oximes were prepared The Schmidt reaction of the ketones and the Beckmann rearrangement of the oximes gave the same lactams, which were isolated and their structures proved. The steric structures of the oximes, *i.e.* the configuration of the oxime hydroxyl group with respect to the 5α-H atom of the skeleton were established.

The oximes of 3β-acetoxycholest-5-en-7-one and 3β-acetoxycholestan-7-one were also prepared, but the isomers were not separated. Both in the case of cholest-5-ene and cholestane derivatives the Schmidt reaction of the ketones and Beckmann rearrangement of the oximes gave the corresponding lactams.

After a comparative examination of the rearrangements of 17-ketosteroids and their oximes [1—3], as well as a preliminary communication [4] dealing with the compounds specified in the title of this paper, the present publication is concerned with the detailed investigation of the Schmidt reaction of 3β-acetoxycholestan-6-one and 7-one, 3β-benzoyloxycholestan-6-one, 3β-acetoxycholest-5-en-7-one, and the Beckmann rearrangement and isomerism of the corresponding oximes.

Reference should be made at this point to the work of KNOF [5] carried out with some of these compounds for other purposes.

At first the Schmidt reactions of 3β-acetoxy (**I**) and 3β-benzoyloxycholestan-6-one (**II**) will be discussed, which, similarly to the case of other ketones [2], were carried out in several ways:

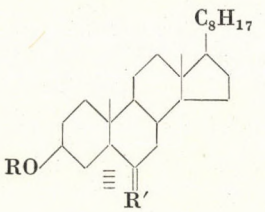

I R = Ac, R′ = O
II R = Bz, R′ = O
III R = Ac, R′ = NOH (*syn*)
IV R = Ac, R′ = NOH (*anti*)
V R = Bz, R′ = NOH (*syn*)
VI R = Bz, R′ = NOH (*anti*)
X R = H, R′ = O
XI R = H, R′ = NOH

The ketones were converted to the corresponding ketoximes (**III—IV**) in the usual way and these were subjected to Beckmann rearrangement.

If the oximes were prepared in alcohol, as it has already been mentioned [4], the *syn* and *anti* isomers could be readily separated, especially in the case of ketone **II.**

A method has also been elaborated for the separation of the two isomers by thin-layer and column chromatography [6].

In the latter case Brockmann II neutral aluminium oxide was used as adsorbent. The column was prepared in benzene as a solvent, and elution was carried out by benzene–ethanol gradually increasing the ethanol concentration in the mixture. Pure ethanol eluted the *syn* isomer in each case (**III, V**).

(It should be noted that in the case of the 6-ketoximes the 5α-hydrogen atom served as the point of reference, and by *syn* and *anti* isomers are meant those stereoisomers in which the hydroxyl of the ketoxime moiety is in the *cis* and *trans* position with respect to the 5α-hydrogen atom, respectively).

The Beckmann rearrangement of ketoximes **III—VI** and **V—VI,** as well as the Schmidt reaction of ketones (**I** and **II**) the following products were isolated:

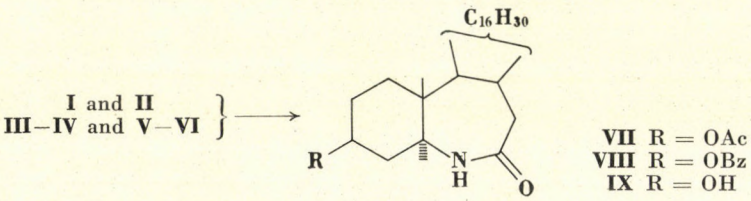

VII R = OAc
VIII R = OBz
IX R = OH

The structure of **IX** was also proved by acetylation to **VII.** At the same time, 3β-hydroxy-cholestan-6-one (**X**), and therefrom its oxime (**XI**), were prepared by alkaline hydrolysis of ketone **I** at room temperature. In this case the reaction led to the formation of one stereoisomer only. The Beckmann rearrangement of this isomer, carried out under identical conditions as in the case of **III—IV,** gave again **IX.** Lactam **VII** is known in the literature, therefore no effort was made to prove its structure.

The B-homolactam **IX** obtained in the above rearrangements was reduced with lithium aluminium hydride and acetylated with acetic anhydride in pyridine to give the following B-homo-aza-steroid and its N-acetyl derivative:

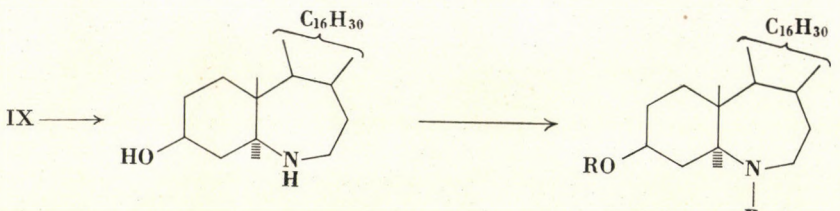

XII **XIII** R=Ac

3β-Hydroxycholest-5-en-7-one (**XIV**), 3β-acetoxycholest-5-en-7-one (**XV**), as well as 3β-hydroxycholestan-7-one (**XVI**) and its acetate (**XVII**) were also converted to the corresponding oximes (**XVIII**—**XXI**) and these subjected to Beckmann rearrangement:

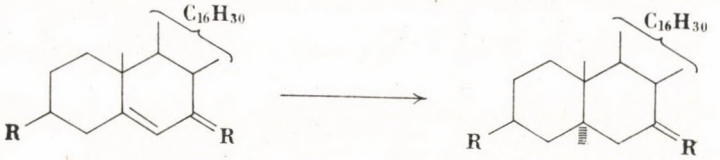

XIV R = OH, R′ = O
XV R = OAc, R′ = O
XVIII R = OH, R′ = NOH
XIX R = OAc, R′ = NOH

XVI R = OH, R′ = O
XVII R = OAc, R′ = O
XX R = OH, R′ = NOH
XXI R = OAc, R′ = NOH

The Schmidt reaction of the ketones and the Beckmann rearrangement of the corresponding oximes gave the same lactams. In neither case could oxime isomers be separated. Only the *syn* oximes (with respect to the 5α-hydrogen atom) are existing in these cases. The structure of lactam **XXIII** is known from the literature [5] and the structures of the other lactams were brought into correlation with it.

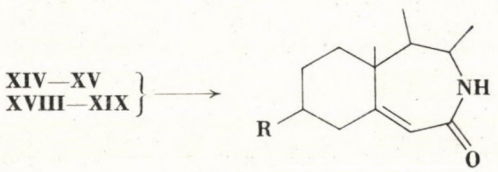

XXII R = OH
XXIII R = OAc

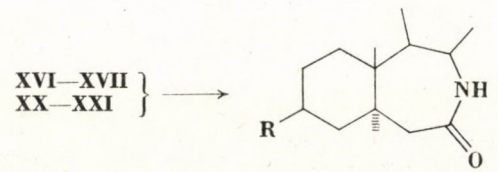

XXIV R = OH
XXI R = OAc

Hydrogenation of lactam XXIII over PtO_2 gave lactam **XXV**:

XXIII ⟶ **XXV**

In contrast to earlier observations, the yields were lower in the Schmidt reaction carried out under the usual conditions and, as it has been mentioned in the preliminary communication [4], side reactions occurred. For instance, the Schmidt reaction of **XV** in polyphosphoric acid (PPA) with sodium azide in the presence of sulfuric acid gave cholesta-3,5-dien-7-one (**XXVI**) [7].

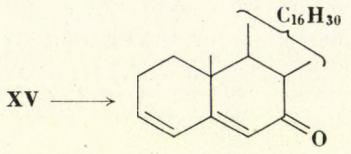

XXVI

Lactam **XXIII** was obtained by the Schmidt reaction of **XV** with hydrazoic acid in benzene in the presence of sulfuric acid only.

Experimental

All m.p.'s were determined on a Böetius-Heiztisch (Dresden) and they are uncorrected. The $[\alpha]_D$ values were measured in most cases in 1% chloroform solution, unless stated otherwise.

The infrared spectra were recorded by a Unicam SP200 and a Perkin Elmer 21 spectrophotometer. The absorptions are expressed in ν_{max}^{KBr} cm^{-1} values throughout this paper.

In the column chromatographic separations Brockmann II neutral aluminium oxide (n. Al_2O_3/II) or Kieselgel für Chromatographie (Merck) adsorbents were employed.

The conditions of the thin-layer chromatography employed in our laboratory have been described in detail in several of our earlier communications [1, 6, 8].

The experimental conditions applied in the Beckmann rearrangement procedures were those described in Organic Reactions [9] and in one of our earlier communications [1].

Similarly, the experimental conditions of the Schmidt reactions were identical with those described in Organic Reactions [10] and also in one of our earlier papers [2].

3β-Acetoxycholestan-6-one (I) [11, 12]

Compound **I** was obtained by nitration of 3β-acetoxycholest-5-ene with conc. nitric acid (sp. gr. 1.52; Merck) in glacial acetic acid in the presence of $NaNO_2$ and reduction of the nitro compound with Zn in glacial acetic acid. M. p. 127—128 °C, $[\alpha]_D$ —16 ± 2° (*c* 1.0; $CHCl_3$) (Lit. m. p. 127—128 °C, $[\alpha]_D$ —14.4 ± 2° (*c* = 1.0; $CHCl_3$).

$C_{29}H_{48}O_3$ (444.7). Calcd. C 78.33; H 10.88. Found C 78.33; H 10.86%.

ν_{max}^{KBr} 1700 (C=O), 1240, 1040 (C—O acetate) cm^{-1}.

3β-Benzoyloxycholestan-6-one (II)

Compound **II** was prepared from 3β-benzoyloxycholest-5-ene by nitration with conc. nitric acid and $NaNO_2$, and reduction of the 6-nitro compound obtained, as in the preceding case. After several recrystallizations from methanol the product melted at 158 °C, $[\alpha]_D$ 7 ± 2° (*c* = 1; $CHCl_3$).

$C_{34}H_{50}O_3$ (506.77). Calcd. C 80.00; H 9.93. Found C 80.04; H 9.98%.

ν_{max}^{KBr} 1700 (C=O), 1260 (C—O benzoate), 715 (Ar) cm^{-1}.

3β-Acetoxycholestan-6-one oxime (III, IV)

The oximes were prepared in two ways.

(*a*) In ethanol, with hydroxylamine hydrochloride, in the presence of anhydrous sodium acetate.

8.88 g (0.02 mole) of **I** was dissolved in 500 ml of abs. ethanol, 6.95 g (0.1 mole) of $NH_2OH \cdot HCl$ and 30 g of anhydrous sodium acetate were added to the solution, and the mixture was refluxed on a water bath for 6 hrs. It was then filtered, 65—70% of the solvent was removed, and the residue allowed to stand in a refrigerator. The crystalline product was filtered and dried, m. p. 191—195 °C. After a recrystallization from methanol the m. p. of the oxime

(**IV**) rose to the literary value: 205 °C. $[\alpha]_D$ —40 ± 2° (*c* = 1.0; $CHCl_3$) (Lit. m. p. 201—202 °C [5]).

$C_{29}H_{49}O_3N$ (459.70). Calcd. C 75.84; H 10.74; N 3.05. Found C 75.82; H 10.77; N 3.10%.

ν_{max}^{KBr} 3280 (OH), 1710 (C=O), 1660 (C=N), 1240 (C—O acetate) cm^{-1}.

On dilution with water the methanolic mother liquor resulted a second crop of crystalline product (**III**), m. p. 196—198 °C, $[\alpha]_D$ —47 ± 2° (*c* = 1.0; $CHCl_3$).

Analysis: (molecular weight, empirical formula and calculated composition are the same as for **IV**); found: C 75.86; H 10.73; N 3.15%.

ν_{max}^{KBr} 3250 (OH), 1710 (C=O), 1650 (C=N), 1230 (C—O acetate) cm^{-1}.

The two oxime isomers can be separated by column chromatography. The n. Al_2O_3/II adsorbent was filled in the column in benzene suspension and elution was done with a mixture of benzene–ethanol gradually increasing the ethanol concentration in the mixture. **III** could be obtained in pure form from the ethanol fractions.

(*b*) With hydroxylamine hydrochloride in pyridine: 10 g (0.022 mole) of **I** was dissolved in 100 ml of pyridine, 4.82 g of $NH_2OH \cdot HCl$ was added to the solution and it was heated on a water bath for 3 hrs. The hot solution was poured into a mixture of 300 ml of 1 : 1 hydrochloric acid and ice. The precipitate was filtered, washed with water and dried, m. p. 201—202 °C.

Recrystallization of the crude product from methanol gave **IV** only, in pure form, m. p. 205 °C.

3β-Benzoyloxycholestan-6-one oxime (V, VI)

The preparation of the oximes was accomplished as in the preceding case. Both methods gave a mixture of the isomers. Thin-layer chromatographic analysis revealed, in addition to the oxime isomers, the presence of starting material (II). Column chromatography on n. Al_2O_3/II adsorbent with benzene–ethanol permitted separation of the isomers.

The isomer eluated with benzene was the *syn* oxime (**V**) (71.4%), m. p. 179—181 °C, $[\alpha]_D$ —14 ± 2° (*c* = 1.0; $CHCl_3$).

$C_{34}H_{51}O_3N$ (521.80). Calcd. C 78.26; H 9.85; N 2.68. Found C 78.29; H 9.82; N 2.80%.

ν_{max}^{KBr} 3300 (OH), 1700 (C=O), 1670 (C=N), 1270 (C—O benzoate), 715 (Ar) cm^{-1}.

The anti isomer (**VI**) (22.5%) was eluted with benzene–ethanol (9:1), m. p. 225—227 °C, $[\alpha]_D$ —11 ± 2° (*c* = 1.0; $CHCl_3$).

Analysis: (*cf.* above.) Found: C 78.27; H 9.83; N 2.88%.

ν_{max}^{KBr} 3500 (OH), 1720 (C=O), 1600 (C=N), 1260 (C—O benzoate), 710 (Ar) cm^{-1}.

Beckmann rearrangement of 3β-acetoxycholestan-6-one oxime (III, IV) [1, 5]

2.3 g (0.005 mole) of **III, IV** (a mixture of the oxime isomers) was subjected to Beckmann rearrangement with 23 ml of thionyl chloride at —20 °C; the reaction time was 5 min. The mixture was neutralized with 4*N* KOH solution, the precipitate was filtered off, washed with water and dried. Chromatogrophy of the product permitted the isolation of two lactams with different physical constants (adsorbent: n. Al_2O_3/II, solvent: petroleum ether–benzene).

3β-Acetoxy-6-aza-B-homocholestan-6a-one (VII)

In the chromatography of the above mentioned crude product, the combined benzene and benzene–petroleum ether fractions contained 48% of the crude material, m. p. 221—222 °C, $[\alpha]_D$ + 34 ± 2° (*c* 1.0; $CHCl_3$). (Lit. m. p. 222—223 °C, $[\alpha]_D$ + 36° (*c* = 0.7; $CHCl_3$) [5].)

Analysis: The empirical formula, molecular weight and composition are the same as of **IV**, see there. Found: C 75.85; H 10.78; N 3.20%.

ν_{max}^{KBr} 3400, 3100 (NH), 1720 (C=O), 1670 (C=O, NH), 1250 (C—O acetate) cm^{-1}.

Elution with petroleum ether–methanol (9 : 1–1 : 1) and ethanol gave the deacetylated B-homolactam.

3β-hydroxy-6-aza-B-homocholestan-6a-one (IX)

M. p. 273—275 °C, $[\alpha]_D$ 52 ± 2°C (*c* = 1.0; $CHCl_3$).

$C_{27}H_{47}O_2N$ (417.67). Calcd. C 77.64; H 11.34; N 3.35. Found C 77.62; H 11.33; N 3.45%.

ν_{max}^{KBr} 3320, 3215, 3105 (OH, NH), 1660, 1640 (O=C—NH), cm^{-1}.

The Beckmann rearrangement of the pure **III** and **IV** oximes gave the same mixture of lactams (**VII** and **IX**) under the same conditions.

Schmidt reaction of 3β-acetoxycholestan-6-one

0.53 g (0.007 mole) of sodium azide was added in portions to a mixture of 2.24 g (0.005 mole) of **I** and 100 g of PPA (Fluka) with stirring. After the violent reaction was over, the mixture was heated at 100 °C for 10 hrs, poured into ice, made alkaline with 50% aqueous KOH solution and extracted with chloroform. The chloroform phase was washed with water, dried over anhydrous $CaCl_2$ and concentrated to give 2.1 g of the product, a brown oil, which was then chromatographed on n·Al_2O_3/II with petroleum ether–benzene.

Altogether three products were obtained in the chromatography of the above product:

(*a*) 0.25 g of unchanged ketone (**I**),

(*b*) 0.30 g of deacetylated lactam, 3β-hydroxy-6-aza-B-homocholestan-6a-one (**IX**), m. p. 274—275 °C. $[\alpha]_D$ 25 ± 2° (*c* = 1.0: $CHCl_3$)

Analysis: (*cf.* **IX**). Found: C 77.69; H 11.38; N 3.45%.

The ν_{max}^{KBr} cm^{-1} values also were identical with that of **IX**.

(*c*) 1.45 g of B-homolactam (72.5% of the end-product), which could be identified as **VII**.

Beckmann rearrangement of 3β-benzoyloxycholestan-6-one oxime

Rearrangement of oxime **VI** at —20 °C in thionyl chloride gave the benzoyl-B-homolactam, *3β-benzoyloxy-6-aza-B-homocholestan-6a-one* (**VIII**), m. p. 272—274 °C, $[\alpha]_D$ 42 ± 2° (*c* = 1.0; $CHCl_3$).

$C_{34}H_{51}O_3N$ (521.80). Calcd. C 78.26; H 9.85; N 2.68. Found C 78.28; H 9.90; N 3.10%.

ν_{max}^{KBr} 3350, 3220, 3090 (NH), 1690, 1650 (O=C—NH), 1280 (C—O benzoate), 720 (Ar) cm^{-1}.

The Beckmann rearrangement of oxime **V** with *p*-aminobenzenesulfonyl (chloride PABSCl) in pyridine gave two products, which were separated by chromatography on n. Al_2O_3/II. One of them was identical with lactam **VIII**, while the other proved to be 3β-hydroxy-6-aza-B-homocholestan-6-one (**IX**), which can also be derived from the *anti* oxime. M. p. 274—275 °C, $[\alpha]_D$ + 51 ± 2° (*c* = 1.0; $CHCl_3$).

Analysis: (*cf.* **IX**). Found: C 77.60; H 11.32; N 3.20%.

ν_{max}^{KBr} 3320, 3215, 3105, (OH, NH), 1660, 1640 (O=C—NH) cm^{-1}.

A 1 : 1 mixture of lactams **VIII** and **IX** showed a considerable m. p. depression; also their thin-layer chromatographic R_f values were different.

Schmidt reaction of 3β-benzoyloxycholestan-6-one

1.26 g (0.0025 mole) of **II** was reacted in 50 g of PPA in the presence of sodium azide at 80 °C [13, 14]. After removal of the solvent from the chloroform extract, an oil containing crystal was obtained, which was then chromatographed on n. Al_2O_3/II with petroleum ether–benzene. The crude product was 1.2 g; on chromatography it gave the following fractions:

(1) 0.8 g of the starting material (**II**)

(2) 0.25 g of **VIII** (21.8%)

(3) 0.1 g of **IX** (8.69%)

A more detailed examination of the reaction conditions and improvement of the yield of conversion require further experiments.

3β-Hydroxycholestan-6-one (X) [11, 12]

It was prepared from **I** by alkaline hydrolysis with 2*N* potassium hydroxide in dioxan–water at room temperature. M. p. 152—153 °C, $[\alpha]_D$ —6 ± 2° (*c* = 1.0; chloroform).

$C_{27}H_{46}O_2$ (402.67). Calcd. C 80.54; H 11.52. Found C 80.56; H 11.54%.

ν_{max}^{KBr} 3420 (OH), 1700, 1685 (C=O) cm^{-1}.

3β-Hydroxycholestan-6-one oxime (XI)

It was prepared with hydroxylamine hydrochloride in pyridine, as described earlier for another oxime. M. p. 214—216 °C, $[\alpha]_D$ 16 ± 2° (*c* = 1.0; chloroform).

$C_{27}H_{47}O_2N$ (417.67). Calcd. C 77.64; H 11.34; N 3.35%. Found C 77.66; H 11.38; N 3.40%.

ν_{max}^{KBr} 3350 (OH), 1650, 1465 (C=N) cm^{-1}.

Beckmann rearrangement of 3β-hydroxycholestan-6-one oxime

Beckmann rearrangement of compound **XI** in thionyl chloride at —20 °C and chromatography of the product on n. Al_2O_3/II gave, besides a small amount of starting material, compound **IX** as the main product, m. p. 273—275 °C. All other physical constants were identical with those of **IX**.

Analysis: Found: C 77.66; H 11.30; N 3.50%.

3β-Acetoxy-6-aza-B-homocholestan-6a-one (VII)

0.0001 mole of **IX** was dissolved in 1 ml of dry pyridine, 1 ml of acetic anhydride was added, the solution refluxed for 30 min, and the product isolated in the usual way to give **VII**, identical in all respects with the product obtained in the Beckmann rearrangement: m. p. 222—223 °C, $[\alpha]_D$ 35 ± 2° (c = 1.0; chloroform).

Analysis: Found: 75.84; H 10.70; N 3.25%.

3β-Hydroxy-6-aza-B-homocholestane (XII)

Reduction of compound **IX** was carried out by the method described by SHOPPEE *et al.* [15].

Accordingly, 0.417 g (0.001 mole) of **IX** was reduced with 5 g of lithium aluminium hydride in an ethereal solution for 48 hrs. At the end of this period, excess lithium aluminium hydride was decomposed with wet ether and ice, the ethereal phase was decanted, the precipitate acidified and extracted with ether several times. The combined ethera! fractions were dried and concentrated to give an oil, which was then chromatographed on n. Al_2O_3/II. The product was eluted with *n*-hexane. M. p. 128—130 °C, $[\alpha]_D$ 16 ± 2° (c = 1.0; methanol).

$C_{27}H_{48}NO$ (402.69). Calcd. C 80.53; H 12.02; N 3.48. Found C 80.54; H 12.04; N 3.60%.

ν_{max}^{KBr} 3330, 3230, 3100 (OH, NH) cm^{-1}.

3β-Acetoxy-6-N-acetyl-B-homocholestane (XIII)

Compound **XII** was acetylated with acetic anhydride in pyridine at room temperature. The reaction mixture was then concentrated in vacuum and the residue chromatographed on n. Al_2O_3/II. The column was prepared with ether and elution was effected with *n*-hexane, to obtain the diacetyl derivative. It was recrystallized from methanol; m. p. 158—160 °C, $[\alpha]_D$ 21 ± 2° (c = 0.15, chloroform).

$C_{31}H_{52}NO_3$ (486.77). Calcd. C 76.49; H 10.77; N 2.88. Found: C 76.46; H 10.74; N 3.10%.

ν_{max}^{KBr} 1630 (C=O), 1240 (C—O acetate) cm^{-1}.

3β-Acetoxycholest-5-en-7-one (XV) [16]

Compound **XV** was prepared by the method of WINDAUS *et al.* [16] from 3β-acetoxycholest-5-ene (cholesterol acetate). The isolated crude product was purified by recrystallization from aqueous ethanol to give a substance with the same physical constants as described in the literature: m. p. 154—155 °C, $[\alpha]_D$ = 90 ± 2° (c = 1.0; chloroform) (lit. m. p. 153—154 °C).

$C_{29}H_{46}O_3$ (442.69). Calcd. C 78.68; H 10.47. Found C 78.70; H 10.51%.

ν_{max}^{KBr} 1720, 1660, 1620 (C=O and C=CHC=CO), 1240 C—O acetate) cm^{-1}.

3β-Acetoxycholest-5-en-7-one oxime (XIX) [17—19]

It was prepared from ketone **XV** by heating with hydroxylamine hydrochloride in ethanol in the presence of anhydrous sodium acetate. The product was recrystallized from ethanol several times; m. p. 190—191 °C, $[\alpha]_D$ —195 ± 2° (c = 2.0; chloroform). (Lit. m. p. 184 °C, $[\alpha]_D$ —194° (c = 2.0; chloroform)).

$C_{29}H_{47}NO_3$ (457.70). Calcd. C 76.08; H 10.35; N 3.06. Found C 76.12; H 10.36; N 3.20%.

ν_{max}^{KBr} 3450 (OH), 1695 (C=O), 1630, 1595 (C=CH—C=N), 1260 (C—O acetate) cm^{-1}.

3β-Acetoxycholest-5-en-7-one oxime (**XIX**) was also prepared in dimethylformamide. 0.91 g (0.002 mole) of **XV** was dissolved in 20 ml of dimethylformamide, 0.28 g (0.004 mole) of

hydroxylamine hydrochloride was added, and the mixture heated on a water bath for 6 hrs. At the end of this period the solution was poured onto ice, the precipitate filtered off and dried. The product (0.87 g) had m. p. 90—110 °C. Chromatography of the crude product on neutral Al_2O_3/II gave 0.8 g of **XIX**.

3β-Hydroxycholest-5-en-7-one (XIV)

Alkaline hydrolysis of **XV** with potassium hydroxide in dioxan at room temperature gave **XIV**. After recrystallization from methanol, the product melted at 160—162 °C, $[\alpha]_D$ —136 ± 2° (c = 1.0; chloroform).

$C_{27}H_{44}O_2$ (400.65). Calcd. C 80.95; H 11.07. Found C 80.98; H 11.12%.

ν_{max}^{KBr} 3420 (OH), 1650, 1630, 1480 (C=CH—C=O) cm^{-1}.

3β-Hydroxycholest-5-en-7-one oxime (XVIII)

Compound **XVIII** was prepared from **XIV** with hydroxylamine hydrochloride in ethanol in the presence of anhydrous sodium acetate. The crude product was recrystallized from methanol several times, m. p. 239—241 °C, $[\alpha]_D$ —204 ± 2° (c = 1.0; chloroform).

$C_{27}H_{45}NO_2$ (415.66). Calcd. C 78.02; H 10.91; N 3.37. Found C 78.06; H 10.94; N 3.45%.

ν_{max}^{KBr} 3290, 3170 (OH), 1615, 1600 (C=CH—C=N) cm^{-1}.

Beckmann rearrangement of 3β-acetoxycholest-5-en-7-one oxime

The Beckmann rearrangement was carried out also in this case with thionyl chloride. 50 ml cold (—20 °C) thionyl chloride (sp. gr. 1.655) was added to 4.57 g (0.01 mole) of **XIX**. As soon as the substance dissolved, 10 ml of cold 4N KOH was added to the solution, which was then made alkaline by the addition of further 4N KOH solution. The suspension was finally neutralized with 2N HCl. The precipitate was filtered off, washed with water and dried; m. p. 115 °C. The crude product (4.3 g) was chromatographed on n. Al_2O_3/II, when 4.02 g of material was recovered:

(1) 0.44 g of the unchanged starting material (**XIX**);

(2) 0.12 g of deacetylated lactam (3β-hydroxy-7a-aza-B-homocholest-5-en-7-one (**XXII**))

(3) 3.46 g of 3β-acetoxy-7a-aza-B-homocholest-5-en-7-one (**XXIII**), m. p. 202 °C, $[\alpha]_D$ —81 ± 2° (c = 1.0; chloroform).

$C_{29}H_{47}NO_3$ (457.70). Calcd. C 76.08; H 10.53; N 3.06. Found C 76.12; H 10.48; N 3.25%.

ν_{max}^{KBr} 3200, 3050 (OH, NH), 1720 (C=O), 1650, 1610 (C=CH—C=O), 1240 (C—O acetate cm^{-1}.

The Beckmann rearrangement was also effected in pyridine in the presence of PABSCl, in the same manner as described earlier, starting with 0.914 g (0.002 mole) of **XIX**. The crude product was recrystallized from methanol to give pure **XXI** in a high yield. Neither the starting material, nor deacetylated lactam contaminated the product.

Schmidt reaction of 3β-acetoxycholest-5-en-7-one

The reaction was carried out in PPA in the same manner as described earlier, starting with 4.42 g (0.01 mole) of **XV**. The reaction mixture was poured onto ice, neutralized with 50% KOH solution and extracted with chloroform. The organic phase was washed with water, dried and evaporated to give 4 g of a brown oil. The crude product was chromatographed on n. Al_2O_3/II to give 0.86 g of *cholesta-3,5-dien-7-one* (**XXVI**) [7] and 2.7 g of the unchanged starting material (**XV**).

Similar result was obtained when the reaction was carried out with sodium azide in chloroform in the presence of conc. sulfuric acid, merely the ratio of the two components in the product was somewhat different.

The desired lactam was obtained as follows: 4.42 g (0.01 mole) of **XV** was dissolved in 30 ml of anhydrous benzene and 5 ml of conc. sulfuric acid was added cautiously to form a lower layer beneath the solution (cooling was necessary in the period of sulfuric acid introduction); a 6% solution of hydrazoic acid in benzene was then added dropwise at room temperature. The mixture was stirred with cooling for 2 hrs, the benzene phase was washed with 2N NaOH and water, and dried over anhydrous calcium chloride. After removal of the solvent a partly crystalline residue was obtained. It was chromatographed on n. Al_2O_3/II to give 1.54 g of the starting material (**XV**) and 1.65 g of **XXIII**, which could be identified with the lactam obtained in the Beckmann rearrangement.

3β-Acetoxycholestan-7-one (XVII)

Compound **XVII** was prepared from **XV**. The latter compound was dissolved in ethyl acetate and hydrogenated in the presence of PtO_2 at atmospheric pressure as described by WINTERSTEINER *et al.* [20]. The crude product was crystallized from methanol several times, m. p. 147—148 °C, $[\alpha]_D$ —36 ± 2° (*c* = 1.0; chloroform).

$C_{29}H_{48}O_3$ (344.47). Calcd. C 78.33; H 10.88. Found C 78.35; H 10.92%.

ν_{max}^{KBr} 1710, 1690 (C=O), 1260 (C—O acetate) cm^{-1}.

3β-Acetoxycholestan-7-one oxime (XXI)

4.44 g (0.01 mole) of **XVII** was dissolved in 100 ml of ethanol; 1.4 g (0.02 mole) of hydroxylamine hydrochloride and 1.64 g anhydrous sodium acetate were added and the mixture refluxed for 2 hrs. It was filtered while hot and allowed to cool, when the ketoxime deposited in crystalline form. The product was filtered off and recrystallized from methanol; m. p. 203—205 °C, $[\alpha]_D$ —92±2° (*c* = 1.0; chloroform).

$C_{29}H_{49}NO_3$ (459.70). Calcd. C 75.84; H 10.74; N 3.05. Found C 75.78; H 10.80; N 3.25%.

ν_{max}^{KBr} 3500 (OH), 1700 (C=O), 1650, 1630 (C=N), 1260 (C—O acetate) cm^{-1}.

Beckmann rearrangement of 3β-acetoxycholestan-7-one oxime

In this case the rearrangement reaction was carried out in two ways:

(a) In thionyl chloride at —20 °C as described earlier. The lactam obtained was recrystallized from ethanol several times, m. p. 165—166 °C, $[\alpha]_D$ 9±2° (*c* = 1.0; $CHCl_3$). The product isolated was *3β-acetoxy-7a-aza-B-homocholestan-7-one* (**XXV**). (Lit. m. p. 167—168 °C, $[\alpha]_D$ 9.5° (*c* = 2.3; $CHCl_3$) [5].

$C_{29}H_{49}NO_3$ (459.70). Calcd. C 75.84; H 10.74; N 3.05. Found C 75.80; H 10.76; N 3.30%.

ν_{max}^{KBr} 3300, 3150 (OH, NH), 1730 (C=O), 1670 (O=C, NH), 1235 (C—O acetate) cm^{-1}.

(b) In pyridine with PABSCl at room temperature. The reaction mixture was poured onto ice and the brown oily product which separated was extracted with a 1 : 1 mixture of chloroform and ether. The organic layer was dried and the solvent removed in vacuum. The residue was chromatographed on a silica gel column to give **XXV**.

In this case the thionyl chloride procedure gave the product of higher purity.

Schmidt reaction of 3β-acetoxycholestan-7-one

2.22 g (0.005 mole) of **XVII** was subjected to the Schmidt reaction as described earlier using a benzene solution of hydrazoic acid.

The solution of hydrazoic acid in benzene was added dropwise, with stirring, to the reaction mixture at room temperature. After stirring with cooling for 2 hrs, the benzene phase was separated, washed with 2*N* NaOH solution and water, dried over anhydrous $CaCl_2$ and concentrated in vacuum. The brown oily residue (2.1 g) was chromatographed on n. Al_2O_3/II to obtain 0.25 g of the starting material (**XVII**), 0.3 g of *3β-hydroxy-7a-aza-B-homo-cholestan-7-one* and 1.38 g of *3β-acetoxy-7a-aza-B-homocholestan-7-one* (**XXV**). The physical properties of lactam **XXV** were identical with those of the product obtained in the Beckmann rearrangement.

Beckmann rearrangement of 3β-hydroxycholest-5-en-7-one oxime

The Beckmann rearrangement was effected in dioxan with thionyl chloride as follows: 0.42 g (0.001 mole) of **XVIII** was dissolved in 20 ml of dry dioxan, the solution was cooled to 10 °C, and a solution of 1.2 ml of thionyl chloride in 2 ml of dioxan was added dropwise at this temperature. The solution was kept 10 min. at 10 °C, 30 min. at room temperature, and then poured onto ice. After neutralization with ammonium hydroxide, the precipitate was filtered off and chromatographed on n. Al_2O_3/II to give *3β-hydroxy-7a-aza-B-homocholest-5-en-7-one* (**XXII**), m. p. 194—196 °C, $[\alpha]_D$ —80±2° (*c* = 1.0; chloroform).

Analysis: (*cf.* **XVIII**). Found: C 78.04; H 10.95; N 3.45%.

ν_{max}^{KBr} 3490, 3420 (OH, NH), 1630, 1600, 1560 (C=C—C=NH) cm^{-1}.

Compound **XXII** was also isolated in the Beckmann rearrangement of **XIX**.

Schmidt reaction of 3β-hydroxycholest-5-en-7-one oxime

The Schmidt reaction of this compound carried out in PPA gave the same (**XXII**) lactam.

Beckmann rearrangemant of 3 β-hydroxycholestan-7-one oxime

Beckmann rearrangement of compound **XX**, carried out as described for **XVII**, gave **XXIV**, *3β-hydroxy-7a-aza-cholestan-7-one*, m. p. 188—190 °C, $[\alpha]_D$ 16±2° (*c* = 1.0; chloroform).

Analysis: (*cf.* **XXI**). Found: C 77.61; H 11.35; N 3.40%.

ν_{max}^{KBr} 3320, 3240, 3100 (OH, NH), 1750, 1720 (O=C—NH) cm^{-1}.

Schmidt reaction of 3β-hydroxycholestan-7-one

The Schmidt reaction in polyphosphoric acid of this compound gave the same B-homolactam (**XXIV**).

3β-Hydroxy-7a-aza-B-homocholestan-7-one (XXIV)

Compound **XXIV** was also obtained by the catalytic reduction of compound **XXII** in the presence of PtO_2.

0.042 g of **XXII** was dissolved in 5 ml of glacial acetic acid, 5 mg of pre-hydrogenated PtO_2 catalyst was added in 5 ml of glacial acetic acid, and the mixture was hydrogenated at atmospheric pressure. After the absorption of the calculated amount of hydrogen the catalyst was removed by filtration, the filtrate evaporated in vacuum and the residue recrystallized from aqueous methanol; m. p. 188—189 °C.

Analysis: Found: C 77.68; H 11.38; N 3.45%.

The infrared spectrum of the product was identical with that of **XXIV**.

3β-Acetoxy-7a-aza-B-homocholest-5-en-7-one (XXIII)

Acetylation of compound **XXII** by refluxing it with acetic anhydride in pyridine gave a product with the following characteristics: m. p. 200—202 °C, $[\alpha]_D$ —81±2° (*c* = 1.0; chloroform).

Analysis: (*cf.* **XXIII**). Found: C 76.10; H 10.55; N 3.25%.

The infrared spectrum of the product was identical with that of compound **XXIII**.

REFERENCES

1. Matkovics, B., Göndös, Gy., Tegyey, Zs.: Magy. Kém. Foly. **72,** 303 (1966)
2. Matkovics, B., Tegyey, Zs.: Magy. Kém. Foly. (In the press)
3. Matkovics, B., Göndös, Gy., Taródi, B.: Acta Chim. Acad. Sci. Hung. **57,** 119 (1968)
4. Matkovics, B., Göndös, Gy., Tegyey, Zs.: Acta Chim. Acad. Sci. Hung. **53,** 417 (1967)
5. Knof, L.: Ann. **642,** 194 (1961)
6. Matkovics, B., Tegyey, Zs., Göndös, Gy., Baláspiri, L.: Microchem. J. **13,** 502 (1968)
7. Norginberski, J. K.: Brit. Pat. 887, 706; 1962; (C. A. **57,** 2292 (1962))
8. Matkovics, B., Tegyey, Zs.: Magy. Kém. Foly. **74,** 516 (1968)
9. Donarum, L. G., Heldt, W. Z.: Organic Reactions, Vol. 11, p. 1. Wiley, London, 1960
10. Wolff, H.: Organic Reactions, Vol. 3, p. 320. Wiley, London, 1964
11. Dodson, R. M., Riegel, B.: J. Org. Chem. **13,** 424 (1948)
12. Hassner, A., Heathcock, C.: J. Org. Chem. **29,** 1350 (1964)
13. Doorenbos, N. I., Wu, M. T.: J. Org. Chem. **26,** 2548 (1961)
14. Doorenbos, N. I., Havranch, R. E.: J. Org. Chem. **30,** 2474 (1965)
15. Shoppee, C. W., Killich, R. W., Krüger, G.: J. Chem. Soc. **1962,** 2275
16. Windaus, A., Lettré, H., Schench, Fr.: Ann. **520,** 102 (1935)
17. Matkovics, B., Göndös, Gy., Kovács, Ö.: IUPAC, London, 10—17th July 1963, Handbook, p. 334, Abstract 9—42

18. ECKHARDT, H.: Ber. **71**, 461 (1938)
19. ELSEVIER's Encyclopaedia of Organic Chemistry, Vol. 14, Suppl. 2684. Spinger-Verlag, Berlin 1959
20. WINTERSTEINER, O., MOORE, M.: J. Amer. Chem. Soc. **65**, 1053 (1943)

Béla MATKOVICS; Szeged, Táncsics M. u. 2.
Zsuzsanna TEGYEY; Budapest, XII. Győri út 2/a
Mária RESCH; Szeged, Dóm-tér 8.
Ferenc SIROKMÁN; Szeged, Aradi vértanuk tere 1.
Endre BOGA; Szeged, Rerrich Béla-tér
Hungary.

BOOK REVIEWS — BUCHBESPRECHUNGEN — РЕЦЕНЗИИ КНИГ

H. F. EBEL: *Die Azidität der CH-Säuren*

Georg Thieme Verlag, Stuttgart 1969, 99 Seiten

Als Motto wählte der Verfasser höchst treffend den vor zwei Jahrhunderten von MORVEAU geprägten Satz: »Tenir la définition des acides, c'est tenir la clef de la chimie.«

In der Tat spielte der Säure-Base-Begriff und das Bestreben nach seiner exakten Definition eine entscheidene Rolle in der Entwicklung der Theorie der Chemie. Zugleich ist es jedoch auch für den organischen Synthetiker von außerordentlicher Bedeutung, zu wissen, in welchem Maße z. B. seine saure CH-Bindungen enthaltenden Moleküle zur Dissoziation, d. h. zur Bildung von Carbanionen neigen. Die Kenntnis derartiger Faktoren erleichtert die Planung der Reaktionen, die Wahl des passenden Lösungsmittels wesentlich.

Im ersten Teil des Buches (31 Seiten) behandelt der Verfasser die verschiedenen Verfahren zur Bestimmung der Azidität, gemeinsam mit den Fragen der Gleichgewichtsazidität sowohl in wäßriger als auch in wenig polarer nichtwäßriger Lösung. In den letzteren Lösungsmitteln ist es notwendig, die Begriffe Ionisation und Dissoziation voneinander zu trennen. Diese Begriffe werden klar und genau abgegrenzt. Im Zusammenhang mit der Protonenbeweglichkeit werden einige charakteristische Reaktionen, wie z. B. durch Basen katalysierte Halogenierung, Racemisierung und Isotopenaustausch behandelt. In Verbindung mit der Austauschreaktion zwischen Wasserstoff und Metallen wird die kinetische und thermodynamische Azidität verglichen.

Im zweiten Teil der Monographie sind Zahlenwerte der Azidität der behandelten organischen Verbindungen angegeben und diskutiert. Die pK_a-Werte zahlreicher Derivate in wäßriger Lösung sowie ihre pK-Werte in nichtwäßriger Lösung bzw. in Lösungsmittelgemischen sind tabellarisch angeführt. Bei der Diskussion der Zusammenhänge zwischen dem sauren Charakter und der Struktur wird der Einfluß von induktiven, konjugativen und hybridisierenden Effekten behandelt.

Infolge der zahlreichen experimentellen Angaben und der recht gut geschriebenen, klaren Übersicht des Themas wird das Buch zur interessanten Lektüre und zugleich zu einem wertvollen Nachschlagewerk.

CS. SZÁNTAY

Ancillary Techniques of Gas Chromatography, Ed. by L. S. ETTRE and W. H. MCFADDEN

Wiley-Interscience, New York, 1969, 395 pp.

Gas chromatography is considered today as one of the most frequently used, indispensable analytical tools. However, it is often forgotten that in essence, gas chromatography is a separation technique. It can be used therefore only with due circumspection for the identification of substances, and still more so for the elucidation of the structure of unknown compounds, even in possession of suitable test substances. Moreover, the number of problems is increasing steadily, which involve the gas chromatographic separation of a mixture containing unknown components, and the subsequent determination of the structure of the single components by some other (physical or chemical) method.

The peculiarity of gas chromatography is that while the mixture to be separated is introduced as a single slug, it is introduced into a continuously moving gas flow and at the end

of the column, the individual fractions emerge separated in time. One technique would be a collection of preparative character of the fractions separated, however, in most of the cases this method is not to the purpose. A better method consists in direct introduction of the fractions leaving the column into a suitable instrument, where the physical parameters characteristic of the structure (spectrum, etc.) are recorded. The manipulations which are directly coupled with the standard gas chromatographic systems may be called the ancillary techniques of gas chromatography.

Two further problems arise from the application of known methods of structural investigation for this purpose: the dimensions of the sample and the speed of recording. The sensitivity of the various methods is different, and the reduction of the sample dimensions may result in a distortion of the recording, which makes its evaluation impossible. The other problem is the speed of recording, because the recording of the single components leaving the column must be terminated before the next component appears. It is due to the advantageous fulfilment of these two precondictions that chromatographs combined with a mass spectrograph appeared first on the market, though recent years brought important developments in this respect also in the field of IR and NMR spectroscopy.

As becomes clear from the Preface, the principal aim of the reviewed book is "not simply to give a literature survey of all the techniques dealing with a particular system, but rather to summarize the aspects of a particular system, discuss its pros and cons, describe the most important instrumental arrangements, and discuss what kind of information can be obtained through its use. It should be emphasized again that we do not want to teach gas chromatography or any of the chemical or physical techniques coupled with the gas chromatography. The subject is how individual techniques are interfaced with gas chromatography".

The book comprises the following chapters:

1. Principles, What are "ancillary techniques"? by Leslie S. Ettre.
2. Microreaction gas chromatographic techniques, by Paul Steingaszner.
3. Pyrolysis gas chromatography, by Robert W. McKinnes.
4. Precolumn reactions for structure determination, by Morton Beroza and May N. Inscoe.
5. Gas chromatography and mass spectroscopy, by J. Throck Watson.
6. Gas chromatography and infrared and Raman spectrometry, by Stanley K. Freeman.
7. Gas chromatography and nuclear magnetic resonance spectroscopy, by Gordon E. Hall.
8. Gas chromatography and thin-layer chromatography, by Rudolf Kaiser.
9. Chemical identification of gas chromatographic fractions, by Charles Merritt, Jr.
10. Special identification detectors, by Charles T. Malone and William H. McFadden.

The authors of the individual chapters are investigators with experience in the various interfaced systems.

This book, excellently edited and containing ample bibliography, similarly to its predecessor "The Practice of Gas Chromatography", is indispensable for those using gas chromatographic methods, and will help to improve the efficiency of their work.

Gy. Deák

R. Paterson: *An Introduction to Ion Exchange*

Heyden and Son Ltd., London 1970, 109 pp.

As indicated by the title, this small volume gives a brief outline of the chemistry and applications of ion exchangers.

After a general discussion of ion exchange processes, a description of ion exchangers is given dealing in particular with inorganic ion exchangers and modern types of ion exchange resins.

This part is followed by a discussion of the Gregor—Glueckauf theory of ion exchange equilibria and selectivity, which can be regarded as classic today; this is complemented by the theory of Curney and Holm, explaining the apparently anomalous behaviour of weak acid ion exchangers and exchangers of the phosphoric acid type.

In the next chapter, problems in the kinetics of ion exchange processes are discussed and the known relationships interpreted, primarily on the basis of Helfferich's works, in a graphic way.

The fifth chapter deals with ion exchange membranes. This chapter is the longest. Material transport occurring in the membrane and electrokinetic phenomena are discussed in terms of irreversible thermodynamics.

The following chapter describes the basic principles of the operation of ion exchange columns, and discusses methods of application.

Finally, the last chapter deals with the properties and the applications of inorganic ion exchangers.

The thermodynamical interpretation of ion exchange equilibria is contained in the Appendix.

The book gives a short but well-constructed and interesting picture of ion exchangers, their mode of operation and their applications according to the present state of scientific knowledge.

The book is to be recommended mainly to readers who wish to obtain information in a form affording good reading, on the basic principles of the operation and the applications of ion exchangers, without requiring details.

The chief merit of the book is that in each case the most essential information, the most important material has been selected by the author, and this is presented in a very lucid form, which is easy to understand, while the addition of irrelevant matter has been avoided. Perhaps occasional lack in proportion between the importance and length of some chapters might give rise to criticism but, in the opinion of the reviewer, it is the author's prerogative to make decisions in this respect; it is not only permissible but desirable that an author should devote greater concern to parts or problems that belong to his special field where he himself has made contributions.

Today, when torrents of new scientific discoveries and research results almost suffocate the research chemist, this book, which presents knowledge of ion exchangers in a concise, clear-cut and perspicuous form at an up-to-date scientific level, must indeed be welcomed.

The rational arrangement of the chapters, the spaced setting of the text and the well selected figures all contribute to the lucidity, descriptiveness and clarity of the book.

J. INCZÉDY

INDEX

INORGANIC AND ANALYTICAL CHEMISTRY – ANORGANISCHE UND ANALYTISCHE CHEMIE – НЕОРГАНИЧЕСКАЯ И АНАЛИТИЧЕСКАЯ ХИМИЯ

KISS, A. B., GADÓ, P., ASZTALOS, I. and HEGEDÜS, A. J.: New Results Concerning the Thermal Decomposition of Ammonium Heptamolybdate Tetrahydrate 235

NYILASI, J., ORSÓS, P. und POMOGÁTS, E.: Die Reaktion von Osmiumtetroxyd mit Äthylendiamin (The Reaction of Osmium Tetroxide with Ethylenediamine)..... 251

RATKOVICS, F., SALAMON, T. and LÁSZLÓ, M.: Investigation of the Dielectric and Volumetric Properties of the Acetic Acid–Chloroform Mixture 259

PHYSICAL CHEMISTRY — PHYSIKALISCHE CHEMIE — ФИЗИЧЕСЧАЯ ХИМИЯ

DÉVAY, J., LENGYEL, B. jr. and MÉSZÁROS, L.: The Elimination of Resistance Polarization in Potentiostatic Investigations 269

MINK, J. and PENTIN, YU. A.: Vibrational Spectra of Organomercuric Compounds, VI. Infrared and Raman Spectra of Divinyl Mercury 277

KOMOR, M., VÉRTES, A., DÉZSI, I. and RUFF, I.: Investigation of the Electron Exchange Reaction between Iron(II) and Iron(III) by Mössbauer Effect in Solution 285

ROCKENBAUER, A. and GÁTI, GY.: Electron Spin Resonance Spectra of the Chromium(III) Oxide–Molybdenum(VI) Oxide System 293

ORGANIC CHEMISTRY — ORGANISCHE CHEMIE — ОРГАНИЧЕСКАЯ ХИМИЯ

KUSZMANN, J. and VARGHA, L.: Synthesis of New Sugar Derivatives Having Potential Antitumour Activity, XIII. Synthesis of 1,2 : 5,6-Diepithio-D-mannitol, -D-glucitol and some of their Derivatives 307

LIPTÁK, A.: Carbohydrate Methyl Ethers, II. A New Synthesis of 3,4-Dimethyl-D-glucose 315

BARTÓK, M. and MOLNÁR, Á.: The Chemistry of 1,3-Bifunctional Systems, IX. The Reaction of 1,3-Butanediol and some of its Cyclic Derivatives with Hydrochloric Acid 319

MATKOVICS, B., TEGYEY, ZS., RESCH, M., SIROKMÁN, F. and BOGA, E.: Rearrangements of Steroids, VI. Comparative Examination of the Schmidt Reaction of 3β-Substituted Cholestan-6- and 7-ones, Cholest-5-en-7-one and the Beckmann Rearrangement of the Corresponding Oximes 333

BOOK REVIEWS — BUCHBESPRECHUNGEN — РЕЦЕНЗИИ КНИГ 345

Printed in Hungary

A kiadásért felel az Akadémiai Kiadó igazgatója — Műszaki szerkesztő: Farkas Sándor

A kézirat nyomdába érkezett: 1970. VIII. 6. — Terjedelem: 10 (A/5) ív, 49 ábra

71.70180 Akadémiai Nyomda, Budapest — Felelős vezető: Bernát György

ACTA CHIMICA

ТОМ 66 — ВЫП. 3

РЕЗЮМЕ

О некоторых новых данных по термическому разложению тетрагидрата аммоний-гептамолибдата

Б. А. КИШ, П. ГАДО, И. АСТАЛОШ и Й. А. ХЕГЕДЮШ

Реакция термического разложения тетрагидрата аммоний-гептамолибдата изучалась различными методами. Было установлено, что во образованию MoO_3 наблюдается два промежуточных фазы неизвестной структуры. На основе данных химического анализа общая формула новых фаз, относимая к 1 R_2O, представляет собой $(NH_4)_2OMo_{14}O_{42}$ и $(NH_4)_2OMo_{22}O_{66}$. Были определены ИК спектрофотометрические характеристики членов серий разложения в области валентных колебаний Mo—O, а также размеры элементарных ячеек 2,5, 14 и 22-молибдата с помощью рентгено-диффракционного метода.

При сравнении твердофазного процесса с реакцией поликонденсации в растворе, были обнаружены отдельные общие и различающиеся особенности относительно образующегося промежуточного конденсата. На основе полученных зависимостей было заключено, что и в твердой фазе протекает реакция поликонденсации.

Реакция тетраокиси осмия с этилендиамином

Й. НИЛАШИ, П. ОРШОШ и Э. ПОМОГАТЧ

Изучалась реакция тетраокиси осмия с этилендиамином в 0,5 N растворе NaOH и при температуре 100°C, причем определялась доля азота, освобождавщегося в виде аммиака, а также доля азота, которая может быть измерена методом Къелдаля после реакции.

Было установлено, что при постоянном содержании этилендиамина увеличение концентрации OsO_4 вплоть до молярного отношения 1 моль диамина: 2 молям OsO_4 благоприятствует дезаминированию, в то время как последующее увеличение количества тетраокиси осмия приводит к уменьшению выхода аммиака. При молярном отношении 1 моль диамина: 8 молям OsO_4 уже вообще не наблюдается выделения аммиака.

После дезаминирования азот не может быть измерен методом Кьелдаля до тех пор, пока на 1 моль диамина не будет приходиться два или более молей тетраокиси осмия. Сумма содержания азота, измеренного в форме аммиака, а также обнаруживаемого недостатка, выраженная в грамматомах, согласуется с количеством грамматомов осмия присутствующем в системе. Количества аммиачного азота, равные с, так называемым, недостатком азота, рассчитанным из сопоставления содержания азота в образце и выделявщегося в форме аммиака, а также измеренного методом Кьелдаля, могут быть измерены, если смеси после дезаминирования подвергать восстановлению в щелочной среде с помощью сплава Деварда.

На основе проведенных исследований в реакции тетраокиси осмия с этилендиамином полагается присутствие комплексов осмия с различным содержанием азота, атомы которого связаны различным образом.

Изучение диэлектрических и объемных свойств смесей уксусной кислоты с хлороформом

Ф. РАТКОВИЧ, Т. ШАЛАМОН и М. ЛАСЛО

Приводятся результаты исследований по изменению объема при смешении уксусной кислоты с хлороформом, по диэлектрическим постоянным смесей, а также их коэффициентом преломления, измеряемым в видимом свете, в зависимости от состава. На основе

этих данных, диэлектрические свойства смесей не могут быть объяснены с помощью модели тройной смеси, типа $A—A_2—B$, предложенной в предыдущем сообщении, т. к. мономер уксусной кислоты, вероятно, образуя водлородный мостик с хлороформом, дает также и ассоциат типа AB.

Исключение поляризации сопротивления при потенциостатических исследованиях

Й. ДЕВАИ, Б. ЛЕНДЬЕЛ, мл. и Л. МЕСАРОШ

Был разработан метод непрерывного измерения поляризации сопротивления в условиях потенциостатических исследований и автоматической компенсации ее. Сущность метода заключается в том, что в измеряемую ячейку направлялся переменный ток, пропорциональный постоянному току, протекающему в ней, и первый суперпонировался на последний. Напряжение переменного тока между стандартным и измеряемым электродом является пропорциональным напряжению постоянного тока, появляющемся на омическом сопротивлении. Последнее, усиливая и выпрямляя, добавляется к напряжению постоянного тока, регулирующего потенциостат. С помощью этого метода удалось достигнуть то, что на изучаемый электрод, независимо от омического сопротивления, всегда поступает напряжение, установленное на потенциостате.

Колебательные спектры ртутноорганических соединений, VI. ИК- и Раман-спектры дивинилртути

Я. МИНК и Ю. А. ПЕНТИН

ИК-спектры дивинилртути были зарегистрированы в газовой и жидкой фазах, а Раман-спектры в жидкой фазе и кристаллической фазе при низкой температуре. Наблюдаемые полосы были отнесены к характерным колебаниям молекулы. На основе наблюдаемой картины предполагается линейный или близкий к линейному скелет CHgC. Следует также отметить, что спектры, полученные в отдельности для газовой, жидкой и твердой фаз, не могут быть интерпретированы при предположении наличия единственного типа из групп симметрии C_2, C_{2v}, C_{2h}, $D_{\infty h}$. Анализ нормальных координат спектра, проведенный с помощью ЭВМ, приводит к значению силовой постоянной валентного колебания CHg, равному $4{,}02 \cdot 10^6$ см$^{-2}$ (2,58 мдин/Å).

Изучение электронного обмена, протекающего между Fe(II) и Fe(III) в растворах, методом Мёссбауэра

М КОМОР, А. ВЕРТЕШ, Й. ДЕЖИ и Й. РУФФ

Электронный обмен между Fe^{2+} и Fe^{3+} изучался на примере следующей реакции

$$^{57}Fe^{3+} + Fe^{2+} = {}^{57}Fe^{2+} + Fe^{3+}$$

Хлорнокислый соль Fe(III) приготовлялось из ^{57}Fe, а хлорнокислый соль Fe(II) — из природного железа. Концентрация смеси по железу составляла 0,13 моль/л и pH изменялось в интервале $pH = 0 \div 2{,}50$. За обменом различных продуктов гидролиза железа(III) следили по появлению в спектре эффекта соответствующего Fe^{2+}. Было установлено, что комплексы $Fe(H_2O)_6^{3+}$ и $FeOH^{2+}$ в изученных экспериментальных условиях почти мгновенно обменивают их электроны. Константа скорости обмена $K \geqq 2{,}6$ моль$^{-1}$ сек$^{-1}$. Продукты более высокой степени гидролиза $[Fe(OH)_2^+$ и $Fe_2(OH)_2^{4+}]$ блокируют электронный обмен.

Концентрации комплексов Fe(III), гидролизованных в различной степени, определялись из интенсивностей эффекта Мёссбауэра и сравнивалась с данными, полученными Хэдстрёмом [1]. В пределах погрешности измерений (10%) и за исключением дигидроксокомплексов результаты хорошо согласуются. В случае же дигидроксокомплексов, концентрация последних намного превышает таковую по литературным данным [1, 2] (и равно около 10%).

Спектр ЭПР системы окись хрома(III) — окись молибдена(VI)

А. РОКЕНБАУЭР и ДЬ. ГАТИ

Изучался спектр ЭПР смешанных окисей в хрома и молибдена, полученных при различных отношениях хрома и молибдена, из различных исходных веществ и при различных температурах прокаливания. В спектре наблюдается два типа линий: один широкий синглет без стс, который относится к ионам Cr^{+3} в $Cr_2(MoO_4)_3$ и один узкий сигнал, обладающий g-анизотропией и стс, который согласно нашим предположениям, может быть отнесен к ионам Cr^{+5} в решетке MoO_3. Эти ионы образуются лишь в ограниченном количестве и для их образования необходимо присутствие группы $(OH)^-$. Ионы Cr^{+5} окружены кислородом в виде тетрагональной пирамиды, причем наиболее сильной связью между хромом и кислородом является связь с кислородом, находящимся в вершине пирамиды. Структура связей аналогична со структурой в $(CrOCl_4)^-$, но б-связь, лежащая в плоскости, сильнее и энергии возбуждения «переноса заряда» больше. В спектрах на частоте 93 000 Мгц X полосе мопимо линий изотопа Cr^{53}, наблюдается также суперсверхтонкое расщепление, вызванное водородом.

Синтез новых сахарных производных, обладающих потенциальной противоопухольной активностью XIII

Й. КУСМАНН и Л. ВАРГА

Был разработан синтез 1,2 : 5,6-диэпитио-D-маннита и -D-сорбита, а также их некоторых производных, исходя из 1,2 : 5,6-диангидро-3,4-0-изопропилиден-L-идита и 3,4-0-изопропилиден-D-сорбита, соответственно. Изучались свойства полученных соединений.

Метиловые эфиры углеводов, II. Новый синтез 3,4-диметил-D-глюкозы

А. ЛИПТАК

α-Метил-D-глюкозид дает при взаимодействии с 2-мя молями бензоилхлорида в пиридине и при 0°С 2,6-дибензоил-α-метил-D-глюкозид(II), который в присутствии каталитического количества эфирата трехфтористого бора в дихлорметановом растворе метилируется с помощью диазометана до 2,6-дибензоил-3,4-диметил-α-метил-D-глюкозида(III). Дебензоилированием последнего с помощью метилата натрия и последующим кислотным гидролизом удалось получить 3,4-диметил-D-глюкозу(V) с 70%-ным выходом.

Химия 1,3-бифункциональных систем, IX. Реакция взаимодействия бутандиола-1,3 и его некоторых циклических производных с соляной кислотой

М. БАВТОК и МОЛНАР

Обсуждается механизм процессов и направления превращений протекающих под влиянием концентрированной соляной кислоты, а также сухого хлористого водорода на бутандиол-1,3 и его некоторые циклические производные, а именно: циклический сульфит, циклический карбонат и циклический формаль.

Перегруппировки в стероидах, VI. Сравнительное изучение реакции Шмидта для 3β-замещенных-6- и -7-кетохолестанов, а также 7-кетохолест-5-ена с перегруппировкой Бекманна для оксимов

Б. МАТКОВИЧ, Х. ТЕДЕИ, М. РЕШ, Ф. ШИРОКМАН и Е. БОГА

Были синтезированы 3β-ацетокси- и 3β-бензоилоксихолестан-6-кетоны и их оксимы. Проведя для кетонов реакцию Шмидта, а для оксимов перегруппировку Бекманна, изолировались лактамы и определялось их строение. Изучение пространственного строения оксимов позволило определить расположение гидроксильной группы оксима по сравнению к 5α—H скелета.

Также были получены оксимы 3β-ацетокси-7-кетохолест-5-ена и 3β-ацетокси-7-кетохолестана. Однако, в данном случае изомеры оксимов не удалось разделить. Как для холест-5-ена, так и для холестанового скелета были получены соответствующие лактамы с помощью реакции Шмидта для кетонов и Бекманновской перегруппировки для оксимов.

The Acta Chimica publish papers on chemistry in English, German, French and Russian.

The Acta Chimica appear in volumes consisting of four parts of varying size, 4 volumes being published a year.

Manuscripts should be addressed to

Acta Chimica
Budapest 112/91 Műegyetem

Correspondence with the editors should be sent to the same address.

The rate of subscription is $16.00 a volume.

Orders may be placed with "*Kultúra*" Foreign Trade Company for Books and Newspapers (Budapest I., Fő utca 32. Account No. 43-790-057-181) or with representatives abroad.

Les Acta Chimica paraissent en français, allemand, anglais et russe et publient des mémoires du domaine des sciences chimiques.

Les Acta Chimica sont publiés sous forme de fascicules. Quatre fascicules seront réunis en un volume (4 volumes par an).

On est prié d'envoyer les manuscrits destinés à la rédaction à l'adresse suivante:

Acta Chimica
Budapest 112/91 Műegyetem

Toute correspondance doit être envoyée à cette même adresse.

Les prix de l'abonnement est de $16.00 par volume.

On peut s'abonner à l'Entreprise pour le Commerce Extérieur de Livres et Journaux «*Kultúra*» (Budapest I., Fő utca 32. Compte-courant No. 43-790-057-181) ou à l'étranger chez tous les représentants ou dépositaires.

«*Acta Chimica*» издают трактаты из области химической науки на русском, французском, английском и немецком языках.

«*Acta Chimica*» выходят отдельными выпусками разного объема. 4 выпуска составляют один том. 4 тома публикуются в год.

Предназначенные для публикации рукописи следует направлять по адресу:

Acta Chimica
Budapest 112/91 Műegyetem

По этому же адресу направлять всякую корреспонденцию для редакции.

Подписная цена — $16.00 за том.

Заказы принимает предприятие по внешней торговле книг и газет «*Kultúra*» (Budapest I., Fő utca 32. Текущий счет № 43-790-057-181) или его заграничные представительства и уполномоченные.

Reviews of the Hungarian Academy of Sciences are obtainable at the following addresses:

ALBANIA
Drejtorija Qëndrone e Përhapjes dhe Propagandimit të Librit
Kruga Konferenca e Pazes
Tirana

AUSTRALIA
A. Keesing
Box 4886, GPO
Sydney

AUSTRIA
GLOBUS
Höchstädtplatz 3
A-1200 Wien XX

BELGIUM
Office International de Librairie
30, Avenue Marnix
Bruxelles 5
Du Monde Entier
5, Place St. Jean
Bruxelles

BULGARIA
HEMUS
11 pl Slaveikov
Sofia

CANADA
Pannonia Books
2, Spadina Road
Toronto 4, Ont.

CHINA
Waiwen Shudian
Peking
P. O. B. 88

CZECHOSLOVAKIA
Artia
Ve Směčkách 30
Praha 2
Poštovní Novinová Služba
Dovoz tisku
Vinohradská 46
Praha 2
Mad'arská Kultura
Václavské nám. 2
Praha 1
SLOVART A. G.
Gorkého
Bratislava

DENMARK
Ejnar Munksgaard
Nörregade 6
Copenhagen

FINLAND
Akateeminen Kirjakauppa
Keskuskatu 2
Helsinki

FRANCE
Office International de Documentation et Librairie
48, rue Gay Lussac
Paris 5

GERMAN DEMOCRATIC REPUBLIC
Deutscher Buch-Export und Import
Leninstraße 16
Leipzig 701
Zeitungsvertriebsamt
Fruchtstraße 3—4
1004 Berlin

GERMAN FEDERAL REPUBLIC
Kunst und Wissen
Erich Bieber
Postfach 46
7 Stuttgart S.

GREAT BRITAIN
Blackwell's Periodicals
Oxenford House
Magdalen Street
Oxford
Collet's Subscription Import Department
Dennington Estate
Wellingsborough. Northants.
Robert Maxwell and Co. Ltd.
4—5 Fitzroy Square
London W. 1

HOLLAND
Swetz and Zeitlinger
Keizersgracht 471—487
Amsterdam C.
Martinus Nijhof
Lange Voorhout 9
The Hague

INDIA
Hind Book House
66 Babar Road
New Delhi 1

ITALY
Santo Vanasia
Via M. Macchi 71
Milano
Libreria Commissionaria Sansoni
Vie La Marmora 45
Firenze

JAPAN
Kinokuniya Book-Store Co. Ltd.
826 Tsunohazu 1-chome
Shinjuku-ku
Tokyo
Maruzen and Co. Ltd.
P. O. Box 605
Tokyo-Central

KOREA
Chulpanmul
Phenjan

NORWAY
Tanum-Cammermeyer
Karl Johansgt 41—43
Oslo 1

POLAND
RUCH
ul. Wronia 23
Warszawa

ROUMANIA
Cartimex
Str. Aristide Briand 14—18
Bucureşti

SOVIET UNION
Mezhdunarodnaya Kniga
Moscow G—200

SWEDEN
Almquist and Wiksell
Gamla Brogatan 26
S—101 20 Stockholm

USA
F. W. Faxon Co. Inc.
15 Southwest Park
Westwood Mass. 02090
Stechert Hafner Inc.
31. East 10th Street
New York, N. Y. 10003

VIETNAM
Xunhasaba
19, Tran Quoc Toan
Hanoi

YUGOSLAVIA
Forum
Vojvode Mišića broj 1
Novi Sad
Jugoslovenska Knjiga
Terazije 27
Beograd

ACTA CHIMICA

ACADEMIAE SCIENTIARUM HUNGARICAE

ADIUVANTIBUS

V. BRUCKNER, GY. DEÁK, K. POLINSZKY,
E. PUNGOR, G. SCHAY, Z. G. SZABÓ

REDIGIT

B. LENGYEL

TOMUS 66 FASCICULUS 4

AKADÉMIAI KIADÓ, BUDAPEST

1970

ACTA CHIM. ACAD. SCI. HUNG.

ACTA CHIMICA

A MAGYAR TUDOMÁNYOS AKADÉMIA KÉMIAI TUDOMÁNYOK OSZTÁLYÁNAK IDEGEN NYELVŰ KÖZLEMÉNYEI

SZERKESZTI

LENGYEL BÉLA

TECHNIKAI SZERKESZTŐK

DEÁK GYULA és HARASZTHY-PAPP MELINDA

Az Acta Chimica német, angol, francia és orosz nyelven közöl értekezéseket a kémiai tudományok köréből.

Az Acta Chimica változó terjedelmű füzetekben jelenik meg, egy-egy kötet négy füzetből áll. Évente átlag négy kötet jelenik meg.

A közlésre szánt kéziratok a szerkesztőség címére (Budapest 112/91 Műegyetem) küldendők.

Ugyanerre a címre küldendő minden szerkesztőségi levelezés. A szerkesztőség kéziratokat nem ad vissza.

Megrendelhető a belföld számára az „Akadémiai Kiadó"-nál (Budapest V., Alkotmány utca 21. Bankszámla 05-915-111-46), a külföld számára pedig a „Kultúra" Könyv- és Hírlap Külkereskedelmi Vállalatnál (Budapest I., Fő utca 32. Bankszámla: 43-790-057-181) vagy annak külföldi képviseleteinél és bizományosainál.

Die Acta Chimica veröffentlichen Abhandlungen aus dem Bereiche der chemischen Wissenschaften in deutscher, englischer, französischer und russischer Sprache.

Die Acta Chimica erscheinen in Heften wechselnden Umfanges. Vier Hefte bilden einen Band. Jährlich erscheinen 4 Bände.

Die zur Veröffentlichung bestimmten Manuskripte sind an folgende Adresse zu senden:

Acta Chimica
Budapest 112/91 Műegyetem

An die gleiche Anschrift ist auch jede für die Redaktion bestimmte Korrespondenz zu richten. Abonnementspreis pro Band: $ 16.00.

Bestellbar bei dem Buch- und Zeitungs-Außenhandels-Unternehmen »*Kultúra*« (Budapest I., Fő utca 32. Bankkonto No. 43-790-057-181) oder bei seinen Auslandsvertretungen und Kommissionären.

Acta Chimica Academiae Scientiarum Hungaricae. Tomus 66 (4), pp. 349—371 (1970)

THERMOKONDENSATION VON WO_3 AUS 12-WOLFRAMATOKIESELSÄUREHYDRATEN

A. J. HEGEDŰS, P. GADÓ, G. SCHLOSSER und J. NEUGEBAUER

(TUNGSRAM Forschungslaboratorien, Grundstoffprüfung, Budapest-Ujpest)

Eingegangen am 2. Juni 1969

Es wurde erläutert warum die Hydrate der 12-Wolframatokieselsäure in verschiedenen Kristallsystemen kristallisieren, weshalb und inwiefern die Reanal- bzw. Merck-Präparate sich voneinander unterscheiden. Der Existenzbereich der bisher als 6-Hydrat bekannten kubischen Keggin-Phase der Si-Heteropolysäure erstreckt sich nur auf 100 ± 25 °C und ihre richtige Formel ist nicht $H_4[SiW_{12}O_{40}] \cdot 6\,H_2O$, sondern $H_4[SiW_{12}O_{34}(OH)_{12}]$. Die Struktur des daraus thermolytisch entstehenden $H_4[SiW_{12}O_{40}]$ weicht von der Struktur der Keggin-Phase ab und war bisher unbekannt. Die Stabilität dieser Grundsäure erstreckt sich auf $\sim$150—480 °C, doch macht sich schon oberhalb von $\sim$320 °C eine gewisse Amorphisierung bemerkbar. Beim Abkühlen wird sie mit einer vom Wasserdampfpartialdruck abhängigen Geschwindigkeit zur Keggin-Phase rehydratiert. Fehlordnung des Keggin-Anions kann die Kristallisation der Säurehydrate in verschiedenen Kristallsystemen bewirken und die Verschiebung der Menge der mit verschiedener Stärke gebundenen Wassermoleküle verursachen. Aus der Grundsäure entsteht in einem endothermen Amorphisationsvorgang und einem exothermen Kristallisationsvorgang zuerst tetragonales, dann bei höheren Temperaturen monoklines WO_3. Im Rahmen der Diskussion wurde die bisherige Literatur zusammengefaßt. Anstelle der thermischen Zersetzung der 12-Wolframatokieselsäure wurden die Vorgänge von der Seite der Entstehung des WO_3 betrachtet, weil dadurch auf den Mechanismus der Thermokondensation des WO_3 und auf den Einbau des Siliziums in das WO_3-Gitter größeres Gewicht gelegt werden konnte.

Ein wichtiger Zusatztoff der in den Glühlampen verwendeten Wolframspiralen ist das Si, das vor der Hochtemperaturreduktion mit Wasserstoff in Form von Kaliumsilikat dem Ausgangsstoff hinzugefügt wird. Dieser Ausgangsstoff ist entweder ein bei 300 °C dehydratiertes $(WO_3 \cdot nH_2O)_x$ oder ein Zwischenprodukt des in N_2+H_2-Atmosphäre thermisch teilweise zersetzten und reduzierten $(NH_4)_{10}[W_{12}O_{36}(OH)_{10}]$ Ammoniumparawolframats. Hinsichtlich einer allgemeineren Kenntnis des Einbaumechanismus der Zusatzstoffe und der Verunreinigungen ist also die Erforschung des thermischen Verhaltens der früher Silikowolframsäure genannten und ein zentrales Si-Atom enthaltenden 12-Wolframatosilikoheteropolysäure bzw. ihrer Hydrate sehr wichtig.

Die Struktur und die thermische Dissoziation der Wolframatokieselsäure wurde bereits durch viele Forscher untersucht. Auf ihre Ergebnisse werden wir später noch ausführlich zurückkommen. Da jedoch die Literaturangaben nicht eindeutig sind und vom Vorleben der angewendeten Präparate abhängig zu sein scheinen, führten auch wir die Untersuchung der bei uns zugänglichen

Tabelle I

Auswertung der Thermokurven

Nr.	Herkunft der Probe	Gravimetrische Angaben in mg and die daraus berechnete Zahl der H_2O-Moleküle in mol/mol								Temperatur, °C der Inflexionen		
		Einwaage	1. Inflexion	2. Inflexion	Auswaage	$n_2 + n_1 + n$	$n_1 + n$	n	$(n_1 + n)/n$	1	2	3
1	Merck	1429,4	1331,2	1288,2	1274,6	19,2	7,01	1,68	4,16	125	325	550
2	Merck	1425,5	1327,5	1286,2	1272,8	18,9	6,78	1,66	4,08	130	330	550
3	Merck	957,0	892,5	864,3	855,5	18,7	6,83	1,62	4,20	115	330	540
4	Merck	1245,6	1168,0	1130,0	1118,7	17,9	6,95	1,68	4,14	115	330	540
5	Merck	—	1199,9	1159,7	1147,2	—	7,25	1,72	4,22	—	325	550
6	Reanal	1462,3	1331,2	1286,3	1271,3	23,7	7,43	1,86	3,99	130	300	545
7	Reanal	3455,1	3175,0	3060,0	3020,0	22,7	8,10	2,09	3,88	160	360	530
8	Reanal	3370,0	3090,0	2975,0	2935,0	23,4	8,33	2,15	3,87	185	380	560
9	Reanal	1203,3	1095,3	1058,2	1045,3	23,9	7,55	1,95	3,88	—	300	545
10	Reanal	1200,3	1095,9	1057,9	1045,2	23,4	7,66	1,92	3,99	120	300	540
11	Reanal	—	1167,4	1125,9	1113,0	—	7,71	1,83	4,22	—	300	550
12	Reanal	2444,0	2313,4	2233,5	2208,2	16,9	7,52	1,81	4,08	130	330	545
13	Reanal	1159,7	1155,6	1116,7	1103,7	7,98	7,39	1,83	4,04	120	310	540
14	Reanal	1608,5	1531,4	1480,7	1464,9	15,5	7,19	1,72	4,17	135	330	545

Bemerkungen: *Probe* **5** und **11** wurden vorher 5 Stunden lang bei 80 °C getrocknet und dann 20 Stunden lang stehen gelassen, *Probe* **12** wurde ähnlich behandelt jedoch 5 Stunden lang bei 100 °C getrocknet und 7 Tage stehen gelassen. *Probe* **13** 5 Stunden bei 120 °C getrocknet, 20 Stunden gelagert. *Probe* **14** wurde durch Umkristallisierung in Wasser auf dem Wasserbad erhalten.

$SiO_2 \cdot 12WO_3 \cdot 26H_2O$ p.a. (Reanal, Budapest) und $SiO_2 \cdot 12WO_3 \cdot xH_2O$ (Merck, Prod. Nr. 916489) Präparate durch, in erster Reihe mit thermo- und röntgenanalytischen Methoden.

Versuchsergebnisse

Die GTA-Ergebnisse der mit beiden Präparaten öfter wiederholten Messungen sind in Tab. 1 zusammengefaßt. Eine der voneinander kaum abweichenden, mit der Chevenardschen Thermowaage erhaltenen Kurven ist in Abb. 1, eine der mit dem Derivatograph von Paulik—Paulik—Erdey erhaltenen in Abb. 2 wiedergegeben.

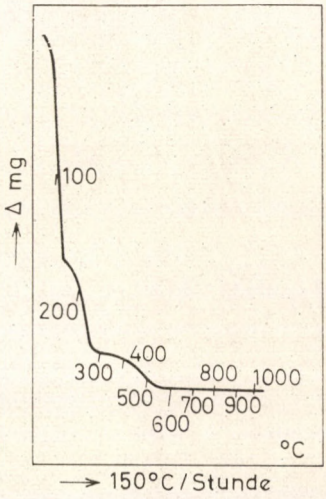

Abb. 1. Thermogramm des 12-Wolframatokieselsäurehydrats

Aufgrund der Thermogramme können drei, mit verschiedener Stärke gebundene H_2O-Arten unterschieden werden. Bei einer Heizgeschwindigkeit von 150 °C/Stunde wird das am schwächsten gebundene Wasser (n_2) bis ~125 °C, das mittelmäßig stark gebundene (n_1) zwischen 125—315 °C und das am stärksten gebundene (n) zwischen 320—545 °C abgespalten. Auf den mit 600 °C/Stunde aufgenommenen Derivatogrammen gehören zu diesen thermischen Dissoziationsvorgängen endotherme Spitzen mit Minima bei 180, 330 und ~540 °C. Die DTA-Kurve des Reanal-Präparates weist mit der Inflexion bei ~110 °C auch auf die Abspaltung von noch lockerer gebundenem Wasser (n_3) hin. Auf diesen Aufnahmen sind auch exotherme Spitzen mit Maxima bei 590 und 890 °C zu sehen, von denen die Erstere die endotherme Spitze bei 540 °C teilweise überdeckt.

Die wäßrige Lösung des Reanal-Präparates war opalisierend, die des Merck-Präparates klar. In Gegenwart von Methylrot ergab das Reanal-Präparat, auf 1 g $H_4[Si(W_{12}O_{40})]$ berechnet, einen Verbrauch von 13,6 ml 0,1 *n* NaOH. Während der Verbrauch beim anderen Präparat 11,5 ml betrug.

Der Si-Gehalt wurde kolorimetrisch [1] bzw. nach Abtreiben mit CCl_4 [2] und Abrauchen mit HF gravimetrisch bestimmt, wobei folgende Ergebnisse erhalten wurden:

	Reanal	Merck
g SiO_2/g $SiO_2 + WO_3$ kolorimetrsch	0,0209	0,0179
g/g Rückstand beim Abtreiben mit CCl_4	0,0285	0,0378
g/g Rückstand beim Abrauchen mit $HF + H_2SO_4$	0,0071	0,0184
g SiO_2/g $SiO_2 + WO_3$ gravimetrisch	0,0214	0,0194

Die Ergebnisse der Spektralanalysen nach Entwässerung bei 600 °C sind in Tab. II enthalten. Die in der Tabelle nicht angeführten verunreinigenden Elemente waren entweder in beiden Präparaten in gleichen Mengen vorhanden oder ihre Menge blieb unterhalb der Nachweisgrenze.

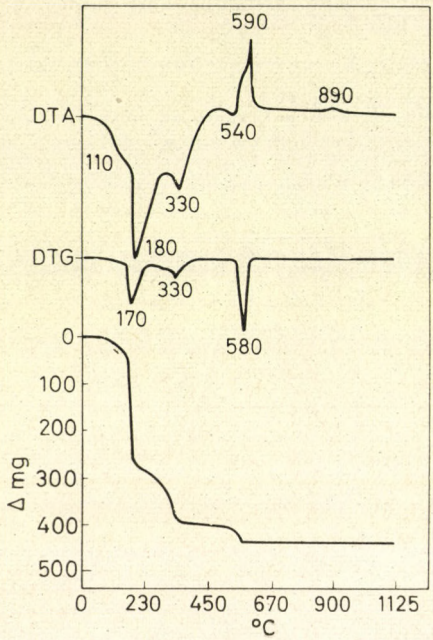

Abb. 2. Derivatogramm des 12-Wolframatokieselsäurehydrats bei einer Heizgeschwindigkeit von 600 °C/Stunde

Tabelle II

Quantitative und vergleichende qualitative Spektralanalysen

Element		Reanal	Merck
Al	Gew.%	$5{,}6 \cdot 10^{-4}$	$23 \cdot 10^{-4}$
Ca	Gew.%	$5{,}5 \cdot 10^{-4}$	$22 \cdot 10^{-4}$
Fe	Gew.%	$20 \cdot 10^{-4}$	$23 \cdot 10^{-4}$
Ba	relative Einheiten, nur für ein und dasselbe Element vergleichbar	Spuren	2
Be	relative Einheiten, nur für ein und dasselbe Element vergleichbar	—	2,5
Cu	relative Einheiten, nur für ein und dasselbe Element vergleichbar	Spuren	1
Mg	relative Einheiten, nur für ein und dasselbe Element vergleichbar	1	2,5
Mn	relative Einheiten, nur für ein und dasselbe Element vergleichbar	Spuren	2,5
Mo	relative Einheiten, nur für ein und dasselbe Element vergleichbar	2	—
Na	relative Einheiten, nur für ein und dasselbe Element vergleichbar	2	3,5
Sr	relative Einheiten, nur für ein und dasselbe Element vergleichbar	—	1,5

Mit Hilfe der Thermowaage wurden intermediäre Präparate bei den in Abb. 1 angegebenen Temperaturen von 130 und 330 °C hergestellt und mit den Ausgangsstoffen zusammen röntgenanalytisch untersucht. Die linienreichen Röntgenspektren der sechs Proben zeigten keine wesentlichen Strukturunterschiede. Es konnte festgestellt werden, daß die Ursache hierfür darin lag, daß sämtliche Proben vor der Röntgenaufnahme einige Tage lang im selben Raum, bei ~25 °C und in Normalatmosphäre aufbewahrt wurden. Während dieser Zeit egalisierte sich nämlich der H_2O-Gehalt bei jeder Probe zu 12—18 $H_2O/SiO_2 \cdot 12\ WO_3$. Die teilweise dehydratierten Präparate hydratierten sich (Tab. I, Probe 12), beim Reanal-Ausgangsstoff erfolgte eine Wasserabgabe, die durch das Verreiben vor der Röntgenaufnahme wahrscheinlich noch verstärkt wurde, so daß der Wassergehalt sämtlicher Proben dem H_2O-Gehalt des Merck-Präparates ähnlich wurde.

Diese reversible Wasserabgabe und Wasseraufnahme wird durch die Thermokurven des Reanal-Präparates in Abb. 3 veranschaulicht. Die bis 330 °C, d. h. bis zur Säure ($n = 2\ H_2O$) dehydratierte Probe nahm bei Raumtemperatur im Laufe von zwei Tagen ~10 H_2O auf, die etwas lockerer gebunden wurden als die ursprünglich außer den beiden Säurewassermolekülen vorhandenen 23—24 H_2O-Moleküle. Nach Dehydratierung bis 540—550 °C, also bis zum Säureanhydrid wurden innerhalb drei bzw. vier Tagen 2 H_2O aufgenommen was zwar stöchiometrisch der Grundsäure entsprach, aber die Bindung blieb in diesem Fall viel schwächer (Kurve *a* und *b* in Abb. 3). Die bei 600 °C dehydratierte Probe erwies sich im Laufe von vier Tagen als kaum mehr hygroskopisch (Kurve *c* in Abb. 3).

Nach mehr als einem Jahr wiederholten wir die Dehydratierungen derart, daß beide Ausgangsstoffe bei 100, 290 und 500 °C in gleicher Weise wärmebehandelt wurden (Aufheizung + 30 Minuten). Danach folgte eine kurze schonend ausgeführte Zerreibung und sofort die Röntgenaufnahme bei Zimmertemperatur. Die Aufnahmen der Ausgangsstoffe ergaben zwar wieder linienreiche Diffraktionsspektren, die sich jedoch jetzt untereinander gering, aber ausgesprochen und von den früheren Röntgendiagrammen der Ausgangsstoffe wesentlich unterschieden. Es sah so aus, als ob auf der neuen Aufnahme des Reanal-Präparates die Linien der früheren Kristallphase nur als die Linien einer verunreinigenden Komponente vorhanden wären.

Nach der Behandlung bei 100° und Abkühlen vergrößerte sich der Strukturunterschied zwischen den beiden Präparaten. Das Reanal-Präparat zeigte die bekannte kubische Keggin-Struktur ($a = \sim 12{,}10$ Å) [3, 4], mit wenig Ausgangsstoff gemischt, wobei letzterer in struktureller Hinsicht gewissermaßen dem früher untersuchten Reanal-Präparat ähnlich war. Das Merck-Präparat bestand nach dieser Vorbehandlung noch nicht aus der Keggin-Phase, nur die Ausgangskristallstruktur wurde etwas verändert, wodurch sie sich jener Struktur annäherte, welche beide Ausgangsstoffe ein Jahr früher — voneinander praktisch nicht unterscheidbar — besaßen. Nach zweiwöchiger Lagerung an der Luft bei Raumtemperatur verwandelte sich jedoch auch das Merck-Präparat in die scharfe Diffraktionslinien aufweisende Keggin-Phase mit ungefähr 13—16 H_2O.

Das bei 290 °C dehydratierte Reanal-Präparat hatte eine reine, aber ungeordnete Keggin-Struktur, während das Merck-Präparat neben der Keggin-Phase auch mit der nach der Behandlung bei 100 °C entstandenen Kristallmodifikation verunreinigt war.

Nach Erhitzung bis 500 °C lag bereits bei beiden Proben eine gleiche Kristallstruktur mit tetragonaler Symmetrie vor. Die Gitterparameter waren $a = 5{,}28$ Å und $c = 3{,}82$ Å, ebenso wie bei den früheren Untersuchungen, als die Säure bis 540 °C erhitzt wurde. Diese Phase, welche in Zusammenhang mit der $WO_3 \cdot SiO_2$ festen Lösung zuerst von BABAD-ZACHRJAPIN [5] beschrieben wurde, ist strukturell mit der bekannten, über 740 °C stabilen Kristallmodifikation des WO_3 [6] identisch.

Die mit einer Heizgeschwindigkeit von 150 °C/Stunde in Luft bis auf 600 °C erhitzten Proben ergaben ebenfalls identische Röntgenaufnahmen. Diese konnten mit der bei Zimmertemperatur stabilen monoklinen Modifikation des WO_3 identifiziert werden. Das gleiche ergab sich bei den bis auf 1000 °C geglühten Proben, doch waren die Interferenzlinien im letzteren Fall wesentlich schärfer.

Wurde der thermische Abbau der Wolframatokieselsäurehydrate anstelle von Luft in reinem Stickstoff durchgeführt, so ergab sich bei den bis 600 °C oder darüber erhitzten Proben statt der monoklinen Form eine orthorhombische WO_3-Struktur, mit folgenden Gitterparametern:

$$a = 7{,}32\ \text{Å}, \qquad b = 7{,}50\ \text{Å}, \qquad c = 3{,}85\ \text{Å}.$$

Aufnahmen mit dem Hochtemperaturdiffraktometer in Luft, wobei die Temperatur in 50 °C-Etappen gesteigert wurde, bewiesen, daß sich die Reanal-Säure, die bei Zimmertemperatur ein linienreiches Diffraktogramm lieferte, bei 100 °C in eine hochgeordnete, scharfe

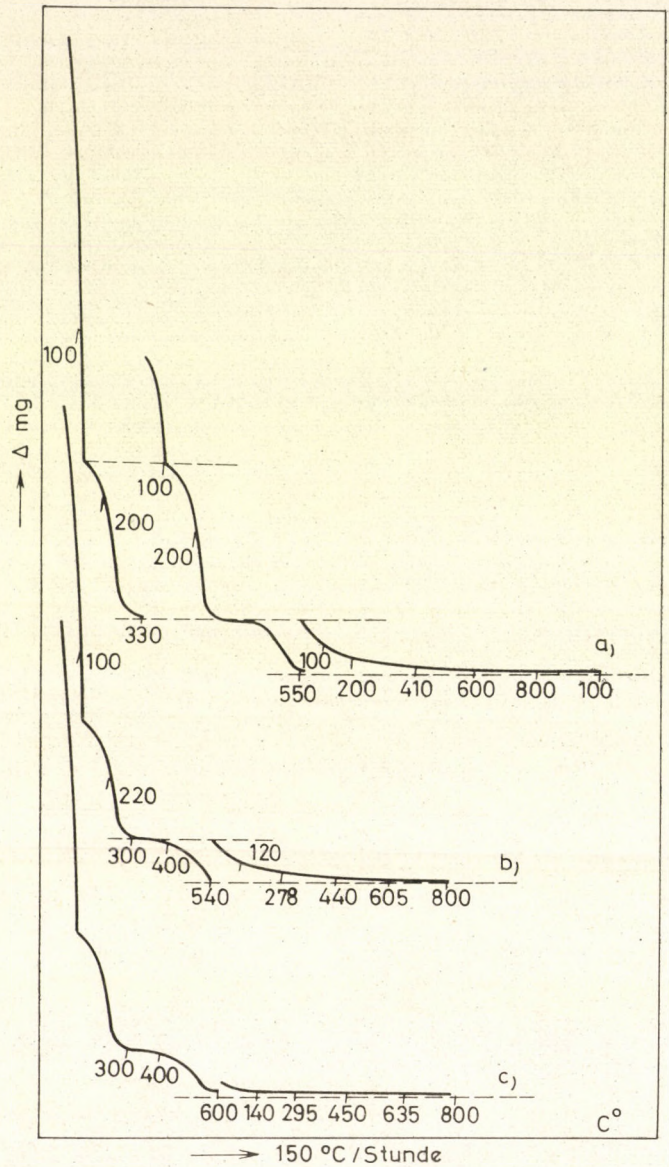

Abb. 3. Dehydratierungs- und Rehydratierungsthermogramme des 12-Wolframatokieselsäurehydrats in Luft (Erklärung im Text)

Linien liefernde, zeitlich stabile kubische Keggin-Phase umwandelt. Die weitere Steigerung der Temperatur führt bei ungefähr 200 °C zum Verschwinden der kubischen Keggin-Struktur und es erscheinen nur einige schwache, sehr breite (Halbwertbreite $\sim 1°$), auf die Gegenwart einer ungeordneten kristallinen Phase hinweisende Diffraktionslinien, in einer wesentlich stärker gewordenen Untergrundstrahlung. Die d-Werte der bei 300 °C gemessenen bezeichnendsten Linien dieser neuen Phase und ihre visuell geschätzten Intensitäten sind in Tab. III angegeben. Dieses Diffraktionsbild bleibt mit geringen Abweichungen bis ungefähr 450—480 °C

bestehen d. h. bis zum Erscheinen der bereits erwähnten 12 $WO_3 \cdot SiO_2$festen Lösung mit tetragonaler Symmetrie.

Wenn man die neue Hochtemperaturphase von 400, 300 oder 200 °C abkühlte, so erschien erst nach längerem Stehen die Keggin-Phase, aber nie in einer so geordneten Form wie bei 100 °C. Die hochgeordnete Keggin-Struktur läßt sich durch langsames (~30 °C/Stunde) Abkühlen von 100 °C gewissermaßen bewahren, bei etwa 40 °C bemerkt man jedoch auch in diesem Fall eine wesentliche Abnahme der Intensität und die Verschwärzung des Untergrundes, was auf Erhöhung der Kristallfehlstellen, auf die Änderung der Kristallstruktur hindeutet. Dieser Vorgang konnte selbst durch 90stündiges Lagern an der Luft bei Zimmertemperatur nicht verändert werden. Wenn die Probe in einer Minute rasch von 100 °C abgekühlt wurde, so verschwand die kubische Struktur vorübergehend fast vollständig und sie erschien nur nach 20—30stündigem Stehen wieder, aber auch dann nur in einer ungeordneten Form.

Tabelle III

Auswertung des Röntgendiffraktionsspektrums der 12-Wolframatokieselsäure bei 200—400 °C

d Å	I_{rel}
4,71	mittelmäßig
3,77	schwach
3,60	stark
3,48	mittelmäßig
3,40	mittelmäßig
3,26	mittelmäßig
3,00	stark
2,69	mittelmäßig
2,56	stark
2,45	mittelmäßig

Auswertung und Abstimmung mit den bisherigen Literaturergebnissen

Bekanntlich wurde die Silikowolframsäure vor mehr als einem Jahrhundert durch MARIGNAC [7, 8] hergestellt und ihre Zusammensetzung als $SiO_2 \cdot 12WO_3 \cdot 26H_2O$ angegeben. Er unterschied davon ausdrücklich die Wolframsilikosäure $SiO_2 \cdot 12WO_3 \cdot 32H_2O$ und die Silikodeciwolframsäure $SiO_2 .10WO_3 .7H_2O$.

Ihre erste Formel erhielt sie durch die Auswirkung der Werner-Pfeifferschen Koordinationstheorie [9, 10] aufgrund der $P_2O_7^{2-}$, $Cr_2O_7^{2-}$ Pyrosäureanalogie [11] von MIOLATI [12], bzw. ROSENHEIM [13]. Sie gaben, von der Annahme eines zentralen Si-Atoms mit der Koordinationszahl 6 ausgehend, eine allgemeine Formel für die Heteropolysäuren an $H_{12-m}[X(Me_2O_7)_6] \cdot nH_2O$, wo X das Heteroatom (Si, P, B, usw.), m die Wertigkeit des Heteroatoms, *Me*

das Metall der zum Heteroatom koordinierten Liganden (W, Mo, usw.) und n die Zahl der Kristallwassermoleküle ist. Demgemäß ist die Formel der Silikoheteropolysäure $H_8[Si(W_2O_7)_6]\cdot nH_2O$ und da sie auf die hypothetische Hexaoxokieselsäure H_8SiO_6 zurückführbar ist, wurde sie nicht als Silikowolframsäure, sondern als Wolframatokieselsäure benannt. Die Benennung der Marignac-Säuren lautet also: 12-Wolframatokieselsäure-22-hydrat, -28-hydrat und 10-Wolframatokieselsäure-3-hydrat.

Basizitäts-[8—11], [14—16] und thermoanalytische [8, 11, 17, 18] Untersuchungen untergruben inzwischen die auf ein zentrales Heteroatom mit der Koordinationszahl 6 aufgebaute Konzeption und Formel von MIOLATI und ROSENHEIM beträchtlich, zumindest im Falle der zur Familie der Metawolframate [24, 25] gehörenden Wolframatokieselsäure, und Röntgenuntersuchungen [4, 17, 19—23] stürtzten sie dann endgültig. Anders ist die Lage bei den Parawolframaten [24, 25], wo das $[W_{12}O_{36}(OH)_{10}]^{10-}$ Polyanion noch vor kurzem aufgrund röntgenanalytischer Angaben als $W_{12}O_{46}^{20-}$ [26], aufgrund von chemisch-analytischen Angaben hingegen als $W_{12}O_{41}^{10-}\cdot 5H_2O$ geschrieben wurde und neuestens von LIPSCOMB [27] genau so wie von MIOLATI—ROSENHEIM als $W_{12}O_{42}^{12-}$ angegeben wird. Im Käfiggitter des Parawolframatanions ist der durch den in der Mitte befindlichen Polyeder gebildete Hohlraum größer als beim Metawolframatanion, so daß darin ein größeres Metallion (Ce, Th usw.), oder mehrere kleinere Metallionen (2 Co usw.) Platz haben, mit einer Koordinationszahl von insgesamt 6. Die Metawolframatokieselsäure und die Metawolframsäure wurde bereits hergestellt, die Parawolframatokieselsäure und die Parawolframsäure dagegen noch nicht.

Kurz nach der Entdeckung der Strukturuntersuchung mit Hilfe von Röntgenstrahlen nahm PAULING [19], aus den Ergebnissen der röntgenanalytischen Untersuchungen der Silikate ausgehend an, daß auch bei der 12-Wolframatokieselsäure ein zentrales SiO_4-Tetraeder vorliegt, welches von einer Hülle aus WO_6-Oktaedern umgeben wird, wobei diese WO_6-Oktaeder nur mit den Ecken miteinander verbunden sind und gegenüber den Spitzen des SiO_4-Tetraeders, infolge der Wirkung des Kraftfeldes des zentralen Si-Atoms, zu $W_3O_{13,5}^{9-}$ Polyliganden aus je 3—3 WO_6-Oktaedern verdichtet werden. Im Falle des 18-Hydrats besetzte PAULING die freigebliebenen 4×9 Spitzen mit OH-Gruppen und gab somit die Formel $H_4[SiO_4(W_{12}O_{18}/OH/_{36})]$ an. Die wesentlichen neuen Züge dieser Konzeption kann man folgenderweise zusammenfassen:

1. Ein zentraler SiO_4-Tetraeder mit zentralem Si-Atom, das die Koordinationszahl 4 besitzt, womit die Struktur der Heteropolysäure auf die bekannte H_4SiO_4 Ortho- oder Hexaoxokieselsäure zurückgeführt werden kann.

2. Die WO_6-Oktaeder und ein aus diesen gebildeter Käfig, bei welchem die WO_6-Oktaeder gegenüber den Spitzen des zentralen Tetraeders verdichtet sind.

3. Die Anwesenheit von OH-Gruppen.

4. Die Tatsache, daß die Grundsäure problemfrei hergestellt werden kann [28, 29].

Die Röntgenuntersuchungen von KEGGIN [4] führten zu der seitdem mehrfach bestätigten und heute noch gültigen Kristallstruktur des 12-Wolframatophosphorsäure-5-hydrats. Die Hypothese von PAULING [19] mußte nur insofern modifiziert werden, daß die WO_6-Oktaeder sich in den Liganden nicht mit den Spitzen, sondern mit den Kanten berühren, also noch enger gepackt sind, und $W_3O_{10}^{2-}$-Liganden bilden. Kurz danach stellten KEGGIN [20], sowie BRADLEY und ILLINGWORTH [21] fest, daß das Anion des 12-Wolframatophosphorsäure-19-hydrats dieselbe Kristallstruktur besitzt, nur ist bei dieser die Kantenlänge der kubischen Zelle nicht 12,4 Å, sondern 23,28 Å. Vor kurzem wurde die Gegenwart des Keggin-Anions auch in wäßriger Lösung (d.h. $n_2 = \infty H_2O$) nachgewiesen [22]. Fernerhin konnten SIGNER und GROSS [23] zeigen, daß die 5-6-Hydrate der 12-Wolframatophosphorsäure, -kieselsäure, -borsäure und der Metaisowolframsäure isomorph sind. Aufgrund dieser Ergebnisse kann das Anion der Metawolframate mit der allgemeinen Formel

$$[X^{m+}(W_3O_{10})_4]^{(8-m)-} \qquad (1)$$

beschrieben werden, wo X bei Heteropolysäuren und ihrer Salze das zentrale Heteroatom (P^V, As^V, Si^{IV}, Ge^{IV}, Sn^{IV}, Ti^{IV}, Zr^{IV} usw.) ist, bei der Metaisopolysäure und ihrer Salze gegebenenfalls Protonen bedeutet und m die Wertigkeit des Heteroatoms ist.

Dem Wassergehalt nach wurden bis jetzt sehr viele (etwa 18) Wolframatokieselsäurehydrate hergestellt und untersucht [30], jedoch nur vier sind davon kristallographisch anerkannt [9, 31]. p_{H_2O} vs. $Mol_{H_2O}/Mol_{SiW_{12}O_{38}}$ Gleichgewichtsdiagramme von verschiedenen Hydraten wurden bei 18 °C von RODE [18] aufgenommen. Seine Diagramme deuten auf die Existenz von 5 Hydraten hin. Die bisher anerkannten Hydrate sind in Tab. IV zusammengefaßt.

Das trigonale Hydrat wandelt sich in wäßriger Lösung beim Erhitzen unter Druck auf 150 °C in das tetragonale Hydrat [11, 32] um, welches eine metastabile polymorphe (?), mit dem 12-Wolframatophosphorsäure-29-hydrat isomorphe kubische Modifikation besitzt. Die an der Luft bei 100 °C ($n_1 + n = 8$), bzw. 220 °C ($n = 2$) getrockneten Säurehydrate haben bei Zimmertemperatur identische Röntgendiffraktionsspektren [17], deshalb wurde bis jetzt ziemlich allgemein angenommen, daß auch die Grundsäure $H_4[SiW_{12}O_{40}]$ eine kubische Keggin-Struktur besitzt.

Isotopenprüfungen [33] bestätigen fernerhin, daß die n_2-Wassermoleküle ziemlich mobil sind und daß in der Bindungsstärke kein Unterschied zwischen ihnen besteht.

Tabelle IV

Durch kristallographische [31] *und thermodynamische* [18] *Messungen unterstützte Hydrate der 12-Wolframatokieselsäure*

Röntgenanalyse			Bestimmung des chemischen Gleichgewichtes	
$n_2 = 24$	tetragonal	$H_{64}SiW_{12}O_{70}$	$n_2 = 25$	$H_{66}SiW_{12}O_{71}$
$n_2 = 18$	trigonal	$H_{52}SiW_{12}O_{64}$	$n_2 = 18$	$H_{52}SiW_{12}O_{64}$
			$n_2 = 11$	$H_{38}SiW_{12}O_{57}$
$n_2 = 8$	triklin	$H_{32}SiW_{12}O_{54}$	$n_2 = 8$	$H_{32}SiW_{12}O_{54}$
$n_1 = 6$	kubisch	$H_{16}SiW_{12}O_{46}$	$n_1 = 6$	$H_{16}SiW_{12}O_{46}$

Anmerkung: Der $n_1 = 5$-Wert von JAHR [9] und KRAUS [31] ist offensichtlich unrichtig' deshalb korrigierten wir auf $n_1 = 6$.

Die eventuell bestehende abweichende Bindungsstärke von n_2-Kristallwassermolekeln könnte mit thermoanalytischen Untersuchungen bei verschiedenen Wasserdampfdrucken ausfindig gemacht werden. RODE [18] gab aufgrund von Messungen in Normalatmosphäre folgende Zersetzungsstufen für das $n_2 = 25$ Hydrat an:

40— 44 °C Schmelzen des $H_{66}SiW_{12}O_{71}$, Bildung von $H_{52}SiW_{12}O_{64}$, endotherme Dehydratierung, Umkristallisation;
44— 50 °C Bildung von $H_{38}SiW_{12}O_{57}$, endotherme Dehydratierung, Umkristallisation;
74— 76 °C Schmelzen und Bildung einer Lösung;
108—115 °C Ausscheiden von $H_{32}SiW_{12}O_{54}$, endotherme Dehydratierung, Kristallisation;
115—148 °C Bildung von $H_{16}SiW_{12}O_{46}$, endotherme Dehydratierung, Umkristallisation;
178—248 °C Bildung von $H_4SiW_{12}O_{40}$, endotherme Dehydratierung ohne Strukturänderung;
400—478 °C Dehydratierung, endotherme Zersetzung zu amorphem WO_3;
505—530 °C exotherme Kristallisation des WO_3;
710—895 °C polymorphe Umwandlungen des WO_3.

Bis zur Amorphisation ist die Dehydratierung reversibel; oberhalb von 400 °C spielen sich jedoch irreversible Vorgänge ab. Die Thermoanalyse der bei Raumtemperatur in Vakuumexsikkator über Schwefelsäure (10^{-3}—$5 \cdot 10^{-4}$

Torr p_{H_2O}) getrockneten Wolframatokieselsäure wies eine endotherme Spitze bei 140—280 °C und eine exotherme Spitze bei 470—500 °C auf, während sie unter gleichen Umständen, aber bei 300 °C getrocknet nur eine exotherme Spitze bei 490—510 °C zeigte. Vor dem exothermen Vorgang waren beide Proben farblos und hatten die gleiche Röntgenstruktur, während sie nach dem exothermen Vorgang gelb waren und die Struktur des WO_3 besaßen [34].

In Laufe unserer Messungen konnten gravimetrisch nie ganzzahlige Werte für das Molverhältnis $H_2O/SiW_{12}O_{38}$ erhalten werden, und der H_2O-Gehalt von zwei 12-Wolframatokieselsäuren verschiedener Herkunft zeigte sowohl vor, als auch nach einem De- und Rehydratierungsvorgang bedeutende Unterschiede. Die gemessenen Durchschnittswerte sowie die theoretischen Werte von n, n_1 und n_2 sind in Tab. V zusammengefaßt. Unabhängig davon, welches Präparat reversibel dehydratiert wurde, lief die Rehydratierung immer bis $n_2 = 8$.

Tabelle V

Vergleich der aus den Meßdaten in Tabelle I berechneten durchschnittlichen und der theoretischen n-Werte

	Reanal	Reanal wärmebehandelt	Merck	theoretisch
n_2	15,6	8,9	11,8	24 20 16 12 8
n_1	5,28	5,66	5,29	6
n	1,99	1,80	1,67	2
$(n_1 + n)/n$	3,92	4,13	4,16	4

Die Untersuchungen bewiesen, daß nicht nur die Zusammensetzung des Reanal-Präparats, der rehydratierten Proben und des Merck-Präparats verschieden sind, sondern auch ihre ungeordneten, linienreiche Röntgendiffraktiogramme liefernden Kristallgitter. Da aber die exakte kristallographische Identifizierung dieser Gitter nicht das Ziel unserer Arbeit war, begnügten wir uns mit der Feststellung, daß das Keggin-Anion in allen Kristallarten der 12-Wolframatokieselsäurehydrate anwesend ist und nur das Kristallsystem oder die Kristallklasse dieser Hydrate mehr oder weniger voneinander abweicht, während mit der Änderung des Wassergehalts nur die Si-Si-Abstände verändert werden.

Gemäß der n-Werte in Tab. V kann die thermische Zersetzung des Reanal-Präparats (Tab. I, Proben 6—10) mit der folgenden schematisierten

Bruttogleichung beschrieben werden:

$$H_{46,82}SiW_{12}O_{61,01} \rightarrow H_{15,62}SiW_{12}O_{45,81} \rightarrow H_{3,98}SiW_{12}O_{39,99} \rightarrow SiW_{12}O_{38} \,. \quad (2)$$

Die Abweichung von der theoretischen

$$H_{48}SiW_{12}O_{62} \rightarrow H_{16}SiW_{12}O_{46} \rightarrow H_4SiW_{12}O_{40} \rightarrow SiW_{12}O_{38} \quad (3)$$

Gleichung ist minimal und kann sowohl auf Gitterfehler und H_2O-Defizit, als auch in geringerem Maße auf die Ungenauigkeiten der thermogravimetrischen Messungen und ihrer Auswertung zurückgeführt werden.

Dies ist jedoch für das Merck-Präparat nicht der Fall (Tab I, Proben 1—4), da die Zersetzungsreihe

$$H_{37,52}SiW_{12}O_{56,76} \rightarrow H_{13,92}SiH_{12}O_{44,96} \rightarrow H_{3,34}SiW_{12}O_{39,67} \rightarrow SiW_{12}O_{38} \quad (4)$$

in diesem Fall wesentlich von der Theorie (Gleichung 3) abweicht. Halten wir nach Tab. V die Zusammensetzung $n_2 = 12$ für richtig, so ergibt sich eine andere theoretische Gleichungsreihe

$$H_{40}SiW_{12}O_{58} \rightarrow H_{16}SiW_{12}O_{46} \rightarrow H_4SiW_{12}O_{40} \rightarrow SiW_{12}O_{38} \quad (5)$$

mit welcher der Vergleich — abgesehen von den Wasserstoffatomen der Grundsäure — wesentlich günstiger wird.

Zur Klärung dieser letzten Abweichung von der Theorie wurde die im experimentellen Teil beschriebene nicht absolute Titration durchgeführt, wobei sich für die Merck-Säure $H_{3,39}$ ergab, wenn für die Reanal-Säure der in Gl. 3 verwendete und mit den Meßergebnissen in Einklang stehende Wasserstoffindex 4 angenommen wurde. Aus der guten Übereinstimmung folgt noch sozusagen selbstverständlich die Kontrolle der Si-Indexe, weil die betreffenden Wasserstoffatome vom Si koordiniert werden. Die Si-Bestimmungen führten beim Reanal-Präparat zu $Si_{1,00}$, beim Merck-Präparat zu $Si_{0,88}$. Diese Werte sind ebenfalls in guter Übereinstimmung mit den thermogravimetrischen Messungen. Wenn wir also die thermogravimetrisch gewonnenen Werte für n beibehalten, so muß für die thermische Zersetzung des Merck-Präparates die Bruttogleichung

$$\begin{aligned} H_{37,52}Si_{0,835}W_{12}O_{56,43} &\rightarrow H_{13,92}Si_{0,835}W_{12}O_{44,63} \rightarrow \\ &\rightarrow H_{3,34}Si_{0,835}W_{12}O_{39,34} \rightarrow Si_{0,835}W_{12}O_{37,67} \end{aligned} \quad (6)$$

als gültig angenommen werden. Daraus ergeben sich, auf $Si_{1,00}$ zurückgerechnet die Indexe $H_{44,93}$, $H_{16,67}$ und H_4, wodurch die Annäherung an die theoretische Gleichung (3) bereits befriedigend wird.

Demnach müßte das Merck-Präparat ebenfalls eine $H_{48}SiW_{12}O_{62}$-Säure mit H_2O-Defizit sein, die aber wahrscheinlich auch solche Heteroanionen enthält, in denen der WO_6-Oktaederkäfig leer geblieben ist (wie z. B. beim Anion der Metawolframsäure), oder in denen fremde, andersartig oder überhaupt nicht koordinierende zentrale Heteroatome (eventuell mehrere) im WO_6-Oktaederkäfig drinnensitzen. Um diese letztere Annahme zu bekräftigen, wurden die Proben spektralanalytisch untersucht. Die erhaltenen Werte in Tab. II beweisen eindeutig, daß mit einem solchen Fremdstoffeffekt gerechnet werden kann. Die größte Abweichung zeigt sich beim Na, weil bei der verwendeten Spektralmethode der Nachweis von Na am wenigsten empfindlich ist.

Die Zahlen in Tab. I, besonders die zusammengeklammerten praktisch konstanten Werte von $(n_1 + n)/n$ verraten, daß $n + n_1$ unabhängig vom absoluten Wert von n und n_1 konsequent viermal so groß wie n ist. Zu den am stärksten gebundenen Säurewassermolekeln werden also stets dreimal soviel, mittelstark gebundene H_2O-Wassermoleküle koordiniert. Außer der Möglichkeit also, daß bei der Herstellung nicht ein jedes Keggin-Anion von einem zentralen Si-Atom besetzt, oder daß das Si-Atom aus irgendeinem Grunde aus seiner zentralen Lage verdrängt und entfernt wird, kann auch jener Fall vorkommen, daß ein Teil des Si abhydrolysiert (z. B. opalisierende Lösung, Erwärmung, usw.), oder aus irgendeinem anderen Grund seine komplexbildende bzw. koordinierende Fähigkeit verliert, ohne dabei entfernt zu werden. In diesem Fall ergibt sich zwar ein richtiges Si : W Verhältnis, der $(n + n_1)/n$ Wert bleibt auch unverändert, aber der Säurewasserstoffindex nimmt ab, d.h. die thermoanalytischen Eigenschaften der Säure, nähern sich den thermoanalytischen Eigenschaften einer solchen Säure die über ein von 1 : 12 abweichendes Si : W-Verhältnis verfügt (Tab. I, Probe 11—14). Diese Annahme scheint auch jene Tatsache zu unterstützen, daß das Röntgenspektrum des Reanal-Präparates nach der thermischen Behandlung und Rehydratierung praktisch identisch mit dem Diffraktogramm des dehydratierten und rehydratierten Merck-Präparates wurde, und daß die Wärmebehandlung des Merck-Präparates bei 80 °C keine thermoanalytisch erfaßbare Änderung mit sich brachte (Tab. I, Probe 5), weil das Verhältnis des wirksamen Si zu W durch eine derartige Wärmebehandlung nicht mehr verändert wurde.

Es war nur teilweise bekannt, daß die Iso- und Heteropolysäuren des Wolframs aus wäßrigen Alkalimonowolframatlösungen bei der Steigerung der

H^+-Konzentration gemäß folgendem Schema entstehen:

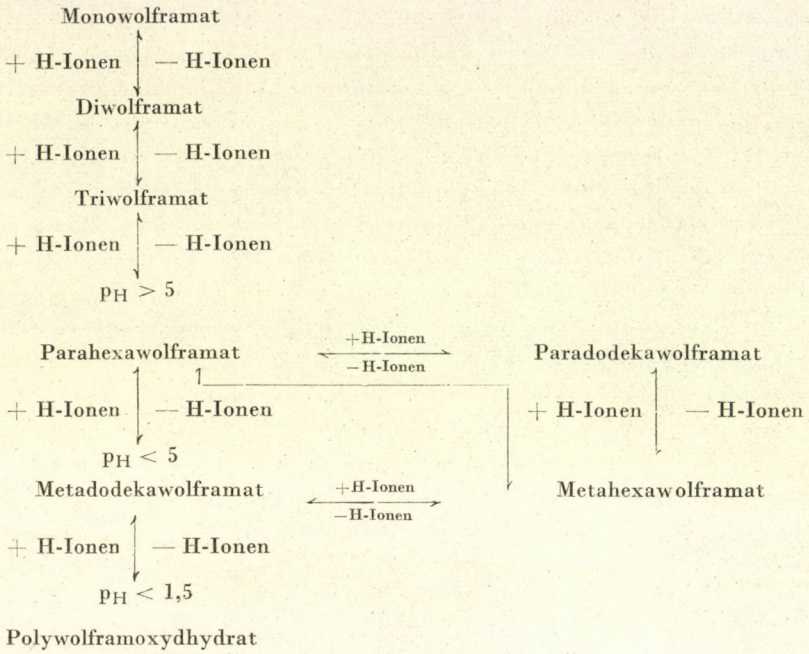

Das Keggin-Anion ohne zentralem Heteroatom ist im allgemeinen labiler und leichter kondensierbar, d.h. aus den Isosäuren wird das Oxydhydrat bereits bei höherem pH ausgeschieden. Aus dem Schema geht einerseits hervor, daß der H^+-Verbrauch zugleich Aggregation, die H^+-Abgabe Desaggregation bedeutet und andererseits, daß HOLLEMAN und WIBERG [35], im Gegensatz zu GLEMSER und Mitarbeiter [25], die Entstehung der Para- bzw. Metawolframsäure in Abhängigkeit vom pH irrtümlicherweise verkehrt geschrieben haben.

Die Ansäuerung von Alkaliwolframat- oder z.B. Alkaliwolframat + Alkalisilikat-Lösungen befördert außer der Kondensation auch die innere Ordnung der gebildeten festen Phase. So sind die Parasäuren im Grunde genommen kristallographisch weniger geordnet als die Metasäuren, die Keggin-Phase [4] ist dichter gepackt als die Lindqist-Phase [26], und die hypothetische Jahr-Phase [9] nimmt eine Zwischenstellung ein. Wenn dazu noch bemerkt wird, daß die Steigerung der H^+-Ionenkonzentration im allgemeinen zu einer Abnahme der Reaktionsgeschwindigkeit der Bildung von kondensierten Phasen führt, so ist leicht einzusehen wie stark die Qualität des zustandegekommenen Anions, ob ein Si-Atom in das Zentrum des Anions eingebaut wird oder nicht, von der Herstellungsweise abhängig ist. So kann z.B. auch der Kristallwassergehalt des aus der Lösung kristallisierenden Wolframatokieselsäurehydrats mit

Hilfe des pH eingestellt werden [18]. Dabei bleibt natürlich die Frage weiterhin offen, ob das fehlerfreie Keggin-Anion imstande ist, in Form von Hydraten mit verschiedenen Kristallwassergehalten und im verschiedenen Kristallsystem zu kristallisieren; ob sämtliche Hydrate kubisch bleiben und nur die Kantenlänge der Elementarzelle mit dem höheren H_2O-Gehalt ansteigt und schließlich ob gerade die mehr oder weniger ausgeprägten Gitterfehler des Anions zur Bildung von verschiedenen Hydraten führen.

Unsere Versuche weisen darauf hin, daß das zentrale Si-Atom nicht nur die $W_3O_{10}^{2-}$-Liganden, sondern auch die Kristallwassermoleküle koordiniert, und zwar mit umso geringerer Kraft, je mehr H_2O-Moleküle vorhanden sind, bis es schließlich zur Lösungsbildung kommt. Die von SIGNER und GROSS [23] beschriebene kubisch-tetragonale Polymorphie des $n_2 = 24$ Hydrats scheint zu beweisen, daß die Kristallform des Hydrats auch bei größerem H_2O-Gehalt kubisch bleiben kann.

Die Beweglichkeit der Kristallwassermoleküle im Kristallgitter ist verhältnismäßig hoch, und zwar umso höher, je weiter sie vom zentralen Si-Atom entfernt sind. Demzufolge werden die Kristalle mit steigendem Wassergehalt labiler, und es kann leicht zu Kristallumwandlungen kommen. Auch eine Strukturänderung während der Lagerung läßt sich dadurch ohne weiteres erklären.

Kristallographisch sind zur Zeit drei Wolframatokieselsäurehydrate bekannt, die in verschiedenen Kristallsystemen kristallisieren. Werden auch die anderen Wolframatoheteropolysäuren beachtet, dann sind es insgesamt fünf. Theoretisch können bis $n_2 = 24$ ebenfalls fünf existieren, wenn man berücksichtigt, daß die Wassermoleküle durch ein zentrales Heteroatom mit der Koordinationszahl 4 koordiniert werden.

Die Keggin-Phase selbst verfügt nur im Bereich von 80—130 °C über ein geordnetes, stabiles Kristallgitter. Beim Abkühlen wird es ausnahmslos defekt, und zwar desto mehr, je schneller die Abkühlung erfolgt. Manchmal findet vorübergehend eine fast vollständige Umordnung statt. Die Gegenwart von Verunreinigungen verzögert die Ausbildung der Keggin-Phase.

Die Frage, welche Rolle die Verunreinigungen bei Entstehung von verschiedenen Kristallsystemen spielen, bleibt ebenfalls offen. Es ist fraglich, ob die verschiedenen Kristallsymmetrien aus derselben oder aus einer hochreinen Wolframatokieselsäure herstellbar sind. Möglicherweise sind die in der Literatur angegebenen Hydratphasen nicht die Kristallphasen der »reinen« Wolframatokieselsäure.

Der H_2O-Gehalt der Hydrate hängt vom Partialdruck des Wasserdampfes in der umgebenden Atmosphäre ab, demzufolge können Hydrate mit verschiedenen n_2-Werten aus demselben Ausgangsstoff durch Einstellung des H_2O Gleichgewichtdruckes erhalten werden. Wir wissen aber nicht, ob die so hergestellten Hydrate mit verschiedenen p_{H_2O}—T Existenzgebieten gleichzeitig

auch in verschiedenen Kristallsystemen kristallisieren oder nicht. Das bedeutet aber, daß ganzzahlige $H_2O/H_{16}SiW_{12}O_{46}$ Molverhältnisse in Normalatmosphäre praktisch unerreichbar sind, und daß die Angabe solcher Formeln mit ganzen H_2O Molzahlen höchstens einen theoretischen Wert hat. Aufgrund der n_2-Werte in Tab. IV und V dürfte dann zu den von uns untersuchten rehydratierten Proben ein triklines Kristallsystem und $n_2 = 8$, zum Reanal-Ausgangsstoff ein trigonales Kristallsystem und $n_2 = 16$ und zum Merck-Präparat ein neues Kristallsystem und $n_2 = 12$ gehören. Bei dem ersten Präparat sind dann die Kristalle wegen H_2O-Überschuß, bei den zwei letzteren dagegen infolge H_2O-Defizit ungeordnet.

Es soll hier ausdrücklich betont werden, daß die Ergebnisse solcher Untersuchungen wie z.B. die kristallographische Bestätigung der Existenz von kubischen, triklinen, trigonalen und tetragonalen $H_4[SiW_{12}O_{40}]$-Hydraten [9] oder die Aufnahme von chemischen Gleichgewichtsdiagrammen der Wolframatokieselsäurehydrate [18], ja daß im allgemeinen die Bestimmung von physikalisch-chemischen Eigenschaften verschiedener Stoffe heute bereits einen viel geringeren Wert hat und die Ergebnisse keineswegs verallgemeinert werden dürfen, wenn keine ausreichend exakte chemische Analysendaten zu den untersuchten Stoffen vorliegen.

Was nun die weitere thermische Zersetzung anbelangt, können wir aufgrund von Literaturangaben und eigener Messungen folgende Schritte unterscheiden: In Normalatmosphäre beginnt bei ~ 125—130 °C die endotherme Wasserabgabe der kubischen Keggin-Phase, deren Zusammensetzung $H_{16}SiW_{12}O_{46}$ ist und deren Elementarzelle eine Kantenlänge von $a = 12{,}4$ Å hat. Es entsteht dabei die $H_4SiW_{12}O_{40}$ Grundsäure mit der von uns erkannten neuen Struktur, die beim p_{H_2O} der Normalatmosphäre zwischen ~ 150 und 350 °C stabil ist. Die genauen Existenzbereiche können durch die Aufnahme von Gleichgewichtsdiagrammen mit strömenden Gasgemischen von bekannter Zusammensetzung bestimmt werden.

Bei etwa 350 °C beginnt die endotherme Abspaltung der beiden letzten Wassermoleküle. Diese verläuft bis 450—480 °C, d. h. fast bis zur quantitativen Abspaltung beider Säure-H_2O-Moleküle, ohne wesentliche Strukturänderung, vielleicht nur von einer geringen Zunahme der Hintergrundstrahlungsintensität begleitet. Die Dehydratation bleibt reversibel, solange die erwähnte neue Kristallstruktur, d.h. vermutlich das Gitter des Keggin-Anions, unbeschädigt bleibt. Die nachträgliche Hygroskopizität des erhaltenen Produktes nimmt jedoch mit der vorschreitenden Amorphisation immer besser ab, und nach Erhitzung auf eine höhere Temperatur, genauer gesagt nach der exothermen Reaktion, wird der Vorgang irreversibel, die Regeneration zur gefundenen neuen, bzw. zur Keggin-Phase findet nicht mehr statt. Bei der röntgenamorphen Phase handelt es sich also nicht um das WO_3, wie Rode [18] behauptet, sondern um die Grundsäure als Ausgangsgitter.

Nach der Amorphisation erfolgt zwischen 500 und 530 °C die exotherme Umkristallisation zur tetragonalen festen Lösung $W_{12}O_{36} \cdot SiO_2$ und bei $\sim$ 600 °C eine erneute Umordnung zum monoklinen WO_3. Oberhalb von 700 °C verlaufen dann noch die bekannten polymorphen Umlagerungen des WO_3 [18, 36], und zwar mit steigender Temperatur als endotherme, mit abnehmenden Temperaturen als exotherme Vorgänge. Diese Umlagerungstemperaturen sind von der Menge des Si, von der Fehlstellenkonzentration abhängig.

Um ein ausreichend genaues Bild vom Einbau des Si bzw. SiO_2 in das Gitter des WO_3 zu erhalten, müßte die eingehende kristallographische Analyse der Umwandlung der einzelnen Kristallphasen ineinander durchgeführt werden, etwa so wie es GADÓ [37] im Fall der α-W-Oxyd $\longrightarrow$ β-W-Oxyd Unwandlung getan hat. Eine derartige Untersuchung bildete jedoch nicht den Gegenstand unserer vorliegenden Arbeit.

Wenn man in der Literatur über die kubische Keggin-Phase mit $a = 12{,}14$ Å spricht, so wird darunter das 6-Hydrat der Grundsäure d. h. $H_4[Si(W_3O_{10})_4] \cdot 6H_2O$ verstanden. Wo abweichende Formulierungen, z. B. 5-Hydrat usw. vorkommen, dort muß es sich — wie aus unseren Untersuchungen folgt — um irgendeine Anomalie, um die Verschiebung des Si:W- und/oder des $Si_{zentral}$: W-Verhältnisses, um Defektstellen in der Struktur des Keggin-Anions, um die Gegenwart von Verunreinigungen, oder um anomale Dehydratierung usw. handeln. Thermogravimetrische Messungen haben gezeigt, daß diese sechs Wassermoleküle stärker gebunden sind bzw. werden, nicht nur bei der Dehydratierung, sondern auch bei der Rehydratierung. Diese Wassermenge ist konsequent das Dreifache der noch stärker gebundenen Säurewasser-Moleküle. Vor uns wurde die Dehydratierung der Keggin-Phase nur derart untersucht, daß die Röntgenanalyse nach der thermischen Dehydratierung bei Raumtemperatur durchgeführt wurde. Demgemäß konnte immer wieder nur die Gegenwart des Keggin-Anions festgestellt werden. Durch Röntgendiffraktometrie bei der Zersetzungstemperatur ist es uns jedoch gelungen, nachzuweisen, daß die Keggin-Phase mit $a = 12{,}41$ Å bei der Dehydratierung des 6-Hydrates zersetzt wird; daß die Keggin-Phase im Grunde genommen nur in einem engen Temperaturbereich von $100 \pm \leq 25$ °C kristallographisch geordnet ist, während sie oberhalb und unterhalb dieses Bereiches zerfällt, bzw. defekt wird.

Laut dieser Ergebnisse erweist sich die Annahme von WEST und AUDRIETH [34], wonach das Wasser der kubischen Keggin-Phase zeolitisch gebunden wäre, als unrichtig. Aufgrund ihrer Angaben dehydratierten sie bei Zimmertemperatur bis zur Keggin-Phase und bei 300 °C bis zu einem Wassergehalt unter $n = 2$, d.h. bis zur sogenannten Amorphisation. Sie haben aber nicht die getrockneten Proben bei der Trocknungstemperatur und bei konstantem P_{H_2O} der Röntgenanalyse unterworfen. Hätten sie das getan, so hätten sie keine identischen Strukturen gefunden. Die Abgabe und Wiederaufnahme von

Zeolithwasser wird dagegen im allgemeinen von keiner Strukturänderung begleitet und verläuft nicht stufenweise, wie bei der Wolframatokieselsäure.

Unsere bisherigen Darlegungen lassen allein die Möglichkeit offen, daß von den Kristallwassermolekeln sechs darum besonders stark gebunden werden, weil sie sich in besonders ausgebildeten Hohlräumen des Kristallgitters befinden. Solche Hohlräume sind im Gitter des Keggin-Anions nur an den beiden Enden der drei zweizähligen Symmetrieachsen, gegenüber den sechs Kanten des zentralen Koordinationstetraeders vorhanden. Somit kann zwar geometrisch erklärt werden, weshalb die Zahl der ausgezeichneten Kristallwassermoleküle 6 ist, eine energetische Erklärung, weshalb diese Zahl nicht einer vierer Koordination entspricht, bleibt jedoch dahingestellt. Es ist weiterhin unklar, wie über 500 °C bei der ohne Gewichtsänderung verlaufenden Umwandlung zur WO_3-Phase, aus den 12 freien Sauerstoffspitzen des Keggin-Anions gemeinsame WO_6-Oktaedersauerstoffe des WO_3-Kristallgitters entstehen.

Diesen Widerspruch konnten wir beheben, wenn wir von der Annahme ausgingen, daß eine Ähnlichkeit zwischen dem oben behandelten Vorgang der pH-Abnahme und dem Vorgang der thermischen Dehydratierung vorliegt, und daß bei beiden Vorgängen gleichzeitig auch eine Kondensation stattfindet. Demgemäß sitzen an den drei freien Spitzen der $W_3O_{10}^{2-}$-Liganden der Keggin-Phase nicht Sauerstoffatome, sondern Hydroxylgruppen [19], und man kann anstelle $H_4[SiW_{12}O_{40}] \cdot 6H_2O$ $H_4[SiW_{12}O_{34}(OH)_{12}]$ schreiben. Statt Kristallwasser ist also hier strukturell gebundenes, sogenanntes Kondensationswasser vorhanden. Demzufolge werden die Keggin-Anionen in der kubischen Keggin-Phase eigentlich nicht durch Wasserbrücken —O—H—O—H—O—, sondern durch Wasserstoffbrücken —O—H—H—O— zusammengehalten, was darum notwendig ist, weil das Keggin-Anion selbst nur einen geringen Teil der Elementarzelle der kubischen $a = 12{,}14$ Å Keggin-Phase ausfüllt. In diesem Zusammenhang seien die Worte von JAHR [9] zitiert: » . . . in konzentriert-wäßriger Lösung müssen auch höherbasische, also konstitutionswasserreichere Formen der 12-Heteropolysäuren existieren . . .«.

Verläuft beim Erhitzen der Keggin-Phase gleichzeitig auch eine Kondensation, so entstehen infolge der zwischen den freien Spitzen der WO_6-Oktaeder zustandekommenden chemischen Bindung aus 6 Sauerstoffatomen der 12 OH-Gruppen gemeinsame WO_3-Sauerstoffe und es treten 6 Wassermoleküle aus:

$$X \cdot Y\left(H_4[SiW_{12}O_{34}/OH_{/12}]\right) \rightarrow X\left(H_4[SiW_{12}O_{40}]\right)_Y + X \cdot Y(6H_2O), \qquad (7)$$

wenn $Y \rightarrow \infty$, wo Y die Zahl der in geordneten Kristalleinheiten vorkommenden Moleküle ist.

Bei weiterer Erhöhung der Temperatur werden auch die am stärksten gebundenen Säurewassermoleküle abgespalten, wobei gleichzeitig auch die

Bildung des immer metastabiler werdenden aber vorübergehend noch isomorphen Säureanhydrids, d.h. die Amorphisation beginnt. Daraufhin folgt dann der Zusammensturz des Gitters und weitere Aggregation, die zur Bildung der tetragonalen festen Lösung führen

$$X(H_4[SiW_{12}O_{40}])_Y \rightarrow (W_{12}O_{36}SiO_2)_{X \cdot Y} + X \cdot Y(2H_2O). \quad (8)$$

Eine selbstverständliche Folge des parallel laufenden Polykondensationsvorganges ist, daß beim Erhitzen der kubischen Keggin-Phase niemals mit der Abspaltung der theoretischen Menge von 6 Kondensationswassermolekeln gerechnet werden darf, weil nie $Y = \infty$ ist. Je größer, geordneter und fehlerfreier die Kristallite → Kristalle der hergestellten $H_4SiW_{12}O_{40}$ Grundsäure sind, d.h. je vollkommener die Kondensation durchgeführt wurde, umso mehr nähern wir uns dem theoretischen Wert, der Abspaltung von 6 H_2O Kondensationswasser. Die Ursache der Ausbildung von Gitterfehlern kann u.a. Si-Defizit oder die Gegenwart von Verunreinigungen sein, wie das z.B. bei dem durch uns untersuchten Merck-Präparat der Fall war.

Diejenigen Wassermoleküle, die nicht als Kondensationswasser, sondern größtenteils aus den an der Oberfläche, an den Spitzen der WO_6-Oktaeder zurückgebliebenen OH-Gruppen, in geringerem Maße auch aus den Hydroxylgruppen im Inneren der Teilchen zustandegekommen sind, lassen bei ihrer Entfernung Gitterfehler zurück. Auf der Oberfläche ist die Konzentration dieser Fehler so groß, daß eine metastabile sog. Randschicht zurückbleibt, die eine abweichende Struktur und abweichende Stoffeigenschaften aufweist. Bei erneuter Abkühlung resorbiert oder sorbiert diese Randschicht Sauerstoff und/oder Wasser, gegebenenfalls auch andere Stoffe, weist Sauerstoffdefizit auf usw., verhält sich also anders, als das aus WO_6-Oktaedern mit gemeinsamen Sauerstoffatomen bestehende Innere der WO_3-Kristalle.

Diskussion

Es wurde die thermische Zersetzung der 12-Wolframatokieselsäurehydrate, in erster Reihe mit Hilfe von thermoanalytischen und röntgenanalytischen Methoden untersucht. Beim Erhitzen dieser Heteropolysäure konnte die Abspaltung von drei verschieden stark gebundenen Wassermolekülarten beobachtet werden, namentlich:

n_2-Kristallwassermoleküle, die als Wasserüberschuß über der Zusammensetzung der sog. Keggin-Phase $H_{16}SiW_{12}O_{46}$ vorhanden und am schwächsten gebunden sind;

n_1-Kondensationswassermoleküle, maximal $6H_2O$, die als Konstitutionswasser in Form von OH-Gruppen in der Keggin-Phase $H_4[SiW_{12}O_{34}(OH)_{12}]$ anwesend sind, und schließlich

n-Säurewassermoleküle, maximal $2H_2O$, die den Konstitutionswassergehalt der Grundsäure bilden und am stärksten gebunden sind.

Weil $n = 2$ ist, kann die Koordinationszahl des zentralen Si-Heteroatoms nur 4 sein und die beiden Wassermoleküle werden in Form von 4 OH koordiniert. KEGGIN hat bewiesen, daß das Kraftfeld des zentralen Si-Atoms bei den Spitzen seines Koordinationstetraeders auch die umgebenden 12 WO_6-Oktaeder »mit großer Kraft« zu vier $W_3O_{10}^{2-}$-Liganden verdichtet. Wir konnten nachweisen, daß nach den beiden Säurewassermolekülen stets dreimal soviel Wasser eingebaut, bzw. vorher immer dreimal soviel Wasser abgespalten wird, als der Wert von n ist, d.h. $(n_1 + n)/n = 4$. Dies bedeutet, daß auch die mit mittlerer Stärke gebundenen sechs H_2O-Moleküle durch das zentrale Si-Atom koordiniert werden. Bei der Koordinationszahl 4 ist dies nur so vorstellbar, daß die Koordination in der Form von 4·3 OH-Gruppen geschieht. Die Übereinstimmung mit der Zahl der 4·3 freien WO_6-Oktaederspitzen an den vier Liganden $W_3O_{10}^{2-}$ des Keggin-Anions bewog uns, im Gegensatz zu KEGGIN und in Einklang mit PAULING, die von KEGGIN angenommenen O-atome an den freien Spitzen des Polyanions der kubischen Keggin-Phase $a = 12{,}14$ Å durch OH-Gruppen zu ersetzen und damit die Formel $H_4[SiW_{12}O_{40}]$ für die Grundsäure, sowie die Formel $H_4[SiW_{12}O_{34}(OH)_{12}]$ für die Keggin-Phase vorzuschlagen.

Weitergehend nehmen wir an, daß auch die n_2-Wassermoleküle koordiniert werden, selbstverständlich in umso geringerem Maße, je höher der Wert von n_2 ist, d.h. je weiter sie vom zentralen Si-Atom entfernt sind, bis schließlich die wässerige Lösung entsteht. Theoretisch sind also Hydrate mit n_2-Werten von 4, 8, 12, 16 und eventuell noch 24 vorstellbar. Von diesen wurden die Hydrate $n_2 = 8$ und $n_2 = 24$ bereits hergestellt (RODE gab irrtümlicherweise $n_2 = 25$ an). In unseren rehydratierten Proben fanden wir ebenfalls $n_2 = 8$ und bei dem Reanal-Präparat konsequent $n_2 = 16$, anstelle des am häufigsten angegebenen, aber möglicherweise nicht richtigen Wertes von $n_2 = 18$. RODE fand das Hydrat $n_2 = 11$, statt dem unserer Meinung nach theoretisch möglichen $n_2 = 12$ Hydrat. Zur Deutung solcher Abweichungen wiesen wir auf die Möglichkeit hin, daß die Gegenwart von Verunreinigungen, der Wasserdampfdruck der umgebenden Atmosphäre, die Verschiebung des Si : W-, bzw. $Si_{zentral}$: W-Verhältnisses zu Änderungen der Struktur und/oder der n_2-, n_1- und n-Werte führen können. Hiermit taucht natürlich die Frage auf, ob es bei einer hochreinen Wolframatokieselsäure überhaupt solche Hydrate gibt, die in verschiedenen Kristallsystemen kristallisieren. Sind nicht vielleicht die Kristalle sämtlicher Hydrate kubisch und nimmt mit steigender Kristallwassermenge nicht nur die Kantenlänge der Elementarzelle zu. Sind nicht vielleicht die bisher gefundenen, in verschiedenen Systemen kristallisierenden Hydrate nur die Folge von verschieden defekten Keggin-Anionen?

Aufgrund von Literaturangaben schließen wir uns der Meinung an, daß das Keggin-Anion im Gebiet $n_2 = \infty \rightarrow n = < 2$, bzw. $\sim 20 \rightarrow \sim 500$ °C

stabil ist. Weitergehend weisen wir jedoch auf die Parallelität der Vorgänge bei der pH-Abnahme in wässeriger Lösung und bei der thermischen Zersetzung hin, und sind der Meinung, daß pH-Abnahme in Lösung $\triangleq$ Polykondensation; kontinuierliche Temperaturerhöhung der festen Phase $\triangleq$ Aggregation ist. Daraus stellen wir fest, daß die Kristallstruktur bei unversehrt bleibenden Keggin-Anionen infolge Änderung ihrer gegenseitigen Lage verändert werden kann. Die kubische Keggin-Phase selbst ($a = 12{,}14$ Å) besitzt nur im Temperaturgebiet 100 ± 25 °C ein geordnetes Gitter. Unterhalb dieser Temperatur wird das Gitter defekt, oberhalb dieser Temperatur erfolgt Zersetzung zur Grundsäure, die bereits eine andere, ebenfalls aus unversehrten Keggin-Anionen bestehende, bisher unbekannte Struktur besitzt. Auch das aus WO_6-Oktaedern bestehende Käfiganion durchmacht im Laufe seiner Herstellung einen Gitterordnungsvorgang, u. zw. bis zu dem geordnetesten, am dichtesten gepackten Keggin-Anion. Eine 12-Wolframato-Heteropolykieselsäure mit idealer Struktur besteht nur aus solchen fehlerfreien Keggin-Anionen. Der Ordnungsvorgang kann gegebenenfalls auch über die Pauling- [19], Lindqist- [26] und Jahr-Phasen [9] verlaufen und wenn wir bei der Herstellung irgendwo auf halbem Wege, an einer falschen Stelle Halt machen, dann treten später die beschriebenen Anomalien in Vordergrund.

Die Grundsäure kommt derart zustande, daß viele Keggin-Anionen mittels ihrer freien OH-Spitzen kondensieren. Die Benennung »Keggin-Phase« ist also nur für die Zusammensetzung $H_{16}SiW_{12}O_{46}$ gültig. Aus den ohne Kondensationspartner gebliebenen OH-Gruppen bildet sich natürlich ebenfalls H_2O, welches beim Erhitzen entweicht. Befinden sich diese Wassermoleküle im Inneren der sich ordnenden Kristallite, dann bleiben nach dem Abkühlen Gitterfehler zurück. Auf der Oberfläche ist die Konzentration der OH-Gruppen offensichtlich wesentlich höher und deswegen verfügt die Oberfläche nach dem Entweichen des aus ihnen entstandenen Wassers über eine wesentlich höhere Fehlstellenkonzentration und über eine vom Inneren der Teilchen abweichende Struktur mit besonderen Eigenschaften. Beim Abkühlen regeneriert sich diese Randschicht gierig, sie reagiert mit der umgebenden Gasphase, physikalische Sorption und Chemisorption treten auf, usw.

Bei der Entfernung des Säurewassers wird bereits auch das Keggin-Anion angegriffen. Dieser Vorgang setzt sich aus einer endothermen Amorphisation (kristallin → amorph) und einer exothermen Kristallisation (amorph → kristallin) zusammen. Der erste Vorgang wird von keiner Aggregation begleitet, beim zweiten tritt jedoch Aggregation auf. Die entstehende Phase ist WO_3, welches sich wegen der Gegenwart von Si schwerer ordnen kann und deshalb zuerst die tetragonale und erst bei höherer Temperatur die stabilere monokline Kristallform annimmt. Das Kegginsche Käfiganion mit zentralem Si-Heteroatom kann also praktisch bis zum Beginn der Amorphisation, d.h. bis ~ 500 °C als stabil betrachtet werden.

Wir sind der Meinung, daß unsere Ergebnisse dadurch anschaulicher geworden sind, daß wir die Vorgänge nicht von der Seite der thermischen Zersetzung der Heteropolysäure, sondern von der Seite der thermischen Synthese des WO_3 betrachtet haben.

*

Wir danken auch an dieser Stelle Frau Klara HORKAY für die Durchführung der Spektralanalysen und Frau Margarete SZÉKELY für die Ausführung der chemischen Analysen.

LITERATUR

1. MILLNER, T., NEUGEBAUER, J.: Magy. Kém. Foly. **57,** 321 (1951)
2. HEGEDŰS, A. J., NEUGEBAUER, J., DVORSZKY, M.: Magy. Kém. Foly. **65,** 159 (1959); Microchim. Acta **1959,** 282
3. REMY, H.: Lehrbuch der anorganischen Chemie, Band 2. 11. Ausgabe, Akademische Verlagsgesellschaft Leipzig, 1961
4. KEGGIN, J. F.: Nature **131,** 908 (1933): Proc. Royal Soc. Ser. A **144,** 75 (1934)
5. BABAD-ZACHRJAPIN, A. A. und Mitarb.: Isw. Nauk. Otd. Chim. Nauk **1963,** Nr. 1, 14; **1963,** Nr. 2, 215; **1964,** Nr. 5, 799
6. KEHL, W. L., HAY, R. G., WAHL, D.: J. Appl. Physics **23,** 212 (1952)
7. MARIGNAC, J. C.: Comptes-rendus hebd. Séances Acad. Sci. **55,** 888 (1862)
8. Gmelins Handbuch der anorganischen Chemie, System-Nr. 54, Verlag Chemie, Weinheim/Bergstr.—Berlin, 1933
9. JAHR, K. F.: Naturwissenschaften **29,** 505, 528 (1941) und die dort angeführte Literatur
10. EMELÉUS, H. J., ANDERSON, J. S.: Ergebnisse und Probleme der modernen anorganischen Chemie. Springer, Berlin—Göttingen—Heidelberg, 1954
11. HÜCKEL W.: Anorganische Strukturchemie. F. Enke, Stuttgart, 1948
12. MIOLATI, A.: J. prakt. Chem. **77,** 417 (1908)
13. ROSENHEIM, A. und Mitarb.: Z. Elektrochem. **17,** 694 (1911); Z. anorg. allg. Chem. **70,** 73 (1911); **100,** 304 (1917); **101,** 215 (1917)
14. COPAUX, H.: Z. anorg. allg. Chem. **74,** 355, 360 (1912); Bull. Soc. Chim. Biol. Paris **13,** 324 (1913); Comptes-rendus hebd. Séances Acad. Sci. **156,** 71 (1913)
15. SOUCHAY, P.: Bull. Soc. Chim. France **9,** 289 (1942)
16. KEPERT, D. L.: Progress in Inorganic Chemistry **4,** 199 (1962) und die dort angeführte Literatur (Ed. F. A. Cotton. Interscience, New York—London)
17. SCROGGIE, A. G., CLARK, G. L.: Proc. Nat. Acad. Sci. **35,** 1 (1929)
18. RODE, E. J.: Zh. Neorg. Chim. **3,** 2707 (1958); **4,** 1782 (1959); Thermal Analysis Proc. Conf. Aberdeen, 1965, Ed. J. P. Redfern, MacMillan, London 1965
19. PAULING, L.: J. Amer. Chem. Soc. **51,** 2868 (1929)
20. KEGGIN, J. F.: Nature **132,** 351 (1933)
21. BRADLEY, A. J., ILLINGWORTH, J. W.: Proc. Royal Soc. Ser. A, **157,** 113 (1936)
22. LEVY, H. A., AGRON, P. A., DANFORD, M. D.: J. Chem. Physics **30,** 1486 (1959)
23. SIGNER, R., GROSS, H.: Helv. Chim. Acta **17,** 1076 (1934)
24. COTTON, F. A., WILKINSON, G.: Anorganische Chemie. Verlag Chemie, Weinheim/Bergstr., 1967
25. GLEMSER, O., HOLZNAGEL, W., HÖLTJE, W., SCHWARZMANN, E.: Z. Naturforsch. **20b.** 725 (1965)
26. LINDQIST, I.: Acta Cryst. **5,** 667 (1952)
27. LIPSCOMB, W. N.: Inorg. Chem. **4,** 132 (1965)
28. BRAUER, G.: Handbuch der präparativen anorganischen Chemie, Band 2, Seite 1474 und 1488. F. Enke, Stuttgart, 1962
29. TOURKY, A. R., ELSHAMY, H., ISSA, J.: J. Appl. Chem. **2,** 262 (1952)
30. NIKITINA, E. A., BURISS, E. V.: Zh. Obschtsch. Chim. **25,** 621 (1956)
31. KRAUS, O.: Z. Krist. **91,** 402 (1935); **93,** 379, 902 (1936); **94,** 256 (1936); **96,** 330 (1937); **100,** 394 (1939); Naturwissenschaften **25,** 250 (1937); **28,** 304 (1940)
32. COPAUX, H.: Bull. Soc. Chim. France **3,** 107 (1908)

33. SPIZIN, W. I.: Acta Chim. Acad. Sci. Hung. **12,** 119 (1957)
34. WEST, S. F., AUDRIETH, L. F.: J. Phys. Chem. **59,** 1069 (1955)
35. HOLLEMAN, A. F., WIBERG, E.: Lehrbuch der anorganischen Chemie. 57—70. Ausgabe, Seite 530. Walter de Gruyter, Berlin, 1964
36. HEGEDÜS, A. J., MILLNER, T., NEUGEBAUER, J., SASVÁRI, K.: Z. anorg. allg. Chem. **281,** 77 (1955)
37. GADÓ, P.: Acta Physica **18,** 111 (1965)

András J. HEGEDÜS
Pál GADÓ
György SCHLOSSER
Jenő NEUGEBAUER

Budapest IV., Váci út 77.

Acta Chimica Academiae Scientiarum Hungaricae, Tomus 66 (4), pp. 373—382 (1970)

SOME QUESTIONS OF THE SEPARATION OF TRACE ELEMENTS BY PRECIPITATION, VII

DETERMINATION OF SMALL AMOUNTS OF COPPER, ZINC, NICKEL, COBALT AND SILVER IN ROCKS AFTER PRECIPITATION WITH AMMONIUM HYDROXIDE

M. GÖRBICZ and E. UPOR

(Mecsek Ore Mining Enterprise, Pécs, Hungary)

Received July 21, 1969

A combined method has been developed for the determination of copper, cobalt, nickel, zinc and silver present in small amount in rocks. Copper, cobalt and zinc have been determined by spectrophotometry, measuring the optical density of the copper complex with diethyldithiocarbamate, of cobalt with nitroso R-salt, of zinc with dithizone. Nickel was determined by means of dimethylglyoxime, silver on the basis of its catalytic effect on the oxidation of Mn^{2+}. Iron and other interfering ions were removed with a solution 2 *M* in NH_4OH and 2 *M* in NH_4Cl. Cobalt and silver can be determined from this solution directly, whereas copper, nickel and zinc only after separation by extraction.

Introduction

Several reagents are available for the photometric determination of small amounts of copper, cobalt, nickel and zinc. Of these the following proved to be best in analytical practice.

For copper: dithiocarbamate [1, 2, 3], dioximes [4], dithizone [3, 5, 6]; for cobalt: nitroso naphtol derivatives [7—12], pyridylazo derivatives [13, 14], dithiocarbamates [15], rhodanide [16]; for nickel: dioximes [17, 3, 10, 18], dithiocarbamates [19]; for zinc: dithizone [9, 3, 5, 20, 21].

These reagents, however are not selective. It is known that dithizone and sodium diethyl-dithiocarbamate are widely used besides 8-hydroxyquinoline in the spectrophotometric determination of trace elements in water, since the majority of metal ions can be extracted by them [22, 23, 24]. Methods recommended for rock and ore analysis are also based on the use of these reagents in combination with separation.

For determining copper the extraction and photometric measurement of its diethyldithiocarbamate complex is most generally applied [1, 25], although dithizone has also been used [5].

For determining cobalt the extraction and photometric measurement if its complex with nitroso R-salt proved to be best due to selectivity of the reagent and simplicity of the method [2, 10, 26]. Nickel is most often determined by means of dimethylglyoxime [26—30], although diethyldithiocarba-

mate can also be used [19]. Dithizone has been used for the determination of zinc in bauxite [20] and soil [21].

p-Aminobenzylidenerhodanine [31] and dithizone [32] are applicable to the photometric determination of silver; neutron-activation [33, 34] and catalytic [35] methods are also widely used due to their higher sensitivity.

Investigation of elements interfering with the analysis

In developing methods for the determination of various elements the authors have started with the data given in Table I. Since no data were available in the literature concerning interfering effects, thorough investigations had to be performed in this direction. A number of masking methods partially known from the literature were also tried.

Table I

Ion	Clark-value in granite [36] ppm	Reagent	Conditions of determination	Molar extinction coefficient	Interfering ions
Cu^{2+}	30	Na-diethyl-dithiocarbamate	extraction with $CHCl_3$ at pH = 9	12 800 (λ = 436 nm)	Ni^{2+}, Co^{2+}, Bi^{3+}, Fe^{3+}, Mn^{2+}
Co^{2+}	7	nitroso R-salt	complex formation at pH = 5.5; determination in HNO_3 medium	8 000 (λ = 525 nm)	—
Ni^{2+}	15	dimethylglyoxime	in alkaline medium, in the presence of oxidant	15 000 (λ = 470 nm)	Cu^{2+}, Co^{2+}, Mn^{2+}, Fe^{3+}
Zn^{2+}	60	dithizone	extraction at pH = 5.5	90 000 (λ = 530 nm)	Ag^+, Bi^{3+}, Cd^{2+}, Co^{2+}, Cu^{2+}, Hg^{2+}, Ni^{2+}, Pb^{2+}, Fe^{3+}
Ag^+	0.05	$Mn^{2+} + K_2S_2O_8 \downarrow Ag^+$ MnO_4^- [36]	in H_3PO_4 medium, colorimetry of MnO_4^-	—	Pd^{2+}, Fe^{3+}, oxidizing and reducing ions

Copper

For determining copper, the extraction of Cu-diethyldithiocarbamate with carbon tetrachloride at a pH of 8—11 and the measurement of the optical density at 435 nm is most expedient (at this wavelength the reagent does not show light absorption). Under the same conditions the respective absorptions of 200 μg of Fe^{3+}, 300 μg of Fe^{2+}, 25 μg of Mn^{2+}, 6 μg of Co^{2+}, 6 μg of Ni^{2+} are

equal to that of 1 μg Cu^{2+}, while 500 μg of UO_2^{2+} or 25 μg of Zn^{2+} do not give any absorption under these conditions. Mn^{2+}, Fe^{3+} and Fe^{2+} can be effectively masked by pyrophosphate, which does not affect the extraction of the Cu-DDTC complex. Co^{2+} ions can be masked by CN^- or CNS^- ions, but these bind also Cu^{2+} ions, therefore they cannot be used. Co^{2+} forms a yellow complex with $[Fe(CN)_6]^{3-}$. The complex is of low stability and partly decomposes when DDTC is added. Dimethylglyoxime cannot be used for the complete masking of Ni^{2+} and Co^{2+}, and also hinders the quantitative formation of the Cu-DDTC complex. Nitroso R-salt is suitable for masking Co^{2+}.

As shown by the above description, the main problem is the separation of copper from nickel.

Cobalt

Co^{2+} ions form a yellowish brown complex with nitroso R-salt at a pH of 5.5—6.0, of which a stable Co^{3+} complex can be produced upon boiling with nitric acid. Due to the light absorption of the reagent, the optical density of the complex is not to be measured at the maximum but at 525 nm. Under the conditions of colour development, Fe^{2+} ions give a green complex, while Fe^{3+} forms an interfering coloured complex with acetate ions present in the buffer. The absorption of 6 μg of Cu^{2+} is equal to that of 1 μg of Co^{2+}. The interfering effect of all the ions mentioned can be eliminated by boiling with HNO_3.

Thus Co^{2+} ions can be readily determined. Reducing and oxidizing agents (*e.g.* ascorbic acid and H_2O_2) interfere.

Nickel

Ni^{2+} can be extracted by dimethylglyoxime from ammonia solution and the optical density of the pink complex can be measured. 500 μg of Mn^{2+} show a light absorption equal to that of 10 μg of Ni^{2+}, and Co^{2+} and Cu^{2+} show absorption as well. Co^{2+} and Cu^{2+} can be masked by tartrate. It is more favourable to re-extract Ni^{2+} with hydrochloric acid and determine it in alkaline solution after oxidation. (According to some authors the greater sensitivity is due to the Ni^{4+} complex, while some other authors ascribe it to the formation of a compound with the oxidation products of dimethylglyoxime).

The interference from Mn^{2+} can also be eliminated by re-extraction. Fe^{3+} can be masked by tartrate to some extent, but its interference can be only eliminated completely by separation.

Zinc

At pH 5, Zn^{2+} can be extracted by dithizone dissolved in $CHCl_3$ or CCl_4 and the light absorption of the complex can be measured. In the presence of excess dithizone the optical density has to be measured at two wavelengths viz. 530 and 610 nm, while without excess dithizone at 530 nm only. Under

these conditions several metal ions produce coloured complexes with dithizone. The absorption of 10 μg of Co^{2+}, Ni^{2+}, Cr^{3+} or V^{5+} is equal to that of 2.5 μg, 1.2 μg, 0.9 μg and 0.4 μg of Zn^{2+}, respectively. The interference from Pb^{2+}, Cu^{2+} and Fe^{3+} is even greater.

The light absorption of 1 μg of Ag^{+} is equal to that of 0.3 μg of Zn^{2+} and the absorption of 1 μg of Cd^{2+} to that of 0.5 μg Zn^{2+}. Since in samples occurring in practice the elements mentioned are present in amounts by at least two orders of magnitude smaller than zinc, their effect can be ignored.

α-Benzoinoxime, thiourea and thiosulfate have been tried for masking Cu^{2+} but without success. The re-extraction of Zn^{2+} by 0.1 *n* HNO_3 proved to be good for separating Zn^{2+} from Co^{2+} and Cu^{2+}. Zn^{2+} ions get into the aqueous phase without losses while Co^{2+} and Cu^{2+} ions are retained quantitatively by the organic phase. Ni^{2+} is extracted and re-extracted together with Zn^{2+}, therefore it has to be removed by means of dimethylglyoxime. This operation can be suitably included in the course of analysis.

Silver

For determining silver the method given by NAKAGAWA [35] for the estimation of silver in soils and rocks has been used, in which the catalytic effect of Ag^{+} ions on the oxidation of Mn^{2+} to MnO_4^{-} is utilized. Ag^{+} was separated from interfering ions by extraction with tri-iso-octyl thiophosphate. This way only the interference from Pd^{2+} could not be eliminated (and also that from reducing and oxidizing agents which influence the redox potential of the system). According to the investigations of the authors, 10 μg of Cd^{2+}, Cu^{2+}, Ni^{2+} and Zn^{2+}, 5 μg of Co^{2+} and great amounts of alkali and alkaline earth metals do not interfere. NH_4^{+} and Cl^{-} ions interfere. 10 mg of NH_4^{+} completely eliminate the catalytic effect of Ag^{+}. The interfering effect of both ions can be eliminated by evaporating the solution to dryness with HNO_3. The determination has been carried out as suggested by NAKAGAWA, with the difference that since, according to the authors, the large amounts (5—6 g) of $K_2S_2O_8$ recommended by NAKAGAWA reduce the catalytic effect of Ag^{+} and so decrease the sensitivity of determination, only 100 mg of $K_2S_2O_8$ were added to the solution.

Separation of the ions to be determined in ammonium hydroxide solutions

As shown above, in spite of the great variety of available masking agents, the determination of some ions in the presence of iron, chromium, vanadium, lead and other interfering ions is not possible without separation. At higher concentrations it is difficult to keep some other ions in solution (*e.g.* Al^{3+}) the

hydroxides of which are insoluble. It has already been mentioned in an earlier paper [37] that, in contrast to most statements in the literature, copper, nickel, silver, zinc and cobalt can be separated nearly quantitatively (with losses smaller than 2%) from metal hydroxides in solutions containing ammonia and ammonium salts. The condition of quantitative separation is that the pH and ammonium salt concentration be higher than a certain value. For Co^{2+} ions forming the least stable complex and being most strongly adsorbed on hydroxide precipitates these limiting values are pH = 9.5, and $(NH_4^+) = 2$ *M*.

Utilizing this phenomenon a separation method has been developed for determining small amounts of zinc in rocks, by measuring the absorption of zinc dithizonate [37].

In the paper cited it was pointed out that interfering nickel, copper and cobalt ions are removed in such a way as to enable also these elements to be determined. In the combined method the extraction of Co^{2+}, Cu^{2+} and Zn^{2+} with dithizone is an important procedure besides separation by means of ammonium hydroxide. The pH of the solution obtained after separation with ammonium hydroxide is suitable for extraction and ammonium salts present do not influence the completeness of extraction.

Taking the interference from various ions into consideration, the following scheme has been developed for the determination of Cu^{2+}, Ni^{2+} and Zn^{2+} (silver and cobalt can be determined directly from the ammonia stock solution) (Fig. 1).

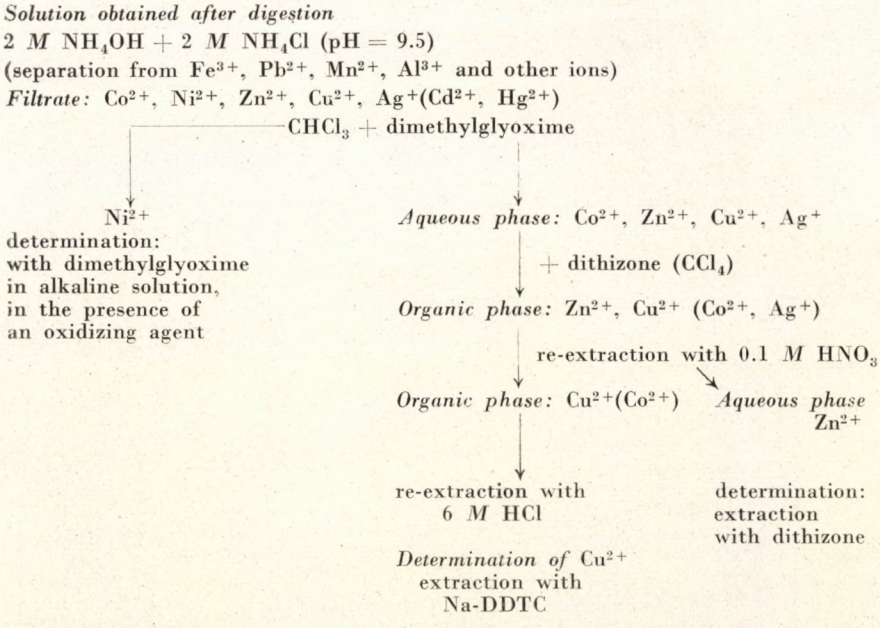

Fig. 1

Note: Co^{2+} and Ag^+ can be determined from the aqueous solution obtained after separation with NH_4OH.

The efficiency of separation has been checked by radioactive tracer technique (using ^{65}Zn, ^{60}Co and ^{63}Ni). The loss was found not to exceed 1% in any of the operations. The scheme given is suitable for the determination of every element studied.

Experimental

Reagents

HF, a.g. (Analytical grade),
HNO_3, a.g. distilled,
HCl, a.g. distilled,
NH_4OH, a.g. distilled or purified by isothermal distillation,
NH_4Cl, a.g.
1% solution of dimethylglyoxime in alcohol,
$CHCl_3$, a.g.
CCl_4, a.g.
0.01% and 0.001% solutions of dithizone in $CHCl_3$,
0.1 *M* HNO_3,
buffer solution of pH = 5.5 (1 : 4 mixture of 1/15 *M* Na_2HPO_4 and 0.1 *M* sodiumcitrate, purified with dithizone),
33% solution of sodiumcitrate,
10% NaOH, a.g.
5% ammonium peroxidsulfate,
1% solution of dimethylglyoxime dissolved in 5% KOH,
6 *M* HCl,
10% sodiumpyrophosphate,
0.1% Nitroso R-salt,
0.5% sodium diethyldithiocarbamate,
1 *M* HCl,
33% sodium acetate,
1 : 1 HNO_3, a.g.

Procedure

Transfer 1—2 g of rock sample powdered to a grain size smaller than 100 μ into a platinum vessel, dissolve in 5 ml HF + 10 ml $HClO_4$ + a few drops of HNO_3 and evaporate to dryness on a sand bath. Dissolve the residue in 10—15 ml of 1 : 1 HCl, then transfer to a glass beaker. Heat to boiling, add 10 g of NH_4Cl and an amount of purified NH_4OH corresponding to 30 ml of cc. NH_4OH. After a few minutes' standing filter the precipitated hydroxides (on prolonged storage losses may occur due to ageing). Wash the precipitate 2—3 times with warm washing liquid (100 g of NH_4Cl + 70 ml cc. NH_4OH in 1 l) and fill up the filtrate to 100 ml.

Determination of nickel

Dilute 5 to 20 ml (depending on the expected nickel, zinc, copper and cobalt content) of the solution to 50 ml in a 100 or 200 ml separatory funnel, add 2 ml 1% solution of dimethylglyoxime in alcohol, and after 2 minutes extract nickel dimethylglyoxime with 2×5 ml $CHCl_3$ shaking for 1 minute each time. Re-extract nickel with 2×5 ml 0.5 *n* HCl and analyze the aqueous phase as follows.

Add 1 ml of 33% sodium citrate, 4 ml of 10% NaOH, 5 ml 5% ammonium peroxidsulfate and 2 ml of alkaline dimethylglyoxime, and dilute to 25 ml after 10 minutes.

Measure the optical density at 470 nm with a spectrophotometer, or an S-47 filter on a Pulfrich photometer, in 5 cm cell. Reference solution: blank containing the reagents. Prepare a calibration graph using 1—10 μg of nickel. 10 μg of Ni correspond to an optical density of 0.48.

Extraction of zinc and copper with dithizone

Extract zinc and copper from the aqueous phase retained after the extraction of nickel with small portions (0.5—2 ml) of 0.01%, then 0.001% dithizone in $CHCl_3$ until the green colour of dithizone remains unchanged.

(Cobalt is determined from the original ammonia stock solution, but it has to be taken into consideration during analysis that cobalt is also extracted by dithizone.)

Determination of zinc

Shake the organic phase containing also zinc with 10 ml of 0.1 *M* HNO_3 in a separatory funnel for 1 minute. This way zinc is transferred into the aqueous phase. After separating the two phases, neutralize the aqueous solution with NH_4OH, add 5 ml of phosphate–citrate buffer and extract zinc with small portions of 0.001% dithizone. Continue extraction until the extracting solution remains green, but do not add this last portion to the combined organic phase. Dilute the solution to 10 ml with $CHCl_3$ (if the volume of the organic phase is greater, to 25 ml) and measure the optical density of the solution at 530 nm with a spectrophotometer in 1 or 5 cm cells. Use pure $CHCl_3$ as the reference solution. Prepare a calibration graph using 0.5—5 μg Zn. The optical density of 5 μg Zn in a 1 cm cell is 1.00.

Alternately, to remove excess dithizone shake the combined organic phase with 10 ml of 0.1% Na_2S. Then act as described.

Determination of copper

Re-extract copper from the solution retained after re-extracting zinc with 0.1 *M* HNO_3, with 2×5 ml of 6 *M* HCl. Completeness of re-extraction is indicated by the green colour of dithizone (cobalt also gets into the aqueous phase).

Discard the organic phase, neutralize the aqueous phase with NH_4OH (checked by indicator paper), then add 2 ml of NH_4OH to adjust the pH. Mask cobalt with 3 ml of 0.1% nitroso R-salt and add 5 ml of 0.5% sodium diethyldithiocarbamate. Extract the yellow copper diethyldithiocarbamate complex with 2×4 ml of CCl_4 and fill up the combined organic solution to 10 ml with CCl_4. Measure the optical density at 435 nm in 1 or 5 cm cells.

Reference solution: the extract of the reagent solutions with CCl_4. Optical density of 5 μg Cu in a 5 cm cell is 0.50.

Determination of cobalt

Use the stock solution obtained after precipitating metal hydroxides. Transfer 5—20 ml (according to the expected cobalt content) of stock solution to a 50 ml beaker, remove part of NH_4OH by boiling and acidify the solution with a few drops of 1 *M* HCl. Add 1 ml of 33% sodiumacetate (to adjust the pH), heat to boiling and add 0.5 ml of nitroso R-salt to form the cobalt complex. After a few minutes' standing add 0.5 ml 1 : 1 HNO_3 to decompose interfering complexes, heat to boiling and after cooling dilute to 25 ml in a volumetric flask and measure the optical density at 520 nm with a spectrophotometer, or with an S-50 filter on a Pulfrich photometer, in a 5 cm cell. Reference solution: solution of the reagent. Optical density corresponding to 10 μg Co is 0.50.

Determination of silver

Evaporate to dryness 0.5—2.0 ml (according to the expected silver content) of the ammonia stock solution with 2×1 ml HNO_3 in a beaker, dissolve the residue in some distilled water and transfer the solution into a test tube (volume should not exceed 6 ml). Then add 1.0 ml of 1 : 1 H_3PO_4, 1.0 ml of 0.1% solution of $MnSO_4$ and 2.0 ml 5% solution of $K_2S_2O_8$. Place the test tubes containing samples and standards into boiling water and keep there for 10 minutes. Then place the tubes into cold water in order to stop the reaction. The determination can be carried out a few minutes later by the simultaneous comparison method of BOGNÁR [38]. Prepare a calibration series with 0.00; 0.01; 0.03; 0.05; 0.10; 0.20; 0.30; 0.40 and 0.50 μg of silver. Sensitivity of the method is 10^{-4}%, the accuracy, however being limited due

to the way of evaluation. In the n. $10^{-4}\%$ range the result may be uncertain to a few units, while at n. $10^{-3}\%$ the error is less than a unit. (Photometry cannot be used due to the low absorption). A great advantage of the method is that if the stock solution is available, 25—30 determinations can be made in one day.

Experience concerning the application of the method

1. According to the authors, digestion with mineral acids does not result complete dissolution of cobalt and silver present in rocks, the loss being 20—60% in the case of silicate rocks. This makes digestion with hydrogen fluoride necessary. Small amounts of hydrogen fluoride do not interfere during analysis, but can also be removed by means of boric acid.

2. Humic acid interferes with the determination of cobalt and nickel. Hence, if soils are analyzed, samples have to be ignited at 5—600 °C prior to digestion.

3. If the sample contains only a small amount of iron, 20 mg Fe^{3+} has to be added to the solution before separation with ammonium hydroxide, which is a good carrier for coprecipitation of interfering ions (Pb^{2+}, etc.).

4. The procedure may be modified if not all the elements mentioned are to be determined. Thus *e.g.* if copper, nickel and zinc are to be determined, hydrogen fluoride is not necessary, aqua regia suffices.

In such cases the analysis can be simplified. In determining copper, only nickel has to be extracted with dimethylglyoxime; zinc can be masked with pyrophosphate, and cobalt with nitroso R-salt.

5. Since the method is sensitive, the reagents have to be of high purity and glassware and vessels should be thoroughly cleaned. The good quality of distilled water used is very important. Double distillation in a quartz equipment following deionization was found to be most effective for preparing water of high purity. Nitric acid was also purified by distillation, whereas hydrochloric acid and ammonium hydroxide by isothermal distillation. Buffers and masking solutions were purified with dithizone before use.

The solution of dithizone was freshly prepared every three–four days and stored in a dark bottle, since stray light may cause oxidation which leads to alteration of the absorption spectrum. In contrast to literature data, the purification of dithizone before use was found unnecessary.

The glassware used during analysis has to be cleaned thoroughly and rinsed with dithizone solution before use.

It is not advisable to allow glass vessels to stand in concentrated acids since this could lead to the exchange of ions with glass. It is, however, useful to store the vessels filled with water to reduce the amount of dust getting into them. Impurities, however, cannot be eliminated completely. For this reason a blank test has to be carried out with the reagents, which has to be taken into consideration in calculating the result of analysis. If this correction exceeds

10%, the analysis has to be repeated after cleaning glassware and purifying reagents. The most difficult task is to remove zinc to the desired extent.

6. The accuracy of the method is difficult to give reliably due to the danger of contamination. In the cases studied the error was found not to exceed ± 10—15% in the determination of Cu, Co, Ni and Zn at concentrations of the order of 10^{-3}%.

The method has been applied to the analysis of standard rock samples supplied by the Geological Institute in Berlin [39], the results of which are given in Table II.

Table II

Results of the analysis of rock samples supplied by the Geological Institute in Berlin by the method described

Designation of sample	Cu	Co	Ni	Zn
GM (granite)	16	4	8	50
BM (basalt)	48	28	38	90
TB (argillitic shale)	50	20	32	90
KS (limestone)	11	6	14	10

REFERENCES

1. Gottschalk, G.: Z. Anal. Chem. **194,** 321 (1963)
2. Алимарин, И. П., Фрид, Б. Й.: Количественный микрохимический анализ минералов и руд. Гос. Хим. Изд. Москва, 1961.
3. Соколов, Й. Ю.: Методическое руководство по определению микрокомпонентов в природных водах при поисках рудных месторождений. Москва 1961.
4. Vanitsh, T., Cserveniak, J., Belop, M.: Glasnik Khim. drustva Beograd **30,** 97. (1965)
5. Grillot, H., Béquiot, J., Boucette, C., Sina, C.: Méthodes d'analyse quantitative appliquées aux roches et aux prelèvements de la prospection géochimique. Mémoires du Bureau de Recherches Géologiques et Minier. No. 30.
6. Zelada, E. E.: An. Fac. Quim. y farmac. Univ. Concepcion. **12,** 1968 (1961)
7. Klooster van H. S.: J. Am. Chem. Soc. **43,** 746 (1921)
8. Пятницкий, И. В.: Аналитическая химия кобальта. Изд. Наука, Москва, 1965.
9. Степин, В. В., Силаева, Е. В., Курбатова, В. И., Ханова, Т. Ф., Барбан, Т. Л., Поносов, В. И.: Анализ цветных металлов. Изд. Металлургия, Москва, 1965.
10. Финкенштейн, Д. Б., Борецкая, В. А.: Методы анализа минерального сыря. Госгеолтехиздат. Москва, 1958.
11. Методы химического анализа минерального сыря. Вып. 10. Изд. Недра. Москва.
12. Ondrejcin, R. S.: Anal. Chem. **36,** 937 (1964)
13. Cheng, K. L., Brau, R. H.: Anal. Chem. **27,** 782 (1955)
14. Бусев, А. И., Иванов, В. М.: Ж. анал. хим. **18,** 208 (1963).
15. Столяров, К. П.: Ж. анал. хим. **26,** 452 (1961).
16. Young, R. S., Hall A. J.: Ind. Eng. Chem. Anal. Ed. **18,** 474 (1946)
17. Пешкова, В. М., Савастина, В. М.: Аналитическая химия никеля. Изд. Наука. Москва, 1966.

18. Чуйко, В. Т., Лотарева, В. И.: Зав. лаб. **17,** 1037 (1951).
19. Borges, P. A.: Rev. portug. quim. **6,** 63 (1964)
20. Monnier, D., Prodilom, G.: Anal. Chim. Acta **30,** 358 (1964)
21. Koter, M., Krauze, A., Bardziczka, B.: Chem. Analit. **10,** 1247 (1965)
22. Minczewski, J., Karczewska, B., Marczenko, Z.: Chem. Analit. **6,** 501 (1961)
23. Freiser, H., Morrison, G.: Ann. Rev. Nucl. Sci. **9,** 221 (1959)
24. Соколов, Й. Ю.: Методическое руководство по определению микрокомпонентов в приходных водах при поисках рудных месторождений. Госгеолтехиздат, Москва, 1961.
25. Исследование и разработка фотометрических методов для микроколичеств элементов в минеральном сыре. Алма-Ата, 1967.
25. Методы химического анализа минерального сыря. Вып. 8. Изд. Недра, Москва.
26. Пахомова, К. С., Волкова, Л. П., Горшков, В. В.: Бюлл. научно-техн. информ. гос. геол. ком-та. СССР 1965. № 1 (56).
28. Малюга, Д. П.: Докл. АН СССР **43,** 216 (1944).
29. Midzumo Hacharo: Japan Analyst **16,** 38 (1967)
30. Kunz, K.: Rudy i metala niezel **9,** 35 (1964)
31. Wojczechowska, J.: Rudy i metala niezel **13,** 75 (1968)
32. Леонтова, К. Д.: Сб. трудов гос. геол. ком. **19,** 706 (1952).
33. Morris, D. F. C., Killick, R. A.: Talanta **4,** 51 (1960)
34. Szabó, E., Elek, A., Ördögh, M., Upor, E.: KFKI Közlemények **12,** 355 (1964)
35. Nakagawa, H. M., Lakin H. W.: U. S. Geol. Surv. Profess. Paper, 1965, No 525, 172
36. Rankama, K., Sahama, T. G.: Geochemistry. Chicago, 1950
37. Upor, E., Rónai, Á., Nagy, Gy.: Acta Chim. Acad. Sci. Hung. **61,** 1 (1969)
38. Bognár, J.: Microchim. Acta, **1963,** 397
39. Schindler, R.: Z. f. Angew. Geologie **12,** 188 (1966)

Margit Görbicz; Kazincbarcika, Pollack M. u. 28. Hungary
Endre Upor; Pécs, 39-es dandár út 3/a. Hungary.

Acta Chimica Academiae Scientiarum Hungaricae, Tomus 66 (4), pp. 383—394 (1970)

PREPARATION, X-RAY, DERIVATOGRAPHIC AND INFRARED STUDY OF ALUMINIUM-SUBSTITUTED GOETHITES

K. JÓNÁS* and K. SOLYMÁR**

*(*Institute of General and Inorganic Chemistry, University of Chemical Industries, Veszprém, Hungary, and **Research Institute for Metal Industry, Budapest)*

Received August 15, 1969

Goethites of different aluminium content (alumo-goethites) have been prepared by ageing iron and aluminium hydroxides together at 40—50 °C. Under these conditions a maximum of 21—23 mole% aluminium substitution could be attained. The aluminium content of the samples was determined by chemical analysis and by X-ray diffraction method elaborated on the basis of the gradual shift of the goethite reflections on the action of the aluminium substitution. The dehydration temperature of both synthetic and natural goethites was found to increase, while the extinction coefficient of infrared bands to decrease, with increasing aluminium substitution. The wave number of the infrared bands also depends on the aluminium content. This phenomenon can be used, after calibration, for the determination of aluminium in alumo-goethites.

α-FeOOH (goethite) and α-AlOOH (diaspore) are isomorphous minerals, therefore iron and aluminium can substitute each other in the lattice. There is a number of papers in the literature which deal with the investigation of aluminium-containing natural and synthetic goethites (henceforth, alumo-goethites). The most important papers are those by SCHWERTMANN *et al.* [1, 2, 3], WEFERS [4, 5], GLEMSER [6], SCHELLMANN [7] and THIEL [8]. According to the authors mentioned, goethite and alumo-goethite can be prepared by precipitating the hydroxides with ammonia from aqueous solution of an iron salt, or from the mixture of an iron and aluminium salt, and ageing the formed primary amorphous hydroxides. The conditions of ageing, first of all the pH and temperature, greatly influence the properties of the product.

Views concerning the mechanism of ageing are often contradictory.

It is generally accepted that the transformation

$$Fe_2O_3.x\,H_2O(Fe(OH)_3) \rightarrow \alpha-FeOOH + H_2O$$

can only occur if iron enters in the solution, *i.e.* if $FeOH)_4^-$ intermediate is formed. This mechanism is supported by the significant role of the OH^- concentration in the aged suspension on the formation of the goethite.

The views are less uniform as to whether the transformation

$$\alpha-FeOOH \rightarrow \alpha-Fe_2O_3$$

takes place in solid phase or in solution.

A review of the most important results on the extent of aluminium substitution in natural goethites is given by WEFERS [5]. On the basis of the literature one can conclude that natural goethites generally contain some aluminium. The extent of substitution however only rarely exceeds 20 mole%, being in most cases about 10 mole%. Higher than 20 mole% substitution was found by BALKAY and BÁRDOSSY [9] in laterites from Guinea. The upper limit of the aluminium substitution has been given by THIEL [8] as 33 mole%. This value has been attained in hydrothermally aged synthetic alumo-goethites. There is no reference in the literature for such a high degree of aluminium substitution in the case of natural samples.

Aluminium incorporated in the goethite lattice is not dissolved during the industrial treatment of the goethite-containing bauxites and so it gets in the red mud. In chemical analysis, however, this aluminum is also determined as part of the total aluminium oxide content. Thus chemical analysis does not give information about the amount of aluminium which is present in the goethite and cannot be recovered during the usual bauxite treatment processes. There is demand therefore for a method by which the aluminium content of the goethite can be determined.

The X-ray diffraction data published by THIEL [8] concerning the gradual shift of the goethite reflections caused by the aluminium can be used for this purpose. The authors of the present paper have reproduced the results of THIEL using synthetic and natural samples [10]. On the basis of these calibration graphs about 50 Hungarian bauxites have been investigated. It was found that the amount of aluminium present in the goethite lattice increases quadratically with the original goethite content of the bauxite in the case of Hungarian samples [11].

It has been observed by BALKAY and BÁRDOSSY [9] that the dehydration temperature of the laterites is shifted to higher values when aluminium is incorporated in the lattice. The authors of the present paper have already mentioned [12] that the wave number of the infrared absorption bands of alumo-goethites differ from those of pure goethite. These two phenomena were the starting points of the present work aimed at finding new methods for determining the aluminium in alumo-goethites.

Experimental

Preparation of goethite and alumo-goethite

The hydroxides were precipitated with ammonia under vigorous stirring from cold solutions containing $Fe(NO_3)_3 \cdot 9\ H_2O$ and $Al(NO_3)_3 \cdot 9\ H_2O$ in different proportions. The slurry was allowed to stand 24 hours, then washed ammonia-free with water. A suitable amount of 1 *M* KOH solution was then added to the precipitate. The KOH ageing solution also contained some dissolved aluminium salt (except in cases when pure goethite was required). According to THIEL [8], the aluminium content of the ageing solution prevents the sudden dissolution

of the aluminium from the iron hydroxide, and so promotes the incorporation of aluminium into the goethite. On the basis of preliminary experiments the concentration of the suspension was adjusted so as to ensure 30—50 ml liquid for every 10^{-2} mole of Al + Fe hydroxide. The suspension was then aged for 150 hours on steam bath. Water was added at intervals to compensate the evaporated amount. During ageing the deep colour of the amorphous iron hydroxide changed gradually, and finally the typical yellowish-brown goethite colour appeared. The shade of that colour depended greatly on the aluminium and hematite content, being the 'darker' the more aluminium was present, and the more hematite has been formed beside the goethite. The darkening effect of the aluminium is explicable by morphology changes. Practically hematite-free series was obtained by keeping the temperature below 50 °C during ageing, and avoiding even temporary concentration of the suspension. Free $Al(OH)_3$ possibly present was washed out from the end product with warm 1 *M* KOH. After washing to neutrality with water the samples were dried on air at 40—50 °C. Drying at higher temperatures led to darkening of the samples, *i.e.* to goethite → hematite transformation.

Derivatograms were taken on a MOM Paulik—Paulik—Erdey-type derivatograph using 250 mg sample and 5 °C/min heating rate. Infrared spectra were recorded on Zeiss UR 10 spectrophotometer in KBr discs. The aluminium content of samples was determined by X-ray diffraction; using Müller Mikro 111 X-ray generator and a Philips goniometer, with CuKα radiation and discrimination. The results of X-ray diffraction measurements were checked by chemical analysis.

Results and discussion

It has been found during the preparation of the alumo-goethites that aluminium was incorporated into the lattice even if pure, aluminium-free iron(III) hydroxide has been aged in an aluminium-containing KOH solution. This supports the assumption that ageing is going through dissolution and reprecipitation of the iron hydroxide. Generally the pH and temperature are mentioned as the most important ageing parameters. Our experiments proved that the concentration of the aged suspension (the solid–liquid ratio) also has a great role. The more concentrated the suspension, the more hematite was formed, under otherwise identical conditions. Practically hematite-free goethite could only be prepared in dilute suspensions of suitable concentration. This seems to support the assumption of the authors that the goethite → hematite transformation is a solid-phase dehydration process. As the concentration of suspension increases, that of the dissolved $Fe(OH)_4^-$ decreases, and the solid phase α-FeOOH → α-Fe_2O_3 reaction comes into prominence.

This effect was even more pronounced in aluminium-containing suspensions. In this case the strongly alkaline ageing solution dissolved a large amount of aluminium hydroxide at the beginning of ageing, thus the solution was saturated with $Al(OH)_4^-$ ions. This led to a reduction of the solubility of iron. In this case the reaction is even more shifted towards solid-phase dehydration, *i.e.* hematite formation. In samples containing aluminium, the amount of the formed hematite was always higher than in aluminium-free ones. The properties of the product depend strongly on the preparation conditions and the reproduction is difficult even at rigorously identical conditions. On the basis of several ageing experiments a relationship was found between the iron-aluminium ratio in the initial amorphous hydroxide (taking also the aluminium content of the ageing solution into consideration) and the amount of aluminium

incorporated into the goethite lattice. It has been established that a relatively large excess of aluminium is needed in the primary amorphous hydroxide for the introduction of even small amounts in the goethite lattice. Above a certain aluminium excess however the degree of substitution approaches a limiting value (Fig. 1). This limit was 21—23 mole% in the case of samples aged at atmospheric pressure. This is in agreement with data reported in the literature on natural goethites, according to which the aluminium substitution in these rarely exceeds 20 mole%. Higher substitution — *e.g.* with some laterites — may be accounted for by the effect of higher pressures, as observed on samples aged by THIEL hydrothermally.

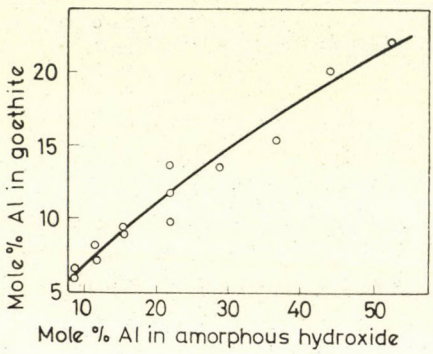

Fig. 1. Amount of aluminium incorporated into goethite lattice, as a function of the aluminium content of aged amorphous hydroxide

X-ray diffraction studies on alumo-geoethites

The aluminium content of the alumo-goethite samples was determined using diagrams given by THIEL based on the shift of the d_{130}, d_{021}, d_{111} and d_{140} goethite reflections. In Fig. 2 the shift of the d_{111} reflection, which is most suitable for the determination, is plotted as a function of the aluminium substitution. The curve was drawn using THIEL's data [8] (the circlets on the graph). The reflections of the synthetic samples corresponding to the aluminium oxide content determined by chemical analysis are marked with triangles. As shown by the figure the results got from the THIEL graph agree well with those of the chemical analysis up to an about 15 mole% aluminium content. In the case of samples containing more aluminium the chemical analysis yields higher aluminium content (with about 4—5 mole%), than that obtained from THIEL's curve. It has been found that the surplus aluminium is present as less crystalline, X-ray amorphous free aluminium hydroxide. Unfortunately, the aluminium hydroxide cannot be washed out completely from goethites aged in the presence of large excess of aluminium, since the temperature of the alkali wash-

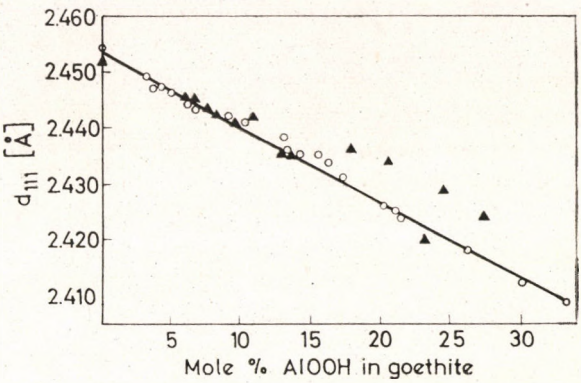

Fig. 2. Shift of the d_{111} goethite reflection as a function of aluminium content. Notations: ○ THIEL's data; ▲ data measured by the authors

ing solution cannot be raised above 40—50 °C without the danger of a subsequent goethite → hematite transformation. Accordingly, THIEL's diagrams were accepted and used for determining the degree of aluminium substitution. Chemical and X-ray analysis data of hematite-free synthetic samples are summarized in Table I. X-ray diagrams of some synthetic samples are presented in Fig. 3.

Table I

The aluminium content of synthetic alumo-goethites

(Chemical analysis and X-ray diffraction data)

Mole% AlOOH (chemical analysis)	d_{130} Å	Substitution (mole%)	d_{021} Å	Substitution (mole%)	d_{111} Å	Substitution (mole%)	d_{140} Å	Substitution (mole%)	Substitution (mole% Al) Average of d_{130}, d_{021} d_{111} and d_{140}
0	2.694	—	2.584	—	2.452	—	2.188	—	∅
6.3	2.690	5.3	2.577	5.5	2.446	5.8	2.184	7.5	6.0
6.8	2.688	6.8	2.576	6.1	2.445	6.3	2.184	7.5	6.7
7.7	2.687	7.5	2.576	6.1	2.444	7.3	2.183	8.2	7.3
8.3	2.687	7.5	2.574	7.4	2.443	8.0	2.182	9.3	8.1
9.3	2.687	7.5	2.573	8.0	2.4415	9.0	2.182	9.3	9.0
9.8	2.685	9.0	2.573	8.0	2.4415	9.0	2.180	10.8	9.2
11.0	2.684	10.0	2.570	9.8	2.442	8.8	2.181	10.0	9,6
12.8	2.680	12.5	2.564	13.5	2.436	13.3	2.175	15.1	13,6
13.4	2.682	11.1	2.567	11.7	2.436	13.3	2.179	11.6	11.9
17.8	2.680	12.3	2.561	15.0	2.436	13.0	2.177	13.5	13.4
20.3	2.677	14.5	2.559	16.8	2.434	14.3	2.174	15.7	15.3
24.4	2.669	20.8	2.549	22.4	2.429	18.5	2.170	19.3	20.2
27.2	2.670	20.0	2.547	23.5	2.424	22.1	2.166	22.6	22.0

The comparison of X-ray diagrams of synthetic and natural samples proves, that the synthetic ones are always less crystalline. In this respect the BET specific surface areas are also of interest. The surface area of natural goethites is around 1—2 m^2/g, while about 30 m^2/g BET area has been measured both with aluminium-free and aluminium containing synthetic samples. Similar result was attained (about 27 m^2/g) if the natural occurrence contained great quantity of aluminium (*i.e.* Guinean laterite).

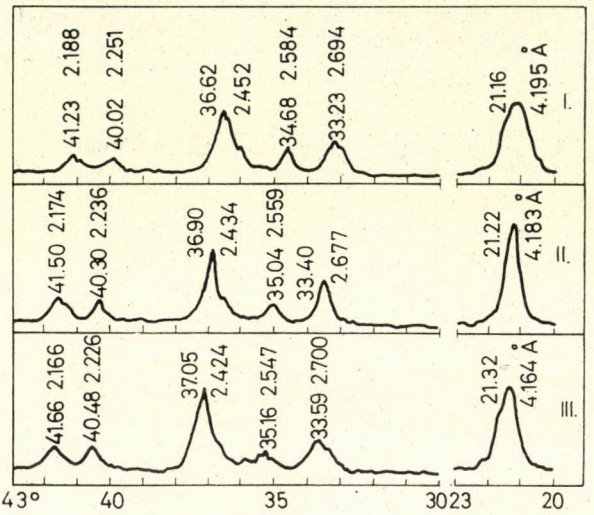

Fig. 3. X-ray diffractogram of synthetic goethite and alumo-goethite. Degree of aluminium substitution: I: 0; II: 15.3; III: 22.0 mole%

Thermal properties of goethites and alumo-goethites

The thermal behaviour of goethites has so far been studied mostly for practical purposes, *e.g.* for determining the goethite in bauxites and red muds. A general treatment of the problem is given by MACKENZIE [13]. According to this the dehydration of α-FeOOH to hematite occurs in one step, indicated by a strong and sharp endothermic peak on the DTA curve. The peak temperature greatly depends on the degree of crystallinity and grain size of the sample. The derivatograms show that the peak of less crystalline, fine-grain synthetic goethites is at about 300 °C, while natural goethites undergo dehydration at considerably higher temperatures. Papers available in the literature are mainly concerned with the effect of grain size, and do not take the possibility of the aluminium-substitution and the effect of this on the peak temperature into consideration. Taking into account, that in addition that the substitution itself causes a shift of the dehydration temperature, it influences the grain

size too, much more importance is to be attached to this phenomenon. It must be remarked that the grain size of alumo-goethites is always smaller than that of pure goethites produced under the same conditions.

The DTA curves of some synthetic and natural alumo-goethites of different aluminium content are presented on Figs 4 and 5. We found that pure, aluminium-free synthetic goethites undergo dehydration in the range of 290—

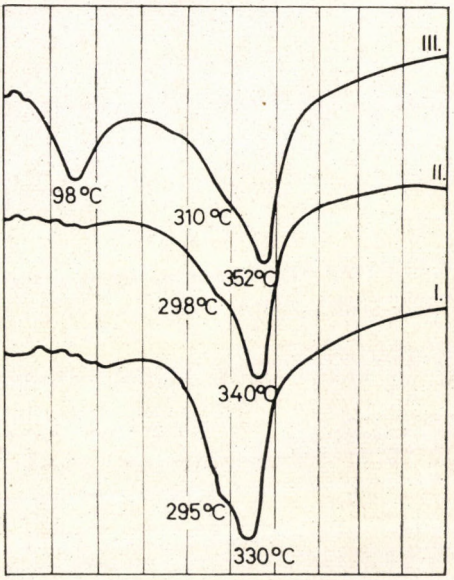

Fig. 4. DTA curves of synthetic alumo-goethites. Degree of aluminium substitution: I: 9.6; II: 13.4; III: 22.0 mole%

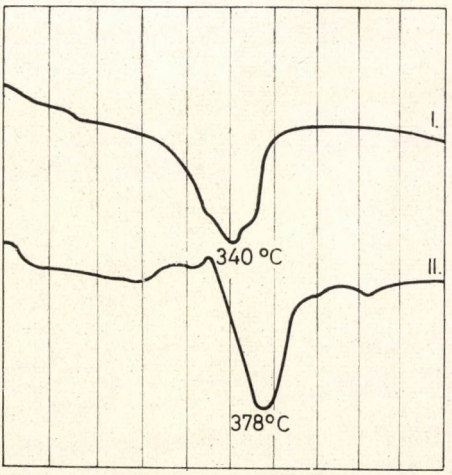

Fig. 5. I: DTA curve of natural goethite (Al-substitution: 1—2 mole%). II: DTA curve of laterite (Al-substitution: 27 mole%)

310 °C, or even at lower temperatures (*cf.* Table II). The dehydration of synthetic alumo-goethites took place between 320 and 360 °C. There appeared on the endothermic peak a shoulder at about 280—305 °C, probably due to some gibbsite which could not be removed by washing.

The derivatograms prove the observation of BALKAI and BÁRDOSSY and show the peak-modifying effect of the aluminum substitution also on natural occurrences.

Some other smaller endothermic peaks between 80—220 °C indicate the loss of non-stoichiometric water. It was found that the amount of that water increases with increasing hematite content. This is explicable by the fact that under ageing conditions favourable for hematite formation, more amorphous (less crystalline) sample is formed.

There is not such an unequivocal relation between the dehydration temperature and aluminium content of the goethite, which would allow a quantitative aluminium determination. Many other hardly controllable parameters have also role. In any case, the possible effect of the aluminium substitution on the goethite peaks must be taken into consideration in the derivatographic analysis of bauxites, which often contain alumo-goethite.

The infrared spectra of goethites and alumo-goethites

The most intensive goethite bands are those corresponding to the Fe—O—H deformation at about 800 and 900 cm^{-1}. The O—H stretching band is broad and flat, thus it cannot even be used for qualitative purposes. There are no papers in the literature dealing with the effect of aluminium substitution on the goethite bands. As mentioned, the present authors have already referred to the gradual frequency shift of goethite deformation bands with increasing aluminium substitution [12]. This phenomenon is now studied systematically. The wave number and absorbance $\left(E = \lg \frac{I}{I_0}\right)$ of the bands at the band maximum were determined. In hematite containing samples the exact goethite content was determined by X-ray analysis, and so ε, the extinction coefficient (E/g goethite) has been calculated in each case. The data are summarized in Table II. It can be seen, that ε decreases with increasing original hematite content. This is explicable by the fact already mentioned, that under conditions favourable for hematite formation less crystalline goethite was formed. Beside the influence of the hematite, the aluminium substitution causes much greater reduction in the specific absorbance, due probably to the presence of less ordered crystalline structure. In Fig. 6, the absorption coefficient of the 900 cm^{-1} band is plotted against the aluminium content. The decrease of ε is approximately proportional to the amount of aluminium present in goethite for samples obtained under identical conditions, *i.e.* having

Table II

Sample number	Hematite content (w%)	Dehydration peak (°C)	Wave number of the band around 900 cm^{-1} (cm^{-1})	E/g goethite (ε)	Al content (mole%) (X-ray anal. data)
		Synthetic goethites			
I	0	310	893	171	0
II	0	265 !	888	233	0
III	45.5	305	892	148	0
IV	51.3	305	892	118	0
		Synthetic alumo-goethites			Series A
1	4.8	320	903	180	4
2	7.5	340	913	84.4	11
3	35.0	338	918	75.4	13
4	20.5	340	920	52.8	14
5	7.5	336	922	53	15
					Series B
6	0	330	900	191	9.6
7	0	340	913	136	13.4
8	0	343	918	118	15.3
9	0	343	926	101.5	20.2
10	0	352	930	83.5	22.0
					Series C
11	0	300	896	232	6.0
12	0	300	896	223	6.7
13	0	310	898	204	7.3
14	0	305	898	204	8.1
15	0	310	900	189	9.0
16	0	312	900	200	9.2
17	0	324	910	133	11.9
18	0	325	910	136	13.6
		Natural geoethites			
Goethite		340	899	84	1—2
Laterite		378	945	46	27.0

similar structure. Products got from different ageing processes can be characterized by parallel curves. Consequently, the change of the extinction coefficient, like that of the dehydration peaks, cannot be used for the determination of aluminium substitution. The results depend on a number of factors, such as grain size, hematite content, etc.

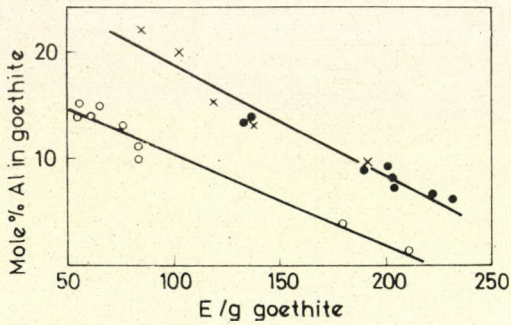

Fig. 6. Change of the extinction coefficient calculated at the 900 cm^{-1} goethite band maximum as a function of aluminium substitution in synthetic alumo-goethites. Notations: ○ Table II, Series A; × Table II, series B; ● Table II, Series C

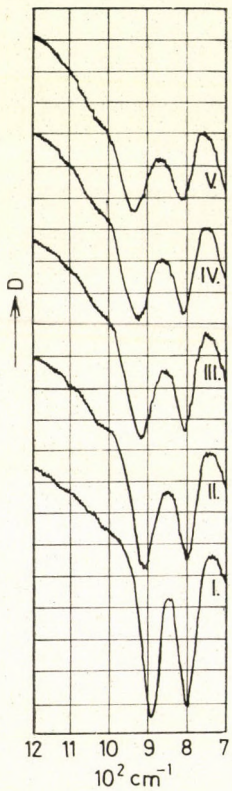

Fig. 7. Infrared absorption of synthetic goethite and alumo-goethite in the 700—1200 cm^{-1} range in KBr discs (sample weight 2.5 mg). Aluminium content of the samples are: I: ∅; II: 13.4; III: 15.3; IV: 20.2; V: 22.0 mole%

The frequency shift of the goethite band maxima — especially that of the 900 cm^{-1} band — is more suitable for aluminium determination, as it is in linear relation with the degree of aluminium substitution and is less sensitive to morphological changes (*cf.* Figs 7 and 8). The calibration curve presented on Fig. 8 can be used for the analysis of synthetic and natural alumo-

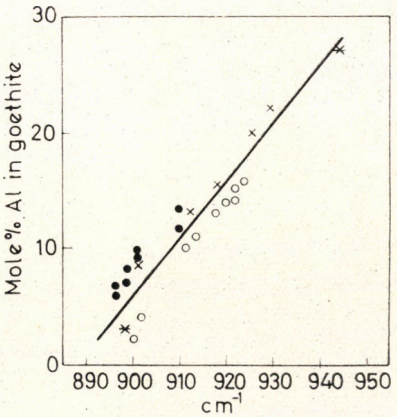

Fig. 8. The shift of the wave number of the 900 cm^{-1} goethite band with aluminium content. Notations: same as in Fig. 6. Natural samples (goethite and laterite) are marked by*

goethites. Unfortunately, the goethite band in question is in a region where other bauxite components (first of all kaolinite and gibbsite) also have absorption. So the proposed method cannot be used for determining goethite or alumo-goethite in bauxite. In this respect one has to rely only on X-ray analysis data.

In red mud which does not contain the above mentioned interfering minerals, the strong absorption of sodalite and cancrinite formed during the bauxite processing disturbs the 900 cm^{-1} goethite band. In that case the frequency shift of the other Fe—O—H deformation band around 800 cm^{-1} might serve for aluminium determination. The effect of the aluminium substitution on this band is much less pronounced, so the analysis is to be used together and as a support of X-ray method.

REFERENCES

1. SCHWERTMANN, U.: Z. anorg. allg. Chem. **298,** 337 (1959)
2. SCHWERTMANN, U., FISCHER, W. R.: Z. anorg. allg. Chem. **346,** 137 (1966)
3. SCHWERTMANN, U.: Z. Pflanzenernähr., Düng., Bodenkunde **108,** 37 (1965)
4. WEFERS, K.: Ber. dtsch. keram. Ges. **43,** 677, 703 (1966)
5. WEFERS, K.: Z. Erzbergbau Metallhüttenwes. **20,** 13, 71 (1967)
6. GLEMSER, O.: Ber. dtsch. chem. Ges. **70,** 2117 (1937)

7. SCHELLMANN, W.: Chem. d. Erde **20**, 104 (1959—60)
8. THIEL, R.: Z. anorg. allg. Chem. **326**, 70 (1963)
9. BALKAY, B., BÁRDOSSY, GY.: Földtani Közlöny *XCVII*, 91 (1967)
10. JÓNÁS, K., SOLYMÁR, K.: V. Dunántúli Analitikai Konferencia, Veszprém, 1969
11. SOLYMÁR, K.: Bauxitföldtani Konferencia, Budapest, 1969
12. JÓNÁS, K., SOLYMÁR, K.: IV. Dunántúli Analitikai Konferencia, Sopron, 1968
13. MACKENZIE, R. C.: The Differential Thermal Investigation of Clays. London, Mineralogical Society, 1957

Klára JÓNÁS
Károly SOLYMÁR } Veszprém, Schönherz Z. u. 12. Hungary.

Acta Chimica Academiae Scientiarum Hungaricae, Tomus 66 (4), pp. 395–406 (1970)

UNTERSUCHUNG DER IONISATION VON METALLEN UND METALLIONENNEUTRALISATION MIT DER ROTIERENDEN RING-SCHEIBEN-ELEKTRODE, V

UNTERSUCHUNG DER ANODISCHEN AUFLÖSUNG VON KUPFER IN SAUREN SULFATLÖSUNGEN

L. KISS und J. FARKAS

(Lehrstuhl für Physikalische Chemie und Radiologie der L. Eötvös Universität, Budapest)

Eingegangen am 8. Juli 1969

Zur Kontrolle der Zusammenhänge, über die in einer früheren Mitteilung [1] berichtet wurde, untersuchten die Autoren den Mechanismus des sich an der Kupferelektrode in sauren Sulfatlösungen abspielenden Anodenvorganges mit Hilfe der rotierenden Ring-Scheibenelektrode. Die bei der anodischen Auflösung des Kupfers erhaltenen Versuchsergebnisse können mit den für einen stufenweisen Mechanismus abgeleiteten Zusammenhängen gut gedeutet werden. Dies beweist, daß sich die anodische Auflösung des Kupfers unter den gegebenen Versuchsumständen stufenweise abspielt.

In einer unserer früheren Mitteilungen [1] ist gezeigt worden, daß der Ionisations- und Neutralisationsmechanismus von Metallen mit Hilfe der rotierenden Ring-Scheibenelektrode untersucht werden kann. In der vorliegenden Arbeit wollen wir uns zwecks Kontrolle der beschriebenen Methode mit der experimentellen Untersuchung der anodischen Auflösung von Kupfer in saurem, sulfathaltigem Medium befassen. Die Wahl des Kupfers für die gegebene Aufgabe erfolgte aus folgenden Gründen: Nach den Untersuchungen von MATTSON und BOCKRIS [2] sowie BROWN und THIRSK [3] geht die Auflösung des Kupfers in zwei aufeinander folgende Einelektronen-Schritten vor sich. MATTSON und BOCKRIS [2] folgern aus dem Neigungswinkel der Polarisationskurven auf einen Stufenmechanismus. BROWN und THIRSK [3] hingegen verwendeten eine kupferne rotierende Scheibenelektrode und folgerten aus dem bei den Messungen auftretenden Effekt auf einen Stufenmechanismus. DIMITREV, MURTAZINA und KOLOSOV [4] bestimmten die Impedanz der Kupferelektrode und gelangten auf Grund der Ergebnisse zu der Schlußfolgerung, daß die Ionisation und Neutralisation des Kupfers in sauren, sulfathaltigen Lösungen nach einem Stufenmechanismus verläuft. LOSEW, SRIBNÜJ und MOLODOW [5] gelangten zum gleichen Ergebnis auf Grund der Analyse der Polarisationskurven bei der Untersuchung von Kupferamalgamen in sauren Perchloratlösungen.

Hingegen herrscht in der Literatur der Hydrometallurgie und Galvanostegie des Kupfers selbst in der letzten Zeit die Auffassung [6, 7], daß sich bei

der anodischen Auflösung des Kupfers in sulfathaltigem Medium zwei parallele Vorgänge abspielen, wobei in dem einen Vorgang Cu(I), im anderen parallelen Vorgang mit dem Übergang von zwei Elektronen in einem einzigen Schritt Cu(II)Ionen gebildet werden.

Auf Grund der obigen Ausführungen glauben wir, daß sich die Untersuchung der anodischen Auflösung des Kupfers zur Kontrolle der von uns ausgearbeiten Methode [1] eignet, und die Messungen mit der rotierenden Ring-Scheibenelektrode weitere Beiträge zur Entscheidung jener Frage liefern werden, nach welchem Mechanismus die anodische Auflösung des Kupfers unter den gegebenen Umständen verläuft.

Im Falle eines stufenweisen Mechanismus spielen sich an der Kupferelektrode fie folgenden Vorgänge ab:

$$Cu \underset{k_{k_1}}{\overset{k_{a_1}}{\rightleftharpoons}} Cu^{+} + e^{-} \qquad \text{(I)}$$

$$Cu^{+} \underset{k_{k_2}}{\overset{k_{a_2}}{\rightleftharpoons}} Cu^{++} + e^{-} \qquad \text{(II)}$$

In diesem Fall kann die Polarisationskurve — wie bereits früher gezeigt worden ist [1] — durch den folgenden Zusammenhang beschrieben werden, falls die Konzentration des Zwischenproduktes Cu^{+} in der Lösung Null ist (1):

$$i = k_{a_1} \frac{X_1 + \dfrac{2k_{a_2}}{k_{k_2}}}{X_1 + k_{k_1} + \dfrac{k_{a_2}}{1 + \dfrac{k_{k_2}}{X_2}}} - \frac{b_\infty}{\dfrac{1}{X_2} + \dfrac{1}{k_{k_2}}} \frac{X_1 + 2k_{k_1}}{X_1 + k_{k_1} + \dfrac{k_{a_2}}{1 + \dfrac{k_{k_2}}{X_2}}} \qquad (1)$$

wobei b_∞ die Konzentration der Cu^{++}-Ionen im inneren der Lösung bedeutet, während

$$X_i = 0{,}62\, F D_i^{2/3} \nu^{1/6} - \omega^{1/2} \qquad i = 1{,}2\,. \qquad (2)$$

F ist die Faradaysche Zahl, D_i die Diffusionskonstante der Cu^{+}- oder Cu^{++}-Ionen, ω die Winkelgeschwindigkeit der rotierenden Elektrode, ν die kinematische Viskosität der Lösung, k_{a_1}, $k_{k_1} \cdot k_{a_2}$, k_{k_2} sind die Geschwindigkeitskonstanten der Teilvorgänge. Zwischen den Geschwindigkeitskonstanten und dem Elektrodenpotential φ besteht der folgende Zusammenhang:

$$k_{a_i} = k'_{a_i} \exp\left(\frac{z_i \alpha_i F \psi}{RT}\right) \qquad (3)$$

$$k_{k_i} = k'_{k_i} \exp\left(-\frac{z_i(1-\alpha_i) F \varphi}{RT}\right) \qquad i = 1{,}2\,, \qquad (4)$$

wo k'_{a_i} und k'_{k_i} vom Potential unabhängige Konstanten, α_i den Übertrittsfaktor, z_i die Zahl der in der entsprechenden Reaktion übertretenden Elektronen bedeuten, während die übrigen Bezeichnungen die üblichen sind.

Falls die Ionisation des Kupfers auf dem Wege (I)—(II) verläuft, können die Cu^+-Ionen laut Gl. (II) an der Ringelektrode oxydiert werden. Der Grenzstrom dieses Vorgangs ist [1]:

$$i_h = N \frac{i + \dfrac{2b_\infty}{\dfrac{1}{X_2} + \dfrac{1}{k_{k_2}}}}{1 + \dfrac{2k_{a_2}}{X_1 + \dfrac{X_1}{X_2} k_{k_2}}}, \tag{5}$$

wo N der geometrische Faktor der Elektrode ist.

Nach der anderen Vorstellung, d. h. wenn die Ionisation des Kupfers in zwei parallelen Schritten verläuft, spielen sich an der Elektrode die folgenden Vorgänge ab:

$$Cu \underset{k_{k_1}}{\overset{k_{a_1}}{\rightleftarrows}} Cu^+ + e \tag{I}$$

$$Cu \underset{k_{k_3}}{\overset{k_{a_3}}{\rightleftarrows}} Cu^{2+} + 2e, \tag{III}$$

wo k_{a_3}, k_{k_3} vom Potential abhängige Reaktionsgeschwindigkeits-Konstanten sind, die durch Gl. (3) und (4) gedeutet werden ($i = 3$)*.

Nun ergibt sich für die Polarisationskurve des Ionisationsvorganges, falls die Konzentration des Zwischenproduktes im Inneren der Lösung Null ist, der folgende Ausdruck:

$$i = \frac{k_{a_3}}{1 + \dfrac{k_{k_3}}{2X_2}} + \frac{k_{a_1}}{1 + \dfrac{k_{k_1}}{X_1}} + \frac{b_\infty}{\dfrac{1}{2X_2} + \dfrac{1}{k_{k_3}}}. \tag{6}$$

Die Deutung von X_1 und X_2 ist durch Gl. (2) gegeben. Der Grenzstrom der weitern Oxydation des im Laufe der Reaktion (I) gebildeten Cu^+:

$$i_h = N \frac{k_{a_1}}{1 + \dfrac{k_{k_1}}{X_1}}. \tag{7}$$

* Falls die anodische Auflösung des Kupfers über den Weg (I)—(III) verläuft, spielt sich laut Annahme der Vorgang (II) nicht ab. Falls jedoch auch diese Möglichkeit berücksichtigt wird, würde sich der Vorgang (II) wegen des hohen Austauschstromes in Vorgang (I) und des verhältnismäßig negative Standardpotentials Cu^+/Cu^{++} mit großer Geschwindigkeit beim gegebenen Potential abspielen, so daß Vorgang (III) neben (I) und (II) nur wenig ins Gewicht fiele, und sich ein Stufenmechanismus ergeben würde. Dies kann auch im Gegensatz zur Meinung anderer Autoren [6] derart gewertet werden, daß auch auf Grund von thermodynamischen Überlegungen der Stufenmechanismus wahrscheinlicher ist.

Wie aus den Gleichungen (1) und (5) sowie (6) und (7) ersichtlich ist, ergibt sich für die Polarisationskurve sowie für den am Ring meßbaren Grenzstrom ein anderer Ausdruck im Falle des stufenweisen Mechanismus, als im Falle eines in parallelen Schritten verlaufenden Vorgangs. Im Besitze entsprechender Versuchsdaten kann also entschieden werden, nach welchem Mechanismus die Ionisation des Kupfers verläuft.

Versuchsergebnisse und Diskussion

Die Messungen wurden in Lösungen von 5,0 *n* H_2SO_4 + x Mol $CuSO_4$ vorgenommen. Zur Bereitung der Lösungen wurde zweimal destilliertes Wasser, *p. a.* H_2SO_4 und *p. a.* $CuSO_4 \cdot 5\ H_2O$ verwendet. Als Scheibenelektrode diente auf Kohle elektrolytisch abgeschiedenes Kupfer, die Ringelektrode wurde aus Kohlenpaste bereitet, die übrigen Teile der Elektrode aus Teflon. Die Versuche wurden in einer von Sauerstoff sorgfältig befreiten Stickstoff-Atmosphäre vorgenommen.

Die verwendete Apparatur stimmte mit der in einer früheren Mitteilung [8] beschriebenen überein. Die Elektrodenpotentiale wurden mit einer Normalkalomel-Vergleichselektrode gemessen, und die im folgenden angegebenen Elektrodenpotentiale sind auf diese Kalomelelektrode bezogene Werte.

Abb. 1 zeigt die an dem aus Elektrolytkupfer verfertigten Scheibenteil der rotierenden Ring-Scheibenelektrode bestimmten Potential-Stromstärke-Zusammenhänge bei drei verschiedenen Drehzahlen der Elektrode, wenn die Kupfersulfat-Konzentration in der Lösung Null ist (der Wert von b_∞ in den vorangehenden Gleichungen ist Null). Wie ersichtlich, verschieben sich die erhaltenen Kurven mit wachsender Drehzahl in negativer Richtung und werden steiler. Diese Änderung der Potential-Stromstärke-Kurven bei Änderung der Drehzahl der Elektrode weist darauf hin, daß Diffusions- und Übertrittspolarisation gleichzeitig auftritt und der Einfluß der Diffusion mit wachsender Drehzahl abnimmt.

Abb. 2 zeigt den Grenzstrom der Oxydation (i_h) der bei der Auflösung der Kupfer-Scheibenelektrode mit einem anodischen Strom i gebildeten Cu^+-Ionen zu Cu^{++}-Ionen, als Funktion von dem anodischen Polarisationsstrom i. Die an der Ringelektrode meßbaren i_h Grenzströme sind im Verhältnis zum Polarisationsstrom i klein. Dies zeigt, daß nur ein vernachlässigbar kleiner Teil des anodischen Polarisationsstromes der Scheibenelektrode für die Erzeugung von Cu^+-Ionen verbraucht wird.

Auf Grund der in Abb. 1 und 2 angeführten Versuchsergebnisse können in den vorangehend aufgeschriebenen Zusammenhängen die folgenden Vereinfachungen gemacht werden:

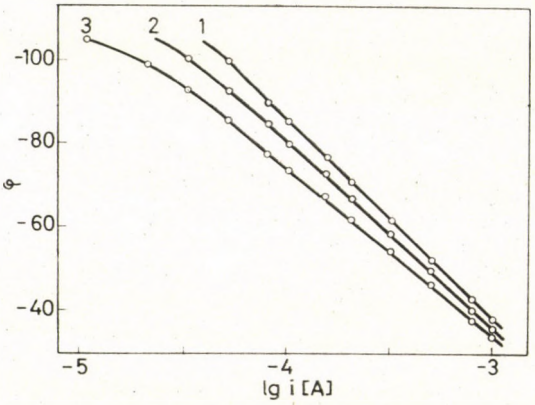

Abb. 1. Die an der elektrolytischen Kupferelektrode bestimmten φ — lg i Zusammenhänge bei verschiedenen Elektrodendrehzahlen. 1. $f = 6500\ \text{min}^{-1}$; 2. $f = 810\ \text{min}^{-1}$; 3. $f = 140\ \text{min}^{-1}$

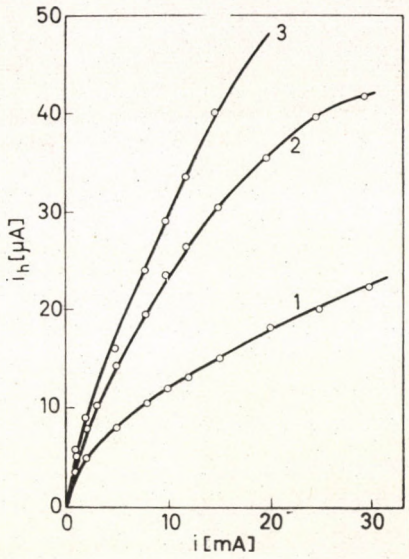

Abb. 2. Der Grenzstrom i_h der Oxydation von Cu^+-Ionen zu Cu^{++}-Ionen als Funktion des anodischen Polarisationsstromes der Scheibe. 1. $f = 350$ min^{-1}; 2. $f = 2120$ min^{-1}; 3. $f = 6500$ min^{-1}

Falls ein stufenweiser Mechanismus angenommen wird, und weil der Grenzstrom der Cu^+-Oxydation klein ist, ergibt sich aus Zusammenhang (1)

$$X_1 \ll \frac{2\,k_{a_2}}{1+\dfrac{k_{k_2}}{X_2}}. \tag{8}$$

Ferner weist der 36—46 mV entsprechende Wert der Neigungswinkel der Polarisationskurven darauf hin, daß

$$k_{k_1} \gg \frac{k_{a_2}}{1+\dfrac{k_{k_2}}{X_2}} \quad \text{ist,} \tag{9}$$

so daß sich aus Gleichung (1)

$$i = \frac{k_{a_1}}{k_{k_1}} \cdot \frac{2\,k_{a_2}}{1+\dfrac{k_{k_2}}{X_2}} \quad \text{ergibt.} \tag{10}$$

Die obigen Feststellungen bedeuten, daß der Austauschstrom des Vorganges (I) bedeutend größer ist als der in Vorgang (II), ferner daß die Größenordnung von k_{k_2} mit der von X_2 vergleichbar ist. Der Wert des Quotienten $\dfrac{k_{k_2}}{X_2}$ kann neben 1 vernachlässigt werden, wenn sich X_2 nicht ändert, und

das Potential sich in positiver Richtung verändert oder die Drehzahl der Elektrode erhöht wird.

Wie aus dem Zusammenhang (5) ersichtlich ist, wird für den Grenzstrom i_h bei $b_\infty = 0$ dann ein kleiner Wert erhalten, falls einen stufenweiser Mechanismus, wenn

$$1 \ll \frac{2\,k_{a_2}}{X_1 + \frac{X_1}{X_2}\,k_{k_2}}. \tag{11}$$

Nun ist also:

$$i_h = N\,\frac{i\,X_1}{2\,k_{a_2}}\left(1 + \frac{k_{k_2}}{X_2}\right). \tag{12}$$

Falls die anodische Auflösung des Kupfers über die Reaktionen (I)—(III) verläuft, muß nach den obigen Versuchsergebnissen und Überlegungen aus den drei Gliedern der rechten Seite des Zusammenhanges (6) über die Polarisationskurve nur das erste Glied beachtet werden:

$$i = \frac{k_{a_3}}{1 + \frac{k_{k_3}}{2\,X_2}}. \tag{13}$$

Aus Gleichung (10) (Stufenmechanismus) ergibt sich der folgende, mit den Versuchsergebnissen vergleichbare Zusammenhang, wenn das Gewicht der Übertrittspolarisation mit dem der Diffusionspolarisation vergleichbar ist:

$$\frac{1}{i} = \frac{k_{k_1}}{2\,k_{a_1}\,k_{a_2}}\left(1 + \frac{k_{k_2}}{X_2}\right). \tag{14}$$

Analoger Ausdruck aus Gleichung (13) (»Simultan-Mechanismus«):

$$\frac{1}{i} = \frac{1}{k_{a_3}} + \frac{k_{k_3}}{k_{a_3}} \cdot \frac{1}{2\,X_2}. \tag{15}$$

Wie aus den Zusammenhängen (14) und (15) ersichtlich ist, besteht im Falle beider Mechanismen zwischen $\frac{1}{i}$ und der reziproken Quadratwurzel der Elektroden-Drehzal ($f^{-1/2}$) unter Berücksichtigung der Gleichung (4) ein linearer Zusammenhang. Abb. 3 zeigt den Zusammenhang $\frac{1}{i} - f^{1/2}$, und die experimentell bestimmten Punkte geben tatsächlich eine Gerade. Wenn die entsprechenden Werte von k_{a_i} und k_{k_i} aus den Ausdrücken (3) und (4) in die Gleichungen (14) und (15) eingesetzt werden, zeigt sich, daß der Neigungs-

winkel (b) der Geraden sich in beiden Fällen identisch mit dem Potential ändert, während der Achsenschnitt (a) der Geraden verschieden ist.

Im Falle eines Stufenmechanismus ist

$$\frac{\partial \ln b_l}{\partial \varphi} = -\frac{2F}{RT}, \tag{16}$$

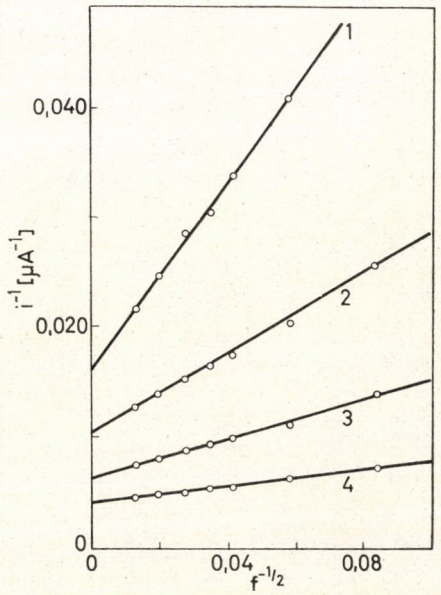

Abb. 3. Zusammenhang $\frac{1}{i} - f^{-1/2}$ bei verschiedenen Elektrodendrehzahlen. 1. $f = 100$ mV; 2. $\varphi = -90$ mV; 3. $\varphi = -80$ mV; 4. $\varphi = -70$ mV

$$\frac{\partial \ln a_l}{\partial \varphi} = -\frac{(1+\alpha)F}{RT}. \tag{17}$$

Im Falle eines Simultanmechanismus ist

$$\frac{\partial \ln b_s}{\partial \varphi} = -\frac{2F}{RT}, \tag{18}$$

$$\frac{\ln a_s}{\partial \varphi} = -\frac{2\alpha F}{RT}. \tag{19}$$

Abb. 4 zeigt die auf Grund der Daten von sieben $\frac{1}{i} - f^{-1/2}$ Geraden dargestellten $\lg b - \varphi$ bzw. $\lg a - \varphi$ Zusammenhänge. Wie ersichtlich, ergibt sich

eine Gerade und aus den Versuchsdaten:

$$\frac{\partial \lg b}{\partial \varphi} = -\frac{1}{30} mV^{-1}, \tag{20}$$

$$\frac{\partial \lg a}{\partial \varphi} = -\frac{1}{47} mV^{-1}. \tag{21}$$

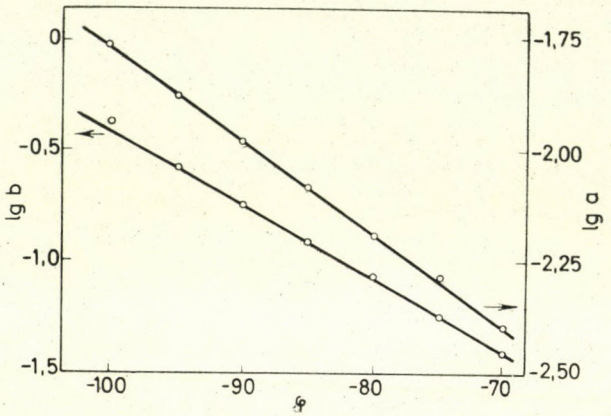

Abb. 4. Änderung des Logarithmus der mit den Gleichungen (14)—(21) gedeuteten Parameter b und a mit dem Potential der Scheibenelektrode (φ)

Auf Grund dieser Daten weist also der Wert der Neigungswinkel der an der Kupferelektrode gemessenen, von Diffusionseinwirkungen freien Polarisationskurven in Einklang mit den Befunden anderer Autoren [2—5] darauf hin, daß sich die anodische Auflösung des Kupfers in Einelektronen-Schritten abspielt. Wir möchten bemerken, daß es sich im Falle eines nicht stufenweisen Mechanismus bei gleichzeitigem Auftreten des Diffusions- und Übertrittvorganges (in einem nicht allzu weiten Stromdichtebereich) ergeben kann, daß die Polarisationskurve einen Neigungswinkel besitzt, der den beim stufenweisen Mechanismus geforderten Wert von 40 mV annähert.

In Abb. 5 ist der Logarithmus des an der Ringelektrode meßbaren Grenzstromes der Cu^+-Oxydation als Funktion des Potentials der Kupfer-Scheibenelektrode dargestellt. Wie ersichtlich, liegen die experimentellen Punkte bei gegebener Drehzahl der Elektrode entlang einer Geraden.

Der Zusammenhang zwischen dem Grenzstrom i_h, dem Potential der Scheibenelektrode und der Drehzahl der Elektrode kann im Falle eines stufenweisen Mechanismus unter Berücksichtigung der Gleichungen (10) und (3) bzw. (4) aus Gleichung (12) erhalten werden:

$$\lg i_h = NX_1 \frac{k'_{a_1}}{k'_{k_1}} + \frac{F\varphi}{RT}. \tag{22}$$

Auch für den Simultanmechanismus ergibt sich aus Gleichung (7) für den Zusammenhang zwischen i_h, X_1 und φ ein Ausdruck, dessen Form mit der von Gl. (22) vollkommen identisch ist, falls die Bedingung

$$1 \ll \frac{k_{k_1}}{X_1} \tag{23}$$

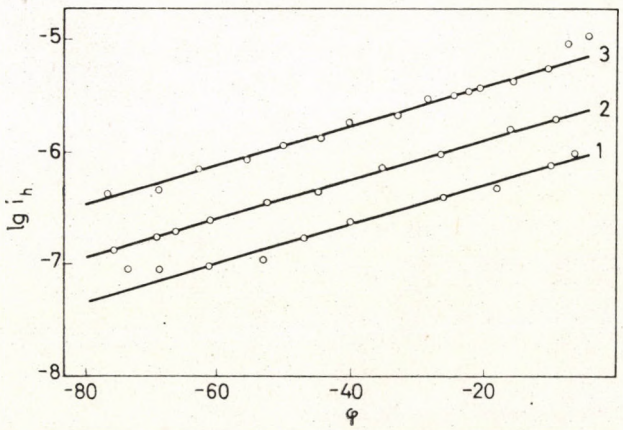

Abb. 5. Abhängigkeit des Logarithmus des an der Ringelektrode meßbaren Grenzstromes i_h vom Potential φ der Scheibenelektrode. 1. $f = 140$ min^{-1}; 2. $f = 810$ min^{-1}; 3. $f = 6500$ min^{-1}

erfüllt wird, was darauf hinweist, daß der Austauschstrom der Reaktion (I) sehr hoch ist. (Wir machen dieselbe Annahme beim stufenweisen Mechanismus [2—5, 10].)

Somit ist für beide Mechanismen:

$$\left.\frac{\partial \lg i_h}{\partial \varphi}\right|_{\omega = \text{konst.}} = \frac{F}{2{,}3\,RT} \qquad \left.\frac{\partial \lg i_h}{\partial \lg \omega}\right|_{\varphi = \text{konst.}} = \frac{1}{2}. \tag{24}$$

Experimentell bestimmte Daten geben die aus den Zusammenhängen (22) bzw. (24) erwarteten Werte:

$$\frac{\partial \lg i_h}{\partial \varphi} = \frac{1}{60}\, mV^{-1}; \qquad \frac{\partial \lg i_h}{\partial \lg \omega} = 0{,}48.$$

Wie ersichtlich, zeigen die Resultate des am Ring meßbaren Grenzstromes gute Übereinstimmung mit dem auf Grund des stufenweisen Mechanismus zu erwartenden Wert, doch würde sich auch im Falle eines Simultanmechanismus dasselbe ergeben.

Wenn die Lösung nicht nur Schwefelsäure, sondern auch Cu^{++}-Ionen enthält, beginnt an der Kupferelektrode in stromlosem Zustand ($i = 0$) die Reduktion der zweiwertigen Kupferionen und die Bildung der einwertigen

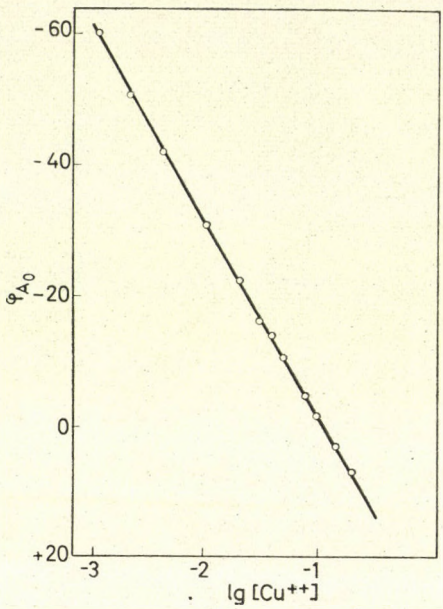

Abb. 6. Änderung des stromlosen Potentials (φ_{A_0}) der Kupferelektrode in 5 *n* H_2SO_4-Lösung in Abhängigkeit vom Logarithmus der Cu^{++}-Ionenkonzentration (b_∞) der Lösung

Kupferionen [9, 11]. Im folgenden soll der an der Ringlektrode meßbare Grenzstrom der im Laufe dieses Vorgangs sich bildenden Cu^+-Ionen untersucht werden.

Wenn sich der Vorgang nach dem stufenweisen Mechanismus abspielt, wird für den am Ring meßbaren Grenzstrom auch in diesem Fall die Gleichung (5) gültig sein. Da $i = 0$ ist und laut der in Abb. 6 angeführten Daten zwischen dem stromlosen Potential der Kupferscheibe φ_{A_0} und der Konzentration b_∞ der Cu^{++}-Ionen der Zusammenhang

$$\varphi_{A_0} = \varphi' + \frac{RT}{2F} \ln b_\infty \tag{25}$$

besteht (wo φ' konstant ist), ergibt sich aus Gleichung (5) unter Berücksichtigung der Gleichungen (3) und (4) der folgende Ausdruck (die Annahme (11) besteht in diesem Fall nicht, hingegen ist $X_i \gg k_{k_2}$):

$$\frac{1}{i_{\bar{h}_0}} = \frac{1}{N}\left\{\frac{1}{K_1 b_\infty^{\frac{1+\alpha_2}{2}}} + K_2 \frac{1}{X_1 b_\infty^{1/2}}\right\}, \tag{26}$$

wobei

$$K_1 = 2\,k'_{k_2} \exp\left(-\frac{(1-\alpha_2)\,F\varphi'}{RT}\right)$$

und

$$K_2 = \frac{k'_{a_2}}{k'_{k_2}} \exp\frac{F\varphi'}{RT}.$$

i_{h_0} ist der am Ring meßbare Oxydations-Grenzstrom für

$$i = 0, \text{ im Falle } b_\infty \neq 0.$$

Aus dem Zusammenhang (7) ergibt sich auf Grund ähnlicher Erwägungen die folgende Gleichung:

$$\frac{1}{i_{h_0}} = \frac{1}{N} K_3 \frac{1}{b_\infty{}^{1/2} X_1}, \tag{27}$$

wo

$$K_3 = \frac{k'_{k_1}}{k'_{a_1}} \exp\left(-\frac{F\varphi'}{RT}\right).$$

Bei der Berechnung des Zusammenhanges (27) ist die Annahme (23) gültig.

In Abb. 7 ist der Reziprokwert des Grenzstromes i_{h_0} als Funktion des Reziproks der Quadratwurzel der Drehzahl dargestellt. Wie aus der Abbildung

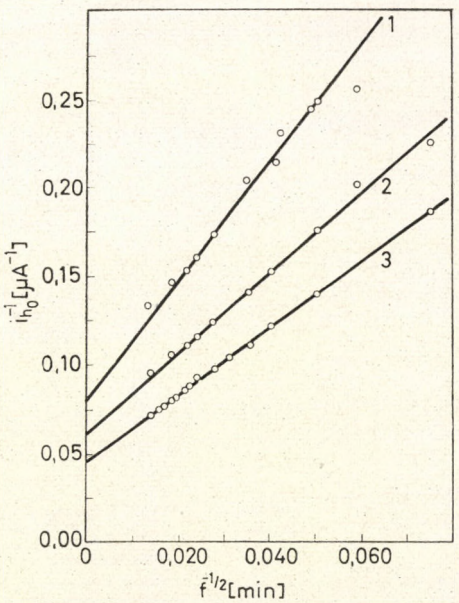

Abb. 7. Reziprokwert des Grenzstromes als Funktion der reziproken Quadratwurzel der Drehzahl bei $i = 0$ im Falle verschiedener $CuSO_4$-Konzentrationen. 1. $b_\infty = 3{,}9 \cdot 10^{-2}$ G. Ion/Lit.; 2. $b_\infty = 6{,}8 \cdot 10^{-2}$ G. Ion/Lit.; 3. $b_\infty = 9{,}6 \cdot 10^{-2}$ G. Ion/Lit

ersichtlich ist, befriedigen die Versuchsdaten den für den stufenweisen Mechanismus gültigen Zusammenhang (26). Dies beweist also ebenfalls, daß die anodische Auflösung des Kupfers auf dem Wege (I)—(II), also nach einem stufenweisen Mechanismus erfolgt.

LITERATUR

1. Kiss, L., Farkas, J.: Magy. Kém. Foly. **76.** 113 (1970); Acta Chim. Acad. Sci. Hung. **64,** 241 (1970)
2. Mattson, E., Bockris, I. O'M.: Trans. Faraday Soc. **55,** 1586 (1959)
3. Brown, O. R., Thirsk, H. R.: Electrochim. Acta **10,** 383 (1965)
4. Дмитриев, Ю. С., Муртазина, А. А., Колосов, А. С.: Электрохимия, **5,** 106 (1969)
5. Лосев, В. В., Сбирный, Л. Е., Молодов А. И.: Электрохимия, **2,** 1431 (1966)
6. Баймаков, Ю. В., Журин, А. И.: Электролиз в гидрометаллургии, Металлургиздат, 1963, стр. 127
7. Лайнер, В. И.: Современная гальванотехника, Изд. Металлургия, 1967, стр. 147
8. Kiss, L., Körösi, A., Farkas, J.: Magy. Kém. Foly. **73,** 551 (1967); Annales Univ. Sci. Budapest, **9,** 3 (1967)
9. Kiss, L., Farkas, J.: Magy. Kém. Foly. **76,** 120 (1970), Acta Chim. Acad. Sci. Hung. **65,** 7 (1970).
10. Некрасов, Л. Н., Березина, Н. П.: Докл. АН СССР **142,** 855 (1962)
11. Tindall, G. W., Bruckenstein, S.: Analitical Chem. **40,** 1402 (1968)

László Kiss
József Farkas } Budapest VIII., Puskin u. 11—13.

Acta Chimica Academiae Scientiarum Hungaricae, Tomus 66 (4), pp. 407—410 (1970)

INTEGRATED RATE-EQUATIONS IN CHEMICAL KINETICS

P. J. ROBINSON

(Chemistry Department, University of Manchester Institute of Science and Technology, Manchester, M60, 1QD, England)

Received July 14, 1969

Integrated rate-equations are presented for chemical reactions with any stoichiometry and with any combination of integral or half-integral orders of reaction up to a maximum order of three. The use of the equations is discussed and illustrated with reference to the reaction between dimethylphosphine and tetrafluoroethylene.

Kinetic studies of a chemical reaction proceeding according to the general equation (1) frequently lead to the postulation of a kinetic rate-equation of the form (2), in which the orders of reaction m and n may or may not be integral.

$$aA + bB \rightarrow \text{Products} \tag{1}$$

$$\frac{-1}{a}\frac{d[A]}{dt} = \frac{-1}{b}\frac{d[B]}{dt} = k[A]^m[B]^n \tag{2}$$

If such a rate-equation is to be useful in the discussion of mechanism or in the calculation of product yields it is clearly important to know if it is applicable over the whole course of the reaction. An equation derived from the observed variation of *initial* rate with concentration (as is common) does not always describe the variation of concentrations throughout a kinetic run. A well known example is the decomposition of acetaldehyde [1], for which the initial rate at different reactant pressures varies as $[CH_3.CHO]^{1.5}$ while the rate during a given run varies approximately as $[CH_3.CHO]^2$. Thus an equation of the type (2) cannot be assumed to represent completely the behaviour of the reaction until it is shown that it predicts correctly the detailed course of any given experiment, and this is most conveniently tested by means of a graph relating to the integrated rate-equation (3), obtained by integration of (2).

$$f([A]_0, [B]_0, a, b, [A], [B]) = kt \tag{3}$$

The graph of f against t will be linear if the corresponding differential equation (2) applies accurately throughout.

FÁY and BALOGH [2] have recently presented in this Journal a least-mean-squares method of determining both the orders of reaction and the values of the rate-constants, using the slopes of composition-time curves at various times throughout the reaction. This procedure has much to recommend it, but relies on the accurate drawing of tangents to curves and involves somewhat laborious computation. In suitable cases one can use instead an integrated equation suggested by the variation of initial rate with concentration, and this should provide nearly linear graphs, whose slopes can be measured accurately. As will be seen in the example below, any slight variation of slope with concentration then provides an accurate correction to the assumed orders of reaction and gives an accurate value for the rate constant.

The main disadvantages of this approach have been that the integration of (2) is rarely straightforward and that the results in the literature are restricted to a very few combinations of reaction orders and stoichiometry. Half-integral orders of reaction often arise in practice, and although one or two of the many possible cases have been treated in connection with particular investigations, the resulting equations do not appear in any compilations and can be located only with great difficulty.

The non-availability of such results has undoubtedly prevented adequate testing of many proposed rate-equations, and the main purpose of the present paper is to present a systematic compilation of the integrated equations for *any stoichiometry* and for *any combination of integral or half-integral orders of reaction*, subject to a maximum total order $(m + n)$ of three. The results are presented in the Table I. In some cases different expressions are required according to which component is in excess ($P > 0$ or $P < 0$), and in most cases the results become indeterminate for stoichiometric or near-stoichiometric mixtures ($P \approx 0$, $[B]_0/b \approx [A]_0/a$). For stoichiometric mixtures the appropriate equation is that for a single reactant disappearing by a reaction of order $(m + n)$, and for near-stoichiometric mixtures a meaningful expression can be obtained by series expansion in a manner similar to that well-known [3, 4] for the case $m, n = 1.1$ or 2.1. The difficulty for near-stoichiometric mixtures is a purely arithmetical one, and usually disappears if a sufficient accuracy is used in the computation. For example, in the investigation referred to below (eqn. 4, $m = 1.5, n = 0.5$), a typical experiment had $[A]_0 = 28.1$ Torr, $[B]_0 = 28.2$ Torr, and $[A]_0 - [A] = [B]_0 - [B] = 4.6$ Torr. If the expression in the Table is computed to 4-figure accuracy we obtain $kt = (2/0.1)\ (1.002 - 1.002) \approx 0$; if eight significant figures are used $kt = (2/0.1)\ (1.0021255 - - 1.0017778) = 6.95 \cdot 10^{-3}$ Torr^{-1}. This is in excellent agreement with the value obtained by assuming $[A]_0 = [B]_0 = 28.15$ Torr and using the relevant expression for a stoichiometric mixture with total order 2; $kt = (1/[A] - - 1/[A]_0) = ([A]_0 - [A])/([A]_0[A]) = 6.95 \cdot 10^{-3}$ Torr^{-1}. Thus even very small values of P need not really be troublesome. In particular, if a digital

Table I

Order w. r. t. A (m)	Order w. r. t. B (n)	Reactant in Excess	$f([A]_0, [B]_0, a, b, [A], [B])\ (= kt)$
$m = 1$	0	A or B	$[a(m-1)]^{-1}\left[[A]^{1-m}\right]_{t=0}^{t}$
1	0	A or B	$a^{-1}\left[1n(1/[A])\right]_{t=0}^{t}$
0.5	0.5	A	$\frac{1}{\sqrt{ab}}\left[1n\frac{\sqrt{b[A]}-\sqrt{a[B]}}{\sqrt{b[A]}-\sqrt{a[B]}}\right]_{t=0}^{t}$
1	0.5	A	$(-2/\sqrt{-aP})\left[\tan^{-1}\sqrt{a[B]/(-P)}\right]_{t=0}^{t}$
		B	$\frac{1}{\sqrt{aP}}\left[1n\frac{\sqrt{P}+\sqrt{a[B]}}{\sqrt{P}-\sqrt{a[B]}}\right]_{t=0}^{t}$
1.5	0.5	A or B	$(2/P)\left[\sqrt{[B]/[A]}\right]_{t=0}^{t}$
2	0.5	A	$(1/P)\left[\frac{\sqrt{[B]}}{[A]}+\frac{b}{\sqrt{-aP}}\tan^{-1}\sqrt{a[B]/(-P)}\right]_{t=0}^{t}$
		B	$(1/P)\left[\frac{\sqrt{[B]}}{[A]}-\frac{b}{2\sqrt{aP}}1n\frac{\sqrt{P}+\sqrt{a[B]}}{\sqrt{P}-\sqrt{a[B]}}\right]_{t=0}^{t}$
2.5	0.5	A or B	$(2/P^2)\left[(a/3)\left([B]/[A]\right)^{3/2}-b\sqrt{[B]/[A]}\right]_{t=0}^{t}$
1	1	A or B	$(1/P)\left[1n[B]/[A]\right]_{t=0}^{t}$
1.5	1	A	$(2/P)\left[\frac{1}{\sqrt{[A]}}-\frac{1}{2}\sqrt{\frac{b}{(-P)}}1n\frac{\sqrt{-P}+\sqrt{b[A]}}{\sqrt{-P}-\sqrt{b[A]}}\right]_{t=0}^{t}$
		B	$(2/P)\left[\frac{1}{\sqrt{[A]}}+\sqrt{\frac{b}{P}}\tan^{-1}\sqrt{\frac{b[A]}{P}}\right]_{t=0}^{t}$
2	1	A or B	$(1/P)\left[\frac{1}{[A]}+\frac{b}{P}1n\frac{[A]}{[B]}\right]_{t=0}^{t}$
1.5	1.5	A or B	$(2/P^2)\left[b\sqrt{\frac{[A]}{[B]}}+a\sqrt{\frac{[A]}{[B]}}\right]_{t=0}^{t}$

$P = (a[B]_0 - b[A]_0)$; $P < 0$ for A in excess, $P > 0$ for B in excess. $\sqrt{}$ refers to the positive square root throughout.

computer is used to process the results the precision will usually be such that the series-expansion technique is not needed with normal experimental results.

The approach suggested here has been useful for a number of reactions studied in the author's laboratory, and is illustrated by some results obtained [5] for reaction (4). The initial slopes

$$Me_2PH + C_2F_4 \rightarrow Me_2PCF_2CF_2H \qquad (4)$$

of the pressure-time curves were plotted logarithmically against the pressure of each reactant, with the other reactant at constant pressure, and the slopes of these plots showed that the orders of reaction with respect to Me_2PH and C_2F_4 were about 0.5 and about 1.5 respectively. Integrated function plots were then constructed, using the sixth equation in the Table; [A] and [B] were evaluated from the initial reactant pressures and the total pressure at time t, correction being made for dead-space [6]. The plots obtained were linear, in many cases up to 75% consumption of the minor component, C_2F_4. The slopes could thus be measured accurately, and were independent of Me_2PH pressure but varied slightly with C_2F_4 pressure according to the expression $[C_2F_4]^{0.10}$. The correct rate equation is therefore (5):

$$d[\text{Product}]/dt = k[Me_2PH]^{0.50}\ [C_2F_4]^{1.60} \qquad (5)$$

and this is applicable over a range of initial conditions and throughout the course of the reaction. The rate constant can clearly be determined more accurately from the slopes of the linear integrated plots than from the slopes of the curved pressure-time plots.

REFERENCES

1. LETORT, M.: J. Chim. Phys. **34**, 206 (1937); Bull. Soc. Chim. France **9**, 1 (1942); EUSUF, M., LAIDLER, K. J.: Can. J. Chem. **42**, 1851 (1964)
2. FÁY, L., BALOGH, A.: Acta Chim. Acad. Sci. Hung. **57**, 391 (1968)
3. FROST, A. A., PEARSON, R. G.: Kinetics and Mechanism, 2nd Edn. p. 18. Wiley, New York, 1961
4. BENSON, S. W.: Foundations of Chemical Kinetics pp. 20, 22. McGraw-Hill, New York, 1960
5. BRANDON, R., HASZELDINE, R. N., ROBINSON, P. J.: unpublished results
6. ROBINSON, P. J.: Trans. Faraday Soc. **63**, 2668 (1967)

P. J. ROBINSON: Manchester, M60 1 QD, England.

Acta Chimica Academiae Scientiarum Hungaricae, Tomus 66 (4), pp. 411—430 (1970)

STUDY OF THERMODYNAMIC PROPERTIES OF BINARY MIXTURES CONTAINING ACETIC ACID

J. Liszi

(Department of Physical Chemistry, University of Veszprém and Research Group for Electrochemistry, Hungarian Academy of Sciences, Veszprém)

Received July 28, 1969

The application of association equilibrium data and molecular properties determined for the acetic acid–carbon tetrachloride mixture [1] was illustrated on the example of calculating isothermal thermodynamic properties of three binary mixtures containing acetic acid. The pairs of acetic acid in these mixtures were *n*-heptane, benzene and toluene, respectively. The present study indicates that the above data properly describe the vapour–liquid equilibrium data of binary mixtures, that they give a good qualitative picture about the excess free enthalpy of mixing but cannot be used to calculate the enthalpy of mixing.

In previous papers [1—4], we have described detailed studies on the thermodynamic properties of acetic acid–carbon tetrachloride mixtures under isothermic conditions. In this paper, the results obtained in the study of acetic acid–carbon tetrachloride mixtures are applied to other acetic acid containing mixtures at 20 °C. The method is illustrated on the examples of the following binary mixtures:

n-heptane–acetic acid
benzene–acetic acid
toluene–acetic acid

1. Thermodynamic model and simplifications used in the calculations

Acetic acid is commonly known to undergo association [5]. The nominally binary mixtures of acetic acid with non-polar substances are, therefore, considered as ternary mixtures consisting of monomeric acetic acid (A), dimeric acetic acid (A_2) and a non-polar component (B). In the mixture, monomeric and dimeric acetic acid molecules are at equilibrium according to the reaction of association.

$$2A \rightleftharpoons A_2 \tag{1}$$

This mixture can exist only in compositions determined by the equilibrium constant of reaction (1). No pair of components of the real (ternary) mixture is regarded as an ideal mixture. All possible pairs of components (A–A_2, A–B,

A_2–B) are supposed to behave as regular mixtures. The thermodynamic model is illustrated by the following scheme

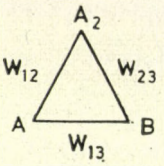

pair	interchange energy
A–A_2	w_{12}
A–B	w_{13}
A_2–B	w_{23}

In the scheme w stands for the interchange energy, subscripts 1, 2, 3 refer to monomeric and dimeric acetic acid, and the non-polar component, respectively, in the true mixture. In the calculation of thermodynamic properties the contribution by both the association reaction (1) and the intermolecular effects to the properties of the mixture are taken into account.

In applying the above thermodynamic model, the same approximations are made as in the study of the acetic acid–carbon tetrachloride mixture [1—4]. Furthermore, we assume that:

1. The non-polar substances studied affect the equilibrium constant of reaction (1) similarly to carbon tetrachloride. In other words, the validity of the relationship

$$\lg K = 1.8261 + 2.4549\, x_B \tag{2}$$

obtained for acetic acid–carbon tetrachloride mixtures at 20 °C is accepted for the systems studied in this work. In Eq. (2), x_B is the mole fraction of the non-polar substance in the nominal (binary) mixture (nominal mole fraction), while

$$K = \frac{x_2}{x_1^2} \tag{3}$$

where x_1 and x_2 are the true mole fractions of monomeric and dimeric acetic acids, respectively.

2. The liquid phases of the systems described in this paper are of the quasi-crystalline structure as are those in the acetic acid–carbon tetrachloride mixtures. On the basis of information on acetic acid–carbon tetrachloride mixtures [2], the liquid phase is modelled by a face-centered cubic lattice.

2. Average molecular interaction energies and interchange energies

Interchange energies play a key role in the calculation of thermodynamic properties. If i and j denote molecules of different kind, u is the average interaction energy of a pair of molecules and z the coordination number, then the interchange energy is defined by the following equation [6]

$$w_{it} = w_{ij} = z\left(u_{ij} - \frac{1}{2}u_{it} - \frac{1}{2}u_{jj}\right) \tag{4}$$

The coordination number for a face-centered cubic lattice is $z = 12$. The average molecular interaction energies were calculated on the basis of SCHOLTE's dielectric model [7], using the following expressions [6]

$$u_{11} = -\frac{2\alpha_1\mu_1^2}{r_{11}^6} \tag{5}$$

$$u_{22} = -\frac{2\alpha_2\mu_2^2}{r_{22}^6} \tag{6}$$

$$u_{33} = 0 \tag{7}$$

$$u_{12} = -\frac{\alpha_1\mu_2^2 + \alpha_2\mu_1^2}{r_{12}^6} \tag{8}$$

$$u_{13} = -\frac{\alpha_3\mu_1^2}{r_{13}^6} \tag{9}$$

$$u_{23} = -\frac{\alpha_3\mu_2^2}{r_{23}^6} \tag{10}$$

where u is the average molecular interaction energy, α the average polarizability, μ the permanent dipole moment, and r the radius of the spherical molecule. Subscripts 1, 2, 3 denote monomeric and dimeric acetic acid, and the non-polar component, respectively, in the real mixture.

The average molecular radii were calculated from the equation

$$r^3 = \frac{\sqrt{2}}{8N_A}v \tag{11}$$

corresponding to the face-centered cubic lattice [6], where N_A is the Avogadro-number and v the molar volume. For pairs of different molecules, the aver-

age molecular radii were calculated:

$$r_{ij} = \frac{r_i + r_j}{2} \tag{12}$$

The data necessary for calculating the average molecular energies are collected in Table I.

Table I

	Monomeric acetic acid	Dimeric acetic acid	*n*-Heptane	Benzene	Toluene
α/cm^3 (mole)	$4.85 \cdot 10^{-24}$ [1]	$15.65 \cdot 10^{-24}$ [1]	$12.46 \cdot 10^{-24}$ [9]	$10.7 \cdot 10^{-24}$ [8]	$12.26 \cdot 10^{-24}$ [8]
μ(D)	1.68 [1]	$0.92(1 - x_3)$]1]	0.0 [10]	0.0 [10]	0.0 [10]
v/cm^3 (mole)	58 [2]	116 [2]	147.5 [10]	87.8 [10]	103.3 [8]

In the Table, x_3 is the true mole fraction of the non-polar component. Molecular radii obtained from Eq. (11) and (12), which are used to calculate values of intermolecular energies, are collected in Table II.

The average molecular interaction energies calculated from Eq. (5)—(10) using the data in Tables I and II, are presented in Tables III, IV and V.

Using the values of the average molecular interaction energies, the interchange energies corresponding to the face-centered cubic lattice ($z = 12$) were determined. For this purpose, Eq. (4) and the data in Tables III, IV, V were used. The results are collected in Table VI.

On the basis of interchange energies collected in Table VI, the following conclusions can be drawn concerning the behaviour of the component-pairs. Monomeric and dimeric acetic acid, monomeric acetic acid and benzene, as well as monomeric acetic acid and toluene form mixtures with strong negative deviations. Monomeric acetic acid and *n*-heptane form a mixture with a positive deviation. Dimeric acetic acid forms mixtures with weak positive deviation with all non-polar components. In the case of the latter mixtures, the deviation

Table II

	Monomeric acetic acid	Dimeric acetic acid
Monomeric acetic acid	$r_{11} = 2.58 \cdot 10^{-8}$ Å	$r_{21} = 2.92 \cdot 10^{-8}$ Å
Dimeric acetic acid	$r_{12} = 2.92 \cdot 10^{-8}$ Å	$r_{22} = 3.27 \cdot 10^{-8}$ Å
n-Heptene	$r_{13} = 3.4 \cdot 10^{-8}$ Å	$r_{23} = 3.38 \cdot 10^{-8}$ Å
Benzene	$r_{13} = 2.77 \cdot 10^{-8}$ Å	$r_{23} = 3.12 \cdot 10^{-8}$ Å
Toluene	$r_{13} = 2.85 \cdot 10^{-8}$ Å	$r_{23} = 3.19 \cdot 10^{-8}$ Å

from ideal behaviour (zero interchange energy) decreases with increasing concentration of the non-polar component. The explanation of this phenomenon was discussed in detail in connection with the study of acetic acid–carbon tetrachloride mixtures [1]. At this point we only mention that such variations

Table III

Average molecular interaction energies in the real acetic acid–n-heptane mixtures

x_B	$u_{11}\frac{(cal)}{2\ mole}$	$u_{22}\frac{(cal)}{2\ mole}$	$u_{33}\frac{(cal)}{2\ mole}$	$u_{12}\frac{(cal)}{2\ mole}$	$u_{13}\frac{(cal)}{2\ mole}$	$u_{23}\frac{(cal)}{2\ mole}$
0.0	−1342.2	−324.7	0.0	−1138.0	−636.1	−107.9
0.2	−1342.2	−148.3	0.0	−1085.0	−636.1	− 49.3
0.4	−1342.2	− 61.8	0.0	−1059.7	−636.1	− 20.5
0.6	−1342.2	− 21.0	0.0	−1047.5	−636.1	− 7.0
0.8	−1342.2	− 4.1	0.0	−1042.5	−636.1	− 1.4
1.0	−1342.2	0.0	0.0	−1041.3	−636.1	0.0

Table IV

Average molecular interaction energies in the real acetic acid–benzene mixtures

x_B	$u_{11}\frac{(cal)}{2\ mole}$	$u_{22}\frac{(cal)}{2\ mole}$	$u_{33}\frac{(cal)}{2\ mole}$	$u_{12}\frac{(cal)}{2\ mole}$	$u_{13}\frac{(cal)}{2\ mole}$	$u_{23}\frac{(cal)}{2\ mole}$
0.0	−1342.2	−324.7	0.0	−1114.7	−960.6	−142.7
0.2	−1342.2	−148.3	0.0	−1063.2	−960.6	− 65.1
0.4	−1342.2	− 61.8	0.0	−1037.4	−960.6	− 27.2
0.6	−1342.2	− 21.0	0.0	−1026.0	−960.6	− 9.2
0.8	−1342.2	− 4.1	0.0	−1021.1	−960.6	− 1.7
1.0	−1342.2	0.0	0.0	−1019.9	−960.6	0.0

Table V

Average molecular interaction energies in the real acetic acid–toluene mixtures

x_B	$u_{11}\frac{(cal)}{2\ mole}$	$u_{22}\frac{(cal)}{2\ mole}$	$u_{33}\frac{(cal)}{2\ mole}$	$u_{12}\frac{(cal)}{2\ mole}$	$u_{13}\frac{(cal)}{2\ mole}$	$u_{23}\frac{(cal)}{2\ mole}$
0.0	−1342.2	−324.7	0.0	−1114.7	−933.7	−141.1
0.2	−1342.2	−148.3	0.0	−1063.2	−933.7	− 64.4
0.4	−1342.2	− 61.8	0.0	−1037.9	−933.7	− 26.9
0.6	−1342.2	− 21.0	0.0	−1026.0	−933.7	− 9.1
0.8	−1342.2	− 4.1	0.0	−1021.1	−933.7	− 1.8
1.0	−1342.2	0.0	0.0	−1019.9	−933.7	0.0

Table VI

x_B	$w_{12}\frac{(cal)}{mole}$	*n*-Heptane		Benzene		Toluene	
		$w_{13}\frac{(cal)}{mole}$	$w_{23}\frac{(cal)}{mole}$	$w_{13}\frac{(cal)}{mole}$	$w_{23}\frac{(cal)}{mole}$	$w_{13}\frac{(cal)}{mole}$	$w_{23}\frac{(cal)}{mole}$
0.0	−3655	+420	+654	−3408	+144	−3086	+161
0.2	−4082	+420	+298	−3408	+ 78	−3086	+ 86
0.4	−4292	+420	+124	−3408	+ 32	−3086	+ 36
0.6	−4391	+420	+ 42	−3408	+ 11	−3086	+ 12
0.8	−4432	+420	+ 8	−3408		−3086	+ 2
1.0	−4458	+420	0	−3408		−3086	0

in the interchange energy are caused by changes in the permanent dipole moment of dimeric acetic acid.

The data in Table VI also indicate that the thermodynamic properties of benzene and toluene must be similar to each other.

3. Enthalpy of isothermal mixing

In the calculation of the enthalpy of mixing, it is taken into account that both the association reaction and intermolecular interactions contribute to the enthalpy of mixing. Consequently, the enthalpy of mixing is calculated by considering the following processes [2].

1. Separation of monomeric and dimeric acetic acid. The enthalpy of the process (Δh_{sep}) is

$$\Delta h_{sep} = - x_1^0 x_2^0 w_{12}^0 x_{ac} \tag{13}$$

where "0" denotes pure acetic acid.

2. Dissociation of dimeric acetic acid in an amount corresponding to the equilibrium constant K^0 (referring to pure acetic acid) expressed in mole fractions. The corresponding enthalpy change is

$$\Delta H_{rd} = - N_{2d}^0 x_{ac} \Delta h_r \tag{14}$$

where N_{2d}^0 is the amount of dimeric acetic acid (moles) in 1 nominal mole of pure acetic acid, h_r is enthalpy of dimerization. Its value [11] is $h_r = -6200$ cal/2 moles of hydrogen bond.

3. Formation of dimeric acetic acid in an amount corresponding to the equilibrium constant K (actual) expressed in mole fractions. The value of K is given by Eq. (2). The enthalpy of the process is

$$\Delta H_{ra} = N_{2a} \Delta h_r \tag{15}$$

where N_{2a} is the amount of dimeric acetic acid (moles) taking part in the association process. Its value referred to 1 mole of the nominal mixture is given by the following expression:

$$N_{2a} = \frac{4Kx_{ac} + 1 - \sqrt{8Kx_{ac} + 1 - 4Kx_{ac}^2}}{2(4K + 1)} \tag{16}$$

4. Mixing of monomeric and dimeric acetic acid and carbon tetrachloride. The enthalpy of the process is

$$\Delta H_e = x_1 x_2 w_{12} + x_1 x_3 w_{13} + x_2 x_3 w_{23} \tag{17}$$

The enthalpies of processes 2 and 3 are referred to 1 mole of the nominal mixture while those of processes 1 and 4 to 1 mole of the real mixture. Since it is the enthalpy of mixing for 1 mole of the nominal mixture that is usually determined experimentally, it is reasonable to refer enthalpies of all processes to 1 mole of the nominal mixture. The true number of moles in 1 mole of the nominal mixture is $(1 - N_2)$ and so the overall enthalpy of mixing and separation (ΔH_e), referred to 1 mole of the nominal mixture, is as follows:

$$\Delta H_e = (\Delta h_e + \Delta h_{sep})(1 - N_2) \tag{18}$$

Hence, the measurable (overall) enthalpy of mixing is

$$H^E = \Delta H_{rd} + \Delta H_{ra} + \Delta H_e = \Delta H_r + \Delta H_e \tag{19}$$

where ΔH_r is the component of the enthalpy of mixing which arises from shift of the association equilibrium.

The results obtained from Table VI and Eq. (2) are collected in Table VII. The data in Table VII refer to 1 mole of the nominal mixture.

Table VII

x_B	ΔH_r (cal/mole)	*n*-Heptane		Benzene		Toluene	
		ΔH_e (cal/mole)	H^E (cal/mole)	ΔH_e (cal/mole)	H^E (cal/mole)	ΔH_e (cal/mole)	H^E (cal/mole)
0.0	0	0	0	0	0	3	0
0.2	−47	139	92	64	17	90	43
0.4	−53	149	96	85	32	107	54
0.6	−46	119	73	79	33	93	47
0.8	−22	67	45	51	29	57	35
1.0	0	0	0	0	0	0	0

The calculated values shown in Table VII were compared with experimental data.

The enthalpy of mixing of the acetic acid–toluene system is taken from the literature [12]. Experimental data taken from the literature are presented in Table VIII.

There were no data on the enthalpy of mixing of the acetic acid–*n*-heptane and acetic acid–benzene systems, therefore, these values were determined experimentally. The method of measurements has been described in a previous paper [2]. The experimental results are given in Table IX. All data in the Table are referred to 1 mole of the nominal mixture.

Table VIII

Enthalpy of mixing of the acetic acid–toluene system at 20°C [12]

X_B	H^E (cal/mole)	X_B	H^E (cal/mole)
0.0	0	0.6	86
0.1	42	0.7	75
0.2	66	0.8	56
0.3	79	0.9	30
0.4	87	1.0	0
0.5	89	—	—

Table IX

Enthalpy of mixing of the acetic acid–n-heptane system at 20°C

X_B	H^E (cal/mole)	X_B	H^E (cal/mole)
0.0	0	0.423	196
0.211	181	0.898	65
0.298	192	1.000	0

Table X

Enthalpy of mixing of the acetic acid–benzene system at 20°C

X_B	H^E (cal/mole)	X_B	H^E (cal/mole)
0.000	0	0.598	86
0.082	52	0.624	82
0.138	70	0.711	66
0.196	82	0.755	68
0.258	88	0.920	23
0.421	93	1.000	0

For comparison, the experimental and calculated data are shown in Figs 1, 2 and 3 as well. The differences between experimental and calculated data are striking. This is probably due to the great sensitivity of the calculated enthalpy of mixing to simplifications introduced in Part 1.

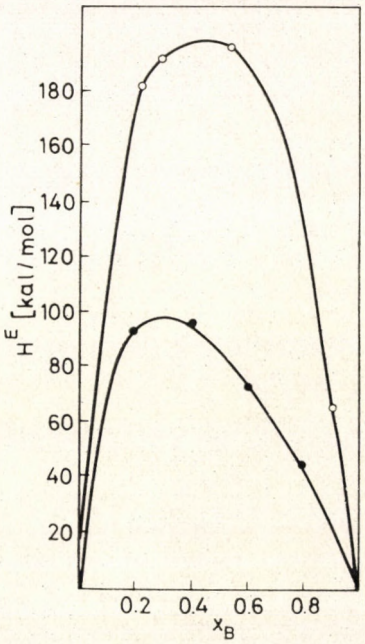

Fig. 1. Enthalpy of mixing of the acetic acid–*n*-heptane mixtures as a function of the *n*-heptane nominal mole fraction at 20 °C. ○ — experimental data, ● — calculated values

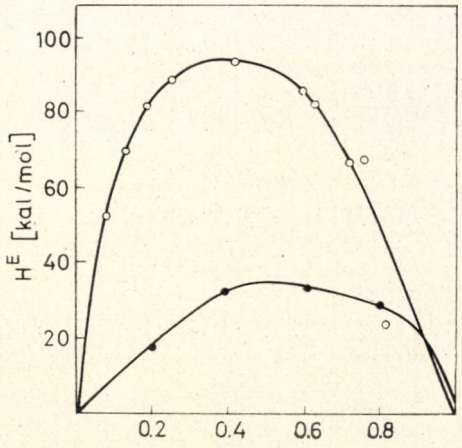

Fig. 2. Enthalpy of mixing of the acetic acid–benzene mixtures as a function of the benzene nominal mole fraction at 20 °C. ○ — experimental data, ● — calculated values

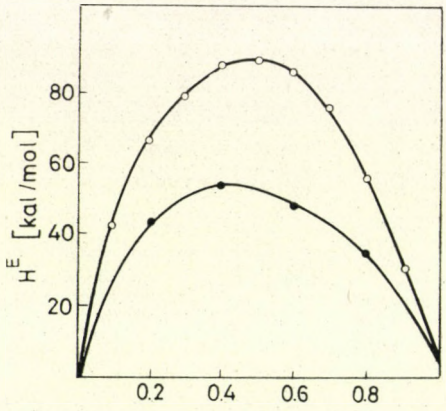

Fig. 3. Enthalpy of mixing of the acetic acid–toluene mixtures as a function of the toluene nominal mole fraction at 20 °C. ○ — experimental data at 15 °C and 20 °C, ● — calculated values for 20 °C

4. Excess free enthalpy of isothermal mixing

When calculating the excess free enthalpy of mixing, effects of both the association reaction (1) and molecular interactions are considered. The excess free enthalpy of mixing is, therefore, presented as a sum of the following two terms

1) G_a^E corresponding to the association reaction, and
2) G_{real}^E corresponding to the real mixing, *i.e.*

$$G^E = G_a^E + G_{\text{real}}^E \tag{20}$$

The terms in Eq. (20) can be expressed as follows [4]:

$$G_a^E = RT\left\{x_{\text{ac}} \ln\left[\frac{1}{x_1^0}\,\frac{x_1}{x_{\text{ac}}}\right] + x_B \ln(1 + x_2)\right\} \tag{21}$$

$$G_{\text{real}}^E = (1 - N_2)\left\{x_1 x_2 w_{12} + x_1 x_3 w_{13} + x_2 x_3 w_{23} - x_1^0 x_2^0 w_{12}^0 x_{ac}\right\} \tag{22}$$

where R is the gas constant and T is the absolute temperature. The calculated values of excess free enthalpies of mixing are listed in Table XI. The data refer to 1 mole of the nominal mixture.

For purposes of comparison, the literature data referring to the systems studied are shown in Tables XII, XIII and XIV. These data were kindly provided by Dr. H. KEHLEN* whose help is gratefully acknowledged. The data in Table XI refer to 20 °C. Unfortunately, there are no data in the literature

* Dr. H. KEHLEN, Martin-Luther-Universität, Halle-Vittenberg, 401, Halle, Mühlpforte 1.

Table XI

x_B	G^E (cal/mole)		
	n-heptane	benzene	toluene
0.0	0	0	0
0.2	205	130	156
0.4	259	194	213
0.6	252	205	226
0.8	174	157	161
1.0	0	0	0

Table XII

Excess free enthalpy of mixing of acetic acid–n-heptane mixtures at 20 °C

X_B	G^E (cal/mole)	X_B	G^E (cal/mole)
0.0	0.0	0.6	315.8
0.1	141.7	0.7	270.0
0.2	235.4	0.8	197.4
0.3	194.8	0.9	103.1
0.4	327.1	1.0	0.0
0.5	334.4	—	—

Table XIII

Excess free enthalpy of mixing of acetic acid–benzene mixtures at 20 and 50°C

X_B	$G^E_{20°C}$(cal/mole)	X_B	$G^E_{50°C}$(cal/mole)
0.0	0.0	0.0000	0.0
0.1	73.0	0.0039	3.7
0.2	128.1	0.0115	10.7
0.3	168.0	0.2265	153.2
0.4	193.3	0.2900	175.8
0.5	204.2	0.4981	205.7
0.6	200.4	0.5811	201.2
0.7	181.3	0.6939	178.1
0.8	144.9	0.8280	119.6
0.9	87.3	0.9354	48.6
1.0	0.0	0.9780	16.6
		1.0000	0.0

Table XIV

Excess free enthalpy of mixing of acetic acid–toluene mixtures at 70 and 80°C

X_B	$G^E_{70°C}$(cal/mole)	$G^E_{80°C}$(cal/mole)
0.0	0.0	0.0
0.1	85.3	86.5
0.2	143.2	145.8
0.3	180.7	184.4
0.4	199.1	203.3
0.5	198.7	202.7
0.6	181.3	184.7
0.7	150.6	153.1
0.8	110.8	112.5
0.9	63.1	64.1
1.0	0.0	0.0

for the acetic acid–toluene system at 20 °C. The data corresponding to 20 °C and 50 °C for the acetic acid–benzene system and to 70 °C and 80 °C for the acetic acid–toluene system indicate (see Figs 5 and 6) that the excess free enthalpy of mixing depends but slightly on the temperature. Consequently, the

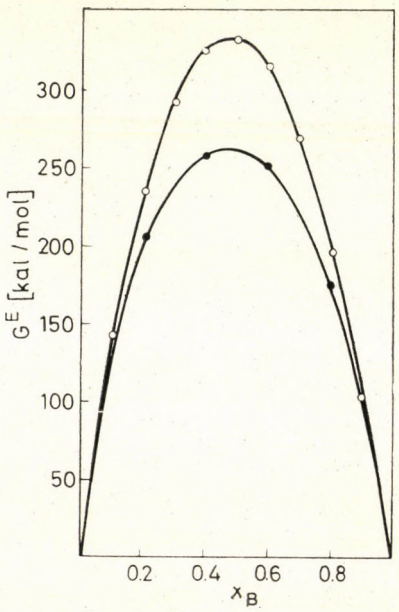

Fig. 4. Excess free enthalpy of mixing of acetic acid–*n*-heptane mixtures as a function of the *n*-heptane nominal mole fraction at 20 °C. ○ — data taken from the literature, ● — calculated values

data referring to the acetic acid–toluene system at 70 °C and 80 °C can be used for the qualitative check of the results. The data in Tables XII, XIII and XIV are referred to 1 mole of the nominal mixture.

For comparison, the calculated data shown in Table XI, and the literature data collected in Tables XII, XIII and XIV are shown in Figs 4, 5 and 6, as well. It can be seen from Fig. 4 that the calculated and literature data are

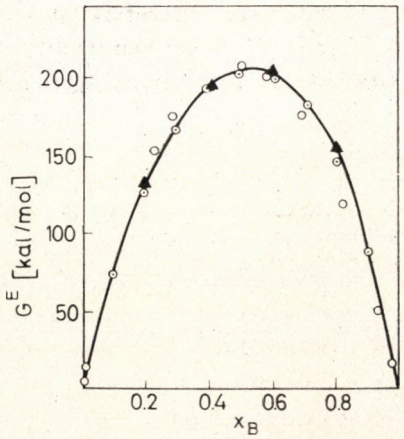

Fig. 5. Excess free enthalpy of mixing of acetic acid–benzene mixtures as a function of the benzene nominal mole fraction at 20 °C. ▲ — calculated values referring to 20 °C; ⊙ — data from the literature, at 20 °C; ○ — same at 50 °C

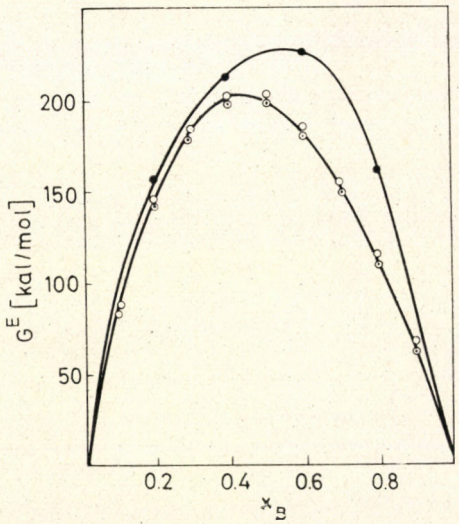

Fig. 6. Excess free enthalpy of mixing of acetic acid–toluene mixtures as a function of the toluene nominal mole fraction. ● — values calculated for 20 °C, ⊙ and ○ — data from the literature referring to 70 °C and 80 °C, respectively

of similar tendency with a maximum deviation of 25%. According to Fig. 5, the calculated excess free enthalpy of mixing for the acetic acid–benzene mixture is in a good agreement with the data in the literature. The data for the acetic acid–toluene system are shown in Fig. 6. The calculated data and those reported in the literature are of the same order of magnitude but the locations of the extrema on the curves are different ($x_B = 0.45$ and $x_B = 0.55$). It should be mentioned at this point that the calculated and the literature data refer to very different temperatures and, therefore, only qualitative agreement can be expected. In summary the conclusion can be drawn that for the systems studied the calculated data are in qualitative agreement with those taken from the literature.

5. Data on isothermal vapour liquid equilibria

Since the nominally binary mixtures of acetic acid with non-polar substances are regarded as ternary mixtures consisting of regular component pairs, the first step toward the calculation of vapour–liquid equilibrium characteristics is the determination of the activity coefficients for the ternary mixture components. The activity coefficients are defined by the following equations as functions of the interchange energies and mole fractions [6].

$$\gamma_1 = \exp\left[\frac{x_2x_3(w_{12} + w_{13} - w_{23}) + x_2^2w_{12} + x_3^2w_{13}}{RT}\right] \tag{23}$$

$$\gamma_2 = \exp\left[\frac{x_1x_3(w_{12} + w_{23} - w_{13}) + x_1^2w_{12} + x_3^2w_{23}}{RT}\right] \tag{24}$$

$$\gamma_3 = \exp\left[\frac{x_1x_2(w_{13} + w_{23} - w_{12}) + x_1^2w_{13} + x_2^2w_{23}}{RT}\right] \tag{25}$$

The activity coefficients calculated from Eqs. (23), (24) and (25) are presented in Tables XV, XVI and XVII.

Equilibrium vapour pressures of the pure substances at 20 °C are listed in Table XVIII.

Considering the vapour phase as an ideal mixture of ideal components and using the activity coefficients and equilibrium vapour pressures, the partial pressures of components can be calculated from the following expression

$$p_i = p_i^0 x_i \gamma_i \qquad (i = 1, 2, 3) \tag{26}$$

Table XV

Activity coefficients in the monomeric acetic acid–dimeric acetic acid–n-heptane mixture as a function of the nominal mole fraction of n-heptane

x_B	γ_1	γ_2	γ_3
0.00	$0.722 \cdot 10^{-2}$	0.920	5.582
0.05	$0.814 \cdot 10^{-2}$	0.891	3.523
0.15	$1.323 \cdot 10^{-2}$	0.899	1.948
0.20	$1.815 \cdot 10^{-2}$	0.909	1.618
0.40	$7.477 \cdot 10^{-2}$	0.942	1.138
0.60	0.275	0.966	1.029
0.80	0.826	0.983	1.004
0.85	1.065	0.986	1.002
0.95	1.618	0.990	1.000
1.00	1.950	0.993	1.000

Table XVI

Activity coefficients in the monomeric acetic acid–benzene mixture as a function of the nominal mole fraction of benzene

x_B	γ_1	γ_2	γ_3
0.0	$0.722 \cdot 10^{-2}$	0.922	1.152
0.2	$0.352 \cdot 10^{-2}$	0.986	1.062
0.4	$0.259 \cdot 10^{-2}$	0.998	1.017
0.6	$0.246 \cdot 10^{-2}$	0.999	1.004
0.8	$0.259 \cdot 10^{-2}$	0.999	1.000
1.0	$0.282 \cdot 10^{-2}$	1.000	1.000

Table XVII

Activity coefficients in the monomeric acetic acid–dimeric acetic acid–toluene mixture as a function of the nominal mole fraction of toluene

x_B	γ_1	γ_2	γ_3
0.0	$0.722 \cdot 10^{-2}$	0.922	1.260
0.2	$0.416 \cdot 10^{-2}$	0.978	1.090
0.4	$0.351 \cdot 10^{-2}$	0.992	1.025
0.6	$0.370 \cdot 10^{-2}$	0.996	1.006
0.8	$0.422 \cdot 10^{-2}$	0.997	1.001
1.0	$0.492 \cdot 10^{-2}$	1.000	1.000

From the partial pressures the nominal mole fraction of the non-polar component in the vapour phase can be calculated in the following way [3]

$$y_B = \frac{p_3}{p_1 + 2p_2 + p_3} \tag{27}$$

The results are shown in Table XIX.

Table XVIII

substance	p (torr)
Monomeric acetic acid	2182.0 [3]
Dimeric acetic acid	12.5 [3]
n-heptane	36.5 [14]
Benzene	77.2 [14]
Toluene	22.5 [14]

Table XIX

x_B	y_B		
	n-heptane	benzene	toluene
0.00	0.000	0.000	0.000
0.05	0.591	—	—
0.15	0.652	—	—
0.20	0.655	0.628	0.337
0.40	0.663	0.810	0.557
0.60	0.683	0904	0.733
0.80	0.764	0.962	0.879
0.85	0.793	—	—
0.95	0.877	—	—
1.00	1.000	1.000	1.000

The calculated data shown in Table XIX were compared with experimental values. Data for the acetic acid–benzene system were taken from the literature [13]. These data are collected in Tables XX and XXI. There are no data in the literature for the acetic acid–toluene system at 20 °C; therefore, the corresponding x–y values were determined experimentally. The experimental procedure was described elsewhere [3]. The experimental values are listed in Table XXII.

For purposes of comparison, the data referring to the vapour–liquid equilibrium, shown in Tables XIX, XX, XXI and XXII, were plotted in Figs 7, 8, 9. The plots indicate a good agreement between the calculated and ex-

Table XX

Nominal composition of the equilibrium vapour phase of acetic acid–n-heptane mixtures at 20°C as a function of the nominal mole fraction of n-heptane in the liquid phase [13]*

x_B	y_B	Δy(%)	x_B	y_B	Δy(%)
0.000	0.000	—	0.581	0.660	−3.0
0.072	0.561	−9.6	0.627	0.669	−3.1
0.094	0.602	−4.8	0.721	0.692	−3.9
0.121	0.616	−4.9	0.786	0.718	−3.5
0.155	0.638	−2.2	0.806	0.718	−7.1
0.191	0.648	−1.5	0.837	0.742	−5.1
0.222	0.650	−1.5	0.865	0.756	−4.0
0.304	0.653	−1.4	0.906	0.793	−5.0
0.375	0.654	−2.0	0.916	0.819	−2.8
0.442	0.655	−2.1	1.000	1.000	—
0.501	0.650	−3.5			

* Note: The last column indicates the deviation (Δy) between the calculated and experimental results.

Table XXI

Nominal composition of the equilibrium vapour phase of acetic acid–benzene mixtures at 20°C as a function of the nominal mole fraction of benzene in the liquid phase [13]*

x_B	y_B	Δy(%)	x_B	y_B	Δy(%)
0.000	0.000	—	0.607	0.880	−3.9
0.124	0.608	+3.6	0.638	0.888	−4.0
0.146	0.640	+8.9	0.671	0.898	−4.5
0.176	0.671	+9.8	0.722	0.909	−3.9
0.216	0.714	+8.7	0.809	0.934	−2.3
0.251	0.743	+7.3	0.880	0.954	−1.9
0.288	0.765	+5.5	0.919	0.965	−1.5
0.333	0.787	+1.6	0.935	0.971	−0.8
0.350	0.795	−0.1	0.970	0.984	−0.6
0.422	0.826	−2.3	1.000	1.000	—
0.486	0.843	−3.4			

* Note: The last column indicates the deviation (Δy) between the calculated and experimental values.

perimental data. The agreement is particularly good in the case of the acetic acid–toluene mixture (Fig. 9). The experimental data on acetic acid–benzene mixture show a slight positive deviation from the calculated values (Fig. 8).

Table XXII

*Nominal composition of the equilibrium vapour phase of acetic acid–toluene mixtures at 20°C as a function of the nominal mole fraction of toluene in the liquid phase**

x_B	y_B	Δy(%)	x_B	y_B	Δy(%)
0.000	0.000	—	0.482	0.631	−1.3
0.061	0.102	−12.7	0.509	0.677	+0.6
0.092	0.156	− 7.7	0.697	0.802	−1.9
0.130	0.212	− 7.5	0.722	0.830	−1.1
0.182	0.285	− 4.6	0.818	0.900	−0.2
0.233	0.368	0.0	0.845	0.908	−1.3
0.328	0.486	+ 1.6	1.000	1.000	—

* Note: The last column indicates the deviation (Δy) between the calculated and experimental values.

The most significant result is the agreement between the experimental and calculated data on the vapour–liquid equilibrium in the acetic acid–*n*-heptane mixture since this system has an azeotropic composition (Fig. 7), *i.e.* it represents the largest deviation from Raoult's law.

In summary the conclusion can be drawn, that the association equilibrium constant determined in the acetic acid–carbon tetrachloride mixture (see Eq. (2)) and the molecular data (molecular sizes, dielectric properties) can be used to calculate vapour–liquid equilibrium data for the mixtures of acetic acid with other non-polar substances. Using the above data, the excess free enthalpy of mixing is qualitatively provided. These data cannot be, how-

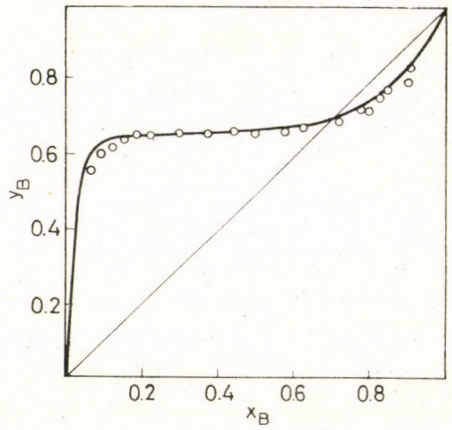

Fig. 7. n-Heptane nominal mole fraction in the vapour phase as a function of its liquid-phase nominal mole fraction at 20 °C. Solid line — calculated values, ○ — experimental data

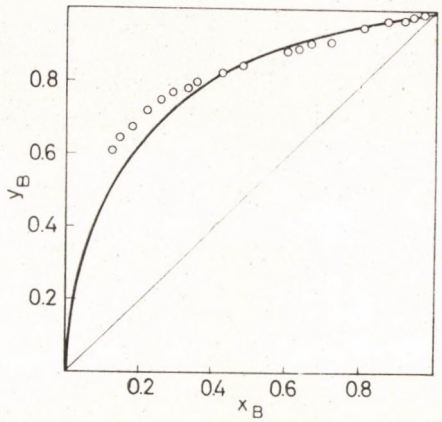

Fig. 8. Benzene nominal mole fraction in the vapour phase as a function of its liquid-phase nominal mole fraction at 20 °C. Solid line denotes calculated values, ○ — experimental data

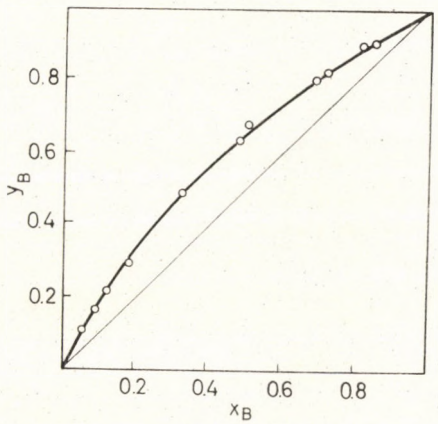

Fig. 9. Toluene nominal mole fraction in the vapour phase as a function of its liquid-phase nominal mole fraction at 20 °C. Solid line corresponds to the calculated values, ○ — experimental data

ever, used to calculate the enthalpy of mixing. It is assumed that the enthalpy of mixing is much more sensitive to simplifications introduced during the application of data obtained for the acetic acid–carbon tetrachloride mixture than are vapour–liquid equilibrium data or the excess free enthalpy of mixing.

Symbols

A — monomeric acetic acid
A_2 — dimeric acetic acid
B — non-polar substance
G^E — excess free enthalpy of mixing
Δh — enthalpy of mixing for 1 mole of the real mixture

ΔH — enthalpy of mixing for 1 mole of the nominal mixture
H^E — enthalpy of mixing
K — association equilibrium constant expressed with mole fractions
N — number of moles
p — partial pressure
p^e — equilibrium vapour pressure
r — molecular radius
R — gas constant
T — absolute temperature
u — average molecular interaction energy
v — molar volume
w — energy of interchange
x — mole fraction in liquid phase
y — mole fraction in vapour phase
z — coordination number
α — average polarizability
γ — activity coefficient
μ — permanent dipole moment

Subscripts

1 — monomeric acetic acid in the real (ternary) mixture
2 — dimeric acetic acid in the real (ternary) mixture
3 — non-polar component in the real (ternary) mixture
a — association
ac — acetic acid in the nominal (binary) mixture
B — non-polar component in the nominal (binary) mixture
d — dissociation
e — mixing
i — component in general
j — component in general
r — reaction
real — real
sep — separation

REFERENCES

1. Liszi, J.: Magy. Kém. Foly. **75,** 158 (1969)
2. Liszi, J.: Magy. Kém. Foly. **75,** 443, 447 (1969)
3. Liszi, J.: Magy. Kém. Foly. **75,** 452 (1969)
4. Liszi, J.: Magy. Kém. Foly. (In the press)
5. Pimentel, G. C., McLellan, A. L.: The Hydrogen Bond. Freeman and Co., 1960
6. Moelwyn-Hughes, E. A.: Physical Chemistry. Pergamon Press, 1964
7. Scholte, T. G.: Physica **15,** 437 (1949)
8. Illic, M.: Technika Beograd **19,** 1877 (1964)
9. Partington, J. R.: An Advanced Treatise on Physical Chemistry, V. Longmans, 1954
10. Bretsnaider, S.: Svoistva gazov i zhidkostiei. Moscow, 1966
11. Freedman, E.: J. Chem. Phys. **21,** 1784 (1953)
12. Zawidski, J.: Z. Phys. Chem. **35,** 129 (1900)
13. Werner, G.: J. Prakt. Chem. **29,** 26 (1965)
14. Reid, R. C. Sherwood, T. K.: The Properties of Gases and Liquids. McGraw-Hill, 1966

János Liszi; Veszprém, Schönherz Z. u. 12. Hungary.

Acta Chimica Academiae Scientiarum Hungaricae, Tomus 66 (4), pp. 431—438 (1970)

SPECTROSCOPIC INVESTIGATION OF SUBSTITUTED CARBONYL GROUPS

Á. I. KISS and G. HORVÁTH

(Department of Physical Chemistry, Technical University, Budapest, and Chemical and Pharmaceutical Works Chinoin, Budapest)

Received August 8, 1969

The ultraviolet and infrared spectra of some benzaldehyde derivatives have been studied in order to obtain information on the relative magnitudes of the $-M$ effect of substituted carbonyl (—COX) groups. The changes in the positions of the $n \rightarrow \pi^*$ and $\pi \rightarrow \pi^*$ bands are interpreted with the electron donor or acceptor character of the X group, respectively, which produces a decrease or increase in the $-M$ effect of —COX, as well as changes in the electronic energy levels of benzaldehyde. As shown by their mesomeric effect, fluorine behaves as a donor, chlorine and bromine seem to be acceptors. For Cl and Br it is supposed that p–d conjugation is playing a role besides p–p conjugation ($+M$ effect). The electronic spectra suggest the following order for the $-M$ effect of the —COX groups investigated:

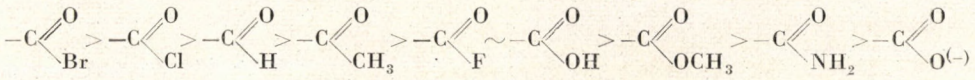

The shifts of the C=O stretching frequencies in the infrared spectra correspond to the changes in the electronegativity values of the X groups.

Only few data are available concerning the relative magnitudes of the $-M$ effect of carbonyl groups substituted by halogen atoms. A survey of the literature shows that primarily the —COCl group has been investigated; the electronic spectra and substituent effects for —COF and —COBr derivatives are not given. It is generally accepted that the $-M$ effect of substituted carbonyl groups decreases in the following order [1]:

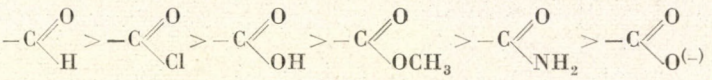

The decrease of the $-M$ effect corresponds to the increase of the $+M$ effect of the donor group linked to the carbon atom of the carbonyl group. It is to be expected that an acceptor group on the carbonyl carbon atom will increase the $-M$ effect.

Recently, FORBES and MYRON [2] have found as a result of the investigation of the K-bands of monosubstituted benzenes and p-substituted benzoyl chlorides that the $-M$ effect decreases in the following order:

$$-NO_2 > -COCl > -CHO > -COCH_3 \,.$$

They concluded that the chlorine atom does not take part essentially in the mesomerism.

It was expected that an investigation of the electronic spectra of carbonyl halides would give information on the substituent effect of halogen atoms. For this reason we studied the electronic spectra of benzoyl halides as well as those of some other aromatic carbonyl derivatives.

Experimental*

Benzoyl fluoride was prepared from benzoic acid and KHF_2 as described in the literature [3]. Benzoyl bromide was obtained from the reaction of benzoyl chloride and PBr_3 [4]. The other compounds investigated were commercial products; they were purified by distillation or recrystallization until the physical constants given in the literature were obtained.

The ultraviolet solution spectra were obtained with a Unicam SP 500 spectrophotometer by standard methods. The infrared spectra were determined in CCl_4 solution as well as in the vapour or liquid state, with a Zeiss UR 10 recording spectrophotometer.

Results and discussion

1. $n \rightarrow \pi^*$ *transition*

As it is known, the $n \rightarrow \pi^*$ transition band in the electronic spectra of carbonyl compounds arises from the excitation of a non-bonding electron of the oxygen atom to the antibonding orbital of the carbonyl group. This band is, in general, characteristic of carbonyl derivatives.

In order to clarify the effect of substituents on the carbonyl $n \rightarrow \pi^*$ transition, it is the most appropriate to consider it without the disturbing effect of $\pi \rightarrow \pi^*$ transitions, that is, in the case of saturated compounds for which a great number of data are available in the literature. As stated, the $n \rightarrow \pi^*$ band of saturated carbonyl compounds is shifted to shorter wavelengths if the carbonyl carbon atom has an electron donating substituent, and to longer wavelengths if it is substituted with an electron acceptor group [5]. For example, the $n \rightarrow \pi^*$ band appearing at 291 nm in the spectrum of acetaldehyde is shifted to 277 nm in acetone [6] because of the weak electron donor behaviour of the methyl group. This short wavelength shift may be explained by hyperconjugation of the methyl group increasing the energy of the π^* level [6, 7]. If a strong electron donor group is present, the band shows a large hypsochromic shift, therefore saturated carboxylic acids, esters, and amides absorb only in the region of 200—210 nm [7, 8]. The $n \rightarrow \pi^*$ band is partly covered by the more intense $n \rightarrow \sigma^*$ and $\pi \rightarrow \pi^*$ bands which appear between 175

* Part of the experimental work was carried out by Á. I. K. at the School of Chemical Sciences, University of East Anglia, Norwich, during a British Council scholarship.

and 195 nm and in the region of 155—165 nm, respectively [9]. On the other hand, the $n \rightarrow \pi^*$ band of pyruvic acid appears at 330 nm [10] because of the bathochromic shift caused by the carboxyl group. This spectral behaviour may be interpreted in the following way [5]. The π-type occupied orbital of

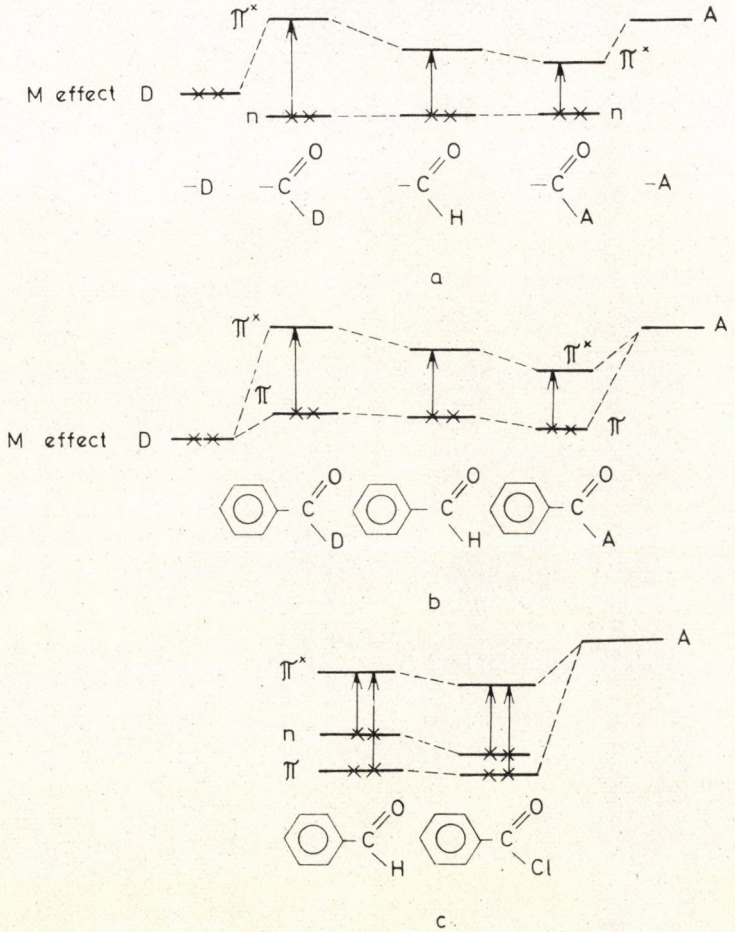

Fig. 1

the donor (D) group interacts with the antibonding π^*-orbital of the carbonyl group hereby increasing its energy. The unoccupied π-type orbital of the acceptor (A) group lowers the energy of the carbonyl antibonding orbital. Since the n level is not altered appreciably, the energy of the $n \rightarrow \pi^*$ transition is increased in the first, and decreased in the second, case (Fig. 1a).

In aromatic compounds, the presence of the $\pi \rightarrow \pi^*$ transition bands of the benzene ring makes more difficult the determination of the position of

the carbonyl $n \rightarrow \pi^*$ band. For an investigation of the ultraviolet spectra of aromatic carbonyl derivatives, benzaldehyde seems to be the most suitable reference compound. In an earlier paper [11] we have shown through solvent effect investigations that the low-intensity band system between 300 and 380 nm may be ascribed to $n \rightarrow \pi^*$ transition.

The substitution of the carbonyl group is expected to have the same spectral effect both in saturated and aromatic derivatives, that is, the shifts of the $n \rightarrow \pi^*$ bands may be interpreted by changes in the energy of the π^* level (Fig. 1a). This is entirely verified by the spectra of the corresponding benzene derivatives. The $n \rightarrow \pi^*$ band appears in the spectrum of acetophenone at shorter wavelengths than in that of benzaldehyde. The band assignment is proved by the short wavelength shift caused by polar solvents (Table I). In the spectra of derivatives whose carbonyl group is substituted with groups having $+M$ effect, the $n \rightarrow \pi^*$ band does not appear. It is probably covered, because of its large blue shift, by the more intense bands of benzene. This may be observed with the spectra of benzoic acid, methyl benzoate, benzamide, benzoyl fluoride, chloride, and bromide. It seems from the non-appearance of the $n \rightarrow \pi^*$ bands as if the halogen atoms had electron donor behaviour.

Table I

Electronic spectral data of

Compound	Solvent	$n \rightarrow \pi^*$ band		
		λ_{max}(nm)	cm^{-1}	log ε
Benzaldehyde	hexane	339	29499	1.44
	ethanol	324	30864	1.48
	0.1 *N* HCl	(324)	(30864)	1.55
Acetophenone	hexane	321	31153	1.61
	ethanol	(312)	(32051)	1.80
Benzoic acid	hexane	—	—	—
	ethanol	—	—	—
	0.01 *N* HCl	—	—	—
Methyl benzoate	cyclohexane		—	
	ethanol		—	
Benzamide	cyclohexane		—	
	ethanol		—	
Sodium benzoate	0.01 *N* NaOH		—	
Benzoyl fluoride	cyclohexane		—	
Benzoyl chloride	hexane		—	
Benzoyl bromide	hexane		—	

Wavelength values in parantheses refer to inflections or shoulders.

2. $\pi \rightarrow \pi^*$ *transitions*

Further information concerning the substituent effect of carbonyl halides may be obtained from the investigation of the $\pi \rightarrow \pi^*$ transitions. In the term scheme of Fig. 1b we consider only one π and π^* level, but it is supposed that all levels of this kind have the same behaviour. The mesomeric interaction of the carbonyl group with the benzene ring is reduced by an electron donor group. The result of the interaction of the donor orbital with the benzaldehyde levels is that the energy of the π^* level of benzaldehyde is raised more than that of the π level (Fig. 1b). This results in a hypsochromic shift of the $\pi \rightarrow \pi^*$ bands as compared with the case of benzaldehyde. According to the experimental data of Table I, the shift increases parallel to the increasing $+M$ effect of the substituent on the carbonyl carbon atom. An electron acceptor group increases the $-M$ effect of the carbonyl bond, thus the interaction between the benzene ring and the carbonyl group is increased. The energy of the π^* level is lowered more than that of the π level (Fig. 1b). In this case the $\pi \rightarrow \pi^*$ bands show red shift in comparison with the spectrum of benzaldehyde.

aromatic carbonyl derivatives

$\pi - \pi^*$ bands					
λ_{max}(nm)	cm^{-1}	log ε	λ_{max}(nm)	cm^{-1}	log ε
278	35971	2.97	240.5	41570	4.03
281	35587	3.08	246	40650	4.01
283	35336	3.19	249	40161	4.10
278	35971	2.95	238	42016	4.13
279	35842	3.02	242	41322	4.08
274	36496	3.02	231	43290	4.20
272	36765	2.90	227	44053	4.08
273	36630	3.00	230	43478	4.09
273	36630	2.98	228	43860	4.10
273	36630	2.95	228	43860	4.08
270	37037	2.90	221—2	45249—45045	4.00
269	37175	2.71	225	44444	3.88
268	37313	2.79	224	44648	3.98
276.5	36166	3.04	230	43478	3.99
282—3	35461—35336	3.10	241	41494	4.18
283	35336	3.25	246	40650	4.27

For bands having vibrational structure only the maximum of highest intensity is given.

The spectra of benzoyl fluoride, chloride, and bromide in hydrocarbon solvent are shown on Fig. 2. According to the hypsochromic shift of the $\pi \rightarrow \pi^*$ bands of benzoyl fluoride, the fluorine atom has donor character. The bands of benzoyl chloride have nearly the same positions as those of benzaldehyde, only with a small bathochromic shift. The $\pi \rightarrow \pi^*$ bands of benzoyl bromide

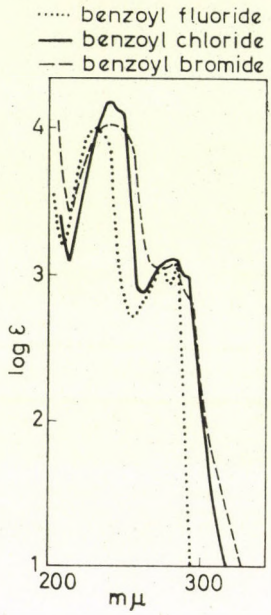

Fig. 2

show bathochromic shift with respect to benzaldehyde which may arise from the acceptor character of the bromine atom. This may be explained if we consider the *p–d* conjugation by which the bromine (and to a smaller extent the chlorine) atom may accept electrons to its unoccupied *d* shell (*cf.* [12]). This effect lowers the π^* level more than the π level.

The non-appearance of the $n \rightarrow \pi^*$ band in the spectrum of benzoyl chloride and bromide may be due to the decrease of the *n* level. This change in the energy of the *n* level may be explained by taking into consideration the inductive effect of the halogen atoms. This decreases the energy of the *n* level of the oxygen atom by means of increasing its ionization potential. It is difficult to estimate the inductive effect exerted on the π levels; energy changes taking place in a similar manner, but to a smaller extent, are probable. In Fig. 1c therefore, we consider the energies of the π and π^* levels to be the same as those given in Fig. 1b. The decrease of the π levels caused by the $-M$ and $-I$ effects seems to be smaller than that of the *n* level, which explains

the hypsochromic shift of the $n \rightarrow \pi^*$ band. It is possible that the inductive effect contributes to the hypsochromic shift also in hydroxy and amino derivatives.

3. *Infrared spectra*

We also studied the infrared spectra of benzoyl halides with a view to investigate the substituent effects, since the frequency of the carbonyl stretching vibration may afford further information. With electron donating substituents, the decrease in the C=O frequency is related to the decrease of the bond strength [13, 14]. The same behaviour is expected for electron-releasing inductive effect and the reversed for electron-attracting effect. This is entirely verified by the spectra studied (Table II). The frequency shifts parallel to the

Table II

Infrared carbonyl stretching frequencies of benzoyl derivatives

Compound	ν(C=O) (cm^{-1})		
	vapour	liquid	CCl_4 solution
Benzaldehyde	—	1706	1712
Benzoic acid	—	—	1702
Acetophenone	1714	1688	1686
Benzoyl fluoride	—	1802	1810
Benzoyl chloride	1796	1771	1772
Benzoyl bromide	1790	1765	1768

The data for the benzoyl halides in the liquid state have been taken from the literature [15].

changes of electronegativity values as stated by FORBES and MYRON [2] for the methyl and chloro groups. Recently DELORME *et al.* [15] published the infrared and Raman spectra of the four benzoyl halides. According to these results, the C=O frequencies are increased parallel to the increase of the electronegativity of the halogen atoms. The vibrational frequencies of benzoyl halides are determined primarily by the electronegativity values, whereas the energies of the electronic transitions are influenced by the effect of the halogen atoms on the π^* levels.

Theoretical calculations of the energy levels of these derivatives are in progress.

*

The authors are greatly indebted to Dr. S. HOLLY for the measurement of infrared spectra, and to Mr. L. PUSZTAY for his very competent assistance in the experimental work.

REFERENCES

1. STAAB, H. A.: Einführung in die theoretische organische Chemie, 3. Auflage. Verlag Chemie, Weinheim-Bergstr. 1963
2. FORBES, W. F., MYRON, J. J. J.: Can. J. Chem. **39**, 2452 (1961)
3. MASHENTSEV, A. I.: J. Gen. Chem. USSR, **15**, 915 (1945), C. A. **40**, 6443 (1946)
4. STAUDINGER, H., ANTHES, E.: Chem Ber. **46**, 1417 (1913)
5. MURRELL, J. N.: The Theory of the Electronic Spectra of Organic Molecules. Methuen, London, 1963
6. RAO, C. N. R., GOLDMAN, G. K., BALASUBRAMANIAN, A.: Can. J. Chem. **38**, 2508 (1960)
7. JAFFÉ, H. H., ORCHIN, M.: Theory and Applications of Ultraviolet Spectroscopy. Wiley, New York, 1962
8. BURAWOY, A.: Tetrahedron, **2**, 122 (1958)
9. TURNER, D. W. in Determination of Organic Structures by Physical Methods, Vol. 2. Edited by NACHOD, F. C. and PHILLIPS, W. D., Academic Press, New York, 1962
10. ERRERA, M., GREENSTEIN, J. P.: Arch. Biochem. **14**, 477 (1947), **15**, 445 (1947); MACKINNEY, G., TEMMER, O.: J. Am. Chem. Soc. **70**, 3586 (1948)
11. KISS, Á. I., HORVÁTH, G.: Acta Chim. Acad. Sci. Hung. **39**, 39 (1963)
12. GOODMAN, L., FROLEN, L. J.: J. Chem. Phys. **30**, 1361 (1959).
13. BARROW, G. M.: J. Chem. Phys. **21**, 2008 (1953)
14. TANAKA, J., NAGAKURA, S., KOBAYASHI, M.: J. Chem. Phys. **24**, 311 (1956)
15. DELORME, P., LORENZELLI, V., ALEMAGNA, A.: J. chim. phys. **62**, 3 (1965)

Árpád István KISS; Budapest, XI. Budafoki út 8
Gábor HORVÁTH; Budapest, VII., Rottenbiller u. 26.

Acta Chimica Academiae Scientiarum Hungaricae, Tomus 66 (4), pp. 439—445 (1970)

SUBSTITUTED BENZAMIDOXIMES ACTING ON THE CENTRAL NERVOUS SYSTEM

G. SZILÁGYI, E. KASZTREINER, K. KOVÁCS* and J. BORSY

*(Research Institute for Pharmaceutical Chemistry, Budapest and *Institute of Organic Chemistry, József Attila University, Szeged)*

Received July 28, 1969

4-Methoxy-3,5-dihalo- and 4-n-octyloxy-3,5-dimethoxybenzamidoximes as well as their O-acyl- and O-alkyl derivatives have been synthesized for a study of the structure-activity (CNS, antibacterial and anticancer) relationships.

Pharmacologial evaluation revealed several correlations between chemical constitution and physiological actions. The CNS actions became weaker on both O-acyl and O-alkyl substitution.

The compounds had no anticancer activity, one of them (V-336), however, showed a medium antibacterial activity *in vitro* against typical strains.

In our previous works [1, 2] several substituted, hypnotic and anticonvulsant benzamides have been prepared. Among these compounds N-cyclopropyl-4-methoxy-3,5-dichlorobenzamide proved to be the most effective hypnotic, and 4-n-octyloxy-3,5-dimethoxybenzamide and 4-n-octyloxy-3,5-dimethoxyphenylacetamide [3] were found the most favourable anticonvulsants. By various structural modifications of the compounds it has been established that — for the above CNS actions — the most convenient structures of the lipophilic part of the molecules are 4-methoxy-3,5-dichlorophenyl- and 4-n-(C_8-C_{10})alkoxy-3,5-dimethoxyphenyl groups; further, nitrogen-containing groups of some kind must be present in the hydrophilic part of the molecule. On the basis of these results, the preparation of other nitrogen-containing acid derivatives seemed interesting for a study of the structure-activity relations.

Concerning physiological actions, the amidoxime group has furnished promising results: *e.g.*, in an investigation of *o*- and *p*-methoxy-, methyl-, chloro-, and trifluoromethylphenoxyacetamidoximes, CAMPBELL [4] showed that the amidoxime group was indispensable for a hypotensive action. 2- and 4-hydroxy-5- (or 3,5-di-)-halobenzamidoximes prepared by BUU-HOI *et al.* [5, 6] had significant antituberculotic action. According to BERGMANN *et al.* [7], the O-acetyl- and O-benzoyl derivatives of *p*-aminobenzenesulphonylbenzamidoxime were active against typhus bacilli; GRAY and LAMBERT [8] demonstrated the antibacterial activity of N- and O-methyl-2-hydroxybenzamidoximes. These examples show that compounds containing the amidoxime group present several important physiological actions. Surprisingly, results have hardly been published on the CNS actions of these compounds.

Table I

Substituted

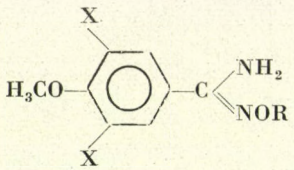

I

Co. No.	Type	X	R	M. p., °C	Yield, %	Recrystallization solvent	Empirical formula	Molecular weight
V-315	I	Cl	H	207—209	72.5	ethanol	$C_8H_8Cl_2NO_2$	235.15
V-316	I	Br	H	199—201	64.5	ethanol	$C_8H_8Br_2NO_2$	324,15
V-317	II		H	87—89	92.5	ethyl acetate	$C_{17}H_{28}N_2O_1$	325,3
V-335	I	Cl	CH_3CO	124—127	82.3	ethanol	$C_{10}H_{10}Cl_2N_2O_3$	277,2
V-336	I	Cl	C_6H_5CO	147—149	65.5	ethanol	$C_{15}H_{12}Cl_2N_2O_3$	337.3
V-347	I	Cl	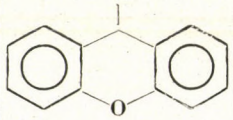	164—166	40.8	ethanol	$C_{22}H_{16}Cl_2N_2O_4$	443,4
V-337	I	Br	CH_3CO	125—126	86.1	ethanol	$C_{10}H_{10}Br_2N_2O_3$	366.2
V-338	I	Br	C_6H_5CO	167—169	56.4	ethanol	$C_{15}H_{12}Br_2N_2O_3$	428.3
V-339	II		CH_3CO	105—107	35.5	ethyl acetate	$C_{19}H_{32}N_2O_5$	367.5
V-340	II		C_6H_5CO	151—153	29.5	ethanol	$C_{24}H_{32}N_2O_5$	427.5
V-349	II		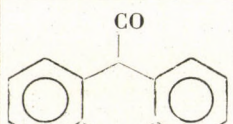	162—163	51.0	ethanol	$C_{31}H_{36}N_2O_6$	533.6

benzamidoximes

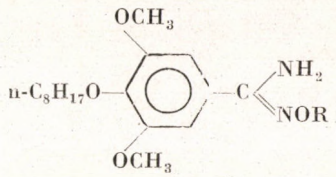

II

Analysis %						IR spectra cm^{-1}	
Calcd.:			Found:				
C	H	N	C	H	N		
40.84	3.41	11.93	41.07	3.35	11.56	ν_{OH}: 3430; $\nu_{NH_3^+}$: 3600—2400; $\gamma_{C=N}$ 1675; $\delta_{NH_3^+}$: 1560; $\delta_{NH_3^+} + \gamma_{OH}$: 800—500	related to the spectra of the hydrochlorides
29.62	2.47	8.65	29.67	2.41	8.47	ν_{OH}: 3370; $\nu_{NH_3^+}$: 3600—2400; $\gamma_{C=N}$: 1670; $\delta_{NH_3^+}$: 1550; $\delta_{NH_3^+} + \gamma_{OH}$: 800—500	
62.54	8.66	8.62	62.63	8.70	8.77	$\gamma_{NH_3^+} + \gamma_{OH}$: 3500—2400 $\gamma_{C=N}$: 1665; γ_{OCH_3}: 1135	
43.37	3.63	10.15	43.42	3.61	10.11	ν_{ester}: 1230 and 1100; $\nu_{C=O}$: 1760; ν_{NH_2}: 3500—3100; ν_{CN}: 1640	
53.52	3.57	8.36	53.51	3.59	8.47	ν_{ester}: 1270 and 1090; $\nu_{C=O}$: 1735; ν_{NH_2}: 3500—3100; ν_{CN}: 1640	
59.58	3.61	6.32	59.71	3.64	6.28	ν_{asNH_2}: 3490; ν_{sNH_2}: 3330; $\nu_{C=O}$: 1750; ν_{CN}: 1630; ν_{ester}: 1265	
32.76	2.74	7.65	32.81	2.70	7.64	ν_{ester}: 1230 and 1010; $\nu_{C=O}$: 1760; $\nu_{C=N}$: 1620; ν_{asNH_2}: 3500; ν_{sNH_2}: 3350	
42.12	2.81	6.55	42.24	2.86	6.59	ν_{ester}: 1260 and 1020; $\nu_{C=O}$: 1740; $\nu_{C=N}$: 1640; ν_{asNH_2}: 3500; ν_{sNH_2}: 3350	
62.46	8.73	7.62	62.67	8.84	7.55	ν_{ester}: 1240 and 1010; $\nu_{C=O}$: 1750; $\nu_{C=N}$: 1630; ν_{asNH_2}: 3500; ν_{sNH_2}: 3350	
67.42	7.48	6.52	67.31	7.56	6.62	ν_{ester}: 1250 and 1020; $\nu_{C=O}$: 1740; $\nu_{C=N}$: 1620; ν_{asNH_2}: 3500; ν_{sNH_2}: 3350	
72.05	6.93	5.25	72.18	6.99	5.49	ν_{ester}: 1265; $\nu_{C=O}$: 1745; $\nu_{C=N}$: 1625; ν_{asNH_2}: 3480; ν_{sNH_2}: 3345	

Table I

Co. No.	Type	X	R	M. p., °C	Yield, %	Recrystallization solvent	Empirical formula	Molecular weight
V-417	I	Cl	CH_3	106—109	37.7	petroleum ether	$C_9H_{10}Cl_2N_2O_2$	245.2
V-409	I	Cl	$CH_2=CHCH_2$	81—84	20.8	petroleum ether	$C_{11}H_{12}Cl_2N_2O_2$	275.2
V-422	I	Br	$CH_2=CHCH_2$	117—119	36.0	ethyl acetate	$C_{11}H_{10}Br_2N_2O_2$	372.2
V-443	I	Br	CH_3, CH_3 $\rangle NCH_2CH_2$	162—163	22.1		$C_{12}H_{18}Br_2ClN_3O_2$	431.6
V-423	II		CH_3	133—135	22.1	petroleum ether	$C_{18}H_{30}N_2O_4$	339.4

* Cl^-(8.23) : 8.29

In our present work 4-methoxy-3,5-dichloro- (and dibromo-) and 4-n--octyloxy-3,5-dimethoxybenzamidoximes, furthermore their O-acyl and O-alkyl derivatives were synthesized and examined pharmacologically.

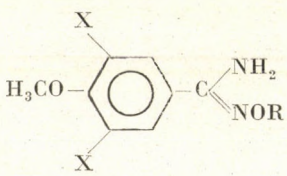

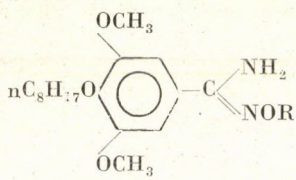

(X = Cl, Br; R = acyl or alkyl group)

Preliminary tests showed that some of these amidoximes and their derivatives had relatively strong CNS (hypnotic, tranquillizing and anticonvulsant) and furthermore antibacterial actions. In order to study these effects, the following structural variations were made on the compounds:

(*a*) In accordance with our previous investigations, 4-methoxy-3,5-dihalo- and 4-*n*-octyloxy-3,5-dimethoxyphenyl groups were employed as the fundamental structures.

(*b*) Concerning the amidoxime part unsubstituted, O-acyl (acetyl, benzoyl and xanthene-9-carbonyl-) and O-alkyl (or basic alkyl) deivatives were prepared.

Data of the compounds prepared are summarized in Table I.

continued

Analysis %						IR spectra cm^{-1}
Calcd.:			Found:			
C	H	N	C	H	N	
44.05	4.08	11.42	43.92	4.14	11.57	$\nu_{C=N}$: 1640; ν_{NH_2}: 3500—2800; $\nu_{C-O(CH_3)}$: 2815, 1060, 995
47.58	4.38	10.42	47.75	4.42	10.26	ν_{C-O-C}: 1270; $\nu_{C=N}$: 1670; $\nu_{C=C}$: 3080 and 1650 ν_{asNH_2}: 3490; ν_{sNH_2}: 3390
35.18	2.68	7.55	35.33	2.74	7.64	ν_{asNH_2}: 3490; ν_{sNH_2}: 3395; $\nu_{C=N}$: 1670; $\nu_{C=C}$: 3080, 1650, 1000, 900
33.38	4.21	9.68	33.42	4.14	9.73*	$\nu_{C=N}$: 1670; $\nu_{NH_3^+}$: 3000
63.53	8.82	4.13	63.42	8.84	4.25	ν_{CH}: 2950—2850; $\nu_{C=N}$: 1670; ν_{NH_2}: 3370 and 3190

The pharmacological evaluation permitted several interesting observations on the structure-activity relationships:

(*a*) Both halogen- and trialkoxy-substituted benzamidoximes showed a medium CNS activity —

(*b*) trialkoxybenzamidoximes had mainly anticonvulsant activity, whereas halogen-substituted compounds had no such activity —

(*c*) acylation or alkylation of the oximino groups caused a significant decrease in CNS activity —

(*d*) O-benzoyl-4-methoxy-3,5-dihalobenzamidoximes showed a medium antibacterial activity *in vitro* against typical strains (*Sarcina subflavia*, *Staphylococcus* strains) —

(*e*) both types of amidoximes were inactive against Yoshida and S-180 sarcomas —

(*f*) all compounds had low toxicity (1000—2000 mg/kg).

The amidoximes were prepared from the appropriately substituted benzonitriles [9]: the nitriles were reacted with hydroxylamine in aqueous ethanol in the presence of a base (*e.g.*, sodium carbonate).

O-Acetylamidoximes were prepared by reaction of the amidoxime with acetic anhydride; other O-acylamidoximes were obtained from the amidoxime with acid chlorides in benzene solution.

The synthesis of O-alkylamidoximes was accomplished by reaction of the amidoxime sodium salts with alkyl halides. The structures of the compounds were supported by their infrared spectra.

Experimental

All m. p.'s are uncorrected.

Amidoximes

A mixture of the appropriate benzonitrile (0.05 mole), Na_2CO_3 (0.05 mole), hydroxylamine hydrochloride (0.125 mole) and 50% aqueous ethanol (180 ml) was refluxed for 24 hrs. After evaporation of the ethanol the residue was triturated with 250 ml of water, and the solid residue was filtered off. After drying, the crude product was recrystallized.

O-Acylamidoximes

O-Acetylamidoximes

A mixture of the amidoxime (1 g) and acetic anhydride (2 ml) was allowed to stand for 2 hrs., then poured into water (10 ml) and the precipitate extracted into ethyl acetate (2×10 ml). The ethyl acetate solution was washed with water (2×10 ml) and dried over Na_2SO_4. After evaporation of the solvent, the residue was recrystallized.

Other O-acylamidoximes

A solution of the acid chloride (0.1 mole) in benzene (100 ml) was added by drops during 30 min to a stirred mixture of the amidoxime (0.1 mole) and benzene (250 ml), then the reaction mixture was stirred for 3 hrs. Next day the benzene solution was filtered, the precipitate washed with benzene (3×50 ml), dried and recrystallized.

O-Alkylamidoximes

The amidoxime sodium salt (0.1mole) was stirred in ethanol (250 ml), and a solution of the alkyl halide (0.1 mole) in ethyl acetate (200 ml) was added dropwise during 30 min; the mixture was refluxed for 8 hrs. The solvents were evaporated in vacuum, the residue was poured into water (200 ml), and the organic product extracted into ethyl acetate (2×200 ml). The ethyl acetate solution was dried over Na_2SO_4, the solvent evaporated and the residue recrystallized.

O-Dimethylaminoethyl-4-methoxy-3,5-dibromobenzamidoxime hydrochloride

A mixture of 4-methoxy-3,5-dibromobenzamidoxime sodium salt (11.6 g; 0.0382 mole), dimethylaminoethyl chloride hydrochloride (5.45 g; 0.0382 mole), and dry ethanol (200 ml) was refluxed for 7 hrs. and the precipitate filtered off after cooling. The ethanol was removed under reduced pressure, the residue dissolved in ether (150 ml) and washed with water (2×40 ml). The ethereal solution was dried over Na_2SO_4, filtered, saturated with gaseous hydrogen chloride and allowed to stand overnight. The crystals were filtered off, washed with ether and dried to give 3.64 g (22.1%) of the hydrochloride.

*

The authors wish to express their thanks to Professor L. VARGHA, Director of the Research Institute for Pharmaceutical Chemistry, for his continuous interest in this work; to the Analytical Department of the Institute for the analyses; to Dr. P. SOHÁR for the infrared spectra; and to Miss M. BITTÓ for her useful technical assistance.

REFERENCES

1. Hungarian Pat.: 152 398 (1965)
2. Hungarian Pat.: 153 246 (1965)
3. SZILÁGYI, G., KASZTREINER, E., VARGHA, L., BORSY, J.: Acta Pharm. Hung. **39**, 66 (1969)

4. US Pat.: 3 139 455 (1967)
5. BUU-HOI, N. P., XUONG, N. D., WELSH, M., THANG, K. V.: Experientia **10,** 169 (1954)
6. BUU-HOI, N. P., XUONG, N. D., THANG, K. V.: Bull. Soc. Chim. France **21,** 294 (1954)
7. BERGMANN, E. D., BENDAS, H., D'AVILLA, V.: J. Org. Chem. **18,** 64 (1953)
8. GRAY, J. D. A., LAMBERT, R. A.: Nature **162,** 733 (1948)
9. SZILÁGYI, G., KASZTREINER, E., VARGHA, L., BORSY, J.: Acta Chim. Acad. Sci. Hung. (In press)

Géza SZILÁGYI
Endre KASZTREINER
József BORSY
Budapest IV., Szabadságharcosok-u. 47/49
Kálmán KOVÁCS
Szeged, Beloiannisz-tér 8. Hungary.

Acta Chimica Academiae Scientiarum Hungaricae, Tomus 66 (4), pp. 447—454 (1970)

REAKTIVITÄT PHENOLISCHER VERBINDUNGEN GEGENÜBER 4-FLUOR-3--NITROACETOPHENON

W. WILDENHAIN, G. HENSEKE und G. BIENERT

(Sektion Chemie, Lehrstuhl für Organische Chemie der Bergakademie Freiberg (Sachs.))

Eingegangen am 15. August 1969

Die Reaktionsfähigkeit verschieden substituierter phenolischer Verbindungen gegenüber 4-Fluor-3-nitroacetophenon in dimethylformamidhaltiger Lösung wird durch deren Nucleophilie und sterischen Bau bestimmt.

Das von ZAHN und WÜRZ [1] zur Abscheidung und Bestimmung von Phenolen eingeführte 2,4-Dinitrofluorbenzol reagiert in dimethylformamidhaltiger Lösung unter modifizierten Versuchsbedingungen [2] quantitativ. 4-Fluor-3-nitroacetophenon läßt sich nach folgendem Chemismus ebenfalls nucleophil substituieren, wenngleich die Beweglichkeit des Fluors abgeschwächt ist [3]:

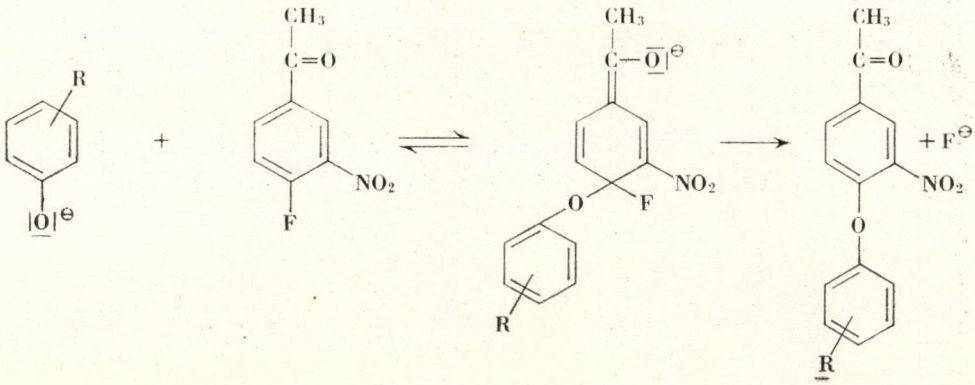

Es sollte untersucht werden, inwieweit unterschiedlich substituierte phenolische Verbindungen nach der für 2,4-Dinitrofluorbenzol angegebenen Arbeitsvorschrift [2] die Ätherbildung mit 4-Fluor-3-nitroacetophenon beeinflussen. Die Reaktionsfähigkeit der phenolischen Komponente wird durch deren Nucleophilie und räumlichen Bau bestimmt. Phenol liefert in 57%iger Ausbeute den entsprechenden 4-Acetyl-2-nitrophenyläther (ANP-Äther) (1). Zur Hydroxylfunktion *p*-ständige Methylgruppen sind ohne nennenswerten Einfluß auf das Ergebnis; befinden sie sich jedoch in *m*- oder *o*-Position, so tritt in zunehmendem Maße sterische Hinderung auf. Übereinstimmend sinkt

Derivate phenolischer Verbindungen mit 4-Fluor-3-nitroacetophenon

Serien-Nr.	ANP-Äther von:	Summenformel (Mol.-Gew.)	Elementaranalyse	C [%]	H [%]	N [%]	Schmp.	Ausbeute [%]
1	Phenol	$C_{14}H_{11}NO_4$ (257,3)	ber.	65,37	4,31	5,44	113 °C (Lit. [3]: 112—114 °C)	
			gef.	65,52	4,41	5,60	Hellgelbe Kristalle (Äthanol)	57
2	*o*-Kresol	$C_{15}H_{13}NO_4$ (271,3)	ber.	66,42	4,83	5,16	78—80 °C	
			gef.	66,62	4,62	5,14	Hellgelbe Kristalle (DMF/verd. Essigsäure)	32
3	*m*-Kresol	$C_{15}H_{13}NO_4$ (271,3)	ber.	66,42	4,83	5,16	99—100 °C	
			gef.	66,48	4,60	5,30	Hellgelbe Kristalle (DMF/verd. Essigsäure)	48
4	*p*-Kresol	$C_{15}H_{13}NO_4$ (271,3)	ber.	66,42	4,83	5,16	81 °C (Lit. [3]: 82—84 °C	
			gef.	66,38	4,78	5,19	Hellgelbe Kristalle (Äthanol)	54
5	2,3-Dimethylphenol	$C_{16}H_{15}NO_4$ (285,3)	ber.	67,36	5,30	4,91	122—123 °C	
			gef.	67,26	5,08	5,00	Hellgelbe Nadeln (DMF/verd. Essigsäure)	26
6	2,4-Dimethylphenol	$C_{16}H_{15}NO_4$ (285,3)	ber.	67,36	5,30	4,91	74—75 °C	
			gef.	67,32	5,06	5,08	Hellgelbe Nadeln (DMF/verd. Essigsäure)	41
7	2,5-Dimethylphenol	$C_{16}H_{15}NO_4$ (285,3)	ber.	67,36	5,30	4,91	85—86 °C	
			gef.	67,36	5,06	5,04	Hellgelbe Kristalle (Äthanol)	31
8	3,4-Dimethylphenol	$C_{16}H_{15}NO_4$ (285,3)	ber.	67,36	5,30	4,91	127—129 °C	
			gef.	67,34	5,13	4,88	Hellgelbe Kristalle (DMF/verd. Essigsäure)	47
9	3,5-Dimethylphenol	$C_{16}H_{15}NO_4$ (285,3)	ber.	67,36	5,30	4,91	90—91 °C	
			gef.	57,33	5,15	4,93	Hellgelbe Kristalle (DMF/verd. Essigsäure)	45

10	Thymol	$C_{18}H_{19}NO_4$ (313,3)	ber. gef.	68,99 68,97	6,11 5,98	4,47 4,64	61—62 °C Hellgelbe Nadeln (DMF/verd. Essigsäure)	42
11	Guajakol	$C_{15}H_{13}NO_5$ (287,3)	ber. gef.	62,72 62,74	4,56 4,54	4,87 4,84	90 °C Hellgelbe Nadeln (DMF/verd. Essigsäure)	56
12	3-Methoxyphenol	$C_{15}H_{13}NO_5$ (287,3)	ber. gef.	62,72 62,45	4,56 4,52	4,87 4,90	95 °C Hellgelbe Kristalle (DMF/verd. Essigsäure)	73
13	2,3-Dimethoxyphenol	$C_{16}H_{15}NO_6$ (317,3)	ber. gef.	60,56 60,73	4,77 4,60	4,42 4,37	114 °C Hellgelbe Nadeln (DMF/verd. Essigsäure)	45
14	2,6-Dimethoxyphenol	$C_{16}H_{15}NO_6$ (317,3)	ber. gef.	60,56 60,55	4,77 4,63	4,42 4,66	95—98 °C Hellgelbe Kristalle (DMF/verd. Essigsäure)	25
15	2-Chlorphenol	$C_{14}H_{10}ClNO_4$ (291,7)	ber. gef.	57,65 57,77	3,46 3,42	4,80 5,03	102—105 °C Hellgelbe Kristalle (DMF/verd. Essigsäure)	75
16	2,4,6-Trichlorphenol	$C_{14}H_8Cl_3NO_4$ (360,6)	ber. gef.	46,63 46,62	2,24 2,15	3,88 4,08	120 °C (Lit. [3]: 121—122 °C) Farblose Nadeln (DMF/verd. Essigsäure)	25
17	2-Nitrophenol	$C_{14}H_{10}N_2O_6$ (302,2)	ber. gef.	55,63 55,70	3,34 3,26	9,27 9,54	88—90 °C (Lit. [3]: 114—116 °C) Hellgelbe Kristalle (DMF/verd. Essigsäure)	66
18	3-Nitrophenol	$C_{14}H_{10}N_2O_6$ (302,2)	ber. gef.	55,63 55,59	3,34 3,14	9,27 9,25	110 °C Hellgelbe Kritalle (DMF/verd. Essigsäure)	73
19	4-Nitrophenol	$C_{14}H_{10}N_2O_6$ (302,2)	ber. gef.	55,63 55,47	3,34 3,26	9,27 9,27	99—100 °C (Lit. [3]: 111—113 °C) Hellgelbe Kristalle (DMF/verd. Essigsäure)	79

Serien-Nr.	ANP-Äther von:	Summenformel (Mol.-Gew.)	Elementaranalyse	C [%]	H [%]	N [%]	Schmp.	Ausbeute [%]
20	4-Hydroxybenzaldehyd	$C_{15}H_{11}NO_5$ (285,3)	ber.	63,15	3,88	4,91	75—76 °C	
			gef.	63,14	3,83	5,14	Hellgelbe Nadeln (DMF/verd. Essigsäure)	42
21	Vanillin	$C_{16}H_{13}NO_6$ (315,3)	ber.	60,95	4,15	4,44	85—90 °C	
			gef.	60,98	4,16	4,47	Hellgelbe Nadeln (DMF/verd. Essigsäure)	65
22	4-Hydroxyacetophenon	$C_{16}H_{12}NO_5$ (299,3)	ber.	64,21	4,38	4,68	125 °C	
			gef.	63,84	4,37	4,67	Hellgelbe Kristalle (DMF/verd. Essigsäure)	45
23	4-Hydroxy-3-methoxy-acetophenon	$C_{17}H_{15}NO_6$ (329,3)	ber.	62,00	4,59	4,25	123 °C	
			gef.	62,08	4,62	4,28	Farblose Nadeln (DMF/verd. Essigsäure)	76
24	4-Hydroxy-2-methoxy-acetophenon	$C_{17}H_{15}NO_6$ (329,3)	ber.	62,00	4,59	4,25	113 °C	
			gef.	62,10	4,59	4,41	Hellgelbe Kristalle (DMF/verd. Essigsäure)	82
25	2-Hydroxy-4-methoxy-acetophenon	$C_{17}H_{15}NO_6$ (329,3)	ber.	62,00	4,59	4,25	108 °C	
			gef.	62,30	4,54	4,31	Hellgelbe Nadeln (DMF/verd. Essigsäure)	27
26	4-Hydroxy-3-methoxy-propiophenon	$C_{18}H_{17}NO_6$ (343,3)	ber.	62,97	4,99	4,08	97 °C	
			gef.	62,87	5,01	4,34	Hellgelbe Kristalle (DMF/verd. Essigsäure)	76
27	α-Naphthol	$C_{18}H_{12}NO_4$ (307,3)	ber.	70,35	4,26	4,56	103 °C	
			gef.	70,43	4,16	4,61	Gelbe Kristalle (DMF/verd. Essigsäure)	85

28	β-Naphthol	$C_{18}H_{13}NO_4$ (307,3)	ber. gef.	70,35 70,64	4,26 4,25	4,56 4,84	115 °C (Lit. [3]: 120—122 °C) Gelbe Blättchen (DMF/verd. Essigsäure)	94
29	4-Hydroxybenzoesäure	$C_{15}H_{11}NO_6$ (301,3)	ber. gef.	59,80 59,64	3,68 3,67	4,65 4,81	191—195 °C Hellgelbe Kristalle (DMF/verd. Essigsäure)	60
30	Vanillinsäure	$C_{16}H_{13}NO_7$ (331,3)	ber. gef.	58,01 57,94	3,96 3,83	4,23 4,36	182—185 °C Hellgelbe Kristalle (DMF/verd. Essigsäure)	45
31	Syringasäure	$C_{17}H_{15}NO_8$ (361,3)	ber. gef.	56,51 56,22	4,18 4,14	3,91 3,96	230—240 °C Hellgelbe Kristalle (DMF/verd. HCl)	33
32	4-Hydroxyzimtsäure	$C_{17}H_{13}NO_6$ (327,3)	ber. gef.	62,39 62,58	4,00 4,01	4,28 4,32	172—185 °C Gelbe Kristalle (DMF/verd. Essigsäure)	46
33	Ferulasäure	$C_{18}H_{15}NO_7$ (357,3)	ber. gef.	60,50 60,48	4,23 4,20	3,92 4,09	220—238 °C Gelbe Kristalle (DMF/verd. Essigsäure)	48
34	N-ANP-3-Aminophenol	$C_{22}H_{17}N_3O_7$ (435,4)	ber. gef.	60,68 60,77	3,94 3,88	9,65 9,84	145—147 °C Gelbe Kristalle (Butanol)	23
35	N-ANP-4-Aminophenol	$C_{22}H_{17}N_3O_7$ (435,4)	ber. gef.	60,68 60,70	3,94 3,82	9,65 9,62	198—202 °C Goldgelbe Blättchen (Äthanol)	23
	Ais-ANP-Äther von:							
36	Brenzcatechin	$C_{22}H_{16}N_2O_8$ (436,4)	ber. gef.	60,55 60,53	3,69 3,70	6,42 6,49	90—91 °C Hellgelbe Kristalle (DMF/verd. Essigsäure)	16

Serien-Nr.	Bis-ANP-Äther von:	Summenformel (Mol.-Gew.)	Elementaranalyse	C [%]	H [%]	N [%]	Schmp.	Ausbeute [%]
37	Resorcin	$C_{22}H_{16}N_2O_8$ (436,4)	ber.	60,55	3,69	6,42	141—143 °C (Lit. [3]: 139—142 °C)	26
			gef.	60,52	3,63	6,56	Hellgelbe Kristalle (DMF/verd. Essigsäure)	
38	Hydrochinon	$C_{22}H_{16}N_2O_8$ (436,4)	ber.	60,55	3,69	6,42	205 °C	30
			gef.	60,55	3,70	6,49	Graubraune Nadeln (DMF/verd. Essigsäure)	
39	Orcin	$C_{23}H_{18}N_2O_8$ (450,4)	ber.	61,33	4,03	6,22	143—144 °C	25
			gef.	61,20	3,98	6,25	Hellgelbe Kristalle (DMF/verd. Essigsäure)	
40	2-Methylresorcin	$C_{23}H_{18}N_2O_8$ (450,4)	ber.	61,33	4,03	6,22	88—90 °C	20
			gef.	61,44	3,97	6,38	Hellgelbe Kristalle (DMF/verd. Essigsäure)	
	Tris-ANP-Äther von:							
41	Methylhydrochinon	$C_{23}H_{18}N_2O_8$ (450,4)	ber.	61,33	4,03	6,22	167—168 °C	24
			gef.	61,34	4,03	6,28	Graubraune Nadeln (DMF/verd. Essigsäure)	
42	Phloroglucin	$C_{30}H_{21}N_3O_{12}$ (615,5)	ber.	58,54	3,44	6,82	165—166 °C (Lit. [3]: 162—163 °C)	19
			gef.	58,36	3,31	6,92	Farblose Kristalle (DMF/verd. Essigsäure)	
43	2,4,6-Trihydroxy-acetophenon	$C_{32}H_{23}N_3O_{13}$ (657,6)	ber.	58,45	3,52	6,39	188—190 °C	12
			gef.	58,51	3,52	6,44	Hellgelbe Kristalle (Rohprodukt über eine Al_2O_3-Säule mit Benzol/Essigester 5 : 1 gereinigt)	
44	N-ANP-Derivat von: 2-Aminophenol	$C_{14}H_{12}N_2O_4$ (272,3)	ber.	61,76	4,44	10,29	214—218 °C	21
			gef.	61,71	4,31	10,42	Orangerote Kristalle (Äthanol)	

die Ausbeute an ANP-Äther in der Reihe *p*-Kresol > *m*-Kresol > *o*-Kresol von 54% über 48% auf 32% (4, 3, 2). Ähnlich verhalten sich Dimethylphenole (5—9). Methoxylgruppen wirken ausbeuteerhöhend, sofern sie die OH-Position nicht zu stark abschirmen (11—14). Auffallend ist ihr reaktivitätsteigernder Einfluß in Gegenwart einer desaktivierenden Acylgruppierung in *p*-Stellung zur Hydroxylfunktion (20 u. 21; 22 u. 23, 24, 26). Substitution durch Chlor bewirkt einen der Einführung von Methoxylgruppen analogen Effekt (15, 16). Phenolcarbonsäuren reagieren nur in Form ihrer Alkalisalze (29—33). Eine Nitrogruppe am Benzolring steigert infolge der größeren Polarisierbarkeit die Ausbeute, in *p*-Stellung stärker als in *m*- und *o*-Position (19, 18, 17). 2,4-Dinitrophenol und 2,4,6-Trinitrophenol bilden keine ANP-Äther. Möglicherweise sind hierfür Solvatationseffekte verantwortlich. Übereinstimmend ist das Verhalten gegenüber 2,4-Dinitrofluorbenzol. Während sich Nitrophenol quantitativ veräthern läßt, bleibt die Reaktion mit 2,4-Dinitrophenol aus [1]. Aminophenole besitzen zwei reaktionsfähige Zentren, die *m*- und *p*-ständig beide in Bindung mit dem Reagens treten (34, 35). Im Falle des 2-Aminophenols erfolgt die Reaktion wegen sterischer Hinderung nur am N-Atom als der Stelle größter Nucleophilie (44). Mehrwertige Phenole zeigen mit zunehmender räumlicher Beeinflussung der Hydroxylgruppen eine verminderte Reaktivität (36—43). Naphthole lassen sich nahezu vollständig in ANP-Äther überführen (27, 28). Zwischen den Dissoziationskonstanten der phenolischen Verbindungen, den Hammett-Konstanten der Substituenten und ihrem Reaktionsvermögen besteht keine Korrelation. Bei höherer Temperatur und Verwendung von Dimethylsulfoxid als Lösungsmittel wird der Substituenteneinfluß weitgehend kompensiert [3].

Experimentelle Methodik

Allgemeine Arbeitsvorschrift zur Darstellung der ANP-Äther: 5 mMol des betreffenden Phenols bzw. des Natriumsalzes der Phenolcarbonsäure und 5,25 mMol 4-Fluor-3-nitroacetophenon werden in 50 ml Dimethylformamid (DMF) gelöst und mit 7,5 mMol $NaHCO_3$ in 25 ml Wasser versetzt. Für polyfunktionelle Verbindungen sind die Mengen an 4-Fluor-3-nitroacetophenon und $NaHCO_3$ entsprechend zu erhöhen. Die Reaktionsmischung erhitzt man 5 min auf dem siedenden Wasserbad und läßt über Nacht bei Raumtemperatur stehen. Dann werden 50 ml Äthanol und 100 ml 2 *N* CH_3COOH zugegeben und weitere 200 ml 2 *N* CH_3COOH unter Rühren langsam zugetropft. Den gebildeten Niederschlag saugt man nach ca. 3 Std. ab, wäscht mit 50%igem Methanol und Wasser und trocknet i. Vak. über P_2O_5. Zur Reinigung wird umkristallisiert, umgefällt oder chromatographiert.

*

Frau S. WILDENHAIN danken wir für geschickte experimentelle Mitarbeit.

LITERATUR

1. ZAHN, H., WÜRZ, A.: Z. Anal. Chem. **134**, 183 (1951/52)
2. POETHKE, W., KÖHNE, H.: Pharm. Zentralhalle **104**, 630 (1965)
3. OELSCHLÄGER, H., TOPORSKI, W., SCHMERSAHL, P., WELSCH, C.: Arch. Pharm. **296**, 107 (1963)

Wolfgang WILDENHAIN
Günter HENSEKE
Gert BIENERT
92 Freiberg (Sachs.), Leipziger Straße. DDR.

Acta Chimica Academiae Scientiarum Hungaricae, Tomus 66 (4), pp. 455—458 (1970)

THE FORMATION AND STRUCTURE OF PSCHORR'S 'BIS-THIOCODIDE'

S. MAKLEIT, R. BOGNÁR, T. MILE and L. RADICS*

*(Department of Organic Chemistry, L. Kossuth University, Debrecen, and *Central Chemical Research Institute of the Hungarian Academy of Sciences, Budapest)*

Received August 15, 1969

It has been established that the compound synthesized by PSCHORR [1] from bromocodide and potassium hydrogen sulfide in alcoholic medium is identical with 8,8'-dideoxy-8,8'-di-pseudocodeinyl disulfide. 8-Deoxy-8-thiol-pseudocodeine is also an isolable product of this reaction and is readily converted by oxidation into the known disulfide.

In 1906 PSCHORR [1] reported that the reaction of bromocodide with potassium hydrogen sulfide in alcohol gave the corresponding disulfide instead of the derivative containing a free thiol group.

BENTLEY [2] accepted the disulfide structure of the product, which was obviously formed by oxidation of the primary product thiol, and assumed on the basis of the well-known interchange reactions of C_8-halogen (Cl, Br) derivatives that the disulfide bond was in position 6,6'. This seems to agree with the usual results of nucleophilic substitutions of halogen derivatives and with the stereochemical aspects of S_N2' reactions, which can be assumed to occur also in this case [3].

In an earlier communication [4a] we have reported the preparation of the hitherto unknown acetylthio and free thiol compounds starting from the 6-O-tosyl and 6-O-mesyl derivatives of the morphine group. These reactions were first interpreted on the basis of BENTLEY's suggestions, since the compound obtained from 6-O-tosylcodeine and containing a free thiol group gave on oxidation a product which was completely identical with PSCHORR's bis-thiocodide [4a].

A detailed comparative investigation of the nuclear magnetic resonance spectra of several C_6- and C_8-substituted morphine derivatives led, however, to the unexpected result [4c, 4d] that the disulfide bond both in our product (obtained from 6-O-tosylcodeine) and in the product of PSCHORR (prepared from bromocodide) displayed chemical shifts and coupling constants characteristic of compounds of the pseudocodeine type [5]; hence the disulfide bond must be in position 8,8'.

Starting with this results in further papers [4b, c, d] we described the mechanism of the nucleophilic substitution reactions occurring between 6-O-

tosyl or 6-O-mesyl derivatives of the morphine group and potassium thiolacetate in dimethylformamide, and we reported the correct structures of the products and their stereochemical properties.

In the present communication we deal with the formation and structure of PSCHORR's bis-thiocodide, giving chemical confirmation of the results.

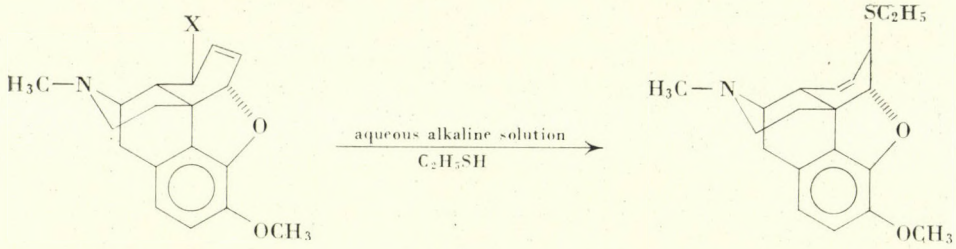

Ia : X = Cl
Ib : X = Br

II

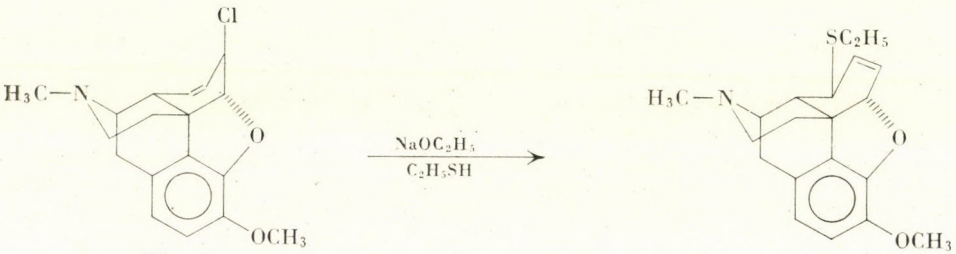

III **IV**

When subjecting PSCHORR's reaction to a closer scrutiny, we have found that, contrary to the statement of this author, a compound containing a free thiol group may also be prepared in this way, provided the appropriate reaction conditions are strictly observed. The thiol is soluble in alkali, and it is readily oxidized into the corresponding disulfide.

In agreement with the NMR measurements position 8 for the thiol group and the disulfide bond can also be proved by chemical methods.

According to MORRIS and SMALL [6], the main product of the reaction of β-chlorocodide (**Ia**) or bromocodide (**Ib**) with ethyl mercaptan in aqueous alkaline medium is α-ethylthiocodide (6-deoxy-6-ethylthioisocodeine); the C_6 position of the ethylthio group has been proved in this compound (**II**).

On the other hand, when α-chlorocodide (**III**) is treated with ethyl mercaptan in the presence of sodium ethoxide, the so-called δ-ethylthiocodide (8-deoxy-8-ethylthiopseudocodeine) is obtained which contains the ethylthio group in position C_8 (**IV**).

The specific rotation of α-ethylthiocodide (**II**) is $-344.6°$ and that of δ-ethylthiocodide (**IV**) $+57.7°$, while the rotation of the disulfide is $+280°$.

The free thiol compound (**V**) which had been prepared by PSCHORR's method was then treated in aqueous alkaline medium with ethyl iodide; the specific rotation of the product (**VI**) was +51°.

From the free thiol compound (**V**) which can be prepared more advantageously from 6-O-tosylcodeine [4a, 4b, 4c, 4d] and in which the C_8 position

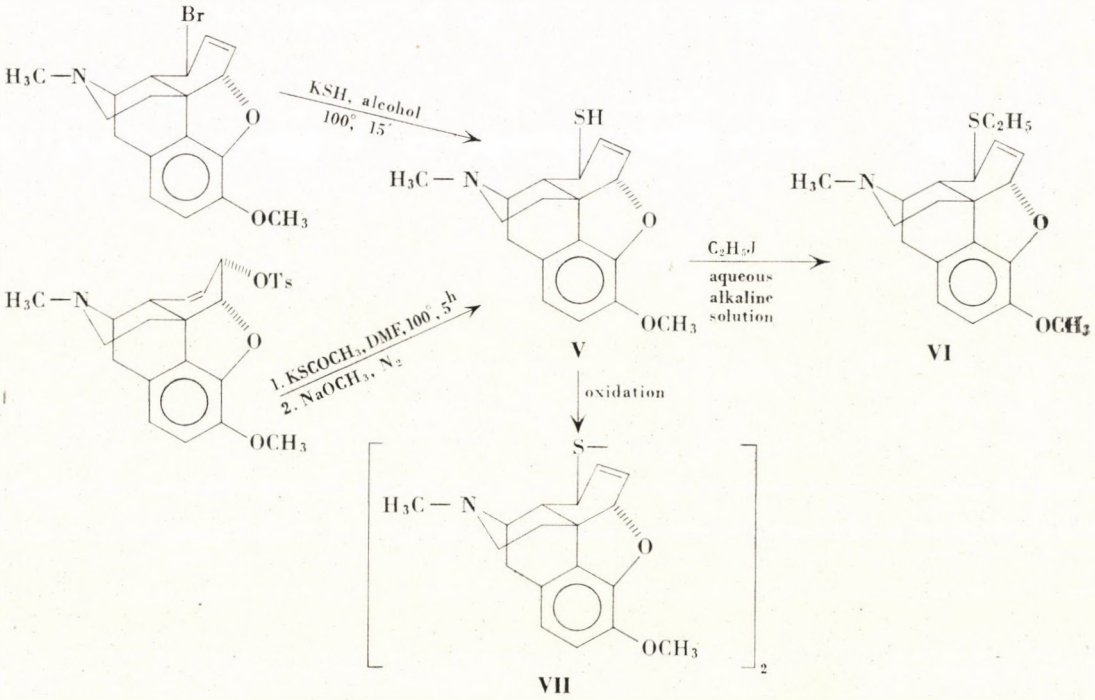

of the thiol group has been proved, a compound with the specific rotation of +50° is obtained by the same method.

Considering these specific rotations, position 8 of the substituents can be regarded as chemically proved; therefore, the structure of PSCHORR's bis--thiocodide (**VII**) is 8,8'-dideoxy-8,8'-di-pseudocodeinyl disulfide.

In view of the constitution and steric structure of the compound, the reaction conditions and the geometrical and stereochemical properties of the morphine molecule (STORK and CLARKE, [3]), compound **VII** is probably formed by S_N1 mechanism, with retention of the configuration.

These investigations show that the structure reported for bis-thiocodide by PSCHORR must be modified, and BENTLEY's [2] statement (which supported the former structure of bis-thiocodide on the basis that the exchange reactions of C_8-halogen (Cl, Br) derivatives always occur according to S_N2' mechanism except in the case of a hydroxyl group) also requires correction. Our results have shown that the thiol group is another exception to this rule.

Experimental

8-Deoxy-8-thiol-pseudocodeine (V)

A solution of 2.0 g of bromocodide [7] was gently refluxed for 15 min in anhydrous ethanol (40 ml) saturated with potassium hydrogen sulfide, under nitrogen. The solution was cooled, and KBr removed by filtration. The filtrate was poured into 100 ml of water. The precipitate consisting mainly of the corresponding disulfide was filtered off and the solution evaporated to 1/3 of its initial volume, filtered again and evaporated to dryness. The residual gum was dissolved in water, and carbon dioxide was allowed to bubble through the solution. The precipitate was filtered off, washed with water and, after short drying by suction, it was recrystallized from ethanol to obtain 140 mg (8%) of a product which was homogeneous to thin-layer chromatography. M. p. 159 °C, $[\alpha]_D$ —21° (chloroform, $c = 0.38$). The IR spectrum had an SH band at 2542 cm^{-1}.

This product was converted into 8,8'-dideoxy-8,8'-di-pseudocodeinyl disulfide as described in earlier communications [4c, 4d], where also a summary of the NMR investigations are given.

The ethylation of the compound containing free thiol group prepared by the above manner, as well as of the thiol obtainable by the deacetylation of the acetylthio derivative prepared by the reaction of 6-O-tosylcodeine with potassium thiolacetate, was effected in aqueous alkaline solution with ethyl iodide, in the usual manner.

Authentic 'δ-ethylthiocodide' **(VI)** was prepared according to MORRIS and SMALL [6].

REFERENCES

1. PSCHORR, H.: Ber. **39,** 3130 (1906)
2. BENTLEY, K. W.: The chemistry of the morphine alkaloids, p. 243. Clarendon Press, Oxford 1954
3. STORK, G., CLARKE, F. H.: J. Am. Chem. Soc. **78,** 4619 (1956)
4/a. BOGNÁR, R., MAKLEIT, S., MILE, T.: Acta Chim. Acad. Sci. Hung. **59,** 161 (1969); b. BOGNÁR, R., MAKLEIT, S., MILE, T.: Magy. Kém. Foly. **75,** 330 (1969); c. BOGNÁR, R., MAKLEIT, S., MILE, T., RADICS, L.: Acta Chim. Acad. Sci. Hung. **64,** 273 (1970); d. BOGNÁR, R., MAKLEIT, S., MILE, T., RADICS, L.: Magy. Kém. Foly. **76,** 102 (1970)
5. BATTERHAM, T. J., BELL, H. K., WEISS, U.: Aust. J. Chem. **18,** 1799 (1965)
6. MORRIS, D. E., SMALL, L.: J. Am. Chem. Soc. **56,** 2159 (1934)
7. RAPAPORT, H., PAYNE, G. B.: J. Org. Chem. **15,** 1093 (1950)

Sándor MAKLEIT
Rezső BOGNÁR
Teréz MILE
Debrecen 10. Hungary
Lajos RADICS; Budapest II., Pusztaszeri út 57—69.

Acta Chimica Academiae Scientiarum Hungaricae, Tomus 66 (4), pp. 459—468 (1970)

PDPDP AND ITS DERIVATIVES, I

PREPARATION AND PROPERTIES OF SYMMETRICALLY AND ASYMMETRICALLY SUBSTITUTED PDPDP DERIVATIVES

G. VASVÁRI and S. HOLLY

(Central Research Institute for Chemistry of the Hungarian Academy of Sciences, Budapest)

Received August 15, 1969

Symmetrically and asymmetrically substituted PDPDP derivatives have been synthesized. The melting points, solubilities, tabulated infrared spectra, and the analyses of the products are given.

For an investigation of the relationship between the molecular structure and optical properties of wavelength shifters used in scintillation counting, it was necessary to synthesize a series of compounds containing different substituents in the same position. These investigations were carried out on five-ring compounds with 1,3,4-oxadiazole rings. The parent compound of the series was 1,4-di-[2-phenyl-1,3,4-oxadiazolyl-(5)]-benzene, called PDPDP. This compound was reported first by HAYES *et al.* [1] who also described its synthesis by cyclization of the corresponding 1,2-diaroylhydrazine with $POCl_3$. Several other methods have become known in the recent years for the preparation of PDPDP, *e.g.* the reaction between benzhydrazide and diethyldiimidoterephthalate hydrochloride in pyridine [2, 3, 4], cyclization of the corresponding diaroylhydrazines by complexes of SO_3–dimethylformamide [5], and acylation of 5-substituted tetrazoles. This latter procedure elaborated by HUISGEN *et al.* [6, 7] seems to be the most suitable for the preparation of the required substances, because the intermediates are easy to purify and the end-products are formed in a comparatively pure state. A number of publications [1—7] have dealt with the properties of the PDPDP; in one publication [7] *p,p'*-dinitro-PDPDP is discussed; the bromo-, methyl-, methoxy- and mono-nitro-derivatives have not been described previously. The way of synthesis is the following:

(a) Symmetrically substituted PDPDP derivatives

Ammonium terephthalate (**I**) is mixed with P_2O_5 and heated in vacuum to 350 °C. The terephtalic acid dinitrile (**II**) obtained is converted into 1,4-di-tetrazolylbenzene (**III**) by a six-day refluxing with LiCl and NaN_3 in methylcellosolve. When **III** is treated with benzoyl chloride suitably substituted in

the *para* position, the symmetrically substituted PDPDP derivatives (**IV**) are obtained.

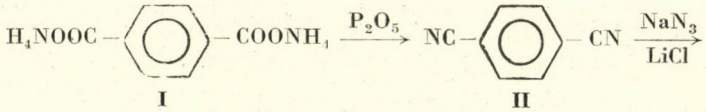

I **II**

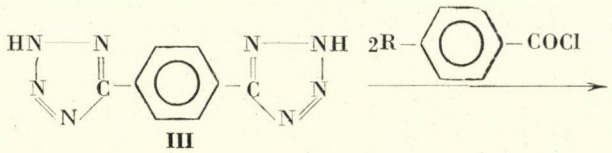

III

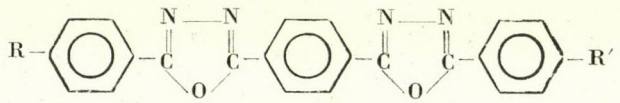

IV

(R′=R=H, CH_3, OCH_3, Br, NO_2)

(b) Asymmetrically substituted PDPDP derivatives

In this case benzonitrile is converted first into 5-phenyltetrazole (**V**), and this is treated with *p*-cyanobenzoyl chloride, obtained from *p*-amino-benzoic acid by the Sandmeyer reaction [8] and subsequent chlorination; the product is 1-[2-phenyl-1,3,4-oxadiazolyl-(5)]-4-cyanobenzene (**VI**). The cyano group of **VI** is transformed to obtain the tetrazole, (**VII**), which is then reacted with a *p*-substituted benzoyl chloride to give the asymmetrically substituted PDPDP derivative, (**VIII**).

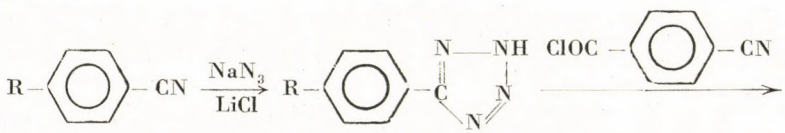

V

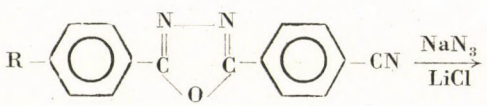

VI

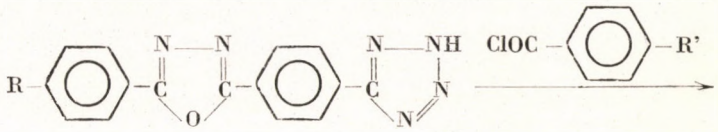

VII

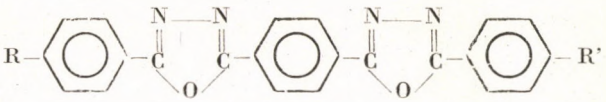

VIII

(R'=H, CH_3, OCH_3, Br, NO_2; R=H)

For the purification of *p*-cyano-benzoic acid, simple recrystallization from water proved to be insufficient to separate the *p*-cyanobenzoic acid from a compound of acidic character formed as a by-product. According to our experiments, the separation may be achieved in the following way: the ammoniacal solution filtered from the cupro-cyanide and containing the ammonium salts of the acids is acidified in two steps. First pH 7 is adjusted, when the main part of the brown by-product separates. This is removed by filtration, and the filtrate is carefully acidified to pH 4. The *p*-cyanobenzoic acid obtained as a white precipitate can be readily purified by recrystallization from water.

For the purpose of the measurements and analyses, the PDPDP derivatives must be prepared in a purity of 'scintillation grade'. It has been found that the unreacted tetrazole compound, occasionally present, cannot be perfectly removed by recrystallization from dimethylformamide. Therefore, after filtration and washing with water, the crude product was heated for a few minutes in a 5% NaOH solution. Owing to the presence of an acidic hydrogen, the unreacted tetrazole is dissolved, thus it can be removed by filtration and washing, or even recovered by acidifying the filtrate. The end-product remaining on the filter was dried and recrystallized from dimethylformamide. The purity of the end-products was checked by thin-layer chromatography. The chromatograms examined in UV light did not show the presence of impurities. The solubilities were determined by making saturated solutions which were shaken for 12 hrs. at room temperature and kept afterwards at 20 ± 0.01 °C for 8 hrs. in an ultrathermostate with shaking from time to time. The 10 ml samples were then carefully evaporated to dryness, and the solid residue was weighed.

The data in Table I show that the melting points change in the same way both in the symmetric and in the asymmetric series. The highest melting points belong to the nitro derivatives, the lowest ones to the methoxy deriva-

Table I

Physical properties of PDPDP derivatives

Compound	R	R'	Colour	Solubility in toluene 20 °C		M. p., °C	Fluor*
				g/l	mole/l		
PDPDP	H	H	white	$3.2 \cdot 10^{-2}$	$8.7 \cdot 10^{-5}$	322**	blue
p-Methyl-PDPDP	H	CH_3	white	$18.0 \cdot 10^{-2}$	$4.75 \cdot 10^{-4}$	321	blue
p-Methoxy-PDPDP	H	OCH_3	white	$24.3 \cdot 10^{-2}$	$6.13 \cdot 10^{-4}$	270	strong blue
p-Bromo-PDPDP	H	Br	white	$11.5 \cdot 10^{-2}$	$2.6 \cdot 10^{-4}$	340(d.)	blue
p-Nitro-PDPDP	H	NO_2	pale yellow	$9.65 \cdot 10^{-2}$	$2.35 \cdot 10^{-4}$	343(d.)	—
p,p'-Dimethyl-PDPDP	CH_3	CH_3	white	$2.75 \cdot 10^{-2}$	$6.97 \cdot 10^{-5}$	361	blue
p,p'-Dimethoxy-PDPDP	OCH_3	OCH_3	white	$3.5 \cdot 10^{-3}$	$0.82 \cdot 10^{-5}$	311	strong blue
p,p'-Dibromo-PDPDP	Br	Br	white	$9.5 \cdot 10^{-3}$	$1.81 \cdot 10^{-5}$	402(d.)	strong blue
p,p'-Dinitro-PDPDP	NO_2	NO_2	yellow	$4.66 \cdot 10^{-2}$	$10.2 \cdot 10^{-5}$	405(d.)***	—

* Fluorescence by UV excitation only

** Lit. m. p.'s: 308—309°C [1], 322°C [6], 322—322.5°C [7], 311—313°C [2, 3], 318—321°C [5]

*** Lit. [7] m. p.: 405—406°C

tives. Solubilities in toluene are very poor, but it may be observed that asymmetric derivatives dissolve better, roughly by an order of magnitude, than the symmetric ones.

Experimental

The infrared spectra were obtained with a double-beam Zeiss UR-10 spectrophotometer. Up to 700 cm^{-1} a KBr prism, from 700 to 1800 cm^{-1} a NaCl prism and above this range a LiF prism was used.

The spectra of the substances were recorded in KBr pellets.

p-Cyanobenzoic acid

20 g of freshly prepared Cu_2Cl_2 and 19 g of anhydrous Na_2CO_3 were added to a stirred solution of 25 g NaCN in 40 ml of water. The solution was maintained at 50—60° and, in the course of 10—15 min., a solution was added which had been obtained from 12.5 g p-aminobenzoic acid, 22 g conc. HCl, 62.5 ml water, and 187.5 g crushed ice, diazotized with 6.25 g $NaNO_2$ in 15 ml water. After the addition, the mixture was maintained at 55° for 30 min. The solution was then allowed to cool, acidified with HCl and the precipitate was filtered off. The solid was treated with conc. NH_4OH on the filter to dissolve the acid which thus could be separated from the insoluble $Cu_2(CN)_2$. The brownish ammoniacal solution was stirred and adjusted by the addition of HCl to pH 7. The brown precipitate was removed by filtration and

Table II

Bands of infrared spectra

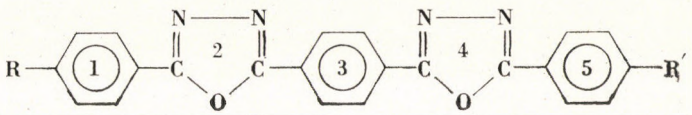

Compound	Band, cm^{-1}	Intensity*	Assignment
R = R' = H	1610 1578 1550 1505 1487 1475 1450 1415	w m s sh vs sh m m	Ring stretching vibrations of the 1st, 2nd, 3rd, 4th and 5th rings
	860	m	Out-of-plane hydrogen wagging vibration of the 3rd ring
	780	m	Out-of-plane hydrogen wagging vibration of the 1st and 5th rings
	717	vs	In-plane bending vibration of the 2nd and 4th rings
	700 690	ms ms	Out-of-plane ring bending vibrations of the 1st, 3rd and 5th rings
R = R' = OCH_3	1617 1588 1555 1500 1475 1445 1417	s mw mw vs sh sh m	Ring stretching vibrations of the 1st, 2nd, 3rd, 4th and 5th rings
	1265 1020	vs s	Asymmetric and symmetric C_{Ar}—O—C stretching vibrations of the ether group
	850	m	Out-of-plane hydrogen wagging vibration of the 3rd ring
	840	m	Out-of-plane hydrogen wagging vibration of the 1st and 5th ring
	740	s	In-plane bending vibration of the 2nd and 4th rings
	710	m	Out-of-plane ring bending vibrations of the 1st, 3rd, and 5th rings + in-plane bending vibration of the 2nd and 4th rings
R = R' = CH_3	1612 1582 1575 1557 1497 1487 1412	m sh m m s s m	Ring stretching vibrations of the 1st, 2nd, 3rd, 4th, and 5th rings

Table II continued

Compound	Band, cm^{-1}	Intensity*	Assignment
R=R'=CH_3	1450	w	Asymmetric and symmetric deformation vibrations of the methyl groups
	1378	w	
	857	m	Out-of-plane hydrogen wagging vibration of the 3rd ring
	830	s	Out-of-plane hydrogen wagging vibration of the 1st and 5th rings
	730	vs	In-plane bending vibration of the 2nd and 4th rings
	710	m	Out-of-plane ring bending vibrations of the 1st, 3rd and 5th rings
R=R'=Br	1605	s	Ring stretching vibrations of the 1st, 2nd, 3rd, 4th and 5th rings
	1579	m	
	1547	m	
	1535	sh	
	1480	vs	
	1460	m	
	1420	w	
	1403	m	
	1080	vs	Radial skeletal vibrations of the bromo-substituted 1st and 5th rings
	860	m	Out-of-plane hydrogen wagging vibration of the 3rd ring
	840	ms	Out-of-plane hydrogen wagging vibration of the 1st and 5th rings
	735	vs	In-plane bending vibration of the 2nd and 4th rings
	708	m	Out-of-plane ring bending vibrations of the 1st, 3rd and 5th rings
R=R'=NO_2	1610	w	Ring stretching vibrations of the 1st, 2nd, 3rd and 5th rings
	1580	m	
	1554	ms	
	1498	m	
	1485	m	
	1413	m	
	1520	vs	NO_2 asymmetric and symmetric stretching vibrations
	1443	vs	
	873	m	Out-of-plane hydrogen wagging vibration of the 3rd ring
	860	ms	Out-of-plane hydrogen wagging vibration of the 1st and 5th rings
	855	sh	Scissoring vibration of the NO_2 group
	723	s	In-plane bending vibration of the 2nd and 4th rings

Table II continued

Compound	Band, cm^{-1}	Intensity*	Assignment
R=OCH_3; R'=H	1612	m	Ring stretching vibrations of the 1st, 2nd, 3rd, 4th and 5th rings
	1585	sh	
	1575	w	
	1548	m	
	1496	vs	
	1486	sh	
	1470	sh	
	1450	w	
	1415	m	
	1258	s	Asymmetric and symmetric $C_{Ar}-O-C$ stretching vibrations of the ether group
	1032	m	
	855	m	Out-of-plane hydrogen wagging vibration of the 3rd ring
	840	m	Out-of-plane hydrogen wagging vibration of the 1st ring
	788	w	Out-of-plane hydrogen wagging vibration of the 5th ring
	741	m	In-plane bending vibrations of the 2nd ring
	730	m	
	715	s	In-plane bending vibration of the 4th ring
	692	m(br)	Out-of-plane ring bending vibrations of the 1st, 3rd and 5th rings
R=CH_3; R'=H	1613	w	Ring stretching vibrations of the 1st, 2nd, 3rd, 4th and 5th rings
	1582	sh	
	1575	m	
	1550	m	
	1545	sh	
	1495	s	
	1487	s	
	1449	mw	
	1413	m	
	857	m	Out-of-plane hydrogen wagging vibration of the 3rd ring
	826	m	Out-of-plane hydrogen wagging vibration of the 1st ring
	777	w	Out-of-plane hydrogen wagging vibration of the 5th ring
	732	s	In-plane bending vibration of the 2nd ring
	714	s	In-plane bending vibration of the 4th ring
	692	m	Out-of-plane ring bending vibrations of the 1st, 3rd and 5th rings

Table II continued

Compound	Band, cm^{-1}	Intensity*	Assignment
R=Br; R'=H	1605	m	Ring stretching vibrations of the 1st, 2nd, 3rd, 4th and 5th rings
	1577	m	
	1550	m	
	1485	sh	
	1480	s	
	1450	w	
	1418	mw	
	1403	m	
	1080	s	Radial skeletal vibration of the bromo-substituted 1st ring
	857	m	Out-of-plane hydrogen wagging vibration of the 3rd ring
	840	m	Out-of-plane hydrogen wagging vibration of the 1st ring
	779	w	Out-of-plane hydrogen wagging vibration of the 5th ring
	732	s	In-plane bending vibration of the 2nd ring
	715	s	In-plane bending vibration of the 4th ring
	692	m	Out-of-plane ring vibrations of the 1st, 3rd and 5th ring
$R=NO_2$; R'=H	1610	w	Ring stretching vibrations of the 1st, 2nd, 3rd, 4th and 5th rings
	1575	m	
	1552	s	
	1485	s	
	1450	w	
	1470	sh	
	1410	vs	
	1530	s	NO_2 asymmetric and symmetric stretching vibrations
	1350	vs	
	868	m	Out-of-plane hydrogen wagging vibration of the 3rd ring
	857	s	Out-of-plane hydrogen wagging vibration of the 3rd ring + scissoring vibration of the nitro group
	780	w	Out-of-plane hydrogen wagging vibration of the 5th ring
	720	vs	In-plane bending vibrations of the 2nd and 4th rings
	692	m	Out-of-plane ring vibrations of the 1st, 3rd and 5th rings

vs = very strong
s = strong
ms = medium-strong
m = medium
mw = medium-weak
w = weak
sh = shoulder
br = broad

the light yellow filtrate acidified with HCl to pH 4. *p*-Cyanobenzoic acid separated as a white solid. Recrystallization from hot water in the presence of some decolorizing carbon gave white plates.
Yield: 3 g (24%); m. p. 219 °C.
Analysis: Mol. wt. (from titration of the carboxyl groups with alkali): 146.7—147. Mol. wt. (calcd.): 147.1.

Symmetrically substituted PDPDP derivatives

1,4-Ditetrazolylbenzene and the double amount of the stoichiometrically needed p-substituted benzoyl chloride were refluxed for 1 hr. in about a tenfold quantity of pyridine. Near the boiling point of the solvent gas evolution began, and the main part of the product soon precipitated. After cooling, the precipitate was filtered off with suction, washed with water and heated for 10 min. in a 5% NaOH solution. After filtration and washing, the crude solid was dried and recrystallized from dimethylformamide.

PDPDP

Yield: 98%.
$C_{22}H_{14}N_4O_2$. Calcd.: C 72.15; H 3.85; N 15.29
Found: C 72.27; H 3.97; N 15.27%.

p,p'-Dimethoxy-PDPDP

Yield: 83%.
$C_{24}H_{18}N_4O_4$. Calcd.: C 67.62; H 4.25; N 13.14
Found: C 67.26; H 4.60; N 13.50%.

p,p'-Dimethyl-PDPDP

Yield: 98%.
$C_{24}H_{18}N_4O_2$. Calcd.: C 73.10; H 4.60; N 14.20
Found: C 73.10; H 4.93; N 14.14%.

p,p'-Dibromo-PDPDP

Yield: 98%.
$C_{22}H_{12}Br_2N_4O_2$. Calcd.: C 50.42; H 2.31; N 10.68; Br 30.48
Found: C 50.63; H 2.57; N 10.90; Br 30.47%.

p,p'-Dinitro-PDPDP

Yield: 98%.
$C_{22}H_{12}N_6O_6$. Calcd.: C 57.90; H 2.65; N 18.42
Found: C 57.94; H 3.26; N 18.44%.

Asymmetrically substituted PDPDP derivatives

1-[2-Phenyl-1,3,4-oxadiazolyl-(5)]-4-[tetrazolyl-(5)]-benzene and the double amount of the stoichiometrically needed p-substituted benzoyl chloride were refluxed in about a tenfold quantity of pyridine for 1 hr. Near the boiling point of the solvent gas evolution began, and soon the main part of the product separated. After cooling, the precipitate was filtered off by suction, washed with water and heated for 10 min. in a 5% NaOH solution. After filtration and washing, the product was dried and recrystallized from dimethylformamide.

p-Methoxy-PDPDP

Yield: 74%.
$C_{23}H_{16}N_4O_3$. Calcd.: C 69.69; H 4.06; N 14.12
Found: C 69.62; H 4.50; N 14.01%.

p-Methyl-PDPDP

Yield: 83%.

$C_{23}H_{16}N_4O_2$. Calcd.: C 72.62; H 4.24; N 14.72
Found: C 72.10; H 4.28; N 14.86%.

p-Bromo-PDPDP

Yield: 98%.

$C_{22}H_{13}BrN_4O_2$. Calcd.: C 59.35; H 2.95; N 12.57; Br 17.95
Found: C 59.47; H 3.23; N 12.19; Br 17.81%.

p-Nitro-PDPDP

Yield: 88%.

$C_{22}H_{13}N_5O_4$. Calcd.: C 64.23; H 3.18; N 17.01
Found: C 64.27; H 3.71; N 17.44%.

REFERENCES

1. HAYES, F. N., ROGERS, B. S., OTT, D. G.: J. Am. Chem. Soc. **77**, 1850 (1955)
2. WEIDINGER, H., KRANZ, J.: Ber. **96**, 1049 (1963)
3. KRANZ, J., WEIDINGER, H.: Festschrift Carl Wurster zum 60. Geburtstag, **1960**, 119
4. WEIDINGER, H., KRANZ, J.: Ger. Pat. 1,067.439. Mar. 20, 1958
5. BALTAZZI, E., WYSOCZKI, A. J.: Chem. et Ind. (London) **26**, 1080 (1963)
6. HUISGEN, R., SAUER, J., STRURM, H. I.: Angew. Chem. **70**, 272 (1958)
7. SAUER, J., HUISGEN, R., STURM, H. I.: Tetrahedron, **11**, 241 (1960)
8. VALBY, E. P., LUCAS, H. J.: J. Am. Chem. Soc. **51**, 2718, (1929)

Gábor VASVÁRI
Sándor HOLLY } Budapest II., Pusztaszeri út 57/69.

Fortschritte der Chemischen Forschung

Herausgeber:

A. Davison — M. J. S. Dewar
K. Hafner — E. Heilbronner
U. Hofman — K. Niedenzu
Kl. Schäfer — G. Wittig

Schriftleitung: F. Boschke

Springer Verlag, Heidelberg—New York. Band 13, Heft 3/4, Jan. 1970 bringt drei Artikel aus dem Gebiet der angewandten physikalischen Chemie.

G. Emig (Institut für Technische Chemie der Universität Erlangen-Nürnberg), behandelt die in den Poren von Katalysatoren gleichzeitig verlaufenden Stoff- und Wärmetransport-Erscheinungen.

Auf Grund einer früheren, ähnlichen Arbeit zusammenfassenden Charakters berichtet der Autor hier über die neuesten Ergebnisse und ist außerdem bestrebt, die wichtigsten Bezeichnungen und Benennungen zu vereinheitlichen.

Der Verfasser stellt die Differentialgleichungen des Wärme- und Stofftransportes auf. Das Gleichungssystem wird unter den folgenden üblichen vereinfachenden Annahmen gelöst: Der Wärmeleitungs- und Diffusionsfaktor ist konstant, die Konzentration und Temperatur an der äußeren Oberfläche der Katalysatorteilchens haben den gleichen Wert wie im Gasstrom, die Reaktionsgeschwindigkeit ist nur von der Konzentration eines einzigen Stoffes abhängig, und die Poren sind von gleichem Querschnitt. Aus der Lösung leitet der Verfasser jene dimensionslosen Kriterien ab, mit deren Hilfe zu entscheiden ist, ob der Verlauf der Reaktion in einem gegebenen Fall durch den Wärme- oder Stofftransport wesentlich beeinflußt wird. Der Einfluß wird mit dem Porenausnützungsfaktor charakterisiert. Dieser ist das Verhältnis der beobachteten Reaktionsgeschwindigkeit und jener Geschwindigkeit, welche dann zu beobachten wäre, wenn die Temperatur und die Konzentration im ganzen Katalysatorkorn den gleichen Wert hätten, wie auf an seiner Oberfläche.

Auf Grund der Untersuchung von elf Reaktionen, die überwiegend technische Bedeutung haben, zieht der Verfasser den Schluß, daß man in der Mehrzahl der Fälle nicht mit einer Überhitzung der Katalysatorteilchen zu rechnen hat, denn die Reaktionen verlaufen praktisch isothermisch.

Für den isothermen Fall läßt der Verfasser die obigen vereinfachenden Annahmen weg und sucht für den Fall von komplizierten Reaktionen und Porenverteilungen die Lösung der Diffusionsgleichungen.

Besonders lobenswert in dieser Arbeit ist, daß die theoretischen Lösungen vom Gesichtspunkt praktischer Aufgaben ausgewertet werden.

(103 Seiten, 169 Literaturangaben)

G. M. SCHNEIDER (Institut für Physikalische Chemie und Elektrochemie der Universität Karlsruhe)

Der Verfasser schreibt über die im Jahre 1894 vorausgesagten und 1940 tatsächlich entdeckten Entmischungsvorgänge in der Gasphase bei hohen Drucken und Temperaturen. Es werden zahlreiche Beispiele angeführt, und es wird gezeigt, daß viele Entmischungsvorgänge nur dann verständlich werden, wenn die Gas-Flüssigkeit-, Flüssigkeit-Flüssigkeit- und Gas-Gas-Phasengleichgewichte im Rahmen einer einheitlichen thermodynamischen Theorie behandelt werden. Gemische hoher Dichte über dem kritischen Punkt werden in der Wissenschaft immer ausgedehnter untersucht und verwendet. So können z. B. in der Hochdruck-Chemie Reaktionsmedien mit kontinuierlich abstufbarer Dichte, und Dielektrizitätskonstante aus Gasen hergestellt werden. In der experimentellen Thermodynamik füllt diese Abhandlung eine Lücke und wird für jeden der sich mit überkritischen Mischungen beschäftigt, nützlich und lehrreich sein.

(37 Seiten, 130 Literaturhinweise).

H. JÜNTGEN und K. H. VAN HEEK (Bergbau Forschung GmbH, Essen-Kray, Forschungsinstitut des Steinkohlenbergbauvereins, Essen) berichten in einer zusammenfassenden Arbeit über Reaktionen, die unter nicht-isothermen Bedingungen verlaufen.

In der chemischen Technik gibt es zahlreiche Fälle bei denen sich die Temperatur gleichzeitig mit dem Reaktionsablauf ändert, z. B.: Reaktionen beim Brennen und Verschwelen von Materialen, thermische Zersetzung von Festkörpern usw. Zur Untersuchung dieser Reaktionen verwendet man Reaktoren, deren Temperatur nach wählbarem Programm zu steuern möglich ist. Die Verbreitung von thermogravimetrischen und thermoanalytischen Messverfahren rechtfertigen dieses systematische Studium.

Ausgehend von den Grundgleichungen für den Ablauf chemischer Reaktionen und physikalischer Prozesse unter ändernder Temperatur, werden die Auswertemethoden zur Bestimmung von Reaktionsordnung, Aktivierungsenergie und Frequenzfaktor dargelegt.

Die Abhandlung wird durch zahlreiche Beispiele ergänzt, an Hand deren ein sehr guter kritischer Überblick über den jetztigen Stand dieses Wissenschaftsgebietes gegeben wird. Die in anorganischen Feststoffumwandlungen, in der Zersetzung organischer Stoffe und Kunststoffe, in Reaktionen in der flüssigen Phase, usw. gemessenen DTA-, TG- oder TV-Kurven stimmen mit den berechneten sehr gut überein, was die Leistungsfähigkeit der Theorie bestätigt.

(90 Seiten, 195 Literaturhinweise.)

Gy. RÁCZ

I. Ya. SLONIM and A. N. LYUBIMOV: *The NMR of Polymers* (Translated from Russian)

Plenum Press, New York 1970. p. 365, 163 illustrations.

This book is an English translation; the original was published in 1966 by Khimia Press, Moscow. The subject is divided into two parts, the first one being introductory about the physical basis and principles of detection of nuclear magnetic resonance. The theoretical basis of NMR is discussed by using the matrix formalism of quantum theory. Magnetic resonance in models and in real chemical systems is also discussed on the basis of quantum chemistry rather than the more usual semiclassical treatment. The last sections of Part One are devoted to a very concise description of the experimental methods. The spin-echo technique for measuring nuclear relaxation times is also discussed.

In the second part of the book the application of NMR spectroscopy for studying the chemical and physical structure of polymers is discussed in detail with many illustrative examples. The possibility of using NMR to study molecular motion in solid polymers is treated in a separate chapter and compared with data obtained by other methods such as mechanical and dielectric relaxation. A separate chapter is devoted to chemical processes (reactions) in polymers and to the application of the method for quantitative analysis. The book is completed by a valuable bibliography containing 1033 references, and by a special subject index to the bibliography which helps the reader to obtain a general picture about the data published in his field.

The intention of the authors to treat NMR entirely on the basis of quantum theory is very attractive. This, however, involves that the reader should be familiar with the theoretical basis of quantum chemistry involving elementary matrix algebra. Thus the introductory sections 1.1 and 1.2 seem superfluous; one feels that this is not the right place for introductory quantum theory. The description of experimental techniques, on the other hand, seems to be too concise and probably somewhat out of date.

The important technical details are discussed too briefly to be understandable for non-specialists; for the specialist, on the other hand, not much new is presented. The specific experimental problems of the polymer work are not discussed in sufficient detail.

Most interesting and probably most valuable is the information collected about NMR in solid polymers mainly in chapters 3 and 4. It is, however, somewhat disturbing that the structural studies obtained by high resolution NMR in solution are not separated from those derived by the wide-line method in the solid phase.

Pioneering work has been done by the authors in reviewing the possibilities of application of NMR to study polymerization processes, crosslinking, radiation damage and degradation of plastics and rubbers. The examples cited in chapter 5 are mainly based on the research work done in the authors' laboratory. The results are very stimulating and open up new perspectives for the application of NMR in the field of polymer chemistry.

The English translation is not very good. The translators are evidently not very familiar with the special terminology of NMR and polymer physics, some expressions used by the translators are different from those generally accepted in the corresponding fields.

The book is strongly recommended to polymer physicists, physico-chemists and other researchers working in the field of NMR. It might be useful for graduate students oriented in this field. It is certainly of high value both as a monograph and a textbook.

P. HEDVIG

INDEX

INORGANIC AND ANALYTICAL CHEMISTRY – ANORGANISCHE UND ANALYTISCHE CHEMIE – НЕОРГАНИЧЕСКАЯ И АНАЛИТИЧЕСКАЯ ХИМИЯ

HEGEDÜS, A. J., GADÓ, P., SCHLOSSER, G. und NEUGEBAUER, J.: Thermokondensation von WO_3 aus 12-Wolframatokieselsäurehydraten. (The Thermocondensation of Tungsten Trioxide from Hydrated 12-Tungstatosilicic Acid) 349

GÖRBICZ, M. and UPOR, E.: Some Questions of the Separation of Trace Elements by Precipitation, VII. Determination of Small Amounts of Copper, Zinc, Nickel, Cobalt and Silver in Rocks After Precipitation with Ammonium Hydroxide 373

JÓNÁS, K. and SOLYMÁR, K.: Preparation, X-ray, Derivatographic and Infrared Study of Aluminium-Substituted Goethites 383

PHYSICAL CHEMISTRY – PHYSIKALISCHE CHEMIE – ФИЗИЧЕСКАЯ ХИМИЯ

KISS, L. und FARKAS, J.: Untersuchung der Ionisation von Metallen und Metallionenneutralisation mit der rotierenden Ring-Scheibenelektrode, V. Untersuchung der anodischen Auflösung von Kupfer in sauren Sulfatlösungen. (Investigation of the Ionization and Neutralization of Metals on the Rotary Ring and Disk Electrode, V. Investigation of the Anodic Dissolution of Copper in Acid Sulfate Solutions) 395

ROBINSON, P. J.: Integrated Rate-Equations in Chemical Kinetics 407

LISZI, J.: Study of Thermodynamic Properties of Binary Mixtures Containing Acetic Acid 411

KISS, Á. I. and HORVÁTH, G.: Spectroscopic Investigation of Substituted Carbonyl Groups 431

ORGANIC CHEMISTRY – ORGANISCHE CHEMIE – ОРГАНИЧЕСКАЯ ХИМИЯ

SZILÁGYI, G., KASZTREINER, E., KOVÁCS, K. and BORSY, J.: Substituted Benzamidoximes Acting on the Central Nervous System 439

WILDENHAIN, W., HENSEKE, G. und BIENERT, G.: Reaktivität phenolischer Verbindungen gegenüber 4-Fluor-3-nitroacetophenon. (The Reactivity of Phenolic Compounds Towards 4-Fluoro-3-nitroacetophenon) 447

MAKLEIT, S., BOGNÁR, R., MILE, T. and RADICS, L.: The Formation and Structure of Pschorr's 'Bis-Thiocodide' 455

VASVÁRI, G. and HOLLY, S.: PDPDP and its Derivatives, I. Preparation and Properties of Symmetrically and Asymmetrically Substituted PDPDP Derivatives 459

BOOK REVIEWS – BUCHBESPRECHUNGEN – РЕЦЕНЗИИ КНИГ 469

Printed in Hungary

A kiadásért felel az Akadémiai Kiadó igazgatója — Műszaki szerkesztő: Farkas Sándor

A kézirat nyomdába érkezett: 1970. IX. 7. — Terjdelem: 11 (A/5) ív, 34 ábra

71.70321 Akadémiai Nyomda, Budapest — Felelős vezető: Bernát György

ACTA CHIMICA 1.

ТОМ 66 – ВЫП 4

РЕЗЮМЕ

Термоконденсация трехокиси вольфрама из гидратов 12-вольфраматокремниевой кислоты

Й. А. ХЕГЕДЮШ, П. ГАДО, ДЬ. ШЛОССЕР и Й. НАЙГЕБАУЭР

С помощью, для большинства случаев, термо- и рентгеноаналитического методов изучалось термическое разложение 12-вольфраматокремниевой кислоты. Принимая во внимание новые аспекты, было установлено, почему гидраты этой гетерополикислоты кристаллизуются в различных кристаллических структурах, а также почему и в чем различаются препараты Реанала и Мерка. Было установлено, что область существования кубической Si-гетерополикислоты фазы Кеггина, известной до сих пор как 6-гидрат, ограничена интервалом 100 $\pm <$ 25°C, и ее правильная формула не $H_4[SiW_{12}O_{40}] \cdot 6H_2O$, а $H_4[SiW_{12}O_{40}]$ $6H_2O$, а $H_4[SiW_{12}O_{34}(OH)_{12}]$. Струкура же образующегося отсюда $H_2[SiW_{12}O_{40}]$ отличается от структуры фазы Кеггина и до сих пор была неизвестна, является стабильной между $\sim$ 150 и 480°C, хотя выше $\sim$ 320°C переходит, до некоторой степени, в аморфное состояние, но при охлаждении регидратируется вновь в фазу Кеггина со скоростью, зависящей от pH_2O. Стурктурно испорченный анион Кеггина вызывает кристаллизацию гидратов в виде различных кристаллических систем, а также изменение количества молекул H_2O, связанных различной силой. С повышением температуры исходная кислота превращается в двухступенчатом процессе, состоящем из эндотермической ступени кристаллическое — аморфное состояние и экзотермической ступени аморфное — кристаллическое состояние в тетрагональную трехокись вольфрама, а затем в моноклинную трехокись вольфрама. Приводится общий обзор и дискутируются литературные данные в этой области. Вместо рассмотрения термического разложения 12-вольфраматокремниевой кислоты, в конце концов, вопрос освещается скорее со стороны образующейся трехокиси вольфрама, т. к. при такой постановке вопроса удалось выяснить и механизм процессов термоконденсации и встраивания Si.

О некоторых вопросах осадительного разделения следов элементов, VII

Определение следов меди, цинка, никеля, кобальта и серебра в рудах после разделения с помощью гидроокиси аммония

М. ГЁРБИЦ и Э. УПОР

Был разработан объединенный метод определения следов меди, кобальта, никеля, цинка и серебра в рудах. Медь, кобальт и цинк определялись на основе светопоглощения их комплексов, а именно комплекса меди с Na-диэтилдитиокарбаматом, кобальта — с нитрозо-R-солью, цинка — с дитизоном. Никель определялся с диметилглиоксимом, а серебро на основе его каталитического влияния на окисление Mn^{+2}. Отделение от железа и других ионов, оказывающих помехи, производилось с помощью раствора 2M NH_4OH и 2M NH_4Cl. Кобальт и серебро определяются из раствора непосредственно, а медь, никель и цинк — после экстракционного разделения.

Получение гетита, замещенного алюминием, и изучение его рентгенодиффракционным, дериватографическим и ИК спектрофотометрическим методами

К. ЙОНАШ и К. ШОЙМАР

Были получеты гетиты с различным содержанием алюминия (алюмо-гетиты) с помощью совместного старения гидроокисей железа и алюминия при 40—50°С. В таких условиях удалось достигнуть максимально 21—23 мол.% замещения алюминием. Содержание алюминия в образцах определялось с помощью химического анализа и рентгенодиффракционного метода. Было установлено, что при встройке алюминия, как в синтетических, так и в природных алюмо-гетитах теплота дегидратации постепенно увеличивается, а удельная экстинкция в ИК полосах поглощения постепенно падает. В зависимости от содержания алюминия смещается также и волновое число ИК полосы. Последнее явление позволяет определить с помощью соответствующей калибровки содержание алюминия в алюмо-гетитах.

Изучение ионизации металлов и восстановления ионов металлов с помощью вращающегося дискового электрода с кольцом, V

Изучение анодного растворения меди в кислых сульфатных растворах

Л. КИШ и Й. ФАРКАШ

Для проверки зависимостей, представленных нами в ранних сообщениях, с помощью вращающегося дискового электрода с кольцом изучался механизм анодных процессов, протекающих в кислых сульфатных растворах на медном электроде. Экспериментальные результаты, полученные при анодном растворении меди, успешно объясняются с помощью зависимостей, выведенных, исходя из ступенчатого механизма. Это доказывает, что анодное растворение меди в изученных условиях протекает согласно ступенчатому механизму.

Интегральные уравнения скоростей в химической кинетике

П. Дж. РОБИНСОН

Приводятся интегральные уравнения скоростей химических реакций с любой стехиометрией и с любой комбинацией интегральных или полуинтегральных порядков, вплоть до максимального порядка, равного трем. Применение уравнений обсуждается и иллюстрируется ссылкой на реакцию между диметилфосфином и тетрафторэтиленом.

Изучение термодинамических свойств бинарных смесей, содержащих уксусную кислоту

Й. ЛИСИ

На примере трех бинарных смесей уксусной кислоты с н-гептаном, бензолом и толуолом, авторами демонстрируется использование данных по ассоциационным равновесиям, и молекулярным свойствам определенных в смеси уксусная кислота — четыреххлористый углерод (1), для расчета термодинамических свойств бинарных смесей уксусной кислоты. Было показано, что вышеупомянутые данные хорошо воспроизводят для бинар-

ных смесей данные равновесий пар-жидкость, качественно описывают изменение добавочной свободной энтальпии при смешении, однако, не используются для расчета изменения энтальпии при смешении.

Спектроскопическое изучение замещенных карбонильных групп

А. И. КИШШ и Г. ХОРВАТ

Изучались УФ и ИК спектры некоторых производных бензальдегида с целью получения информации касательно относительной величины влияния-М замещенных карбонильных групп(-COX). Смещение полос $n-\pi^*$ и $\pi-\pi^*$ объяснялось электронно-донорными или электронно-акцепторными свойствами группы X, приводящими к уменьшению или увеличению эффекта-М группы -COX, и тем самым к изменению электронных уровней бензальдегида. На основе мезомерного эффекта, фтор ведет себя как донор, а хлор и бром — как акцепторы. Для последних полагалось, что наряду с p—p сопряжением (эффект+М) проявляется также и p—d сопряжение. Согласно электронным спектрам эффект—М группы —COX изменяется в следующем порядке:

$$-\underset{\underset{O}{\|}}{C}-Br > -\underset{\underset{O}{\|}}{C}-Cl > -\underset{\underset{O}{\|}}{C}-H > -\underset{\underset{O}{\|}}{C}-CH_3 > -\underset{\underset{O}{\|}}{C}-F \sim -\underset{\underset{O}{\|}}{C}-OH > -\underset{\underset{O}{\|}}{C}-OCH_3 > -\underset{\underset{O}{\|}}{C}-NH_2 > -\underset{\underset{O}{|}}{C}-O^-$$

Смещение полосы валентного колебания C = O в ИК спектре соответствует изменению величины электроотрицательности группы X.

Замещенные производные бензамидоксима, оказывающие действие на центральную нервную систему

Г. СИЛАДИ, Э. КАСТРЕЙНЕР, К. КОВАЧ и Й. БОРШИ

Были синтезированы замещенные бензамидоксимы (4-метокси-3,5-дигалоген- и 4-*п*-октилокси-3,5-диметокси-), а также их О-ацил и О-алкил производные. Изучалась взаимосвязь между их химическим строением и физиологическим действием (на центральную нервную систему, противораковое и антибактериальное влияния).

На основе фармакологических исследований были найдены зависимости между химическим строением соединений и их физиологическим действием. Интенсивность действия на центральную нервную систему уменьшается с введением заместителей (как алкил, так и ацил) по кислороду.

Соединения оказались инактивными с точки зрения их противоракового действия; бактерицидная активность одного из соединений (V-336) оказалась средней на типичных штаммах in vitro.

Реакционная способность фенольных соединений при взаимодействии с 4-фтор-3-нитроацетофеноном

В. ВИЛЬДЕНХАЙН, Г. ГЕНСЕКЕ и Б. БИНЕРТ

Было найдено, что реакционная способность различных замещенных фенольных соединений при взаимодействии с 4-фтор-3-нитроацетофеноном в диметилформамидных растворах определяется их нуклеофильными свойствами и пространственной структурой.

Образование и структура как называемого «бис-тиокодида» Пшора

Ш. МАКЛЕЙТ, Р. БОГНАР, Т. МИЛЕ и Л. РАДИЧ

Так называемый «бис-тиокодид», приготовленный Пшором из бромокодида под действием гидросульфида калия в этаноле, оказался, 8,8'-ди-дезокси-8,8'-псевдокодеинил--дисульфидом. Было найдено, что эта реакция приводит также к образованию 8-дезокси-8-тиол-псевдокодеина, полученного авторами другим путем. Окислением этого тиола был получен вышеупомянутый дисульфид.

ПДПДП и его производные, I

Получение и свойства симметрично и асимметричио замещенных производных ПДПДП

Г. ВАШВАРИ и Ш. ХОЛЛИ

Были синтезированы производные ПДПДП, замещенные симметрично и асимметрично. В сообщении приводятся температуры плавления, растворимости и ИК спектры (в табличной форме), а также результаты элементарного анализа полученных соединений.

The Acta Chimica publish papers on chemistry, in English, German, French and Russian.

The Acta Chimica appear in volumes consisting of four parts of varying size, 4 volumes being published a year.

Manuscripts should be addressed to

Acta Chimica
Budapest 112/91 Műegyetem

Correspondence with the editors should be sent to the same address.

The rate of subscription is $ 16.00 a volume.

Orders may be placed with "*Kultúra*" Foreign Trade Company for Books and Newspapers (Budapest I., Fő utca 32. Account No. 43-790-057-181) or with representatives abroad.

Les Acta Chimica paraissent en français, allemand, anglais et russe et publient des mémoires du domaine des sciences chimiques.

Les Acta Chimica sont publiés sous forme de fascicules. Quatre fascicules seront réunis en un volume (4 volumes par an).

On est prié d'envoyer les manuscrits destinés à la rédaction à l'adresse suivante:

Acta Chimica
Budapest 112/91 Műegyetem

Toute correspondance doit être envoyée à cette même adresse.

Le prix de l'abonnement est de $ 16.00 par volume.

On peut s'abonner à l'Entreprise pour le Commerce Extérieur de Livres et Journaux «*Kultúra*» (Budapest I., Fő utca 32. Compte-courant No. 43-790-057-181) ou à l'étranger chez tous les représentants ou dépositaires.

«*Acta Chimica*» издают трактаты из области химической науки на русском, французском, английском и немецком языках.

«*Acta Chimica*» выходят отдельными выпусками разного объема. 4 выпуска составляют один том. 4 тома публикуются в год.

Предназначенные для публикации рукописи следует направлять по адресу:

Acta Chimica
Budapest 112/91 Műegyetem

По этому же адресу направлять всякую корреспонденцию для редакции.

Подписная цена — $ 16.00 за том.

Заказы принимает предприятие по внешней торговле книг и газет «*Kultúra*» (Budapest I., Fő utca 32. Текущий счет № 43-790-057-181) или его заграничные представительства и уполномоченные.

Reviews of the Hungarian Academy of Sciences are obtainable at the following addresses:

ALBANIA

Drejtorija Qändrone e Pärhapjes
dhe Propagandimit tä Librit
Kruga Konferenca e Päzes
Tirana

AUSTRALIA

A. Keesing
Box 4886, GPO
Sydney

AUSTRIA

GLOBUS
Höchstädtplatz 3
A-1200 Wien XX

BELGIUM

Office International de Librairie
30, Avenue Marnix
Bruxelles 5
Du Monde Entier
5, Place St. Jean
Bruxelles

BULGARIA

HEMUS
11 pl Slaveikov
Sofia

CANADA

Pannonia Books
2, Spadina Road
Toronto 4, Ont.

CHINA

Waiwen Shudian
Peking
P. O. B. 88

CZECHOSLOVAKIA

Artia
Ve Směčkách 30
Praha 2
Poštovní Novinová Služba
Dovoz tisku
Vinohradská 46
Praha 2
Mad'arská Kultura
Václavské nám. 2
Praha I
SLOVART A. G.
Gorkého
Bratislava

DENMARK

Ejnar Munksgaard
Nörregade 6
Copenhagen

FINLAND

Akateeminen Kirjakauppa
Keskuskatu 2
Helsinki

FRANCE

Office International de Documentation
et Librairie
48, rue Gay Lussac
Paris 5

GERMAN DEMOCRATIC REPUBLIC

Deutscher Buch-Export und Import
Leninstraße 16
Leipzig 701
Zeitungsvertriebsamt
Fruchtstraße 3—4
1004 Berlin

GERMAN FEDERAL REPUBLIC

Kunst und Wissen
Erich Bieber
Postfach 46
7 Stuttgart S.

GREAT BRITAIN

Blackwell's Periodicals
Oxenford House
Magdalen Street
Oxford
Collet's Subscription Import
Department
Denington Estate
Wellingsborough. Northants.
Robert Maxwell and Co. Ltd.
4—5 Fitzroy Square
London W. I

HOLLAND

Swetz and Zeitlinger
Keizersgracht 471—487
Amsterdam C.
Martinus Nijhof
Lange Voorhout 9
The Hague

INDIA

Hind Book House
66 Babar Road
New Delhi I

ITALY

Santo Vanasia
Via M. Macchi 71
Milano
Libreria Commissionaria Sansoni
Via La Marmora 45
Firenze

JAPAN

Kinokuniya Book-Store Co. Ltd.
826 Tsunohazu 1-chome
Shinjuku-ku
Tokyo
Maruzen and Co. Ltd.
P.O. Box 605
Tokyo-Central

KOREA

Chulpanmul
Phenjan

NORWAY

Tanum-Cammermeyer
Karl Johansgt 41—43
Oslo I

POLAND

RUCH
ul. Wronia 23
Warszawa

ROUMANIA

Cartimex
Str. Aristide Briand 14—18
Bucureşti

SOVIET UNION

Mezhdunarodnaya Kniga
Moscow G—200

SWEDEN

Almquist and Wiksell
Gamla Brogatan 26
S—101 20 Stockholm

USA

F. W. Faxon Co. Inc.
15 Southwest Park
Westwood Mass. 02090
Stechert Hafner Inc.
31. East 10th Street
New York, N. Y. 10003

VIETNAM

Xunhasaba
19, Tran Quoc Toan
Hanoi

YUGOSLAVIA

Forum
Vojvode Mišića broj 1
Novi Sad
Jugoslovenska Knjiga
Terazije 27
Beograd

24. III. 1971

Index: 26.007